University of Southampton

Faculty of Engineering and Physical Sciences

School of Chemistry

Using synthetic oligonucleotides to modify cellular IRES structures and control gene expression

by

Ane Gutierrez Aguirregabiria

ORCID ID 0000-0002-9905-1945

Thesis for the degree of Doctor of Philosophy

December 2019

University of Southampton

Abstract

Faculty of Engineering and Physical Sciences

School of Chemistry

Thesis for the degree of Doctor of Philosophy

Using synthetic oligonucleotides to modify cellular IRES structures and control gene expression

by

Ane Gutierrez Aguirregabiria

There are different structures and sequences in the 5' UTR of mRNAs that can control the levels of translation, such as G-quadruplexes, upstream open reading frames, hairpins or Internal Ribosome Entry Sites (IRESs). Among all of them, IRESs are particularly interesting as they have the ability to increase translation initiation. IRESs were first discovered in viruses and years later their existence in cellular mRNAs was verified. These elements have the ability to start translation when cap-mediated translation is compromised, such as in hypoxia, heat shock or nutrient depravation. These conditions are usually present in tumors, and it is not surprising IRES activity can be increased in cancer cells.

Researchers have tried to target both viral and cellular IRESs as a possible treatment for different viral infections and cancer. In this sense, antisense therapy could be of particular interest. Antisense therapy uses antisense oligonucleotides to control gene expression by inducing RNA degradation, changes in splicing or blocking the translation machinery. Since antisense therapy was developed, oligonucleotides have been modified in different ways to make them more stable in cellular environments and to increase their targeting or cell penetration abilities.

In this project we have designed oligonucleotides with different modifications to modify the secondary structure of the *BAG1* IRES and in this way to control the expression of the IRES by either decreasing or increasing its activity. *BAG1* is an anti-apoptotic gene implicated in the regulation of many cellular processes, and has been shown to be dysregulated in different cancers.

Being aware of the controversy surrounding the existence of cellular IRESs, we have first verified the presence of an IRES in the p36 *BAG1* 5' UTR using stricter criteria than existed during its initial characterisation. We then designed oligonucleotides based on the proposed structure of the *BAG1* IRES as well as a pool of oligonucleotides targeting different regions of the *BAG1* IRES and generated a luciferase based method to quickly assay the effect of different oligonucleotides on IRES activity. The most promising oligonucleotides were modified with Locked Nucleic Acids, 2'-*O*-Methyl RNAs and phosphorothioate bonds in an attempt to increase their activity and stability in cells.

We have shown to be able to increase the *BAG1* IRES activity in a cell free system using different oligonucleotides and have different oligonucleotides that have shown promising results in cells.

Controlling translation initiation has a direct result on the efficiency of protein synthesis. Understanding the events in this process could lead to the discovery of new therapeutic targets, and thereby, the development of new therapies. In this way, these oligonucleotides could prove to be a treatment for diseases associated with an inappropriate amount of functional proteins and in this sense targeting cellular IRESs could be the key.

Table of Contents

Table of Tables

Table of Tables

Table of Figures

Table of Figures

Table of Figures

Table of Figures

Research Thesis: Declaration of Authorship

Print name:	Ane Gutierrez Aguirregabiria

Title of thesis:	**Using synthetic oligonucleotides to modify cellular IRES structures and control gene expression**

I declare that this thesis and the work presented in it are my own and has been generated by me as the result of my own original research.

I confirm that:

1. This work was done wholly or mainly while in candidature for a research degree at this University;
2. Where any part of this thesis has previously been submitted for a degree or any other qualification at this University or any other institution, this has been clearly stated;
3. Where I have consulted the published work of others, this is always clearly attributed;
4. Where I have quoted from the work of others, the source is always given. With the exception of such quotations, this thesis is entirely my own work;
5. I have acknowledged all main sources of help;
6. Where the thesis is based on work done by myself jointly with others, I have made clear exactly what was done by others and what I have contributed myself;
7. None of this work has been published before submission

Signature:		Date:	12.12.2019

Acknowledgements

I would like to thank all my supervisors, Dr Eugen Stulz, Dr Mark Coldwell, Prof Graham Packham and Dr Tilman Sanchez-Elsner for their help and support during my PhD, and in particular, I would like to thank Mark for accepting me in his team as one of his main PhD students.

I would also like to thank the IFLS for funding this PhD and for giving me the opportunity to present my research in international conferences. Special thanks to Janette Thompson for being a great intermediary and for always being there when I needed help.

My trip over this PhD would not have been the same without the support of my lab-mates. Thank you Christina for helping me with the oligonucleotide synthesis and for making Southampton a great place to be. Thank you Connor and Fuad for all your help in the lab, for listening attentively to all my complaints and for keeping patient with me during my OCD moments. Connor, thank you for helping me with the microscopy, for improving all my texts with your “perfect English” and for all your lessons on England. Thank you Fuad for keeping me entertained in the office and for being always SO supportive.

Thank you to all those fish in B85 for your great banter and good memories. Thank you Aleks (Bestie), for always being there when I needed a conversation, a beer or chocolate.

To Dr James Woodhall, you were the first person that suggested I should do a PhD and I am grateful you believed in me that day. Thank you for being my first mentor in the lab.

Elena y Toni, gracias por iluminar Southampton con esa alegría española que los dos desprendéis. Fernando, gracias por esas conversaciones y por siempre enseñarme los mejores sitios de Southampton.

A toda mi familia, pero sobre todo a Aita, Ama y Eva, gracias por vuestro apoyo durante todos estos años. Gracias por ayudarme llegar hasta aquí y por nunca dejar que me diera por vencida.

Lee, thank you. I would not be here if it was not for you. Thank you for your unconditional support, for always being there for me, for your patience with me, for taking me to University so many weekends… Above all, thank you for giving me the best moments during these last three years.

Definitions and Abbreviations

ASO	Antisense oligonucleotide
ATP	adenosine 5’-triphosphate
Avg	average
BAG1	BCL2 associated athanogene 1
bp	base pairs
BSA	bovine serum albumin
cDNA	complementary DNA
CDS	Coding DNA sequence
CEP-Cl	2-Cyanoethyl N,N-diisopropylchlorophosphoramidite
DCM	DNA-cytosine methyltransferase
DIPEA	N,N-Diisopropylethylamine
DMEM	Dulbecco’s Modified Eagle medium
DMT	4,4’-dimethoxytrityl group
DNA	deoxyribonucleic acid
DOC	deoxycholate
DSMZ	Deutsche Sammlung von Mikroorganismen und Zellkulturen/ German Collection of Microorganisms and Cell Cultures
E. coli	*Escherichia coli*
EDTA	ethylenediaminetetraacetic acid
EGTA	egtazic acid
eIF	eukaryotic initiation factor
EMVC	encephalomyocarditis virus
Fluc	Firefly luciferase
FDA	Food and Drug Administration
FBS	fetal bovine serum
FMDV	Foot and mouth disease virus

GJ	GeneJuice
HFIP	hexafluoro-2-propanol
hnRNPC	Heterogeneous Nuclear Ribonucleoprotein C
HPLC	high-performance liquid chromatography
IRES	internal ribosomal entry site
ITAF	IRES trans-acting factor
kDa	Kilo dalton
LB	Luria-Bertani
LNA	locked nucleic acid
m^7G	7-methylguanosine
MCS	multiple cloning site
miRNA	microRNA
MOE	methoxyethyl
mRNA	messenger RNA
NEB	New England Biolabs
Nluc	Nanoluc Luciferase
NTC	no template control
Nt	nucleotide
ORF	open reading frame
PCBP1	poly (rC) binding protein 1
PIC	Preinitiation complex
PS	Phosphorothioate
PNK	polynucleotide kinase
PTBP1	polypyrimidine tract binding protein 1
RBF	round-bottom flask
RIPA	radioimmunoprecipitation assay
RJ	RiboJuice
RLU	relative light units

RNA	ribonucleic acid
RNAi	RNA interference
RNase H	ribonuclease H
RPM	Revolutions per minute
RRL	Rabbit Reticulocyte Lysate
rSAP	Recombinant Shrimp Alkaline Phosphatase
RT	Reverse transcription
SD	Standard deviation
SDS	sodium dodecyl sulphate
siRNA	small interfering RNAs
SOC	super optimal broth with catabolite repression
TAE	tris-acetate-EDTA
TBE	Tris-borate EDT
TBS	tris-buffered saline
TBS-T	tris-buffered saline-tween
TEA	triethanolamine
TLC	thin layer chromatography
Tm	melting temperature
TnT	transcription and translation
uORF	Upper open reading frame
UTR	untranslated region
UV-VIS	ultraviolet–visible spectroscopy or ultraviolet-visible spectrophotometry
WB	western blot

Chapter 1 INTRODUCTION

1.1 OVERVIEW

The control of gene expression using modified oligonucleotides has evolved to create potential therapies for incurable diseases. The introductory chapter of this thesis will cover the basics of gene expression including nucleic acid structure, and the process of eukaryotic transcription and translation with an emphasis on IRES-mediated translation. The chapter will then discuss the IRES-containing *BAG1* gene, covering topics such as its structure, translation and implication in different diseases. Antisense therapy will also be discussed, with special interest on the different oligonucleotide chemistries developed for therapy and FDA approved antisense oligonucleotides.

1.2 GENE EXPRESSION

Gene expression is the process by which the information in genes is used to synthesise functional products, some of which are proteins, however they could also be functional RNAs such as tRNAs or snRNAs. This process is also known as the Central Dogma of Molecular Biology (see Figure 1.1, A), which was properly defined by Francis Crick in 1970[1] (however the concept was first mentioned by Francis Crick in a public lecture in 1957). Gene expression is divided into two main steps: transcription and translation, where nucleic acids play important roles.

1.2.1 Nucleic acids

The main classes of nucleic acids are deoxyribonucleic acid (DNA) and ribonucleic acid (RNA). Nucleic acids are long polymers composed of an array of nucleotides. A common characteristic of nucleic acids is their solubility in water. Nucleotides are composed of a nitrogen heterocyclic base, a pentose sugar (hydrophobic) and a phosphate residue (hydrophilic) (see Figure 1.1, B). The bases can be monocyclic (pyrimidines), as cytosine (C), thymine (T) and uracil (U) or bicyclic (purines) as adenine (A) and guanine (G) (see Figure 1.1, C). The base joins the carbon-1 of the pentose sugar through a ring nitrogen (N1 in pyrimidines and N9 in purines) by covalent bonds (*N*-glycosidic linkage).

Deoxyribonucleic acid (DNA) is formed by 2'-deoxyribonucleotides, whereas ribonucleic acid (RNA) is formed by ribonucleotides[2] (see Figure 1.1, D). Both ribose and deoxyribose sugars are non-planar molecules, they have a 3D structure, nevertheless a reference plane or "sugar pucker" is defined. The location of the atoms above or below the sugar pucker will determine the

conformation of the nucleotides and thereby the conformation of DNA or RNA molecules. Sugars with atoms puckered above the reference plane will be in the *endo*-form while the *exo*-form will take place when the puckered atoms are located beneath the plane[3] (see Figure 1.1, E).

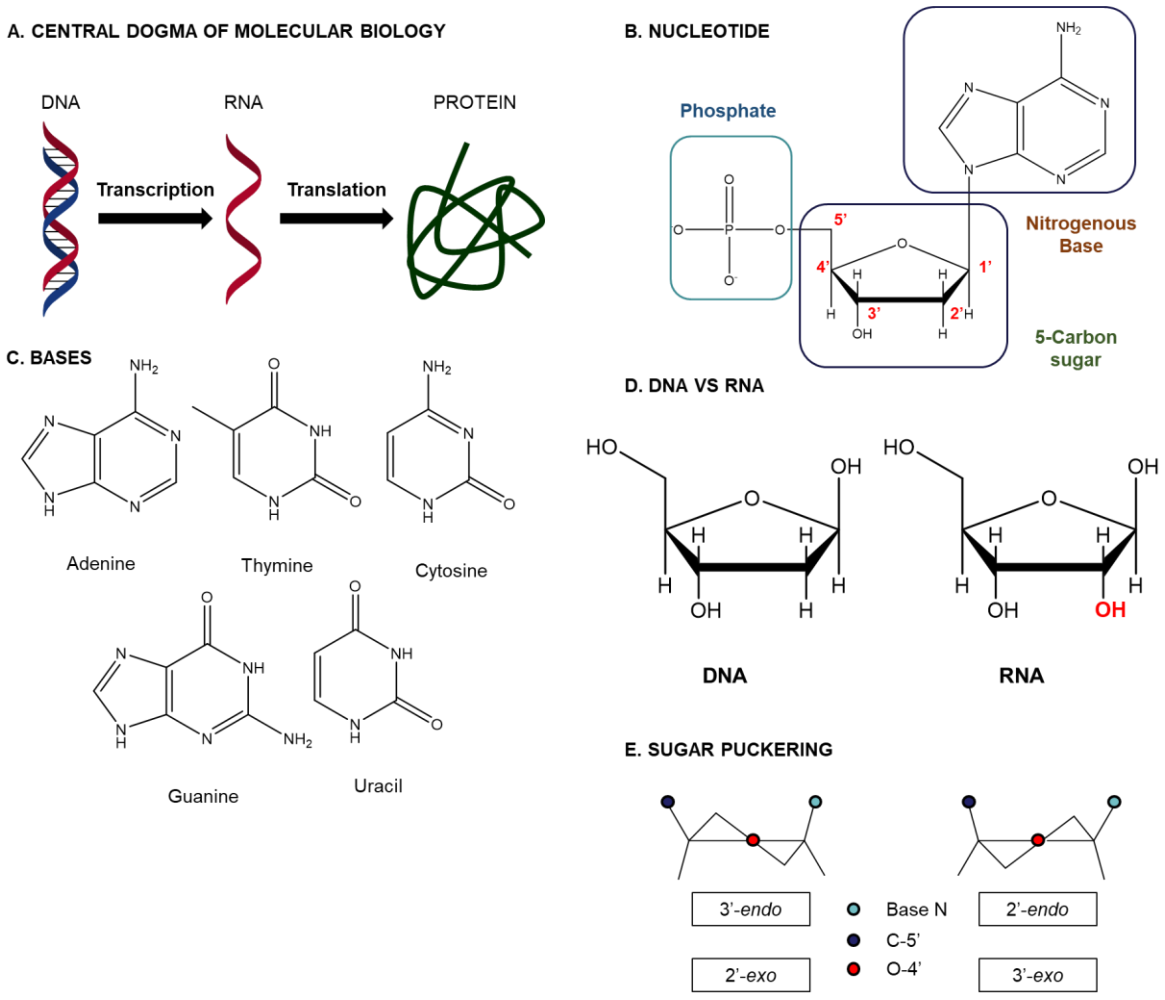

Figure 1.1 **Nucleic acids.** A) Central dogma of Molecular Biology. DNA is transcribed in RNA and RNA is translated into proteins. B) Structure of a nucleotide formed by a 5 Carbon sugar, a nitrogenous base and a phosphate. C) Structure of the bases that can be found on nucleotides. D) Structure of DNA and RNA sugars. E) DNA sugar puckering.

DNA structure:

DNA is the material where the genetic information is stored. Using the X-ray diffraction photographs of DNA fibres obtained by Maurice Wilkins and Rosalind Franklin[4], James Watson and Francis Crick discovered some of the most important aspects in the structure of B DNA. DNA molecules have a double helical nature, where two DNA chains are coiled around a common axis in a right-handed screw sense and in antiparallel directions (see Figure 1.2, A), which gives polarity to the molecule. The bases lie on the inside of the helix, while the phosphate backbones are on the outside. The bases are located almost perpendicularly to the helical axis, where adjacent bases are separated by 3.4 Å. There are 10.5 bases per turn in the double helix and the

helical structure repeats every 34 Å. Each base has a rotation of 36 degrees from the one below. The helix has a diameter of 20 Å[5] (see Figure 1.2, A).

The dominant base pairing in nucleic acids is the so-called Watson-Crick pairing, where adenine binds to thymidine with two hydrogen bonds, whilst cytosine binds to guanine with three hydrogen bonds, in this way all the base pairs have the same size (see Figure 1.2). However, other base pairings do also exist, such as Hoogsteen pairs[6,7] (see Figure 1.2). In any double stranded DNA molecule there is a 1: 1 ratio of purines and pyrimidines, this concept is known as Chargaff's rule[8].

The nitrogen and oxygen atoms present in the bases help form the hydrogen bonding that holds the two DNA strands in a duplex. The interactions between the bases forming the nucleotides are also important in determining the structure of the DNA. Among these interactions, there are repulsive steric interactions between proximate bases and sugars and π-π stacking interactions (non-covalent interactions given between aromatic molecules).

The primary DNA structure consists of nucleosides joined by a phosphate diester from its 5'-hydroxyl group to the 3'-hydroxyl group of the neighbour nucleoside, forming a chain. A DNA molecule is formed by two of these chains located in antiparallel fashion where the bases are joined together by hydrogen bonds, forming a helix. In the helix there can be distinguished the major groove (parts of the helix where the backbones are far apart), and the minor groove (parts of the helix where the backbones are close together). This is known as the secondary structure of the DNA (see Figure 1.2, A).

The two strands forming the DNA molecule can be unwounded by helicases in the cells, or by high temperatures, allowing the processes of replication and transcription to take place. When these processes are complete, the complementary strands can anneal again. The DNA sequence determines the RNA sequence and protein sequence that will carry out most of the activities in the cells.

DNA molecules can adopt different structures under different circumstances (see Figure 1.2, C):

A DNA

Right-handed anti-parallel double helices, forming a cylinder of around 24 Å diameter. Sugar rings are located parallel to the helix axis, whereas the phosphate backbone is on the outside. There are 11 bases in each turn of 28 Å. The major groove is very deep, whereas the minor groove is very shallow. The helix is wider and shorter than B DNA's. Double stranded regions of RNA and some RNA-DNA duplexes adopt a A-like structure[9]. At low humidity and high salt concentration,

the favoured structure is A-DNA[2]. A DNA usually shows a C-3' endo conformation, where the C-3 lies out of the plane, which is formed by the other four atoms of the ring[9].

B DNA

This is the DNA structure defined by Watson and Crick. The B DNA is right-handed, where the base pairs sit on the helix axis, which makes the major and minor groove have a similar depth. Bases on the same strand are predominantly stacked above their neighbours perpendicularly to the helix axis. At high humidity and low salt, under physiological conditions, the dominant secondary structure of the DNA is B-DNA. B DNA usually takes a C-2' endo conformation, where the C-2 lies out of the plane[9].

Z DNA

This structure was discovered by Alexander Rich[10], and consists of a left-handed anti-parallel duplex. This conformation is common in sequences with alternating purine-pyrimidine sequences (dCGCGCG). This DNA conformation has a strong zig-zag pattern in the phosphodiester backbone. Backbone phosphates are closer together in Z DNA than in A or B DNA, hence a high salt concentration is required to minimize the electrostatic repulsion[11].

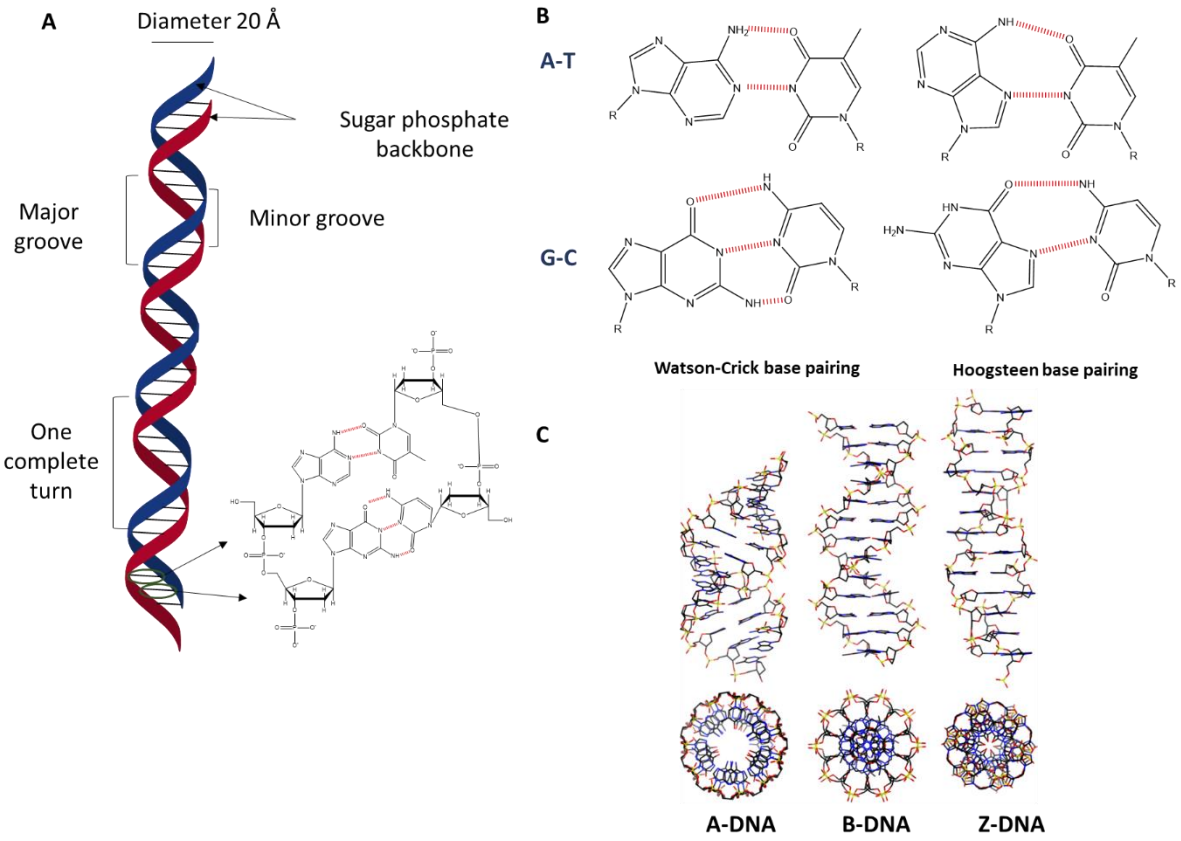

Figure 1.2 **DNA molecule structure.** A) DNA double helix structure showing the major and minor grooves and nucleotide base pairing in the DNA molecule. B) Watson-Crick base pairing versus Hoogsteen base pairing for A-T and G-C base pairs. C) Side and top view of A-DNA, B-DNA and Z-DNA conformation. Image credit: CC BY-SA 4.0 Mauroesguerroto/Wikimedia Commons.

1.2.2 Transcription: RNA

DNA is transcribed into RNA in the nucleus of the cells by an RNA polymerase with the help of different transcription factors[2]. RNA polymerases use a DNA strand as a template for RNA transcription by adding nucleotides to the 3' end of the growing RNA which are complementary to the template DNA strand[2] (see Figure 1.3).

The process of transcription consists of three stages: initiation, elongation and termination. During the initiation step, transcription factors bind to the promoter region in the DNA and recruit the RNA polymerase. Transcription factors also help separating the DNA strands in the double helix to provide access to the RNA polymerase to a single stranded DNA[2].

In prokaryotes there is only one RNA polymerase with five subunits, whereas in eukaryotes three different RNA polymerases can be found with over 10 subunits each. Each of the eukaryotic RNA polymerases will also require different transcription factors. RNA polymerase I transcribes ribosomal RNA, RNA polymerase II transcribes protein coding nuclear pre-mRNAs and RNA

polymerase lll transcribes different structural RNAs as the 5S pre-rRNA, transfer pre-RNAs and small nuclear pre-RNAs[2].

The RNA polymerase is released from the transcription factors to proceed with RNA synthesis in a 5' to 3' direction. The activity of the protein dimer FACT (facilitates chromatin transcription) is required to disassemble nucleosomes (DNA-histone complexes) upstream of the RNA polymerase transcription. RNA polymerases have the ability to unwind the double stranded DNA, allowing the RNA synthesis to occur in a region of single stranded DNA of around 25 nucleotides (see Figure 1.3). The RNA falls off the DNA template as it is synthesised allowing the DNA to rewind again[2].

Termination is different for the three different RNA polymerases, but overall it takes place in response to termination sequences and signals. In the case of RNA polymerase l, the protein TTF-1 is required, which will recognize a specific sequence in the DNA and bind to it, blocking RNA polymerase l from continuing with transcription. RNA polymerase ll lacks any sequence or signal to terminate transcription. The pre-mRNA is cleaved while the RNA polymerase is still transcribing and this is where the process of transcription terminates (see Figure 1.3). It is still not very clear how RNA polymerase lll terminates transcription, however it is known that the poly(T)-terminal signal causes catalytic inactivation and backtracking of the enzyme, which commits polymerase lll to termination[12].

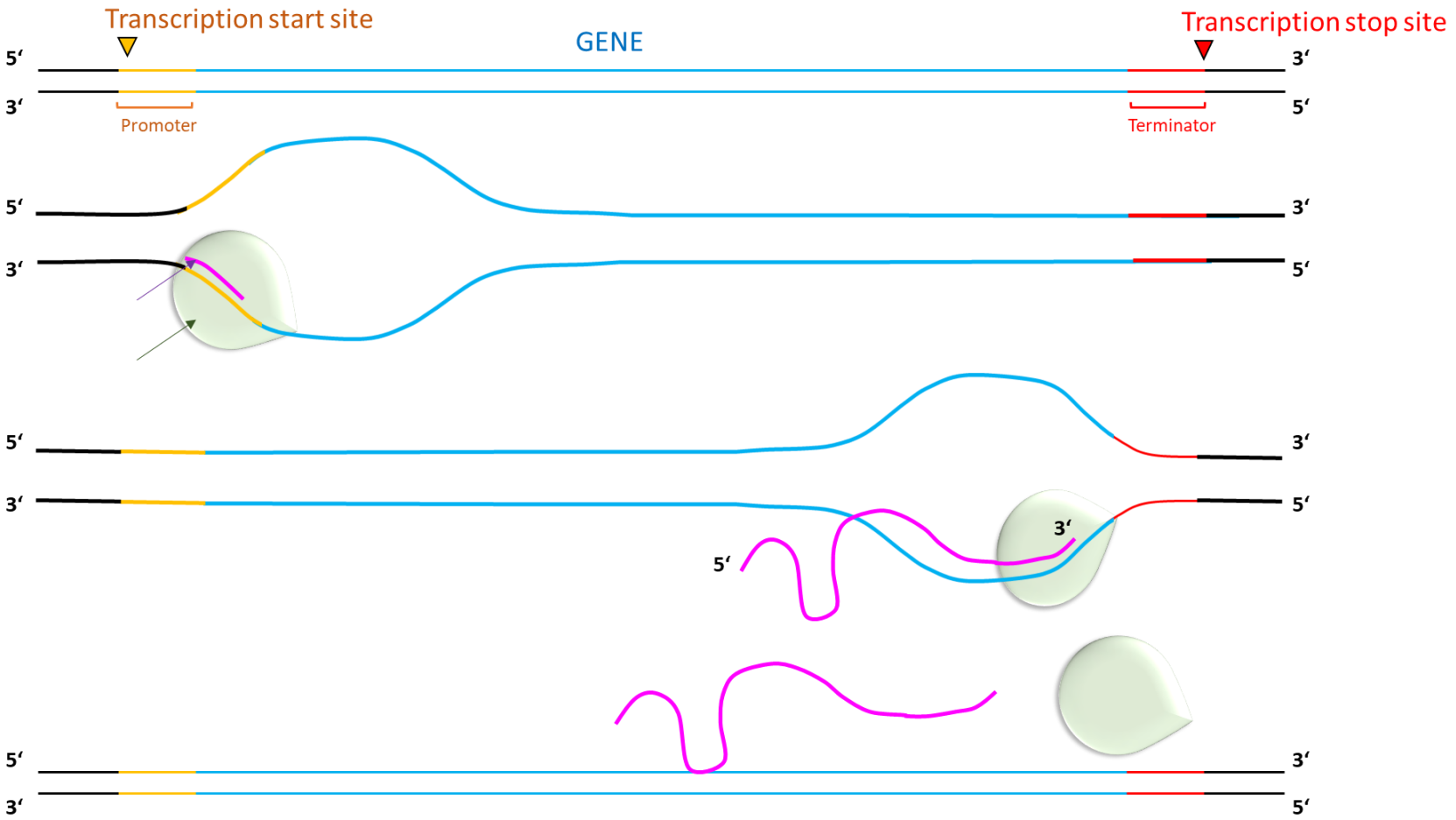

Figure 1.3 **Process of transcription.** RNA polymerase has the ability to unwind the double stranded DNA and start transcription from the transcription start site until the transcription end site. The pre-mRNA is cleaved when the transcription is finished.

Post-transcriptional processes

In eukaryotes, pre mRNAs that code for proteins will still be subject to some modifications in the form of 5' capping, polyadenylation and RNA splicing to become mature mRNAs[13].

Capping:

At the 5' end of the mRNA a guanine residue is added, which is not encoded by the DNA (see Figure 1.4). This guanine residue is bound to the RNA by three phosphate molecules linked *via* a 5' to 5' bond, instead of by a unique phosphate molecule linked by a 3' to 5' bond, as in the rest of the nucleotides forming the RNA molecule. The addition of the extra guanine by a 5'-5' bond is done by the enzyme guanylate transferase. Following this addition, the enzyme guanine methyltransferase adds a methyl group in the position 7 of the purine ring producing a 7-methyl guanine (see Figure 1.4). This cap structure enhances the processes of mRNA export from the nucleus and mRNA translation, and also protects the mRNA from degradation by exonucleases, which would detect a free 5' end and digest the RNA in a 5' to 3' direction.

Polyadenylation:

This process consists of the addition of over 200 adenosine residues in the 3' of the RNA as soon as the transcription process is finished (see Figure 1.4). The polyadenylation site is flanked by two sequences: an AAUAAA sequence upstream and a sequence rich in G and U residues downstream of the polyadenylation site. These two sites are recognized by two protein complexes that will bind to the RNA and cleave the RNA sequence between them. Subsequently the enzyme polyA polymerase will add over 200 adenine residues in the 3' end of the RNA. The polyadenylation of the RNA protects the RNA from degradation by exonucleases and enhances RNA translation.

RNA splicing:

RNA splicing is the process by which intron sequences are removed from an RNA and exons are joined together (see Figure 1.4). The transcribed RNA molecule is formed by introns (RNA sequences that do not code for a protein) and exons (the actual RNA sequences that code for proteins, as well as the 5' and 3' UTRs). The introns need to be removed before the RNA is transported to the cytoplasm for further translation. The process of splicing is carried out by an assembly of proteins and small RNA molecules known as spliceosomes. Spliceosomes can recognise specific splice signals in the pre-mRNA: in most cases introns begin with a GU and end with an AG followed by a pyrimidine rich tract. During the process of splicing the phosphodiester bonds that separate the introns from the exons are cleaved, and exons are joined. Most of the eukaryotic pre-mRNAs can be spliced in different ways giving rise to different proteins.

RNA methylation:

Different RNA types can be methylated post-transcriptionally, in most of the cases at a nucleoside level and not that much in the sugar-phosphate backbone[14]. RNA methylation is a gene expression control system, allowing the activation of protein-coding genes and cellular processes. The most common RNA methylation modification is N^6-methyladenosine (m6A), which is a dynamic and reversible modification. In mammalian cells the m6A modification sites are conserved and regulated by m6A methylatransferases and demethylases[15]. m6A modifications are more abundant near the stop codon and in the 3' and 5' UTRs, which suggests the ability of m6A to affect RNA translation and metabolism[16]. In this instance, m6A modification is known to facilitate translation initiation through the interaction with eIF3 and eIF4E[17]

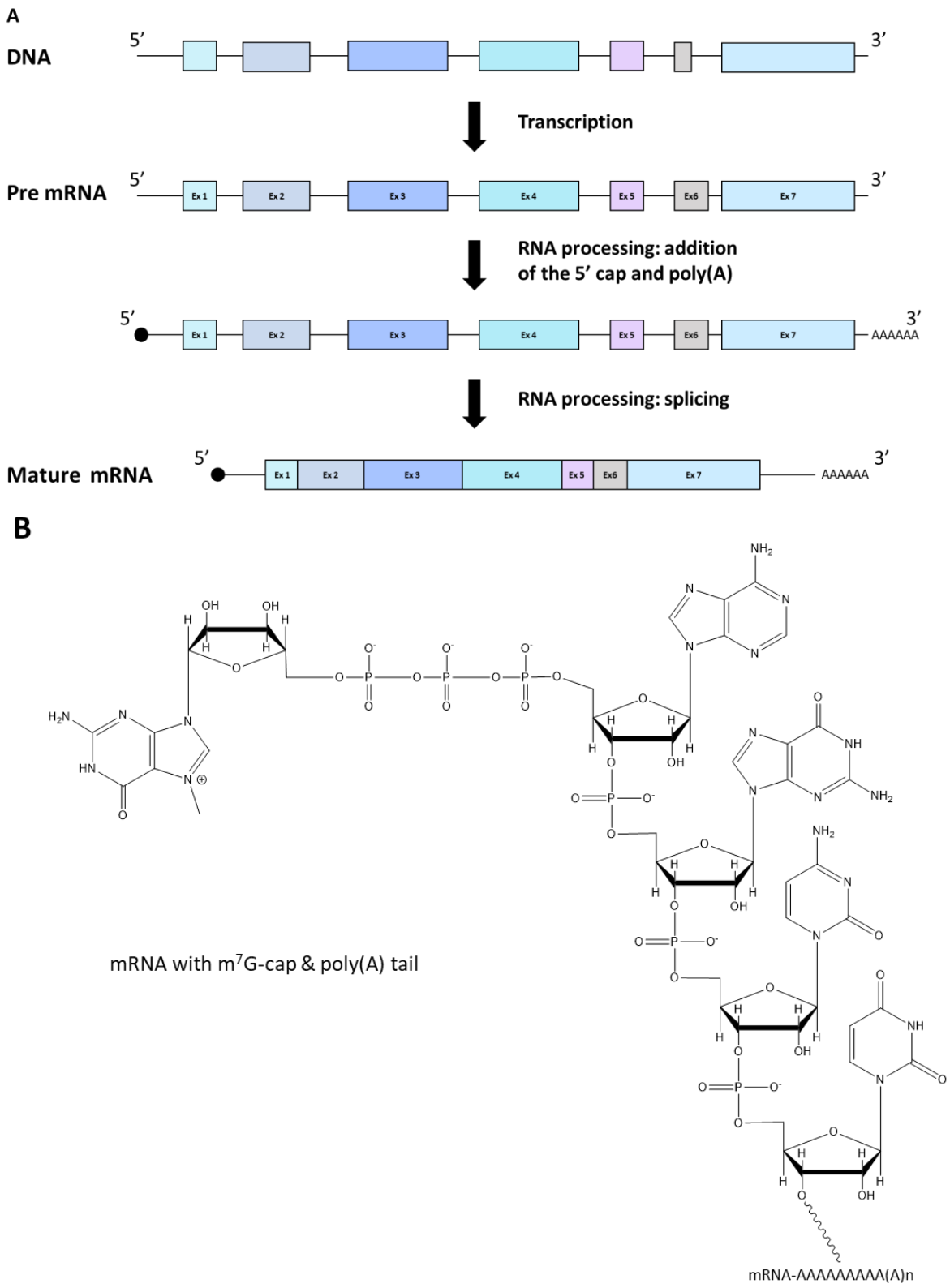

Figure 1.4 **mRNA maturation process.** A) DNA is transcribed into pre-mRNA. That pre-mRNA undergoes a process of maturation where an m^7G-cap is added to its 5' and a poly(A) tail to its 3', followed by the process of splicing, where the exons are removed and the introns are joined together. B) Structure of a mature RNA with a 5' m^7G-cap and a poly(A) tail.

RNA STRUCTURE

RNA molecules require the correct three-dimensional structure to function correctly. Even more, some RNAs require that specific regions have the ability to modify their conformation or to have structural flexibility[18].

RNA shows a greater structural versatility than DNA in terms of its chemical reactivity and conformations[2] and different RNAs can show different structures. They could be long and double stranded or have a globular shape with short duplex domains and single stranded segments[2]. In double stranded RNA molecules Watson-Crick base pairing is the most common one.

There are many different types of RNAs, each found in different kingdoms and species, with different structures and functions. The most known ones are rRNA, mRNA, tRNA, however others are less common, such as non-coding RNAs (ncRNAs), small nucleolar RNAs (snoRNAs), extracellular RNAs (exRNAs), circular RNAs (circRNAs)[19].

RNA has the ability to fold forming three dimensional structures that modulate the ability of the RNA to regulate different functions as translation, gene silencing, RNA splicing and protein trafficking[20,21]. RNA functions rely considerably on secondary and tertiary structures[20]. RNA folding can happen at different levels, it usually starts acquiring a defined structure during transcription[22,23], although that structure will be modulated by different factors such as the cellular environment, the process of transcription itself and RNA chaperones[23,24]. Every RNA molecule in each cell has a unique structure that could differ from the native RNA structure, that is why the conformation of an RNA in a cell could be different from that of a refolded or *in vitro* made RNA[24].

There are different techniques to study the secondary and tertiary structure of RNA: NMR spectroscopy, X-ray crystallography and cryo-electron microscopy can be used to study the three-dimensional structure of RNA molecules. Depending on the RNA length different techniques are accessible to determine the secondary structure of an RNA molecule: for short RNAs of up to 200 nt, gel-based enzymatic and chemical probing could be used. For RNAs of up to 400 nt SHAPE-CE could be used. For bigger RNA molecules SHAPE-seq, SHAPE-MaP or DMS-Map could be used[25]. In general, selective 2'-hydroxyl acylation analysed by primer extension (SHAPE) is the most useful technique to study the structure of a given RNA. This technique uses N-methylisotoic anhydride (NMIA) and 1-methyl-7-nitroisatoic anhydride (1M7) to randomly modify the 2' OH group in the RNA backbone, followed by a reverse primer extension that will be stopped when the reverse transcriptase comes across a modified nucleotide. The cDNA is then sequenced and analysed to determine single and double stranded regions in the RNA[26].

GENETIC STRUCTURE OF A EUKARYOTIC mRNA

The mature eukaryotic mRNA consists of the 5' untranslated region (5' UTR), the coding region and the 3' untranslated region (3' UTR) (see Figure 1.6). Non-coding or untranslated regions mediate the majority of gene expression regulation, as they play important roles in the regulation of post-transcriptional processes. They are implicated in the mRNA transport to the cytoplasm[27], translation efficiency[27], subcellular localization of the mRNA[28] and mRNA stability[29]. RNA binding proteins can interact with different nucleotide patterns or motifs located in the UTRs to regulate different post transcriptional processes, in this case the secondary structure of the RNA plays an important role[30].

5' UTR

The 5' UTR is the region of the mRNA flanked by the m^7G-cap and the start codon. The length of the 5' UTR is roughly constant among different taxonomic classes, with a length of 100-200 nucleotides[30]. However, mRNAs coding for proteins involved in cell regulation, which need a high level of regulation, such as transcription factors, growth factors or proto-oncogenes usually have longer 5' UTRs than average[31]. There is a greater G and C content in the nucleotide sequence of the 5' UTR, usually of around a 60%[30,32].

Post-transcriptional control of mRNA translation is known to be mediated by *cis*-acting elements located in the 5' UTRs[33], such as upstream open reading frames (uORFs), hairpins or stem loops, internal ribosome entry sites (IRESs) or G-quadruplexes.

uORF

Open reading frames (ORFs) are the parts of the mRNA that have the ability to be translated. Upstream open reading frames (uORF), are ORFs located in the 5' UTR, upstream of the start codon and they will contain a start codon in their 5' end location. The 40S ribosomal subunit can detect this AUG in the uORF and start translation from that point[30].

uORFs have the ability to control translation in different ways. If translation of the uORF is terminated alongside the CDS's, then an N-terminal extension will be generated in the translated protein (see Figure 1.5, A). If the uORFs are located near the CDS and their translation is terminated before the CDS's translation is initiated, ribosomes could reinitiate thereby increasing the levels of translation of the CDS (see Figure 1.5, B). If the uORF is located out of frame from the CDS and their translation finishes after the translation start point of the CDS, then the translation of the CDS will be reduced or inhibited[34] (see Figure 1.5, C).

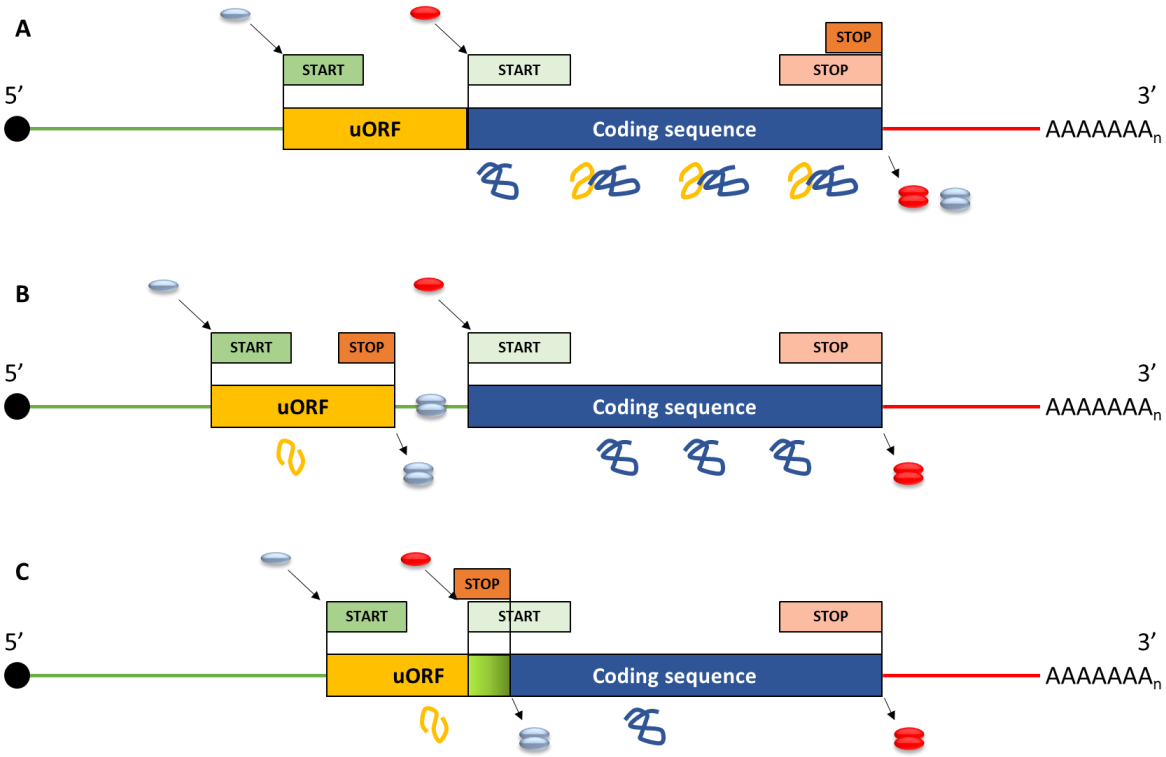

Figure 1.5 **Control of translation of the coding sequence depending on the position of the uORFs and their termination codon.** If the uORF and the CDS share the same termination codon, most of the proteins will contain an extended N-terminal (A). If the uORF's translation is finished before the CDS's translation starts, some ribosomes could reinitiate (if the right conditions are given), increasing the translation of the CDS (B). If the uORF's stop codon is located after the CDS's initiation codon, then the translation of the CDS will be inhibited or reduced (C).

Hairpins or stem loops

Hairpins or stem loops are formed when two regions of nucleotides forming a DNA or RNA molecule form base pairs with each other. It is one of the secondary structures more commonly found in the 5' UTRs. Depending on the thermodynamic stability of the hairpins and their location in respect to the start codon, they could have different effects in the translation efficiency. In general, the further the stem loop is located from the 5' cap, the stronger the stem structure needs to be to inhibit ribosome scanning[35].

IRES

Some of these elements present in the UTRs, as Internal Ribosome Entry Sites (IRESs) for example, can drive translation even when the translation machinery is repressed[36]. It needs to be noted that even though most IRESs are located in the 5' UTR, in some cases they have also been found in the ORF[37,38]. IRESs will be explained in detail in a further section.

G-quadruplexes

G-quadruplexes (G4) are non-canonical, very stable secondary structures that appear in G-rich sequences of DNA or RNA. For a G4 to be formed at least four runs of multiple consecutive guanines, separated by short linker region need to be present, where each G of the tract could then base pair with a G of the next tract through Hoogsteen hydrogen bonds, forming a G-quartet or a co-planar array. When two or more of these G-quartets stack, a G4 is formed. The G-quartets are linked to each other *via* loops formed by random nucleotides. G4s are stabilized by a monovalent cation, which is usually potassium[39].

RNA G4 (rG4) are involved in different post-transcriptional regulatory mechanisms such as polyadenylation, alternative splicing and mRNA localization[40]. rG4s located in the 5' UTR usually inhibit translation by steric blocking of the translation initiation or the ribosomal scanning[41,42]. However, the G4s in *VEGF* and *FGF2* can activate translation, as they are part of the secondary structure of their IRES[43,44].

CODING REGION

The coding region of a mature mRNA is the sequence flanked by the start codon (usually an AUG) and stop codon (UGA, UAA, and UAG), and is formed by triplet codons, each encoding an amino acid, which makes it the region of the mRNA that codes for a protein[30]. Different codons can code for the same amino acid, however different organisms use some codons more regularly than others. Common codons are found in highly expressed genes, are translated more quickly, with a higher fidelity and provide a higher regulatory control than rare codons[45].

3' UTR

The 3' UTR is the sequence defined between the stop codon and the poly(A) in an mRNA. The length of the 3' UTR shows a great variability between different taxonomic classes, and could be between 200-800 nucleotides[30].

RNA turnover is mostly controlled by elements located in the 3' UTR. Among these elements we can find AU-rich elements (AREs), which in response to different signals can promote mRNA decay[30]. On the other hand, GU-rich elements (GREs) cause rapid mRNA decay in short-lived mRNAs[46].

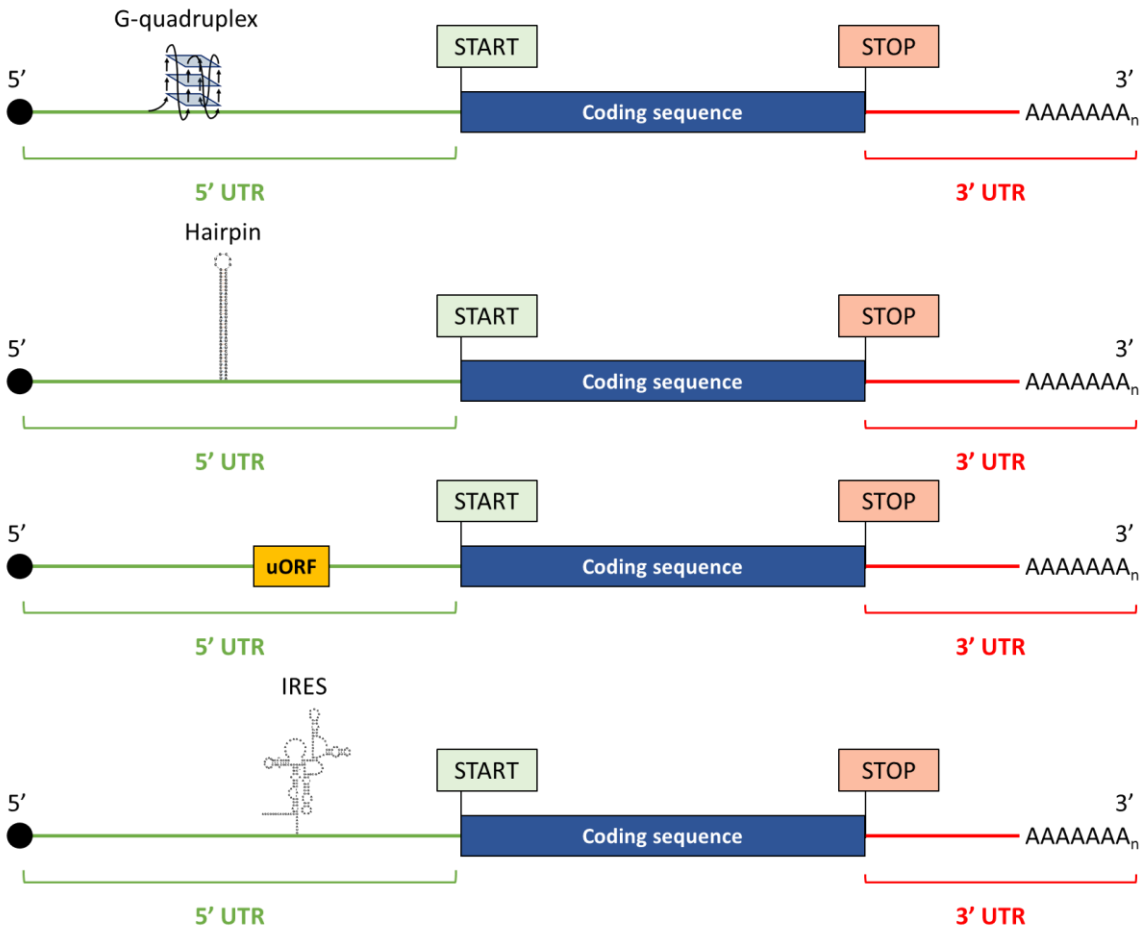

Figure 1.6 **Genetic structure of a mature eukaryotic mRNA.** A mature mRNA is formed by the 5' UTR, (limited by the 5' m^{7}G-cap and the start codon, where G-quadruplexes, hairpins, uORFs and IRESs can be found), the coding sequence (limited by the start and stop codons) and the 3'-UTR limited by the stop codon and poly(A) tail.

1.2.3 Translation in eukaryotes

Translation is the process by which proteins are synthesised based on mRNA templates and it is the process that consumes up to 50% of cellular energy[47]. Mature mRNAs are transported through nuclear pore complexes from the nucleus of the cells to the cytoplasm[48], where the process of translation takes place. As mentioned before, the synthesis of proteins is a complex process that is divided into three phases: initiation, elongation and termination[49,50]. It is believed that initiation is the most complex among the three phases[50].

In most eukaryotic mRNAs, translation is initiated by a process known as cap-dependent translation initiation or canonical translation. This is a well-regulated process that requires various steps and the presence of at least ten initiation factors (eIFs), the roles of which will be discussed in detail below[51].

The first step is the formation of the pre-initiation complex (PIC) formed by the ribosomal 40S subunit and the ternary complex (TC) formed by the initiator methionyl-tRNA (Met-tRNA$_i$) and eIF2 bound to GTP. eIF1, eIF1A, eIF5 and the eIF3 complex promote the binding of the TC to the 40S ribosomal subunit (Figure 1.7, A). This complex will attach to the m^{7}G-cap on the 5' end of the mRNA[52]. This process is facilitated by eIF3, the poly(A) binding protein (PABP), eIF4B, eIF4H and the eIF4F complex (formed by the scaffold protein eIF4G, the cap-binding protein eIF4E and the RNA helicase eIF4A). eIF4G is a scaffold protein that contains binding sites for eIF4E, eIF4A, eIF3 and PABP, with the ability to bind all these components together. eIF4G has the ability to interact with the mRNA *via* the cap and poly(A) tail to form a circular messenger ribonucleoprotein (mRNP), also known as the "closed-loop" structure. When eIF4G and eIF3 interact, a protein bridge is established between the mRNP and the PIC, which stimulates the attachment of the 40S to the mRNA. eIF4E will bind to the m^{7}G-cap, which promotes ribosome binding[51] (Figure 1.7, B). The attachment of the ribosomal 40S subunit to the mRNA requires the unwinding of the mRNA's 5' terminal secondary structure. This unwinding will be done with helicase eIF4A, whose activity is enhanced by eIF4B and eIF4H, generating a single-stranded landing path in the mRNA for the PIC.

Once the ribosome is bound to the m^{7}G and the mRNA is unwound, the ribosome 40S subunit will then scan the mRNA (in the 5' to 3' direction) until the first start codon in a suitable context is recognized. The most common start codon is AUG, however in the late 1980s it was discovered that the ribosome could also take CUG, GUG or UUG as possible start codons[53–55]. ATP, eIF4A, eIF4G and eIF4B are required for the scanning process; the requirement of eIF4A and ATP is proportional to the level of secondary structure in the mRNA[56,57].

The start codon is recognized when the base pairing between the AUG in the mRNA and the anticodon of Met-tRNA$_i$ takes place. The start codon recognition stops the scanning of the PIC. eIF5 and eIF5B will promote hydrolysis of eIF2-bound GTP, so that all the eIFs are displaced and the 60S subunit can join the 40S subunit, forming the 80S ribosome. At this point the initiation complex is formed containing the 80S and the Met-tRNA$_i$ base paired to the AUG (Figure 1.7, C) and protein synthesis will start[52]. While Met-tRNA$_i$ is located in the P site of the 80S ribosome, on the A site an aminoacyl-tRNA with an anticodon complementary to the next codon will be located. The intrinsic peptidyl-transferase activity of the large ribosomal subunit will form a peptide bond between the methionine and the next aminoacyl-tRNA. The tRNA located in the P site leaves the ribosome and this translocates along the mRNA to the next codon, the next aminoacyl-tRNA will bind to the A site (see Figure 1.7, D), this process is GTP dependent. The polypeptide chain will be built in this way in an N-terminal to C-terminal direction. When one of the possible three stop codons (UAG, UAA, and UGA) enters the A site, the tRNA in the P site becomes hydrolysed and the polypeptide is released into the cytoplasm (Figure 1.7, E). The two subunits of the ribosome

dissociate and are ready to start the process of translation again[9] (Figure 1.7, F). However in some cases, the 40S ribosomal subunit can remain attached to the mRNA and start scanning again, which is known as ribosomal reinitiation. If another ORF was found downstream of the original ORF (as in a polycistronic mRNA), those 40S ribosomal subunits could start translation again. Even though at that point the 40S ribosomal subunits cannot effectively start translation because they lack eIF2 ternary complex (eIF2-TC), new eIF2-TC could be acquired to initiate translation[52]. The reinitiation ability depends on the ability of eIF2-TC to bind to the 40S ribosomal subunit, the length of the first ORF and the secondary structures present on it (the longer and more structure in the first ORF, the lower are the chances for ribosomal reinitiation to take place)[58,59].

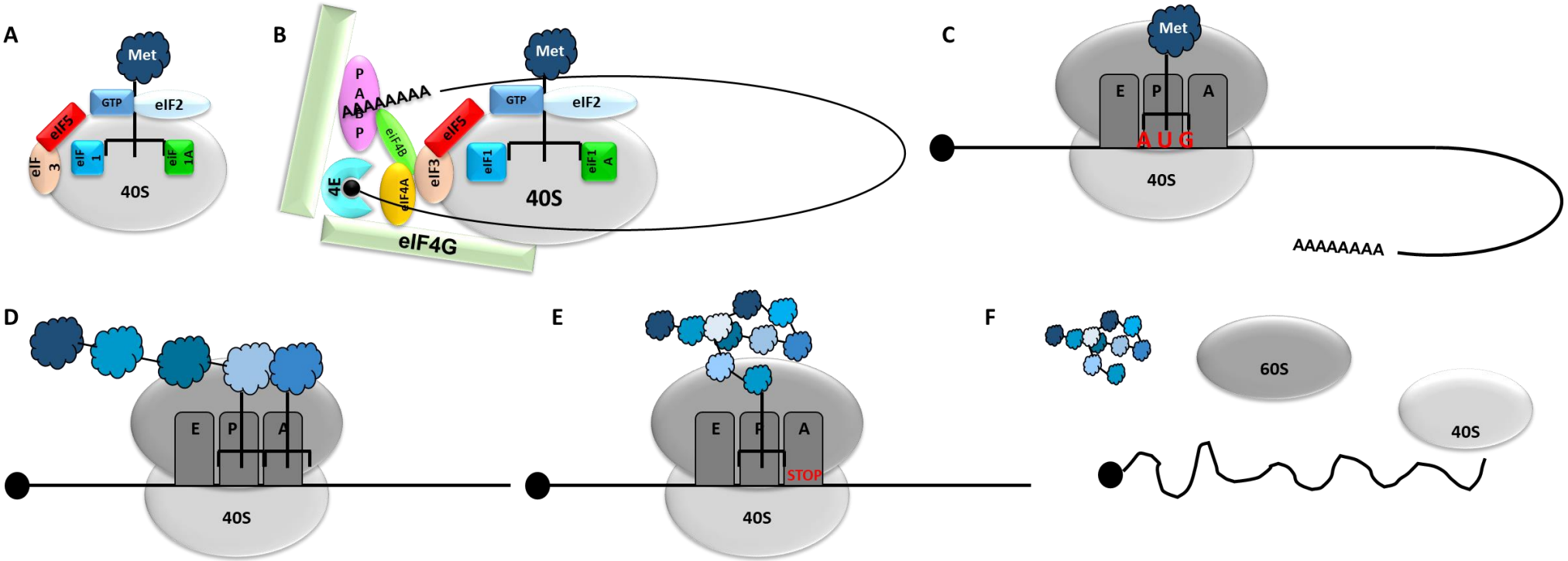

Figure 1.7 **Eukaryotic translation initiation.** A) Representation of the preinitiation complex (PIC), formed by the 40S ribosomal subunit, the eIF2-GTP/Met-tRNA complex, eIF3, eIF1, eIF1A and eIF5. B) The mRNA is unwound thanks to eIF4A, eIF4B and eIF4H. The PIC can now bind to the mRNA cap through eIF4E. eIF4G is a protein scaffold involved in the recruitment of the 40S to the mRNA. C) When the start codon is recognized, usually an AUG, the 60S ribosomal subunit is recruited forming a complete functional ribosome. Protein synthesis will start at this point. D) On the A site an aminoacyl-tRNA with an anticodon complementary to the next codon will be located. Peptide bonds are formed between adjacent amino acids, until a stop codon is found (E). At this point translation terminates, the ribosomal subunits are dissociated (F).

The process of translation can be regulated at different levels. In order for translation to initiate, eIF2 must bind to the 40S ribosomal subunit. However, when the α subunit of eIF2 is phosphorylated (usually by different kinases which are activated in response to cellular stress), eIF2 is unable to couple with GTP and deliver the initiator Met-tRNA$_i$ to ribosomes for the appropriate start codon recognition, and thereby mRNA translation is repressed[60,61] . eIF4E binding proteins (4E-BPs) can also control translation initiation through mTORC1. When mTORC1 phosphorylates 4E-BPs, they dissociate from eIF4E allowing eIF4E to bind to eIF4G and thereby initiate translation[62].

The Kozak consensus plays an important role in the translation of eukaryotic mRNAs. The optimal sequence in mammals for a ribosome to start the translation process is GCCRCCaugG, also known as the Kozak sequence or consensus[63]. It has been demonstrated that the efficiency in translation can vary if the Kozak sequence is not optimal. The A in the AUG codon is considered position number 1 (see Figure 1.8). Changes in positions -3 and +4 of the sequence are the most critical ones for the translation efficiency, a purine (usually A) in position -3 is essential for efficient translation initiation and in its absence a G is required in position +4[64]. Ribosomes tend to initiate translation at the first AUG, but when the match to the optimal Kozak sequence is very weak, some ribosomes can bypass the first AUG and start translation from a start codon positioned further downstream. This process is known as leaky ribosomal scanning[51].

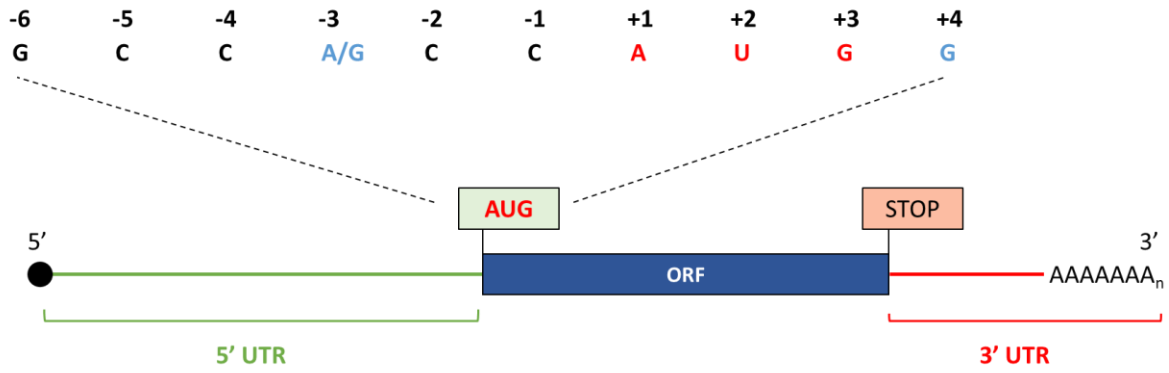

Figure 1.8 **Kozak consensus representing the optimal sequence surrounding the initiation codon (in red) to start translation, where positions -3 and +4 (in blue) play an important role.**

Although translation of mRNAs is normally mediated by the scanning mechanism, an alternative initiation pathway involves the use of internal ribosomal entry sites (IRESs)[52].

1.2.4 IRES-mediated translation initiation

What are IRESs?

IRESs are a segment of mRNA, they are long and often highly structured, with complex secondary and tertiary structures and are usually located near the start codon[50,65]. They are particularly special as they can mediate translation initiation by recruiting the ribosome into an internal position of the mRNA. In this way, the ribosome does not need to associate via the 5'-end of the mRNA[52]. When IRES-driven translation takes place, the ribosomal 40S subunit binds directly to the IRES[66] (Figure 1.9, right hand panel).

Viral IRESs

IRESs were first discovered in poliovirus and in the encephalomyocarditis picornavirus[67,68]. It was in the early 70s when it was discovered that the viral mRNAs had a different structure from the cellular mRNAs, as viruses do not contain the 5' m^7G-cap. Analysing the 5' UTR of the poliovirus, it was seen that this was extremely long, with multiple upstream AUG codons and multiple secondary structures, thus it was hypothesised that the ribosomes could bind the mRNA in an internal position. This was confirmed by using a bicistronic assay[68] (explained in detail in the next section). Viral IRESs are autonomous elements in the RNA, meaning that they can be active outside their natural RNA context. However, viral IRESs function as a single entity, the whole sequence is needed for the IRES to be active[69].

After the discovery of the existence of IRESs in picornavirus, the existence of IRESs in many other viral families was revealed. Nowadays there are a wide range of different IRESs known, all with different qualities in terms of structure, sequence and length. Viral IRESs can initiate translation in two different ways. One of the ways consists of the direct interaction of the 40S ribosomal subunit with the IRES. For the other mechanism, eIFs and RNA binding proteins (RBPs) need to bind to the IRES, which will help with the 40S ribosomal subunit recruitment[70]. These RBPs are also known as IRES trans-acting factors (ITAFs).

Viral IRESs are classified in four different classes according to their ribosome recruitment mode and their secondary/tertiary structure. Type l and ll IRESs are found in picornaviruses. They are long (400-500 nt) and show some conserved sequences within each of the classes. Picornavirus IRESs are classified into five different types, each of them requiring the activity of different eIFs[70]. The main difference between type l and ll IRESs is their position in the 5' UTR. Type l IRESs (for example PV IRES) are located far upstream of the initiation codon, thus after the 40S ribosomal subunit recruitment a process of scanning is required to find the start codon. Type ll IRESs (as EMVC IRES for example) are located just upstream of the initiation codon, and thereby no

scanning process is required to start translation[71]. Type lll IRESs (HCV IRES) are shorter than type l and ll IRESs and have the ability to directly recruit the 40S ribosomal subunit to the start codon. They work by presenting a pseudoknot upstream of the AUG start codon and they require the first 30 nt of the ORF to be active[72,73]. These IRESs require the presence of eIF3 to initiate translation[74]. Type IV IRESs (Intergenic region, IGR IRES) are conserved in the *Dicistroviridae* family, where they present as a bicistronic mRNA and the translation of each ORF takes place by different IRESs. These IRESs have the ability to function in the absence of a start codon and can also form 80S ribosomes in the absence of Met-tRNA[75].

Even though the existence of IRESs was found long ago and despite the research done, it still remains unknown the exact mechanisms each IRES uses to recruit ribosomes[76]. Overall it needs to be kept in mind that different IRESs show different activities and that their activity depends both on the host cell type and on the cellular environment[70].

Cellular IRESs

The discovery of IRESs in viruses suggested the possible existence of these elements in eukaryotic mRNAs. Furthermore, the hypothesis of the existence of IRESs could explain two unknowns in the field of translation in eukaryotes. First, it could explain why some mRNAs with extremely long 5' UTRs, containing various stem loops and with out of frame start codons can be translated efficiently, despite the fact that it has been demonstrated that all those features significantly reduce translation initiation[35,77]. The existence of cellular IRESs could also explain why some mRNAs can still be efficiently translated under stress conditions, even when cap-dependent initiation has been inhibited by cleaving eIF4G[78,79]. The first cellular IRES was discovered in 1991 in the immunoglobulin heavy-chain binding protein (BiP)[80]. Even though the presence of IRESs in cellular mRNAs has been proven, IRES-mediated translation in cells is not as effective as viral IRES mediated translation[81].

It has been suggested that IRES-mediated translation in eukaryotes could skip the regulatory mechanisms required by cap-dependent translation initiation[66]. Nevertheless, IRES-mediated translation is still a regulated process. ITAFs are proteins that bind to the RNA, acting as RNA chaperones whose role is to maintain or to keep the appropriate three-dimensional structure of the IRES for a successful assembly of the 40S complex[82,83]. The involvement of these ITAFs varies in the IRESs of different mRNAs[65] and they include autoantigen La[84], hnRNPC[85], death-associated protein 5[86], members of the poly(rC) protein family[87] and PTBP1 isoforms[88]. Some of these ITAFs are nuclear proteins capable of moving from the nucleus to the cytoplasm, others have known roles in other aspects of RNA metabolism such as splicing or are associated with the translation machinery[71]. Different ITAFs could act in different IRESs, in the same way an IRES could need the

presence of different ITAFs for its activity. An interesting fact is that the same ITAFs could control the activity for both viral and cellular IRESs, which could suggest that the ITAFs could have the same mode of action in both types of IRESs or that one ITAF could act in different ways[71]. The presence and activity of ITAFs is generally more important in cellular IRESs than in viral IRESs. Nevertheless, cellular IRESs show a stronger tissue-specificity than viral IRESs[89].

Much research has still to be done to understand how translation is initiated with IRES elements. It is believed that IRES-mediated translation requires eIFs, ITAFs and the 40S ribosomal subunit, but it is still not known how the 40S ribosomal subunit binds to the IRES and how important is the activity of the eIFs. Studies have been done to analyse the need of different eIFs in the IRES-mediated translation of different genes, which led to the conclusion that different IRESs require different eIFs to be active. In most cases eIF4E (the cap-binding protein) and full-length eIF4G (the scaffold protein) are not required for IRES-mediated translation[90]. C-*myc* and N-*myc* IRESs do not require eIF4E or eIF4G, but they become inactive in the absence of eIF4A and eIF3; L-*myc* IRESs however requires both eIF4E and eIF4G to be active[91]. Some IRESs are more sensitive to the phosphorylation of eIF2 than others; the phosphorylation of eIF2 inhibits protein synthesis, as it reduces the activity of the eIF2-GTP Met-tRNA$_i$ ternary complex and thereby reduces the canonical system of protein synthesis[92]. All this information suggests that cellular IRESs might initiate translation in different ways and thereby require different factors.

There are no large similarities in the structure of the IRES in different genes, most IRESs do not share similarities with one another in terms of structure, sequence and length, which makes difficult the possibility to classify cellular IRESs[52,93]. In general, cellular IRESs show a wide range of structures and are less stable than the folded mRNA in terms of the Gibbs free energy[94]. Cellular IRESs show cell tropism, meaning the grade of activity they have varies from one cell line to other. This suggests that the levels of ITAFs present in different cells lines is different[95].

IRESs can have different levels of activity at different cell stages. *PITSLREp58 kinase*, c-*myc* and *Unr* IRESs are more active during mitosis[96]. *Ornithine decarboxylase (ODC)* has an IRES that is active exclusively in the G2/M phase of the cell cycle, where cap-mediated translation is believed to be blocked[97]. However Coldwell *et al.* showed that cap-mediated translation is still active during G2/M phase[98], which could create some discrepancies in the activity of the ODC IRES. To this day there is no cellular RNA that, under normal circumstances, can only be translated *via* an IRES, all the IRES containing mRNAs can also be translated in the canonical way[52].

It is believed that cellular IRESs could carry out two major physiological functions, one being to support the low levels of translation in mRNAs with highly structured 5' UTRs and the other one to support translation in cells under certain physiological conditions when cap-mediated translation

is compromised such as in apoptosis[99], hypoxia[100], mitosis[101], cell differentiation, nutrient limitation and endoplasmic reticulum stress[92]. Because most of these situations such as amino acid or serum deprivation and hypoxia are observed in tumours, IRESs are believed to be more active in tumour cells[102]. In these situations mRNAs with IRES elements will recruit most of the ribosomes, eIFs and ITAFs[92]. Hypoxia is also observed in cardiovascular diseases as ischemia, and thereby IRESs will also play an important role in these kind of diseases. The IRESs of *FGF1, FGF2, VEFGA, VEGFC* and *VEGFD*, classified as angiogenic genes, are activated in early hypoxia while *EMCV* and *c-myc* IRES, known as non angiogenic, are activated in late hypoxia[103,104]. In this case, IRES-mediated translation allows a quick angiogenic response in an ischemic myocard, contributing with the survival of cardiomyocytes[71].

It is believed that IRES-mediated translation is important in cell-fate decisions, as most of the proteins translated *via* IRESs are involved in apoptosis or protection of cells from stress[92]. Most of the mRNAs that contain IRESs, such as *APAF1, c-myc, XIAP, FGF, p53* and *VEGF* have functions implicated in cell proliferation, survival or death.

Due to the lack of similarities among the different cellular IRESs, the existence of an IRES in a particular mRNA needs to be determined individually. IRES elements have been discovered and studied using bicistronic reporter assays (Figure 1.10). In the case of eukaryotic mRNAs with more than one in frame start codon, ribosomes will efficiently translate the first initiation codon, but they would not efficiently start translation through any of the initiation codons located downstream of the first one, unless any of these start codons were preceded by an IRES. In the presence of an IRES translation of a secondary ORF could be as efficient as the translation of the main ORF[79] (Figure 1.10, A and B). However, bicistronic assays could lead to misunderstandings due to the presence of cryptic promoters (epigenetically silenced and normally inactive promoters that can be activated under certain circumstances and give rise to aberrant peptides) and splice sites present in the bicistronic vectors (Figure 1.10, C). That is why before assuming that a gene contains an IRES, an exhaustive analysis needs to be done, such as the one proposed by Terenin *et al.*[36] (this will be explained in more detail in Chapter 3). Most of the cellular IRESs which have been cloned in bicistronic mRNAs are inactive when they are transfected directly into the cytoplasm of the cells (RNA transfection). This suggests that there must be a vital step taking place in the nucleus of the cell to activate the IRES[82].

A high throughput study was done to study cellular cap independent translation, which showed that around 10% of the mRNAs could translate proteins using IRESs. This very same study also showed that IRESs were present not only in the 5' UTR but also in the 3' UTR of some human mRNAs[105]. In addition, even if the proper analysis is done to verify the existence of an IRES, it still

should not be assumed that the presence of an IRES indicates that a certain protein is translated via an IRES.

Mutations in different IRESs can lead to uncontrolled translation: a mutation in the c-myc IRES leads to c-myc overexpression in multiple myeloma[106]. The IRES activity of *connexin-32* has proven to be essential for the translation of this protein in nerve cells, mutations in different areas of the *connexin-32* IRES lead to a loss or increase of function[107]. More recently it has been reported an increase in the IRES activity of different cancer related genes as *c-myc, IGF1R, FGF1, FGF2* and *VEGFA*[108].

Even though a significant amount of research has been done in the field of cellular IRESs and numerous peer reviewed papers can be found verifying their existence, there has been much debate on this topic, mainly led by Prof Marilyn Kozak. Prof Kozak published several papers (over fifteen years ago) explaining her attitude towards cellular IRESs[35,51,109–113]. Her reticence to accept the existence of cellular IRESs was mainly based on the methods used to determine the presence of an IRES in a cellular mRNA, as she argued that a positive result in a bicistronic assay was not enough evidence to determine the presence of an IRES[113]. She also argued that the structure of the IRESs should be determined to explain how the IRESs function[113]. Prof Kozak also suggested that IRESs in bicistronic mRNAs should be functional when directly transfected in cells, and that the nuclear experience[82] required could simply be splicing or activation of a cryptic promoter[111]. Her disbelief continued due to the lack of similarity found among the sequences of all the putative cellular IRESs found and the lack of knowledge on their mode of action[111]. Prof Kozak brought up some well-documented concerns about the existence of IRESs, however some of her arguments have also been discussed and confronted by William C. Merrick[114], a cellular IRES supporter.

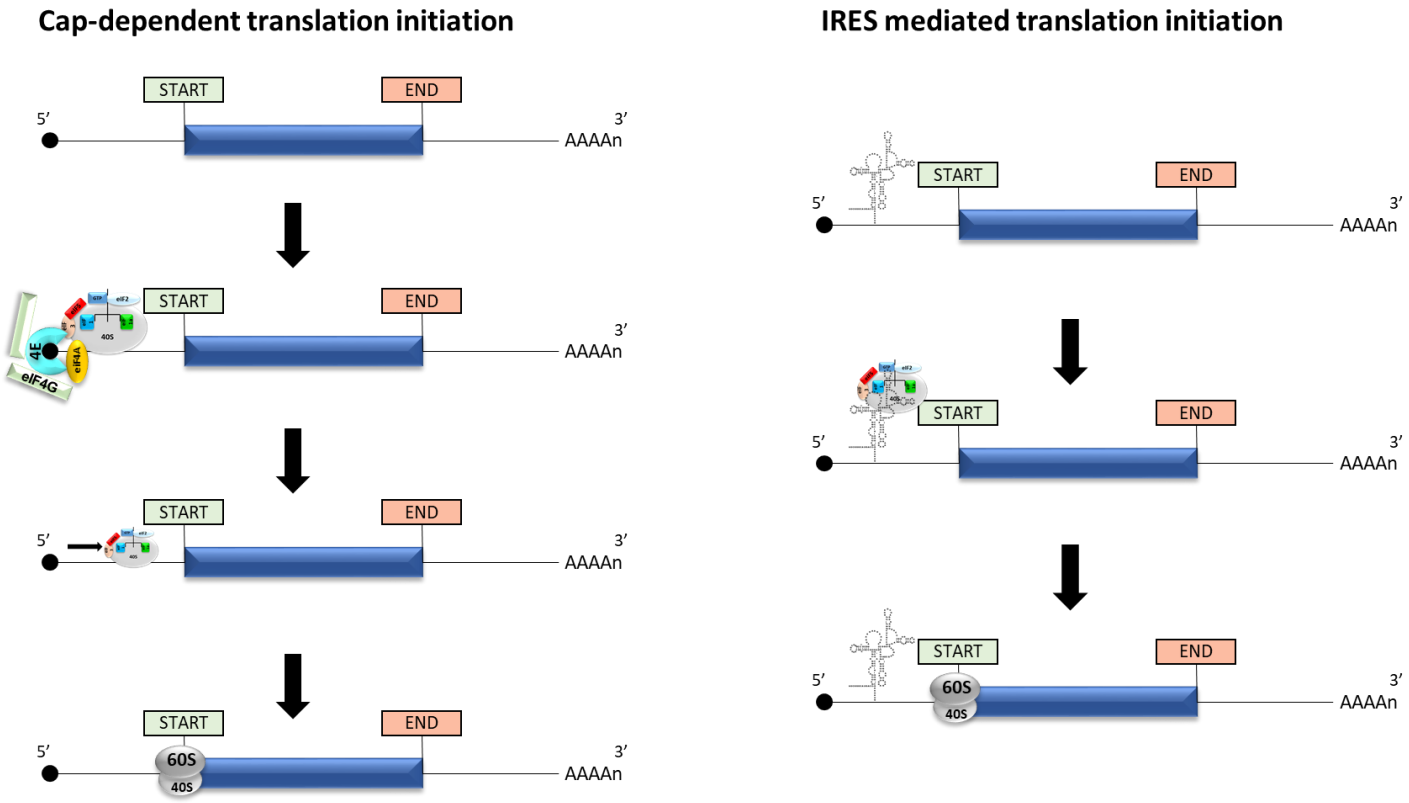

Figure 1.9 **Cap-dependent initiation versus IRES-mediated translation.** In the cap-mediated translation initiation, the preinitiation complex formed by the ribosomal 40S subunit and the eIF2-GTP/Met-tRNA complex binds to the 5′ cap (black circle) and scans the mRNA until it finds the first start codon (AUG). In that moment the 60S ribosomal subunit binds to the initiation complex forming a full functioning ribosome. After this step protein synthesis starts. In the IRES-mediated translation, the IRES element (located nearby the start codon) can directly recruit the preinitiation complex with the 40S ribosome subunit. The ribosome can then scan the mRNA through that point until it finds the first start codon. At that point, the 60S ribosomal subunit will bind to the 40S and protein synthesis will start.

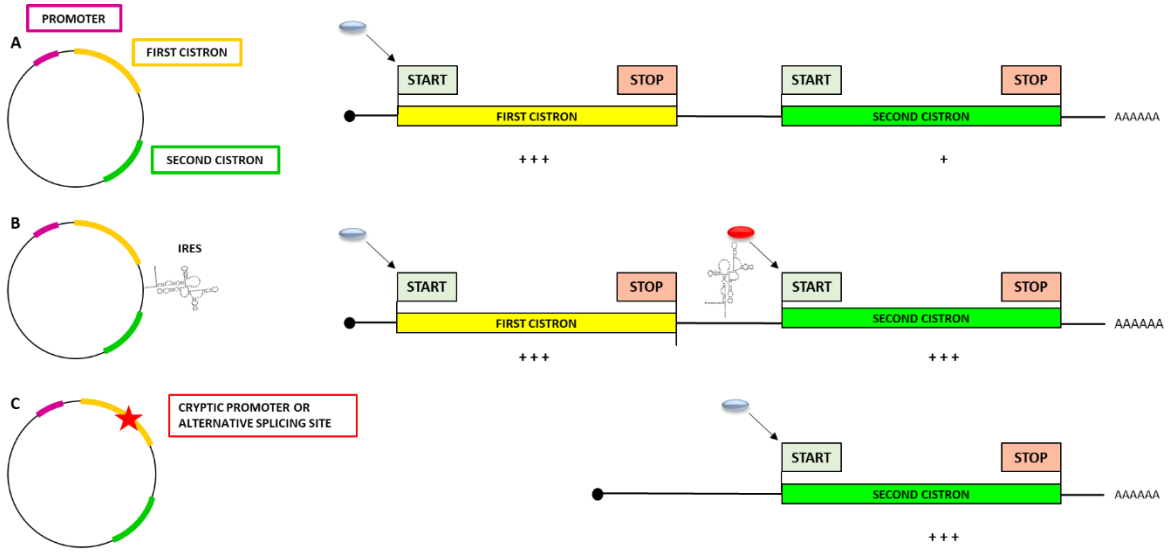

Figure 1.10 **The bicistronic assay system.** On the left hand side circular plasmids are represented, on the right hand side schematic mRNAs are represented. A) In the bicistronic vector system, first cistron will be translated. Due to the presence of a stop codon at the end of the first cistron's sequence, the second cistron will only be translated by a small number of ribosomes by read through reinitiation. B) In the presence of an IRES between both cistrons, an increase in the second cistron's expression can be observed. C) In the presence of cryptic promoters or alternative splice sites upstream of the second cistron's sequence, monocistronic mRNAs can be formed with the sequence of the second cistron on them. When doing a luciferase assay, a strong signal of the second cistron would be detected, which could lead to an erroneous declaration of an IRES present in the mRNA.

TARGETING IRESs AS A THERAPEUTIC APPROACH

Since IRESs were discovered in viruses, several researchers have tried to use drugs and small molecules to inhibit the IRES activity. Most of the research has been focused on the disruption of the IRES structure or preventing interactions of the IRES with the ribosome or ITAFs, in most occasions by targeting the ITAFs themselves[115]. Since IRESs were discovered in cellular mRNAs and their implication in cancer development was observed[116], targeting IRESs has been considered an attractive possibility for anticancer therapy[117].

Viral IRESs have been targeted on various occasions for therapeutic purposes, and HCV IRES is the one that has been studied the most[118–127]. One of the reasons for the research done on targeting the HCV IRES is the relationship between HCV infection and hepatocellular carcinoma[128]. The approaches taken have been to disrupt the structure of the IRES by antagonists or drugs or the disruption of the interaction between the IRES and the ITAFs or canonical initiation factors required for successful IRES-mediated translation. For this purpose antisense oligonucleotides

with different modifications as PNAs[121], LNAs[121] and morpholinos[127] have been used, as well as shRNAS[129] or siRNAs[130].

Different cellular IRESs have also been targeted as a possible cancer treatment using different approaches. Shi *et al.* screened approximately 145 000 compounds by yeast-three hybrid to inhibit the interactions between the *c-myc* IRES and one of its ITAFS, and they successfully found a compound that inhibited the translation of *c-myc* under ER stress conditions (when the IRES was more active)[131]. Du *et al.* discovered that the P/Q-type voltage-gated Ca^{2+} channel (VGCC) gene *CACNA1A* encodes two subunits: α1A and α1ACT, and the translation of the last one takes place through an IRES[132]. When α1ACT is mutated it gives rise to spinocerebellar ataxia type 6 (SCA6). Pastor *et al.* performed a high-throughput screen of FDA-approved small molecules and identified 10 that inhibited the IRES activity[133]. They also found a human miRNA that bound to the *CACNA1A* IRES and inhibited the translation of α1ACT, showing that IRES targeting could be used to treat SCA6. Vaklavas *et al.* screened 135 000 compounds capable of inhibiting the *IGF1R* IRES[134], which is also known to be implicated in different cancers.

1.3 *BAG1* GENE

BAG1 was first found in 1995 by Takayama *et al.*[135], who termed this gene *BAG1*, for *BCL2*-associated athanogene 1. It was then discovered that this gene was identical to the already discovered *RAP46* gene by Zeiner and Geghring[136]. *BAG1* codes for a co-chaperone protein and is implicated in the regulation of different cellular processes as apoptosis, proliferation, signalling, protein refolding, cell survival, transcription and cell motility. It interacts with diverse molecular targets, including the 70-kDa heat shock proteins[100], Hsp70 and Hsc70[137], the *RAF1* kinase[138], nuclear hormone receptors[136], components of the ubiquitination/proteasome machinery[139], different growth factors[140] and the *BCL2* apoptosis regulator[141]. The activity of BAG1 is directly dependent on the proteins it interacts with[142]. Even though BAG1 binds to BCL2, it does not share any sequence similarity with BCL2 or any of the proteins related to BCL2[135].

1.3.1 BAG1 isoforms

The BAG1 protein encoded by the *BAG1* gene is expressed as up to four different isoforms. All these isoforms are generated from the same mRNA, using different translation initiation sites (start codons), caused by leaky scanning[143]. Coldwell *et al.* already showed that the formation of these isoforms is not due to the presence of cryptic promoters or alternative splicing events[144] and according to GenBank, the first exon of the gene contains all the four initiation codons[145]. These isoforms are known as the 50 kDa isoform, p50 or BAG1L, the 46 kDa isoform, p46 or

BAG1M and the 36 kDa isoform, p36 or BAG1S[146] (Figure 1.11). The fourth isoform is not a very common form of BAG1 known as the p29 isoform that is not detected consistently[143]. The translation of p50 is initiated from a non-canonical CUG start codon. This isoform contains a nuclear localisation signal and is thereby mainly localised in the nucleus. The translation of the rest of the isoforms is initiated in different AUG start codons. These isoforms are localized in the cytoplasm. The major form is p36, followed by p50 and p46[146,147]. All the BAG1 isoforms have the same C-terminus (containing the BAG domain and the ubiquitin binding ligand (UBL), required for protein-protein interactions with the proteins named before[39]), but different N-terminus. A DNA binding motif formed by a cluster of arginine and lysine residues in present on p50 and p46, but absent in p36 and p29[139,148]. It is thought that the different isoforms could play different roles in apoptosis, transcription regulation and tumorigenesis, as they are localized in different cell compartments and it has been demonstrated that different isoforms interact with different proteins[82,149]. In this instance, p50 has shown to activate gene transcription in the absence of thermostress[150], whereas p46 has shown to activate it in the absence of the same[139]. Chen *et al.* showed that the different BAG1 isoforms showed different levels apoptotic inhibition in the presence of different apoptosis inducing agents in C33A cells[150]. In this way, p46 was the isoform with the highest ability to suppress apoptosis, followed by p50 and p36. p29 did not show the ability to suppress apoptosis. Different BAG1 isoforms do also have a different effect on hormone receptors: p46 and p26 negatively regulate the transactivation and DNA binding of glucocorticoid receptor and retinoic acid receptor, p50 enhances the activity of androgen receptor[151].

BAG1 can control DNA synthesis by interacting with RAF1 and heat-shock protein Hsp 70. BAG1 has the ability to activate RAF1, a serine/threonine protein kinase essential for the transmission of cell growth control signals from the cell surface to the nucleous[152]. However, when Hsp70 levels are high, as in heat shock, RAF1 is displaced and Hsp70 binds to the BAG1 domain in BAG1, arresting DNA synthesis[153].

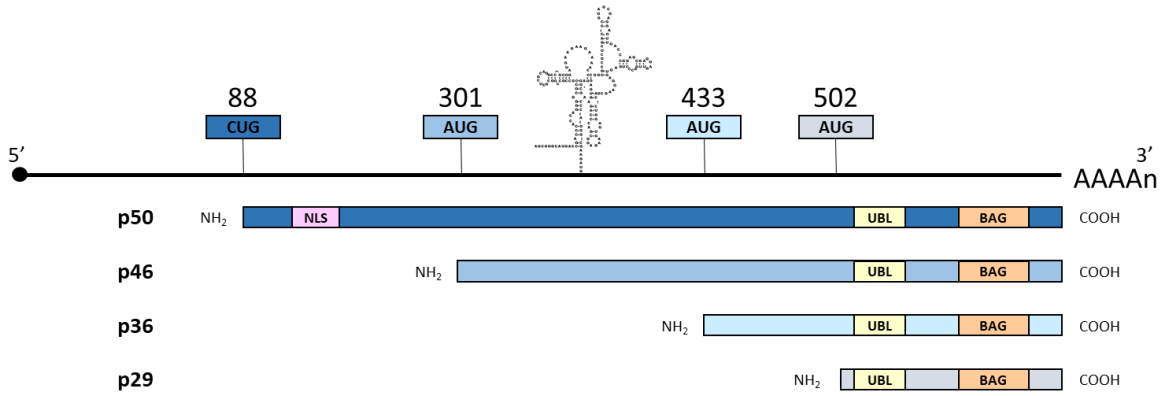

Figure 1.11 **Molecular organization of *BAG1* showing the major isoforms.** Representation of the major BAG1 isoforms (p50, p46, p36), their initiation codon and the position of the same. The translation of p50 is initiated from a CUG codon in position 88. The translation of p46, p36 and p29 is initiated from AUG codons in positions 301, 433 and 502 respectively.

1.3.2 *BAG1* and apoptosis

BAG1 is an anti-apoptotic gene, thereby inhibits apoptosis (programmed cell death)[135]. Apoptosis is a mechanism to regulate the cell population in tissues and it usually occurs during development and ageing. It is also a defence mechanisms that cells have against immune reactions or cell damage by disease or noxious agents. There are different conditions and stimuli that can trigger apoptosis, however not all cells would undergo apoptosis in response to the same stimuli or conditions[154]. The knowledge we have about apoptosis has been used in drug development to increase the levels of this process in cancer cells. Mitochondria play an important role in apoptosis. In stress conditions, cytochrome c (a very potent apoptosis activator) leaves the mitochondria and interacts with apoptotic peptidase-activation factor 1 (APAF1) forming the apoptosome. The apoptosome can then recruit and activate caspase 9 (a proteolytic enzyme) that activates a cascade of other caspases, which then cleave target proteins, (usually proteins that are vital for cell survival)[9].

Proteins of the BCL2 family control mitochondrial apoptosis, where pro-apoptotic and anti-apoptotic proteins can be found. BAG1 interacts, binds and enhances the activity of BCL2 supressing apoptosis[135]. BCL2 has a hydrophobic membrane insertion region in its carboxyl-terminal. This region localizes BCL2 on the outer mitochondrial membrane and it is believed to be involved in the mitochondrial pore formation. BAG1 is believed to act by inhibiting the release of pro-apoptotic factors from the mitochondria, such as cytochrome c[142].

It has also been discovered that BAG1 has the ability to bind to the plasma membrane-associated tyrosine kinase growth factor receptors and enhance their antiapoptotic activity[140]. In this way, dysregulation of apoptosis could be implicated in carcinogenesis[149].

The overexpression of BAG1 has shown to delay or inhibit cell death caused by heat shock, growth factor deprivation and p53 in some cell lines as well as radiation and anti-cancer drugs such as etoposide and cisplatin[135,137,155, 156].

1.3.3 *BAG1* and cancer

The expression of *BAG1* appears to be altered in malignant cells[141], and there is a clear association between the de-regulation of *BAG1* and tumorigenesis[157], however there is some controversy in the literature related to this topic. Yang *et al.* were the first ones to show that BAG1 isoforms can be expressed at different levels *in vivo* and *in vitro* and that the p46 and p36 isoforms are overexpressed in breast carcinoma cell lines and tissues[149]. The over-expression of p46 prevents cells from entering apoptosis and makes the cells resistant to the effects of chemotoxic drugs[158].

It is also known that BAG1 delays cell death and promotes long-term growth in cells[158]. BAG1 can promote cancer progression by avoiding apoptosis. However, in some breast cancer patients, BAG1 expression, as well as the expression of BCL2, has been associated with improved prognosis. This could be because the tumour formed in the presence of high levels of BAG1 and/or BCL2 is less aggressive[158]. The overexpression of BAG1 has shown to increase the metastatic activity of different tumour cells *in vivo*[159].

In breast cancer cells BAG1 has the ability to inhibit the apoptosis caused by chemotherapy, radiation and stress[158,160]. In this way, Kilbas *et al.*[161] showed that the downregulation of BAG1 increased the efficacy of chemotherapeutic drugs in MCF-7 cells. Liu *et al.*[162] also showed that downregulation of BAG1 expression was associated with an increase in the sensitivity to tamoxifen in MCF-7 cells. Recently it has been discovered that it is possible to stop the growth of breast cancer cells by targeting BAG1 interactions using small molecules[163].

BAG1 has also been associated with colorectal cancer (CRC)[164–166]. An overexpression of BAG1 is observed in the late stages of CRC[164] and the overexpression of p50 is associated with a poor prognosis[167,168]. Silencing of BAG1 using gold nanoparticle-delivered siRNA plasmids can increase apoptosis *in vivo* and *in vitro*[169], showing that BAG1 could be a good therapeutic target for cancer.

1.3.4 BAG1 expression in different tissues and cell lines

Yang *et al.* studied the expression of BAG1 in different breast cancer cell lines and normal breast epithelium. They show that *BAG1* mRNA and protein levels were increased in most of the breast cancer cell lines[143].

Takayama *et al.* created three different BAG1 antibodies to study the expression of BAG1 in different human tissues. They showed that not all cell lines contained the four known BAG1 isoforms (p50, p46, p36 and p29). Ovary and testis expressed the three isoforms, however peripheral blood mononuclear cells only expressed p36. Colon, liver, uterine myometrium and breast contained small amounts of p36. They also showed that p36 was the BAG1 isoform with the highest expression in tumor cell lines, and colon, breast and leukemia cell lines were the ones showing the highest p36 expression[147].

Yang *et al.* showed that human cervical cancer cell lines expressed the four BAG1 isoforms, whereas human lung cancer cell lines did not express p29. They also showed that the expression of BAG1 was higher in cervical carcinoma, lung cancer and breast cancer cell lines when compared to normal cervical, lung and breast cells[143].

1.3.5 *BAG1* IRES

Previous work determined that the translation of the p36 isoform of BAG1 is mediated by both an IRES and by cap-dependent translation initiation[144]. To translate p36 in a cap-dependent manner, a ribosome would have to bypass several possible start codons, some in-frame and in a good Kozak consensus, (Figure 1.12). This is a very uncommon event according to the cap-dependent translation initiation theory[141].

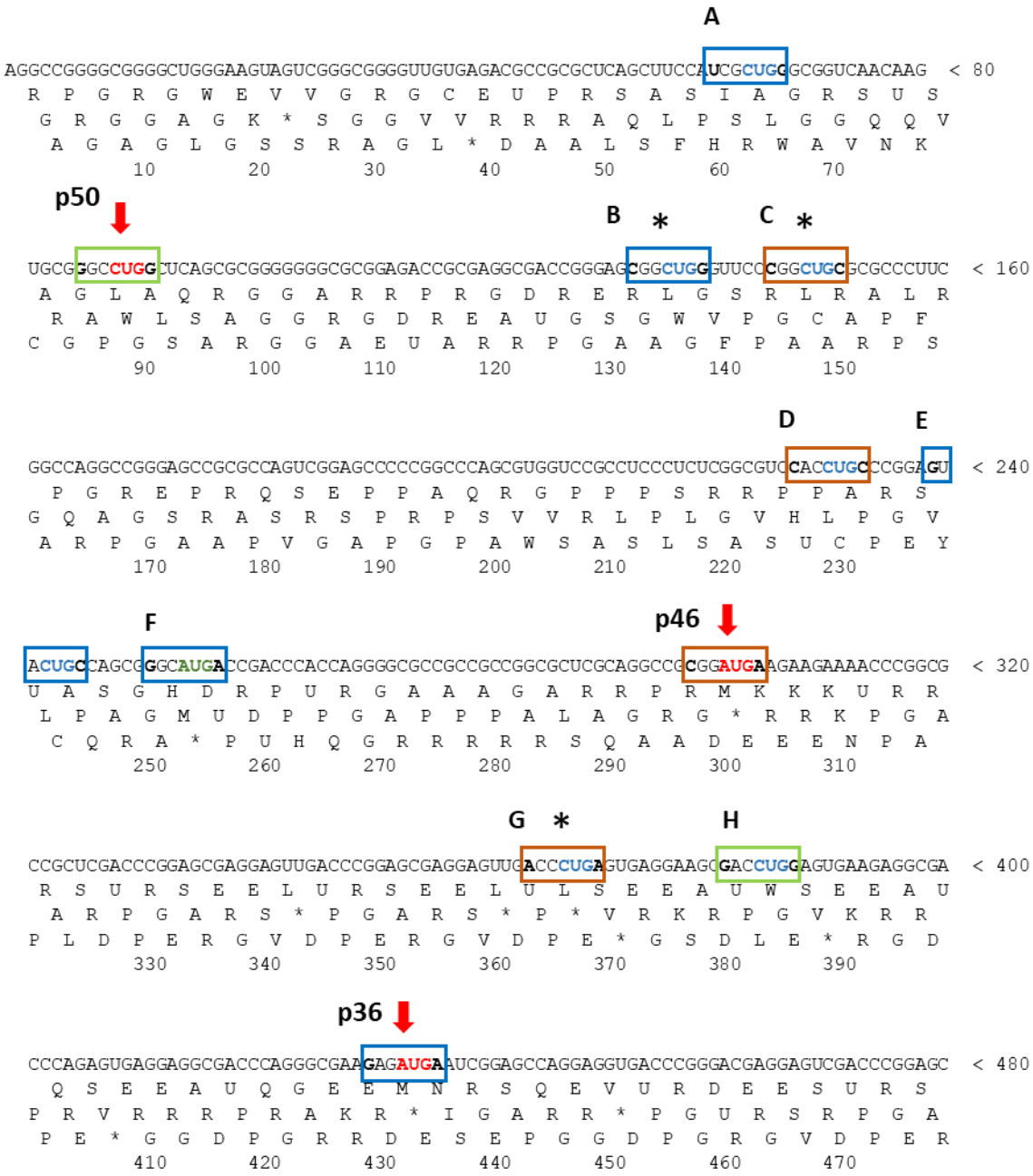

Figure 1.12 **Sequence of *BAG1* 5' UTR.** The p50, p46 and p36 start codon (in the first frame) are highlighted with an arrow and with red letters. The rest of the AUG and CUG start codons are also highlighted, with green and blue colour letters respectively. The Kozak sequence is surrounded by a box. Green, blue and orange boxes are used for start codons in good, medium and bad Kozak consensus respectively. Start codons marked by an asterisk are in frame with the start codons of p50, p46 and p36.

Figure 1.12 shows the 5' UTR of *BAG1*, with the start codons of the three BAG1 isoforms highlighted by arrows. It can be observed that there is one more AUG start codon (F) and 7 CUG start codons (A, B, C, D, E, G and H) before the start codon of p36, not considering the start codons for p50 and p46. Some of the other AUG and CUG start codons are in a relatively good Kozak consensus (marked with a blue box: A, B, E and F) others are in a bad Kozak consensus

(marked with an orange box: C, D and G) and only one is in an optimal Kozak consensus (marked with a green box-H). Three of the CUG codons are in frame (marked with an asterisk: B, C, G), while the rest are not. Before the ribosomes arrive to the start codon of p36, they therefore need to bypass 10 possible start codons.

Stewart *et al.* showed the translation efficiency of different AUG start codons when a different nucleotide was located in the +4 and -3 position (being the A in AUG position 1)[170]. Wegryzn *et al.* showed that translation efficiency is reduced by 80% when it is initiated from a CUG instead of from an AUG[171]. 20% of the ribosomes would initiate translation from a CUG start codon within a good Kozak consensus, that number would be reduced if the Kozak consensus was not ideal. Based on the calculations of Stewart *et al.* and Wegryzn *et al*, the p36 start codon would only capture around 10% of scanning ribosomes (Table 1.1). This strongly suggests that there must be something in the 5' UTR enhancing translation initiation to start through that start codon.

Table 1.1 Possible translation initiation codons in the 5' UTR of *BAG1* and their translation efficiency. We have shown the number of ribosomes that would initiate translation from each of the possible start codons based on their Kozak consensus.

NAME	SEQUENCE	KOZAK CONSENSUS	TRANSLATION EFFICIENCY (% RIBOSOMES TRANSLATING)	40S SUBUNITS THAT CONTINUE SCANNING
		Starting with the suggested number of 1 000 ribosomes.		
A	UCG**CUG**G	MEDIUM	10%	900
p50	GGC**CUG**G	GOOD	20%	720
B	CGG**CUG**G	MEDIUM	20%	576
C	CGG**CUG**C	POOR	0	576
D	CAC**CUG**C	POOR	0	576
E	GUA**CUG**C	MEDIUM	10%	518
F	GGC**AUG**A	MEDIUM	40%	311
p46	CGG**AUG**A	POOR	20%	249
G	ACC**CUG**A	POOR	0	249
H	GAC**CUG**G	GOOD	20%	199
p36	GAG**AUG**A	MEDIUM	40%	119

Pickering *et al.*[82] suggested that the *BAG1* IRES adopts a very complex structure with 4 stem loops and a RNA pseudoknot (Figure 1.13). They used a process of chemical structure probing to

determine it, using Dimethylsulfate (DMS), kethoxal and RNase V1. DMS methylates unpaired cytosine and adenine residues; kethoxal can react and modify single stranded guanine, whereas RNaseV1 cleaves the RNA prior to a residue forming a base-pair. The process followed to determine the *BAG1* IRES structure was the following: *BAG1* IRES RNA was synthesised *in vitro* and renatured by heating it at 80°C and slowly cooling it to 4°C. It was then treated individually with DMS, kethoxal and RNaseV1 and a primer extension reaction was carried out. The generated cDNA was then run in agarose gels to determine the single stranded or double stranded regions in the *BAG1* IRES.

Pickering *et al.*[82] also demonstrated that the ribosome binds to the *BAG1* 5' UTR between position 308 and 326. They showed this by introducing AUG codons at different points of the *BAG1* IRES by site-directed mutagenesis. They hypothesised that those AUG codons would only affect translation if located downstream of the ribosome landing site, but their effect would be minimal if located upstream of the ribosome landing site. *BAG1* internal translation happens by a land and scan type of mechanism, as the *BAG1* initiation codon is situated 100 nucleotides after the ribosome entry window[82]. To start translation, the 40S subunit of the ribosome needs to bind to the mRNA and this requires a tract of 26 to 31 unpaired nucleotides. To get a tract of such an amount of unpaired nucleotides, the mRNA needs to undergo a structural remodelling[82].

The activity of the *BAG1* IRES is stimulated by the binding of proteins polypyrimidine tract binding protein 1 (PTBP1) (57 kDa) and poly (rC) binding protein 1(PCBP1) (38 kDa)[95] (Figure 1.13). It is known that PTBP1 plays a role in mRNA splicing. PTBP1 binds from nucleotide 328 to 351, the binding is especially strong from 332 to 335 and from 346 to 351. PCBP1 binds from nucleotide 320 to nucleotide 347[82]. This was shown by carrying out electrophoretic mobility shift assays (EMSA) where *BAG1* IRES RNA, containing mutations in different sites, was incubated with PCBP1 or PTBP1. Both proteins bind to the IRES in a region not far from the ribosome landing site. When PTBP1 or PCBP1 bind to the mRNA of the *BAG1* IRES, they create a single-stranded region of around 40 nucleotides. This conformational change located near the ribosome entry window in the IRES stimulates the binding of the ribosome[82]. Modifications in the binding sites of PTBP1 and PCBP1 that open the structure of loop lll and avoid the binding of PTBP1 and PCBP1 reduce the internal ribosome entry, as the ability of PTBP1 and PCBP1 to bind the IRES and activate it is lower. PCBP1 acts as a RNA chaperone, it binds to the *BAG1* IRES mRNA and opens stem-loop lll to help PTBP1 binding the mRNA. The binding of PTBP1 to the mRNA is a vital step for the *BAG1* IRES function[82]. The presence of both proteins doubles the activity of the IRES compared to the IRES activity when only one of these proteins is present. In this way, the activity of the IRES will vary according to the amount of PTBP1 and PCBP1 present[82]. Both PCBP1 and PTBP1 can act in the

nucleus and the cytoplasm, this suggests that the binding of the ITAFs to the IRES of *BAG1* could also happen in the nucleus[82].

Pickering *et al.* studied the activity of the *BAG1* IRES in different cells lines (HeLa (human cervical epithelioid carcinoma cell line), COS7 (monkey epithelial cell line), HEK293 (human embryonic kidney cell line), MCF7 (breast cancer derived cell line), CAL51 (breast cancer derived cell line), CALU1 (human lung cancer derived cell line) and CAMA1 (breast cancer derived cell line)). They showed that the *BAG1* IRES exhibits different levels of activity in each cell line. The *BAG1* IRES has a very high activity in CAMA-1 cells, a high activity in HeLa, COS7 and HEK293 cells and it is quite inactive in MCG7, CAL51 and CALU1 cells[95]. These results differ from the ones obtained when doing the same experiments in the c-*myc* IRES[172] and *APAF1*[173] IRES. This clearly states that each cellular IRES requires different ITAFs.

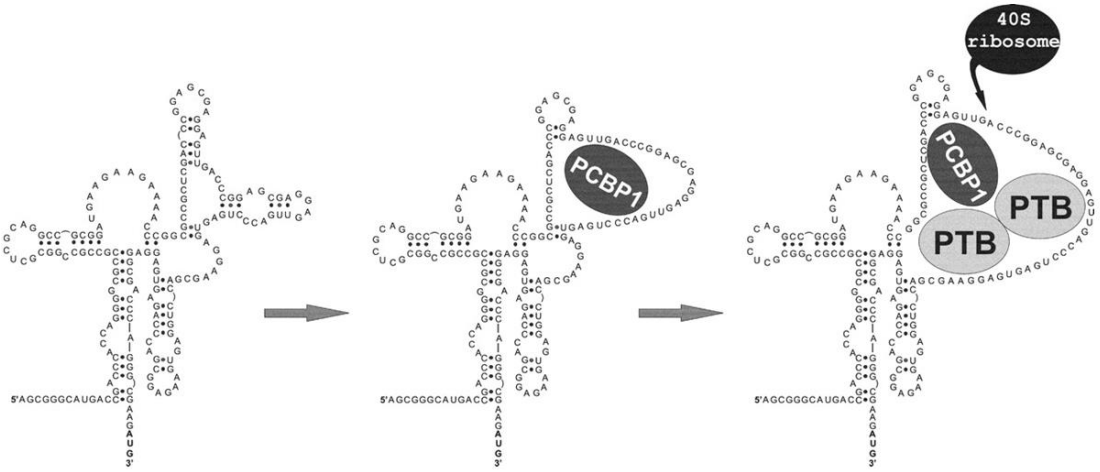

Figure 1.13 **IRES of the gene *BAG1.*** Model of the *BAG1* IRES proposed by Pickering *et al*. The binding of PCBP1 and PTBP1 to the IRES opens the IRES facilitating the 40S ribosome subunit to bind to the mRNA. From Pickering, B. M. *et al*. Molecular and Cellular Biology **24,** 5595–605 (2004)[82].

1.3.6 BAG1 G-quadruplex

In the 5' UTR of *BAG1*, upstream of the IRES and all the isoform initiation codons, very close to the 5' m^7G, the presence of a G4 has been discovered[174]. Jodoin *et al.* studied the effect of the *BAG1* G4 in colorectal cancer cells[39]. This G4 can control the cap-mediated translation initiation and IRES-mediated translation initiation of the different BAG1 isoforms by maintaining the secondary structure of the 5' UTR. In this way, the cap-mediated translation of the BAG1 isoforms can be repressed by small molecule ligands targeting the *BAG1* G4. On the other hand, even if the *BAG1* G4 is not part of the *BAG1* IRES, it is required for the correct IRES-mediated translation of p36[39]. Jodoin *et al.* believe that the *BAG1* G4 can modify the conformation of the *BAG1* 5'UTR and thereby modulate different types and levels of translation.

1.4 ANTISENSE THERAPY

The use of oligonucleotides to supress gene expression is known as antisense therapy. Suppressing the expression of genes that are therapeutically relevant has become a big goal in the treatment of different diseases in the past years and oligonucleotides have shown to have the potential to do so. Antisense oligonucleotides (ASOs) have the potential to treat a wide range of diseases such as neurodegenerative or cardiovascular disease, viral infections or cancer.

One of the main goals in therapy, particularly in cancer therapy, is to stop using untargeted cytotoxic therapy and to start using selective molecular targeted therapies. This is a difficult, costly and a time-consuming process. In this field, RNA therapeutics provides the characteristics to selectively target specific types of mRNA that have been unable to be targeted using more conventional methods, such as pre-mRNAs, noncoding RNAs and microRNAs[175].

In 1977 Paterson *et al.* wrote about the use of nucleic acids to control gene expression[176]. But it was not till 1978 when Zamecnik and Stephenson used oligonucleotides as tools in this respect[177]. They proposed that oligonucleotides could be designed to selectively bind the target RNA based on Watson-Crick base-pairing rules and inhibit or modulate the mRNA function[177]. These oligonucleotides are known as antisense oligonucleotides (ASO). Thanks to all the improvements that took place since the late seventies, nowadays it is possible to design oligonucleotides that behave like drugs by modulating the RNA splicing, degrading the target RNA by the recruitment of RNase H and inhibiting translation or disrupting the RNA structures needed for the regulation of the RNA.

There are two different mechanisms that antisense oligonucleotides use to inhibit translation: a degradative pathway or a non-degradative pathway also known as steric hindrance. The first one implies the activation of the RNase H. The enzyme RNase H cleaves RNA-DNA hybrids. When DNA oligonucleotides bind to the target mRNA, RNase H is activated and it degrades the mRNA. RNAse H has a RNA binding domain in the N-terminus covering around 7-10 nucleotides, which allows the binding and cleavage of the RNA from the 5' end[178]. After mRNA degradation, the oligonucleotides are free again to bind to other copies of the target mRNA. In this way, they can inhibit gene expression in a more efficient way. Not all the oligonucleotides can recruit RNase H, but they can still be used as antisense agents.

Steric hindrance or steric block consists on the formation of an RNA-DNA duplex to physically block mRNA translation in different ways. Antisense oligonucleotides are designed to block the ribosomal machinery at different levels of the process of translation. The 5' m7G-cap[179] or the translation initiation site[180] could be blocked preventing the binding of the PIC to the mRNA and

thereby inhibiting translation. Oligonucleotides could also be designed to block 40S ribosomal subunit scanning to find the start codon, as well as the assembling of the 40S and 60S ribosomal subunits required to initiate translation or elongation. mRNA polyadenylation[181] could also be blocked using oligonucleotides. ASOs have also been used to regulate splicing. As previously explained, splicing is one of the processes in the creation of a mature mRNA. Via alternative splicing different proteins could be formed from the same mRNA. Increasing or decreasing the quantity of some of those proteins could have a therapeutic interest. ASOs targeting sequences near intron/exon junctions, blocking the binding of splicing factors, could be used for this purpose. In this case as well, ASOs would act through the steric block system[182,183]. Antisense therapy can also be used as antiviral therapy by designing oligonucleotides capable of blocking protein binding sites in the viral RNA required for viral gene regulation[2].

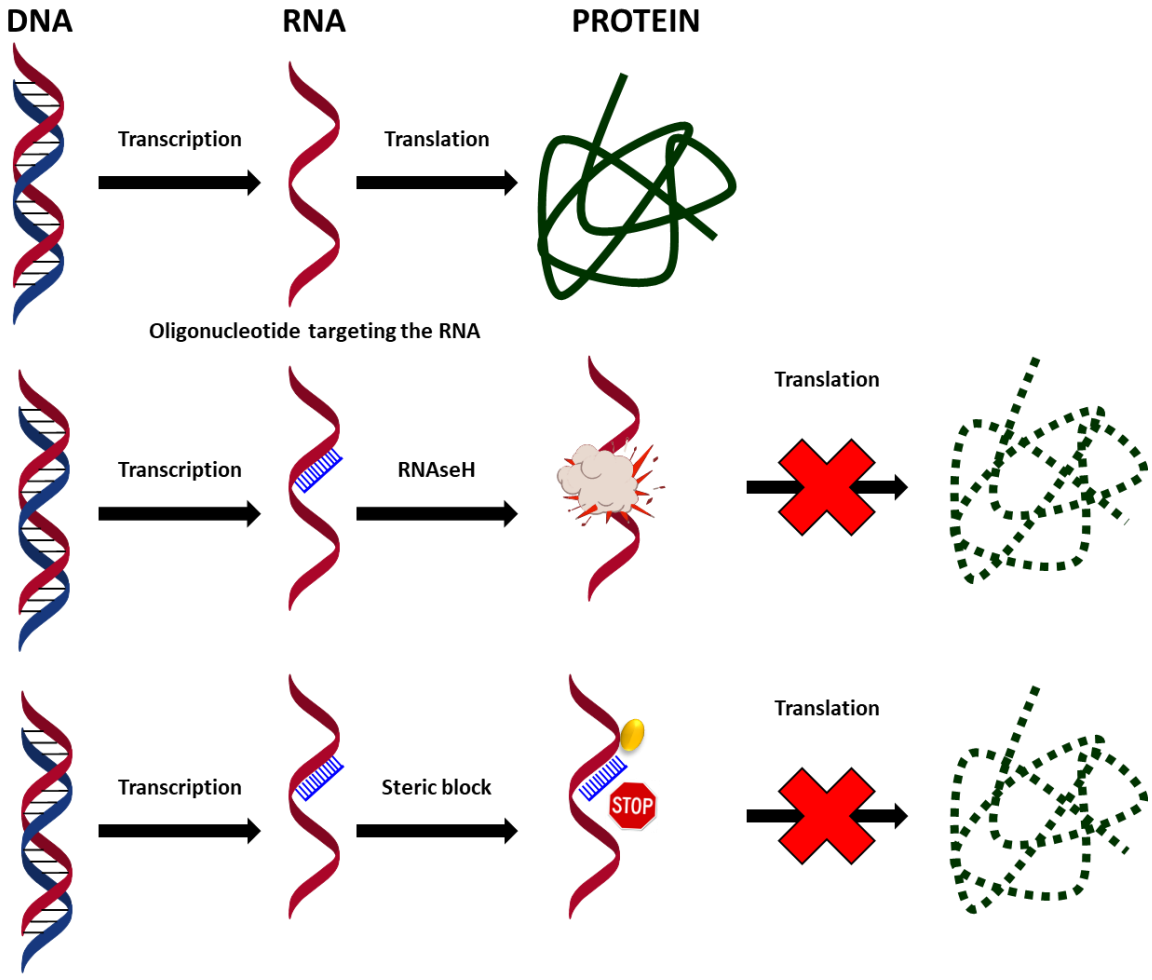

Figure 1.14 **Representation of the mode of action of antisense oligonucleotides.** Antisense oligonucleotides can inhibit translation by two methods: the degradative pathway, where oligonucleotides are designed to recruit RNase H, which will degrade any DNA-RNA duplex, or the steric hindrance/block method, where oligonucleotides will be designed to physically block the ribosomal scanning.

Gene expression could also be upregulated with the use of novel antisense mechanisms. The strategy in this case would be to target naturally occurring translation inhibitors in the 5' UTRs with oligonucleotides and disrupt their structure, such as upstream open reading frames, stem loops or G-quadruplexes[184–186].

One of the most interesting characteristics of ASOs is that only the sequence of the oligonucleotide will change from one target drug to another. The chemistry of the oligonucleotides will not change from one oligonucleotide to the other, this means that many of the properties of the drugs can be predictable[175]. RNA-DNA duplexes generally are less stable than DNA-DNA or RNA-RNA duplexes due to the differences in sugar puckering, but they can have a greater stability than DNA-DNA duplexes if suitable modifications are used (see below), and they usually show A structure[2], in general the higher the content of pyrimidines in the DNA strand the more stable the RNA-DNA duplex is[2].

However not everything is straightforward in the field of antisense therapy. Unlike traditional drugs, oligonucleotides are relatively big amphipathic compounds that have the ability to interact with different molecules forming electrostatic interactions with positively charged proteins as well as sequence specific interaction with proteins. Nevertheless, oligonucleotides could also form Watson-Crick and non-canonical base-pairing with themselves and other non-specific oligonucleotides[187].

It has been argued that antisense oligonucleotides could not be effective systematically as they do not meet the Lipinski rules. Lipinski formulated five characteristics to differentiate drug-like molecules from non-drug-like molecules, these rules help predicting the probability of success of different molecules[188]. A good drug molecule should have these 5 characteristics: a molecular mass smaller than 500 Dalton, high lipophilicity, less than five hydrogen bond donors, less than 10 hydrogen bond acceptors and a molar refractivity between 40 and 130. However, monoclonal antibodies do not meet Lipinski rules either, yet they are used for therapeutic applications[189].

The first ASOs used in antisense therapy were unmodified. These ASOs faced many biological difficulties, as a difficult absorption by the cells and a high degradation rate by nucleases in plasma, tissues and the cells itself. The release of deoxyribonucleoside-5' phosphates (dNMPS), and in particular dGMP, when the oligonucleotides are enzymatically degraded when introduced in the cells induce cytotoxicity and anti-proliferative effects in different cell lines[190–192]. These toxic effects could be correlated with the dephosphorylation of nucleotides by the cell surface enzyme ecto-5'-nucleotidase[190]. This enzyme can dephosphorylate dNMPs to their corresponding nucleosides, which could inhibit the function of critical proteins such as thymidine kinase[193]. To overcome all these issues, the so-called first generation ASOs were evolved.

1.4.1 First generation ASOSs

This first generation ASOs are also known as **Phosphorothioates (PS)**, formed by the substitution of sulphur for one of the non-bridging oxygen in the phosphodiester bond (Figure 1.15). That sulphur atom provides the molecule with more chirality, but the overall charge is still preserved, they are also more soluble in the membranes than unmodified oligonucleotides[194]. These modified oligonucleotides are one of the most efficient ones to inhibit the degradation by nucleases[195]. On the other hand, PS are not the most efficient ones when targeting the mRNA, as the melting temperature of the duplex PS-mRNA decreases around 0.5°C per nucleotide[196]. PSs can activate RNase H and have a good antisense activity. However, when RNase H activation is not required, PS oligonucleotides can be fully 2'-modified to use them as steric blockers (2' modifications will be explained in the next section)[197]. PS oligonucleotides can be synthesised on a polymer support, in the same ways as unmodified oligonucleotides[198] but including an oxidation step that will add a sulphur instead of an oxygen. Several different reagents are commercially available.

PS linkages have two stereoisomers and during the chemical synthesis of the PS oligonucleotides a 1:1 mixture of the two diastomers (Rp and Sp) is obtained. However, if only one of the isomers was of interest, this could be obtained by the use of stereodefined Rp or Sp diastereomers of either nucleoside oxathiaphospholanes or nucleoside oxazaphospholidines as monomer units instead of nucleoside phosphoramidites for solid phase synthesis[199,200]. The two configurations have different properties: Rp configuration binds in a stronger way to RNA (has a higher melting temperature) than Sp analogs[201] and they can stimulate RNase H more strongly than Sp ones, however Sp analogues show a higher resistance to nucleases[202]. For an antisense approach it is required to generate oligonucleotides with both diastomers, to have a combination of each ones properties[203].

The substitution of PO for PS increases the hydrophobicity of the molecule, increasing its capability to bind to proteins. They can easily bind to serum proteins like albumin, which increases their circulation time in plasma and decreases the clearance by the kidney. These non-specific protein binding properties can induce sequence-independent effects. Phosphorothioates are polyanions, as well as phosphodiesters, which have the ability to bind to proteins containing polyanion binding sites such as the heparin binding proteins bFGF, PDGF, VEGF, EEGF-R among others[204]. The affinity of the PS oligonucleotides to these proteins is sequence-independent[205]. Thereby to increase the specificity of PS oligonucleotides the length needs to be optimized and the concentration reduced[206]. Naked PS oligonucleotides (oligonucleotides transfected without

transfection reagent) can also interact with different cell surface proteins, which could cause a physiological response in the cell unrelated to the antisense activity of the oligonucleotides[204].

PS containing ASOs can be delivered into cells naked, without the use of any transfection reagent, which is also known as gymnotic delivery[207]. This would avoid any possible toxicity produced by the transfection reagent, it could make possible the transfection of difficult-to-transfect cells and it would decrease the time required for an antisense experiment. However, this method requires a very high concentration of oligonucleotide, which could be over ten times higher than with the use of a transfection reagent, which would extremely increase the price of the experiments.

PSs are easily degraded *in vivo,* which is the main reason why they were not very useful clinically. Nevertheless some PS ASOs have made it to clinical trials and have been approved by the FDA. Fomivirsen (Vitravene) was the first antisense drug approved and marketed. It is a 21 nucleotide phosphorothioate oligonucleotide capable of inhibiting CMV retinitis when injected into the human eye[208]. There are other FDA approved oligonucleotides or oligonucleotides in clinical trials composed of PSs in combination with other modifications that will be covered later.

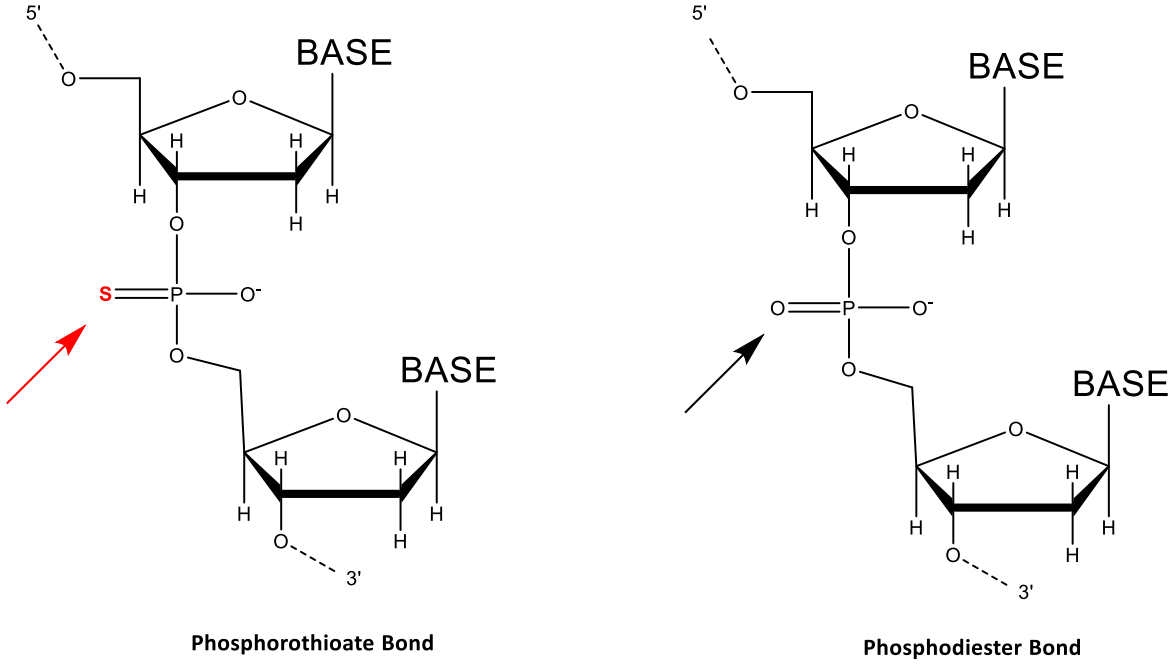

Figure 1.15 **Representation of phosphorothioate bond and a phosphodiester linkage.**

1.4.2 Second-generation ASOs

Second-generation ASOs were designed to increase the nuclease resistance and the binding affinity to the target mRNA. The tissue distribution of these ASOs is similar to the first generation ASOs, they concentrate in the liver and kidneys but the intracellular intake is bigger[194]. **2'-*O*-methoxyethyl (2' MOE)** or **2'-*O*-methyl (2' OME)** modifications form the second generation ASO.

In these modified nucleotides, the hydrogen in the 2' position of the ribose is replaced by a methoxyethyl or a methyl (Figure 1.16) group. The modification in the C2' position with electronegative substituents of the ribose favours the C3'-*endo* sugar puckering, which would favour the A-form conformation of the oligonucleotide increasing its binding affinity[209]. Due to their structural similarity to RNA, these oligonucleotides do not recruit RNase H. However, to increase their antisense activity and recruit RNase H, gapmers composed of 2' MOE or 2' OME modified nucleotides in the 5' and 3' of the oligonucleotides with a central deoxyribose chain can be used. MOE or OME oligonucleotides could also have PS linkages to help recruit RNase H activity[210,211].

They form heteroduplexes with a high melting temperature when bound to the targeting mRNA[212]. They show a higher stability against nucleases as the nucleophilic 2' hydroxyl moiety is blocked[213]. This also confers higher stability and a longer tissue half-life. They also show a smaller non-specific protein binding capability[175]. 2' MOE ASOs have shown to be more successful than 2' OME ASOs in gene knockdown studies[214].

These oligonucleotides can be formulated in saline solutions, delivered to cells and these will introduce them by endocytosis or other mechanisms, which will lead to the drugs being released intact in the cytoplasm or nucleus of the cells[175]. 2'-*O*-methyl oligonucleotides have proven to be useful not only as antisense elements, but also to increase protein levels, when used to target uORFs[215].

These ASOs also have less proinflamatory capacity than first generation ASOs, making them safer to be used as therapeutic agents[175]. Mipomersen was approved in 2012 by the FDA for the treatment of familiar hypercholesterolemia. It is a 20-mer phosphorothioate oligonucleotide 2'-*O*-(2-methoxyethyl) nucleosides[216].

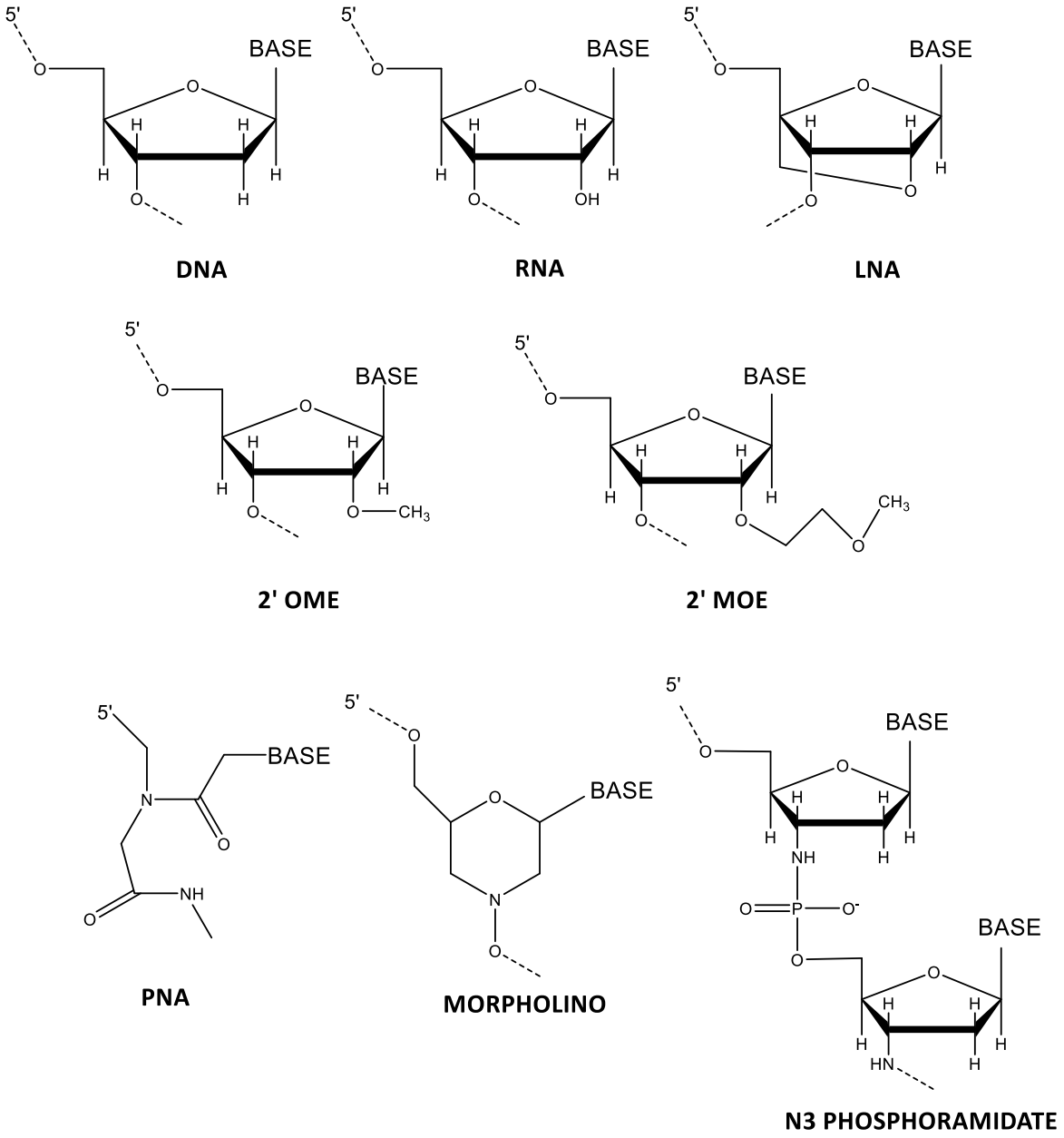

Figure 1.16 **Chemical structure of DNA, RNA, LNA 2'-OME, 2'-MOE, PNA, Morpholino and N3 phosphoramidates nucleosides.**

1.4.3 2.5 or third generation ASOs include

2.5 or third generation ASOs include PNA, morpholino and LNA among others.

Peptide nucleic acids (PNA). PNAs are nucleic acid analogues, composed of a flexible and uncharged polyamide backbone formed by the repetition of N-(2-aminoethyl) glycine units (Figure 1.16). The nucleobases are then attached to those units using methylene carbonyl linkers. PNAs can attach in a strong way to single or double stranded RNA or DNA, which gives them the ability to inhibit not only the process of translation but also transcription. In fact PNAs were designed to use where very high binding affinities were required[194]. PNA oligomers are not negatively charged,

thereby they are not electrostatically repelled by the DNA or RNA[217]. RNase H does not cleave PNA-DNA or PNA-RNA duplexes or triplexes, and their antisense mechanisms depends on steric hindrance (no-degradative pathway). They are also very stable in serum, as they are resistant to nuclease and protease mediated degradation. PNAs have shown to inhibit translation in *in vitro* studies[218]. PNAs have not been used as therapeutic agents mainly due to their inadequate *in vivo* pharmacokinetic properties and their poor cellular penetration[194].

Morpholino. On these nucleotides, the deoxyribose is replaced by a morpholino ring (Figure 1.16). To make these ASOs even more efficient, the charged phosphodiester linkage is replaced by an uncharged phosphoramidite linkage, making phosphorodiamidate morpholinos. Morpholino-DNAs are very stable in cells, as they show high resistance to nucleases and proteases. They do not activate RNase H. However, they are difficult to transfect into cells, as they do not form complexes with commonly used lipid delivery agents. Morpholino-DNAs were generated for applications where a high target specificity is required such as in developing embryos[194]. They bind to the target RNA with a higher affinity than DNA or PS ASOs bind to the RNA[219]. Morpholinos do not show high interactions with cellular proteins, showing low toxicity levels compared to other ASOs chemistries[219].

N3 phosphoramidates. In these oligonucleotide analogues, the 3' amino group is substituted for the 3'-oxygen of the 2'-deoxyribose ring[220] (see Figure 1.16). These oligonucleotides are characterised by their high stability to target ssRNA and even dsDNA and their high nuclease resistance. They do not activate RNaseH and possess a low non-specific protein binding activity as well as a high specificity thanks to their good mismatched discrimination properties[221]. These oligonucleotides have shown to be potential antisense agents in cell systems[222]. They have the ability to increase the melting temperature in around 1°C when bound to DNA and 2°C when bound to RNA[221].

Locked Nucleic Acid (LNA). In the LNA nucleotides the 2'-oxygen and the 4'-carbon of the ribose are connected by a methylene bridge (Figure 1.16). This bridge induces a locked 3'-*endo* (N-type) (see Figure 1.17) conformation on the ribose, which is the preferred conformation found in RNA (compared to the 3'-*exo* conformation in DNA) and the ideal one for binding complementary sequences. This conformation increases the local organization of the phosphate backbone and reduces the conformational flexibility of the ribose[223]. This increases the thermodynamic stabilisation of the RNA-LNA duplex. It has been suggested that the high stability of oligonucleotides containing LNA nucleotides could be due to the conformational changes from C2'-*endo* to C3'-*endo* of the LNA-nucleotide and the neighbouring DNA nucleotides combined with a bigger stacking of the bases[224].

As the link between LNA modifications is the same as that of the DNA or RNA nucleotides, LNA oligomers can be synthesised using automated synthesisers and standard reagents[223]. As LNA oligomers and DNA or RNA are synthesised by a similar process, it is possible to make chimeric oligonucleotides of LNA and DNA or LNA and RNA, also known as mixmers. LNAs are as soluble as DNA and RNA, which facilitates working with them. As they have a charged phosphate backbone, it is possible to deliver LNA into cells using standard transfection protocols with the use of cationic lipids or other transfection agents[223].

LNAs have a high affinity for complementary DNA and RNA sequences. The addition of just one LNA nucleotide into an oligonucleotide sequence can increase the *Tm* by 9.6°C. When introducing more than one LNA into an oligonucleotide sequence, the increase in the *Tm* induced by each LNA is reduced. The biggest increase in *Tm* will be in LNA-DNA mixmers where the LNA modifications are distributed over the length of the oligonucleotide[225]. LNA-RNA duplexes show a higher stability than 2'OME-RNA duplex[226].

The introduction of LNA modifications to a DNA strand induces a conformational change towards the A-type helix, which is found in RNA-RNA or RNA-DNA duplexes. In LNA-DNA mixmers, the structural effects of the LNA only affect the DNA nucleotides that are next to the LNA modifications[225]. Oligonucleotides formed exclusively by LNAs are not very efficient as they have a smaller ability to form a stable complex with the target gene than LNA-DNA mixmers[227]. These oligonucleotides would have a very high *Tm* that would increase the auto-formation of stem loops. LNA has a very rigid conformation and it is the nucleotide analogue able to increase the stability with RNA or DNA strands the most, by increasing the melting temperature[228].

DNA containing natural nucleotides activate RNase H more efficiently than those oligonucleotides made with LNAs, however LNA-DNA mixmers forming gapmers can easily activate RNase H. In these gapmers, LNAs confer stability to the oligonucleotides inside the cells, while the DNA when binding to the RNA makes the perfect substrate for RNase H[229]. LNA-DNA gapmers with 7-8 DNA nucleotides can easily activate RNase H[225].

LNA is resistant to nuclease degradation and thereby LNA-DNA mixmers are more resistant to degradation by nucleases than the analogous DNA oligonucleotides. The degree of resistance to nucleases varies depending where the LNA modifications are placed in the oligonucleotide. To effectively avoid degradation of the oligonucleotides by nucleases, LNA modifications should be located at the edges (3' and 5'-termini) of the oligonucleotides[229]. Three LNAs at the 5'-and 3'-end are sufficient to increase the half-life of the mixmers in human serum from 1.5 hours in unmodified DNA to 15 hours in the mixmers[225], increasing their half-lives 10 fold[230]. It has been

shown that intravenous injection of oligonucleotides containing LNA in mice can be successfully done with a high antisense efficiency and with no toxicity shown[229].

LNA containing ASOs have a lower capacity to stimulate an immune response than PS ASOs, however they have a high potential for hepatotoxicity[231].

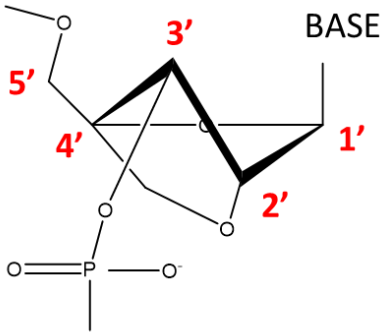

LNA C3'- endo

Figure 1.17 **LNA nucleotides sugar puckering.**

1.4.4 miRNA and siRNA

Gene expression is naturally altered in cells by short noncoding RNA molecules such as microRNA (miRNA) and small interfering RNAs (siRNAs). miRNAs and siRNAs play an important role in gene regulation, and this ability makes them good candidates for therapy[232,233]. miRNAs and siRNAs are small RNA molecules that target mRNA and thereby inhibit gene expression, although they differ in their mechanism of action[234].

siRNAs are fragments of RNA that occur naturally in cells, which promote mRNA degradation (see Figure 1.18). The enzyme Dicer cleaves the precursor RNAs into siRNAs, leaving a 2 nucleotide overhang on the 3' strand[235]. Synthetic siRNAs, the ones used in antisense therapy, are short (around 20 nucleotides) double-stranded RNAs, which often have 2 nucleotide overhangs in the 3' end. They have a guide or active strand and a complementary inactive strand known as the passenger strand.

When siRNAs enter the cells, they are bound by a multiprotein component called the RNA induced silencing complex (RISC)[236]. At this point the siRNA strands are separated and the antisense strand (the one with the less thermodynamically stable 5'-end) is integrated in the RISC complex. The antisense siRNA strand guides the RISC complex to the target mRNA, once the RISC complex is aligned with the target mRNA, the Ago2 protein, which is part of the RISC complex, cleaves the mRNA[237–239]. The activity of siRNAs is mainly in the cytoplasm and in smaller cases in the nucleus.

siRNAs can be produced by chemical synthesis or through gene expression, by cell transfection of an expression vector expressing the short-hairpin RNA precursor of the siRNA[240].
siRNAs show a high level of specificity and low toxicity, however they can also show off-target effects.

In the cells, miRNA genes code for miRNAs, which will be processed in the nucleus and exported to the cytoplasm where they will be further processed by Dicer. At this point miRNAs consist of two strands: the active or mature strand, which is incorporated into RISC to initiate gene silencing, and the inactive or passenger strand[240] (see Figure 1.18).

miRNAs used in antisense therapy show two modes of action: they could act as replacement for pre-existing miRNAs or as miRNAs inhibitory elements. When the goal is miRNA inhibition, miRNAs are used in a similar way as ASOs: a single stranded RNA is designed to acts as a miRNA antagonist, inhibiting the action of target miRNA. When the target miRNA is deactivated or repressed, the miRNA replacement scope is employed. In this case, double stranded miRNAs are used that mimic the activity of the target miRNA, producing target mRNA silencing[240,241].
Two of the biggest difference between miRNAs and siRNAs is that siRNAs act on a specific target mRNA, whereas miRNAs can regulate the expression of multiple RNAs, and that siRNAs result in mRNA degradation, whereas miRNAs do not neccessarily[234].

The fact that siRNAs and miRNAs are double stranded RNA molecules whereas ASOs are single stranded confers some differences to the antisense experiments, apart from the increase in the price that synthesising two strands instead of one means. The cellular uptake of double stranded nucleic acids is lower than the one of single stranded ones. In addition, double stranded RNAs require some help for a successful delivery such as the use of nanoparticles or other targeting agents as N-acetylgalactosamine (GalNac) (GalNac has the ability to bind to asialoglycoprotein receptor in hepatocytes, which increases the internalization of the dsRNAs)[242]. On the other hand, dsRNAs do not need to be chemically modified to be effective, whereas ASOs need to be modified and in some cases the required modifications can be expensive or commercially unavailable[213].

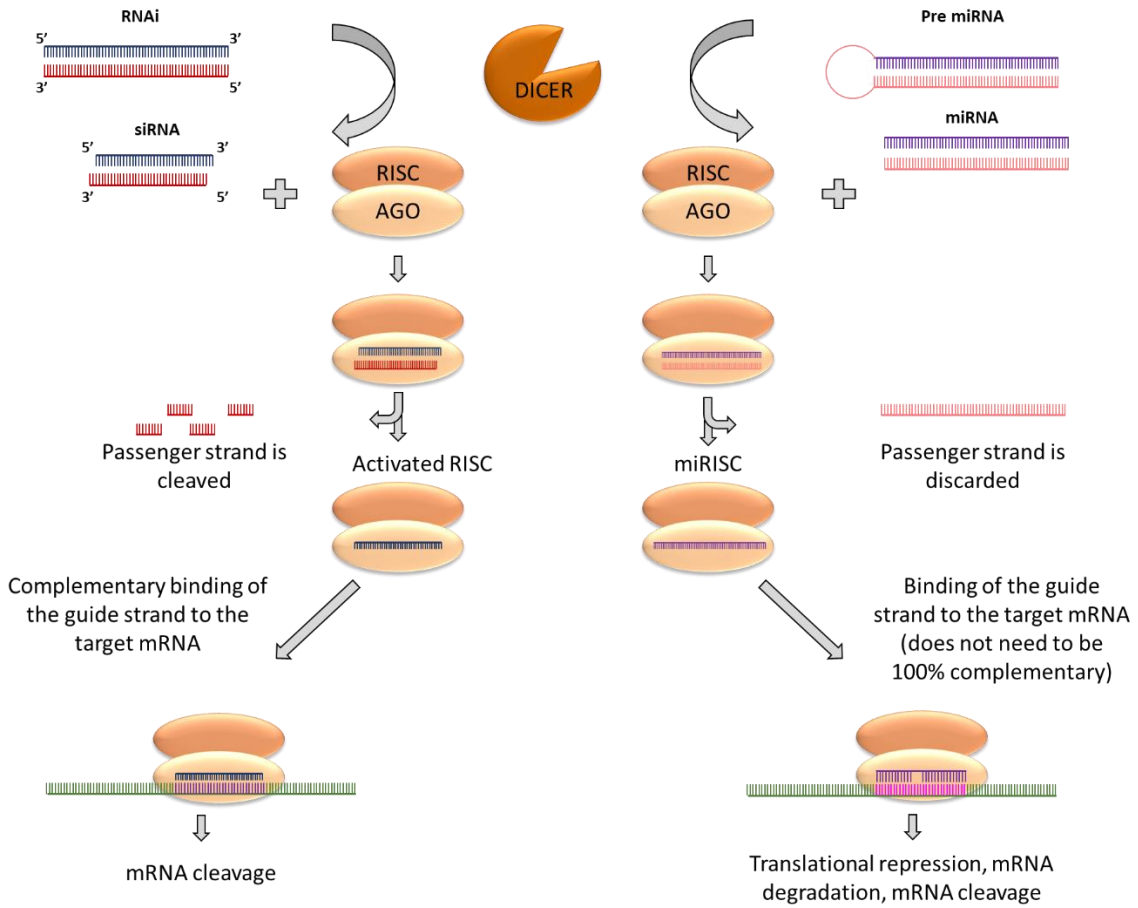

Figure 1.18 **Representation of the mode of action of siRNA and miRNA.** Dicer can process RNAi into siRNA and a pre-miRNA into a miRNA. The siRNA and miRNA will then be loaded into the RISC, where AGO (a component of RISC) will cleave the passenger strand of both the siRNA and miRNA. The siRNA and miRNA guide strand will guide the RISC to the target mRNA. siRNA will be 100% complementary to the target mRNA and it will cleave the mRNA. miRNA can also bind to the mRNA even if they are not fully complementary and inhibit it via degradation, cleavage or translational repression.

1.4.5 Design of antisense oligonucleotides

The ASOs designed to be used in antisense therapy need to have some characteristics to increase their activity. They need to be able of forming a stable duplex with the target RNA at 37°C. Duplex stability can be increased by increasing the G:C content and the length of the oligonucleotide as well as with the use of modified nucleoside analogues that could increase the binding affinity by forming a more compact A-helix. In this context, the accessibility of the RNA sequence to target also needs to be considered, highly structured RNA sequences could be harder to access by the oligonucleotides. The oligonucleotides need to be specific for the target sequence, which could again be achieved by increasing the length of the oligonucleotide. However, increasing the oligonucleotide length also increases the chances to bind non-specifically to random RNA regions

as well as the possibilities of formation of secondary structures that could inhibit the activity of the oligonucleotides. The usual length of the oligonucleotides is 12-25 residues[206].

One of the biggest challenges of antisense therapy is the cellular uptake of the ASOs. In most of the *in cellulo* experiments ASOs are delivered using transfection reagents based on cationic lipids, that can form complexes with the negatively charged oligonucleotides, the cell will uptake the lipids with the ASOs through the endosomal pathway and the ASOs will be released into the cytosol by endosome destabilisation. Once in the cytosol oligonucleotides are able to enter in the nucleus if required. However, the availability of carriers for *in vivo* studies is limited. ASOs need to be stable in the presence of nucleases, minimizing the intra or extra cellular degradation, the only effective way of doing this is by the used of modified nucleosides[2,243].

Even if nowadays there are multiple computer-based approaches that could be useful when designing antisense oligonucleotides, it is still required to analyse a number of different oligonucleotides to verify the antisense activity instead of focussing on studying the activity of the oligonucleotide that showed the best computer-based results[206,244].

1.4.6 Toxicology of antisense oligonucleotides

ASOs can show different toxic effects that depend mostly on the ASO backbone chemistry and less on the specific sequence of the ASO itself. Nevertheless, ASOs could also show some toxicity if they bound to non-target RNAs by full or partial complementarity. This type of toxicity is particular to individual ASOs and could be avoided by a proper ASO design[194].

The toxicity generated by ASOs is usually due to their ability to non-specifically bind to proteins and to plasma proteins in particular, which is facilitated by the negative charge of the ASOs. In this sense, PS ASOs are the ones that show the highest toxicity[196].

Another common toxic effect of the ASOs is immune stimulation. Cytosine-phosphorus-guanine (CpG) motifs in ASOs can be recognized by Toll-like receptor-9 in immune cells, which results in B cell proliferation, the release of cytokines, antibody production and the activation of natural killer cells and T lymphocytes[245]. However, the introduction of LNA modifications in the ASOs has shown to reduce and even eliminate the effect of the CpG motifs[246].

ASOs do also generate cell toxicity *in vivo* when accumulated in the cytoplasm. This has been particularly observed in epithelial cells and in kidney and liver most notably[247]. The level of toxicity in this case will depend on the accumulated ASO concentration as well as the inherent potency of the ASO itself[194].

In the clinical aspect, thrombocytopenia could be considered as one of the most worrying toxic effects ASOs. Thrombocytopenia is a condition characterized by low levels of platelets in the cells, which can decrease clot formation and increase the risk of bleeding[194,213].

1.4.7 Antisense oligonucleotides in clinical trials and FDA approved oligonucleotide therapies

In 2017 there were 6 approved oligonucleotide therapies by the FDA[248]:

Vitravene or *Fomivirsen*, as explained previously, is a 21 nucleotide long phosphorothioate oligodeoxynucleotide, with a CpG motif near the 5' terminus, used to treat patients with cytomegalovirus retinitis. It was directly administered by intravitreal injection into the eye. It was discontinued due to low demand.

Macugen or *Pegabtanib*, a 27 nucleotide long phosphorothioate 3'-3' deoxythymidine cap. All the pyrimidine ribose sugars are 2'-fluorinated and the purine ribose sugars 2'-*O*-methylated. To the 5' terminus, a 40 kDa polyethylene glycol substituent was fused. This drug was approved as treatment for age-related macular degeneration of the retina.

Kynamro or *Mipomersen* (Ionis Pharmaceuticals) is a 20 nucleotide long gapmer phosphorothioate with 2'-*O*-methoxyethoxy (MOE) modifications located in positions 1-5 and 15-20. This drug is used as a treatment for homozygous familial hypercholesterolemia, administered once per week by injection. It was the first ASO that proved able to have an effect on protein expression. Since its approval in 2013, *Mipomersen* has not shown a big commercial success, which is believed to be due to its way of administration[213].

Exondys 51 or *Eteplirsen* (Sarepta) is a 30 nucleotide long phosphomorpholidate oligonucleotide. With a mode of action *via* modifying splicing, it is used as a treatment for Duchenne muscular dystrophy (DMD). It was approved in 2016 by the FDA, however it is still in phase lll clinical trials hoping to get favourable statistical results on its efficacy.

Defitelio or *Defibrotide,* indicated for severe hepatic veno-occlusive disease, is a polydisperse mixture of double stranded (10%) and single stranded (90%) phosphodiester oligonucleotides, with a length of 9-80 nucleotides.

Nusinersen (Spinraza*,* Ionis Pharmaceuticals and Biogen) is a 19 nucleotide phosphorothioate 2'-*O*-methoxyethoxy, indicated for the treatment of type 1, 2 and 3 spinal muscular atrophy. Administered by intrathecal injection into the central nervous system. This has been the most successful ASO for both patients and from a commercial point of view.

Other key clinical ASO candidates were[213]:

Oblimersen or *Genesense* (Genta), a 18 nucleotide PS DNA, targeting the initiation codon of mRNA with the objective to downregulate BCL2 expression and make cancer cells sensible to chemotherapy[249]. The ASO reached phase lll clinical trials, however efficacy remained unproven and it was never commercialised[250].

GRN163L (Imetelstat, Geron) is a 13 nucleotide phosphoramidate oligonucleotide conjugated with a 5'palmitoyl. It targets the RNA component of the ribonucleoprotein telomerase, blocking the telomerase activity and thereby decreasing cell proliferation. The particularity of this ASO is that as it targets telomerase, it could be used in the treatment of different cancers. However, its difficulty relies on the poor efficiency of cancerous cell uptake. Actually in clinical trials[213,251,252].

Drıaspersen (BioMarin), a 2'-*O*-methyl phosphorothioate oligonucleotide, with a mode of action of modifying splicing. Used in treatment of DMD. It reached phase lll clinical trials, but it never showed significant evidence of success and some patients showed thrombocytopenia, hence it was never approved[213].

The key message to take home here is that, even though antisense therapy started over thirty years ago, there have not been many successful approved ASOs. This is mainly due to the delivery system and toxicity of the ASOs. Antisense therapy looks very promising in the treatment of neurological disorders and cancer principally, but much research needs to be done to reach its full potential.

1.5 OBJECTIVE AND AIMS

Antisense therapy was evolved as an innovative therapy for diseases that could not be treated using more conventional techniques and it has been of special interest to treat neurodegenerative diseases as well as cancer. This technique consists of the use of antisense oligonucleotides that specifically target the mRNA and inhibit its translation by inducing mRNA degradation or inhibiting the translation machinery, furthermore, they could also be used to modify splicing. Even if most oligonucleotides are designed to decrease protein expression, antisense oligonucleotides could also be used to increase protein expression. However this last approach is harder to achieve and it has shown to be successful on only a few occasions, where researchers used oligonucleotides to target regions in the mRNA inhibiting translation[184,186,215].

On most occasions, eukaryotic translation takes place *via* a very well regulated method known as cap-mediated translation. However, when this process is compromised, some mRNAs can initiate translation via IRESs[52]. IRESs are often highly structured RNA sequences located in the 5' UTR, usually close to the start codon and they have the ability to directly recruit the 40S ribosomal subunit and start translation from that point[50,65]. It is known that cancer cells tend to initiate translation via IRESs[104], thereby targeting IRESs could be an interesting approach in cancer treatment.

In this project we propose the use of antisense oligonucleotides to control IRES-mediated translation, not only to decrease it, but also to increase it. Antisense oligonucleotides will be specifically designed to target the *BAG1* IRES and modified to increase their efficiency.

The specific objectives of the project are:

- To verify the presence of an IRES in the *BAG1* 5' UTR.
- To study the *BAG1* IRES activity *in vitro* and *in cellulo*.
- To generate a dual luciferase reporter assay to study the IRES activity of *BAG1* post cell transfection with the oligonucleotides.
- To design antisense oligonucleotides (modified and unmodified) targeting the *BAG1* IRES with the aim to either decrease or increase protein expression.
- To develop an effective transfection protocol for the oligonucleotides.
- To study the effect of the oligonucleotides *in vitro* and *in cellulo*.

Chapter 2 MATERIALS AND METHODS

2.1 MOLECULAR BIOLOGY

2.1.1 General techniques

2.1.1.1 Polymerase chain reaction: PCR

PCRs were carried out using the Q5 Hot Start High-Fidelity DNA Polymerase (NEB). The reaction was set up as indicated in Table 2.1. The reactions were transferred to a thermal cycler and they were cycled as explained in Table 2.2.

Table 2.1 PCR master mix composition.

5X Q5 Reaction Buffer	10 µl
10 mM dNTP	1 µl
10 µM Forward primer	2.5 µl
10 µM Reverse primer	2.5 µl
DNA template	10 ng
Q5 enzyme	1 unit
Enhancer	10 µl
H_2O	To a final volume of 50 µl

Table 2.2 PCR thermocycling conditions.

Initial Denaturation	98°C	30 seconds
25–35 Cycles	98°C	10 seconds
	55-72°C*	20 seconds
	72°C	30 seconds/kb
Final Extension	72°C	5 minutes
Hold	4–10°C	

*NEB Tm Calculator was used to calculate the right temperature for the different primers used.

PRIMERS USED FOR CLONING:

Name	**Primer sequence 5'-3'**
NanoLuc R	CTTATCATGTCTGCTCGAAGC
T7-afterSV40 F	TAATACGACTCACTATAGGGGAAGTAGTGAGGAGGCTTT
AfterSV40	GAAGTAGTGAGGAGGCTTT
T7Pphi2.5-afterSV40	TAATACGACTCACTATTA**GG**GAAGTAGTGAGGAGGCTTT
F-BAG1-Hindlll	TTTTTT**AAGCTT**GGAGGCCTAGGCTTTTGC
R-Nano-BamHl	TTTTTT**GGATCC**ATCTTATCATGTCTGCTCG
F-CMV-Mfel	TTTTTT**CAATTG**TTCGCG ATGTACGGGC
R-CMVPA-ClaI	TTTTTT**ATCGAT**AGAGCCCCAGCTGGTT

2.1.1.2 Restriction enzyme digestion

Restriction enzyme digestion was performed in two different occasions: 1) in the cloning process to digest the insert and the vector, prior to the ligation and 2) in the verification process of the cloning. The enzymes used were purchased from New England Biolabs.

The reaction conditions in the cloning process were:

- **Cloning:**

Table 2.3 Digestion master mix for the cloning step.

Digestion master mix:	
DNA	2 µg
Enzyme 1	15 units
Enzyme 2 (optional)	15 units
10X Buffer	5 µl
H_2O	
Total volume	50 µl

- **Verification of the cloning:**

Table 2.4 Digestion master mix for the verification of the minipreps.

Digestion master mix:	
DNA	1 µl (usually corresponding to 100-250 ng of miniprep DNA)
Enzyme 1	5 units
Enzyme 2 (optional)	5 units
10X Buffer	1 µl
H_2O	7.5 µl
Total Volume	10 µl

The digestions were carried out using the appropriate buffer indicated for each enzyme according to New England Biolabs. The reactions were incubated for 90 minutes at 37°C.

2.1.1.3 Phosphatase treatment

Phosphatase treatment was done straight after digestion, adding 1.5 units of Shrimp Alkaline Phosphatase (rSAP, New England Biolabs). Mixture was kept at 37°C for 30 minutes.

2.1.1.4 Oligonucleotides resuspending and annealing procedure

The oligonucleotides were annealed following the protocol suggested by Sigma-Aldrich:

The oligonucleotides were resuspended in milliQ water to a final concentration of 100 µM. Following the resuspension, 45 µl of forward oligonucleotide were diluted with 45 µl of the reverse oligonucleotide and 10 µl of annealing buffer. The dilution was placed in a thermal cycler at 95°C for 5 minutes and was ramp cooled to 25°C over a period of 45 minutes.

Annealing Buffer: 10 mM Tris, 50 mM NaCl, 1 mM EDTA, pH 7.5.
Table 2.5 Annealing buffer recipe.

Annealing Buffer recipe	
H_2O	380 µl
NaCl	500 µl
EDTA	20 µl
Tris	100 µl
Total volume	1 ml

2.1.1.5 Polynucleotide Kinase Reaction

After annealing the oligonucleotides, polynucleotide kinase (PNK) was used to add a phosphate on.

Table 2.6 Polynucleotide kinase reaction conditions.

Polynucleotide kinase reaction	
Buffer A	2 µl
1 mM ATP	16.5 µl
PNK	10 units
Annealed Oligonucleotides	0.5 µl
Total volume	20 µl

The PNK reaction was incubated at 37°C for 20 minutes followed by a further incubation at 75°C for 10 minutes. Once this was done, the annealed oligonucleotides were cleaned-up as explained in section 2.1.1.14 on page 59.

2.1.1.6 Ligation

The ligation processes (vector insert ligation or religation of the digested vector after the removal of the desired sequence) was done using T4 DNA ligase (New England Biolabs).

The ligation reaction was done in different insert:vector mass ratio when necessary, following the equation (for a 3:1 insert:vector ratio):

$$\frac{ng\ of\ vector\ x\ length\ of\ insert\ (bp)}{length\ of\ vector\ (bp)}\ x\ \frac{3}{1} = ng\ of\ insert$$

As controls, ligation of the vector without insert in the presence and absence of T4 ligase were used. The ligation reaction was incubated for 1 hour at room temperature using 1 µl of 10X Lig Buffer, 0.5 µl of T4 DNA ligase (400 000 units/ml) with the required amount of vector and insert in a final volume of 10 µl.

When the ligation reaction was done to religate a digested vector, the ligation reaction was done for an hour at room temperature under the same conditions, without the addition of the insert.

2.1.1.7 Blund end fill in reaction

When the process of digestion left incompatible 3’ or 5’ overhangs, those incompatible overhangs needed to be removed or filled in to promote the blunt-end ligation.

Blunt end reaction was carried out using the Klenow fragment of DNA polymerase I (New England Biolabs). The fill in reaction was incubated for 30 minutes at 37°C. The fill in reaction was usually done straight after the 90 minutes of digestion, without any cleaning step in between.

Table 2.7 Blunt end fill in reaction master mix conditions.

Blunt end fill in reaction master mix	
DNA	1-3 µg
Klenow enzyme	10 units
10X Buffer	3 µl
dNTP(final concentration 0.5 mM each dNTP)	1 µl
H_2O	14 µl
Total volume	30 µl

2.1.1.8 Bacteria transformation

To get good yields of the constructs formed, we transformed competent *E.coli* bacteria with the ligated products. The bacteria used for the purpose were NEB® 5-alpha Competent *E. coli* (Subcloning Efficiency) (C2988). 5 µl of ligation mixture were mixed with 50 µl of competent bacteria, and kept on ice for 30 minutes. After the incubation, the mixture was placed in a 42°C water bath for 30 seconds and back on ice for 2 more minutes. 150 µl of SOC outgrowth medium (New England Biolabs) were added and put in a shaking incubator at 37°C for an hour. The mixture was spread on LB Agar plates with ampicillin (100 µg/ml). Plates were incubated at 37°C overnight.

Multiple colonies were picked and put in 5 ml of LB broth with ampicillin and grown overnight (no more than 16 hours) in a 37°C shaker (200 rpm).

SOC outgrowth medium: 2% (w/v) Vegetable Peptone, 0.5% (w/v) Yeast Extract, 10 mM NaCl, 2.5 mM KCl, 10 mM $MgCl_2$, 10 mM $MgSO_4$, 20 mM Glucose.

LB Agar: 1% (w/v) Bacto-tryptone, 0.5% (w/v) bacto-yeast extract, 1% (w/v) NaCl and 1.5% (w/v) agar in deionised water.

LB Broth (for 1 L): 10 g Tryptone, 10 g NaCl, 5 g Yeast extract, 950 ml ddH_2O. Adjust pH to 7.0, make up to 1 L with ddH_2O.

2.1.1.9 Miniprep

To carry out a small-scale plasmid DNA purification, the NucleoSpin® Plasmid kit (Macherey-Nagel) was used. The 5 mL of bacterial culture that had been grown overnight (see 2.1.1.8, page 56) were pelleted by centrifuging at 3,000 x *g* for 10 minutes and the supernatant was discarded. Cells were lysed by the addition of 250 µl of Buffer A1, containing RNase A to digest bacterial RNA after lysis. To liberate the DNA plasmid from the *E.coli* cells, 250 µl of SDS/alkaline Buffer A2 (containing NaOH) were added to each sample and they were gently mixed by inversion, no mechanical mix was used to avoid shearing of genomic DNA. To neutralise the lysate, precipitate genomic DNA and proteins and create the appropriate high salt conditions required by the plasmid DNA to bind to the silica membrane, 200 µl of Buffer A3 (containing sodium acetate) were added and samples were gently mixed again. Samples were centrifuged for 5 minutes at 11,000 x *g* and a clear supernatant was obtained, genomic DNA, proteins and cell debris are pelleted. The supernatant was decanted in a NucleoSpin® Plasmid/Plasmid Column and centrifuged for 1 min at 11,000 x *g*. Flow-through was removed and the membrane was washed with 500 µl of Buffer AW (centrifuged at 11,000 x *g* for one minute). 600 µl of Buffer A4 (supplemented with ethanol) were added to get rid of possible contaminants as metabolites, salts and soluble cellular components and centrifuged for 1 min at 11,000 x *g*, flow-through was discarded. The silica membrane was dried by centrifuging it for 2 minutes at 11,000 x *g*. The DNA was eluted in 50 µl of Buffer AE (slightly alkaline buffer, containing low ionic strength conditions).

The obtained DNA was quantified using the NanoDrop 2000c UV-Vis spectrophotometer.

2.1.1.10 Midiprep

To carry out a large-scale plasmid DNA purification, the QIAGEN Plasmid Plus Midi Kit was used. Colonies were picked and put in 5 ml of LB broth with ampicillin and grown for around 8 hours. 100 µl of that broth was taken and grown in 100 ml of LB broth with ampicillin overnight. 25 ml of the bacterial culture was pelleted by centrifugation at 6,000 x *g* for 15 minutes at 4°C. The pellet was resuspended in 4 ml of Buffer P1 containing RNaseA. 4 ml of P2 buffer were added and the solution was mixed by inverting and incubated at room temperature for 3 minutes. 4 ml of Buffer S3 (which precipitates proteins, genomic DNA and cell debris) were added to the lysate and it was mixed by inverting. The lysate was transferred to a QIAfilter Cartridge, incubated at room temperature for 10 minutes and filtered. 2 ml of Buffer BB were added to the cleared lysate and it was mixed by inverting 4-6 times and filtered through the QIAGEN Plasmid Plus spin column by applying vacuum. DNA was washed with 0.7 ml of Buffer ETR and vacuum was applied, this process was repeated with Buffer PE. The column was centrifuged at 10,000 x *g* for 1 minute to

completely remove the residual wash buffer. DNA was eluted in 200 µl of Buffer EB. The obtained DNA was quantified using the NanoDrop 2000c UV-Vis spectrophotometer.

2.1.1.11 DNA quantification by NanoDrop

To determine the concentration and purity of the DNA extracted, the NanoDrop 2000 UV-Vis spectrophotometer (Thermo Scientific) was used. The DNA was read at a wavelength of 260 nm and the concentration was calculated using 50 ng-cm/µl as extinction coefficient. The purity ratios were calculated at 260/280 nm and 260/230 nm using the NanoDrop 2000/2000c software (Thermo Scientific). Pure DNA was considered to have a ratio of around 1.8 of absorbance at 260/280 nm and a ratio of absorbance between 1.8 and 2.2 at 260/230 nm.

2.1.1.12 Agarose gel electrophoresis

Agarose gels were used for the analysis of the correct size of the DNA products. 0.8% and 2% agarose gels were used. The most commonly used gels were the 0.8% ones, whereas the 2% agarose ones were only used when the interest was in very small DNA fragments.

The appropriate amount of agarose was mixed with 100 ml of 1X TAE buffer. Agarose was melted in the microwave. Gel casting tray was assembled on a flat surface.

Agarose solution was cooled and 4 µl of Gel Red were added. Solution was mixed and poured into the tray, and comb was placed. Once the gel had set, comb and gel casting gates were removed and placed in a horizontal electrophoresis tank. The tank was filled with 1X TAE buffer.

The required amount of 6X loading dye was added to the DNA solutions. The samples were loaded into the gel. GeneRuler mix (Thermo Fisher Scientific) was used as a ladder.

1 µg of GeneRuler mix was mixed with 10 µl of water and 2 µl of loading dye. The ladder was also loaded.

Gel was run at 120 V for at least 45 minutes.

Gel was visualised using the image analysis system Syngene PXi or using a UV transilluminator.

TAE Buffer (pH 8): 1X solution containing 40 mM Tris base (Fisher Scientific), 20 mM NaOAc (Sigma), 26.9 mM acetic acid (Sigma) and 2 mM EDTA (Sigma).

2.1.1.13 Agarose gel clean-up

For the purification of the DNA from an agarose gel the NucleoSpin® Gel and PCR clean-up (Macherey-Nagel) kit was used.

The band corresponding to the DNA of interest was excised from the gel using a scalpel and the weight of the gel slice was determined. For each 100 mg of agarose gel, 200 µl of Buffer NTI (containing a chaotropic salt, providing the right conditions for the binding of the DNA to the silica membrane) were added. Sample was incubated for 5-10 minutes at 50°C to dissolve the agarose. Once the agarose was totally dissolved, the sample was loaded in a NucleoSpin®Gel and PCR clean-up column and centrifuged for 1 minute at 11,000 x *g*. The silica membrane was washed with 700 µl of buffer NT3 (containing ethanol) and centrifuged at 11,000 x *g* for 1 minute. The silica membrane was dried by centrifugation for 1 minute at 11,000 x *g*. The DNA was eluted in 30 µl of buffer NE (slightly alkaline buffer).

The obtained DNA was quantified using the NanoDrop 2000c UV-Vis spectrophotometer.

2.1.1.14 DNA clean-up

To get rid of the undesired reagents after a digestion process, phosphatase treatment or blunt end fill in reaction, and get clean DNA, a DNA clean-up process was required. For the DNA clean-up the NucleoSpin® Gel and PCR clean-up (Macherey-Nagel) kit was used.

Reactions of less than 50 µl were adjusted to a final volume of 50 µl with water. 1 volume of sample was mixed with 2 volumes of buffer NTI (containing a chaotropic salt, providing the right conditions for the binding of the DNA to the silica membrane). The dilution was loaded in a NucleoSpin® Gel and PCR clean-up column and centrifuged for 1 minute at 11,000 x *g*. Flow-through was discarded. 700 µl of buffer NT3 (containing ethanol) were added and sample was centrifuged at 11,000 x *g* for 1 minute. Flow-through was discarded. The silica membrane was dried by centrifugation at 11,000 x *g* for 1 minute. DNA was eluted in 30 µl of buffer NE.

The obtained DNA was quantified using the NanoDrop 2000c UV-Vis spectrophotometer.

2.2 CELL ASSAYS

All the cell experiments were done in HeLa (human cervical epithelioid carcinoma) cells, HEK293 (human embryonic kidney) cells, CAL51 (breast cancer derived) cells and hpBN-HEK cells (a stable cell line generated form HEK293 cells expressing hpBN. This cell line will be covered in detail in future sections of this thesis).

Cells were maintained in gamma-sterilised, tissue culture-treated 75 cm^2 flasks, in a 37°C incubator (5% CO_2).

2.2.1 Cell maintenance

Cells were maintained by passaging them every 2-3 days with Dulbecco's Modified Eagle Medium with Glutamax™ (DMEM) (Gibco® by Life Technologies™) supplemented with 10% heat-inactivated fetal bovine serum (FBS). Old medium was removed and cells were washed with 7 ml of Mg^{2+} and Ca^{2+} free PBS. Cells were detached from the culture flasks with 2 ml TrypLE™ Express (Gibco® by Life Technologies™) and incubated at 37°C for a few minutes, until cells were detached. 3 ml of supplemented medium was used to stop the cell detachment. For the maintenance of the cells, 1 ml of the detached cells were kept in the flask. Cells were transferred to a new flask once a week.

2.2.2 Cell counting

Cells were counted the day before transfection. As explained before, the old growth medium was removed from the cells and cells were washed with 7 ml of D-PBS. 2 ml of TrypLE were added and cells were put at 37°C until they were detached. 8 ml of growth media were added to the cells. 10 µl of the diluted cells were pipetted into one of the sides of a Neubauer Chamber. Cells in the four corners were counted. The amount of cells per ml was calculated using the following equation:

$$\frac{cell}{ml} = \frac{total\ number\ of\ cells\ in\ the\ four\ corners}{4}\ x\ 10\ 000$$

A master mix was made containing the right amount of cells and growth medium.

2.2.3 Cell transfection

Transfections were done in the different plate or well types. Seeding conditions were also done depending on cell line. General seeding conditions for HEK293 cells:

- 96 well plate: 2 000 cells per well in 200 µl of growth medium.
- 60 mm plates: 200 000 cells per plate in 5 ml of growth medium.

Cell transfection was done using different transfection reagents for each different type of transfection:

- GeneJuice (Novagen) for plasmid transfection.
- RiboJuice (Novagen) for oligonucleotide transfection.
- Lipofectamine 2000 (Thermo Fisher Scientific) for RNA, RNA & oligonucleotide and oligonucleotide transfections. The use of Lipofectamine 2000 will be covered in section 2.14 on page 79.

GENEJUICE

GeneJuice was used to transfect plasmids on their own, to study their expression with a luciferase assay. All the plasmid transfections were carried out in 96 well plates in triplicate (three wells with the same transfection). All the procedure shown is based on a single well transfection.

20 ng of plasmid was transfected per well. 0.06 µl of GeneJuice were mixed with 1.94 µl of serum free DMEM (this was done as a master mix, where the total GeneJuice required for the whole set of transfections was mixed with the required serum free DMEM). Mixture was incubated for 5 minutes. 20 ng of plasmid were added to the mixture and it was incubated for 5-15 minutes. All the volume was added to the well.

RIBOJUICE

RiboJuice was used on its own to transfect the cells with the oligonucleotides in 10 cm plates for the purpose of harvesting for a western blot and qPCR or in combination with GeneJuice to co-transfect oligonucleotides and plasmid.

Co-transfection of plasmid and oligonucleotides:

Plasmid and oligonucleotide co-transfections were carried out in 96 well plates in triplicate, seeding 2 000 cells per well in 200 µl of DMEM. The final volume per well after the transfection was 250 µl.

Oligonucleotides were diluted to a working solution of 1 µM.

To transfect a final concentration of 25 nM of oligonucleotides in a final volume of 250 µl, 6.25 µl of the stock solution are required.

In a tube, 17.75 µl of serum free DMEM was mixed with 1 µl of RiboJuice. In a separate tube, 0.06 µl of GeneJuice was mixed with 1.94 µl of serum free DMEM (in a master mix for all the transfections required). After five minutes, the 2.56 µl of oligonucleotides and the 20 ng of plasmid DNA were added to the RiboJuice and the GeneJuice tubes respectively. The tubes with GeneJuice were topped up with serum free DMEM to a final volume of 25 µl. Mixtures were incubated for 5-15 minutes, and the total volume (50 µl) were added to the cells.

Transfection of oligonucleotides:

Oligonucleotides were only transfected on their own with the purpose to do western blots and qPCRs. 60 mm plates were used and 200 000 cells were seeded per plate in 5 ml of growth medium.

Prior to the transfection, the 5 ml of media were removed from each plate and 3.5 ml of fresh media were added. 683 µl of DMEM without serum were mixed with 17 µl of RiboJuice. They were incubated at room temperature for 5 minutes and a final concentration of 25 nM (62.5 µl of the 1 µM stock) of oligonucleotide added.

2.3 LUCIFERASE ASSAY- Nano-Glo® Dual-Luciferase® Reporter Assay System

To study gene expression a luciferase assay was done. Most of the constructs for the luciferase assay contained Firefly (Fluc) and/or Nanoluciferase (Nluc) reporter genes.

The kit Nano-Glo® Dual-Luciferase® Reporter Assay System (Promega) was used to detect Fluc and Nluc activities. In this kit, ONE-Glo™ EX Luciferase Assay Reagent acts as the substrate for the Fluc and NanoDLR™ Stop & Glo reagent stops the luminescence emission of the Fluc and acts as a substrate for the Nluc.

For the luciferase assays cells were seeded in white or clear 96 well plates (where cells could be monitored and the reagent requirement was five times smaller):

Cells seeded in white plates:

2 days after transfection, growth medium was removed from the wells, and 50 µl of fresh media were added to each well. 50 µl of ONE-Glo™ EX Luciferase Assay Reagent was added to each well and the plate was placed on an orbital shaker for 5 minutes at room temperature. The activity of Fluc was measured using GloMax® 96 Luminometer.

50 µl of NanoDLR™ Stop & Glo reagent were added to each well and plate was placed on an orbital shaker for 10 minutes. The luminescence emitted by Nluc was measured on the luminometer.

Cells seeded in clear plates (protocol to reduce the volume of reagents used):

2 days after transfection, growth medium was removed from the wells and cells were washed with 1X PBS. Cells were lysed in 20 µl of 1X Passive Lysis Buffer (PLB) (Promega) and put in a

rocker for at least 20 minutes. 10 µl of the PLB with the cells were transferred to a white 96 well plate, 10 µl of ONE-Glo™ EX Luciferase Assay Reagent was added to each well and the plate was placed on an orbital shaker for 5 minutes at room temperature. The activity of Fluc was measured using GloMax® 96 Luminometer. The Linear Dynamic Range of the luminometer is greater than 8 decades[253] and an error message is displayed when saturated.

10 µl of NanoDLR™ Stop & Glo reagent were added to each well and the plate was placed on an orbital shaker for 10 minutes. The luminescence emitted by Nluc was measured on the luminometer.

Data were analysed using Instinct software (Promega).

2.4 DATA ANALYSIS OF LUCIFERASE ASSAYS

One of the ways used to study IRES activity was the use of a luciferase assay. Cells were transfected with a bicistronic plasmid expressing two reporter genes (Fluc and Nluc) where the 5' UTR of *BAG1* was located between both of them, or with two monocistronic plasmids, one expressing Fluc and the other one Nluc. The 5' UTR of *BAG1* was cloned upstream of the Nluc sequence. Each transfection was done in triplicate, where n=1 means a unique assay done in triplicate and n=3 is considered when the same assay is repeated three individual times, each done in triplicate.

The luciferase assay data analysis was adapted from the model proposed by J. L. Jacobs *et al.* on the paper "Systematic analysis of bicistronic reporter assay data" [254].

Once the Fluc (*Fluc* $_{\mathrm{RLU}}$) and Nluc (*Nluc* $_{\mathrm{RLU}}$) values were measured for each sample, the Nluc to Fluc ratios were calculated:

$$x_i = \frac{Nluc_{\ \mathrm{RLU}}}{Fluc_{\ \mathrm{RLU}}}$$

Where x_i is the ratio obtained from each sample.

Statistical analysis were carried out to analyse if the oligonucleotides had significantly modified the IRES activity. The normality or Gaussian distribution of the results was analysed using a Shapiro-Wilk normality test on GraphPad (normal distribution was accepted if P>0.05). To determine the significant difference between the different oligonucleotide treatments a one-way ANOVA with a Tukey's multiple comparison test was carried out using GraphPad. To determine the significant difference between the oligonucleotide treated cells and the control cells (no oligonucleotide treated cells or Scramble transfected cells) a one-way ANOVA with a Dunnett's

multiple comparison test was carried out using GraphPad. The statistical analysis showed more reliable results as the sample number increased.

2.5 PROTEIN EXTRACTION AND QUANTIFICATION

2.5.1 Protein extraction

48 hours after transfection, growth media was removed from the plates and the plates were chilled on ice. 1 ml of cold PBS was added. Cells were scraped with the 1 ml of PBS and transferred into an Eppendorf tube. Cells were kept on ice all the time. Samples were centrifuged at 2500 x *g* and 4°C for 5 minutes.

After the centrifugation, the supernatant was removed. 80 µl of RIPA buffer were added. Tubes were vortexed every minute during 5 minutes. After the 5 minutes, the samples were centrifuged at 14,000 x *g* and 4°C for 15 minutes. The supernatant was taken to another tube and the pellet was discarded.

Table 2.8 RIPA buffer composition.

RIPA Buffer component	**Stock concentration**	**Vol to add µl**
150 mM NaCl	2 M	225
1% igepal/NP-40	10%	300
1% DOC	10%	300
0.1% SDS	10%	30
50 mM Tris HCl, pH 7.6	1 M	150
1 mM EDTA	0.5 M, pH 8.0	6
1 mM EGTA	100 mM, pH 8.0	30
H_2O (adjusting for addition of Halt*)	0	1929

*Supplemented with 30 µl Halt protease and phosphatase inhibitor cocktail (100 x stock) immediately before use.

2.5.2 Protein quantification

A Bradford assay was done to calculate protein quantity in the samples. The assay was done using an appropriate 96 well plate, each read was done in triplicate. Bio-Rad Protein Assay Dye Reagent

Concentrate (Bio-Rad) was diluted to a 1X concentration. A standard curve was prepared using a stock solution of 0.5 µg/µl of BSA. The standard curve was done with 0 µg, 0.5 µg, 1 µg, 2 µg, 3 µg and 4 µg of BSA.

The standard curve preparation was done adding the necessary amount of BSA to 200 µl of Bio-Rad Protein Assay Dye Reagent Concentrate.

150 µl of each tube were added to a well of the 96 well plate.

1 µl of protein extract were added to 200 µl of 1X Bio-Rad Protein Assay Dye Reagent Concentrate. Tubes were mixed and 150 µl of the mixture were added to a well of the 96 well plate.

Absorbance was read in a spectrophotometer set to 380 nm and at 595 nm. The values from the standard curve were used to generate a formula used to determine the concentration of protein in each sample.

2.6 WESTERN BLOT

The detection of the expression of *BAG1* in cells treated with the oligonucleotides was done by western blot using Tris-glycine SDS-Polyacrylamide Gel Electrophoresis in a 10% gel. The resolving gel was done in a total volume of 10 ml composed of 2 ml of H_2O, 1.7 ml of protogel, 1.25 ml of 1.5 M Tris-HCl (pH 8.8), 50 µl of 10% (w/v) SDS, 25 µl of 10% (w/v) ammonium persulfate and 5 µl of TEMED. The stacking gel was done in a total volume of 4 ml composed by 1.2 ml of H_2O, 260 µl of protogel, 0.5 ml of 0.5 M Tris-HCl (pH 6.8), 40 µl of 10% (w/v) SDS, 20 µl of 10% (w/v) ammonium persulfate and 5 µl of TEMED.

Using the known concentration of lysate samples, the volume of lysate required for 16 µg of protein was calculated. To this, 8 µl of sample buffer (containing 1:10 volume β-Mercaptoethanol) was added and made up to a total volume of 40 µl adding RIPA buffer. To denature proteins, samples were heated at 70°C for 10 minutes.
The gel was set in the tanks such that the wells faced into the central chamber. The central chamber was filled with 1X Laemmli Running Buffer. 20 µl of the denatured lysate were loaded per well. Gel was run at 120 V until the dye-front reached the bottom.

Proteins were transferred from the gel to a 0.45 µm nitrocellulose membrane *via* semi dry transfer. For this purpose The Trans-Blot® Turbo™ transfer system (Bio Rad) was used.
6 pieces of 3 mm filter paper and the membrane were soaked in 1X Tris Glycine buffer. In the tray of the Trans-Blot® Turbo™ transfer machine 3 of the wet papers were placed followed by the

membrane, the gel and the other 3 wet papers. The tray was closed with the lid. The standard minidry protocol was run.

After the transfer, the membrane was blocked in TBS-Tween (TBS-T) containing 3% (w/v) Bovine Serum Albumin (BSA) for 30 minutes.
The membrane was incubated in primary antibody in the require dilution (see Table 2.9) on 3% BSA in TBS-T overnight at 4°C. The following morning, the membrane was washed with TBS-T, three washes of 10 minutes each, and was incubated with the required secondary antibody (see Table 2.9) protected from light, for one hour at room temperature while on the rocker.
The membrane was washed twice for 10 minutes each time with TBS-T, followed by a last wash with PBS.

The detection was done by a Near Infrared fluorescence detection method, with Licor Odyssey using both 700 nm and 800 nm channels. Results were analysed with the software Image Studio Lite (LI-COR), where the bands corresponding to each of the protein signals were selected and the signal intensity was quantified. The expression of the gene of interest was quantified relative to a housekeeping gene (actin) using densitometry.
Laemmli buffer: 200 ml of Laemmli buffer 10X diluted in 1800 ml dH_2O giving a final concentration of 25 µM Tris (HCl), 0.1% SDS, 192 mM glycine, adjusted to pH 8.5.

1X Tris Glycine buffer: 100 ml 10X Tris Glycine (Bio Rad), 700 ml water and 200 ml ethanol.

TBS-T: 50 mM Tris (HCl), 150 mM NaCl, 0.1% (v/v) Tween-20, pH 7.5-8.0.

Table 2.9 Antibody dilutions.

	Company	**Antibody**	**Raised in**	**Dilution**
Primary	Cell Signaling Technology, #3920	Anti-BAG1	Mouse	1:1000
	Sigma, AC-40	Anti-α actin	Rabbit	1:5000
	Abcam, ab8227	Anti-β actin	Mouse	1:5000
	Promega	Anti-Nluc	Rabbit	1:1000
Secondary	Invitrogen, a32734	Rabbit 680 nm	Goat	1:15000
	Invitrogen, a32735	Rabbit 800 nm	Goat	1:15000
	Invitrogen, a21050	Mouse 680 nm	Goat	1:15000
	Invitrogen, a32730	Mouse 800 nm	Goat	1:15000

2.7 SEQUENCING

All the constructs made were sent for sequencing to Eurofins Genomics. In most of the cases the constructs were sequence in forward and reverse directions to get more robust results. The software Serial Cloner was used to analyse the sequencing results.

Table 2.10 Primers used for sequencing.

Primer name	**Sequence 5'-3'**
RV 3 PRIMER	5'-CTAGCAAAATAGGCTGTCCC-3'
3'Luc2 seq F	5'-GGTTACAACCGCCAAGAAG-3'
SV40 pA seq R	5'-CTTATCATGTCTGCTCGAAGC-3'
pcDNA3_for	5'-GGC TAA CTA GAG AAC CCA CTG-3'
pcDNA3_rev	5'-GGC AAC TAG AAG GCA CAG TC-3'
AfterSV40 F	5'-GAAGTAGTGAGGAGGCTTT-3'

2.8 RNA EXTRACTION AND QUANTIFICATION

48 hours after transfection, growth media was removed from the plates and the plates were chilled on ice. Cells were scraped with the 1 ml of PBS, transferred into a clean tube and centrifuged at 2500 x *g* and 4°C for 5 minutes. Supernatant was removed.

For RNA extraction the kit "Macherey Nagel™ NucleoSpin™ RNA Columns" was used.

350 µl of Buffer RA1 and 3.5 µL β-Mercaptoethanol were added to the cell pellet and it was vortexed vigorously. Viscosity was reduced and the lysate was cleared by filtration through the NucleoSpin® Filter (violet ring) by centrifugation at 11,000 x *g* for 1 minute. 350 µL of 70% ethanol were added to the homogenised lysate and it was placed in a NucleoSpin® RNA Column (light blue ring) and centrifuged for 1 minute at 11,000 x *g*. 350 µl of Membrane Desalting Buffer were added and sample was centrifuged at 11,000 x *g* for one minute. To get rid of the DNA, 95 µl of DNase reaction mixture were applied to the centre of the silica membrane and it was incubated at room temperature for 15 minutes. The first wash and rDNase inactivation was done by the addition of 200 µl of Buffer RAW2. The second and third washes were done by adding 600 µl and 250 µl of Buffer RA3 respectively and by centrifugation at 11,000 x *g* for 1 minute each time. The RNA was eluted in 60 µl of RNase-free water and centrifuged at 11,000 x *g* for 1 minute.

2.8.1 RNA quantification by NanoDrop

To determine the concentration and purity of the RNA extracted, the NanoDrop 2000 UV-Vis spectrophotometer (Thermo Scientific) was used. The RNA was read at a wavelength of 260 nm. The purity ratios were calculated at 260/280 nm using the NanoDrop 2000/2000c software (Thermo Scientific). Pure RNA was considered to have a ratio between 1.9 and 2.1 of absorbance at 260/280 nm.

2.8.2 Reverse transcription

To carry out a reverse transcription (RT) the "ImProm-II™ Reverse Transcription System" from Promega was used.

All the work was done on ice unless otherwise stated.

Up to 1 µg of RNA was combined with nuclease-free water and random primer (0.5 µg/reaction) to a final volume of 5 µl. Tubes were heated at 70°C for 5 minutes and immediately chilled in ice-water for 5 minutes.

The reverse transcription reaction mix was prepared in the following way:

Table 2.11 Master mix for the reverse transcription reaction.

Experimental Reaction	**1 sample**
Nuclease-Free Water (to a final volume of 15 µl)	X µl
ImProm-II™ 5X Reaction Buffer	4.0 µl
$MgCl_2$ (final concentration 1.5–8.0 mM)	4 µl
dNTP Mix (final concentration 0.5 mM each dNTP)	1.0 µl
Recombinant RNasin® Ribonuclease Inhibitor	0.5 µl
ImProm-II™ Reverse Transcriptase	1.0 µl
Final volume	15.0 µl

The 5 µl or the RNA samples were mixed with 15 µl of RT reaction mix. A thermocycler was used to reverse transcribe the RNA into cDNA. The following conditions were used:

Table 2.12 Conditions to reverse transcribe the RNA into cDNA.

Process	**Temperature**	**Time**
Anneal	25°C	5 minutes
Extend	42°C	60 minutes
Inactivate Reverse Transcriptase	70°C	15 minutes

2.8.3 Real time PCR

RNA levels were measured using real time PCR or quantitative PCR (qPCR). As an internal control *B2M* mRNA levels were measured[255]. *B2M* had previously shown to have stable RNA expression in HEK293 cells[244]. By comparing the BAG1 expression to the B2M expression we could ensure that any effect in the BAG1 levels is due to a translational effect.

The primers used were:

Table 2.13 *BAG1* and *B2M* qPCR primers sequence.

Primer name	**Sequence 5'-3'**
BAG1 after 5UTR F	CTTGGATGGAGCCTGTGGTT
BAG1 after 5UTR R	CCACCTGCCTGCTTTACTCA
B2M F	TTCATCCATCCGACATTGAAG
B2M R	ATCCAATCCAAATGCGGC

Prior to testing any of the samples, a standard curve was done to calculate the efficiency of the primers. One of the cDNA samples was used as a template for the standard curve. From that sample a series of serial dilutions were created. The serial dilutions had 5 points of 1:10 dilutions (undiluted, 1:10, 1:100, 1:1000, 1:10 000). A no template control (NTC) was also used. Each sample or dilution was done in triplicate.

qPCR master mix was prepared in the following way:

Table 2.14 qPCR master mix composition.

	Volume in µl
H_2O	6.2
2X Luna qPCR Master Mix	7.5
Primer forward (10 µM)	0.15
Reverse primer (10 µM)	0.15
Template DNA	1 (of the RT reaction)

The qPCR was run on a PCRmax Eco 48 under the following conditions:

Table 2.15 qPCR conditions.

Stage	**Temperature**	**Duration**	**Cycles**
UDG Incubation	50°C	2 min	1
Polymerase Activation	95°C	10 min	1
PCR Cycling	95°C	10 sec	40
PCR Cycling	60°C	30 sec	40
Melt Curve	95°C	15 sec	1
Melt Curve	55°C	15 sec	1
Melt Curve	95°C	15 sec	1
Total Cycle Count	40		

The software Eco Study was used to do all the qPCR analysis, as the calculation of the efficiency of the primers and the relative amplification. For the efficiency of the primers, values between 95% and 105% were considered appropriate.

To analyse the *BAG1* mRNA levels of the samples, they were normalised to the *B2M* (reference gene) mRNA levels. The method chosen was the Livak method[256]. On this method, the expression of a targeted gene (*BAG1*) is normalised to a reference gene (*B2M*) and expressed relative to a reference sample (usually mock transfected cells). The calculations done were the following ones:

$$\Delta Cq = avg\ Cq\ (BAG1) - avg\ Cq\ (B2M)$$

$$\Delta\Delta Cq = \Delta Cq\ (oligonucleotide\ treatment) - \Delta Cq\ (mock)$$

$$RQ = 2^{-\Delta\Delta Cq}$$

The RQ values of the different oligonucleotide treatments were then compared to study variations in the RNA levels.

2.9 MICROSCOPY

Fluorescent microscopy techniques were used to check the presence of the oligonucleotides in the cells. For this purpose the fluorescent oligonucleotide B6FAM, purchased from Sigma-Aldrich was used (check appendix B.2. on page 271 for the sequence). B6FAM was modified with a 6-FAM™ (fluorescein) on the 5' end. The excitation maximum of 6-FAM™ is 495 nm, the emission maximum 520 nm and the fluorescent colour is green.

One coverslip was placed in each well of a 24 well plate. 20 000 HEK293 cells were seeded per well. The following day a final concentration of 25 nM of B6FAM were transfected, using 1.2 µL of RiboJuice.

48 hours after transfection cells were fixed.

2.9.1 Cell fixation

As the fluorescent oligonucleotide B6FAM was used, work was carried out in the dark/low light as much as possible to avoid photo bleaching of the samples.

The medium was removed from the wells and the cells were washed with 1 ml of PBS. Cells were incubated with 1 ml of 4% paraformaldehyde during 15 minutes, in darkens. Cells were quickly washed with ammonium chloride (NH_4Cl_2) followed by three PBS washes and a final wash of water. A blob of ProLong mounting medium (with DAPI nuclear stain) (Invitrogen) was placed in a microscope slide. Coverslips were removed from the well. Excess water was removed. The coverslip was laid on top of the mounting mediums (cell side down) and air bubbles were pushed out. Mounted coverslips were stored in the dark at 4°C.

2.9.2 Microscopy analysis

Mounted coverslips were imaged on a DeltaVision Elite system (GE Life Sciences) with an SSI 7-band light-emitting diode (LED) for illumination. The objective used was an X60/1.42 numerical aperture (NA) Oil Plan Apo objective and the camera used was a monochrome sCMOS camera running SoftWoRks software (version 6). FITC, Cy-5, TRITC 4',6-diamidino-2-phenylindole (DAPI) and differential interference contrast (DIC) channels were used. The data from multiple z-stacks were compressed into single images through obtaining the maximum projection of the stack and

combining it into one image. Brightfield images of cells in culture were taken on an EVOS XL Core Imaging System (Thermo Fisher).

Autostitch software (University of British Columbia) was used to reconstitute composite overview images from multiple single images. Images were deconvolved using SoftWoRks software (version 6) iterative deconvolution and were analysed using the Fiji image processing package. Plot profiles were generated using FIJI by analysis of the pixel intensity for the corresponding regions.

2.10 *IN VITRO* RNA SYNTHESIS

2.10.1 DNA template preparation

Forward and reverse primers were designed to amplify the desired regions in the plasmids pFBN, pFN, pBN, pN and pGL4.13SV40. Primers were designed to amplify the region including the coding sequence for Fluc and Nluc in pFBN (with the *BAG1* 5' UTR between both promoter genes) and pFN; *BAG1* 5' UTR and Nluc in pBN; Nluc in pN and Fluc in pGL4.13SV40. The forward primer contained the T7 promoter region on its 5' extreme and two guanines after the T7 promoter sequence to increase transcription yields (TAA TAC GAC TCA CTA TAG **GG**).

Primers used to insert the T7 promoter in pFBN, pFN, pBN and pN:

NanoLuc R good: 5'-CTTATCATGTCTGCTCGAAGC-3'

T7-afterSV40 F: 5'-TAATACGACTCACTATAGGGGAAGTAGTGAGGAGGCTTT-3'

Primers used to amplify pFBN, pFN, pBN, pN lacking the T7 promoter:

AfterSV40 F: 5'-GAAGTAGTGAGGAGGCTTT-3'

NanoLuc R good: 5'-CTTATCATGTCTGCTCGAAGC-3'

Primers used to amplify *BAG1* 5' UTR:

BAG1 F: 5'-TAATACGACTCACTATAGGGAAGCCTAGCCTCGAGGAAT-3'

BAG1 R: 5'-CCAACGAAATCTTCGAGTGT-3'

DNA was amplified by PCR using "Q5® High-Fidelity DNA Polymerase" (New England Biolabs).

The reactions were assembled on ice:

Table 2.16 Reaction setup to amplify the desired products with the T7 promoter.

	25 µl REACTION	**50 µl REACTION**	**FINAL CONCENTRATION**
5X Q5 Reaction Buffer	5 µl	10 µl	1X
10 mM dNTPs	0.5 µl	1 µl	200 µM
10 µM Forward Primer	1.25 µl	2.5 µl	0.5 µM
10 µM Reverse Primer	1.25 µl	2.5 µl	0.5 µM
Template DNA	10 ng	10 ng	10 ng
Q5 High-Fidelity DNA Polymerase	0.25 µl	0.5 µl	0.02 U/µl
5X Q5 High GC Enhancer	5 µl	10 µl	1X
Nuclease-Free Water	to 25 µl	to 50 µl	

The DNA was amplified on a thermal cycler under the following conditions:

Table 2.17 Thermocycling conditions for the PCR.

Initial Denaturation	98°C	30 seconds
35 Cycles	98°C	10 seconds
	62°C	30 seconds
	72°C	70 seconds
Final Extension	72°C	2 minutes
Hold	10°C	

The DNA was purified as specified in 2.1.1.13 on page 58 or 2.1.1.14 page 59.

2.10.2 *In vitro* RNA synthesis

For the *in vitro* synthesis of RNA the kit “HiScribe™ T7 Quick High Yield RNA Synthesis Kit” (New England Biolabs) was used.

The necessary kit components were mixed and pulse-spun prior to their use. The components were kept on ice at all times, but the reaction was assembled at room temperature following the instructions on Table 2.18.

Table 2.18 RNA synthesis reaction assembly.

Nuclease-free water	X µl
NTP Buffer Mix (20 mM each NTP)	10 µl 10 mM each NTP final
Template DNA	0.5 µg of the purified PCR product
T7 RNA Polymerase Mix	2 µl
Total reaction volume	20 µl

The reaction was incubated for 2 hours at 37°C.

After two hours, a DNase treatment was carried out to remove the DNA template. 30 µl of nuclease-free water were added to the reaction followed by 4 units of DNase l (RNase-free), the reaction was incubated for 15 more minutes at 37°C.

2.10.3 *In vitro* capped RNA synthesis

3´-O-Me-m^{7}G(5')ppp(5')G RNA Cap Structure Analog, also known as Anti-Reverse Cap Analog (ARCA) (NEB) was used to *in vitro* synthesise the RNAs with a m^{7}G-cap and G(5')ppp(5')A RNA Cap Structure Analog (NEB) was used to *in vitro* synthesise the RNAs with an A-cap.

Primers used to insert the T7 promoter in pFBN, pFN, pBN and pN, required for the m^{7}G-capped RNAs:

NanoLuc R good: 5’-CTTATCATGTCTGCTCGAAGC-3’

T7-afterSV40 F: 5’-TAATACGACTCACTATAGGGGAAGTAGTGAGGAGGCTTT-3’

Primers used to insert the T7 phi2.5 promoter pFBN, pFN, pBN and pN, required for the A-capped RNAs:

T7Pphi2.5-afterSV40 F: 5’-TAATACGACTCACTATTAGGGAAGTAGTGAGGAGGCTTT-3’

NanoLuc R good: 5’-CTTATCATGTCTGCTCGAAGC-3’

Table 2.19 Capped RNA synthesis reaction assembly.

Nuclease-free water	X µl
NTP Buffer Mix (20 mM each NTP)	2 µl 2 mM each NTP final
Cap Analog (40 mM)	4 µl 8 mM final
Template DNA	0.5 µg of the purified PCR product
T7 RNA Polymerase Mix	2 µl
Total reaction volume	20 µl

The reaction was incubated for 2 hours at 37°C.

After two hours, a DNase treatment was carried out to remove the DNA template. 30 µl of nuclease-free water were added to the reaction followed by 4 units of DNase l (RNAse-free), the reaction was incubated for 15 more minutes at 37°C.

2.10.4 *In vitro* RNA Poly(A) tailing

E.coli Poly(A) Polymerase (NEB) was used to introduce a poly(A) tail in the *in vitro* transcribed RNA.

The following components were mixed:

Table 2.20 Poly(A) addition reaction master mix.

RNA	1-10 µg in 15 µl nuclease free water
10X *E.coli* Poly(A) Polymerase Reaction Buffer	2 µl (1X)
ATP (10 mM)	2 µl
E.coli Poly(A) Polymerase	1 µl
Total	20 µl

The reaction was incubated at 37°C for 30 minutes.

The reaction was stopped by proceeding directly to the clean-up step.

2.10.5 Purification of synthesised RNA by LiCl precipitation

LiCl precipitation of the RNA is an effective technique to remove the enzymes and most of the unincorporated NTPs from the reaction.

25 µl of LiCl solution (7.5 M LiCl, 10 mM EDTA) were added to each reaction tube. Reactions were incubated at -20°C for 30 minutes and then centrifuged at 4°C for 15 minutes at 13,000 rpm to pellet the RNA. Supernatant was removed and the pellet was rinsed with 500 µl of ice cold 70% ethanol. The RNA was resuspended in 50 µl of 0.1 mM EDTA. The RNA concentration was measured using the NanoDrop (see 2.1.1.11 on page 58). The RNA was stored at -20°C.

2.10.6 RNA agarose gel electrophoresis

Transcript length and integrity was evaluated on 0.8% agarose gels. 0.8 g of agarose were mixed with 100 ml of 1X TBE buffer. Agarose was melted in the microwave. Gel casting tray was assembled on a flat surface.

Agarose solution was cooled and 6 µl of Gel Red were added. Solution was mixed and poured into the tray, and comb was placed. Once the gel had set, comb and gel casting gates were removed and placed in a horizontal electrophoresis tank. The tank was filled with 1X TBE buffer.

0.2-1 µg or *in vitro* synthesised RNA were mixed with 2X RNA Loading Dye (NEB). Single strand RNA ladder (NEB) was used a ladder. 2 µl of the ladder were mixed with 1 µl of loading dye. RNA was denatured by heating it at 70°C for 10 minutes. The gel was run at 120 V for at least 45 minutes.

Gel was visualised using the image analysis system Syngene PXi or using a UV transilluminator.

***1X TBE Composition**:* 89 mM Tris, 89 mM boric acid, 2 mM EDTA.

2.11 TnT® QUICK COUPLED TRANSCRIPTION/TRANSLATION SYSTEMS

TnT® Quick Coupled Transcription/Translation Systems (Promega) was used to study IRES activity *in vitro*. The T7 pFBN, pFN, pBN, pN and pGL4.13SV40 DNA templates were prepared as in section 2.10.1 on page 72. The TnT reactions were carried out following manufacturer's instructions:

Table 2.21 TnT reaction master mix for the T7 DNA samples.

TnT® T7 Quick Master Mix	40 µl
Methionine (1mM)	1 µl
PCR-generated DNA template	4 µl
T7 TnT® PCR Enhancer	1 µl
Nuclease-Free Water	4 µl
Final volume	50 µl

The kit contains a Luciferase control plasmid, to verify that the transcription and translation work correctly:

Table 2.22 TnT reaction master mix for the luciferase control.

TnT® T7 Quick Master Mix	40 µl
Methionine (1 mM)	1 µl
Luciferase Control DNA (0.5 µg/µl)	2 µl
Nuclease-Free Water	7 µl
Final volume	50 µl

Reactions were incubate at 30°C for 90 minutes.

Fluc and Nluc activities were measured doing a Nano-Glo® Dual-Luciferase® Reporter Assay. The TnT reactions were diluted 1:100 in PBS and the Fluc and Nluc activities were measured as explained in section 2.3 on page 62.

2.12 *IN VITRO* TRANSLATION-RETIC LYSATE IVT™ KIT

To study the translation rates of the synthesised RNA, we used the RETIC LYSATE IVT™ KIT (Invitrogen™). This kit has been optimised to generate high level of proteins from both capped and uncapped mRNAs. The Rabbit Reticulocyte Lysate (RRL) is prepared from reticulocytes isolated from rabbits treated with acetylphenylhydrazine, the isolation process results in a system that can translate mRNA in a very active way. The endogenous mRNA present in the reticulocytes is degraded with micrococcal nuclease.

In vitro transcribed uncapped RNA was prepared as explained in section 2.10.2 page 73, capped RNA as explained in section 2.10.3 on page 74 and a poly(A) tail was added when required as

explained in section 2.10.4 on page 75. *In vitro* generated RNAs were purified by LiCl precipitation as explained in section 2.10.5 on page 75 before programming the RRL. The following amounts of the indicated reagents were added per RRL reaction:

Table 2.23 RRL reaction mix.

	Just RNA	RNA & oligonucleotide
20X Translation Mix – met	0.136 µl	0.136 µl
20X Translation Mix – leu	0.136 µl	0.136 µl
Retic Lysate	3.7 µl	3.7 µl
RNA template (500 ng/µl)	1 µl	1 µl
Oligonucleotide (10 µM)	-	0.53 µl
Final volume	5.45 µl	

Reactions were incubated at 30°C for 90 minutes, 2.5 µl of RNase A (1 mg/ml) were added to the reaction and this was incubated for 10 minutes at 30°C. Samples were placed on ice for 5 minutes to stop the reaction.

Fluc and Nluc activities were measured doing a Nano-Glo® Dual-Luciferase® Reporter Assay. The RRL reactions were diluted 1:50 in PBS and the Fluc and Nluc activities were measured as explained in section 2.3 on page 62.

2.13 RNA TRANSFECTION IN HEK293 CELLS

On day 1, 3000 HEK293 cells were seeded in a 96 well plate. The following day transfections were done. 150 ng of RNA were transfected per well using Lipofectamine 2000 (Thermo Fisher Scientific). 150 ng of RNA were mixed with 10 µl of serum free DMEM in a tube. In another tube 0.3 µl of Lipofectamine 2000 were mixed with 10 µl of serum free DMEM (this was done as a master mix for all the reactions required). The contents in both tubes were mixed, incubated for 5 minutes at room temperature and added to the cells.

Translation levels of the RNA were measured 6 and 24 hours after transfection by a luciferase assay as explained in section 2.3 on page 62.

2.14 RNA AND OLIGONUCLEOTIDE TRANSFECTION IN CELLS

For this experiment *in vitro* transcribed FBN RNA was used, with an m^7G-cap and a poly(A), the RNA was synthesised as explained in section 2.10. On day 1, 5 000 CAL51 cells were plated out in a 96 well plate. The following day transfections were done. In each 96 well plate 150 ng of FBN RNA were transfected with a final concentration of 1 µM of oligonucleotide (0.159 µl of a 10 µM oligonucleotide). Before the transfection, the RNA and oligonucleotide were mixed and incubated at 37°C for 10 minutes. The RNA and oligonucleotide mixture were mixed with 10 µl of serum free DMEM. In a different tube, 10 µl of serum free DMEM were mixed with 0.3 µl of Lipofectamine 2000 (Thermo Fisher Scientific). Both tubes were mixed, incubated at room temperature for 5 minutes and added to the cells.

2.15 SOFTWARE USE

For the analysis of the sequencing results and the genetic engineering experiments, the software Serial Cloner (version 2.6.1) and pDraw32 (version 1.1.141) were used.

For the analysis of the luciferase assays GloMax®-Multi+ Detection System with Instinct™ Software was used.

The western blot analysis were carried out using Licor Image Studio (version 5.2) software.

The analysis of the agarose gels was done using GeneSys software.

The analysis of the qPCR results was done using the software Eco Study (version 5.0).

The statistical analysis was done using GraphPad Prism 8.

Chapter 3 VERIFICATION OF THE PRESENCE OF AN IRES IN *BAG1*

3.1 INTRODUCTION

The first aim of the project was to verify the presence of an IRES in *BAG1.* Coldwell *et al.*[144] showed in 2001 the existence of an IRES in the *BAG1* mRNA, that encourages the translation of the p36 isoform. However, since then, the existence of cellular IRESs has been questioned multiple times and new assays have been developed to show their existence more definitively. In this chapter we have used these different experiments to verify the presence of an IRES in *BAG1*.

One of the main reasons why the existence of cellular IRESs has been questioned was due to the difficulty in generating a method to determine the unequivocal presence of an IRES in a eukaryotic mRNA. The first step when it comes to determine if certain mRNA has an IRES is the study of the 5' UTR: long and highly structured 5' UTRs are common in mRNAs with IRES elements. Then, internal initiation, independent from 5' cap-mediated initiation, should we assessed.

The most common technique to study IRES-dependent translation is *via* a dual luciferase reporter assay system. Many studies related to the IRES activity have been published using a bicistronic vector containing Firefly luciferase (Fluc) and *Renilla* (*Renilla reniformis* or sea pansy), commonly referred to as pRF, from the Willis laboratory[82,95,144,257]. A bicistronic vector has both reporter genes transcribed on the same RNA, with at least one stop codon at the end of the first cistron, which will be translated by the usual cap-dependent mechanism. The suspected IRES sequence is inserted between the cistrons (Figure 3.1). If the downstream cistron has increased expression relative to the upstream cistron, it is assumed that an IRES is present, although further experiments are necessary to definitively prove this. The explanation to this is based in the fact that when in the same mRNA there are two ORFs, the efficiency of the eukaryotic ribosomes to reinitiate translation of the downstream ORF is smaller unless an IRES is present between the two ORFs[79]. We will also use a bicistronic luciferase assay as the first step to determine the presence of an IRES in *BAG1*.

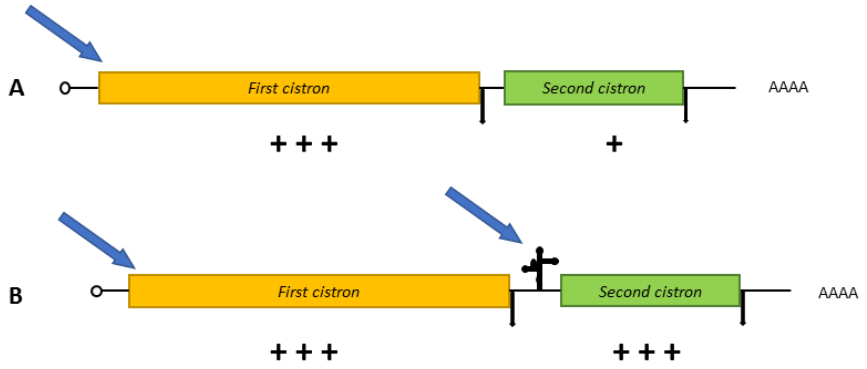

Figure 3.1 **The bicistronic assay system. A)** In the bicistronic vector system, the first cistron will be translated. Due to the presence of a stop codon at the end of the first cistron's sequence, the second cistron will only be translated by a small number of ribosomes by read through reinitiation. **B)** In the presence of an IRES between both cistrons, an increase in the second cistron's expression can be observed.

More recently, the reporter gene Nanoluc (Nluc) has been developed from the shrimp *Oplophorus gracilirostris.* Nanoluc® Luciferase is a small enzyme (19 kDa), and in the presence of the substrate furimazine, light is produced. This bioluminescent capability of Nluc is very useful for dual reporter assays, as it provides clear and quantitative signal, and a low level of background signal. The half-life of the luminescence signal of Nluc is greater than two hours and the activity of Nluc is 150-fold greater than that of either *Renilla* or Fluc luciferases[258]. Therefore we wished to determine if Nluc could be employed in assaying IRES activity.

Furthermore, the luciferases used in pRF correspond to the respective wild type cDNAs from *Renilla reniformis* and *Photinus pyralis*, but since then, Promega has codon-optimised these for mammalian expression and also to remove potential cryptic promoters, creating hRluc and luc2 for *Renilla* and Fluc respectively. The vector used for the generation of the rest of the vectors was pGL4.13 [luc2/SV40] (Promega), see Figure 3.2. This vector was designed to have a high expression and was optimised for mammalian expression. It encoded the luciferase reporter gene luc2 (*Photinus pyralis*) and contained the SV40 early enhancer/promoter. The qualities of the vector made it ideal to be used as an expression control or a co-reporter vector[259].

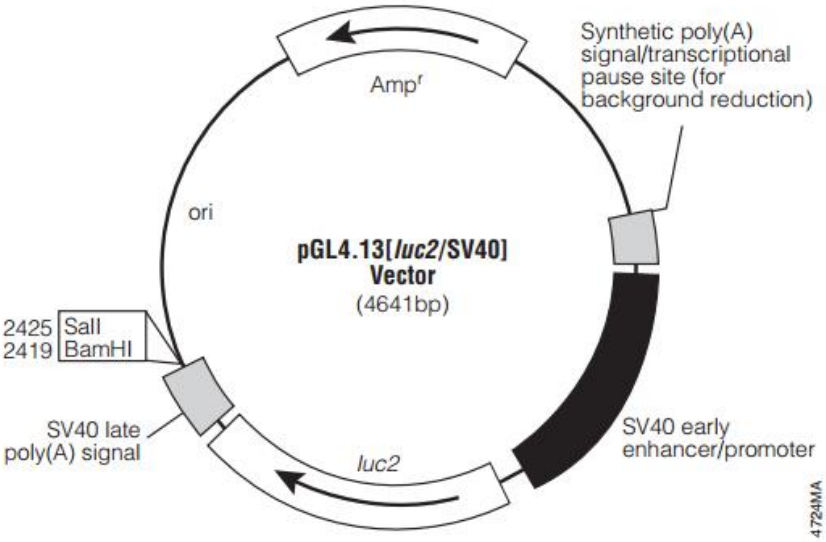

Figure 3.2 **Representation of the pGL4.13SV40 vector**.

pGL4.13 [luc2/SV40] was modified to generate all the constructs needed for the purposes of the project.

When working with bicistronic assays different problems could be found that would produce misleading results. If a silent or inactive promoter sequence (a cryptic promoter) was inserted between both cistrons or a potential splice site was present between both cistrons, the reporter activity of the second cistron would be activated. In this case, instead of measuring the activity of a bicistronic plasmid, the activity of two independent monocistronic mRNAs would be measured (as illustrated in Figure 1.10 on page 26). That is why a positive bicistronic assay is not evidence enough to argue that a certain mRNA has an IRES. To check for the presence of cryptic promoters promoterless plasmids should be constructed and tested in cells. A strong hairpin could also be used to inhibit or at least strongly reduce cap-mediated translation. *In vitro* synthesised RNA could also be transfected in cells and study its effect.

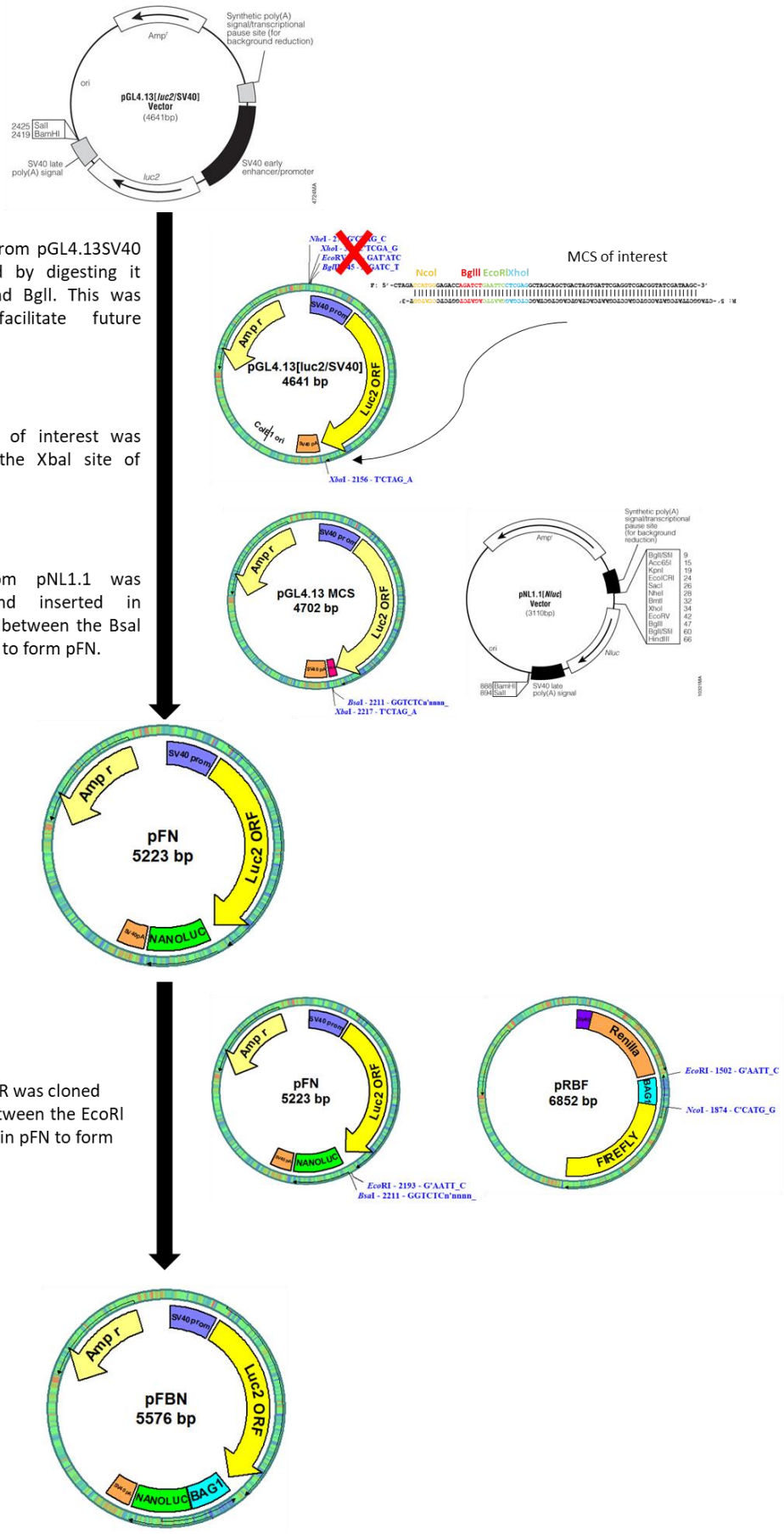

Figure 3.3 **Diagram of the cloning process to construct the bicistronic plasmids.** Each of the steps will be fully explained in the next sections.

3.2 BICISTRONIC PLASMID CONSTRUCTION

3.2.1 Modifications of the pGL4.13SV40 vector:

As previously mentioned the plasmid pGL4.13SV40 (Figure 3.2) was used to determine the presence of an IRES in *BAG1*. To this plasmid containing Fluc, Nluc and the *BAG1* 5' UTR needed to be inserted (this will be explained in detail) (see Figure 3.3). The plasmid was originally designed with the multiple cloning site (MCS) upstream of the Fluc open reading frame (ORF). However, for the purpose of our experiments, we had to eliminate that MCS and introduce a different MCS downstream of the Fluc ORF before cloning in the Nluc ORF and *BAG1* 5' UTR.

3.2.1.1 Deletion of the MCS, making pGL4.13SV40 no MCS

The first modification done to the vector was the removal of the multiple cloning (MCS) site flanked by NheI and BglII (NheI-XhoI-EcoRV-BglII) between positions 27 and 45 (Figure 3.4). The removal of all those restriction sites from that area was required to facilitate future cloning experiments downstream the Fluc ORF that would require the presence of the restriction sites present in that MCS.

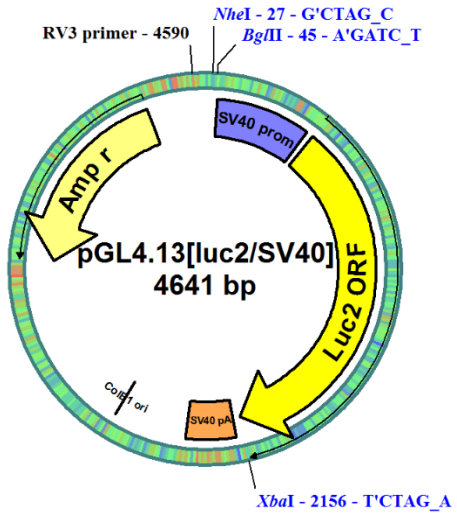

Figure 3.4 **Representation of the pGL4.13SV40 vector**. The NheI and BglII restriction sites are also represented, showing the localization of the removed MCS. RV3 primer was used for sequencing. XbaI was used to check the minipreps for the correct removal of the MCS.

The vector was digested with NheI and BglII, a Klenow fill in reaction was done and it was religated. One of the minipreps was picked and sent for sequencing, RVprimer3 was used for the sequencing (check for primer sequence in section 2.7 on page 67). The sequencing results showed that the deletion was successful.

The pGL4.13SV40 without that MCS will be called pGL4.13SV40 no MCS.

3.2.1.2 Introduction of the desired MCS

We introduced a multiple cloning site of interest in pGL4.13SV40 no MCS straight after the Fluc ORF. This multiple cloning site would be used to allow convenient introduction of selected sequences in a future. Two oligonucleotides were designed to clone them in the Xbal restriction site (after the Fluc ORF) of pGL4.13SV40 no MCS, to create a new MCS (Figure 3.5).

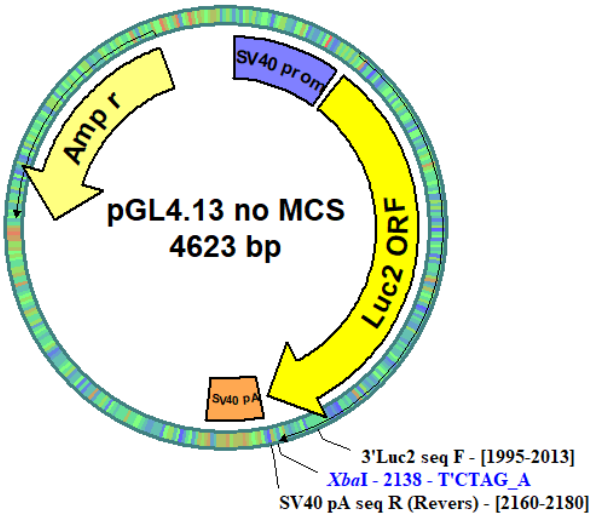

Figure 3.5 **Illustration of the pGL4.13 no MCS.** The restriction site Xbal shows the place where the MCS was introduced. 3'Luc2seqF and SV40-pA seqR primers were used for the sequencing.

The oligonucleotides were designed to contain restriction sites for multiple restriction enzymes that would be useful for future cloning experiments as Ncol, Bglll, EcoRl and Xhol (Table 3.1).

Table 3.1 Oligonucleotides used for the construction of the MCS of interest.

F	5'CTAGACCATGGGAGACCAGATCTGAATTCCTCGAGGCTAGCAGCTGACTAGTGATTCGAGGTCGACGGTATCGATAAGC3' NcoI BglII EcoRI XhoI
R	5' CTAGGCTTATCGATACCGTCGACCTCGAATCACTAGTCAGCTGCTAGCCTCGAGGAATTCAGATCT GGTCTCCCATGG T 3' XhoI EcoRI BglII NcoI

The oligonucleotides were annealed following the protocol in section 2.1.1.4 on page 54 and phosphorylated using PNK as explained in section 2.1.1.5 on page 55.

pGL4.13 no MCS was digested with Xbal and treated with phosphatase as explained in section 2.1.1.3 on page 54. The digested vector was cleaned-up as described in section 2.1.1.14 on page 59.

The Xbal digested pGL4.13 no MCS vector and the annealed phosphorylated oligonucleotides were ligated overnight at 4°C as explained in 2.1.1.6 on page 55.

The sequencing results (using the primers 3'Luc2 seq F and SV40 pA seq R, (check for primer sequence in section 2.7 on page 67)) suggested that the construct generated had the insert in the correct orientation, and so this was renamed as pGL4.13SV40 MCS.

3.2.2 Construction of pFN

At this point the plasmid pGL4.13SV40 was ready to create the bicistronic plasmid pFN containing both Fluc and Nluc reporter genes. The next step was to clone the Nluc ORF in the pGL4.13SV40 MCS vector, from the vector pNL1.1 [Nluc] (Promega) (Figure 3.6, B).

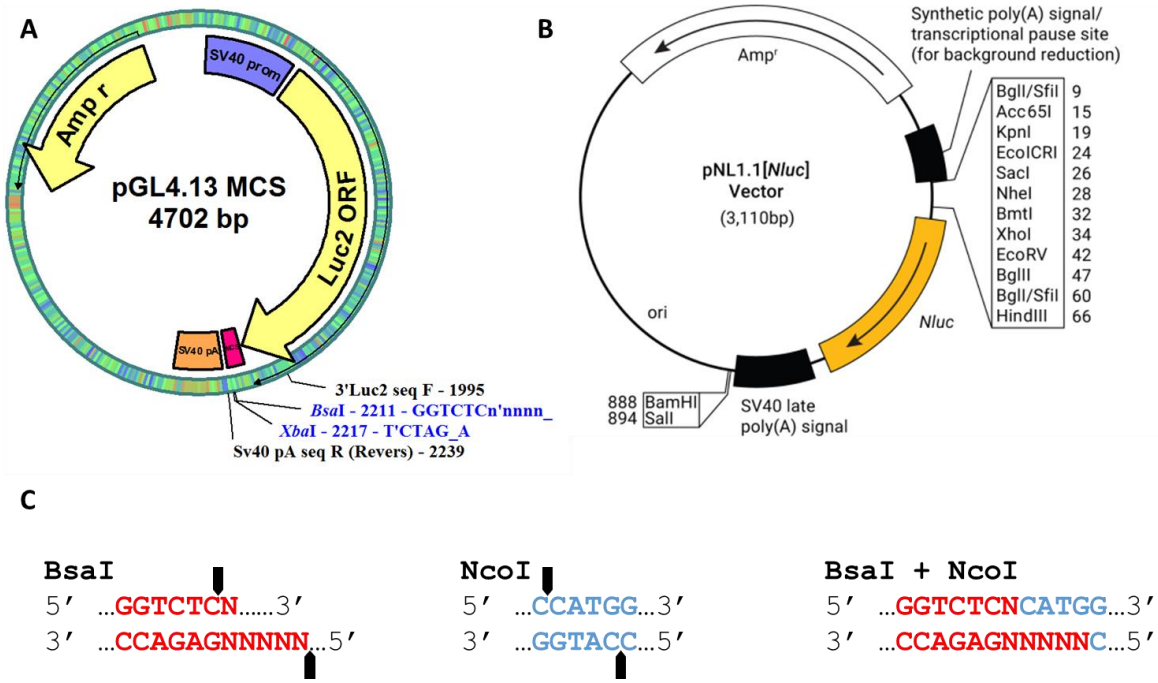

Figure 3.6 **A) Illustration of the pGL4.13SV40 MCS.** The restriction sites BsaI and XbaI were marked to show where the Nluc was inserted. The vectors used to send pFN sequencing were also marked. **B) Illustration of pNL1.1.** Nluc was excised from the vector pNL1.1 and introduced in pGL4.13SV40 MCS. **C) Restriction map of BsaI and NcoI and the consensus sequence after the ligation.**

pGL4.13SV40 MCS was digested with BsaI and XbaI. The restriction enzyme BsaI is a type IIS restriction enzyme, which digests the DNA outside its recognition points (see Figure 3.6, C). This would open the vector and allow the further ligation of the Nluc insert. The Nluc vector was digested with NcoI and XbaI, this would separate the Nluc sequence from the rest of the vector. The sticky ends created by the digests were compatible (see Figure 3.6, C) and so following ligation and transformation, the miniprepped DNA was digested with XbaI and BsaI.

Successful subcloning was found for all the minipreps by agarose gel electrophoresis and thereby one of the minipreps was sent for sequencing using the primers 3'Luc2 seq F and SV40 pA seq R

(see primer sequences in section 2.7 page 67), and the results showed the successful insertion of the Nluc in the vector.

Therefore the pGL4.13SV40 MCS vector with the Nluc was called pFN, meaning that our novel bicistronic vector had been constructed, with the Fluc and Nluc reporter genes on it.

3.2.3 pFBN: insertion of *BAG1* 5' UTR in pFN

The next step was to introduce a region of cDNA encoding the *BAG1* 5' UTR between the two promoter genes in the pFN vector, and this was obtained from the vector pRBF[144].

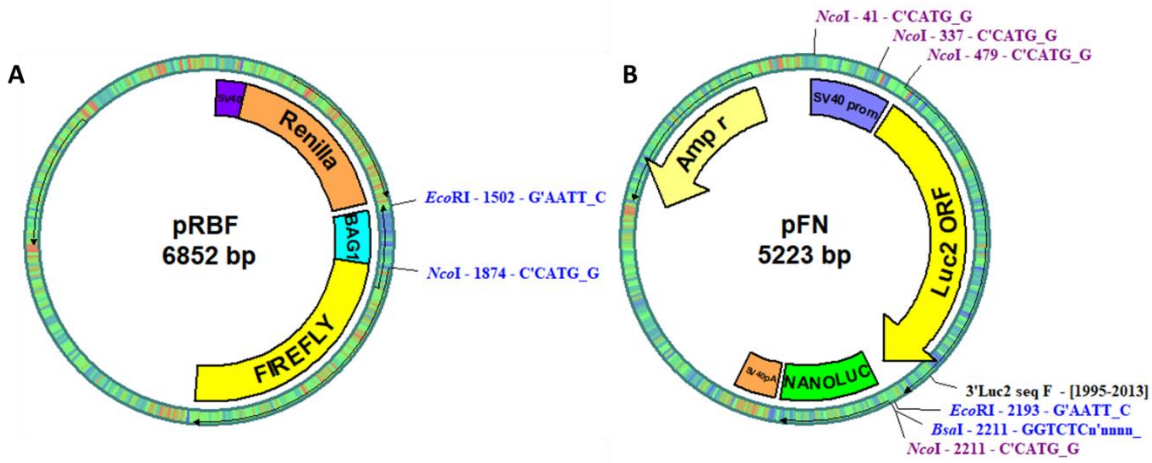

Figure 3.7 **A) Illustration of the pRBF vector.** pRBF was digested with EcoRl and Ncol to extract the *BAG1* 5' UTR. **B) Illustration of pFN.** The restriction sites EcoRl and Bsal were marked to show where the *BAG1* 5' UTR sequence was inserted. The Ncol restriction sites were also marked as they were used to check the minipreps.

pRBF was digested with Ncol and EcoRl to separate the full *BAG1* 5' UTR sequence from the rest of the vector. pFN was digested with Bsal and EcoRl to open the vector between the two reporter genes and to allow the insertion of the *BAG1* 5' UTR. See Figure 3.7.

The sticky ends created by the digests were compatible and so following ligation and transformation, the miniprepped DNA was digested with EcoRl and Ncol to check for the successful introduction of the *BAG1* 5' UTR in the pFN vector.

Restriction digests of plasmids extracted observed that the *BAG1* 5' UTR was successfully inserted in all the minipreps tested. One of the minipreps was sent for sequencing, using the primer 3'Luc2 seq F. The sequencing results confirmed that the 5' UTR *BAG1* DNA was successfully introduced in the pFN vector. Sequencing results can be seen in Appendix C. The new vector was named pFBN.

At this point the main vector was made, with the *BAG1* 5' UTR containing the IRES cloned between the two reporter genes Fluc and Nluc, with the p36 AUG initiation codon positioned as the AUG initiation codon of the Nluc ORF.

3.3 BICISTRONIC VECTOR TRANSFECTION-LUCIFERASE ASSAY

The constructed bicistronic plasmids (pFN and pFBN) were transfected in cells to study their activity. In these experiments HeLa cells were transfected with the different vectors using GeneJuice (GJ) as explained in section 2.2.3 on page 60. A luciferase assay was carried out 48 hours post transfection, where the Fluc activity was measured first, followed by the activity of Nluc (see section 2.3 on page 62 for more detail). The transfections were done in triplicate. Luminescence was measured in Relative Light Units (RLUs).

In this bicistronic assay, the upstream cistron (Fluc) in pFBN indicated cap-dependent translation and the downstream cistron (Nluc) measured the IRES activity (see Figure 3.8).

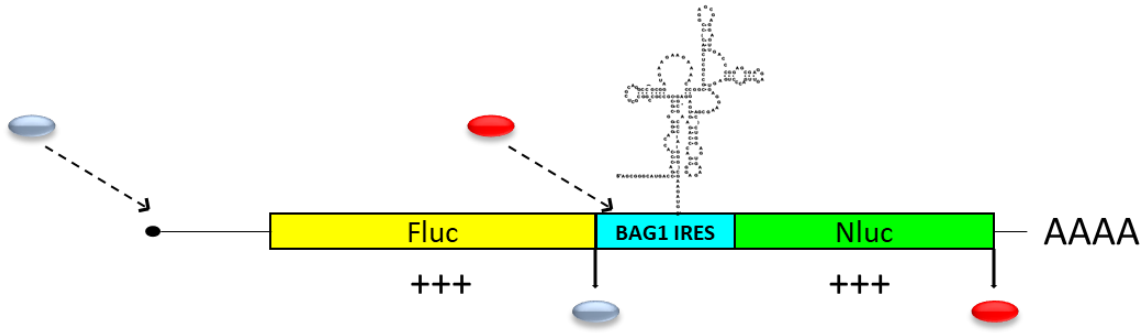

Figure 3.8 **FBN translation representation.** Fluc was translated *via* cap-mediated translation (see grey 40S ribosomal subunit), whereas Nluc was translated *via* IRES-mediated translation (see red 40S ribosomal subunit).

3.3.1 The presence of the *BAG1* 5' UTR decreases the Fluc expression and increases the Nluc expression

In white 96 well plates 2 000 HeLa cells per well were seeded and the following day 20 ng of plasmid were transfected. Luciferase assays were carried out 48 hours after the transfection. pFN and pFBN were transfected in HeLa cells under the same conditions on five different occasions (each of them in triplicate), the results in Figure 3.9 A show the average raw RLU values of the five independent experiments. At this point, the results were not normalised to account for transfection efficiency or transcription levels. Cells were seeded in white 96 well plates, which made impossible to monitor the cells. The objective of the experiment was to measure how the

presence of the *BAG1* 5' UTR, which is supposed to contain an IRES, in pFBN could modify the expression of both Fluc and Nluc.

When comparing the Fluc activity in cells transfected with pFN and pFBN it could be observed that the presence of the *BAG1* 5' UTR significantly decreased the Fluc activity over four times (Figure 3.9, A). This could be due to the complicated structure sequence of the *BAG1* 5' UTR making it difficult for the ribosome to bind the mRNA. It is known that adding a structure between the cistrons can disrupt the expression of the upstream one, and this had been observed in the equivalent pRF vectors when either *BAG1* or *APAF1* 5' UTRs were inserted between the *Renilla* and Fluc cistrons[144,173]. In the case of the Nluc activity (Figure 3.9, A), the presence of the *BAG1* 5' UTR slightly increased the activity of Nluc in a 70%. This must be related to the presence of the *BAG1* 5' UTR and the IRES that has been proved to be located there. The effect of the *BAG1* 5'UTR was bigger in the Fluc activity than in the Nluc activity.

On a second data analysis, Nluc to Fluc ratios were calculated (Figure 3.9, B). The average of the Nluc to Fluc ratio obtained in all the experiments was calculated for both pFN and pFBN and the results were compared.

The presence of the *BAG1* 5' UTR significantly increased the Nluc to Fluc ratio more than seven times, as can be seen in Figure 3.9, B. These results suggest that the higher Nluc emission obtained in pFBN was due to something present in the 5' UTR, possible the IRES. Another possibility could be that after termination, some ribosomes could reinitiate downstream if there is plenty of ternary complex and enough sequence between the cistrons; in this case, the presence of the *BAG1* 5' UTR would provide this necessary extra sequence. It cannot be ignored that the increase in the Nluc to Fluc ratio in pFBN is also due to both the increase of the Nluc expression and the decrease of the Fluc expression, as shown in Figure 3.9, A. In fact, the decrease in the Fluc activity was stronger than the increase in the Nluc activity.

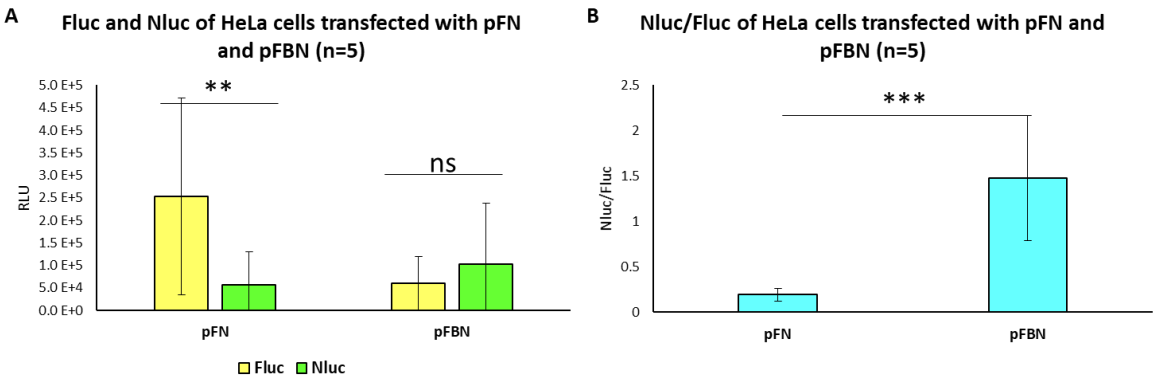

Figure 3.9 **Luciferase assay results of HeLa cells transfected with pFN and pFBN.** A) Comparison of the Fluc and Nluc activity in HeLa cells transfected with pFN and pFBN. Transfections were done five times, each transfection was done in triplicate. B) Measurement of the Nluc to Fluc ratio in HeLa cells transfected with pFN and with pFBN. pFBN showed a higher Nluc to Fluc ratio than pFN. Error bars show the standard deviation. Statistical analysis done with an unpaired t-test (two-tailed). ($P<0.05$)

When pFN is transfected, only translation of Fluc should be observed. This is due to the presence of three stop codons at the end of the Fluc ORF. Even so, there are a few situations where Nluc could be translated at low levels. One possibility is that ribosomes did not terminate translation at the stop codon after the Fluc and, as the Fluc and Nluc are in frame, kept translating the Nluc sequence *via* ribosomal read-through. Ribosomal read-through takes place when the ribosomes do not recognize the stop codons and translation continues. It is known that not all stop codons have the same efficiency to end the process of translation[260] and that different factors such as the expression levels of the genes[261] could affect the read-through ability. Another possibility could be the presence of cryptic promoters upstream of the Nluc sequence. It also needs to be kept in mind that raw RLU values can vary hugely depending on the freshness and temperature of reagents and the ambient light levels (observations by members of the laboratory). It also needs to be acknowledged that there is always an RLU signal in untransfected cells (significantly smaller than the one found in transfected cells), which suggests some inherent instability of the furimazine substrate. Moreover, it cannot be forgotten that the furimazine substrate was specifically developed to be brighter than luciferin substrates of Fluc.

The fact that pFN showed Nluc signals (Figure 3.9) suggested the presence of a cryptic promoter in the Fluc sequence, although as many of these as possible had supposedly been engineered out during the development of the pGL4 vectors[262]. In the case of pFN, the reads for Fluc were over four times higher than the reads for Nluc. This suggested that the cryptic promoter enabling the expression of Nluc was weak.

To check if the Nluc signal in pFN was due to the presence of a cryptic promoter, pFN no SV40 was constructed, as well as pFBN no SV40. The removal of the SV40 promoter should inhibit the expression of both Fluc and Nluc. After the removal of the SV40 promoter, transcription of the RNA cannot start, making it impossible to translate the protein. Only in the presence of cryptic promoters Nluc would be expressed.

3.4 PROMOTERLESS AND MONOCISTRONIC VECTORS

3.4.1 Removal of the SV40 promoter from pFN and pFBN

It is known that when cells are transfected with a bicistronic vector, aberrant RNA cleavage or RNA splicing can occur. There is also the possibility of the appearance of cryptic promoters. This could lead to the formation of monocistronic transcripts that could be translated independently to the IRES[111] (see Figure 1.10 on page 26).

In order to ensure that the increased expression of the downstream cistron (Nluc) is due to the activity of the IRES and not due to the presence of cryptic promoters upstream of the Nluc sequence, the SV40 promoter was removed from pFN and pFBN. The removal of the SV40 promoter, in the absence of cryptic promoters, would decrease to a minimum the luminescence emitted by both Fluc and Nluc.

pFN and pFBN were digested with SacI and HindIII (see Figure 3.10). The digested vectors were run in an agarose gel, the band corresponding to the vectors without the SV40 promoter (over 5000 bp) was excised from the gel and DNA was extracted. A Klenow fill in reaction was carried out. pFN without the SV40 and pFBN without the SV40 were religated.

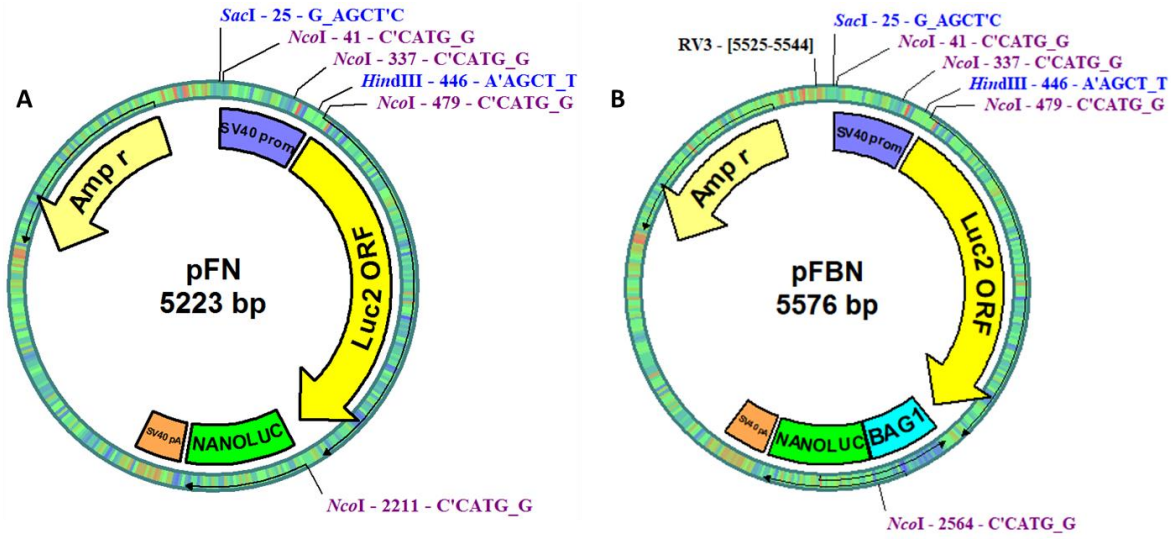

Figure 3.10 **Illustration of pFN (A) and pFBN (B).** The vectors were digested with SacI and HindIII to remove the SV40 promoter. NcoI was used to check the subsequent minipreps.

The minipreps were checked for the correct removal of the SV40 promoter by digesting them with Ncol. There were two Ncol restriction sites in the SV40 promoter and another in the vector. The cloning worked in all the checked minipreps.

One miniprep for pFBN no SV40 and another one for pFN no SV40 were sent for sequencing. RV3 primer was used for sequencing (see primer sequence in section 2.7 on page 67). The sequencing results confirmed the removal of the SV40 promoter.

3.4.2 Construction of pN, pBN, pN no SV40 and pBN no SV40

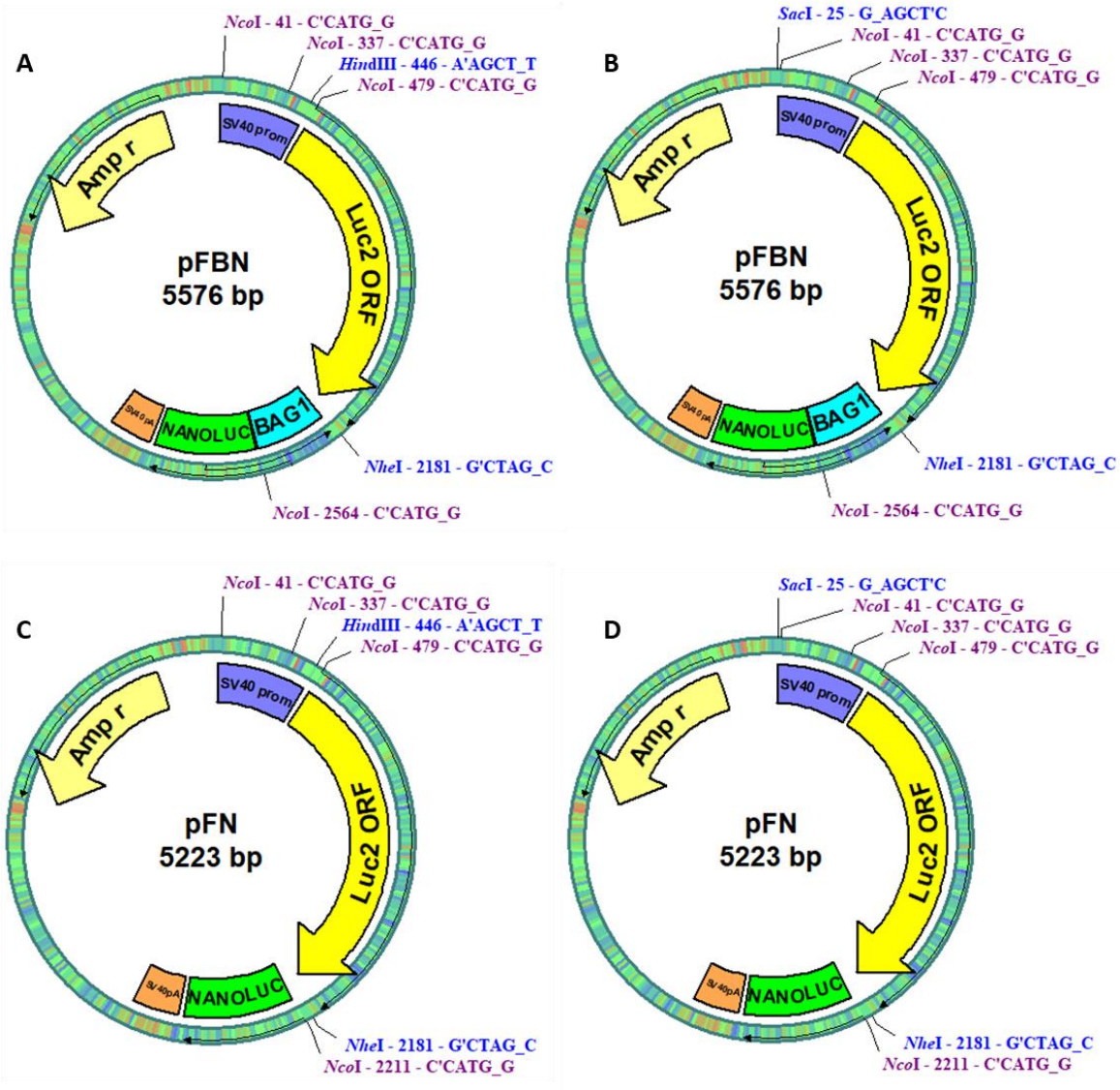

Figure 3.11 **pFBN and pFN with the restriction sites used to make pFBN no SV40, pFN no SV40, pBN and pN marked.**

As well as doing the experiments with bicistronic vectors, monocistronic vectors based on the bicistronic vectors were made. This approach would solve the problems related to the bicistronic vectors mentioned before, as the presence of cryptic promoters and ribosome reinitiation.

Besides, the expression of monocistronic vectors is more effective than the expression of the bicistronic vectors.

The original pGL4.13SV40 with the Fluc reporter gene integrated would be used as a co-transfection control, and our intent was to create monocistronic vectors containing the Nluc reporter. Therefore, the Fluc sequence was removed from all the vectors constructed (pFN, pFBN, pFN no SV40 and pFBN no SV40): pFBN and pFN were digested with HindIII and NheI to get pBN and pN, whereas pFBN and pFN were digested with SacI and NheI to get pBN no SV40 and pN no SV40 (Figure 3.11). A fill in reaction was done in both vectors. The digested samples were run in an agarose gel, and the bands corresponding to pBN, pN, pBN no SV40 and pN no SV40 were excised from the gel. DNA was extracted from the gel and vectors were religated. Minipreps showed the expected band pattern after digestion with NcoI.

3.4.3 No SV40 promoter plasmid analysis in cells

In clear 96 well plates, 2 000 HeLa cells were seeded per well, the following day 20 ng of plasmid were transfected per well. The new constructs were transfected in HeLa cells, and 48 hours after transfection a luciferase assay was done. The experiment was done three individual times in triplicate.

In the case of cells transfected with the bicistronic constructs, both Fluc and Nluc activities were undetectable in the promoterless constructs when compared to their SV40 analogues (Figure 3.12, A). Cells transfected with pFN no SV40 and pFBN no SV40 did not give any Fluc signal, as expected but both of them gave some Nluc signal (Figure 3.12, A and B). Cells transfected with pFBN no SV40 showed almost double the Nluc expression than cells transfected with pFN no SV40 (Figure 3.12, B). This could be explained with different hypothesis. One of them would be the presence of more than one cryptic promoters, one of them being within the *BAG1* 5' UTR sequence. This promoter would be absent in pFN no SV40. The other hypothesis would be that there is a cryptic promoter located upstream of the *BAG1* 5' UTR sequence, which would generate a monocistronic mRNA including the *BAG1* 5' UTR and therefore, any structure present in that UTR (an IRES, for example) could alter the Nluc expression in cells transfected with pFBN no SV40.

The fact that the Nluc expression of cells transfected with pFN no SV40 and pFBN no SV40 were over ten times smaller compared to the Nluc expression of cells transfected with pFN and pFBN (Figure 3.12, C and D) suggested that the cryptic promoters present were weak.

The fact that in the absence of the *BAG1* 5' UTR (in cells transfected with pFN and in pFN no SV40) there was also a signal for Nluc suggested the presence of a promoter in the Fluc sequence and

not in the *BAG1* sequence. To check if the promoter could be present in the Fluc sequence, pN no SV40 and pBN no SV40 were constructed.

In the case of the monocistronic constructs, the Nluc activity of the cells transfected with promoterless constructs was undetectable when compared to cells transfected with their SV40 analogues (Figure 3.13, A). In cells transfected with pN no SV40 and pBN no SV40, no Fluc signal was detected, as expected, but Nluc signal was detected in both cases (Figure 3.13, B). The Nluc signal emitted by cells transfected with pBN no SV40 was over seven times stronger than the one emitted by cells transfected with pN no SV40. These results suggested the presence of a cryptic promoter within the *BAG1* 5' UTR sequence. The fact that cells transfected with pBN no SV40 showed a higher Nluc expression could indicate that the cryptic promoter is located upstream the *BAG1* 5' UTR sequence. If the cryptic promoter was located upstream the 5' UTR, the UTR would be transcribed and any structure present there (an IRES for example) could modify the expression of the Nluc.

When compared the Nluc activity of cells transfected with pN no SV40 and pBN no SV40 to cells transfected with pBN (Figure 3.13, C and D), the Nluc signal of the cells transfected with the promoterless plasmids was undetectable. This suggested that the putative cryptic promoters were weak.

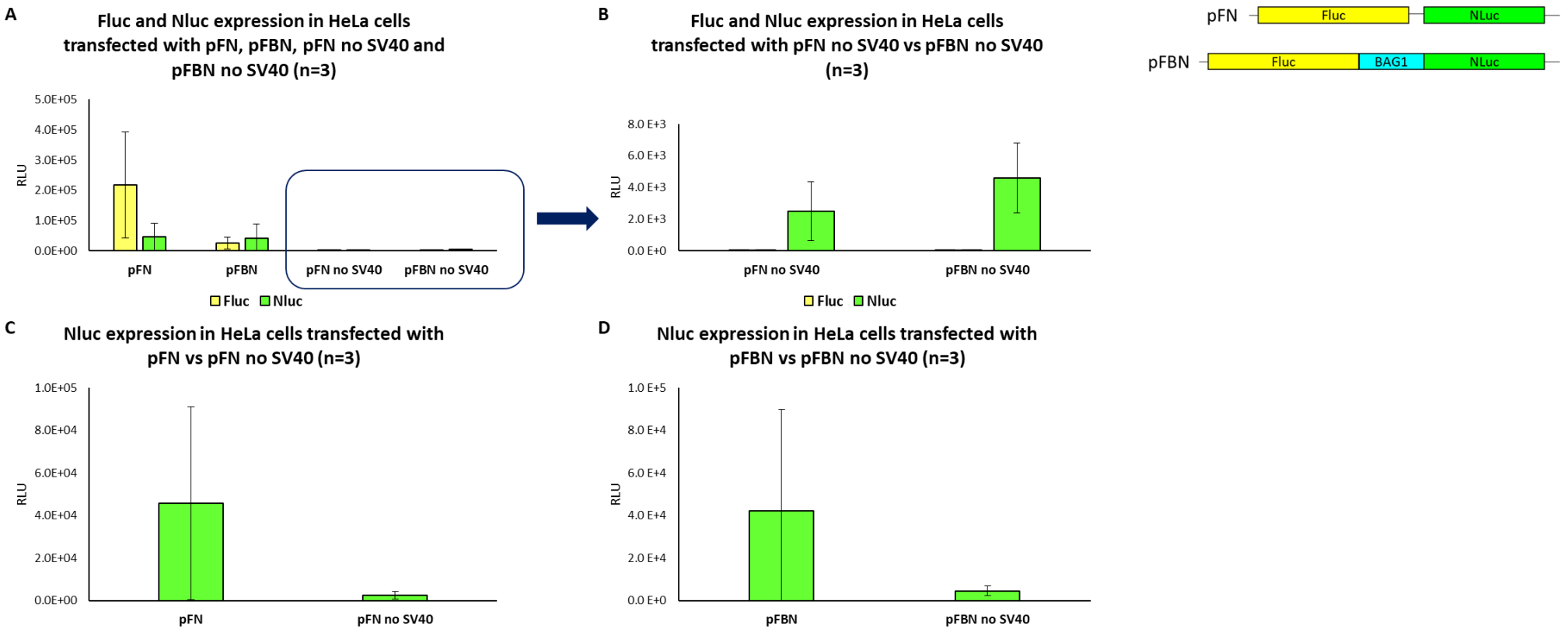

Figure 3.12 **Luciferase assay results of HeLa cells transfected with pFN, pFBN, pFN no SV40 and pFBN no SV40.** A) Fluc and Nluc expression in HeLa cells transfected with pFN, pFBN, pFN no SV40 and pFBN no SV40. B) Fluc and Nluc expression in HeLa cells transfected with pFN no SV40 vs pFBN no SV40. C) Nluc expression in HeLa cells transfected pFN vs pFN no SV40. D) Nluc expression pFBN vs pFBN no SV40. Error bars represent standard deviation values.

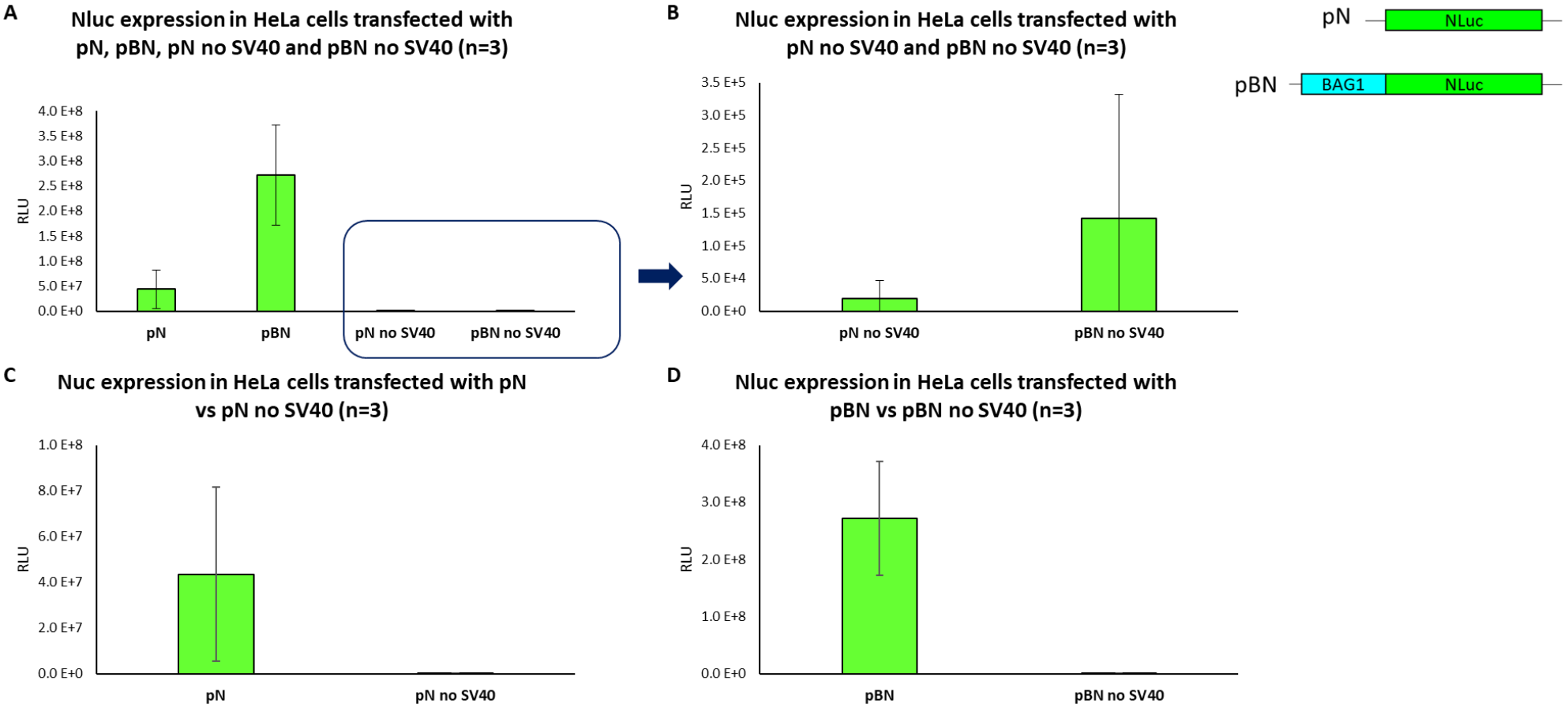

Figure 3.13 **A) Nluc expression in HeLa cells transfected with pN, pBN, pN no SV40 and pBN no SV40**. **B) Nluc expression pN no SV40 and pBN no SV40. C) Nluc expression in HeLa cells transfected with pN and pN no SV40. D) Nluc expression in HeLa cells transfected with pBN and pBN no SV40.** Error bars represent standard deviation values.

3.5 COMPARISON OF Fluc AND Nluc ACTIVITY

At this point we had pGL4.13SV40 expressing Fluc and pN (which came from the removal el Fluc in pGL4.13SV40 and the introduction of Nluc in its place), which allowed us to study the activity of both Fluc and Nluc. In 96 well plates 2000 HEK293 cells were seeded and the following day 20 ng of each plasmid were transfected. Fluc and Nluc activities were measured 2 days after transfection. Transfections were done once in triplicate.

As it can be seen in Figure 3.14, in the case of pGL4.13SV40 transfection, only the activity of Fluc could be measured and in the case of pN only Nluc's. These results show that the Nano-Glo® Dual-Luciferase® Reporter Assay System is specific for the reporter genes of interest and that there is no cross-contamination between them. The results also show that Nluc is around 37 fold brighter than Fluc, these results are in the limits to the ones already published[258,263].

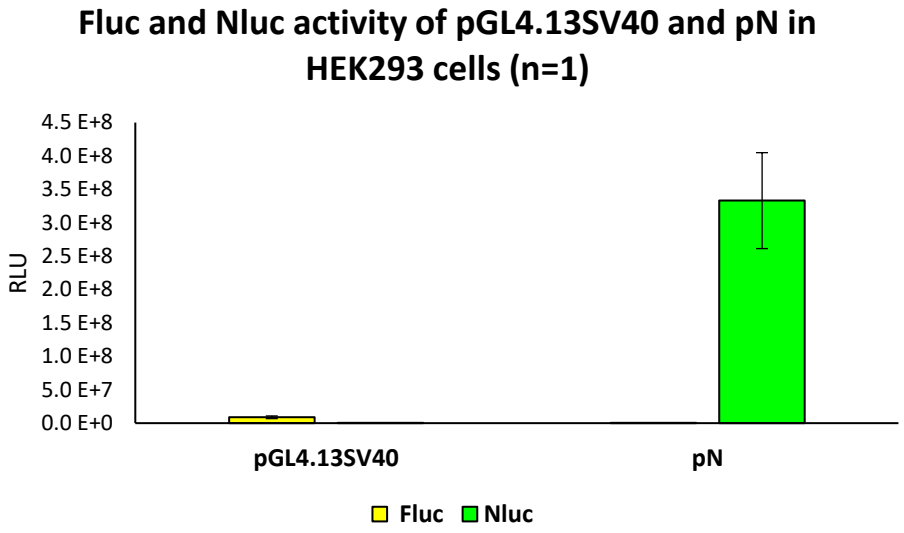

Figure 3.14 **Fluc and Nluc activity of HEK293 cells transfected with 20 ng of pGL4.13SV40 and pN for 2 days.** The experiment was done once in triplicate (n=1). Error bars indicate ± SD.

3.6 INTRODUCTION OF A HAIRPIN

It is known that secondary structures present in the 5' UTR can inhibit the binding and/or scanning of the preinitiation complex. The activity of stem loops to do so depends on their thermodynamic stability and position[215]. Hairpins are particularly efficient at inhibiting translation when they are positioned close to the 5' m^7G-cap, locking the ribosome entry[51]. Liang *et al.*[215] showed that when a hairpin of moderate strength (-30 kcal/mol) was located at position +12 relative to the 5' cap, the association with the PIC was inhibited, but this did not happen when the

same hairpin was located in position +52. When a stronger hairpin of -61 kcal/mol was located at position +72, the PIC stopped scanning at that same point. A model has been established regarding the inhibitory activity that secondary structures in the 5' UTRs could have: the presence of a hairpin near the 5' cap can inhibit the binding of the PIC, whereas a stem structure far from the 5' cap should not affect the binding of the PIC to the mRNA. The scanning could be stopped if the thermodynamic stability of the secondary structure is too strong[35,264].

3.6.1 Construction of phpBN and phpN

In the pBN and pN vectors, a palindromic sequence that formed a hairpin was cloned just before the 5' UTR sequence of the *BAG1* and Nluc respectively to form phpBN and phpN (see Figure 3.16 for the hairpin structure). The objective of the hairpin was to compromise cap-mediated translation by blocking the scanning process of the ribosomes before they reached the IRES (see Figure 3.15). We chose a very stable hairpin ($\Delta G \geq$-50 kcal/mol), as it had already been shown to be a good system to completely block ribosome scanning[35].

The hairpin we introduced on pBN and pN was ΔG = -78 kcal/mol. The hairpin structure was very similar to the one used by Stoneley *et al.*[265] to study the presence of the *c-myc* IRES using a luciferase assay based on the pRF vector, where the *c-myc* IRES was cloned between the two reporter genes.

The presence of a hairpin would inhibit the cap-dependent translation of the downstream cistron, in this case Nluc. If any Nluc expression was detected in the phpBN vector, this would have occurred mainly due to elements present in the 5' UTR of *BAG1,* as the presence of an IRES. The hairpin introduction is a reliable way to study IRES-mediated translation.

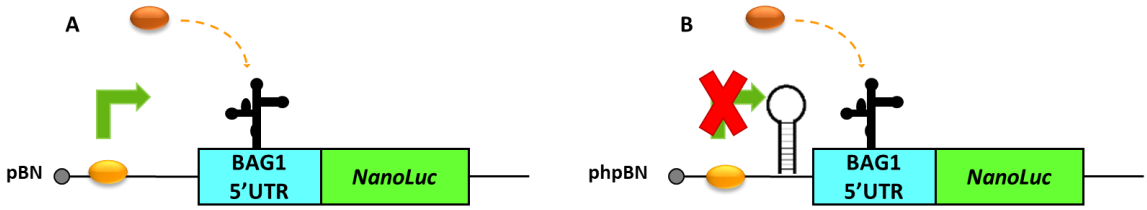

Figure 3.15 **pBN and phpBN translation representation.** When ribosomes bind to the 5' cap, they start scanning the mRNA looking for the first start codon. In pBN, the ribosomes would scan the mRNA until they found the start codons located in the 5' UTR. The Nluc signal would be representative of the efficiency of the cap-mediated and IRES-mediated translation (IRES-mediated translation is usually less efficient than cap-mediated translation). If a stem loop is introduced just before the *BAG1* 5' UTR as in phpBN, ribosomes are stopped at the point of the stem loop and cannot continue the scanning process. If an IRES is present in the *BAG1* 5' UTR, the IRES could recruit the ribosomes and start translation from that point. Any Nluc signal detected from phpBN would be due to the IRES-mediated translation.

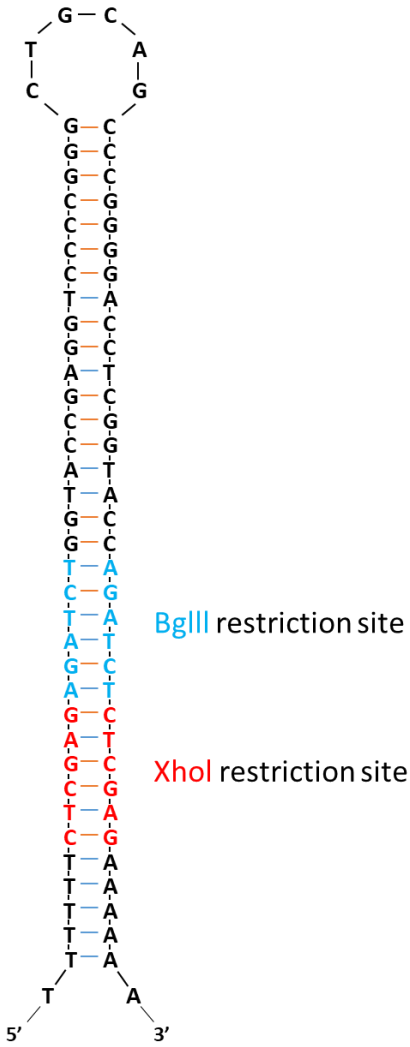

Figure 3.16 **Illustration of the palindromic sequenced introduced in pBN to form a hairpin generating phpBN.**

XhoI and BglII restriction enzyme sites were introduced in the hairpin (Figure 3.16) to facilitate future cloning experiments. The hairpin was synthesised by Eurofins.

The oligonucleotides forming the hairpin were annealed as explained in section 2.1.1.4 on page 54 and digested with XhoI, as it would then be cloned in the XhoI site of pBN and pN .

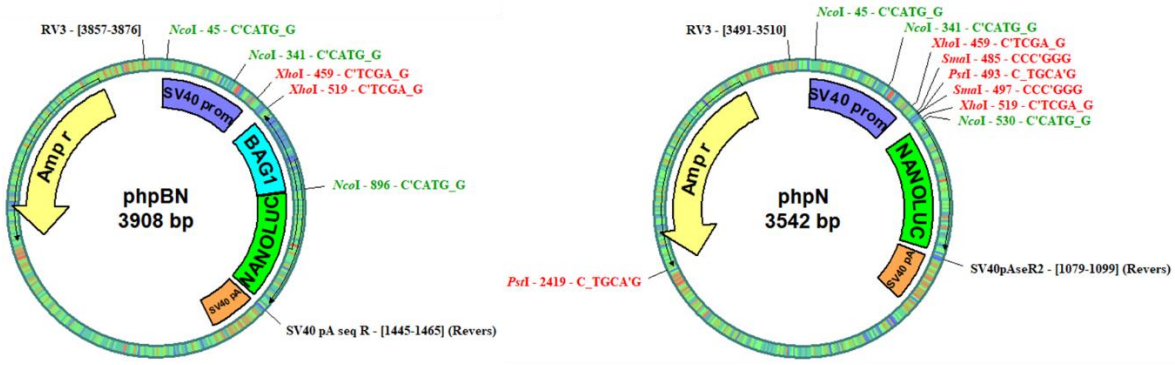

Figure 3.17 **Illustration of the phpBN and phpN vectors.** The phpBN vector had a hairpin just before the sequence of the *BAG1* 5' UTR. The phpN vector had a hairpin just before the sequence of Nluc. The hairpin localisation is limited by the Xhol restriction sites. Ncol was used to check the minipreps for the presence of the hairpin in phpBN. Ncol, Pstl and Smal were used to check the minipreps for the presence of the hairpin in phpN.

pBN and pN were digested with Xhol prior to the insertion of this hairpin (see Figure 3.17). Six phpBN and two phpN colonies were screened with Bglll to check for the insertion of the hairpin. Bglll had two cutting sites in phpBN in position 465 and 513. Bglll did not have any cutting site in pBN. phpN minipreps were digested with Ncol, Smal and Pstl individually. Xhol, Smal and Pstl had two restriction sites in phpN in positions 460 and 520, 486 and 498 and 494 and 2433 respectively. Ncol had three cutting sites in pN in positions 45, 341 and 484 and Pstl had a unique cutting point in position 2373, Smal did not have any cutting point.

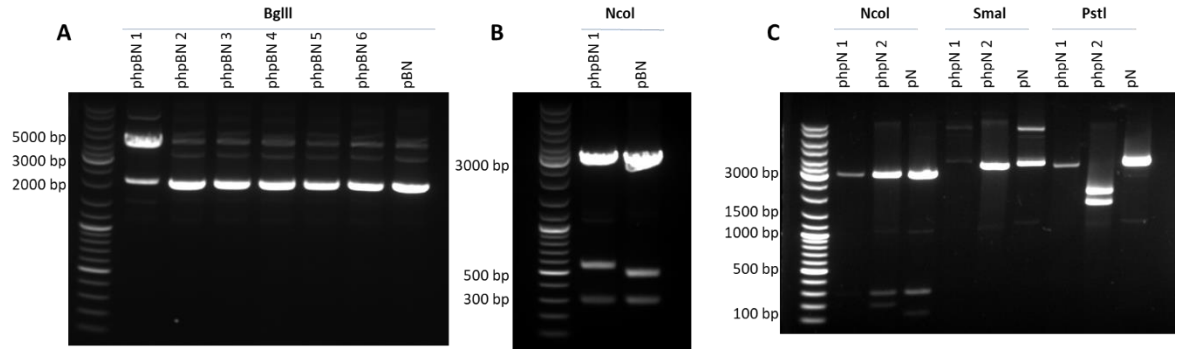

Figure 3.18 **A) phpBN minipreps digested with Bglll to check for the insertion of the hairpin in a 0.8% agarose gel. B) phpBN1 and pBN digested with Ncol. C) phpBN minipreps digested with Ncol, Smal and Pstl.**

As seen in Figure 3.18 A, only phpBN1 had a different pattern to the rest of the minipreps and the control pBN. It did not show the expected pattern, though. phpBN 1 was digested with Ncol along with pBN to double check if the hairpin was inserted and the digested vectors were run in an agarose gel (Figure 3.18, B). After the digestion with Ncol, the band pattern expected for pBN was three bands of 3057 bp, 495 bp and 296 bp respectively. Whereas in phpBN the expected pattern

was three bands of 3057 bp, 555 bp and 296 bp. In Figure 3.18 A and B it can be observed that phpBN1 showed the pattern expected for the correct insertion of the hairpin.

In the case of phpN minipreps, phpN2 showed the expected band pattern (Figure 3.18, C). Both minipreps were digested alongside with pN with NcoI, SmaI and PstI. The expected band pattern showing the successful insertion of the hairpin in the pN vector was the following: NcoI digestion should show three bands of 3057 bp, 29 bp and 210 bp; PstI should show two bands of 1946 bp and 1616 bp and SmaI should show two bands of 3550 bp and 12 bp. In Figure 3.18 C it can be observed that phpN2 showed the expected pattern.

phpBN1 and phpN2 were sent for sequencing using RV3 and SV40pAseR2 primers (see primer sequences in section 2.7 on page 67). Both forward and reverse sequencing stopped just at the beginning of the hairpin. phpBN1 was sent for sequencing again with the AfterSV40 F primer (see primer sequences in section 2.7 on page 67), and the sequencing service was upgraded to "Power Read", where special conditions are applied to allow the sequencing of hard to sequence sequences such as hairpins. However, this upgrade also failed on showing the full sequence of the hairpin. An experimental approach was taken to verify the presence of the hairpin in phpBN and phpN. Sequencing results can be seen in Appendix C.

Nluc expression of cells transfected with phpN and phpBN plasmids will be measured to study the activity of the putative IRES present in the *BAG1* 5' UTR. In future experiments, cells will be transfected with phpBN and pGL4.13SV40 and the oligonucleotides. phpN will be used as a control.

3.6.2 Transfecting phpBN and phpN to measure IRES-mediated translation

To reduce cap-mediated translation initiation and measure the activity of the IRES, a hairpin was inserted in the vectors pBN and pN, forming phpBN and phpN (Figure 3.17). In phpBN the hairpin was located just before the *BAG1* 5' UTR sequence and in phpN just upstream of the Nluc ORF. The role of the hairpin was to inhibit cap-mediated translation by blocking the scanning of the ribosomes from the cap through the mRNA. Thereby, any Nluc signal obtained from phpBN would be due to structures present in the 5' UTR of *BAG1*, ideally due to the presence of an IRES (Figure 3.15). Any Nluc signal obtained from phpN would be indicative of the presence of cryptic promoters or would be evidence of the weakness of the introduced hairpin.

pBN, phpBN, pN and phpN were co-transfected in HEK293 cells along with pGL4.13SV40, transfecting a total of 20 ng (10 ng of each plasmid) per 2 000 cells. Transfections were done one day after seeding the cells and the luciferase levels were assayed 2 days after transfection. In each

experiment the transfections were done in triplicate. These results show the data obtained from a single experiment. All the experiments done until this moment were done in HeLa cells, however after this experiment HEK293 cells were used. It is known that both HEK293 and HeLa cells have a very similar *BAG1* IRES activity[95], while HEK293 showed to have a higher transfection efficiency.

As was previously mentioned, the sequencing of phpBN and phpN stopped at the point where the hairpin was introduced, so the only way to check the presence of the hairpin, apart from the restriction enzyme analysis (see Figure 3.18), was by transfecting the vector in cells and studying its expression.

The Fluc values showed the levels of cap-mediated translation in cells as well as the transfection efficiency of the plasmids (see Figure 3.19). Most of the Fluc levels were similar, however, in the case of pN, this was over three times smaller than in the rest of the cases. This could be due to transfection issues, however we could not discard the fact that pN could have an inhibitory effect of pGL4.13SV40. As can be seen in Figure 3.19 B, the presence of the hairpin strongly decreased the Nluc expression in cells transfected with both phpBN (over 10 times) and phpN (over 5 times). However, to study more efficiently the IRES activity the Nluc to Fluc ratios were calculated (Figure 3.19, C). Cells transfected with phpBN had an Nluc to Fluc ratio 9 times smaller than cells transfected with pBN, and cells transfected with phpN 34 times smaller than cells transfected with pN. Cells transfected with phpBN showed a higher Nluc to Fluc ratio than cells transfected with phpN, as well as a higher Nluc activity, this shows that there is something in the *BAG1* 5' UTR (an IRES) increasing the Nluc activity.

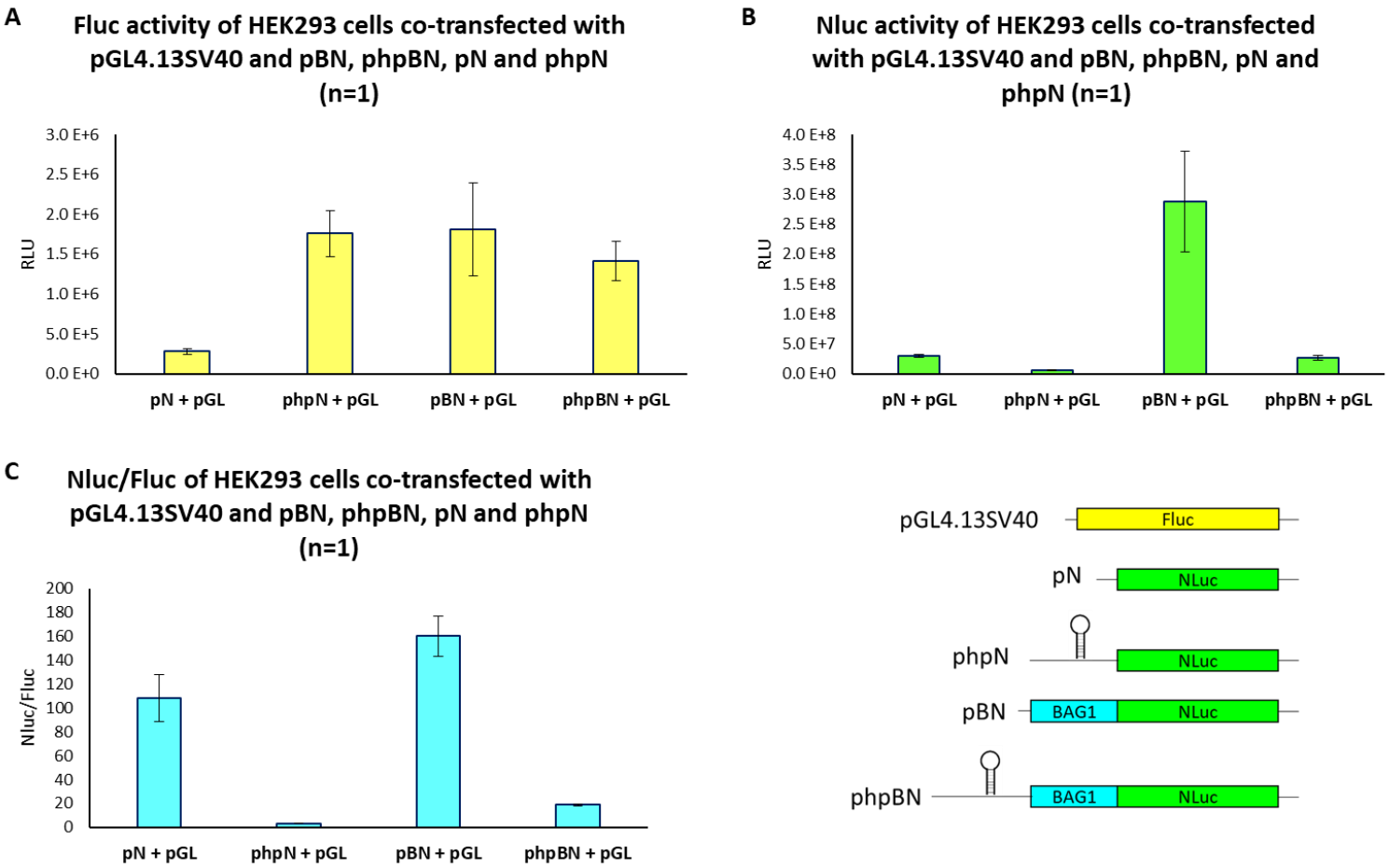

Figure 3.19 **Luciferase assay results of HEK293 cells transfected with pGL4.13SV40 and pBN, phpBN, pN and phpN.** Fluc (A) and Nluc (B) activity and C) Nluc to Fluc ratio in HEK293 cells co-transfected with pGL4.13SV40 and pBN, phpBN, pN and phpN. Error bars show ± SD.

The efficiency of the hairpin plasmids was also analysed by western blot. HEK293 cells were transfected with pN, phpN, pBN and phpBN and the expression was measured using an anti Nluc antibody (Promega). The size of Nluc is of around 19 kDa, therefore p36 should show a band of that size. p46 and p50 should show bands of around 20 kDa and 36 kDa respectively. As seen in Figure 3.20, the introduction of a hairpin in phpN reduced to undetectable levels the Nluc expression. In the case of cells transfected with phpBN it could clearly be noticeable that there was a decrease in the Nluc expression when the hairpin was inserted. The fact that in cells transfected with phpN no Nluc signal was detected, but in cells transfected with phpBN some was could be explained by the presence of the *BAG1* 5' UTR. The possible presence of an IRES in the 5' UTR of *BAG1* could have driven the translation of the weak signal of Nluc detected in phpBN.

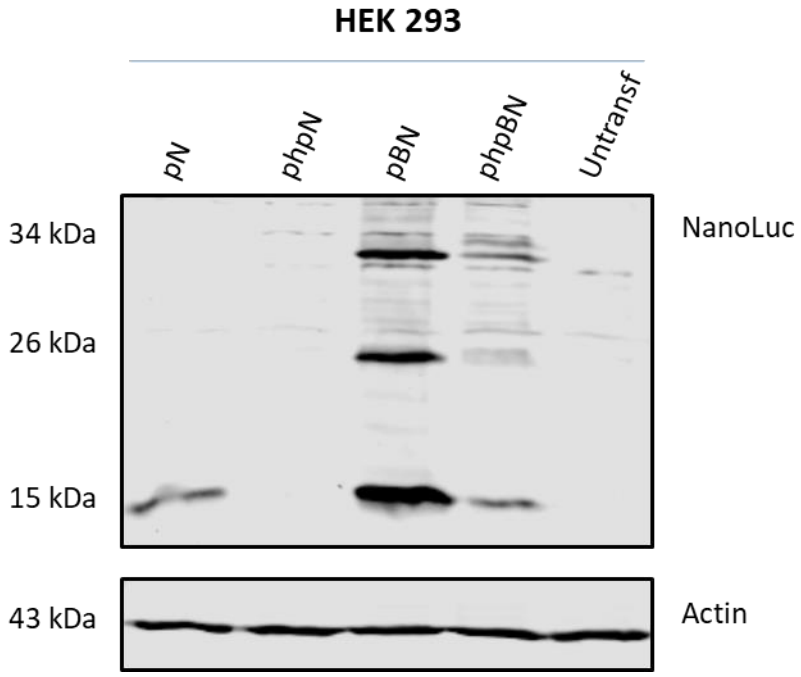

Figure 3.20 **Nluc expression of HEK293 cells transfected with pN, phpN, pBN and phpBN.** The introduction of a hairpin reduced the Nluc expression in both cases.

3.7 PROGRAMMING TnT AND RRL

The activity of the IRES was also studied in the cell free *in vitro* transcription and translation systems as TnT and Rabbit Reticulocyte Lysate (RRL).

For the TnT assays, the TnT® Quick Coupled Transcription/Translation Systems (Promega) was used. In this system a coupled transcription/translation reaction is created for eukaryotic cell-free protein expression, in our case from templates containing a T7 phage promoter.

To study the IRES activity in RRL, the Retic Lysate IVT™ Kit (Invitrogen) was used, where mRNAs had been synthesised separately. The kit contains RRL that had been optimised for efficient translation by the addition of calf liver tRNA, hemin and an ATP-regenerating system. The reticulocytes are isolated from rabbits that have been treated with acetylphenylhydrazine to increase immature red blood cells (reticulocytes). The endogenous mRNA from the reticulocytes is degraded with micrococal nuclease, to ensure that exogenous RNA is the only one being translated. *In vitro* RNAs were first generated and IRES activity was then studied by programming the RRL.

Few people have studied the IRES activity in these two *in vitro* systems (TnT and RRL) and there is some controversy in the use of them to study IRES activity. Rhinovirus and enterovirus IRESs are not efficient in RRL, unless HeLa cell proteins are added to the system[266,267]. On the other hand, the IRES elements of cardiovirus and aphthovirus picornaviruses, as encephalomyocarditis virus (EMCV) and foot-and-mouth disease virus (FMDV), function very efficiently in RRL[268]. Shih-Ting Kang *et al.*[269] showed in TnT the activity of the IRES located in the vp31/cp39b coding region of the genome of the white stop syndrome virus. Christina L. Topliff *et al.* studied the IRES activity of eight Bovine viral diarrhea virus (BVDV2) field isolates in RRL and in different cell lines, and saw a variability in the expression levels in each of the systems, explained by the different secondary structures the RNA could take in the systems. It has also been shown that the XIAP cellular IRES is functional in RRL[270]. Terenin *et al.*[36] do not support the idea of using *in vitro* systems to study the presence of an IRES, as they suggest that some IRESs have a weak activity in RRL due to some inexplicable property of the cell free system.

3.7.1 TnT experimental design

Primers were designed to introduce the T7 promoter in the constructs of interest (pFBN, pFN, pBN, pN and pGL4.13SV40) to facilitate the transcription of a single stranded RNA by the T7 RNA polymerase (see section 2.1.1.1 on page 52 for NanoLuc R, AfterSV40 F and T7-afterSV40 F primer sequences). In the primers, the T7 promoter ((5'-TAATACGACTCACTATAG-3') was followed by two Gs to increase transcription yields, as recommended by NEB. As a control, primers lacking that T7 promoter were also designed, to verify that the presence of the promoter was crucial for translation to take place. Primers were designed to amplify from the end of the SV40 promoter to the end of the Nluc ORF, as shown in Figure 3.21.

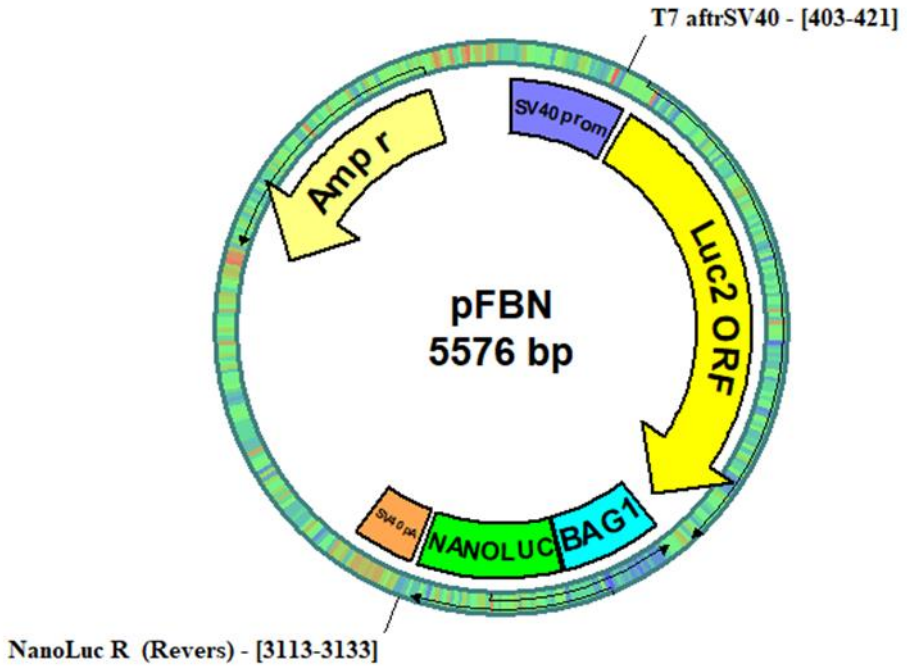

Figure 3.21 **Representation of the primers used to amplify the sequence containing Fluc, *BAG1* 5' UTR and Nluc in pFBN for the synthesis of *in vitro* transcribed RNA.** The same primers were used to amplify the sequences of interest in pFN, pBN and pN.

The amplification of DNA containing the T7 promoter for the correct translation of the constructs of interest was done as specified in section 2.10.1 on page 72. After the PCR amplification, the amplicons were run in an agarose gel and the bands corresponding to the DNA of interest were excised from the gel and cleaned-up. Amplicons were also checked for the right size, to verify that the amplified DNA was the expected one.

When TnT lysates were programmed, only the TnT programmed with T7 promoter containing DNA showed Fluc activity (Figure 3.22, A). No Fluc activity was detected in any of the TnT programmed with DNAs lacking the T7 promoter. TnT programmed with pBN and pN did not show any Fluc activity either, as expected. In the case of Nluc, the TnT programmed with no T7 constructs showed Nluc levels higher than background values (around ten times higher) , but over 25 times smaller than the ones showed by the TnT programmed with constructs with the T7 promoter (Figure 3.22, B). TnT programmed with the monocistronic constructs pBN and pN showed a higher Nluc activity (over 30 times stronger) than the TnT programmed with bicistronic constructs. TnT programmed with pN showed over a threefold increase in its Nluc activity compared to TnT programmed with pBN, suggesting that the presence of the *BAG1* 5' UTR compromises the levels of translation in TnT. In the case of the bicistronic constructs, TnT programmed with pFN showed a 20% increase in its Nluc activity compared to TnT programmed with pFBN, which again suggested that the presence of the *BAG1* 5' UTR affected the Nluc translation in a negative way. As controls pGL4.13SV40 and Luc control (a luciferase control

included in the TnT kit) were used, both showing high Fluc activities and no Nluc activity (see Figure 3.22, A).

TnT programmed with pFBN only showed a 10% increase in the Nluc to Fluc ratio when compared to TnT programmed with pFN (Figure 3.22, C), which suggested that the activity of the presence of the *BAG1* 5' UTR did not affect the Nluc activity in TnT as much as it did in cells, this would also mean that the *BAG1* IRES in TnT was not very strong. This could be due to the lack of ITAFs required (PTBP1 and PCBP1) for the IRES' activity in TnT.

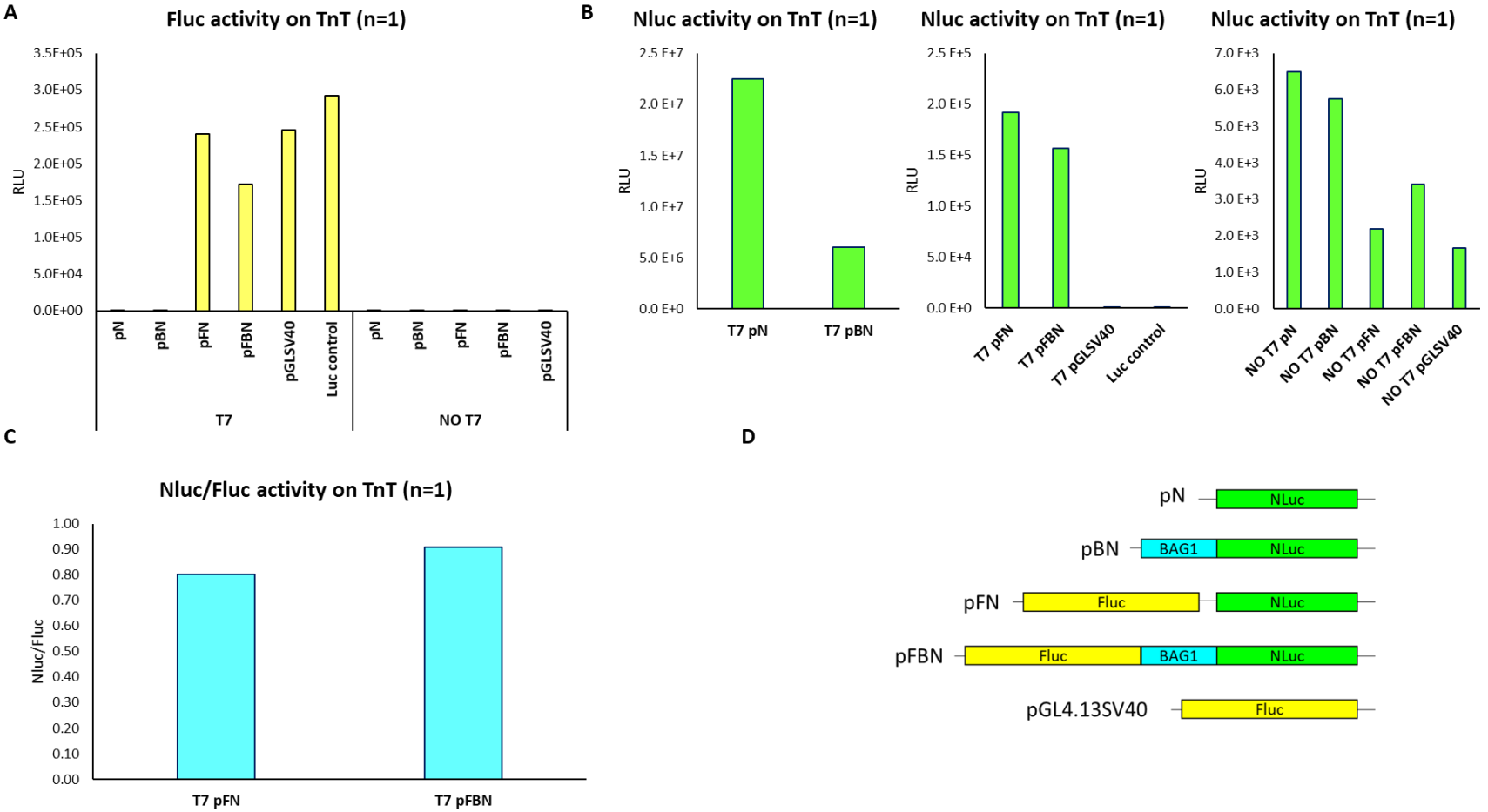

Figure 3.22 **Luciferase assay results of TnT programmed with the different PCR products.** A) Fluc B) Nluc activity of TnT programmed with the PCR products with and without T7 C) Nluc/Fluc of TnT programmed with the PCR products.

3.7.2 RRL experimental design

Using the same amplicons as for the TnT, *in vitro* RNA was synthesised using the HiScribe T7 Quick High Yield RNA Synthesis Kit (NEB) (see section 2.10.2 on page 73). All the constructs with the T7 promoter were transcribed successfully and showed the expected size. The constructs lacking the T7 promoter did not transcribe, as expected (Figure 3.23).

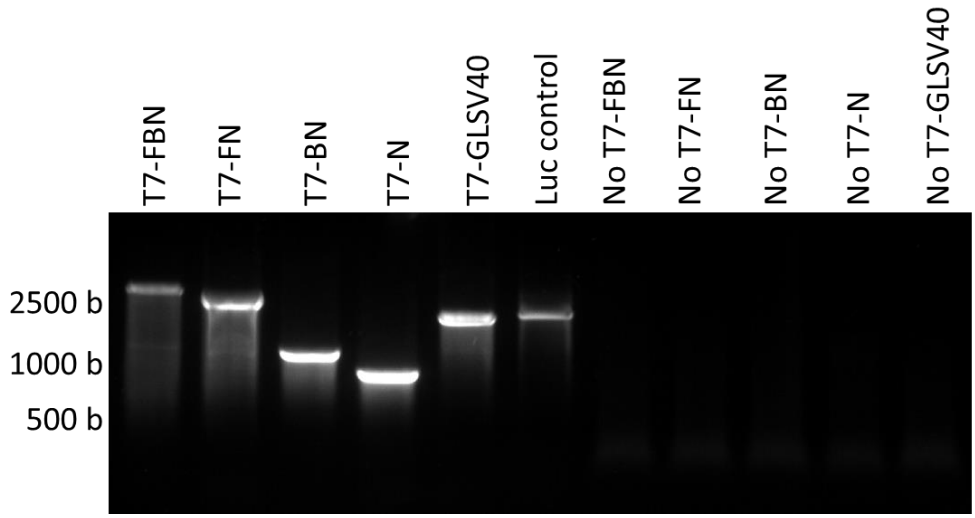

Figure 3.23 **Agarose gel showing *in vitro* synthesised RNA.** The no T7 DNA did not transcribe into RNA, as expected. The T7 amplicons were all successfully transcribed. Expected sizes: T7-FBN 2751 b, T7-FN 2398 b, T7-BN 1019 b, T7-N 667 b, T7-GL4.13SV40 1777 b.

RRL programmed with FBN only showed a 9% increased Fluc activity when compared to RRL programmed with FN (Figure 3.24, A). In the same way as in TnT, RRL programmed with monocistronic RNAs showed at least a 24 times more Nluc activity than RRL programmed with the bicistronic ones (Figure 3.24, B). The presence of the *BAG1* 5' UTR had a negative effect in the Nluc activity both in RRL programmed with FBN and BN when compared to RRL programmed with FN and N. RRL programmed with FN showed almost double Nluc to Fluc ratio than RRL programmed with FBN (Figure 3.24, C). This indicated that the presence of the *BAG1* 5' UTR had a strong effect in the Nluc activity in RRL. If there was an IRES present in *BAG1's* 5' UTR, its activity would be limited. This could be due to the lack of the ITAFs required for the activity of the *BAG1* IRES[82,95].

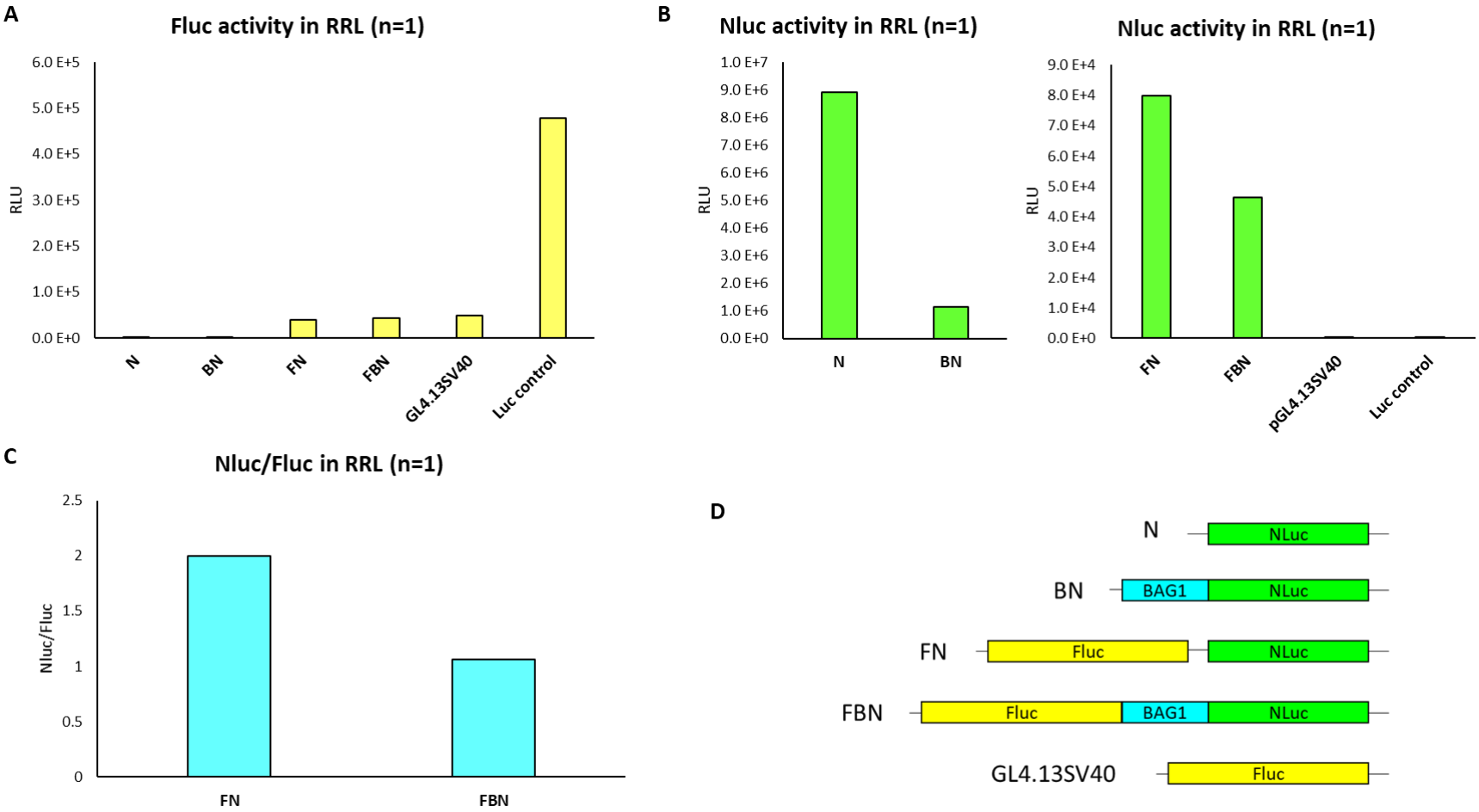

Figure 3.24 **Luciferase assay results of RRL programmed with the *in vitro* synthesised N, BN, FN, FBN, pGL4.13SV40 and Luc control RNA.** Fluc (A), Nluc (B) activity and C) Nluc to Fluc ratio of the *in vitro* synthesised RNA in RRL.

3.8 TRANSFECTION OF *IN VITRO* SYNTHESISED RNA IN HEK293 CELLS

IRES activity was also studied by transfecting the *in vitro* synthesised RNA in HEK293 cells. The RNA transfected was the same used in the RRL experiment (3.7.2, page 110). The RNA was transfected as explained in section 2.13 on page 78.

Fluc and Nluc activity was measured 6 hours and 24 hours after RNA transfection. The Fluc and Nluc values of untransfected cells was also measured, which showed no activity for either of the reporter genes. The Fluc activity was slightly smaller 24 hours after transfection rather than 6 hours after transfection and the presence of the *BAG1* 5' UTR in FBN decreased the Fluc activity when compared to FN (Figure 3.25, A).

Cells transfected with monocistronic RNAs showed at least a 20 times higher Nluc activity (Figure 3.25, B) than bicistronic RNAs (Figure 3.25, C). In all the cases the Nluc activity 24 hours after transfection was at least double the Nluc activity when the transfection was done for 6 hours, this could be due to the accumulation of Nluc in the cells due to its long half-life when compared to Fluc. The presence of the *BAG1* 5' UTR decreased the Nluc activity in cells transfected with both the monocistronic BN RNA and the bicistronic FBN when compared to cells transfected with N and FN.

6 hours after RNA transfection, cells transfected with FBN showed a 40% higher Nluc to Fluc ratio than cells transfected with FN, that difference increased 24 hours after transfection to a 70% (Figure 3.25, D). The fact that the Nluc Fluc ratio was stronger in cells transfected with FBN than in cells transfected with FN corroborated the presence of an IRES in the *BAG1* 5' UTR. The fact that the Nluc to Fluc ratio increased from 6 hours to 24 hours after transfection could also be due to the higher stability and half-life of Nluc compared to Fluc[271].

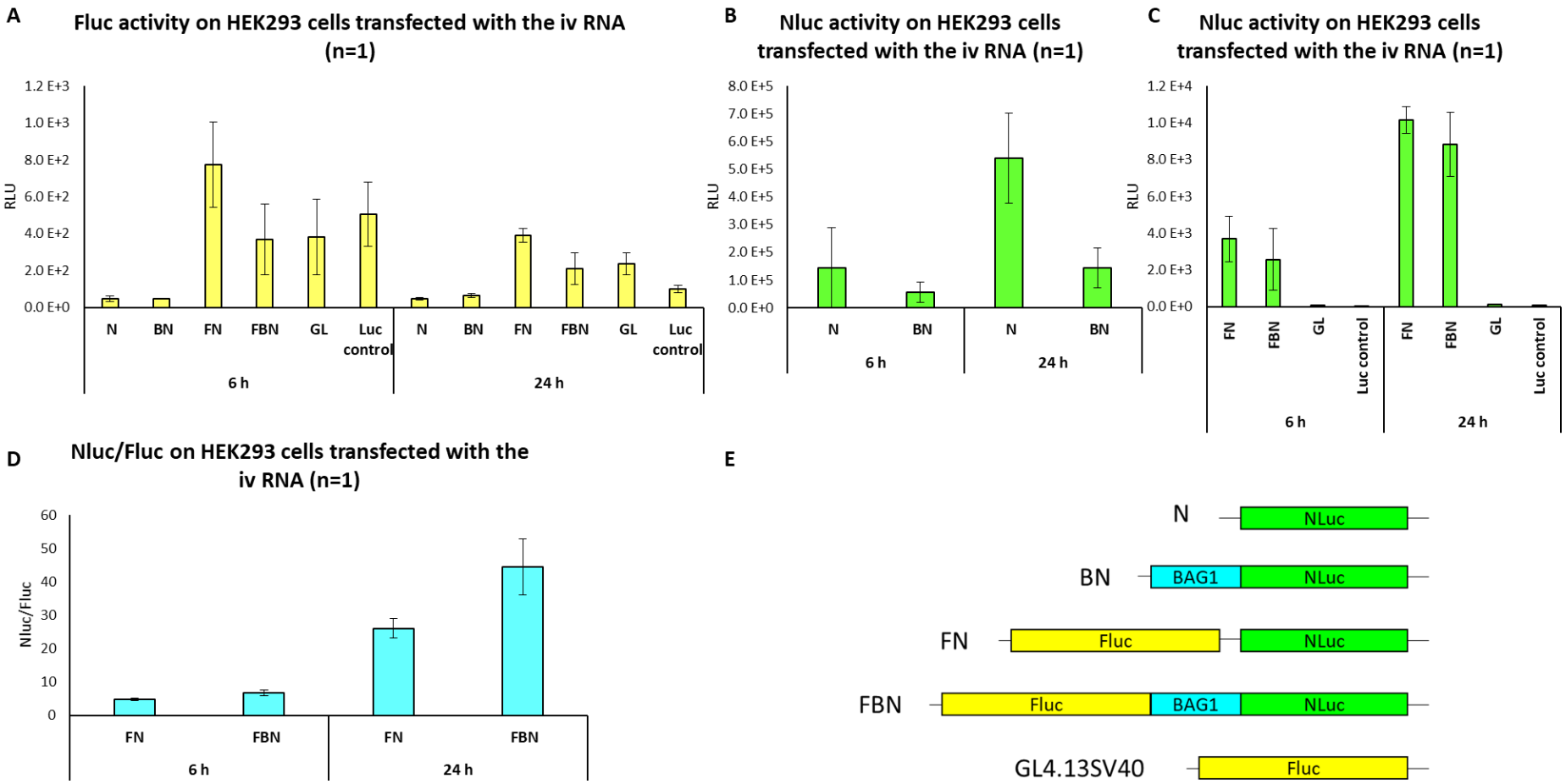

Figure 3.25 **Luciferase assay results in HEK293 cells transfected with the *in vitro* synthesised RNA (N, BN, FN, FBN, GL4.13SV40 and Luc control) for 6 and 24 hours.** A) Fluc, B and C) Nluc and D) Nluc/Fluc activities in HEK293 cells. Error bars show ± SD.

3.9 THE ULTIMATE EXPERIMENT TO VERIFY THE PRESENCE OF AN IRES

To verify the presence of the *BAG1* IRES, we carried out the "ultimate" experiment proposed by Terenin *et al* [36]. They proposed to design a bicistronic construct containing the putative IRES element between two reporter genes (pFBN in our case, where the putative *BAG1* IRES is located between Fluc and Nluc). Those constructs should then be transcribed *in vitro*. The RNA should be capped with a non-functional cap (A-cap) and a functional cap (m^7G-cap). A poly(A) tail should also be added to the RNAs. As controls, the process should be repeated with the bicistronic construct lacking the putative IRES (pFN in our case), and their monocistronic analogues (pBN and pN). In Figure 3.26 it can be seen all the RNAs synthesised. The generated RNAs should then be transfected in cells and the expression of the reporter genes should be studied to verify the presence of the IRES. In a standard cap-dependent system, m^7G-capped RNAs should translate more efficiently than A-capped RNAs. An m^7G-capped monocistronic RNA should also be translated more efficiently than the same sequence in an m^7G-capped bicistronic construct.

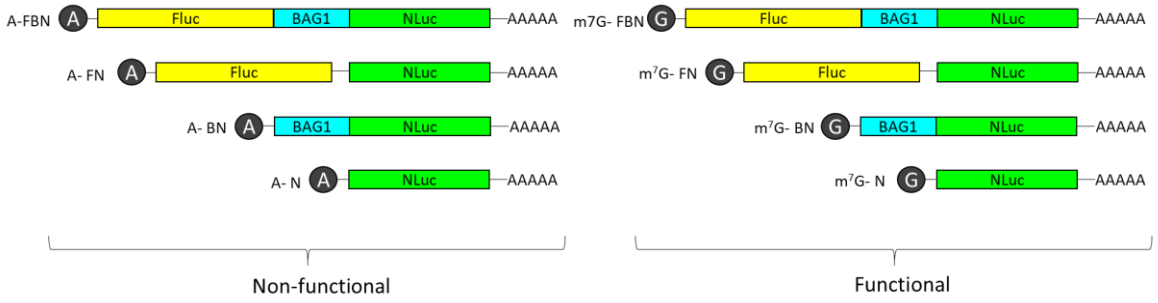

Figure 3.26 **Diagram of the *in vitro* synthesised RNAs**. FBN, FN, BN and N were *in vitro* transcribed and a functional cap (m^7G-cap) and non-functional cap (A-cap) were attached in the 5'.

We first designed primers to introduce the T7 promoter in the RNAs that would be m^7G-capped and the T7 phi 2.5 promoter in the RNAs that would be A-capped (see primer sequences on section 2.10.1 on page 72). Primers were designed to amplify the DNA from the end of the SV40 promoter to the end of the Nluc sequence (including the full length Nluc ORF, (see Figure 3.21)). The primers used to introduce the T7 promoter in the constructs were the same ones used to amplify the DNA for TnT and RRL experiments (section 3.7.1, page 106). The primers designed to synthesise RNA with an A-cap contained the T7 phi 2.5 promoter (5'-TAATACGACTCACTATTAG-3') followed by two Gs to increase the synthesis yield (see section 2.10.1 on page 72).

The DNA was amplified as explained in section 2.10.1 on page 72 and *in vitro* RNA was synthesised using the HiScribe™ T7 Quick High Yield RNA Synthesis Kit (NEB) as explained in sections 2.10.2 and 2.10.3 on page 73. The poly(A) tail was added as explained in see section 2.10 on page 72.

3.9.1 Verifying the correct insertion of the cap analogues and poly(A) tail in the RNA

We then did an assay to verify if the cap analogues and poly(A) had been integrated in the RNA correctly. To do so, we made the following *in vitro* RNA: m^7G-FBN-poly(A), FBN-poly(A), m^7G-FBN, FBN, m^7G-FN-poly(A), FN-poly(A), m^7G-FN and FN (see Figure 3.27).

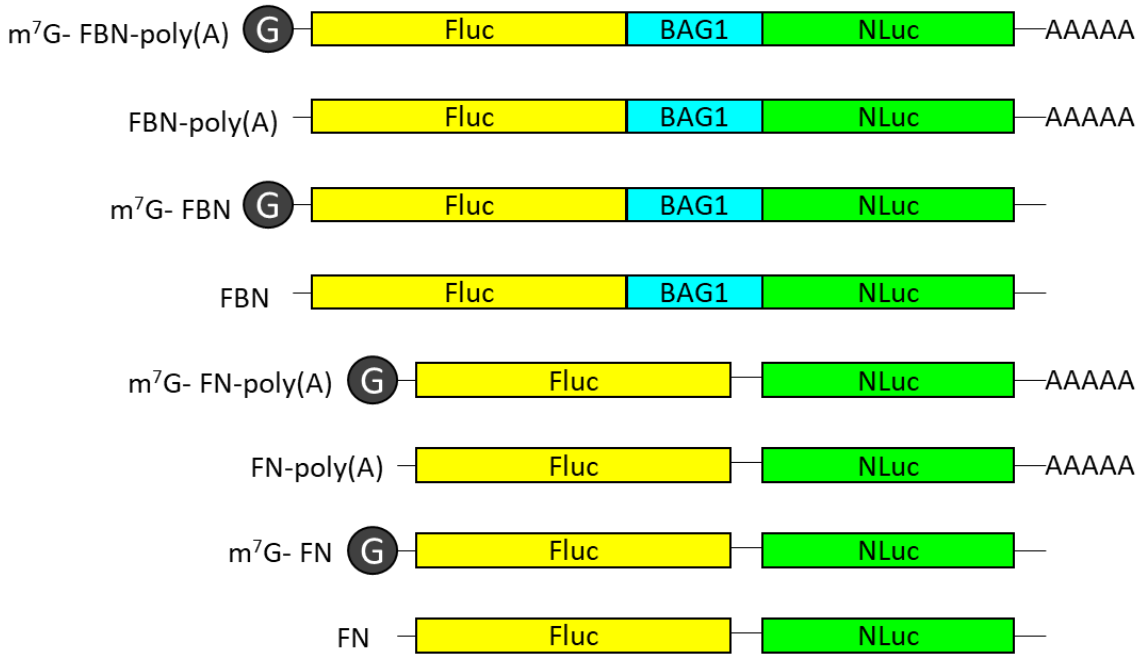

Figure 3.27 **Representation of the RNA synthesised *in vitro* to verify the correct insertion of the m^7G-cap and poly(A) tail.**

As it can be seen in Figure 3.28, all the constructs showed a unique band of the expected size. We were unable to see differences in the gel between the non-tailed and A-tailed RNA. This was expected as the maximum numbers of adenosine monophosphates that could be integrated in the RNA with the method used (explained in section 2.10.4 on page 75) was 150, and the total size of the RNA was big enough (over 2000 nucleotides) to distinguish a difference of less than 150 nucleotides.

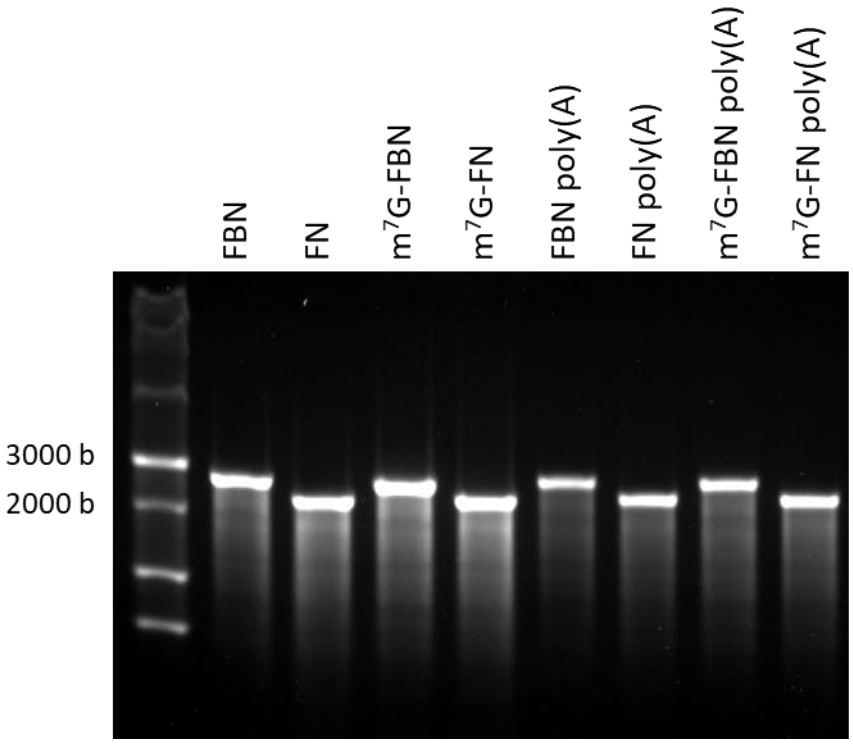

Figure 3.28 **Agarose gel showing the *in vitro* synthesised FBN, FN, m^{7}G-FBN, m^{7}G-FN, FBN-poly(A), FN-poly(A), m^{7}G-FBN-poly(A) and m^{7}G-FN-poly(A).**

We then transfected 150 ng of each of the RNAs in HEK293 cells as explained in section 2.13 on page 78 and the Fluc and Nluc activities were analysed 6 and 24 hours after transfection.

Cells transfected for 6 hours with uncapped FN and FBN RNAs showed an Nluc activity at least 80% stronger than the Fluc activity (see Figure 3.29, A) whereas when m^{7}G RNAs were transfected the Fluc activity was at least a 30% higher than the Nluc activity (see Figure 3.29, B). Cells transfected with the uncapped FN RNA with poly(A) for 6 hours showed a threefold increase in the Fluc activity when compared to the cells transfected with the uncapped FN RNA without poly(A) (see Figure 3.29). Cells transfected with uncapped FBN with poly (A) doubled the Fluc activity (see Figure 3.29). The differences were more obvious when capped RNAs were transfected. In this case, cells transfected with m^{7}G-capped FN RNA with poly(A) showed a sixfold increase in their Fluc activity when compared to the cells transfected with m^{7}G-capped FN RNA without poly(A) and cells transfected with m^{7}G-capped FBN RNA with poly(A) showed a threefold increase in their Fluc activity when compared to the cells transfected with m^{7}G-capped FBN RNA without poly(A). In the case of Nluc, the addition of a poly(A) tail to both uncapped FN and FBN increased the Nluc activity over three times (see Figure 3.29, A) and in the case of cells transfected with m^{7}G-capped FN and FBN, the addition of a poly(A) tail increased the Nluc activity over ten times (Figure 3.29, B). The Nluc to Fluc ratio of cells transfected with uncapped FN was the same in the presence or in the absence of a poly(A) tail, which was the same as the Nluc to

Fluc ratio of cells transfected with uncapped FBN without a poly(A); however the addition of a poly(A) tail in FBN increased the Nluc to Fluc ratio over a 50% (see Figure 3.29, C). In the case of cells transfected with m^7G-capped RNAs, the addition of a poly(A) tail increased the Nluc to Fluc ratio in over twofold for both FN and FBN (see Figure 3.29, D). Cells transfected with uncapped RNAs showed over double the Nluc to Fluc ratio than cells transfected with m^7G-capped constructs (see Figure 3.29, C and D). In the case of cells transfected with m^7G-cap, cells transfected with FBN RNAs showed over a fourfold increase in the Nluc to Fluc ratio when compared to the cells transfected with FN RNAs independently on the presence or the absence of a poly(A) tail (see Figure 3.29, D).

When cells were transfected for 24 hours, the Nluc activity was higher than Fluc activity in the presence or absence of both a poly(A) tail and an m^7G-cap (see Figure 3.29, E and F). The Fluc signals of cells transfected with RNAs without a cap was almost at background levels (under 600 RLU) (see Figure 3.29, E). In the case of the Nluc activity, the addition of a poly(A) tail increased its activity at least five times (see Figure 3.29, E). The addition of an m^7G-cap to the RNAs increased both the Nluc and Fluc activity over ten times (see Figure 3.29 F). When a poly(A) tail was added to the m^7G-cap both the Fluc and the Nluc activity was increased, and it was stronger in the case of FBN rather than in FN (see Figure 3.29, G). The Nluc to Fluc ratio was always stronger in the cells transfected with FN and FBN with poly(A) (see Figure 3.29 G and H). The Nluc to Fluc ratio was very similar for uncapped FN and FBN without poly(A), and in the case of the constructs with poly(A) FBN only showed a 10% increase in the Nluc to Fluc ratio compared to FN (see Figure 3.29 G). In the case of m^7G-capped RNAs, cells transfected with FBN no poly(A) showed over a twofold increase in the Nluc to Fluc ratio compared to cells transfected with FN no poly(A), whereas in the case of the constructs with poly(A) cells transfected with FBN showed over a fourfold increase (see Figure 3.29 H).

Overall we could say that both the poly(A) tail and the m^7G-cap were successfully introduced in the RNAs. All the RNAs containing a poly(A) or the m^7G-cap showed a higher level of activity than the ones lacking them. The presence of both the poly(A) tail and the m^7G-cap increased the activity of the RNAs even more. We thereby assumed that the A-cap would also be successfully integrated in the RNA.

The presence of the 5'-m^7G increased the cap-dependent translation, as expected. We need to keep in mind that Nluc is around 37 brighter than Fluc[271] (see Figure 3.14), and the higher Nluc activity observed in the uncapped RNA could be due to that. These results suggest that in the presence of an m^7G-cap there is some IRES activity in FBN. This will be analysed in further detail in section 3.9.2, page 119.

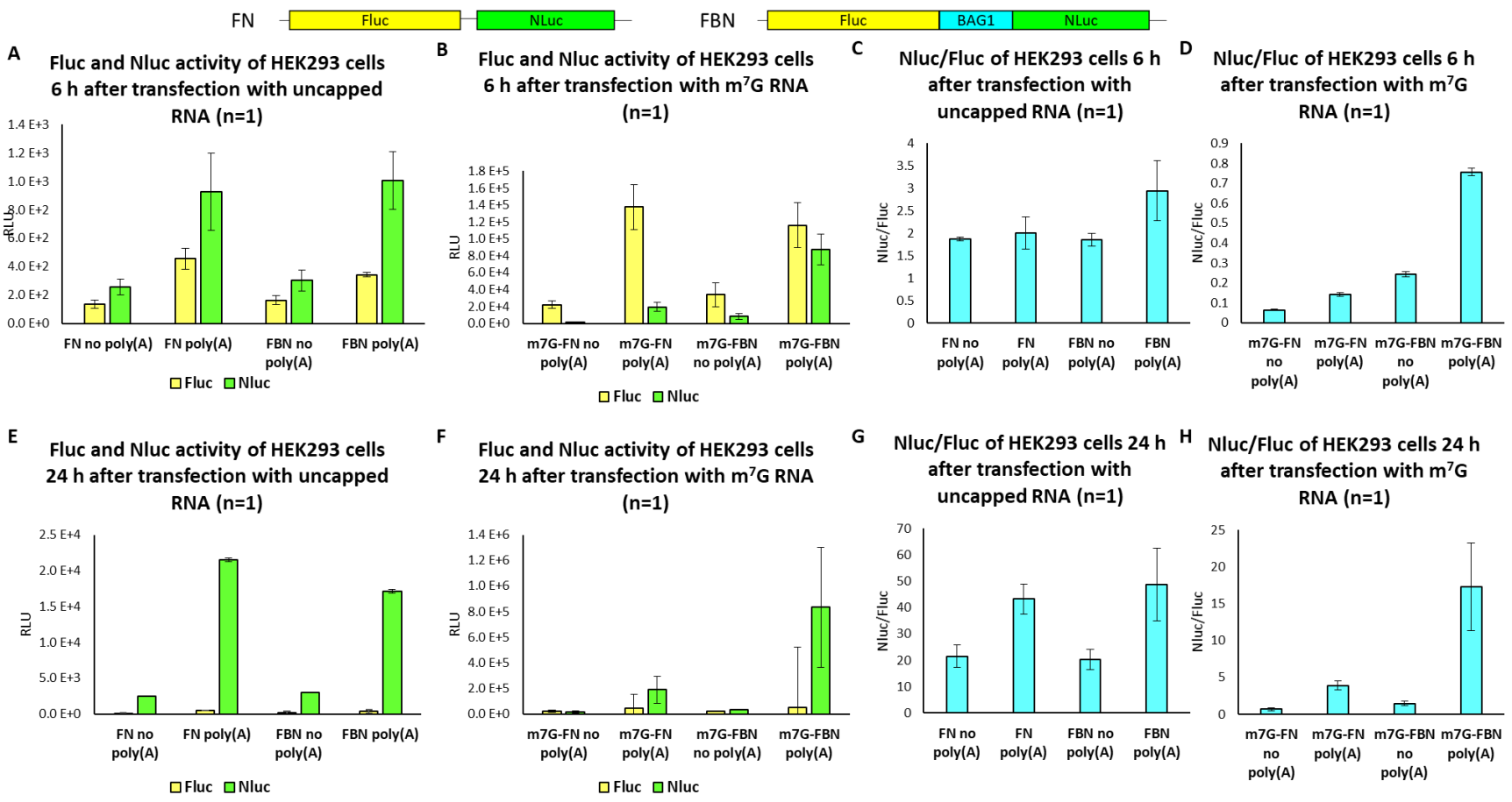

Figure 3.29 **Fluc and Nluc activities of cells transfected with *in vitro* synthesised FBN and FN RNAs, transfected for 6 hours without m^{7}G-cap (A) and in the presence of an m^{7}G-cap (B); transfected for 24 hours without m^{7}G-cap (E) and in the presence of an m^{7}G-cap (F). C, D, G and H show the Nluc/Fluc of the RNA 6 and 24 hours after transfection in the presence and absence of an m^{7}G-cap.** . Error bars show ± SD

3.9.2 Transfection of A-capped and m^{7}G-capped RNA in cells.

The next step was to do the experiment proposed by Terenin *et al.*[36] to verify the presence of the *BAG1* IRES. We first amplified the DNA and introduced the T7 promoter and T7 phi 2.5 promoter sequences required for the *in vitro* transcription and insertion of the m^{7}G-cap and A-cap (see section 2.10.1 on page 72). We analysed the purified PCR product by agarose gel electrophoresis to verify the presence of a unique band of the right size (Figure 3.30). We then transcribed the *in vitro* RNA with an A and m^{7}G cap and added a poly(A) tail (see sections 2.10.3 and 2.10.4 on page 74) and we checked the RNA in an agarose gel to verify the presence of a unique band of the correct size (Figure 3.31).

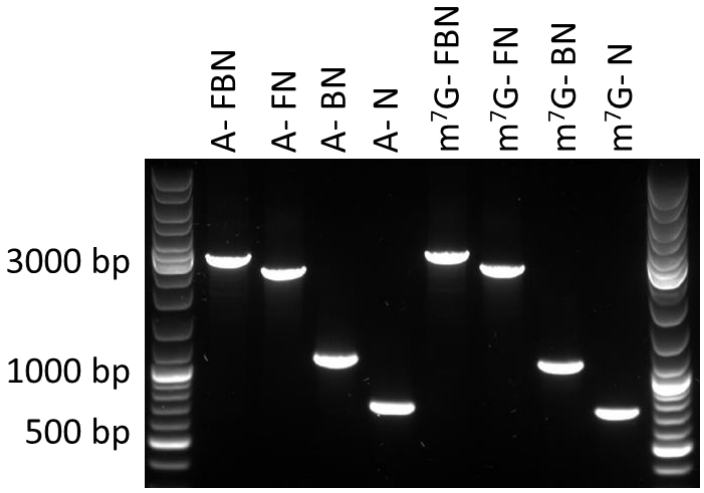

Figure 3.30 **DNA amplicons with the T7 phi 2.5 promoter and the T7 promoter.**

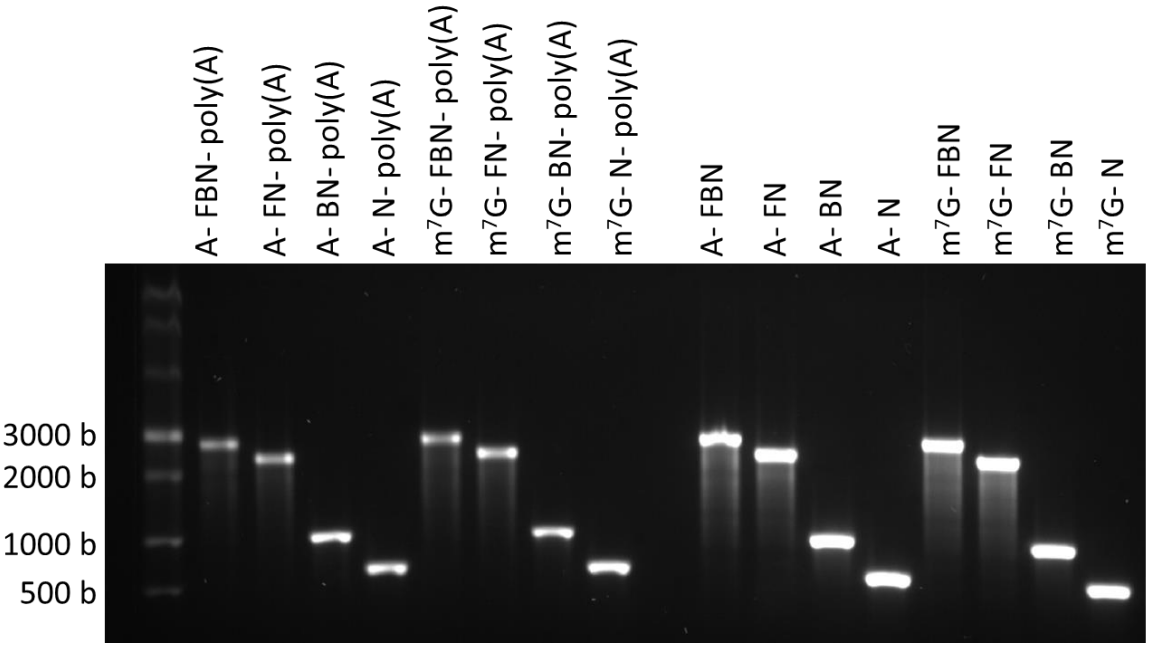

Figure 3.31 **m^{7}G-capped and A-capped *in vitro* synthesised RNA, with and without a poly(A) tail.**

RNA was transfected in HEK293 cells in triplicate and the activity of Fluc and Nluc was measured 6 hours and 24 hours after transfection. The translation levels were also measured in RRL.

Cells transfected with the monocistronic RNAs (N and BN) showed the same trend when the transfections were done for 6 and 24 hours, where cells transfected with N showed at least a fivefold increase in the Nluc activity compared to BN transfected cells. In both cases the m^7G RNAs showed an Nluc activity five times higher than the A-capped RNAs. Doing the transfection for 24 hours increased the Nluc activity over three times (see Figure 3.32, A and B). The results obtained when RRL were programmed with N and BN were very similar, where m^7G-capped RNAs showed a sevenfold increase in the Nluc activity compared to A-capped RNAs and N showed at least a 12 times increased in the Nluc activity over BN (see Figure 3.32, C).

In general, when bicistronic RNAs were transfected in cells, m^7G-capped RNAs showed at least a fivefold increase in the activity of both Fluc and Nluc compared to A-capped RNAs (see Figure 3.32, D and E). The Fluc activity when the transfections were done for 6 and 24 hours suffered small variations between the 10% and the 50%, however cells transfected for 24 hours showed an eightfold increase in their Nluc activity compared to cells transfected for 6 hours (see Figure 3.32, D and E). When cells were transfected for 6 hours, A-capped FN showed double the Fluc activity than the Nluc activity, however when the transfection was done for 24 hours Nluc showed 3 times more activity than Fluc, which could be because Nluc has a higher half-life than Fluc[271]. In both cases, cells transfected with A-FBN showed over double the Nluc activity than Fluc activity. Cells transfected with RNAs containing an m^7G-cap showed a higher Fluc activity than Nluc activity when the transfection was done for 6 hours, however when it was done for 24 hours their Nluc activity was stronger. Cells transfected with m^7G FN and FBN showed a very similar Fluc activity when transfections were done for 6 hours, however cells transfected with FBN showed over five times more Nluc activity (see Figure 3.32, D). When transfections were done for 24 hours, cells transfected with FBN showed over five times more Nluc activity than cells transfected with FN (see Figure 3.32, E).

RRL programmed with bicistronic A-capped RNAs showed at least four times more Nluc activity than Fluc activity (see Figure 3.32, F). The Fluc activity between FN and FBN programmed RRL only differed in a 30% in favour of FBN, however FN programmed RRLs showed three times more Nluc activity. RRL programmed with m^7G-FN RNA showed a 70% higher Fluc expression and a twofold increase in the Nluc expression compared to m^7G-FBN programmed RRL. However the levels of Fluc and Nluc of RRL programmed with FN were very similar, and the same happened with RRL programmed with FBN.

In every cell transfection, FBN showed at least three times more Nluc to Fluc ratio and thereby IRES activity than FN. The difference between the Nluc to Fluc ratio of cells transfected with FBN and FN was double when transfections were done for 6 hours compared to when transfections were done for 24 hours, however the ratios were very similar in cells transfected with A-capped or m^7G-capped RNAs (see Figure 3.33, A and B). RRL programmed with FN showed at least a 50% higher Nluc to Fluc ratio than RRL programmed with FBN (see Figure 3.33, C). RRL programmed with A-FN showed an Nluc to Fluc ratio 16 times stronger than RRL programmed with m^7G-FN and A-FBN showed over a fivefold increase in its Nluc to Fluc ratio compared to m^7G-FBN.

Overall we could say that in cells m^7G-cappped RNAs were translated more efficiently than the A-capped ones, as expected. In the case of the monocistronic RNAs, the presence of the *BAG1* 5' UTR reduced the Nluc activity, whereas in the case of the bicistronic constructs it increased it. This could be because the 5' UTR, where the putative IRES is located, is highly structured and ribosomal scanning of ribosomes translating *via* the canonical pathway could get stopped in the presence of such a highly structured sequence, whereas in the bicistronic RNAs the IRES could exercise its function. RRL and cells showed the same trend in the presence of monocistronic and A-capped bicistronic RNAs, however no differences were observed in the Fluc and Nluc activities where RRL were programmed with m^7G-capped RNAs. In terms of the Nluc to Fluc ratio, which corresponds to the IRES activity, FBN always showed a higher Nluc to Fluc ratio than FN, which could be explained by the presence of an IRES in the *BAG1* 5' UTR. In RRL FBN did not show a higher Nluc to Fluc ratio than FN, but this could be due to the lack of ITAFs present in the RRL system that are required for the functioning of the *BAG1* IRES.

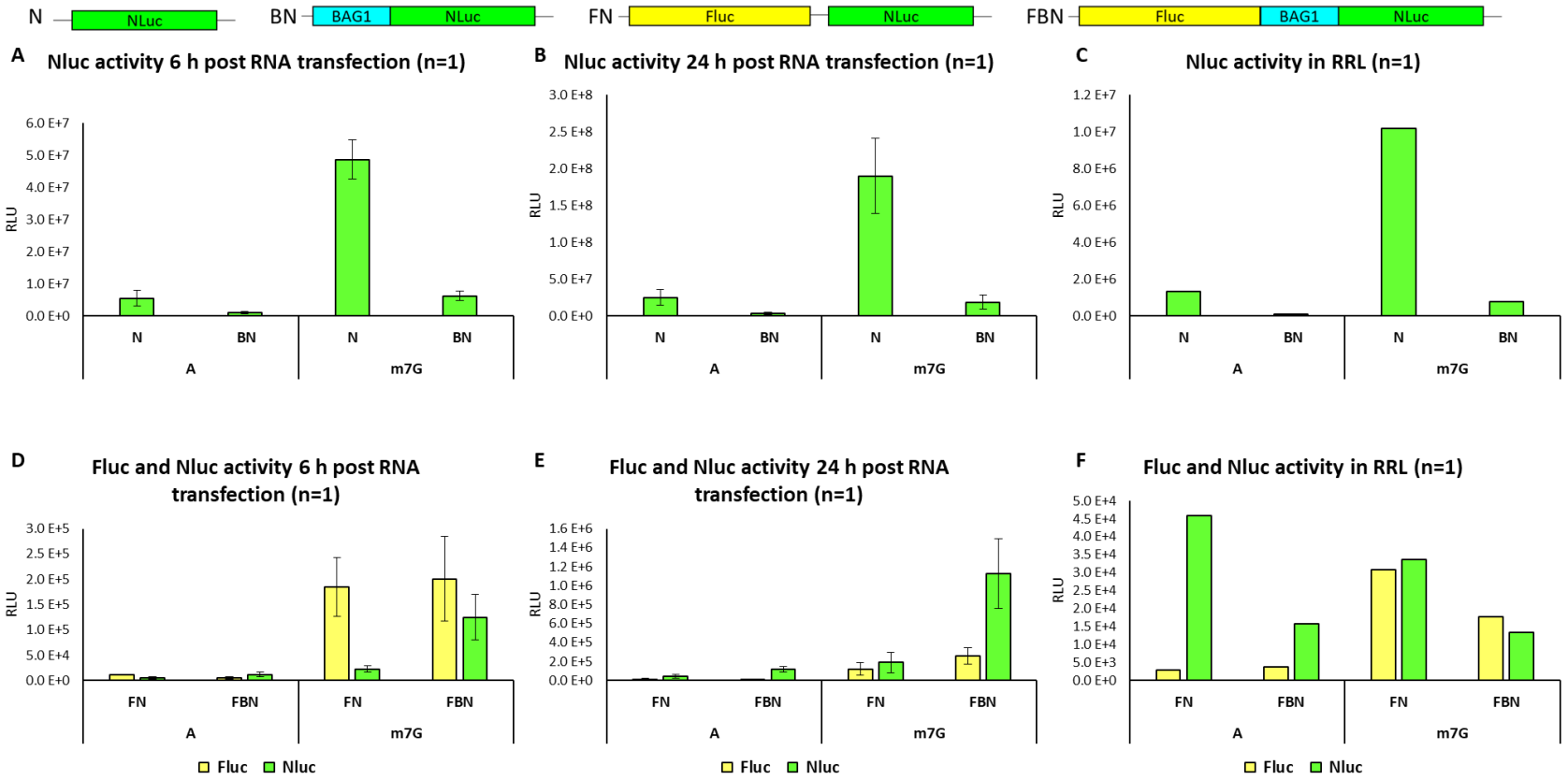

Figure 3.32 **Fluc and Nluc activity of cells transfected and RRL programmed with A-capped and m^{7}G-capped bicistronic mRNAs**. Nluc activity of cells transfected with A and m^{7}G-capped monocistronic RNAs measured 6 hours and 24 hours after the transfection in HEK293 cells (A and B) and in RRL (C). Fluc and Nluc activity was measured 6 and 24 hours after RNA transfection in HEK293 cells (C and D) and in RRL (F). Error bars show ± SD

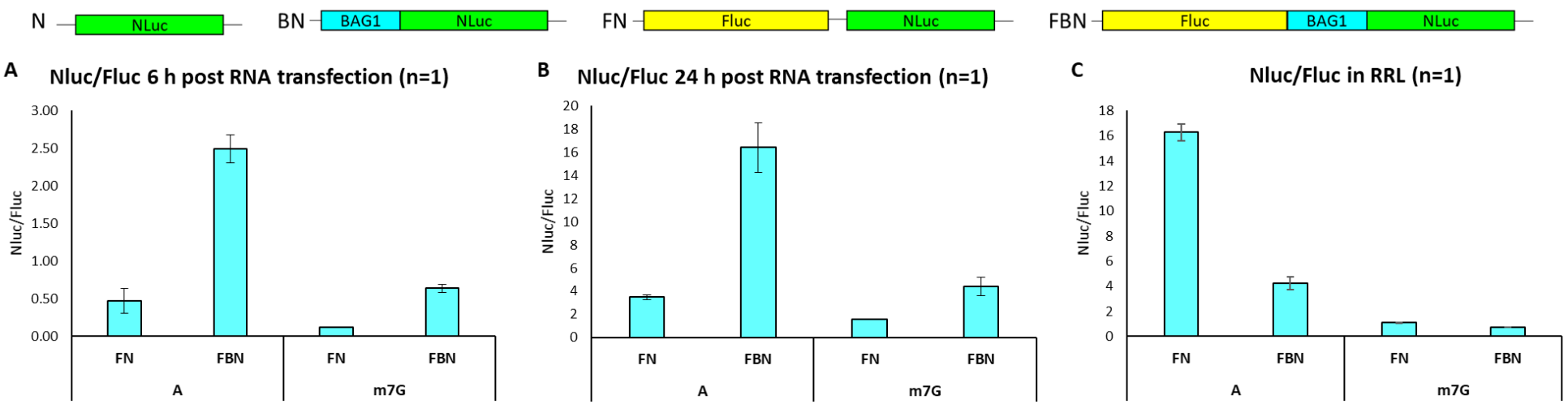

Figure 3.33 **Nluc to Fluc ratio of cells transfected and RRL programmed with A-capped and m^{7}G-capped bicistronic mRNAs.** Nluc/Fluc was measured 6 and 24 hours after RNA transfection in HEK293 cells (A and B) and in RRL (C). Error bars show ± SD

3.10 DISCUSSION

The first aim of the research was to verify the presence of an IRES in the *BAG1* 5' UTR. Since IRESs were discovered in viruses[67,68], the existence of cellular IRESs has been questioned [35,51,109–113]. In eukaryotes translation is usually started by a method known as cap-dependent translation initiation, but in some cases, when this method is compromised, translation can be started from an IRES[52]. IRESs are located in the 5' UTR of the mRNAs, close to the start codon and are able to bypass some of the control steps required in cap-dependent translation initiation as they are able to recruit 40S ribosomes and start translation from the point where they are located[66]. There is a lot of controversy in the world of cellular IRESs and discrepancies about how the presence of an IRES should be demonstrated[79,105,272,273]. That is why in 2016, Terenin *et al.*[36] suggested a step by step method to demonstrate the existence of an IRES in a determined gene.

We have focused our research on the *BAG1* gene. In 2001 Coldwell *et al.*[144] showed the presence of an IRES in the *BAG1* mRNA that could translate the p36 isoform of this gene. It needs to be specified that p36 is mainly translated via cap-mediated translation. Coldwell *et al.* did rigorous research to determine the presence of the IRES at the time, but they did not follow all the steps proposed by Terenin *et al.*[36], which would be expected prior to publication at the current time. In this chapter, we have therefore extended the earlier work and adopted the approaches suggested by Terenin *et al.*[36], to validate the presence of an IRES in the *BAG1* 5' UTR.

DUAL LUCIFERASE REPORTER ASSAY

Once there is some evidence that a certain mRNA could have an IRES (e.g. long and highly structured 5' UTRs, uncommon translation patterns), the first experiment to be done is a bicistronic assay, where the 5' UTR containing the putative IRES is located between two reporter genes, with the pRF dual luciferase vector commonly used. Cap-mediated translation is measured by the activity of the first cistron. At least one stop codon is located at the end of the first cistron, in that way, any activity detected from expression of the reporter in the second cistron should be due to the IRES activity.

We constructed the plasmid pFBN, where the *BAG1* 5' UTR containing the putative IRES was located between the Fluc and Nluc reporter genes. All the experiments carried out were compared to the plasmid pFN, containing the Fluc and Nluc reporter genes but lacking the *BAG1* 5' UTR.

Both plasmids were transfected in HeLa cells five times and the Nluc and Fluc activities were measured. pFBN showed a higher Nluc activity than pFN, as well as a significantly higher Nluc to

Fluc ratio, showing that something in the *BAG1* 5' UTR had the ability to facilitate translation of Nluc. These results suggested that an IRES could be present in the *BAG1* 5' UTR.

In this experiment pFN showed some Nluc activity, which was almost half of what pFBN showed. pFN had three stop codons after the Fluc ORF, so any Nluc signal detected could be due to the presence of cryptic promoters or ribosome reinitiation.

In previous studies the presence of cryptic promoters had been demonstrated in the plasmids used in bicistronic assays to study IRES elements[274] and it has been previously shown that the Fluc gene contains a cryptic promoter[275], however this should have been removed in the pGL4.13SV40 vector as it was designed by Promega to reduce anomalous transcription[262]. To check the presence of cryptic promoters in our vector, the SV40 promoter was removed from all the constructs made. Promoterless vectors (pN no SV40, pBN no SV40, pFN no SV40 and pFBN no SV40) were transfected in HeLa cells and luminescence activity was measured for Fluc and Nluc. In all the cases, the Fluc signal was lost, but it was still possible to detect some Nluc signal, this suggested the presence of at least one cryptic promoter. In the presence of the *BAG1* 5' UTR, the detected Nluc signal was almost double that in the absence of the *BAG1* 5' UTR. This suggested that one of the cryptic promoters at least could be located anywhere between the SV40 promoter sequence and the start of the *BAG1* 5' UTR sequence. We could not discard the presence of cryptic promoters within the sequence of *BAG1* 5' UTR. We know it is not located before the SV40 promoter sequence, as if that was the case we would get some Fluc expression. The presence of that cryptic promoter would transcribe a monocistronic mRNA with the Nluc present on it. If the cryptic promoter was upstream of the *BAG1* 5' UTR sequence, the putative IRES present there could also modify the levels of Nluc (see Figure 3.34). The Nluc expression in the promoterless vectors was over 100 times smaller than in the vectors with the SV40, which suggested cryptic promoters were weak.

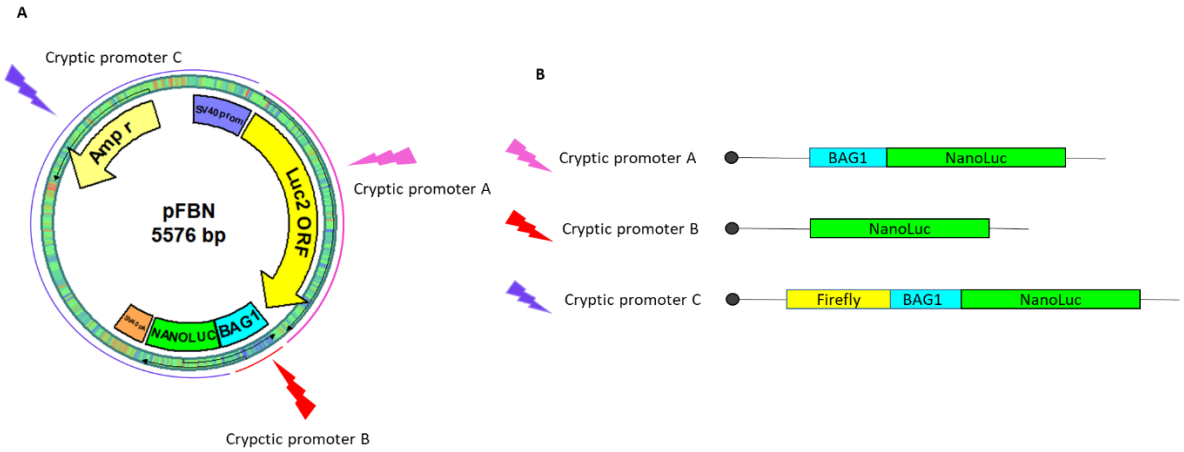

Figure 3.34 **A) Representation of the possible locations of the cryptic promoters in the plasmids.** Cryptic promoter A represents any cryptic promoter located anywhere between the SV40 promoter and the *BAG1* 5' UTR sequence. Cryptic promoters present in the *BAG1* 5' UTR sequence are represented by cryptic promoter B. Cryptic promoter C represents any cryptic promoter present upstream of the Fluc ORF. pFBN is represented, but the idea could be used for any of the other constructs. **B) Representation of the mRNA transcribed if cryptic promoter A, B or C were present.**

phpBN was constructed to inhibit or drastically reduce cap-mediated translation and reduce the effects of the cryptic promoters (it would not affect cryptic promoter B) by introducing a strong stem-loop sequence forming a hairpin just upstream the *BAG1* 5' UTR. phpN was also constructed as a control. The results obtained when transfecting HEK293 cells with both phpBN and phpN showed that the hairpin strongly inhibited cap-mediated translation. In phpBN there was something that recovered the Nluc expression when compared to phpN. A strong suggestion is that the sequence recovering the Nluc expression is present in the *BAG1* 5' UTR, and it could be the IRES proposed by Coldwell *et al* [144].

The second aim of the construction of all these plasmids was to use them to study how the oligonucleotides designed could modify the IRES activity in subsequent chapters. The difference in the Fluc and Nluc measurements in each experiment suggested that the transfection efficiency was not consistent. The ratio Nluc to Fluc also suffered some changes from one experiment to another, but the proportion was kept consistent, which meant that the assay was useful if all the appropriate controls were used.

These results confirmed that the use of pFBN and phpBN in combination with pGL4.13SV40 were a good model to do some preliminary studies about how the oligonucleotides behaved when transfected into cells. We need to keep in mind that those plasmids have some weak cryptic promoters present and that the hairpin in phpBN is not 100% effective.

IRES ACTIVITY IN CELL FREE *IN VITRO* SYSTEMS: TNT AND RRL

IRES activity was also studied *in vitro* using a cell free *in vitro* transcription and translation system (TnT) and by synthesising the RNA *in vitro* and using a cell free *in vitro* transcription system (RRL). Not many people have studied IRES activity in RRL or TnT, and only few of them have proven in repeated occasions to be active in these cell free systems as the EMVC and FMDV IRESs[269]. Others have shown to be against the use of RRL to study IRES activity, as these systems do not always reproduce the behaviour of these IRESs in cells[36].

TnT lysates were programed with DNA sequences amplified from pFBN, pFN, pBN, pN and pGL4.13SV40 containing the sequence of the two full reporter genes (Fluc and Nluc) and the *BAG1* 5' UTR when corresponded. A T7 promoter was incorporated into each of the sequences to facilitate T7 RNA polymerase-driven transcription. As a control, no T7 promoter constructs were also made. RRL were programmed with the same sequences after *in vitro* transcription from them, to determine if any components could give signals in the reporter assays.

When the RNA was transcribed, the RNA transcribed from DNA lacking the T7 promoter did not show any band in the agarose gel done to check for the correct size of the RNA, whereas the RNA transcribed from DNA containing the T7 promoter showed clear bands of the expected sizes. These results showed that the presence of the T7 promoter is vital for the correct transcription of the RNA via the method used (T7 RNA polymerase).

Surprisingly, DNAs lacking the T7 promoter showed some Nluc activity in TnT (but this was relatively undetectable when compared to the DNAs containing the T7 promoter). The DNA sequences were studied to identify any possible T7 promoter or any sequence with high similarity to the T7 promoter after the Fluc ORF, but no sequences were found. The sequences from pBN and pN lacking the T7 promoter had a sequence of only 60 nucleotides from the 5' of the primer until the 5' of the Nluc ORF with no similarity to the sequence of the T7 promoter and they also showed some Nluc activity. This could be due to an artefact of the TnT system being a bit dysregulated for transcription plus the ultra-sensitivity of the Nluc light signal or due to the breakdown of the furimazine in the TnT lysate.

pFN showed a high Nluc activity in TnT and in RRL. We verified the presence of a unique band of the correct size in the *in vitro* transcribed FN RNA, proving that any Nluc activity detected was due to ribosome reinitiation or to the fact that once the RNA was transfected, this could have been cleaved into two monocistronic sequences containing the full Fluc ORF and Nluc ORF.

The Nluc activity did not show an increase in pFBN when compared to pFN in TnT or RRL, suggesting there was no *BAG1* IRES activity in either of the systems. This could be due to the lack

of ITAFs required for the correct functioning of the IRES. These results corroborate the results obtained by Pickering *et al.*[95], where they also showed that the *BAG1* IRES was not active in RRL unless the RRL were stimulated with PTBP1 and PCBP1. The fact that no IRES activity was detected could make TnT and RRL useful systems to study whether the oligonucleotides could be used to increase the IRES activity.

RNA TRANSFECTION IN CELLS

The *in vitro* transcribed RNA that was used to program RRL was also transfected in HEK293 cells and the Fluc and Nluc activity was measured 6 and 24 hours after transfection. Cells transfected with FBN showed a higher Nluc to Fluc ratio than cells transfected with FN in both cases, but it was more obvious 24 hours after transfection. These results showed that there must be something in the *BAG1* 5' UTR that increases the Nluc translation, ideally an IRES.

We looked for the last proof of evidence of the *BAG1* IRES existence by doing the ultimate experiment proposed by Terenin *et al*[36]. We *in vitro* transcribed the sequences containing the Fluc and Nluc ORFs and *BAG1* 5' UTR (when competent) of FBN, FN, BN, N and GL4.13SV40 with an A-cap (non-functional) and m^7G-cap (functional) and a poly(A) tail was added to the capped RNAs. We then transfected the RNAs in HEK293 cells to study the Fluc and Nluc activity.

We first verified that the cap analogues and poly(A) tails were correctly inserted by analysing the activity of Fluc and Nluc in cells transfected with FBN and FN in the presence and absence of an m^7G-cap and a poly(A) tail. This experiment showed that the technique used to introduce the m^7G-cap and poly(A) tail in the RNAs was efficient. We also showed that the addition of both an m^7G-cap and a poly(A) tail increased the translation of *in vitro* synthesised RNAs and that the presence of an m^7G-cap increased the translation levels more than the presence of a poly(A) tail.

m^7G-capped RNAs were translated at least five times more efficiently than A-capped RNAs, this was expected as the A-cap is non-functional. There was not a big difference in the Fluc activities of cells transfected with FBN and FN when compared among A-capped and m^7G-capped RNAs, but cells transfected with FBN always showed at least three times more Nluc activity. These results suggested that there must be an IRES present in the *BAG1* 5' UTR to increase the Nluc activity.

m^7G-capped and A-capped RNAs were also used to program RRL. In this case again, RRL programmed with FBN did not increase the Nluc activity when compared to RRL programmed with FN, which suggested that the presence of a cap analogue and a poly(A)tail did not affect the IRES activity and it kept the IRES inactive.

The uncertainty about the presence of the IRES in *BAG1* was therefore examined by doing some exhaustive experiments. The steps suggested by Terenin *et al.*[36] were followed (with some modifications) in order for us to make a definitive conclusion about the existence of the *BAG1* IRES. p36 is the most expressed BAG1 isoform, but to be translated, the ribosomes need to bypass several possible start codons, some of them in frame and in a good Kozak consensus. This fact strongly suggests that there must be something in the 5' UTR, most probably some kind of structure, that increases translation through that point, and with all these experiments we have successfully concluded the presence of the *BAG1* IRES.

Chapter 4 OPTIMIZATION OF THE OLIGONUCLEOTIDE TRANSFECTION PROTOCOL

4.1 INTRODUCTION

The aim of the project was to use oligonucleotides to control gene expression at the level of translation of genes with IRES elements, in particular the *BAG1* IRES. To do so, we designed a bicistronic plasmid (pFBN) (Figure 4.1, A), where the *BAG1* 5' UTR containing the IRES was cloned between Fluc and Nluc reporter genes. In this way, any Nluc signal detected would be mainly due to the IRES activity. When using the oligonucleotides to control the *BAG1* IRES activity, Nluc expression could easily be measured and oligonucleotide activity could be assessed.

To avoid problems caused by bicistronic plasmids (the presence of cryptic promoters mainly), the monocistronic plasmid phpBN was constructed (Figure 4.1, B), where a strong hairpin was inserted just upstream of the *BAG1* 5' UTR. This hairpin strongly inhibited any cap-mediated translation, which means that most of the Nluc activity detected was due to the IRES (more information about the hairpin can be found in section 3.5 on page 98). Oligonucleotides were then co-transfected with phpBN and their activity was easily assessed by measuring the expression of Nluc.

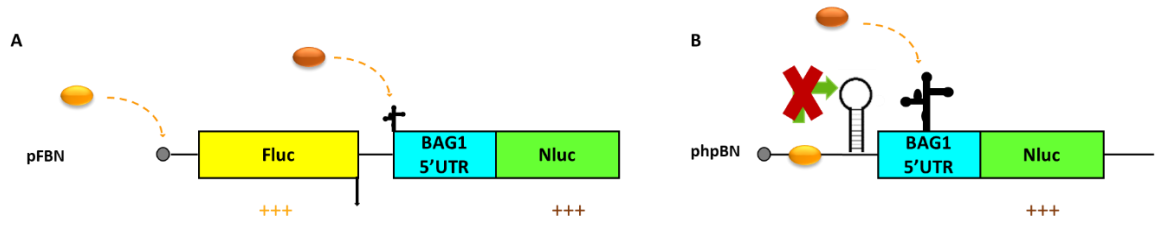

Figure 4.1 **A) pFBN and B) phpBN representation.** In pFBN, ribosomes will initiate translation of Fluc in a cap-dependent way and translation will be finished after the three stop codons present at the end of the Fluc ORF. Due to the presence of an IRES in the *BAG1* 5' UTR, ribosomes can start translation through that point and translate Nluc in an IRES-dependent way. In phpBN, the presence of a hairpin upstream the *BAG1* 5' UTR blocks cap-mediated translation. Most of the Nluc activity detected will be due to the IRES activity.

We also tried to study the effect of the oligonucleotides in the native *BAG1* activity. In this case western blots were carried out and qPCRs to make sure any effect in the BAG1 protein levels was due to modifications in the level of translation.

Following these initial results, we embarked on experiments to optimise the transfection protocol for each of the systems used, to get results in the most time and cost effective way. To optimise the protocol all the possible variables in the protocol were modified in different ways. The modified variables were the following ones:

- Cell line used in the experiments.
- Number of cells seeded.
- Duration of the transfection.
- Transfection reagent used.
- Concentration of oligonucleotide used.
- Concentration of transfection reagent used.

4.2 CHOOSING THE CELLS TO USE TO TRANSFECT THE OLIGONUCLEOTIDES

When Coldwell *et al.*[144] discovered the *BAG1* IRES, all the experiments were done in HeLa cells. Later, Pickering *et al.*[95] studied IRES activity in different cell lines. Both HeLa and HEK293 cells showed similar IRES activity results (HEK293 cells had a slightly higher IRES activity). Previous experience in the lab group had shown that transfection efficiency of plasmids was higher in HEK293 cells than in HeLa cells, and as the IRES activity was very similar in both cell lines, we decided to start with the study of the activity of the oligonucleotides using HEK293 cells.

4.3 SEEDING DIFFERENT NUMBERS OF CELLS

The number of HEK293 cells seeded for the experiment was also modified, as translation rates have been shown to decrease once cells reach confluency[276]. In a 96 well plate, 2 000 cells, 5 000 cells, 7 000 cells and 10 000 cells were plated out. Cells were transfected 24 hours after seeding them and were monitored every 24 hours after transfection. 2 days after transfection the wells where 7 000 cells and 10 000 cells had been transfected were over 90% confluent. 3 days after the cells had been transfected only the wells where 2 000 cells had been seeded presented around an 80% of confluency, while the rest of them were 100% confluent.

These experiments should be done when the cells present 60% to 80% of confluency. A high level of confluency could stress the cells and show anomalous translation levels.

With these results it was concluded that the optimal seeding number of HEK293 cells in a 96 well plate is 2 000. This amount was extrapolated accordingly when cells were seeded in plates with larger growth surface areas.

4.4 DETERMINING TRANSFECTION EFFICIENCY BY FLUORESCENT MICROSCOPY

The first experiment done was to verify that the transfection efficiency of the oligonucleotides in HEK293 cells was good. We did an extensive literature research to decide the amount of oligonucleotide to transfect and the length of the transfection experiment. Based on the oligonucleotide dose used in the literature to achieve similar objectives, we decided to transfect a final concentration of 25 nM of oligonucleotide for two days.

We designed a fluorescent oligonucleotide (B6FAM, purchased from Sigma-Aldrich (see oligonucleotide sequence in Appendix B). B6FAM was modified with a 6-FAM™ (fluorescein) in the 5'. The excitation maximum of 6-FAM™ is 495 nm, the emission maximum 520 nm and the fluorescent colour is green. In a 24 well plate with coverslips, B6FAM was transfected in HEK293 cells using 2 µl of RiboJuice as explained in material and methods (see section 2.2.3 on page 60) for two days.

Most of the cells showed fluorescent green dots (Figure 4.2), showing that B6FAM was successfully transfected in the cells.

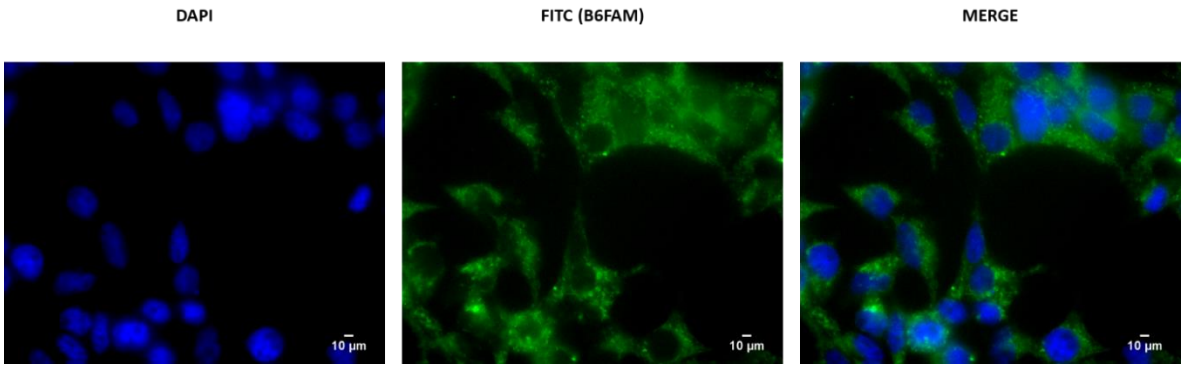

Figure 4.2 **HEK293 cells transfected with B6FAM.** Regions rich in DNA (nucleus) are stained in blue with DAPI, green dots show where B6FAM in present.

4.5 CONTROLS USED IN THE TRANSFECTION OPTIMISATION PROTOCOL

4.5.1 Scramble oligonucleotide

An oligonucleotide with the same chemical properties as the oligonucleotides used, that would not target any gene in the whole human genome was used as the Scramble oligonucleotide. The Scramble oligonucleotides were used as a control to check if the modifications in the Nluc expression being observed were due to the action of the oligonucleotides specifically targeting the 5' UTR of *BAG1* or due to the presence of oligonucleotides (not necessarily targeting *BAG1*) in the system.

The sequence chosen to act as the Scramble oligonucleotide was the sequence from the pSilencer NEG plasmid which gets transcribed and then processed into a double stranded siRNA. The sequence was run through Primer BLAST to verify it did not match any human mRNA targets.

Scramble oligonucleotide sequence:

5'-ACTACCGTTGTTATAGGTGT-3'

4.5.2 BAG1 siRNA as a negative control

A siRNA was designed that would target the *BAG1* IRES (Figure 4.3). As previously explained, siRNAs are double-stranded RNA molecules that act by degrading the mRNA and thereby inhibiting protein expression before translation occurs (more information on siRNAs can be found in section 1.4.4 on page 45). BAG1 siRNA was designed to target the IRES downstream of the putative 40S ribosome binding site and contained overhanging TT dinucleotides, as they have shown to increase the efficiency of siRNAs[277]. The aim of BAG1 siRNA was to use it as a control of BAG1 downregulation via the 5' UTR.

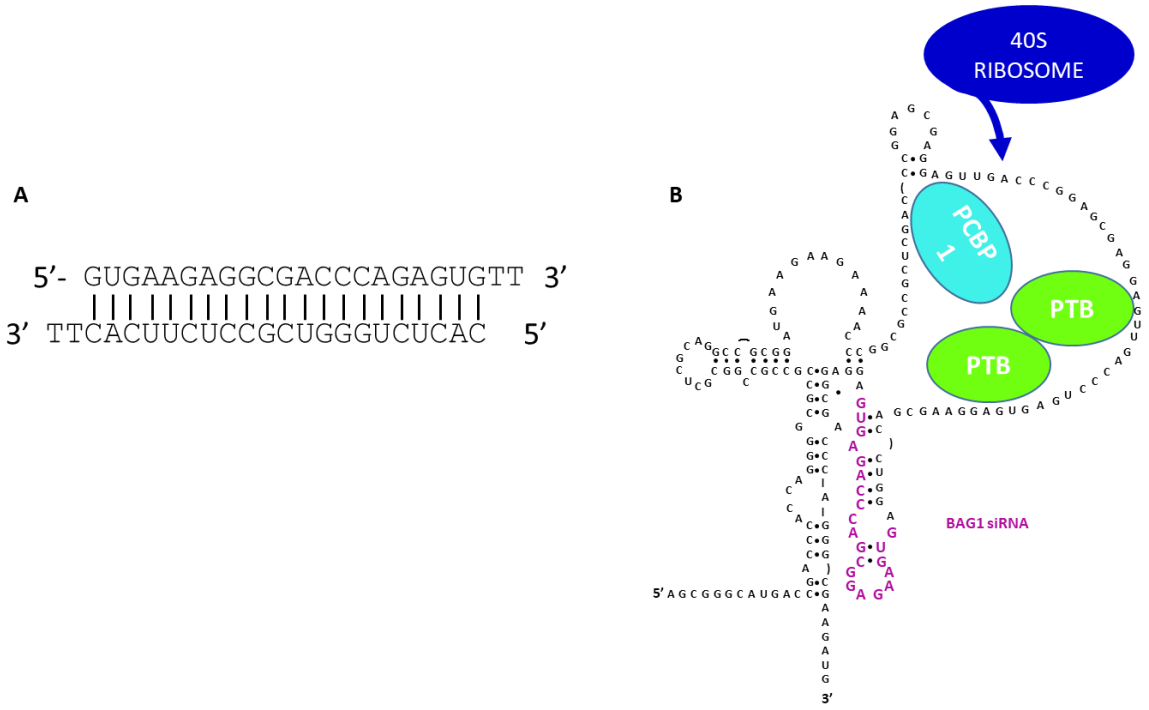

Figure 4.3 **BAG1 siRNA sequence (A) and representation of the *BAG1* IRES, the sequence targeted by the siRNA is represented in fuchsia colour (B).**

4.5.3 SMART pool: ON-TARGET plus Human BAG1 siRNA from Dharmacon (GE Healthcare)

SMART pool: ON-TARGET plus Human BAG1 siRNA (from now on we will refer to it as siRNA pool), is a commercial siRNA pool composed of four different siRNAs targeting different points in the *BAG1* ORF (see the *BAG1* target sequences in Table 4.1). This siRNA pool was used as a more reliable control than the BAG1 siRNA (targeting the 5' UTR of *BAG1*) designed by us (4.5.2).

At this point it needs to be reminded that the aim of the oligonucleotides was to modify the levels of protein expression by modifying translation, thereby keeping the mRNA levels constant. For this reason we needed to avoid the recruitment of RNase H with the oligonucleotides. Using siRNAs (both siRNA pool and BAG1 siRNA) would show the effects it would have in *BAG1* expression the intentional destruction of the mRNA.

Table 4.1 Target sequences of the different siRNAs forming the Smart pool in the *BAG1* ORF.

Target sequence 1	5'-CGAGUGAGGUGUAGCAGAA-3'
Target sequence 2	5'-ACACUGAUCCUGCCAGAAA-3'
Target sequence 3	5'-AAGCACGACCUUCAUGUUA-3'
Target sequence 4	5'-GAAUAAAGAGCUUACUGGA-3'

4.6 TESTING THE EFFICIENCY OF BAG1 siRNA IN CELLS TRANSFECTED WITH PLASMIDS

In this experiment the efficiency of the BAG1 siRNA to downregulate the *BAG1* expression in plasmids was tested with a luciferase assay (see section 2.3 on page 62 for the luciferase reporter assay system protocol).

In a 96 well plate, 2 000 HEK293 cells were seeded per well. The following day 20 ng of plasmid were transfected per well. Some of the plasmid transfections were treated with a final concentration of 10 nM of BAG1 siRNA.

The following transfections were done in triplicate:

- pN+ pGL4.13SV40
- pBN + pGL4.13SV40
- phpN + pGL4.13SV40
- phpBN + pGL4.13SV40
- pN+ pGL4.13SV40 + BAG1 siRNA
- pBN + pGL4.13SV40 + BAG1 siRNA
- phpN + pGL4.13SV40 + BAG1 siRNA
- phpBN + pGL4.13SV40 + BAG1 siRNA

Two days after transfections the luciferase assay was done.

For each of the transfections the Nluc to Fluc ratio was calculated and the average of the triplicate was calculated. These results are shown in Figure 4.4. As the BAG1 siRNA targets the *BAG1* IRES, it should only inhibit the Nluc expression in the vectors where the *BAG1* 5' UTR was cloned (pBN and phpBN). The BAG1 siRNA activity was calculated by comparing the Nluc to Fluc ratios of BAG1 siRNA transfected cells with the Nluc to Fluc ratios of cells not transfected with the BAG1 siRNA with a two tailed T-test ($P<0.05$).

BAG1 siRNA did not have a significant effect in pN+pGL4.13SV40, pBN+pGL4.13SV40 or phpN+pGL4.13SV40. BAG1 siRNA should have had an effect in pBN+pGL4.13SV40, however the high standard deviation values could have affected the statistical analysis and thereby the significance. BAG1 siRNA reduced the Nluc to Fluc ratio in cells transfected with phpBN + pGL4.13SV40 in a significant way, as expected.

With this assay we showed that BAG1 siRNA could effectively decrease the expression of the reporter containing the BAG1 sequence.

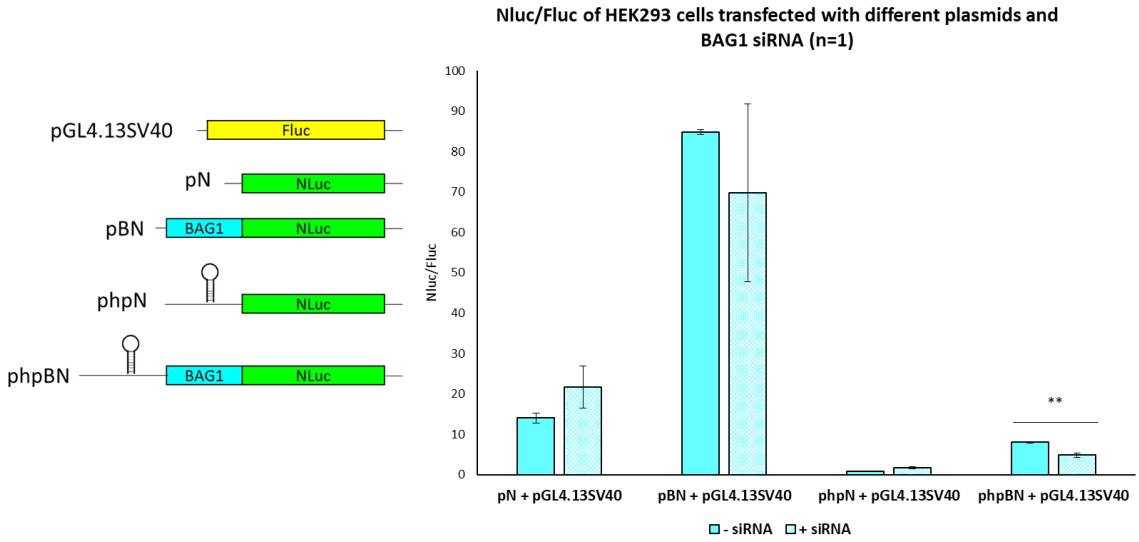

Figure 4.4 **Average Nluc to Fluc ratio of HEK293 cells transfected with the different constructs previously made and the BAG1 siRNA to check the efficiency of the siRNA.** Error bars showing standard deviation values of the triplicate values. Statistical analysis was done with an unpaired T-test (two-tailed) ($p<0.05$).

The Fluc and Nluc activity of the results of this experiment can be found on Appendix D, Figure D.1 on page 288.

4.7 MODIFICATION OF THE OLIGONUCLEOTIDE CONCENTRATION AND THE TRANSFECTION DURATION – LUCIFERASE ASSAY

HEK293 cells were transfected with 10 ng of pGL4.13SV40 and 10 ng of phpBN and a final concentration of 10 nM or 50 nM of oligonucleotides. The oligonucleotides transfected in this occasion were BAG 1, BAG 2, BAG 3 and BAG 4 DNA and LNA-DNA mixmers (see oligonucleotide sequences in Appendix B). The aim was to study the effect of the oligonucleotides in the *BAG1* IRES expression when transfecting cells with different oligonucleotide concentrations during different transfection durations. Transfections were done for two and three days.

This experiment was done just once. For each of the wells the ratio Nluc to Fluc was calculated. The Nluc to Fluc ratios were normalised to the average of the Nluc to Fluc ratio of the control phpBN+pGL4.13SV40 (no oligonucleotide) (see Figure 4.5). Even due the low sample size, a multiple comparisons ANOVA with a Dunnett test was done to compare the Nluc to Fluc ratio of oligonucleotide treated cells normalised to the Nluc to Fluc ratio of phpBN+pGL4.13SV40 cells to phpBN+pGL4.13SV40 (no oligonucleotide) transfected cells. An unpaired T-test (two-tailed) was done to compare the Nluc to Fluc ratio of oligonucleotide transfected cells normalised to the Nluc to Fluc ratio of phpBN+pGL4.13SV40 cells with a final concentration of 10 nM to cells transfected

with a final concentration of 50 nM as well as to compare cells transfected for 2 days with cells transfected for 3 days. $P<0.05$.

When a final oligonucleotide concentration of 10 nM was transfected (for 2 or 3 days) and when a final oligonucleotide concentration of 50 nM were transfected for 2 days, there were no significant differences among the Nluc to Fluc ratios of cells treated with different oligonucleotides, however when a final oligonucleotide of 50 nM was transfected for 3 days, all the oligonucleotide transfected cells showed significantly different Nluc to Fluc ratio from the phpBN+pGL4.13SV40 cells.

In most of the occasions there were no significant differences in the Nluc to Fluc ratio when the transfection timing was increased from 2 to 3 days, however when a final concentration of 10 nM of BAG 1 DNA, BAG 1 LNA and BAG 4 LNA were transfected and when a 50 nM final concentration of BAG 3 LNA were transfected significant differences were observed in the Nluc to Fluc ratio alongside the increase in the transfection timing.

An increase in the final oligonucleotide concentration from 10 nM to 50 nM strongly decreased the Nluc to Fluc ratio of cells transfected with BAG 3 DNA, BAG 4 DNA and BAG 1 LNA for 2 days and that of BAG 2 DNA and BAG 3 LNA for 3 days.

These preliminary results suggested that the 10 nM (final concentration) treatment had a lower effect on the IRES expression than the 50 nM treatment after a three day treatment. The reduction in the Nluc to Fluc ratio was more pronounced when a final concentration of 50 nM was transfected for 3 days. The smaller the Nluc to Fluc ratio, the stronger should be the effect of the oligonucleotides blocking IRES-mediated translation.

It also needs to be considered that the confluency of the cells after a 3 day transfection is greater than after a 2 day transfection, and an increase in the amount of cells to be assayed could induce some kind of stress in the cells making the results less consistent. On the other hand, an increase in the oligonucleotide concentration means that there is an increase in the volume of transfection reagent, inducing more toxicity in the cells, which again could have an effect on the translation levels.

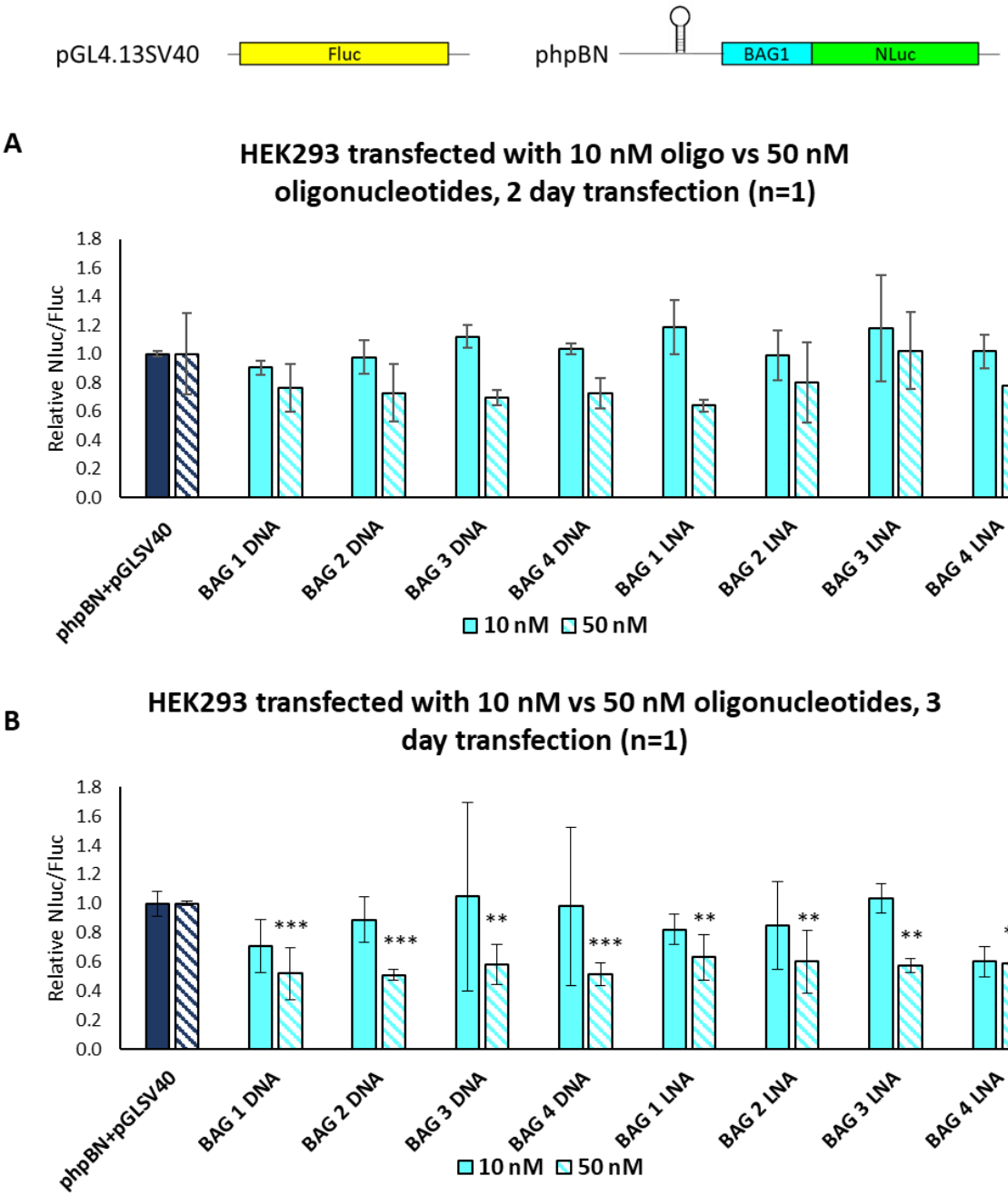

Figure 4.5 **Nluc to Fluc ratio of HEK293 cells transfected with a final concentration of 10 nM and 50 nM of oligonucleotides for 2 (A) and 3 days (B) normalised to the Nluc to Fluc of phpBN+pGL4.13SV40 transfected cells.** Error bars showing standard deviation values of the triplicate values. Statistical analysis was done with a multiple comparisons ANOVA with a Dunnett test to compare the Nluc to Fluc ratio of oligonucleotide treated cells normalised to the Nluc to Fluc ratio of phpBN+pGL4.13SV40 cells to phpBN+pGL4.13SV40 (no oligonucleotide) transfected cells. ($P<0.05$).

The Fluc and Nluc activity of the results of this experiment can be found on Appendix D, Figure D.2 and Figure D.3 on pages 289 and 290 for 2 day and 3 day transfection respectively.

4.8 MODIFYING THE AMOUNT OF RIBOJUICE

To study how the modification of the amount of oligonucleotide transfection reagent (in our case RiboJuice, Merk) could affect the transfection efficiency, a different amount of RiboJuice was used to transfect different concentrations of oligonucleotides. The transfections were done for two and three days. In this case, the oligonucleotide transfected was B1 (see oligonucleotide sequence on Appendix B and targeting site on Figure 4.6).

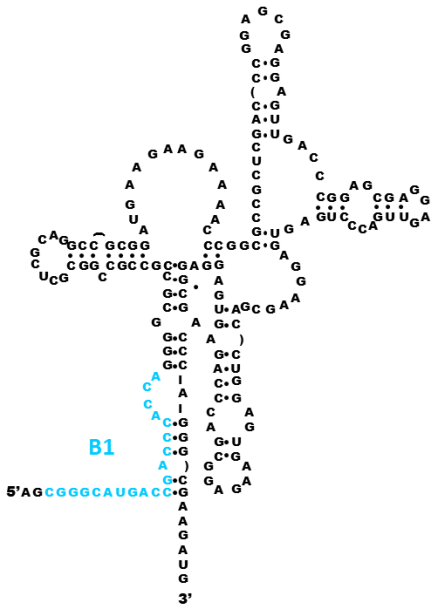

Figure 4.6 **B1 targeting site on the *BAG1* IRES.**

Before this experiment, all the transfections were done based on the first protocol used: 1 µl of RiboJuice was used to transfect a final concentration of 25 nM of oligonucleotide in a well of a 96 well plate. The RiboJuice volume used was scaled up or down with the concentrations of oligonucleotides used.

In this experiment, 10 nM, 25 nM and 50 nM (final concentrations) of B1 were transfected using 0.4 µl, 1 µl and 2 µl of RiboJuice in a 96 well plate (Figure 4.7).

	Increase in the RiboJuice concentration →		
Increase in the concentration of B1 ↓	10 nM B1 0.4 µl RiboJuice	10 nM B1 1 µl RiboJuice	10 nM B1 2 µl RiboJuice
	25 nM B1 0.4 µl RiboJuice	25 nM B1 1 µl RiboJuice	25 nM B1 2 µl RiboJuice
	50 nM B1 0.4 µl RiboJuice	50 nM B1 1 µl RiboJuice	50 nM B1 2 µl RiboJuice

Figure 4.7 **Representation of the B1 transfections done in HEK293 cells using different final concentrations of B1 (10 nM, 25 nM and 50 nM) and different concentrations of RiboJuice (0.4 µl, 1 µl and 2 µl).**

Cells transfected using 2 µl of RiboJuice showed a high toxicity level, independently of the amount of B1 transfected. For this reason, the use of 2 µl of RiboJuice was discontinued.

Each experiment was done three individual times in triplicate. For each of the oligonucleotide transfections the ratio between the Nluc and the Fluc values was calculated and that value was then normalised to the Nluc to Fluc values of phpBN+pGL4.13SV40 transfected cells. The results shown are an average result of the three experiments (Figure 4.8). The results were analysed with a multiple comparison ANOVA with a Tukey's correction ($P<0.05$) to compare the Nluc to Fluc ratio normalised to phpBN+pGL4.13SV40 of each condition among each other.

We compared the Nluc to Fluc ratios normalised to phpBN+pGL4.13SV40 of cells transfected for 2 days vs 3 days under the same conditions. In this case there were no significant differences observed, meaning that an increase in the transfection timing did not have an effect on the oligonucleotide activity.

We also compared the Nluc to Fluc ratio of cells normalised to phpBN+pGL4.13SV40 when the RiboJuice volume was increased from 0.4 µl to 1 µl (see Table 4.2). In this case all the transfection reactions showed to be significantly different, showing that increasing the RiboJuice concentration had an effect in the Nluc to Fluc ratio of the transfected cells.

We also compared the Nluc to Fluc ratio normalised to phpBN+pGL4.13SV40 of cells to compare the Nluc to Fluc ratios when a final concentration of 10 nM, 25 nM or 50 nM of oligonucleotide were transfected. In this case the increase in the oligonucleotide concentration did not show a significant effect in any case.

We also compared the Nluc to Fluc normalised to phpBN+pGL4.13SV40 to the Nluc to Fluc of phpBN+pGL4.13SV40 transfected cells when transfections were done for 2 and 3 days (see Table

4.3). In both cases, all the Nluc to Fluc ratios of cells transfected using 1 µl of RiboJuice showed to be significantly bigger than the Nluc to Fluc of cells transfected with phpBN+pGL4.13SV40.

The results suggested that the volume of RiboJuice used was the factor that modified the Nluc to Fluc ratio of oligonucleotide transfected cells in a stronger way.

The transfections where a final concentration of 50 nM of B1 were used showed the strongest variability and the highest amount of outliers, which is why transfecting a final concentration of 50 nM of oligonucleotide was discontinued.

After this experiment the conclusion was to transfect the oligonucleotides in HEK293 cells for 2 days, transfecting a final concentration of 25 nM of oligonucleotide using 1 µl of RiboJuice (in 96 well plates).

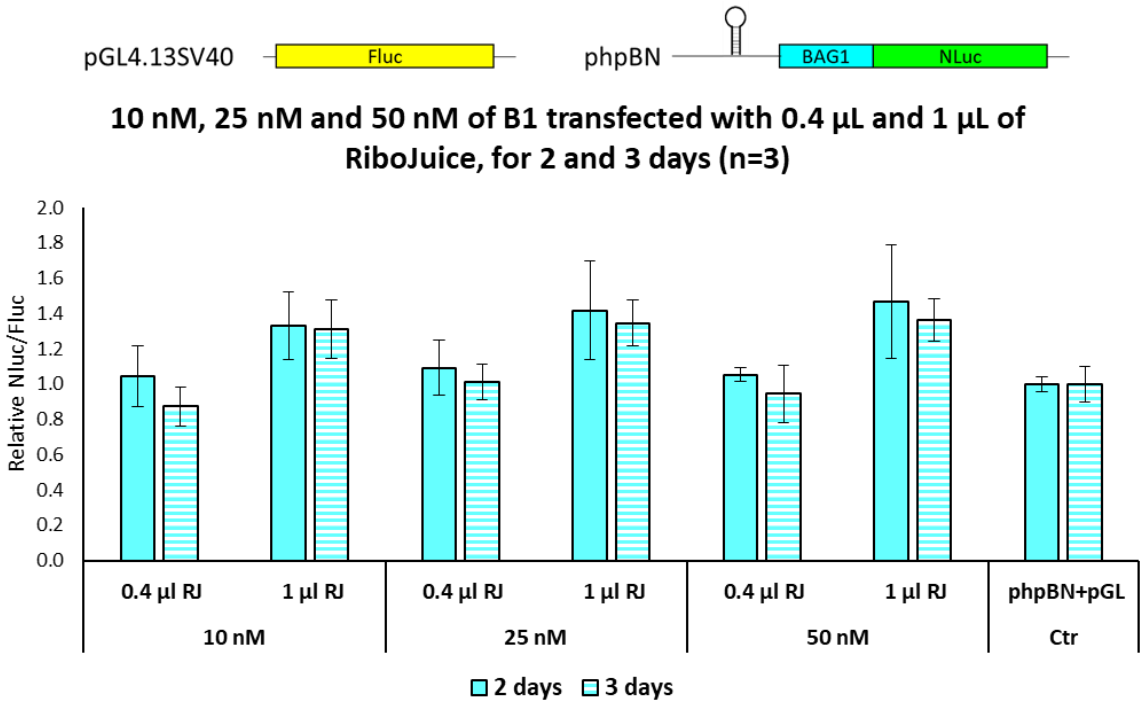

Figure 4.8 **Average Nluc to Fluc expression of HEK293 cells transfected with a final concentration of 10 nM, 25 nM and 50 nM of B1 using 0.4 µl, 1 µl and 2 µl of RiboJuice.** Error bars show standard deviation values of each of the three independent replicates, each of them done in triplicate.

The Fluc and Nluc activity of the results of this experiment can be found on Appendix D, Figure D.4 on page 291.

Table 4.2 A multiple comparison ANOVA with a Tukey's correction analysis result comparing the Nluc to Fluc ratio of cells transfected with the oligonucleotides normalised to the Nluc to Fluc ratio of cells transfected with phpBN+pGL4.13SV40 when the RiboJuice volume was increased from 0.4 µl to 1 µl. P<0.05

CONDITION 1			CONDITION 2			STATISTICAL SIGNIFICANCE
Days of transfection	RiboJuice Volume (µl)	Oligonucleotide final concentration (nM)	Days of transfection	RiboJuice Volume (µl)	Oligonucleotide final concentration (nM)	
2	0.4	10	2	1	10	*
2	0.4	25	2	1	25	**
2	0.4	50	2	1	50	***
3	0.4	10	3	1	10	***
3	0.4	25	3	1	25	*
3	0.4	50	3	1	50	***

Table 4.3 A multiple comparison ANOVA with a Tukey's correction analysis result comparing the Nluc to Fluc ratio of cells transfected with the oligonucleotides normalised to the Nluc to Fluc ratio of cells transfected with phpBN+pGL4.13SV40 with the Nluc to Fluc ratio of cells transfected with phpBN+pGL4.13SV40. P<0.05

	Oligonucleotide final concentration (nM)	RiboJuice Volume (µl)	2 days transfection	3 days transfection
phpBN+ PGL4.13SV40 vs Oligonucleotide	10	0.4	ns	ns
	10	1	**	***
	25	0.4	ns	ns
	25	1	***	****
	50	0.4	ns	ns
	50	1	****	****

4.9 STUDYING ISOFORM EXPRESSION IN UNTRANSFECTED HEK293 CELLS-WESTERN BLOT

The aim of the experiment was to study the level of expression of the different BAG1 isoforms in untransfected HEK293 cells. Different number of cells were plated out (100 000 and 200 000 cells) in 6 cm plates and harvested 3 and 4 days after seeding them, as if they had been harvested 2 and 3 days after transfection. This was done in duplicates, to be able to compare the isoform expression in identical conditions. Western blots were done (Figure 4.9, A) and each of the bands expressing a different BAG1 isoform was quantified. The total amount of BAG1 was also measured and normalised to actin:

$$Total\ \mathrm{BAG1} = p50 + p46 + p36 + p29$$

The percentage of expression of each of the isoforms was measured, x being any of the BAG1 isoforms:

$$\%\ px = \frac{\mathrm{px\ quantification}}{\mathrm{Total\ BAG1}}$$

Looking at the total BAG1 expression a big difference could be observed between identical replicates (Figure 4.9, B). It was only in the experiment where 250 000 cells were seeded and harvested 3 days after the hypothetical transfection, that both duplicates showed the same amount of BAG1. In the rest of the cases (100 000 cells seeded and harvested 2 and 3 days after the hypothetical transfection and 250 000 cells seeded and harvested 2 days after the hypothetical transfection), one of the duplicates showed an expression of *BAG1* 50% higher than the other.

When the expression of the individual isoforms was studied, differences were also found between replicates (Figure 4.9, C). Only the expression of p50 and p36 was analysed here, as the expression of p46 and p29 was smaller in comparison, and p50 and p36 would still give an indication of cap- versus IRES-dependent translation efficiency. When 100 000 cells were seeded and harvested after 2 days of the hypothetical transfection (2-100 A) and when 250 000 cells were seeded and harvested 3 days after the hypothetical transfection (3-250 A), p50 and p36 were expressed at very similar levels. When 250 000 cells were seeded and harvested after 2 days of the hypothetical transfection (2-250 A) and when 250 000 cells were seeded and harvested 3 days after the hypothetical transfection (3-250 B), the levels of p36 were higher than that of p50. However, in the rest of the conditions, the expression of p50 was higher than the p36 isoform.

Our aim was to study the changes in expression of p36 (the only isoform partially translated via the *BAG1* IRES) when oligonucleotides targeting the IRES were used. Unfortunately, western blot is the only technique that allows us to do so, as other techniques widely used to study protein expression (ELISA, for example) would not be able to detect differences in expression of p50, p46, p36 and p29. These results emphasise the fact that western blot is a semi quantitative technique. Therefore, to verify the activity of the oligonucleotides, western blots will need to be repeated several times and we should focus more on the trends of BAG1 isoform expression observed, rather than finite amounts.

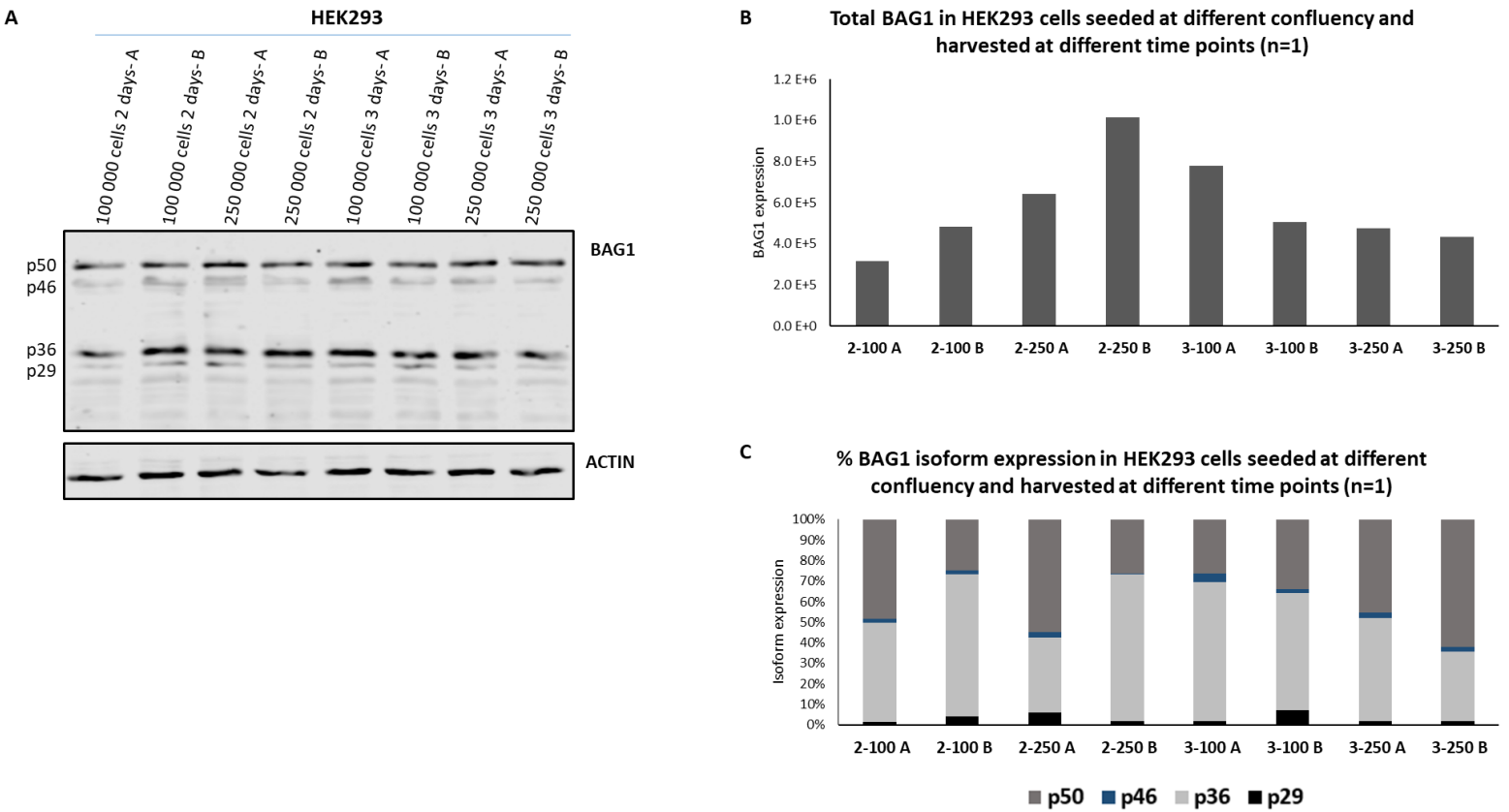

Figure 4.9 **A) *BAG1* expression of HEK293 cells after seeding 100 000 and 250 000 cells and harvesting the cells 2 and 3 days after a hypothetical transfection.** The seeding and harvesting was done in duplicates for each of the individual conditions. **B) Total BAG1 quantification and C) BAG1 isoform quantification of HEK293 cells seeded at different levels and harvested at different times.** Difference in *BAG1* expression were observed among duplicates.

4.10 MODIFYING THE OLIGONUCLEOTIDE CONCENTRATION AND DURATION

In this experiment HEK293 cells were transfected with a final concentration of 10 nM and 25 nM of BAG 1 DNA, BAG1 siRNA, BAG 1 LNA, siRNA pool and the Scramble oligonucleotide (see section 4.5 for more details about BAG1 siRNA, siRNA pool and Scramble oligonucleotide, see Appendix B for oligonucleotide sequences). Cells were harvested 2 and 3 days after transfection.

Looking at the blots (Figure 4.10) it can be seen that the BAG1 siRNA and the siRNA pool had a major effect when a final concentration of 25 nM of each of them was transfected in the cells. There was not a big difference when the transfection period was increased from 2 to 3 days.

The total expression of BAG1 was quantified and normalised to actin (Figure 4.11, A) and the expression of each of the isoforms was quantified after the different oligonucleotides were transfected, however only the expression of p50 and p36 was considered, as they were the most relevant ones (Figure 4.11, B).

Looking at the total expression of BAG1 (Figure 4.11, A), there were no big changes when a final concentration of 10 nM of any of the oligonucleotides were transfected for 2 or 3 days. When a final concentration of 25 nM of BAG1 siRNA and siRNA pool were transfected for 2 or 3 days a significant decrease of over 50% of total BAG1 expression was observed. There was no difference observed when any of the other oligonucleotides were transfected.

The Scramble oligonucleotide did not change the expression of p50 independently of the concentration transfected or the timing of the transfection (Figure 4.11, B). Both BAG1 siRNA and siRNA pool decreased the expression of p50 when a final concentration of 25 nM were transfected, increasing the transfection timing slightly increased the efficiency. BAG 1 DNA increased the p50 expression when a final concentration of 10 nM were transfected for 2 days, it did not have any effect the rest of the occasions. BAG 1 LNA decreased the expression of p50 when a final concentration of 10 nM were transfected for 3 days, and increased its expression when a final concentration of 25 nM were transfected for 3 days. It did not have any effect the rest of the occasions.

Both BAG1 siRNA and siRNA pool decreased the expression of p36 in every transfection, but the decrease was more significant when a higher dose of siRNA was used (Figure 4.11, B). Harvesting the transfected cells after 2 days instead of 3 increased the effect when a concentration of 10 nM

was transfected. When 25 nM were transfected increasing the transfection timing did not make a big difference.

The results provided by BAG 1 LNA and BAG 1 DNA were somehow contradictory, transfecting 10 nM or 25 nM (final concentration) of oligonucleotide gave opposite results, however this could also be due to experimental error. The results provided by both siRNAs were more stable, as they decreased the expression of BAG1 in every occasion. Therefore, the results provided by both siRNAs were used. In this way, it was concluded that transfecting 25 nM (final concentration) of oligonucleotide was more effective than transfecting a final concentration of 10 nM. In terms of the transfection timing, as no big differences were observed when the timing was increased, it was concluded that transfecting cells for 2 days was enough to show the effect of the oligonucleotides.

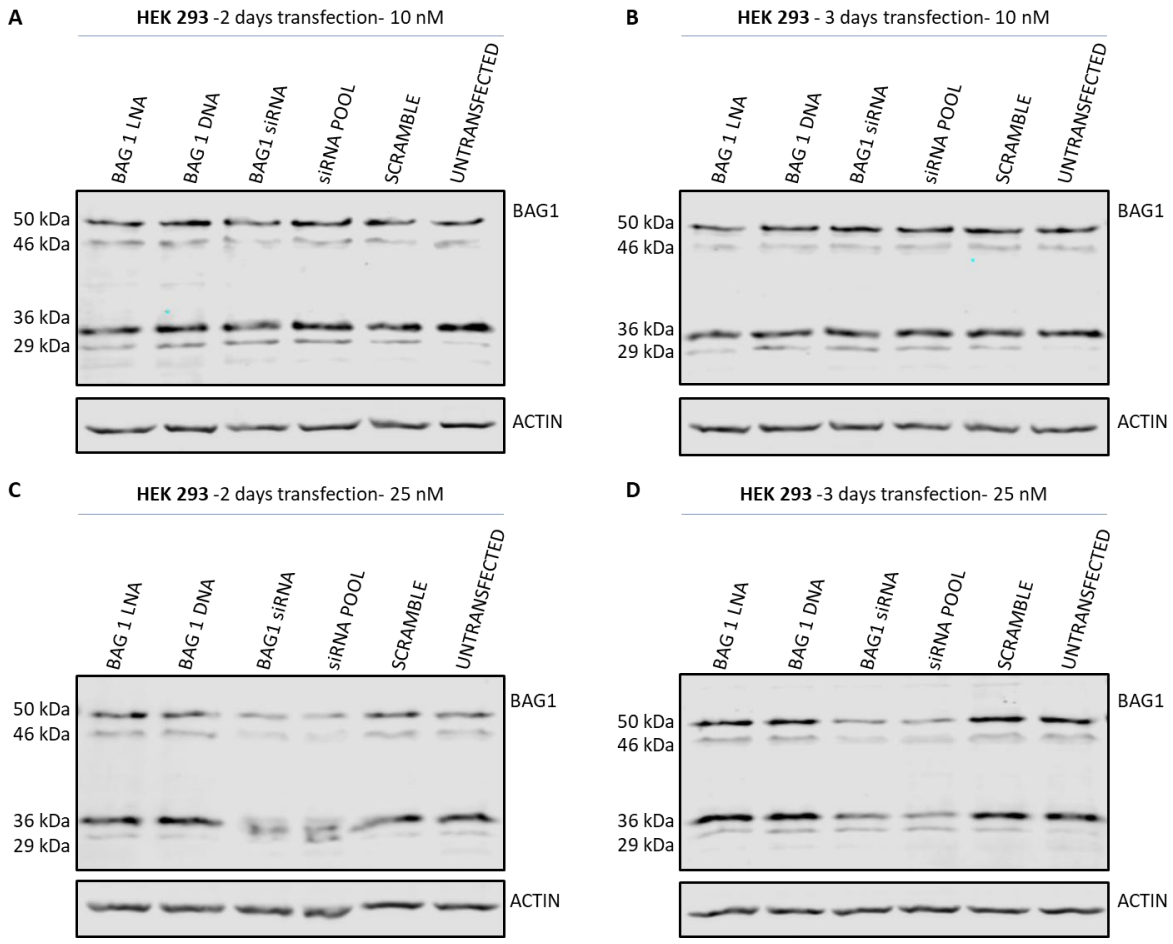

Figure 4.10 **BAG1 expression of HEK293 cells transfected with a final concentration of 10 and 25 nM BAG 1 LNA, BAG 1 DNA, BAG1 siRNA, siRNA pool and Scramble for 2 and 3 days.** When 25 nM of BAG1 siRNA and siRNA pool were transfected for 2 and 3 days a clear decrease in *BAG1* expression was observed.

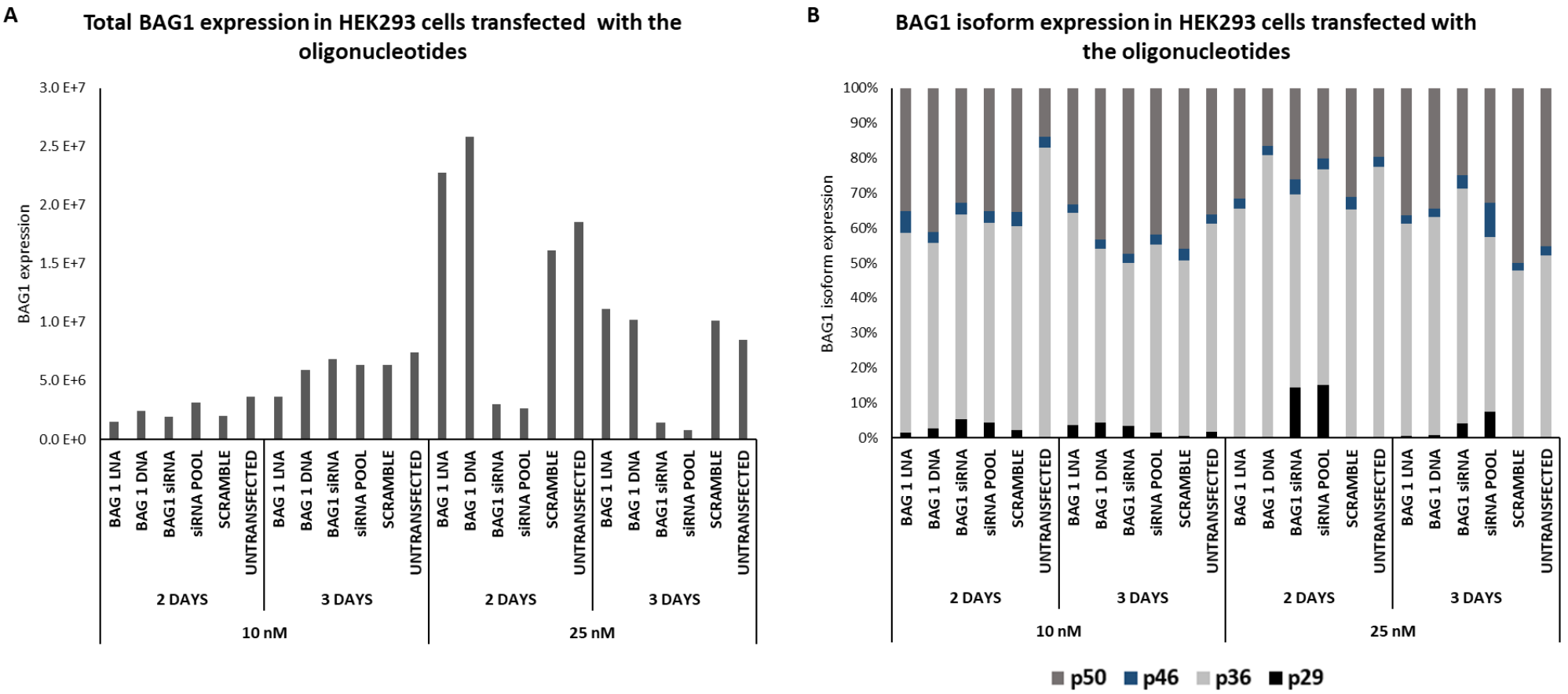

Figure 4.11 **Quantification of the total BAG1 expression (A) and the expression of p50, p46, p36 and p29 (B) after transfecting HEK293 cells with a final concentration of 10 and 25 nM of BAG 1 LNA, BAG 1 DNA, BAG1 siRNA, siRNA pool and Scramble for 2 and 3 days.** Quantified from the western blot in Figure 4.10.

4.11 CONSTRUCTION OF THE STABLE CELL LINE hpBN-HEK

As seen in the previous experiments, transiently transfecting in two plasmids (pGL4.13SV50 and phpBN) as well as the oligonucleotides can lead to variations in experimental replicates. Therefore, with the idea to reduce this variability, a stable cell line expressing Nluc was generated.

A stable HEK293 cell line was generated expressing the hairpin (see section 3.5 on page 98), *BAG1* 5' UTR and Nluc ORF present in phpBN. To make this stable cell line, the lentivirus pLVTHM[278] was used (see Figure 4.13), alongside the packaging plasmid psPAX2 (see Figure 4.15 A) and the envelope plasmid pMD2G (see Figure 4.15 B). The three plasmids were a gift from Didier Trono (Addgene plasmid # 12247, # 12260, # 12259; http://n2t.net/addgene:12247 ; RRID:Addgene_12247)[278]. This lentivirus was chosen as it was the only one available in the lab at the moment. pLVTHM is a second generation lentivector designed to efficiently express shRNA from H1 promoter and containing GFP. H1, alongside U6 and 7SK, is one of the polymerase lll type 3 promoters and it is used for shRNA stable expression in cells. Polymerase lll terminates transcription when it finds a stretch of 4 or more thymidines[279]. This characteristic of the H1 promoter makes it useless for our purpose as there are over fifteen 4T stretches in the phpBN sequence, for that reason the H1 promoter had to be replaced with an appropriate promoter. The use of the pGL4.13SV40 backbone was avoided, as its translation is driven by a SV40 promoter, and this promoter is also present in the pLVTHM lentivirus (Figure 4.13, marked in blue). For this purpose, the hpBN sequence (hairpin, *BAG1* 5' UTR and Nluc ORF) was cloned in the pcDNA 3.1 vector, whose transcription is driven by a CMV promoter.

4.11.1 Construction of pcDNA-hpBN

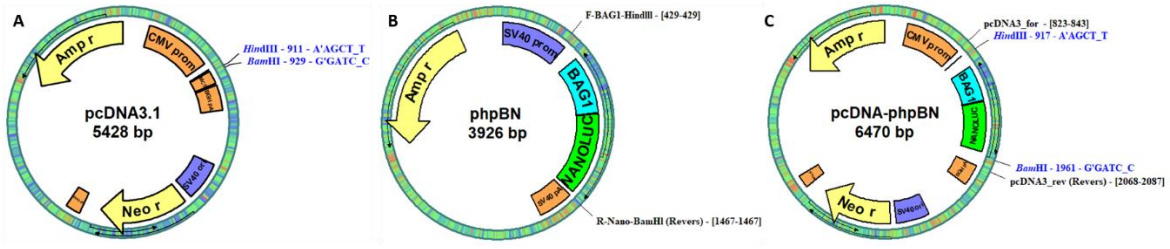

Figure 4.12 **Representation of the construction of pcDNA-phpBN.** A) pcDNA3.1 with the restriction sites used for the cloning BamHI and HindIII highlighted. B) phpBN with the primers used for the cloning highlighted. C) pcDNA-phpBN with the BamHI and HindIII restriction sites used to verify the presence of the insert highlighted, as well as the primers used for the sequencing.

The aim of the experiment was to clone phpBN from the start of the hairpin to the end of the Nluc ORF downstream the CMV promoter in pcDNA 3.1 to form pcDNA-phpBN (Figure 4.12).

Primers were designed to amplify phpBN from the start of the hairpin to the end of the Nluc ORF (Figure 4.12, B). To facilitate the insertion of the amplified products in the pcDNA vector, HindIII and BamHI restriction sites were introduced in the forward and reverse primers respectively. The primers used for the cloning were F-BAG1-HindIII and R-Nano-BamHI (see primer sequences in section 2.1.1.1 on page 52).

pcDNA3.1 was digested first with BamHI and then with HindIII. The fragment desired from phpBN was amplified by PCR as explained in section 2.1.1.1 on page 52.

The amplified product was run in an agarose gel to verify the presence of a unique band of 1020 bp, cleaned-up and digested with BamHI and HindIII. The digested plasmid and digested amplified product were ligated. Competent bacteria were transformed, colonies were picked and minipreps were done. Minipreps were digested with BamHI and HindIII to check the correct cloning of the desired products in the plasmid.

One of the minipreps was sent for sequencing with the primers pcDNA3_for and pcDNA3_rev (see primer sequences in section 2.7 on page 67). The sequencing results showed the phpBN insert was successfully cloned in the pcDNA vector, generating pcDNA-phpBN.

4.11.2 Cloning of the insert of interest from pcDNA-phpBN in pLVTHM

Once pcDNA-phpBN was constructed, the sequence starting from the start of the CMV promoter until the end of the poly(A) tail (Figure 4.14) were cloned in the pLVTHM lentiviral vector between the ClaI and EcoRI restriction sites (Figure 4.13).

The primers used for the amplification of the desired sequence in the pcDNA-phpBN plasmid were F-CMV-MfeI (with an MfeI restriction site) and R-CMVPA-ClaI (with a ClaI restriction site) (Figure 4.14) (for sequences go to section 2.1.1.1 on page 52).

MfeI and EcoRI are compatible enzymes, a sequence digested by MfeI (5'-C'AATTG-3') can be ligated to a sequence digested with EcoRI (5'-G'AATTC-3'). The amplified pcDNA-phpBN product was introduced between the EcoRI and ClaI sites in pLVTHM (see Figure 4.13).

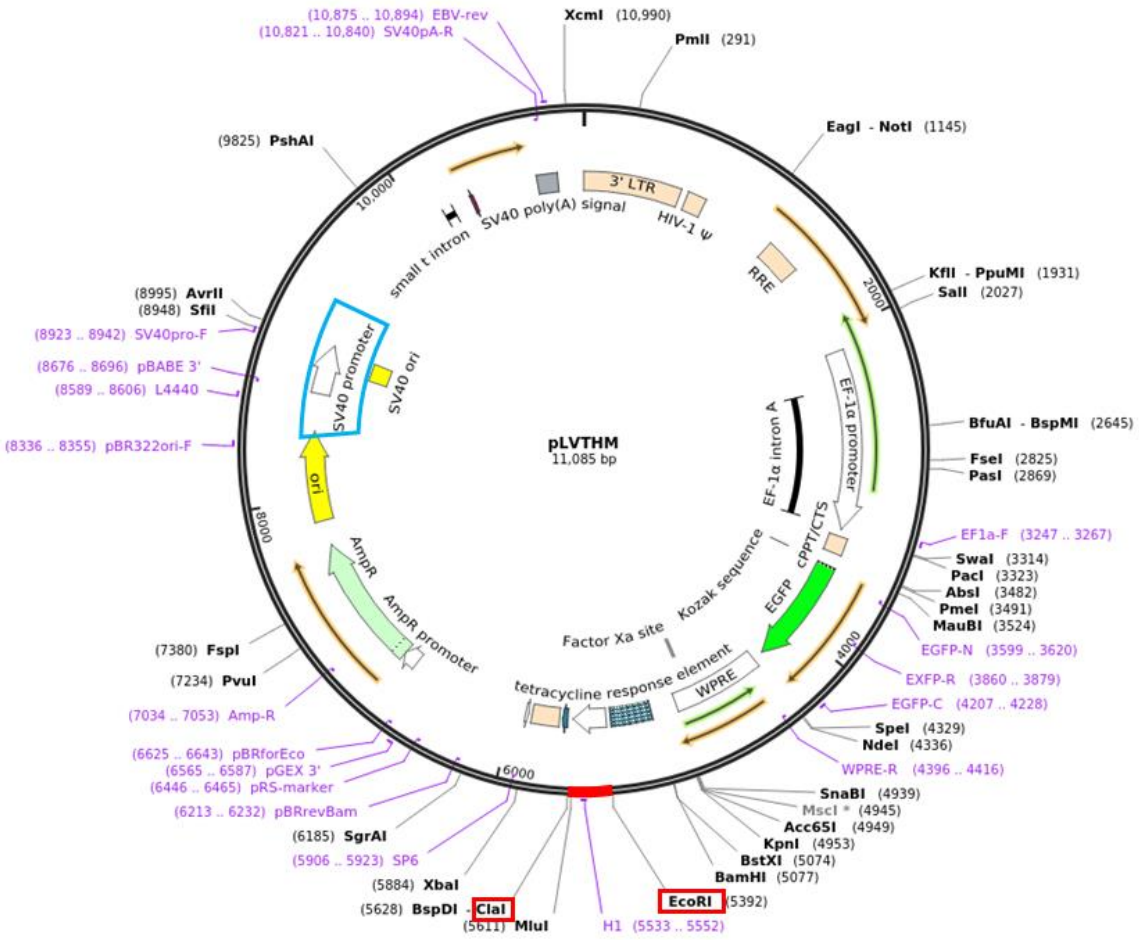

Figure 4.13 **Representation of the pLVTHM lentiviral vector.** SV40 promoter is highlighted in blue. ClaI and EcoRI restriction sites, used to clone the CMV-phpBN sequence, are also highlighted in red.

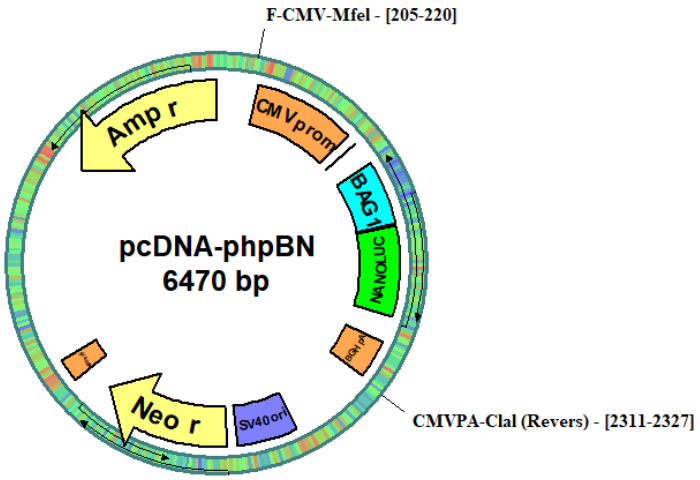

Figure 4.14 **Representation of the pcDNA-phpBN vector with the primers used to clone it in the pLVTHM lentivirus.**

The sequence of interest was amplified from the pcDNA-phpBN vector by PCR as explained in section 2.1.1.1 on page 52. The correct amplification of the sequence was verified by agarose gel electrophoresis.

pLVTHM was digested with EcoRl and Mfel (with this digestion the H1 promoter was removed), and treated with rSAP (see 2.1.1.2 and 2.1.1.3 on pages 53 and 54). The amplified PCR product and the digested lentivirus were cleaned-up (see 2.1.1.14 page 59) and ligated (see 2.1.1.6 page 55). Minipreps were checked by digestion with the restriction enzymes BamHl. The successful results showed two bands of 10890 and 2078 bp respectively.

pLVTHM-phpBN was sent for sequencing using the same primers that were used to amplify the CMV-phpBN insert F-CMV-Mfel and R-CMVPA-Clal (primer sequences can be found in section 2.7 on page 67). Sequencing results verified the presence of the insert in the lentivirus. Sequencing results can be seen in Appendix C.

pLVTHM-phpBN was extracted by midiprep to get plasmid DNA of higher purity.

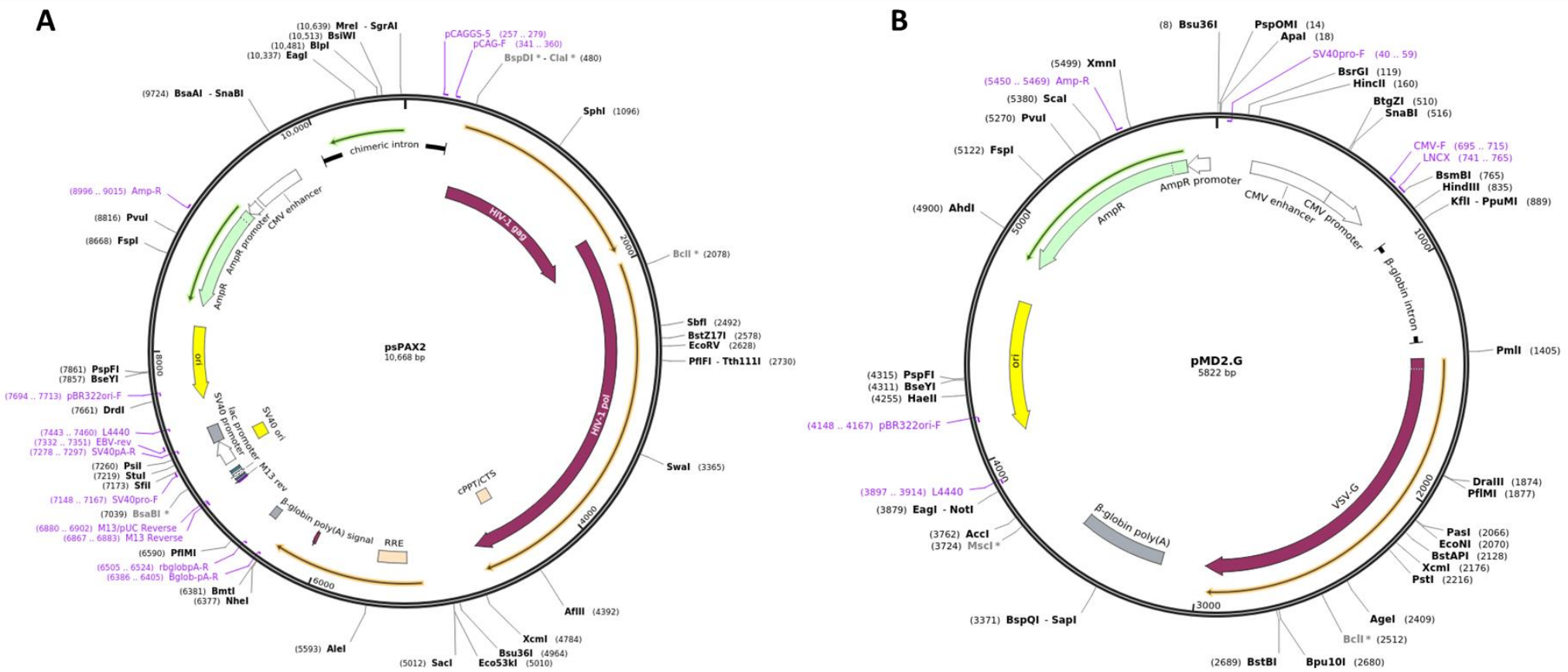

Figure 4.15 **psPAX2 (A) and pMD2-G (B) plasmid representation**.

4.11.3 Stable transfection (transduction) of pLVTHM-phpBN in HEK293 cells.

As previously mentioned, pLVTHM is a second generation lentivirus. To reduce the risks that working with lentiviruses could produce, in the second generation lentiviruses the components needed for the production of a fully functional virus are split across three plasmids: the lentiviral transfer plasmid encoding the insert of interest (pLVTHM-hpBN), the packaging plasmid (psPAX2, see Figure 4.15 A) and the envelope plasmid (pMD2G -expressing VSV-G, see Figure 4.15, B).

In pLVTHM, the transgene sequence (hpBN) is flanked by long terminal repeat (LTR) sequences (see Figure 4.13). These sequences facilitate the integration of the sequence of interest into the host genome. For safety reasons, pLVTHM is replication incompetent and contains a deletion in the 3' LTR that self-inactivates (SIN) the virus after integration. The lentiviral genes that are required for the viral replication are only present in the packaging plasmids (psPAX2 and pMD2G). When the three plasmids (pLVTHM, psPAX2 and pMD2G) are co-transfected in cells, lentiviral particles containing the RNA transcribed from pLVTHM are produced.

SuperFect (Qiagen) was used to transfect HEK293 cells according to the following protocol. On day one, $2x10^6$ HEK293 cells were plated in a 10 cm dish. The following day the 3 plasmids (pLVTHM, pPAX2 and pMD2G) required were transfected with SuperFect: 5 µg of pLVTHM, 3.75 µg of pPAX2 and 1.5 µg of pMD2G were mixed with 260 µl of OptiMEM and incubated for 10 minutes at room temperature. Meanwhile, cells were washed with PBS and 3 ml of DMEM (10% FBS) were added to the plates. After the 10 minutes had passed, the DNA complexes were added to the cells and the cells were placed in the incubator. 4 hours later, the medium was removed and replaced with 6 ml of DMEM (10% FBS). These cells were the ones making the viral particles that would be used to infect the target cells.

On day three, 50 000 HEK293 cells were seeded in each well of a 6 well plate, these were our target cells. Target cells were transduced the following day (day four): medium was removed from the wells and replaced with 2 ml of DMEM supplemented with 8 µg/ml of Polybrene (Sigma-Aldrich). Polybrene increases retroviral vector transfection efficiency from 100 to 1 000 fold in some cells. Cells were put back in the incubator. The supernatant of the HEK293 cells with the viral particles was taken and centrifuged at 2 000 rpm for 15 minutes, the pellet was discarded. The supernatant was filtered with a 0.22 µm filter. The medium was removed from the target cells and the filtered virus-containing medium, supplemented with 8 µg/ml of Polybrene, was added to the cells. The plate was centrifuged at 2 200 rpm for 90 minutes at 37°C. Plates were put back in the incubator. When the virus infects the target cells, viral genomic RNA is retro-transcribed and

the cDNA is integrated in the cellular genomic DNA. After 6 hours, the medium containing viruses was removed and replaced by 3 ml of DMEM.

On the following two days (day five and six), the procedure on day four was repeated.

As pLVTHM had GFP, it was easy to monitor by fluorescence microscopy the transfection levels (see Figure 4.16). Cells were maintained and monitored for two weeks, to make sure that the transfection was stable and not transient. After two weeks, the transduced GFP positive cells were sorted using a BD FACS Aria lll cell sorter by Dr Carolann McGuire at Southampton General Hospital. Sorted cells were kept for two more weeks and were sorted again for GFP (see Figure 4.17 and Figure 4.18). The stable cell line expressing hpBN was called hpBN-HEK.

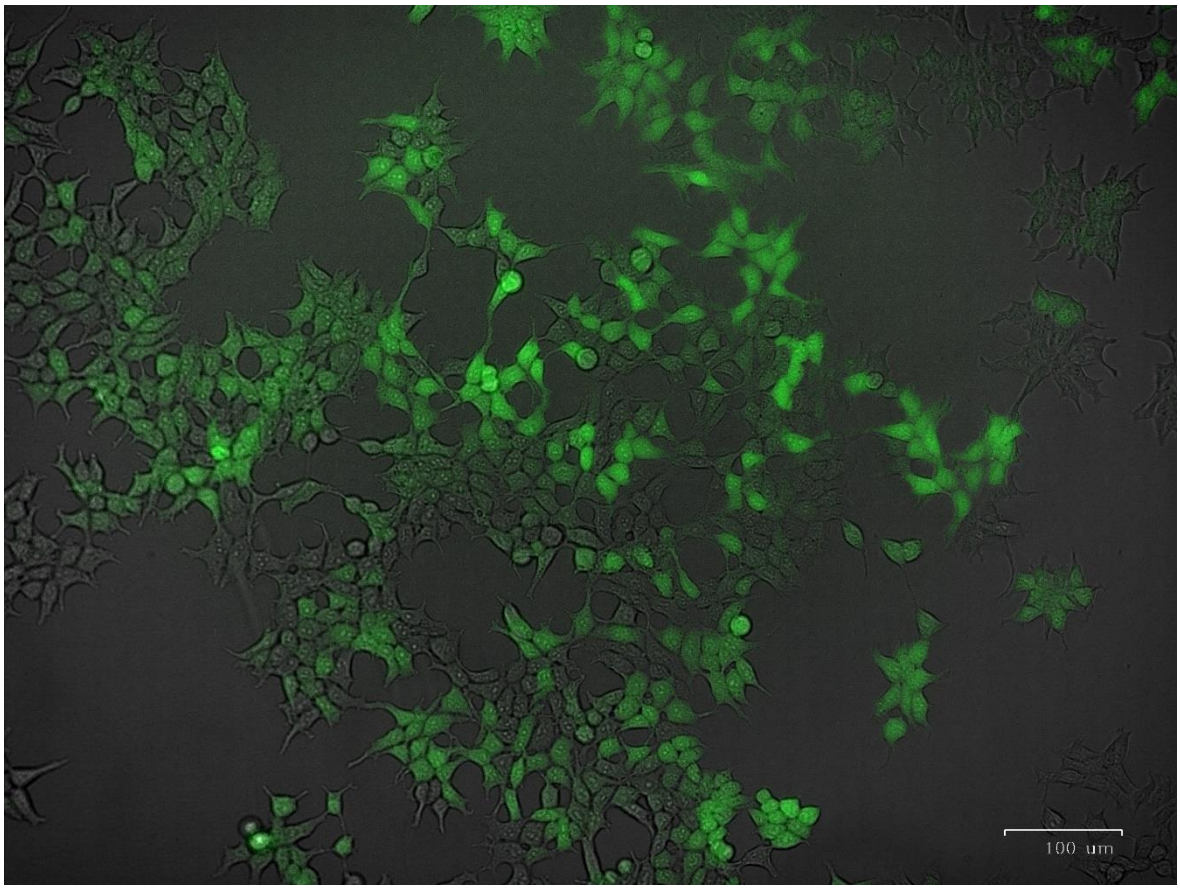

Figure 4.16 **hpBN-HEK cells expressing GFP.** Most of the cells express GFP, the expression levels differ between cells.

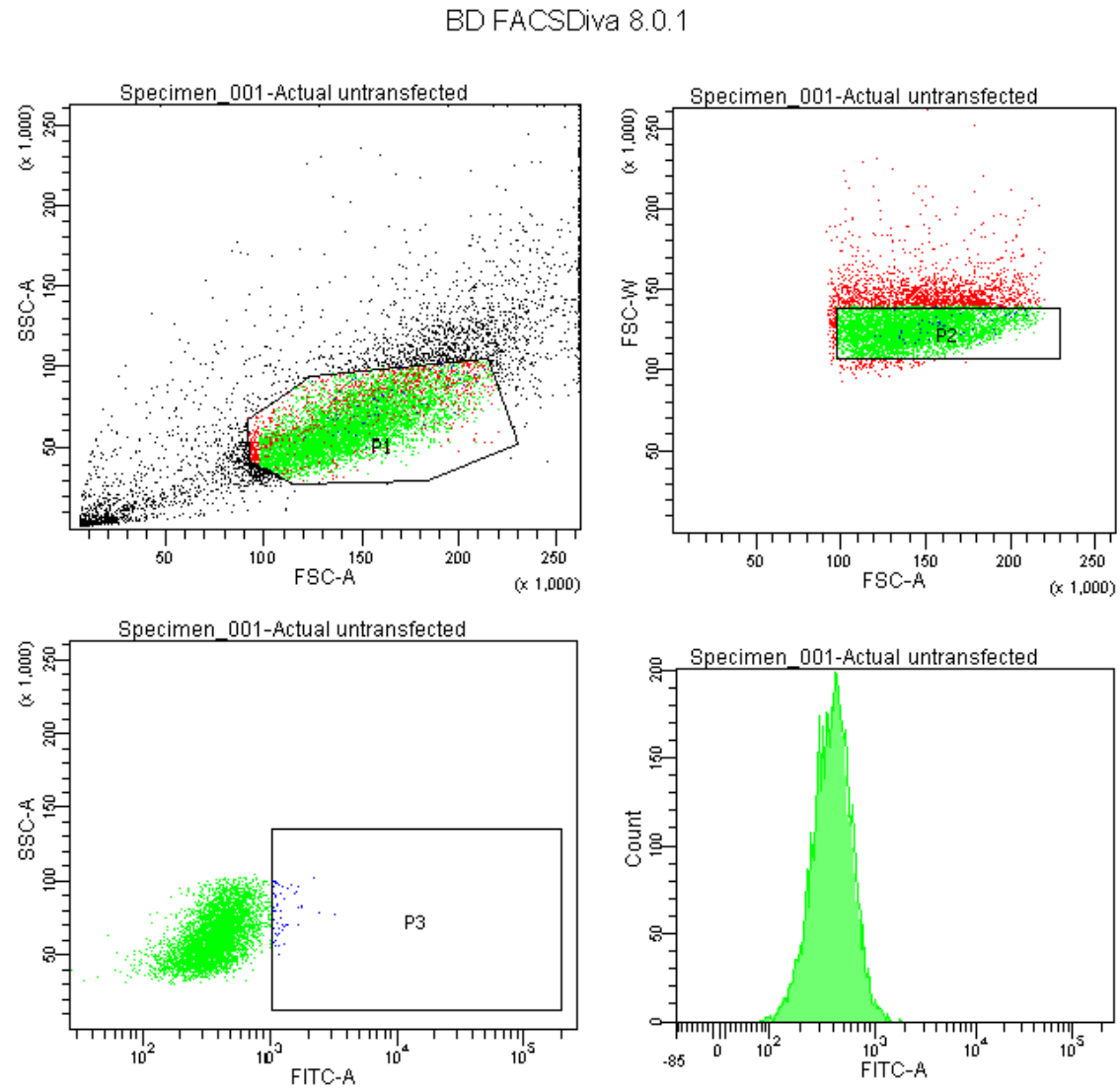

Experiment Name:	Ane GFP_001
Specimen Name:	Specimen_001
Tube Name:	Actual untransfected
Record Date:	02-Jul-2018 12:43:27
$OP:	TobyM
GUID:	5228a5db-dd6f-4e27-bc54-e57...

Population	#Events	%Parent	SSC-A Mean	FITC-A Mean
P2	5,190	74.7	62,170	401
P3	52	1.0	79,685	1,286

Figure 4.17 **GFP FACS reads for HEK293 cells.**

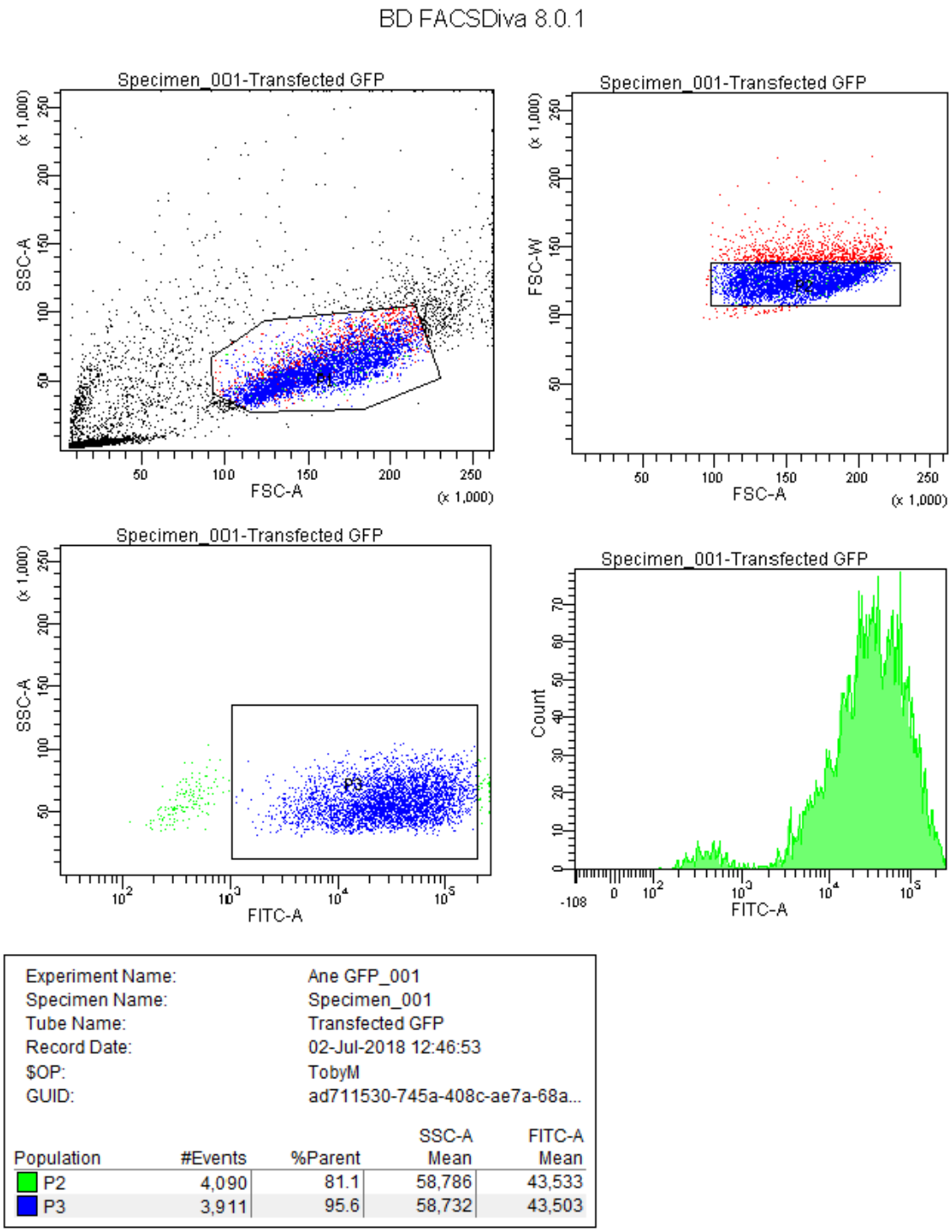

Figure 4.18 **Selection of transduced HEK293 cells expressing GFP by FACS.**

4.11.4 Nluc activity of stable cell line

On two different days, 2 000 and 5 000 hpBN-HEK cells were plated in 3 wells in a 96 well plate. Two days after seeding the cells the Nluc activity was measured, and the experiment was repeated twice. The results in Figure 4.19 show the average value of each of the triplicates. The small error bars indicated that the Nluc activity in hpBN-HEK cells is consistent.

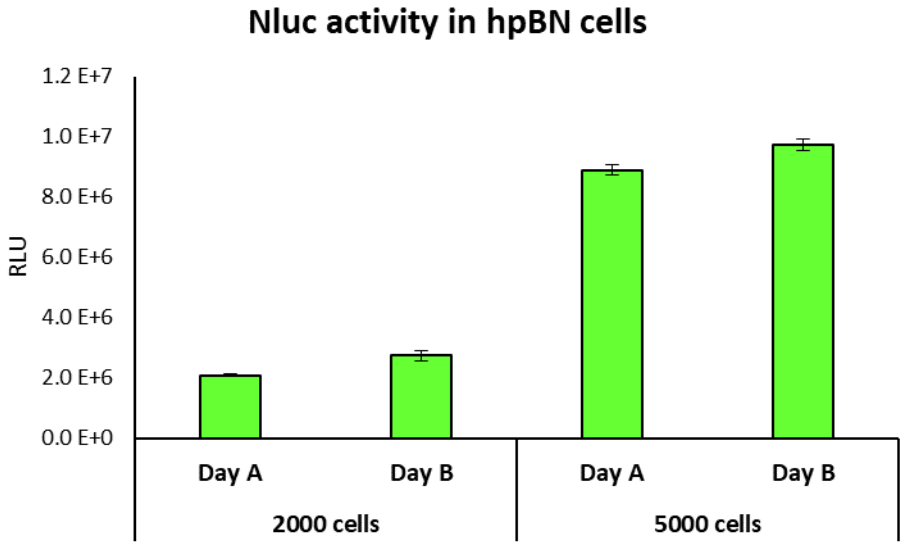

Figure 4.19 **Nluc activity of hpBN-HEK cells, after seeding 3 wells of a 96 well plate with 2 000 and 5 000 cells.**

4.11.5 hpBN-HEK cells expressing Nluc and GFP

50 000 hpBN-HEK cells were seeded in a 35 mm glass bottom dish (with a 14 mm diameter glass microwell). The following day GFP and Nluc expression was measured by microscopy using a custom built bioluminescence microscope, operated with the help of Pete Johnson.

DMEM was removed from the plate, cells were washed with 1X PBS and 100 µl of recently made NanoDLR™ Stop & Glo® were added. Ten minutes after the addition of NanoDLR™ Stop & Glo®, the bioluminescence activity of the hpBN-HEK cells was measured.

Differential interference contrast (DIC) microscopy was used to visualise the outline of cells as a method to verify that the signal visualised was coming from the cells (Figure 4.20, A). Fluorescence microscopy was then used in conjunction with DIC to visualise GFP expression (Figure 4.20, B) and bioluminescence microscopy was used in conjunction with DIC to visualise Nluc expression (Figure 4.20, C).

Bioluminescence microscopy (Figure 4.21, A and A') and fluorescence microscopy (Figure 4.21, B and B') were used to study Nluc and Fluc activity respectively. hpBN-HEK cells were naturally expressing GFP, and therefore emitting light in response to the excitation, but to measure the Nluc activity a chemical reaction produced by a substrate needed to take place. It is therefore not surprising that the Nluc signal was much more difficult to detect than the fluorescence.

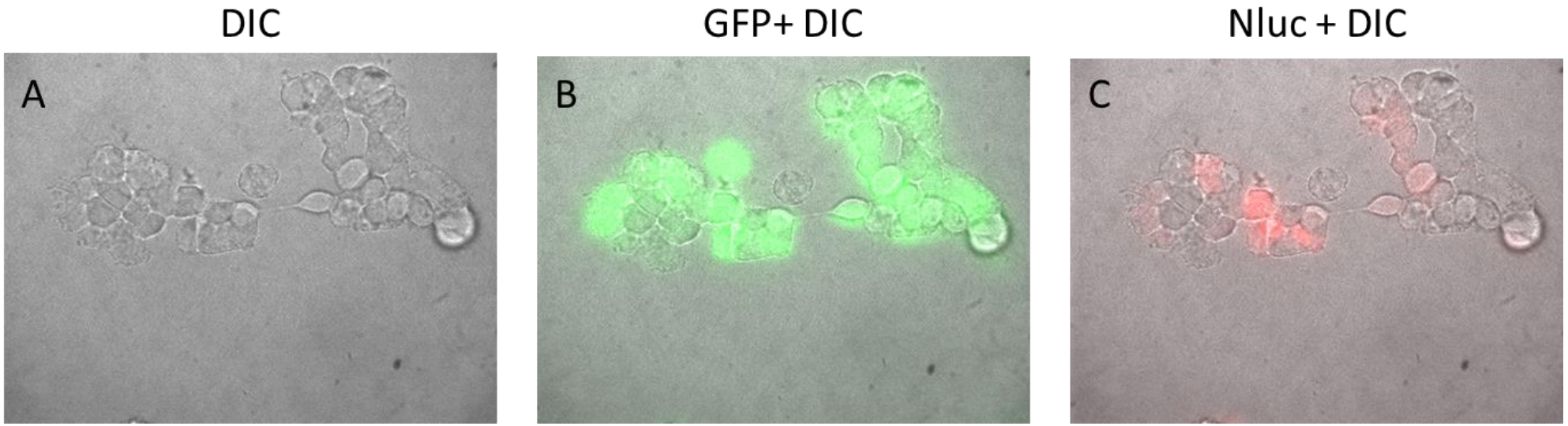

Figure 4.20 **hpBN-HEK cells images using DIC microscopy (A), DIC microscopy in conjunction with fluorescence microscopy (B) and DIC microscopy in conjunction with bioluminescence microscopy (C).**

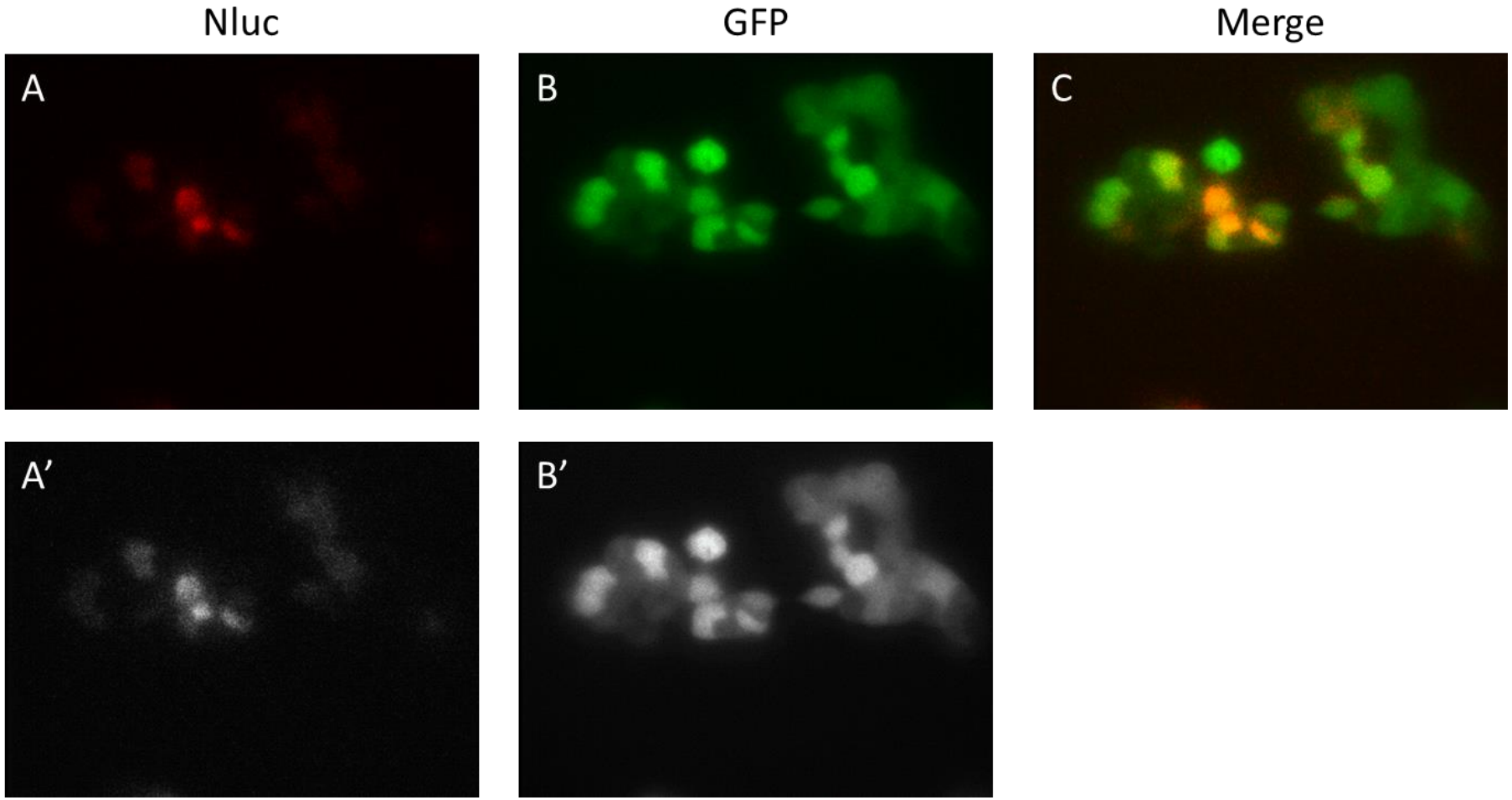

Figure 4.21 **Image of hpBN-HEK cells using bioluminescence microscopy (A and A'), fluorescence microscopy (B and B') and merging both (C).**

4.12 DISCUSSION

To evaluate the efficiency of the oligonucleotides controlling the expression of the *BAG1* IRES two different techniques were used: a dual reporter luciferase assay and western blot. Both techniques have been validated for this purpose and the best protocol has been suggested.

Initial experiments were done in HEK293 cells due to their high transfection efficiency. Before doing any experiment, different numbers of cells were seeded and monitored over several days, to determine which should be the best seeding density of the cells for our purpose.

A fluorescent oligonucleotide (B6-FAM) was used to successfully verify that the oligonucleotides were transfected in HEK293 cells. However, we could not verify that the oligonucleotide was successfully targeting *BAG1* mRNA or if it had suffered from any degradation. Some people believe that if an oligonucleotide can modify gene expression, its cellular localization should be appropriate[187]. This experiment was not useful to study cell localization of the oligonucleotide, as the presence of a fluorescent tag could affect the localization and the fluorescent tag could detach[187]. It has also been proven that the use of fixatives, as was the case in this experiment, could alter the localization of tagged molecules[280].

Different controls were used to study the oligonucleotide activity, such as a commercial siRNA pool targeting *BAG1*'s ORF and a siRNA targeting the *BAG1* IRES. These controls were used to study the best transfection protocol, by analysing when were they more effective. As none of the siRNAs forming the BAG1 siRNA pool targeted the *BAG1* IRES, it could not be used as control for the luciferase assays. A Scramble oligonucleotide with a similar chemical composition and with the same length as the oligonucleotides targeting the *BAG1* IRES, which would not target any sequence in the whole human genome, was also used. All controls were tested by luciferase assays and western blot to verify their efficiency. siRNA pool always managed to reduce protein expression, but BAG1 siRNA (targeting the *BAG1* IRES) was not always effective. This was not surprising, as it had previously been shown that siRNAs targeting 5' UTR regions were not as efficient. The main reason behind this is that 5' UTRs are rich in regulatory protein binding sites and these proteins could prevent binding of the siRNA to RISC and void the silencing effect[281].

Extensive research was carried out on the literature to understand the best ways to transfect the oligonucleotides in cells. Unfortunately, we did not find a definitive protocol that suggested how oligonucleotides should be transfected to successfully modify gene expression. What we found were protocols that varied in the final concentration of oligonucleotide used from 5 nM to 200 nM, the length of the transfection timing, transfection reagent used etc. [184,185,215,229,230,282–286].

We modified the final concentration of oligonucleotide transfected (10-50 nM) and the length of the transfection (1-3 days) and we concluded that the best results were obtained when a final concentration of 25 nM were transfected for two days.

Luciferase assays where different oligonucleotides were co-transfected with different plasmids containing reporter genes were also carried out to verify the best oligonucleotide concentration to use and transfection length. In this case it was observed that the amount of transfection reagent used was more important than the concentration of the oligonucleotide itself, which could mean that a higher amount of transfection reagent is required to make sure that most of the oligonucleotides are successfully transfected, or that the transfection reagent itself can somehow modify the expression of BAG1.

When the objective of the experiment is to see a change in protein expression, as in our case, western blot is the gold standard technique, as it provides convincing evidence of the relative expression level of the protein of interest[187]. In addition, it is the only technique where we could differentiate the expression levels of the different BAG1 isoforms at the same time. However, we showed that western blot is a semi quantitative technique that can sometimes show inconsistent results. Western blots would need to be repeated several times, and the results obtained from them would only be reliable if the oligonucleotides and control siRNAs would always show the same trend in the BAG1 expression. Related to this, we cannot forget that IRES-mediated translation is less efficient than cap-mediated translation and that, at the moment, we cannot differentiated how much protein is translated through one way or the other. The differences in the expression levels among replicate samples could be due to the difference in the synthesis rate or decay rate of the different BAG1 isoforms. This could be directly related to the N-end rule pathway of protein degradation, which states that the rate of protein degradation is directly related to the recognition of the N-terminal residue of the protein[287]. Different algorithms have been developed to measure the protein decay and stability levels[288,289], however when using them, no big differences could be observed among the different BAG1 isoforms. To verify the half-life of the different BAG1 isoforms, their expression should be measured by western blot after treating the cells with cycloheximide from 1 to 24 hours. Cycloheximide inhibits protein synthesis at the level of elongation and is widely used to determine the half-life of proteins[290,291]. In our case, we could also compare the BAG1 isoform expression of cells treated with the siRNA pool with untreated cells and calculate if there are variations on the levels of decay of the different isoforms.

One of the biggest challenges of the luciferase assays is the high variability obtained among replicates. This could be due to the fact that most of the times two plasmids (phpBN and

pGL4.13SV40) and the oligonucleotide were transfected in the cells. This could lead to differences in the transfection efficiencies of the different components. To solve this issue, a stable HEK293 cell line expressing phpBN was constructed: hpBN-HEK.

Chapter 5 USING OLIGONUCLEOTIDES TO MODIFY THE *BAG1* IRES ACTIVITY IN CELLS (I)

5.1 RATIONAL DESIGN OF OLIGONUCLEOTIDES TARGETING THE *BAG1* IRES

The main objective of this project is to control expression of genes with IRES elements using modified oligonucleotides. *BAG1* continued to be our focus, following the verification of the presence of an IRES in this gene. Our first oligonucleotide design considered the model of the *BAG1* IRES secondary structure determined by Pickering *et al.* [82] (model represented in Figure 5.1). In this publication, apart from trying to determine the secondary structure of the *BAG1* IRES, Pickering *et al.* showed that the RNA binding proteins PTBP1 and PCBP1 stimulated IRES-mediated translation. Some of the oligonucleotides were designed to mimic the activity of these two proteins on the *BAG1* IRES, others were designed to inhibit their activity. The oligonucleotides BAG 1 and BAG 2 were designed with the aim to keep the IRES of the *BAG1* gene closed or inactive by avoiding the binding of PTBP1 and PCBP1 (see Figure 5.1, A and B). BAG 3 was designed with the aim to open the IRES and BAG 4 with the aim to keep it opened (see Figure 5.1, C). BAG 1 and BAG 2 only differed from each other in a nucleotide. An extra thymine was added to BAG 2 to increase the flexibility. All the oligonucleotides were checked for specificity for BAG1 with a BLAST analysis.

We decided to start working with LNA-DNA mixmers, due to their higher affinity of binding to complementary sequences and their higher melting temperature compared to DNA oligonucleotides. Furthermore, LNA-DNA mixmers show a higher resistance to nucleases, that makes them more biologically stable[225]. For more information about LNA-DNA mixmers see section 1.4.3 on page 42. The LNA-DNA mixmers were designed containing an LNA nucleotide every one to five DNA nucleotides (see oligonucleotide sequences in Appendix B). Gene expression was studied after cell treatment with the oligonucleotides. Unmodified strands analogous to the LNA-DNA mixmers were also synthesised. The ability to control gene expression of the unmodified and modified oligonucleotides was compared.

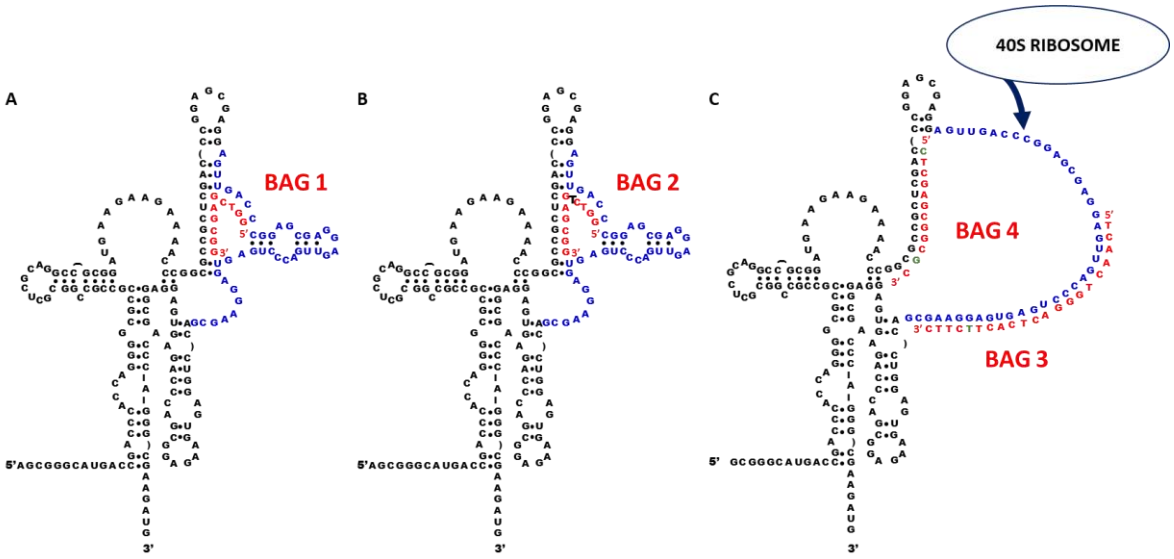

Figure 5.1 **Oligonucleotides targeting the *BAG1* IRES**. BAG 1 (A) and BAG 2 (B), which had the same sequence as BAG 1 with an additional T-nucleobase (see in black colour), were designed to maintain the IRES in a closed confirmation. BAG 3 and BAG 4 (C) were designed to open the IRES. The sequence in blue represents the single stranded region formed when the IRES is active where the 40S ribosomal subunit could land. In green it can be observed the mismatches introduced in BAG 3 and BAG 4 by error (more information on this can be found in section 5.2.1 on page 174).

The oligonucleotides were transfected in HEK293 cells following the optimised protocol as determined by the experiments in Chapter 4. Protein expression was measured using Nano-Glo® Dual-Luciferase® Reporter Assay System (Promega), when studying the effect on reporter vectors, and western blot, when considering native BAG1 protein. Despite our previous work showing that the isoform expression of BAG1 is inconsistent in untreated cells (see section 4.3 on page 132), western blot is the only technique we can use to quantify the total amount of protein. Therefore western blots were repeated on various occasions to make the results obtained as reliable as possible, and qPCR was also used to quantify the levels of *BAG1* mRNA.

5.1.1 . Co-transfection of pGL4.13SV40 and phpBN and the oligonucleotides

Due to the expression problems that the bicistronic vectors show, such as the presence of cryptic promoters (see section 3.4.3 on page 94), instead of studying the effect of the oligonucleotides in pFBN, we decided to co-transfect the two monocistronic vectors phpBN and pGL4.13SV40 in cells (Figure 5.2). In this scenario, pGL4.13SV40 was the cap-dependent translation control and with phpBN the IRES activity was measured. It needs to be kept in mind that in phpBN a hairpin was introduced upstream of the sequence of the 5' UTR of *BAG1*, which blocked most of the cap-mediated translation (see section 3.6.2 on page 102).

2 000 cells were seeded and transfected the following day with a final concentration of 25 nM of oligonucleotide and 10 ng of each plasmid (phpBN and pGL4.13SV40). Media was changed 5 hours after transfection and 48 hours post transfection luciferase assays were carried out using the Nano-Glo® Dual-Luciferase® Reporter Assay System.

The Fluc and Nluc expression were measured and the Nluc to Fluc ratios were normalised to the phpBN+pGL4.13SV40 in each plate. The Nluc to Fluc ratios were analysed by a one-way ANOVA with a Dunnett's multiple comparison test, to study the effect of the oligonucleotides compared to phpBN+pGL4.13SV40 (no oligonucleotide) transfected cells. The results shown were from three independent experiments performed in triplicate, ±SD (Figure 5.2).

The Fluc activity of the phpBN+pGL4.13SV40 (no oligonucleotide) transfected cells was over threefold stronger than the Fluc activity of cells transfected with the oligonucleotides (as well as the plasmids), suggesting that the oligonucleotides somehow had the ability to decrease the Fluc activity of pGL4.13SV40 (Figure 5.2, A). There were no big differences observed in the Fluc values of the oligonucleotide treated cells, which suggests that it was the oligonucleotide transfection (independently of the sequence or chemistry) that affected the Fluc activity.

Similar effects on Nluc activity were observed (Figure 5.2, B). phpBN+pGL4.13SV40 (no oligonucleotide) transfected cells had an Nluc activity over fivefold that of the oligonucleotide transfected cells, but there was not a large difference among the different oligonucleotide transfected cells. In this case there were no significant differences in the Fluc and Nluc activities between unmodified oligonucleotides and LNA-DNA mixmers.

When the Nluc to Fluc ratios of the different oligonucleotide treated cells were compared to untreated cells (Figure 5.2, C), all the oligonucleotides appart from BAG 3 decreased the Nluc to Fluc ratio in a significant way. The fact that some of the oligonucleotides designed to increase the IRES activity had the opposite effect could be due to a poor oligonucleotide design or it could be proof that the *BAG1* IRES structure proposed by Pickering *et al.*[82] was not accurate.

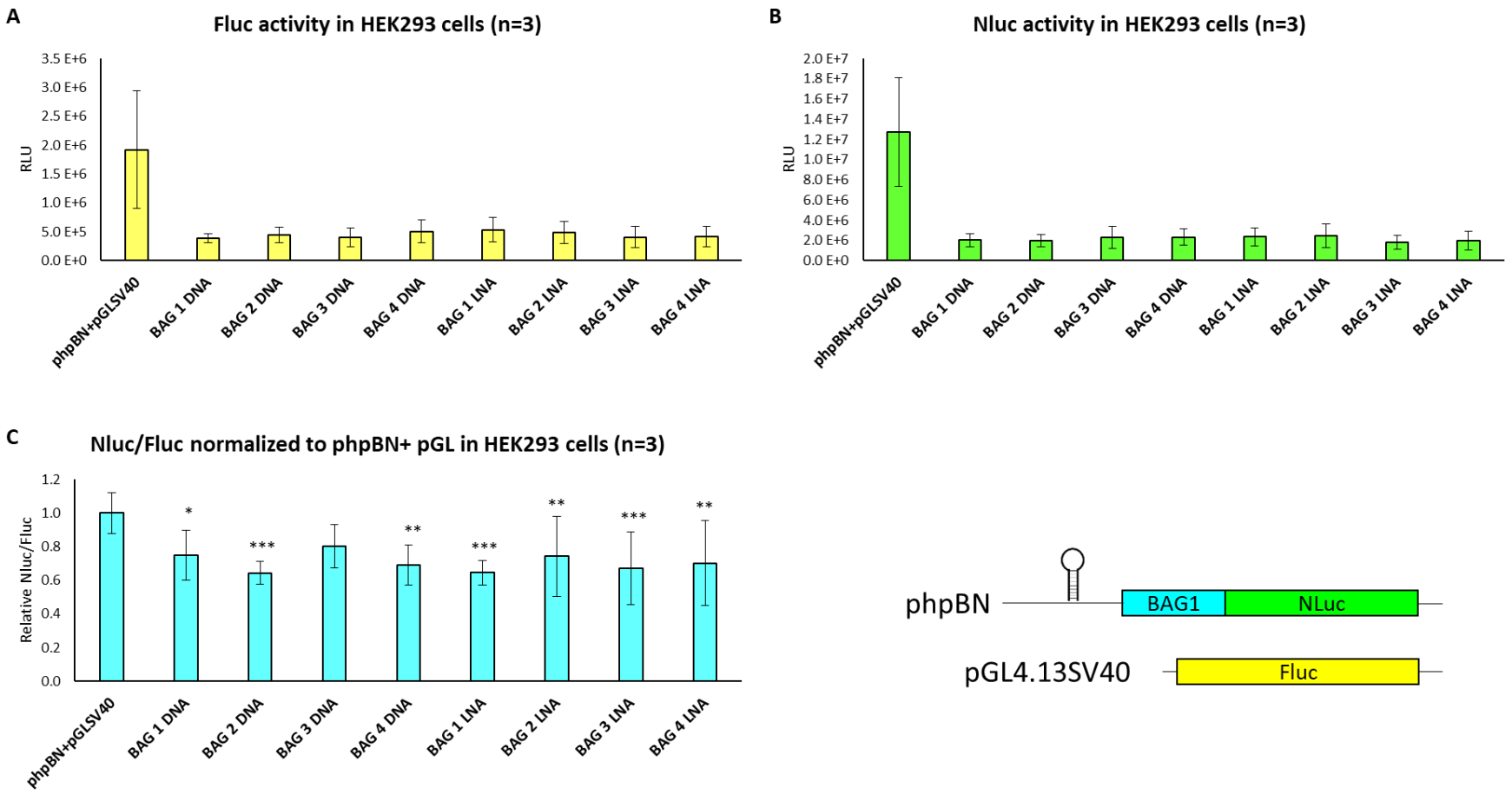

Figure 5.2 **Dual luciferase reporter assay results of HEK293 cells transfected with 20 ng of phpBN+pGL4.13SV40 and 25 nM (final concentration) of oligonucleotides for 2 days.** Fluc (A) and Nluc (B) activity were measured and Nluc to Fluc ratio was measured and normalised to phpBN+pGL4.13SV40 transfected cells (C). Results from three independent experiments performed in triplicate, ±SD. Data analysed by one-way ANOVA with a Dunnett's multiple comparison test, to compare the oligonucleotide transfected cells to phpBN+pGL4.13SV40 (no oligonucleotide) transfected cells. $P<0.05$.

5.1.2 Study of the effect of the oligonucleotides targeting the endogenous *BAG1* by western blot

As the oligonucleotides were designed to target the *BAG1* IRES, which drives part of the translation of p36, the most significant result for the aim of the project would be the modification of the expression of p36, and so this was examined in the context of the expression levels of the endogenous protein isoforms

HEK293 cells were transfected with a final concentration of 25 nM of the oligonucleotides BAG 1 DNA, BAG 2 DNA, BAG 3 DNA, BAG 4 DNA, BAG 1 LNA, BAG 2 LNA, BAG 3 LNA and BAG 4 LNA for 2 days. Proteins were extracted and BAG1 expression was studied by western blot (Figure 5.4). The experiment was repeated twice, on the second repetition RNA was extracted, as well as proteins, to carry out qPCRs as well as western blots (see blots in Figure 5.3)

The expression of each of the isoforms was quantified (Figure 5.4, A), added up and normalised to actin to calculate the total BAG1 expression (Figure 5.4, B). The expression of p46 was not measured due to the presence of non-specific bands (due to probable contamination of the BAG1 antibody stock with an actin antibody) of around 46 kDa.

By looking at the blots on their own, it was hard to conclude the effects that the oligonucleotide treatment had on the expression of BAG1 (Figure 5.3), however it seemed that all the oligonucleotides decreased the expression of p36 when compared to the untransfected cells. These results were verified for both experiments when the total BAG1 expression was quantified (Figure 5.4, B). In experiment l LNA-DNA modified oligonucleotides decreased the BAG1 expression the most, whereas in experiment ll it was the unmodified oligonucleotides that decreased it the most.

When comparing the isoform expression (Figure 5.4, A) we could verify that all the oligonucleotides decreased the p36 expression, and in experiment l the oligonucleotides had a stronger effect decreasing the expression of p36. In experiment l, BAG 2 DNA was the oligonucleotide that strongest decrease the p36 expression, whereas in experiment ll BAG 4 DNA was the oligonucleotide that had the largest effect and BAG 2 DNA was the oligonucleotide with the smallest effect. The reduction in the p36 levels caused an increase in the p29 levels of all the oligonucleotide treated cells. This could perhaps be explained by the landing of the ribosomes downstream of the p36 initiation codon after some form of modified internal initiation.

The amount of *BAG1* mRNA was measured by qPCR for experiment ll (see section 2.8 on page 67). The *BAG1* mRNA levels were normalised to the *B2M* internal control mRNA levels and then to the untransfected (no oligonucleotide) cells (Figure 5.4, C). qPCR data was analysed by a one-way ANOVA with a Dunnett's multiple comparison test, where the BAG1 mRNA levels of oligo transfected cells (normalised to unmodified cells) were compared to the mRNA levels of unmodified cells. Unfortunately only BAG 1 DNA and BAG 1 LNA transfected cells maintained similar *BAG1* mRNA levels as untransfected cells, the rest of the oligonucleotides decreased the *BAG1* mRNA levels in a significant way.

Total mRNA and protein content were combined (Figure 5.4, D), in order to determine the amount of protein translated from the mRNA. This was done by calculating the ratio of BAG1 protein normalised to the untransfected cells to *BAG1* mRNA normalised to the untransfected cells. A protein to mRNA ratio of >1, would mean that from the same amount of mRNA more protein was translated. This would implicate that the oligonucleotides were increasing translation levels. On the other hand, a protein to mRNA ratio of <1 would mean that from the same amount of mRNA less protein was translated. This would mean that the oligonucleotides decreased translation levels. A ratio protein to mRNA ratio close to 1, indicated that the translation levels had not been modified by the oligonucleotides.

The results showed that all the oligonucleotides decreased the translation levels, but unmodified oligonucleotides had a stronger effect than LNA-DNA mixmers. BAG 1 DNA and BAG 4 DNA showed to be the most effective oligonucleotides at decreasing the translation levels. However, as BAG 1 DNA in combination with BAG 1 LNA were the only two oligonucleotides that did not decrease the mRNA levels, we could say that these two oligonucleotides were the most effective ones in decreasing the translation levels of BAG1 without modifying the mRNA levels. BAG 1 DNA and BAG 1 LNA only had nine nucleotides each, whereas the rest of the oligonucleotides had between 10 and 21. There is the possibility that the DNA-RNA duplex formed when those oligonucleotides targeted the mRNA could not be big enough to recruit RNase H in a very effective way.

As a conclusion we could say that the modified LNA-DNA mixmers were not effectively reducing the RNA degradation. This could be due to our LNA-DNA mixmer design, so a different modified oligonucleotide design could be used to check where the LNA modifications should be located to avoid RNA degradation.

All the oligonucleotides decreased the total BAG1 protein levels, even the ones that were designed to increase protein levels. This could be due to our poor oligonucleotide design when choosing the areas in the IRES that should be targeted. Another possible explanation could be

that the IRES in HEK293 cells is already very active, which makes it harder to increase its activity even more.

Overall we could say that these two experiments showed that BAG 1 DNA and BAG 1 LNA successfully decrease the BAG1 protein levels, while they kept the *BAG1* mRNA levels constant. This was considered a successful result, as both oligonucleotides were designed to have this effect. Fortunately, the luciferase assay results in section 5.1.1 and these results show similar results in terms of the oligonucleotide activity, in both cases most of the oligonucleotides decreased the IRES activity.

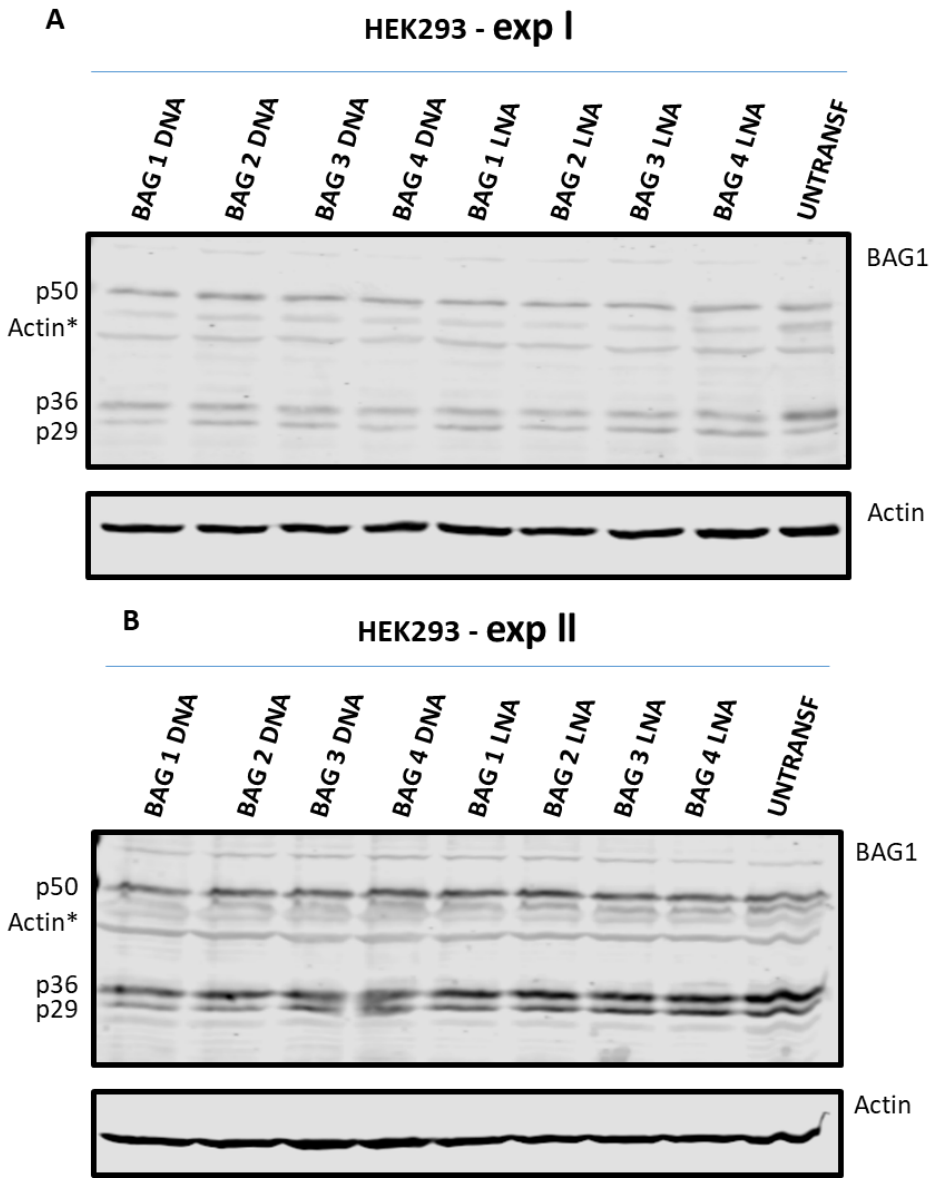

Figure 5.3 **Western blots of HEK293 cells transfected with a final concentration of 25 nM of oligonucleotide for two days.** The experiment was repeated twice (A and B).

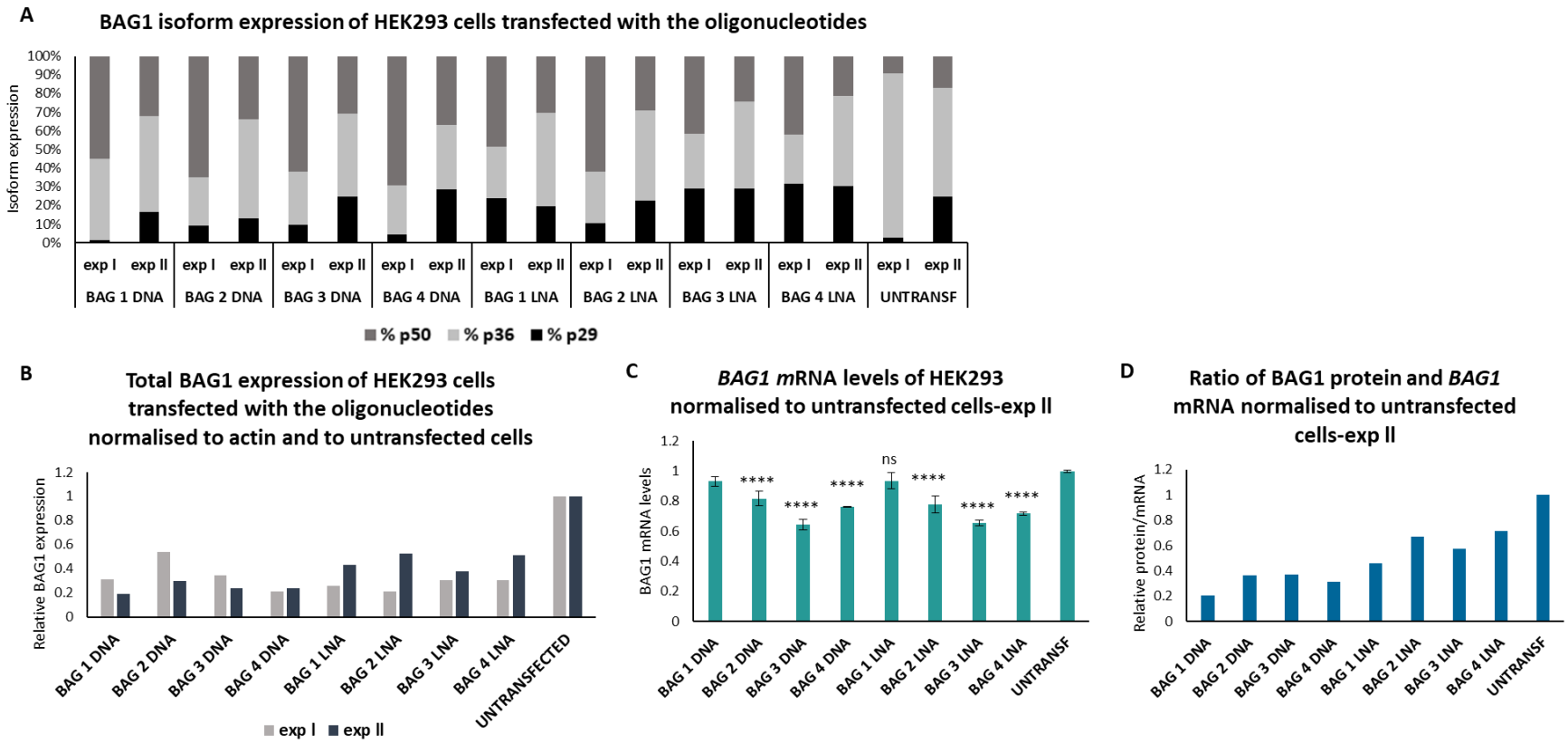

Figure 5.4 **Analysis of western blots of HEK293 cells transfected with a final concentration of 25 nM for two days.** A) BAG1 isoform expression, B) Total BAG1 expression normalised to actin and untransfected cells. C) *BAG1* mRNA levels normalised to *B2M* mRNA levels and to untransfected cells, Statistical analysed done by one-way ANOVA with a Tukey's multiple comparison test. Error bars show ± SD. D) BAG1 protein to *BAG1* mRNA ratio normalised to untransfected cells.

5.2 AN OVERLAPING OLIGONUCLEOTIDE POOL COVERING THE MINIMAL *BAG1* IRES SEQUENCE

All the experiments done up to this point used oligonucleotides that were specifically designed to modify the structure of the *BAG1* IRES proposed by Pickering *et al*[82]. Those oligonucleotides were carefully selected and designed to target the areas of the *BAG1* IRES where the ITAFs PCBP1 and PTBP1 bound and the area where the 40S ribosome bound to the IRES, according to the aforementioned paper.

As all the oligonucleotides decreased the BAG1 IRES activity, even the ones designed to increase it, and keeping in mind that the IRES structure proposed by Pickering *et al.* might not be fully representative of the real one, oligonucleotides of 20 nucleotides covering the full length of the IRES were designed.

17 unmodified oligonucleotides that targeted the reduced IRES sequence of BAG1 proposed by Pickering et al.82 were purchased from Sigma-Aldrich (Figure 5.5), with the first nine covering consecutive regions, and the last eight again covering consecutive regions, but offset by 10 nucleotides. All the oligonucleotides showed the max score and query cover for BAG1 when run on a BLAST, however some oligonucleotides showed a smaller similarities with other genes. Due to time and resource limitations, we could not study how that affected the effectivity of the oligonucleotides.

The plan was to study how each of the oligonucleotides affected the expression of *BAG1* using the already mentioned luciferase assay. The objective was to choose the five oligonucleotides showing the most promising results and to study in more depth how those oligonucleotides could modify the expression of *BAG1*.

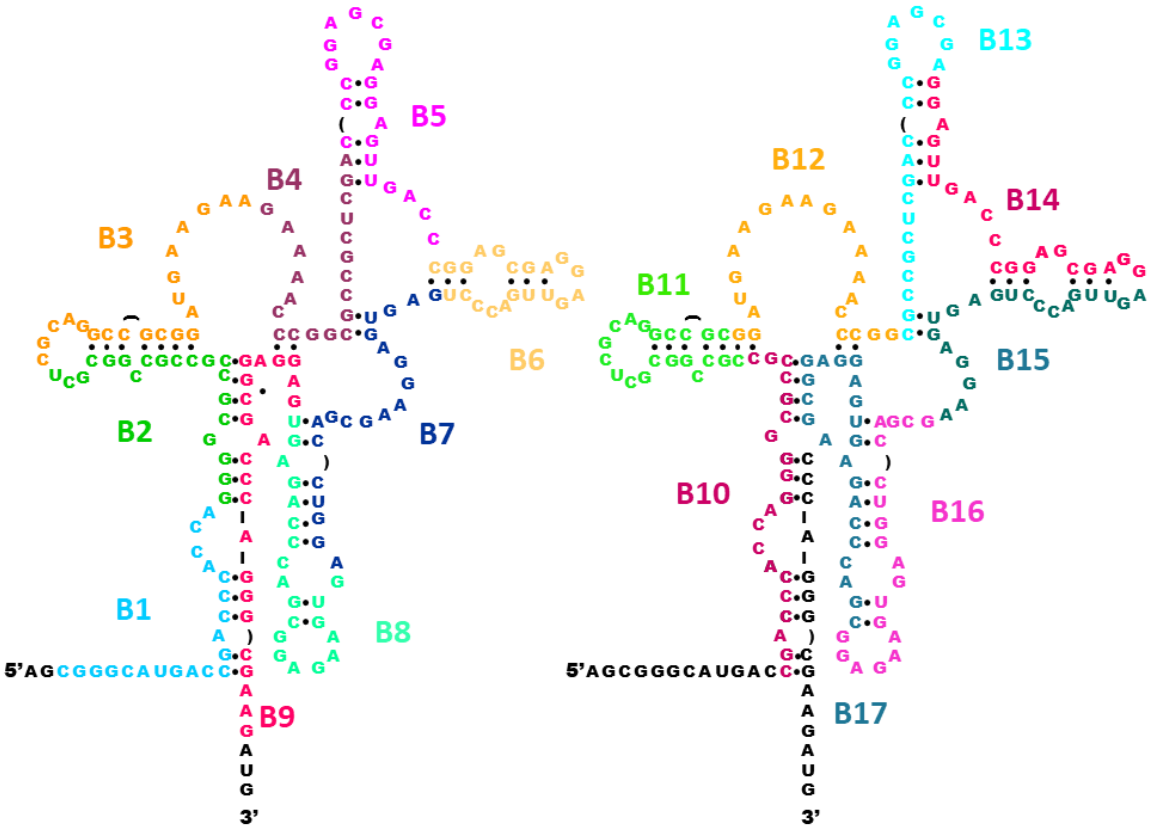

Figure 5.5 **Illustration of the target sites in the *BAG1* IRES of the oligonucleotides B1-B17.**

5.2.1 Transfecting HEK293 cells with the oligonucleotide pool for *BAG1* IRES.

The experiment was done in 96 well plates as explained in section 2.2.3 on page 60, 25 nM final concentration oligonucleotide was transfected. After 2 days the luciferase assay was done as explained in section 2.3 on page 62.

The following oligonucleotides were transfected:

- Oligonucleotide pool for *BAG1* IRES: B1-B17.
- Old oligonucleotides (BAG 1 DNA, BAG 2 DNA, BAG 3 DNA, BAG 4 DNA, BAG 1 LNA, BAG 2 LNA, BAG 3 LNA and BAG 4 LNA).
- BAG 3 NEW and BAG 4 NEW (some nucleotide mismatches were found in BAG 3 DNA and BAG 4 DNA that were corrected in BAG 3 NEW and BAG 4 NEW).
- BAG1 siRNA.
- Scramble oligonucleotide.
- B6-FAM.

From now on we will be only showing the results of Fluc to Nluc ratio. We will not show the raw Fluc and Nluc data unless they show any relevant information. However, the Fluc and Nluc values

for every experiment can be found in Appendix D on page 287. The Fluc and Nluc values of this experiment, as well as the statistical analysis results, can be found in Figure D.5 on page 292.

The Nluc to Fluc ratio values normalised to the phpBN+pGL4.13SV40 (no oligonucleotide) values were used to study the effect of the oligonucleotides on the IRES activity. As seen in Figure 5.6 all the oligonucleotides increased the Nluc to Fluc ratio. This was surprising, as the first set of oligonucleotides (BAG 1, BAG 2, BAG 3DNA and BAG 4, unmodified and modified with LNAs) had shown the opposite results in previous experiments (see section 5.1.1 on page 166).

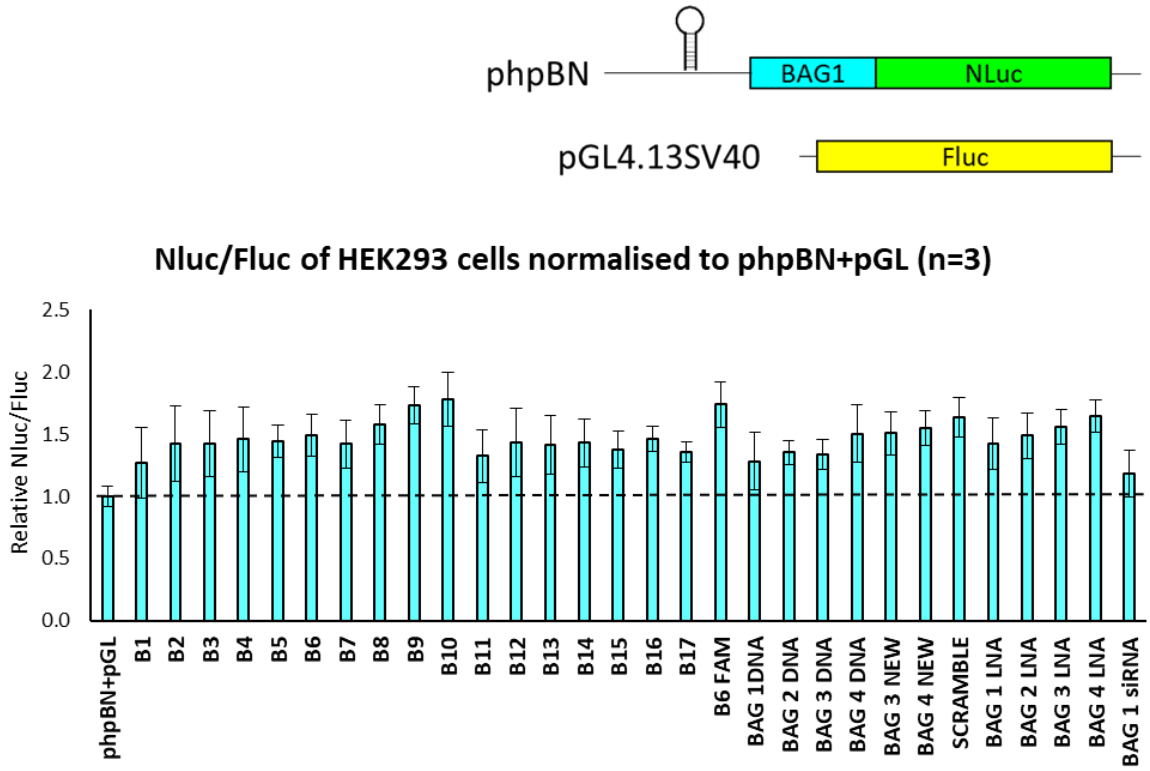

Figure 5.6 **Dual luciferase reporter assay results of HEK293 cells transfected with a final concentration of 25 nM of oligonucleotides for two days.** Nluc/Fluc normalised to phpBN+pGL4.13SV40 transfected cells. Results from three independent experiments each done in triplicate. Error bars show ±SD.

As the main objective of the experiment was to choose the top five effective oligonucleotides (both to increase and decrease gene expression), the Nluc to Fluc ratios were analysed with a one-way ANOVA with a Tukey's multiple comparison test ($P<0.05$) (see Table D 1 on page 294). This test compares the mean of all the oligonucleotide treatments against each other, providing a good technique to study which of the oligonucleotides were most different from each other. The results of the statistical analysis can be found in Appendix D on page 294.

B9, B10 were the oligonucleotides that increased the Nluc to Fluc ratio the most and B1, B11, B15, B17, BAG 1 DNA, BAG 2 DNA, BAG 3 DNA, BAG 4 DNA, BAG 3 NEW were the ones that decreased

it the most (see Figure 5.7). Most of the oligonucleotides Nluc to Fluc ratio was significantly different from that of phpBN+pGL4.13SV40. To compare the Nluc to Fluc ratios of the oligonucleotide treated cells to the phpBN+pGL4.13SV40 (no oligonucleotide) transfected cells and to Scramble transfected cells, a one-way ANOVA with a Dunnett's multiple comparison test was done ($P<0.05$) (see Table D 2 on page 295). This test compares the mean of all the oligonucleotide treatments against the mean of the phpBN+pGL4.13SV40 (no oligonucleotide) or Scramble transfected cells. Surprisingly, the Scramble oligonucleotide transfected cells had a significantly different Nluc to Fluc ratio when compared to the no oligonucleotide cells. The Scramble sequence was designed to study the effect that the transfection of an oligonucleotide could have in the cells, but it should not target any sequence in the whole human genome or in the plasmids transfected. The fact that none of the oligonucleotide transfected cells was significantly different from the Scramble transfected cells could mean that in reality none of the oligonucleotides was really having an effect. BAG1 siRNA did not decrease the Nluc to Fluc ratio either, which could support the hypothesis that none of the oligonucleotides was really affecting the IRES activity. On the other hand, BAG1 siRNA was designed to target the *BAG1* 5' UTR, and as it has been previously explained, siRNAs targeting regions in the 5' UTR are not always efficient.

A unique experiment (in triplicate) was done where the oligonucleotides were transfected as previously explained, but instead of comparing them to cells transfected with phpBN+pGL4.13SV40 (no oligonucleotide), they were compared to Mock transfected cells. Mock transfected cells were transfected with phpBN+pGL4.13SV40 (in the same way as the rest of the cells), and contained the same amount of RiboJuice (the transfection reagent used for the oligonucleotide transfection) as the cells transfected with the oligonucleotides.

The Nluc to Fluc ratios were calculated and normalised to the Mock transfected cells (Figure 5.7). The Fluc and Nluc values of this experiment can be found in Figure D.6 on page 293.

In this case some of the oligonucleotides decreased the Nluc to Fluc ratio, whereas others increased it. A one-way ANOVA with a Tukey's multiple comparison test ($P<0.05$) was done to study which of the oligonucleotides were more different from each other (see Table D 3 on page 295). A one-way ANOVA with a Dunnett's multiple comparison test ($P<0.05$) was done to study which of the oligonucleotide transfected cells had a significantly different effect from Mock transfected cells. However it needs to be reminded that this experiment was done only once (in triplicate), so the sample size to do a proper statistical analysis was very small.

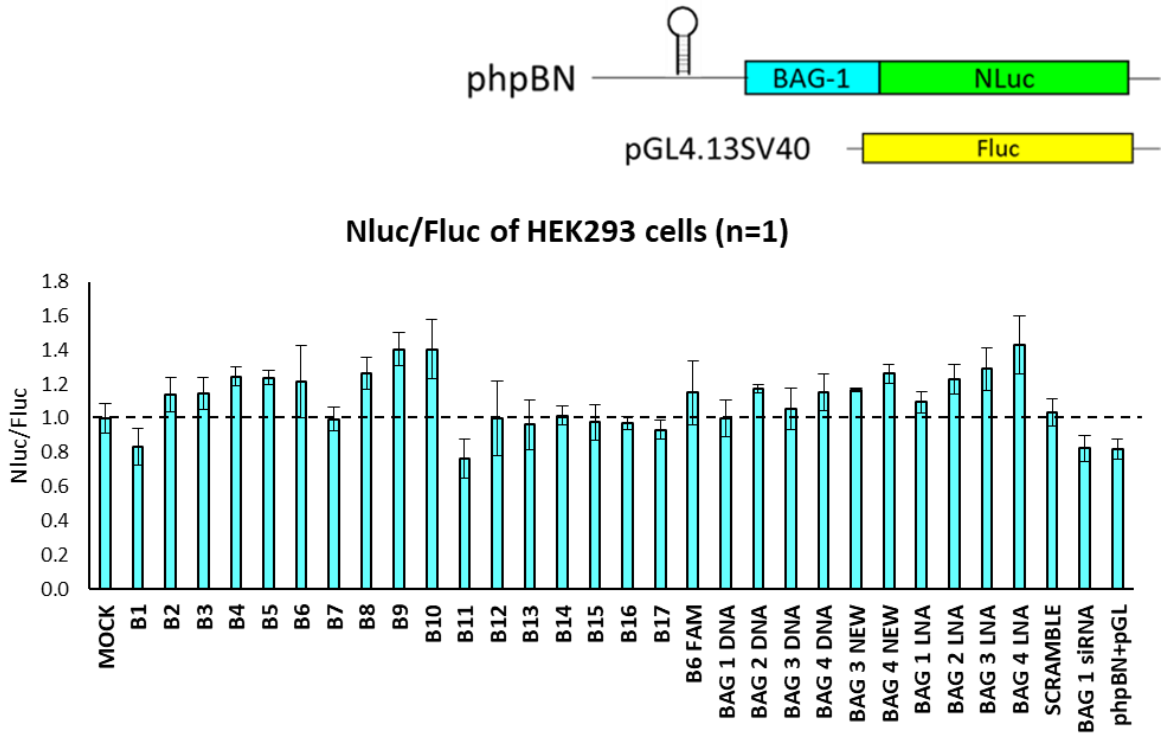

Figure 5.7 **Dual luciferase reporter assay results of HEK293 cells transfected with a final concentration of 25 nM of oligonucleotides for two days.** Nluc/Fluc normalised to Mock transfected cells. Results from one independent experiments each done in triplicate. Error bars show ±SD**.**

B9, B10, BAG 3 LNA and BAG 4 LNA transfected cells showed to have a significantly different Nluc to Fluc ratio when compared to Mock transfected cells. B1 and B11 transfected cells were the ones that decreased the Nluc to Fluc ratio the most, whereas B9, B10 and BAG 4 LNA were the ones that increased it the most.

With all these results, we decided to focus our research in using B1, B9, B10, B11 and BAG 4 NEW to modify the expression of the *BAG1* IRES, where B1 and B11 would decrease the IRES activity and B9, B10 and BAG 4 NEW would increase it.

5.3 THE EFFECT OF MODIFIED B1, B9, B10, B11 AND BAG 4 NEW ON THE *BAG1* IRES ACTIVITY

At this point we had five oligonucleotides that had shown to have the largest effect in modifying IRES-mediated translation in *BAG1*. B1 and B11 had previously shown to be the oligonucleotides that decreased the IRES activity the most. B9, B10 and BAG 4 had shown to be the oligonucleotides increasing the IRES activity the most. B1, B10 and B11 targeted a similar region of the *BAG1* IRES (see Figure 5.8), however B10 had the opposite effect to the other two.

The next step was to modify these oligonucleotides in different ways, to make them more nuclease resistant and hopefully increase their activity in cells. LNA-DNA mixmers had previously shown not to be the ideal candidates for our purpose, we thereby decided to increase their nuclease resistance by introducing phosphorothioate bonds forming B1 PS LNA, B9 PS LNA, B10 PS LNA, B11 PS LNA and BAG 4 PS LNA. Phosphorothioate (PS) oligonucleotides with DNA nucleotides were synthesised as control oligonucleotides, as they could recruit RNase H and thereby degrade the mRNA (B1 PS, B9 PS, B10 PS and B11 PS). BAG 4 PS did not meet our quality control criteria and it was discarded from the experiments. An LNA-DNA mixmer with phosphodiester linkages (BAG 4 LNA, with the mismatches from the old BAG 4 LNA corrected) was also designed to compare the activity of the PS LNA-DNA mixmers to the phosphodiester LNA-DNA mixmers. The modified oligonucleotides were synthesised by Dr Eugen Stulz. For each of the modifications a Scramble sequence was synthesised. Oligonucleotide sequences can be found in section B.3 on page 272.

The activity of the oligonucleotides was studied with the luciferase assay that was previously developed, by western blot and qPCR in HEK293 cells and hpBN-HEK cells.

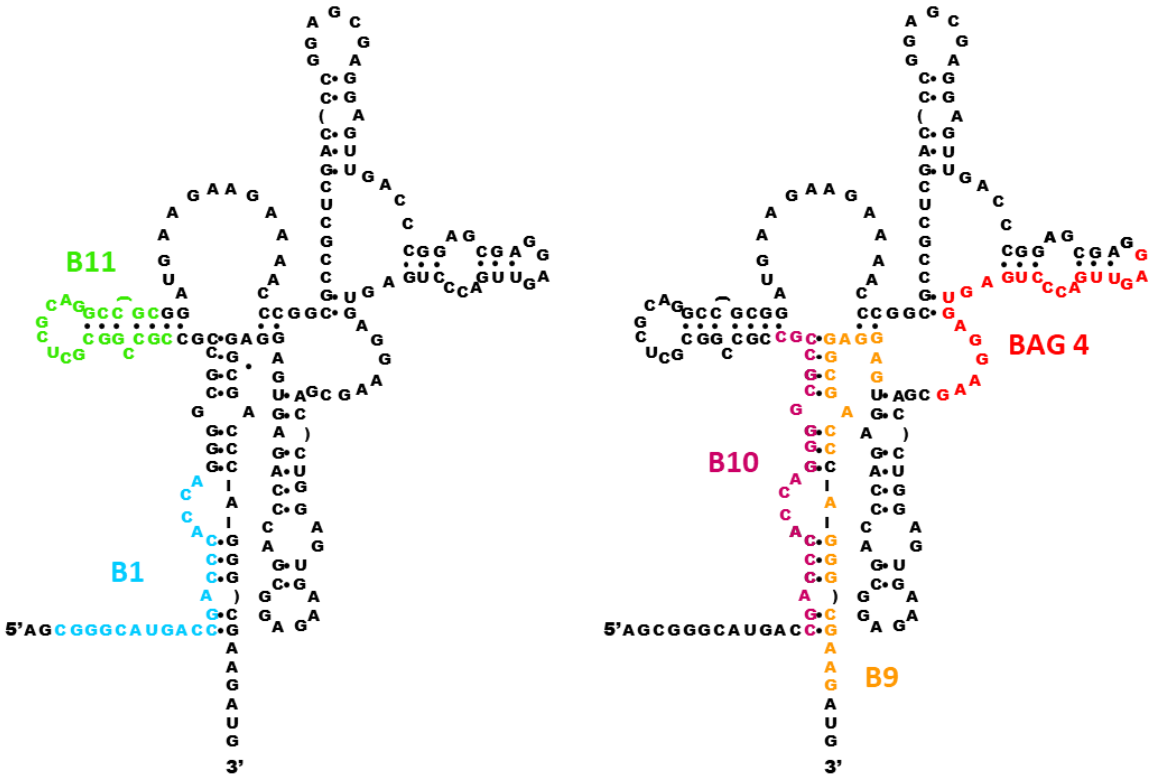

Figure 5.8 **Representation of the regions targeted by the oligonucleotides B1, B11, B9, B10 and BAG 4 in the *BAG1* IRES.** B1 and B11 had shown to decrease the IRES activity, whereas B9, B10 and BAG 4 had shown to increase it.

5.3.1 Luciferase assay

Cells were seeded and transfected with phpBN and pGL4.13SV40 as explained in section 2.2.3 on page 60 and in the same way as in the previous experiment (section 5.2.1 on page 174). Each experiment was done in triplicate on three independent occasions. The results were analysed by normalising the Nluc to Fluc ratios of oligonucleotide transfected cells to the Nluc to Fluc ratio of Mock transfected cells and comparing them to the Nluc to Fluc ratio of Scramble transfected cells.

5.3.1.1 Luciferase assay in HEK293 cells

None of the unmodified oligonucleotides had a significant different Nluc to Fluc ratio when compared to Scramble transfected oligonucleotides, only B9 PS and B9 PS LNA showed significantly smaller Nluc to Fluc ratio values than Scramble PS and Scramble PS LNA respectively (Figure 5.9). Some of the oligonucleotide transfected cells showed a significantly smaller Nluc to Fluc ratio than Mock transfected cells, as B1 PS, B9 PS, B10 PS, B11 PS, B1 PS LNA, B9 PS LNA, B10 PS LNA, Scramble PS LNA and BAG1 siRNA. In this case, BAG1 siRNA showed to efficiently target the *BAG1* mRNA, as it significantly decrease the Nluc to Fluc activity. In the case of the other

oligonucleotides, any effect shown when compared to Mock transfected cells could be due to sequence independent activity of the oligonucleotides.

After this experiment we could conclude that B9 is the oligonucleotide that had the largest effect in decreasing the Nluc to Fluc ratio, and thereby the *BAG1* IRES activity. These results showed the opposite of what we were expecting, as B9 was chosen because in previous experiments its presence had been observed to increase the IRES activity. Unmodified oligonucleotides did not show any effect on the IRES activity, which did not match the results obtained before. Modifying the oligonucleotides with phosphorothioate linkages showed a stronger effect on decreasing the Nluc to Fluc ratio compared to LNA modifications.

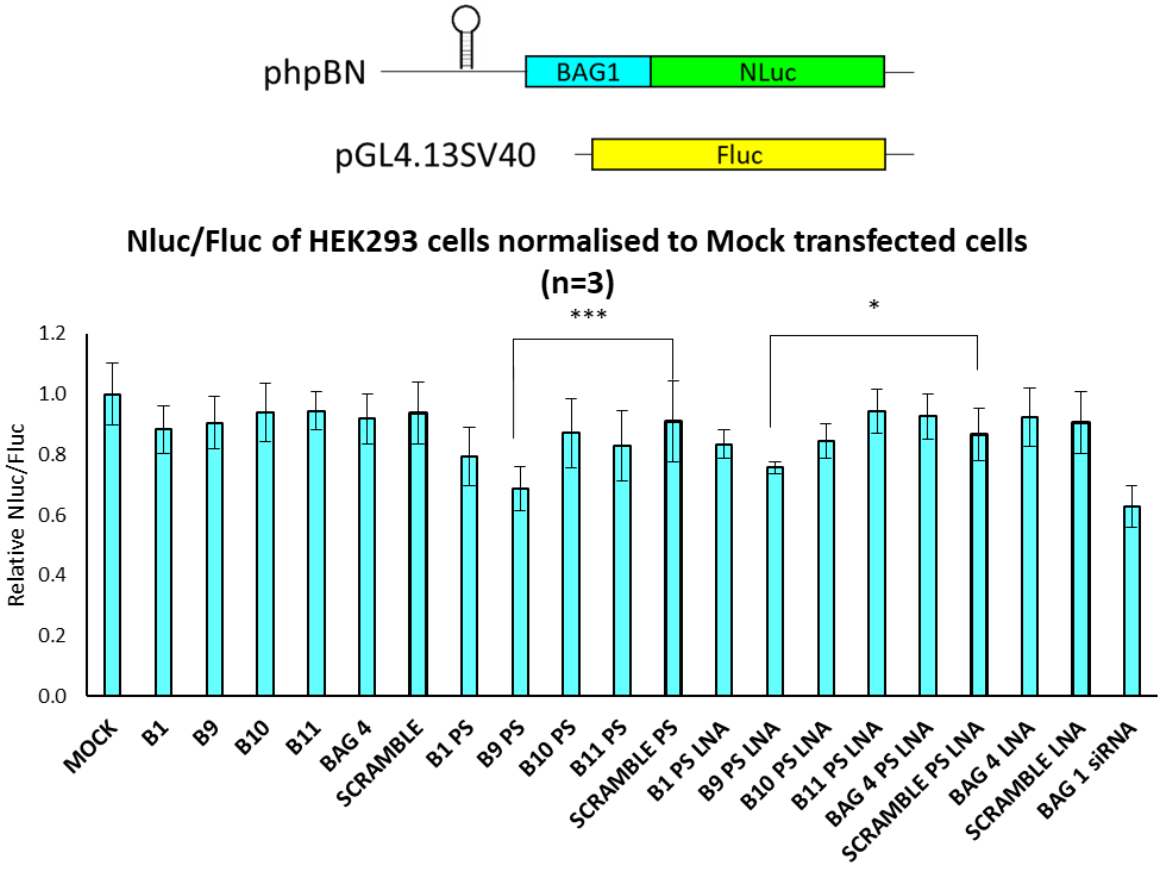

Figure 5.9 **Dual luciferase assay results of HEK293 cells transfected with phpBN and pGL4.13SV40 and a final concentration of 25 nM of the selected oligonucleotides for two days.** Nluc to Fluc ratio normalised to Mock transfected cells. Results from three independent experiments, each done in triplicate. Error bars show ± SD. Statistical analysis was done using a one-way ANOVA with a Dunnett's multiple comparison test ($P<0.05$), where the means of the Nluc to Fluc ratio of each oligonucleotide treated cells normalised to Mock transfected cells were compared against the Nluc to Fluc ratio of Scramble transfected cells.

The Fluc and Nluc values of this experiment can be found in Figure D.7 on page 297.

5.3.1.2 Luciferase assay in hpBN-HEK

The stable cell line hpBN-HEK was constructed to reduce the number of plasmids transfected and thereby try to reduce the variability in the assay. We still transfected pGL4.13SV40, to be able to compare the IRES-mediated activity from the hpBN expressed in the cells from the cap-mediated translation.

When compared to the Scramble transfected cells, only BAG 4 LNA significantly increased the Nluc to Fluc ratio. When compared to Mock transfected cells, BAG1 siRNA was the only one that significantly decreased the Nluc to Fluc ratio (Figure 5.10). B9 PS showed to be the oligonucleotide that decreased the Nluc to Fluc activity the most, but it did not do it in a significant way.

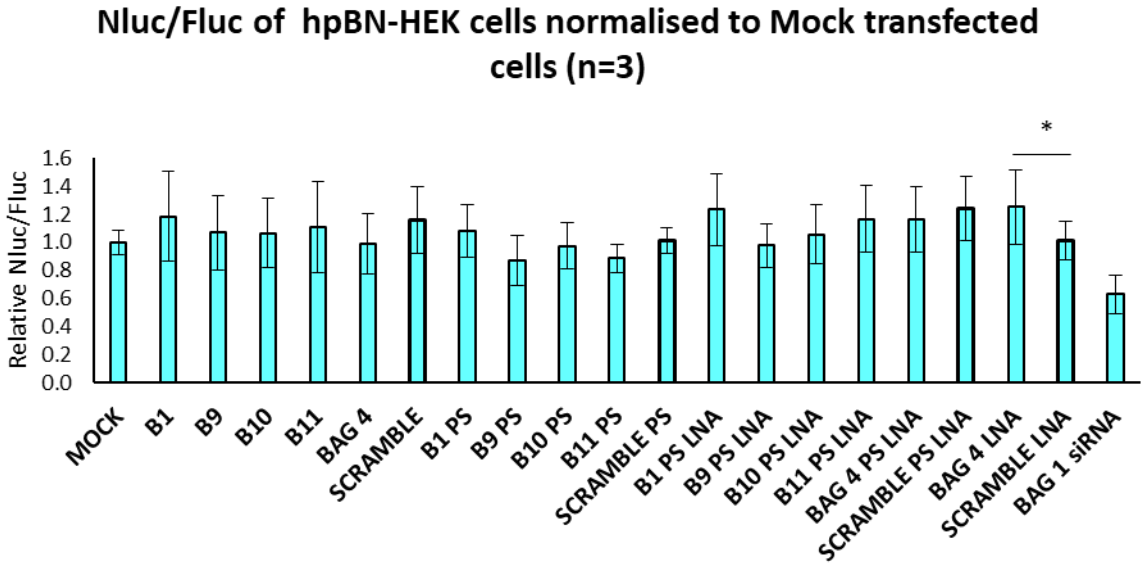

Figure 5.10 **Dual luciferase assay of hpBN-HEK cells transfected with pGL4.13SV40 and a final concentration of 25 nM of the selected oligonucleotides for two days.** Nluc to Fluc ratio was calculated and normalised to the Nluc to Fluc of Mock transfected cells. Error bars represent ± SD. Statistical analysis was done using a one-way ANOVA with a Dunnett's multiple comparison test ($P<0.05$), where the means of the Nluc to Fluc ratio of each oligonucleotide treated cells normalised to Mock transfected cells were compared against the Nluc to Fluc ratio of Scramble transfected cells.

The Fluc and Nluc values of this experiment can be found in Figure D.8 on page 298.

5.3.2 Western blot and qPCR

With the luciferase assay we were able to study the effect that the oligonucleotides had on the *BAG1* IRES present in the phpBN plasmid or in the integrated *BAG1* IRES in the case of hpBN-HEK cells. We also wanted to study the effect of the oligonucleotides in the endogenous BAG1

expression. To do so, oligonucleotides (25 nM final concentration) were transfected in HEK293 cells, and 2 days after transfection cells were harvested, protein and RNA was extracted to study BAG1 protein expression and mRNA levels by western blot and qPCR respectively. Western blot results were compared to Scramble transfected cells and qPCR results to Mock transfected cells (cells treated with the transfection reagent, without oligonucleotides).

The experiment was done three independent times. To study the effect of the oligonucleotides in the BAG1 protein expression, the main BAG1 isoforms p36 and p50 expression was quantified in each western blot. The total amount of BAG1 expression was calculated by adding up the p36 and p50 expression and the relative expression of p50 and p36 was also calculated (%p36 and %p50). The total BAG1 expression was normalised to the actin expression and normalised to Mock transfected cells. *BAG1* mRNA levels of cells transfected with the oligonucleotides were also normalised to Mock transfected cells. BAG1 protein to *BAG1* mRNA ratios were calculated to study the effect that the oligonucleotides could have in the levels of translation.

To assess the activity of the oligonucleotides in the BAG1 expression and mRNA or translation levels, a one-way ANOVA with a Dunnett's multiple comparison test was done ($P<0.05$), comparing the oligonucleotide treated cell results to Scramble transfected cells in the case of the western blot analysis and to Mock transfected cells in the case of qPCR results .

None of the unmodified oligonucleotides or phosphorothioate DNA oligonucleotides showed any difference when compared to the Scramble transfected cells (Figure 5.12, A). However, B1 PS LNA, B9 PS LNA and B11 PS LNA transfected cells showed a decrease in total BAG1 expression when compared to Scramble PS LNA transfected cells. The BAG1 levels of siRNA pool transfected cells were compared to Pool control transfected cells with an unpaired t-test (two-tailed), and showed that the siRNA significantly decreased the BAG1 expression. Both BAG1 siRNA and siRNA pool transfected cells decreased the total BAG1 protein expression, but the statistical analysis did not show that levels were significantly different from the Mock transfected cells. B10 PS, Scramble PS, B11 PS LNA, Scramble PS LNA and Pool control transfected cells significantly increased the total BAG1 amounts when compared to Mock transfected cells. The fact that cells transfected with the Scramble oligonucleotide showed a significant increase in the BAG1 expression could mean that the oligonucleotide transfection itself (independently of the sequence), had an effect on the BAG1 expression.

None of the oligonucleotides significantly modified the p50 and p36 expression when compared to Scramble transfected cells and the same result was observed when compared to Mock transfected cells (Figure 5.12, B).

As seen in Figure 5.12 C, only siRNA pool transfected cells showed a decrease in *BAG1* mRNA levels, as expected. BAG1 siRNA, however, did not decrease the *BAG1* mRNA levels, which suggests that it was not functioning very efficiently. None of the oligonucleotide transfected cells exhibited a decrease in the levels of *BAG1* mRNA. B1 PS LNA, B9 PS LNA significantly increased the *BAG1* mRNA levels. None of the oligonucleotide treated cells showed a difference in *BAG1* mRNA compared to the mRNA levels of the cells transfected with the Scramble oligonucleotide. These results show that none of the oligonucleotides (the unmodified oligonucleotides included) recruited RNase H, and it suggests that any effect seen in the protein expression levels (apart from the effect seen in the B1 PS LNA and B9 PS LNA transfected cells) will be at the level of translation.

BAG1 protein to *BAG1* mRNA ratio was calculated to see the effect of the oligonucleotides in the translation of BAG1 (see Figure 5.12 D). When compared to the Scramble transfected cells, only B1 PS LNA and B9 PS LNA showed a significant decrease in the BAG1 protein to mRNA ratio. Only Scramble PS significantly increased the BAG1 protein to mRNA ratio when compared to Mock transfected cells.

The results of this experiment did not match up to the hypothesis behind the experiment in the first place, as none of the oligonucleotides modified the expression of p36, whose translation is partially driven by the IRES. However, some of the oligonucleotides modified the total BAG1 protein levels when compared to Scramble transfected cells. None of the oligonucleotide transfected cells showed a decrease in the *BAG1* mRNA levels, as expected, but some increased it. When looking at the BAG1 protein to mRNA ratios, B1 PS LNA and B9 PS LNA showed a decrease in BAG1 protein when compared to Scramble PS LNA transfected cells. These two oligonucleotides were the ones that also showed an increase in the *BAG1* mRNA levels.

It seems that B1 PS LNA and B9 PS LNA are the oligonucleotides showing the most promising results. To obtain definitive results of the oligonucleotide activity on *BAG1* IRES-mediated translation, this experiment should be repeated to increase the n value in the statistical analysis.

One of the biggest problems faced in this experiment is that oligonucleotides showed different, and many times opposite, effects in each of the three individual experiments, as can be observed by the error bars showing the standard deviation in Figure 5.12. To this we need to add the fact that we know that western blot is a semi quantitative technique and that we had previously observed the difficulty to use it as a reliable technique to quantify the expression of BAG1 and its isoforms (see section 4.3 on page 132).

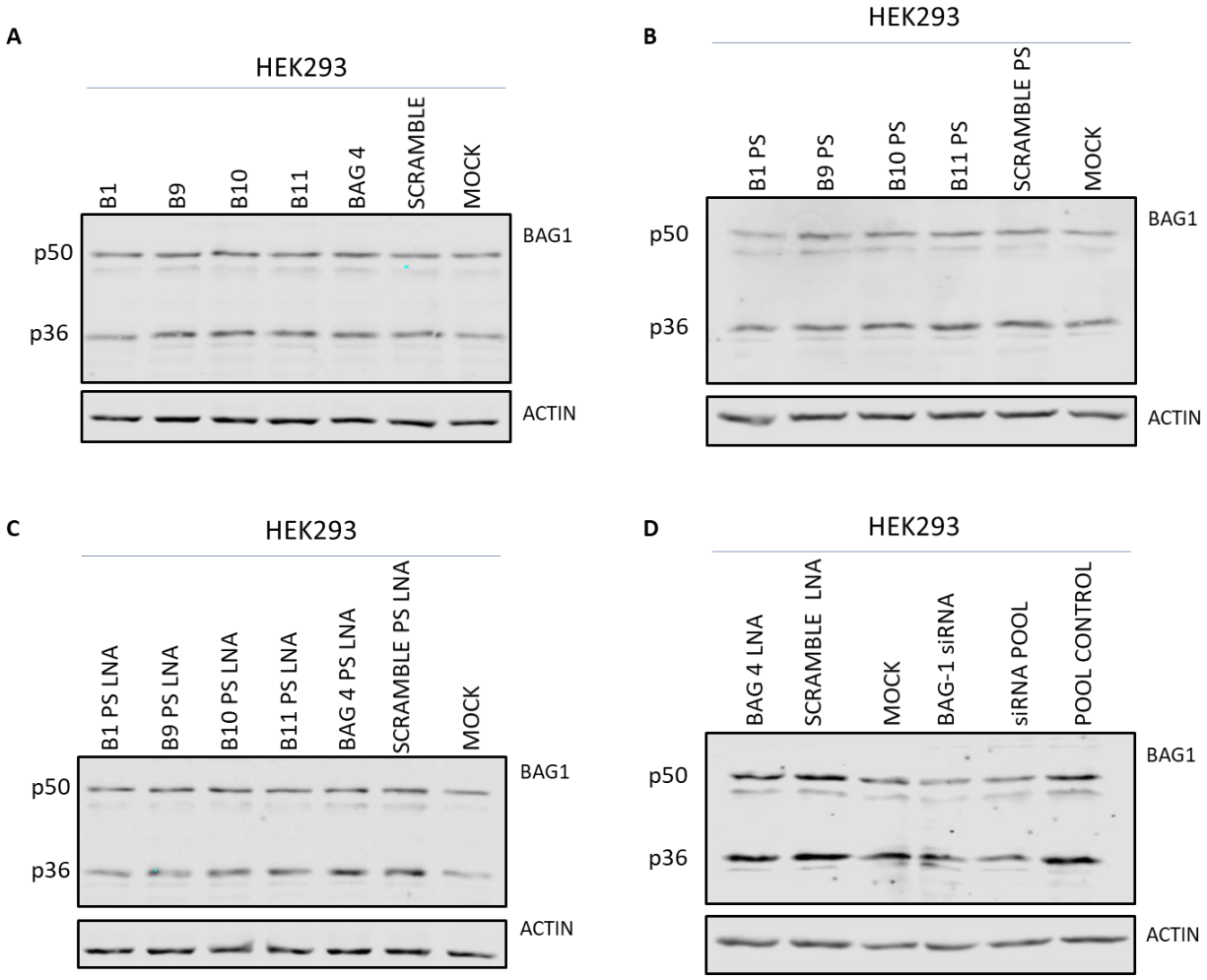

Figure 5.11 **One of the three western blots to study the effect of the oligonucleotides in the endogenous BAG1.**

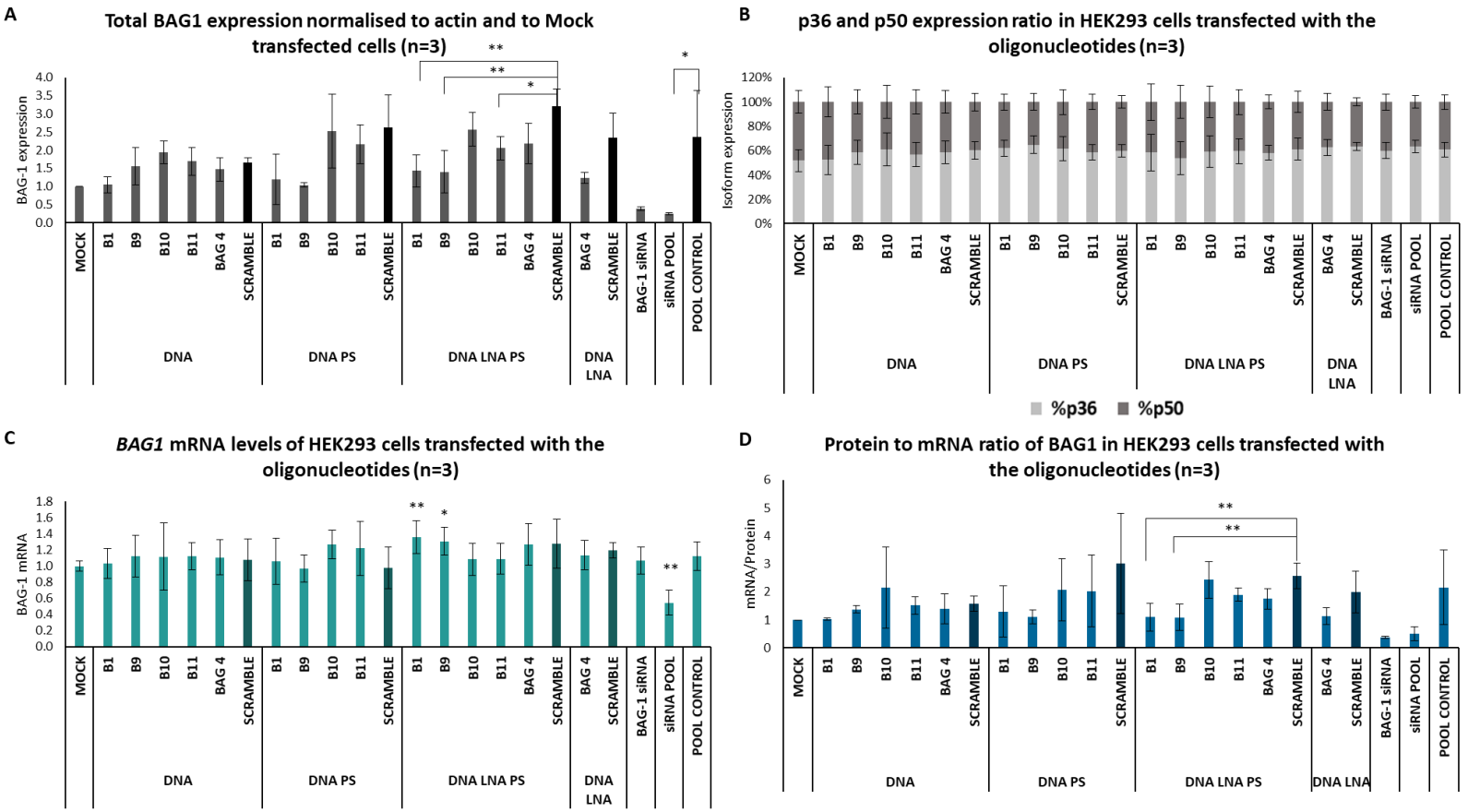

Figure 5.12 **Western blot quantification and qPCR results of HEK293 cells transfected with a final concentration of oligonucleotide of 25 nM for two days.** A) Total BAG1 expression normalised to acting and Mock transfected cells. B) %p36 and %p50 expression. C) *BAG1* mRNA levels, normalised to *B2M* and to Mock transfected cells. D) BAG1 protein to mRNA ratios normalised to Mock transfected cells. Error bars show ±SD. Statistical analysis was done using a one-way ANOVA with a Dunnett's multiple comparison test ($P<0.05$).

5.4 DISCUSSION

The overall aim of the project was to use oligonucleotides to modify gene expression at the translation level of mRNAs containing IRESs. We have focused our research in the *BAG1* gene. In 2001 Coldwell *et al.*[144] showed the presence of an IRES in the *BAG1* mRNA that could translate the p36 isoform of this gene and we have corroborated the presence of that IRES (see Chapter 3). It needs to be specified that p36 can also be translated *via* cap-mediated translation.

OLIGONUCLEOTIDE DESIGN BASED ON THE *BAG1* IRES STRUCTURE

It was three years after the discovery of the *BAG1* IRES that Pickering *et al.*[82] proposed the structure of the *BAG1* IRES based on chemical and enzymatic probing data. They also suggested that according to its conformation, the activity of the IRES could be compromised. Based on this structure, we designed several oligonucleotides that would target key sequences in the IRES (BAG 1 DNA, BAG 2 DNA, BAG 3 DNA, BAG 4 DNA, BAG 1 LNA, BAG 2 LNA, BAG 3 LNA and BAG 4 LNA). BAG 1 and BAG 2 were designed to keep the IRES closed, and thereby reduce IRES-mediated translation, while BAG 3 and BAG 4 were designed to open the IRES and thereby activate IRES-mediated translation initiation.

Scramble and BAG1 siRNA were used as control sequences. Scramble should not target any gene in the whole genome, but it should show us how the transfection of an oligonucleotide could affect the physiology or morphology of the cells. BAG1 siRNA was designed to target the 5' UTR of *BAG1.*

To avoid all the problems unmodified oligonucleotides might cause, such as degradation by endonucleases and cell toxicity[190,191] LNA-DNA mixmers were designed. An LNA modification was introduced every one to five DNA nucleotides, to increase the targeting effect, specificity and avoid recruiting RNase H[225].

The effect of the oligonucleotides controlling the *BAG1* IRES-mediated translation was first studied by a dual luciferase reporter assay and later on by western blot.

We started studying the effect of the oligonucleotides in the activity of the *BAG1* IRES using reporter RNAs expressed from the phpBN vector. phpBN was generated to decrease the cryptic promoter activity present in pFBN, plus the presence of the hairpin showed a decrease in cap-mediated translation allowing this reporter to be a clearer way to assay *BAG1* IRES activity. phpBN was co-transfected alongside pGL4.13SV40, as a transfection control as well as to compare the cap-mediated translation and IRES-mediated translation. This experiment was done in triplicate

three independent times. In this case we could not observe large differences in the activity of the unmodified and modified oligonucleotides. All the oligonucleotides but BAG 3 DNA decreased the Nluc to Fluc ratio, and thereby the IRES activity.

The effect of the oligonucleotides modifying the expression of the endogenous BAG1 in HEK293 cells was also analysed by western blot. In the two independent western blot experiments that were done, all the oligonucleotides reduced the total BAG1 expression when compared to no oligonucleotide transfected cells. In one of the experiments the LNA-DNA mixmers reduced the total BAG1 protein levels more than the unmodified oligonucleotides, whereas in the other experiment the results obtained showed the opposite. All the oligonucleotides decreased the p36 expression in both experiments. BAG 4 LNA and BAG 4 DNA were the oligonucleotides that decreased the p36 expression in a stronger way when comparing both experiments. This suggests that the effect of the oligonucleotides depends more on the region they target rather than on the chemistry of the same. On the other hand, BAG 1 DNA and BAG 2 DNA were the oligonucleotides that decreased the p36 expression less efficiently. This result corroborates our previous hypothesis, as BAG 1 and BAG 2 target the same area of the IRES (BAG 2 differs from BAG 1 in the addition of an extra thymidine to increase its flexibility).

BAG1 mRNA levels of HEK293 cells transfected with the oligonucleotides were also measured for the cells used to obtain the second western blot. Unfortunately, only BAG 1 DNA and BAG 1 LNA transfected cells maintained similar *BAG1* mRNA levels as untransfected cells, the rest of the oligonucleotides decreased in a significant way the *BAG1* mRNA levels. Unmodified oligonucleotides did not have any protection against nuclease degradation in the cells, we thereby did not expect to see a difference in the *BAG1* mRNA levels of cells transfected with the unmodified oligonucleotides. However, a decrease in the *BAG1* mRNA levels of cells transfected with the unmodified oligonucleotides could be an indicative that the oligonucleotides had not been degraded by the nucleases in the cells and were thereby targeting the mRNA. The decrease in the mRNA levels could be due to the RNase H activation. What was more surprising was the fact that cells transfected with LNA-DNA mixmers decreased the *BAG1* mRNA levels. These modified oligonucleotides were designed to avoid nuclease degradation in the cells and RNA degradation by RNase H. We did not manage to reduce the mRNA degradation using LNA-DNA mixmers, thereby different oligonucleotide modifications should be considered in the future. Only BAG 1 DNA and BAG 1 LNA kept the mRNA levels constant. These oligonucleotides were the shortest oligonucleotides, composed of only 10 nucleotides. The fact that these two oligonucleotides were the only ones keeping the *BAG1* mRNA levels constant could suggest that they were not properly targeting the *BAG1* mRNA, and this could mainly be because their short length decreased their specificity and they could have miss-targeted other regions in the mRNA.

These results suggested that we should consider increasing the number of nucleotides in future oligonucleotide design.

When BAG1 protein levels were normalised to *BAG1* mRNA levels to study translation levels, all the oligonucleotides decreased the translation levels, but unmodified oligonucleotides had a stronger effect than LNA-DNA mixmers. BAG 1 DNA and BAG 4 DNA were the most effective oligonucleotides decreasing the translation levels.

BAG1 OLIGONUCLEOTIDE POOL COVERING THE WHOLE *BAG1* IRES

As some of the oligonucleotides designed did not show the expected results, we designed 17 oligonucleotides (of 20 nucleotides each) that targeted the whole minimal *BAG1* IRES sequence proposed by Pickering *et al*[82].

The new designed oligonucleotides and the ones from previous experiments were co-transfected with phpBN+pGL4.13SV40 in triplicate three individual times and a dual luciferase reporter assay was carried out, as in previous experiments. On the contrary to what we saw in previous experiments, all the oligonucleotides increased the Nluc to Fluc ratio, even the ones that had previously shown to decrease it. This was very surprising and definitely unexpected, as the oligonucleotides were transfected following the same protocol both times. In this case, most of the oligonucleotides had a significant effect in the Nluc to Fluc ratio when compared to no oligonucleotide transfected cells, which means that most of them had the ability to modify the IRES expression. B9 and B10 were the oligonucleotides that increased the Nluc to Fluc ratio the most and B1 and B11 were the ones that decreased it the most. Nevertheless, Scramble oligonucleotide also showed the ability to modify the IRES activity, which suggests that to have a more reliable effect of the oligonucleotides in the IRES activity, the Nluc to Fluc ratio of oligonucleotide transfected cells should be compared to the ratio of Scramble transfected cells. However when this was done, none of the oligonucleotides showed a significant difference in the Nluc to Fluc ratio. These results suggest that none of the oligonucleotides had a real ability to modify the IRES expression. This could easily be because the oligonucleotides used were unmodified and thereby their activity was not as strong as that of modified oligonucleotides.

In this experiment the concept of Mock transfected cells was introduced: cells treated with transfection reagent in the absence of oligonucleotides. Mock transfected cells represented a more realistic control to normalise the oligonucleotide transfected cells to. B10 and BAG 4 LNA were the only oligonucleotides that showed a significant different Nluc to Fluc ratio when compared to Scramble transfected cells, whereas B9, B10, BAG 3 LNA and BAG 4 LNA transfected cells had a significantly different Nluc to Fluc ratio when compared to Mock transfected cells. B1

and B11 transfected cells were the ones that decreased the Nluc to Fluc ratio the most, whereas B9, B10 and BAG 4 LNA were the ones that increased it the most.

WORKING WITH THE MOST PROMISING OLIGONUCLEOTIDES: B1, B9, B10, B11 AND BAG 4 NEW

After this experiment, we decided to focus our research in using B1, B9, B10, B11 and BAG 4 NEW to modify the expression of the *BAG1* IRES, where B1 and B11 had previously shown to decrease the IRES activity and B9, B10 and BAG 4 NEW to increase it. We decided to modify these oligonucleotides in different ways to study their effect in the *BAG1* IRES. As LNA-DNA mixmers failed to modify the oligonucleotide activity in cells and induced RNA degradation, we decided to make LNA-DNA mixmers with phosphodiester bonds to increase their activity and avoid RNase H recruitment.

Unmodified oligonucleotides did not alter the Nluc to Fluc ratio compared to Scramble or Mock transfected cells. B9 PS and B9 PS LNA were the only oligonucleotides that showed a decrease in the Nluc to Fluc ratio when compared to Scramble transfected cells. All he PS modified oligonucleotides and most of the PS-LNA oligonucleotides significantly decreased the Nluc to Fluc ratio when compared to Mock transfected cells.

These results suggested that the nuclease resistance of the PS oligonucleotides was stronger than that of the unmodified oligonucleotides. The results also suggested that the PS oligonucleotides could have recruited RNase H and thereby decrease the Nluc to Fluc ratio when compared to Mock transfected cells.

Overall B9 PS and B9 PS LNA were the only oligonucleotides able of decreasing the IRES activity. These results were surprising, as B9 was selected to be one of the oligonucleotides capable of increasing the IRES activity in previous experiments.

When the modified oligonucleotides were transfected in hpBN-HEK cells, only BAG 4 LNA had a significant effect when compared to Scramble transfected cells. The fact that BAG1 siRNA decreased the Nluc to Fluc ratio in a significant way when compared to Mock transfected cells suggested that the transfection protocol was efficient in this experiment. However, the transfection protocol could always be optimised for this particular cell line and study the effect of the oligonucleotides again.

The endogenous BAG1 expression of HEK293 cells transfected with the new modified oligonucleotides was also studied by western blot and *BAG1* mRNA levels were measured by qPCR. Western blots and qPCRs were done three independent times.

None of the oligonucleotides modified the p50 and p36 expression when compared to Scramble or Mock transfected cells. Only B1 PS LNA, B9 PS LNA and B11 PS LNA transfected cells significantly decreased the total BAG1 amounts when compared to Scramble transfected cells. siRNA pool also significantly decreased the total BAG1 expression when compared to pool control, suggesting that the experiment worked properly. B10 PS, Scramble PS, B11 PS LNA and Scramble PS LNA showed a significantly stronger BAG1 expression when compared to Mock transfected cells. The fact that the controls Scramble PS and Scramble PS LNA had a significant effect in the BAG1 expression could mean that none of the other two oligonucleotides had a real effect in the BAG1 expression and thereby, the BAG1 expression of oligonucleotide treated cells should be compared to the expression of Scramble transfected cells.

In terms of the *BAG1* mRNA levels, only siRNA pool transfected cells showed a decrease in the *BAG1* mRNA levels. The fact that the DNA PS oligonucleotides did not decrease the *BAG1* mRNA levels was surprising, as these oligonucleotides were designed to recruit RNase H. These results might suggest that the PS oligonucleotides were not as nuclease stable as the literature suggests and were thereby degraded before they had the chance to target the mRNA. It could also suggest that they did not recruit RNase H as the literature suggests, and thereby did not produce RNA degradation or that they did not target the mRNA properly. Surprisingly B1 PS LNA and B9 PS LNA transfected cells, who had previously shown to have the ability to decrease the BAG1 expression, showed significantly higher *BAG1* mRNA levels than Mock transfected cells.

When the BAG1 to protein ratio was calculated to study the effect of the oligonucleotides in the levels of translation, only B1 PS LNA and B9 PS LNA showed a significantly reduced ratio compared to Scramble transfected cells, suggesting they were the only oligonucleotides capable of modifying the levels of a translation in a significant way.

After the study of the effect of the oligonucleotides on modifying the *BAG1* IRES activity, we can conclude that B9 PS LNA was the only oligonucleotide capable of showing a decrease in the *BAG1* IRES activity by a dual luciferase assay and by western blot without decreasing the *BAG1* mRNA levels.

Chapter 6 USING OLIGONUCLEOTIDES TO MODIFY THE *BAG1* IRES ACTIVITY IN RRL

Delivery of oligonucleotides and reporter genes into cells can easily introduce errors and generate inconsistencies in the results due to the different levels in translation efficiency between and within experiments. We thereby decided to go to the simplest possible system: the cell free system RRL. As we had previously shown, *BAG1* IRES is not active in RRL (see 3.7.2 on page 110), therefore this system would be good to study whether we can increase the IRES activity with the oligonucleotides. This would allow us to determine if our oligonucleotides could mimic the activity of ITAFs and modify the IRES structure and activity. RRL were programmed as explained in section 2.12 on page 77. To avoid any RNA degradation and the potential generation of monocistronic RNAs expressing Nluc from FBN, new RNA was synthesised for each one of these experiments. That is why the Fluc and Nluc activities of the FBN (no oligonucleotide) programmed RRLs exhibit differences from one experiment to the other. We were also unable to undertake statistical analysis, as each RNA was only used once. The results show the luminescence reads of two wells containing the same RRL reaction, for that reason no error bars are shown in the results, as they would only indicate the accuracy in the pipetting more than the differences between replicate experiments.

6.1 UNMODIFIED OLIGONUCLEOTIDES IN RRL

All the unmodified oligonucleotides were used to program RRL (B1-B17, BAG 1-2-3-4 DNA, 3 NEW and 4 NEW). As controls Scramble oligonucleotide (should not modify the IRES activity) and BAG1 siRNA were used. There is not much evidence in the literature about the activity of siRNAs in RRL, however Hagerlof *et al.*[292] successfully showed the activity of siRNAs in RRL.

Looking at the literature we found different RRL programming protocols where antisense oligonucleotides were used. Some researchers incubated the oligonucleotide with the RNA at 65-70°C for a few minutes to increase their binding affinity[293,294], whereas others just incubated the RNA and oligonucleotide together at 30-37°C for a few minutes before the RRL reaction[295,296].

RRL was programmed with 1 µM of oligonucleotide and 500 ng of *in vitro* synthesised FBN RNA, meaning that 0.53 µl of oligonucleotide (10 µM) was mixed with 1 µl of RNA (FBN or FN, at 500 ng/µl). We did two different and independent experiments, in one the oligonucleotide and RNA mix was heated at 65°C for 5 minutes, incubated in an ice water bath for 5 minutes and incubated at 37°C for around 10 minutes. In the other one (carried out on a different day, with a different *in*

vitro synthesised RNA), to check if the heating step was a critical step in the ability of the oligonucleotide to modify the IRES activity , the steps of heating the mix at 65°C and incubating it on ice were skipped. The RRL reaction was set up and carried out as described in section 2.12 on page 77. The Fluc and Nluc activity was measured by the dual luciferase assay. To verify that the oligonucleotides were specifically targeting the *BAG1* IRES, RRL were also programmed with FN and the oligonucleotides. In this case, the mixture was also heated at 65°C before the start of the RRL reaction.

To study the effect of the oligonucleotides on the IRES activity, the Nluc to Fluc ratio of the RRL programmed with FBN and the oligonucleotides was calculated and normalised to the Nluc to Fluc ratio of FBN (no oligonucleotide) programmed RRL and the results were compared to RRL programmed with Scramble oligonucleotides. In every case the RRL programmed with the Scramble oligonucleotide kept the Nluc to Fluc ratio at the RRL programmed with FBN (no oligonucleotide) levels, it did not have an effect in the *BAG1* IRES activity, which verifies its activity as a control oligonucleotide and suggests that any other changes in the Nluc to Fluc activity must be due to the ability of the oligonucleotides to modify the *BAG1* IRES. When RRL were programmed with FBN and the oligonucleotide most of the oligonucleotide increased the Nluc to Fluc ratio (Figure 6.2). The increase in the Nluc to Fluc ratio was higher when the oligonucleotide and RNA mixture was heated at 65°C before the RRL reaction was set up. However, the reactions where the heating step was skipped also showed an effect. RRL programmed with BAG1 siRNA showed a decrease in the Nluc to Fluc ratio, verifying its activity in RRL.

When the oligonucleotide and FBN RNA mixture was heated at 65°C, B15, B6, B5 and B14 were the oligonucleotides that increased the Nluc to Fluc ratio the most (see Table 6.1, left hand side), and thereby increased the *BAG1* IRES activity the most (see the oligonucleotide targeting site on Figure 6.1). However, when the heating step was skipped, B3 was the oligonucleotide that increased the Nluc to Fluc ratio the most, followed by B15, B6, B5 and B14 (see Table 6.1, right hand side) (see the oligonucleotide targeting site on Figure 6.1). Surprisingly, B5, B6, B4 and B15 targeted the same area in the *BAG1* IRES where Pickering *et al.*[82] had determined that the ribosome landing area was located (see Figure 6.1).

B1 and B2 were the only oligonucleotide capable of decreasing the Nluc to Fluc ratio when the oligonucleotide and RNA mixture was heated at 65°C (see Figure 6.2 and Table 6.1, left hand side). B1, B10 and B17 were the only oligonucleotides seen to decrease the Nluc to Fluc ratio when the heating step was skipped (see Figure 6.2 and Table 6.1, right hand side).

When studying the Nluc to Fluc ratio of RRL programmed with oligonucleotides and FN to the Nluc to Fluc ratio of RRL programmed only with FN (no oligonucleotide), most of the oligonucleotides

did not have an effect, however some of them did decrease the Nluc to Fluc ratio (Figure 6.2). We were not expecting to see any effect on the Nluc to Fluc ratio values to RRLs programmed with FN and the oligonucleotides, as none of the oligonucleotides targeted any region of the FN plasmid. Each of the oligonucleotides was checked individually and it was verified that all of them showed at least 8 mismatches with the FN plasmid.

Even if the oligonucleotides had a small effect in the FN activity, that activity was minimal when compared to the level of activity the oligonucleotides had in FBN. After this experiment, we believed that the increase observed in the Nluc to Fluc ratio of the RRL programmed with FBN and the oligonucleotides was due to the effect that they were having on the *BAG1* IRES activity.

With this experiment we have shown that heating the RNA and oligonucleotides at 65°C before the RRL reaction was not a critical step for the oligonucleotide activity, even though the heating step could increase the oligonucleotide activity. We also showed that four oligonucleotides consistently increased the IRES activity: B5, B6, B14 and B15. These oligonucleotides target the same area in the *BAG1* IRES, which overlaps the ribosome entry site.

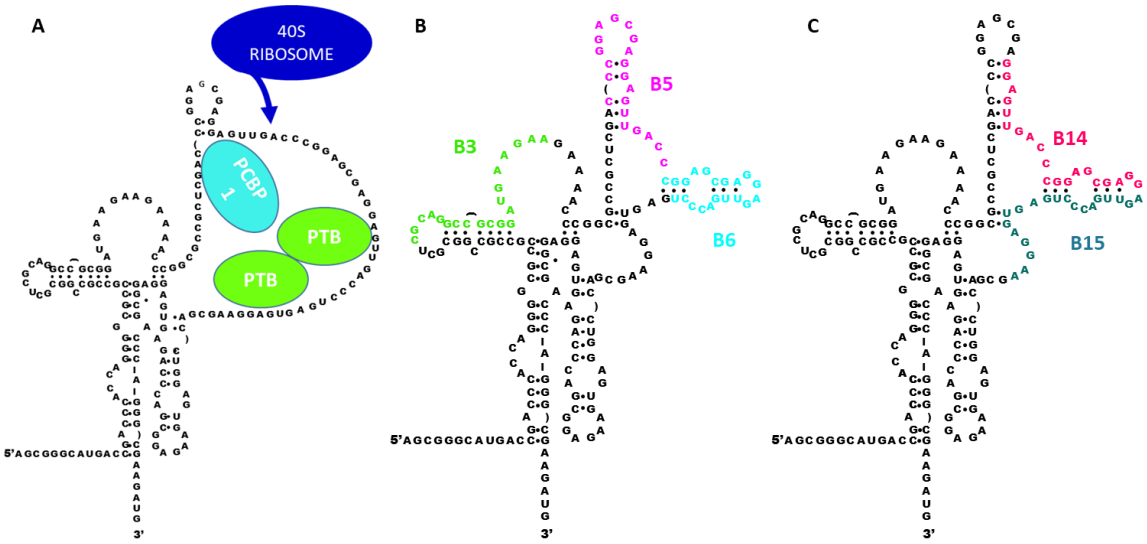

Figure 6.1 **Representation of the target area in the *BAG1* IRES of the oligonucleotides that increased the IRES activity the most in RRL.**

The Fluc and Nluc results of these experiments can be found in Figure D.9, Figure D.10 and Figure D.11 on pages 299, 300 and 301.

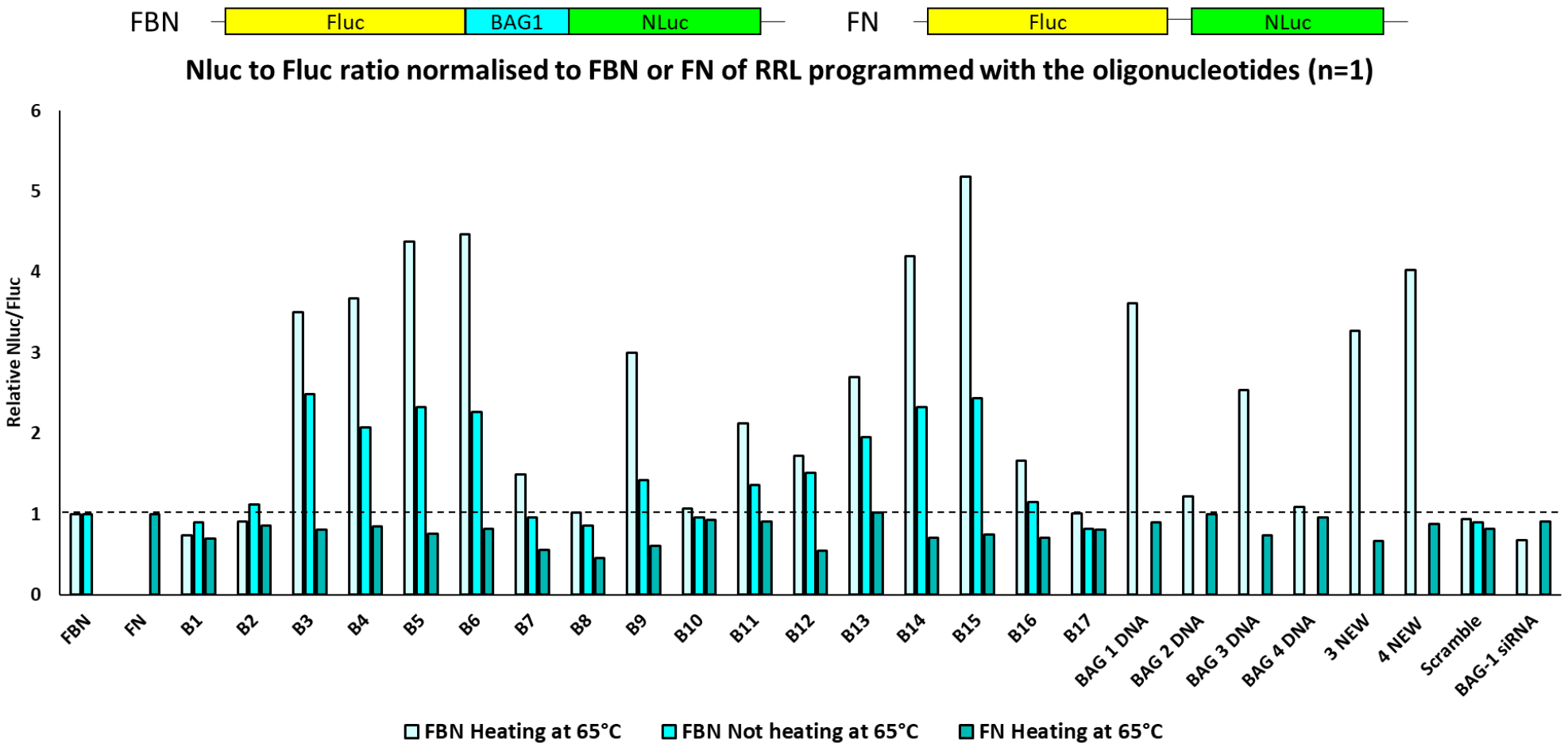

Figure 6.2 **Luciferase assay results of RRL programmed with 500 ng FBN or FN and 1 µM of final concentration unmodified oligonucleotides (heated at 65°C and not heated).** Nluc to Fluc ratio normalised to Nluc to Fluc ratio of RRL programmed with FBN or FN.

Table 6.1 List of oligonucleotides ranked from the highest to the lowest effect they had modifying the Nluc to Fluc activity in FBN. A) According to the results when the RNA mixture were heated at 65°C before the RRL reaction and B) when the heating step was skipped.

A	FBN Nluc/Fluc Heating at 65°C	FBN Nluc/Fluc Not heating at 65°C	FN Nluc/Fluc Heating at 65°C	B	FBN Nluc/Fluc Heating at 65°C	FBN Nluc/Fluc Not heating at 65°C	FN Nluc/Fluc Heating at 65°C
B15	5.18	2.44	0.75	**B3**	3.50	2.49	0.81
B6	4.47	2.27	0.82	**B15**	5.18	2.44	0.75
B5	4.38	2.33	0.75	**B14**	4.20	2.33	0.71
B14	4.20	2.33	0.71	**B5**	4.38	2.33	0.75
4 NEW	4.02		0.88	**B6**	4.47	2.27	0.82
B4	3.68	2.07	0.84	**B4**	3.68	2.07	0.84
BAG 1 DNA	3.61		0.90	**B13**	2.70	1.96	1.02
B3	3.50	2.49	0.81	**B12**	1.73	1.51	0.54
3 NEW	3.27		0.66	**B9**	3.00	1.42	0.61
B9	3.00	1.42	0.61	**B11**	2.13	1.36	0.91
B13	2.70	1.96	1.02	**B16**	1.66	1.15	0.71
BAG 3 DNA	2.54		0.74	**B2**	0.91	1.12	0.86
B11	2.13	1.36	0.91	**FBN**	1.00	1.00	
B12	1.73	1.51	0.54	**B7**	1.49	0.96	0.56
B16	1.66	1.15	0.71	**B10**	1.07	0.96	0.93
B7	1.49	0.96	0.56	**B1**	0.74	0.90	0.70
BAG 2 DNA	1.22		1.00	**Scramble**	0.94	0.90	0.81
BAG 4 DNA	1.09		0.96	**B8**	1.02	0.86	0.46
B10	1.07	0.96	0.93	**B17**	1.01	0.81	0.80
B8	1.02	0.86	0.46	**4 NEW**	4.02		0.88
B17	1.01	0.81	0.80	**3 NEW**	3.27		0.66
FBN	1.00	1.00		**BAG 3 DNA**	2.54		0.74
Scramble	0.94	0.90	0.81	**BAG 2 DNA**	1.22		1.00
B2	0.91	1.12	0.86	**BAG 4 DNA**	1.09		0.96
B1	0.74	0.90	0.70	**BAG 1 DNA**	3.61		0.90
BAG1 siRNA	0.68		0.91	**BAG1 siRNA**	0.68		0.91
FN			1.00	**FN**			1.00

6.2 UNMODIFIED OLIGONUCLEOTIDE COMBINATIONS IN RRL

B5, B6, B14, B15 and B3 were the oligonucleotides that had shown to increase the Nluc to Fluc ratio (and thereby the IRES activity) in RRL in the previous experiments; whereas B1, B8 and B17 had shown to decrease it or to have the lowest effect (Figure 6.3 to check the sequence the oligonucleotides target in the *BAG1* IRES). We decided to combine the oligonucleotides that increased the IRES activity among each other (in pairs) and the oligonucleotides that decreased it. In the case of the oligonucleotide combinations, 0.3 µl of each oligonucleotide (10 µM) were mixed, and the same procedure as in the previous experiments was followed (omitting the 65°C heating step).

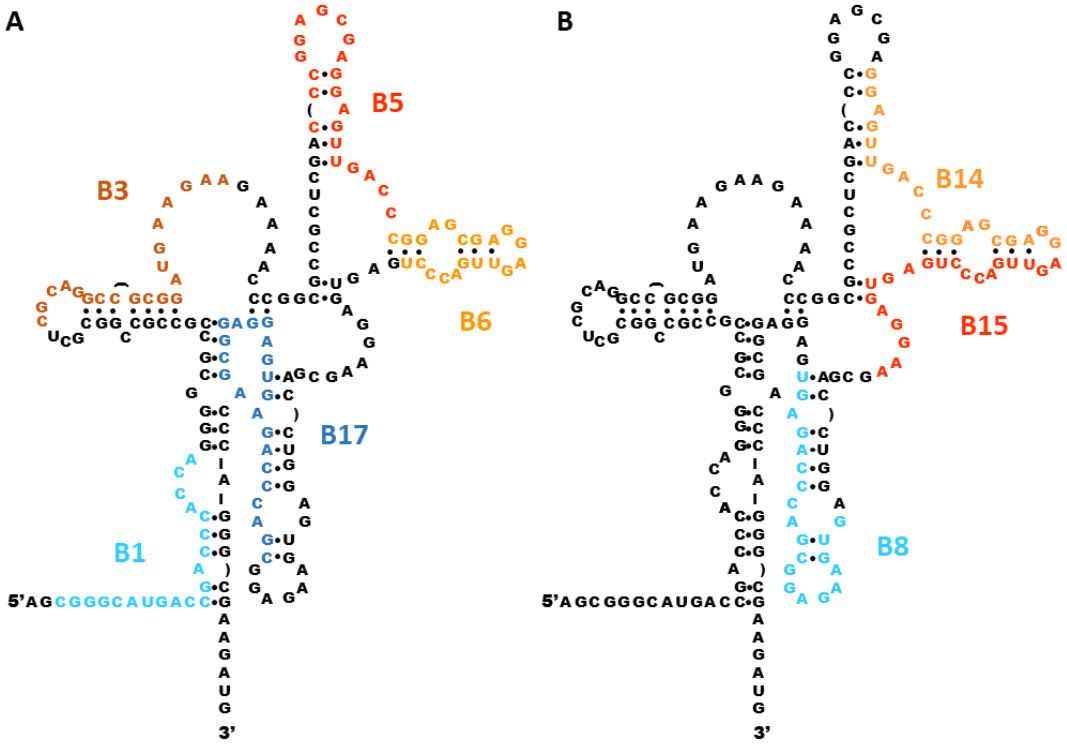

Figure 6.3 **Representation of the targeting sites in the *BAG1* IRES of the oligonucleotides that were used in combination with each other**. B3, B5, B6, B14 and B15 increased the Nluc to Fluc ratio, whereas B1, B8 and B17 decreased it.

To study the effect of the oligonucleotides on IRES activity, the Nluc to Fluc ratio of the oligonucleotide and FBN programmed RRL was normalised to the Nluc to Fluc ratio of the FBN (no oligonucleotide) programmed RRLs (see Figure 6.4). In this case RRL programmed with the Scramble oligonucleotides increased the Nluc to Fluc ratio by 23%. B1, B8 and B17 programmed RRL did modify the Nluc to Fluc ratio when compared to the Scramble programmed RRL. B17 was the only oligonucleotides capable of slightly decreasing the Nluc to Fluc ratio when compared to the Scramble programmed RRL. The oligonucleotide combination did not show any greater effect

than the oligonucleotides used individually. B15 programmed RRL had clearly the greatest Nluc to Fluc ratio, followed by the combination of B5 & B15. The oligonucleotides having the next largest increase in the Nluc to Fluc ratio were B6 and B14, which showed very close values to the combination of B5 & B15.

We thereby concluded that a combination of oligonucleotides did not increase or decrease the IRES activity in an additive or synergistic way. Instead, it was possible that in the reactions where two oligonucleotides were combined, the oligonucleotides could have interacted with each other, reducing their chances to interact with the *BAG1* IRES and thereby having a smaller effect. B15 was again identified as the oligonucleotide with the highest ability to increase the *BAG1* IRES activity in RRL.

The Fluc and Nluc results of these experiments can be found in Figure D.12 on page 302.

A

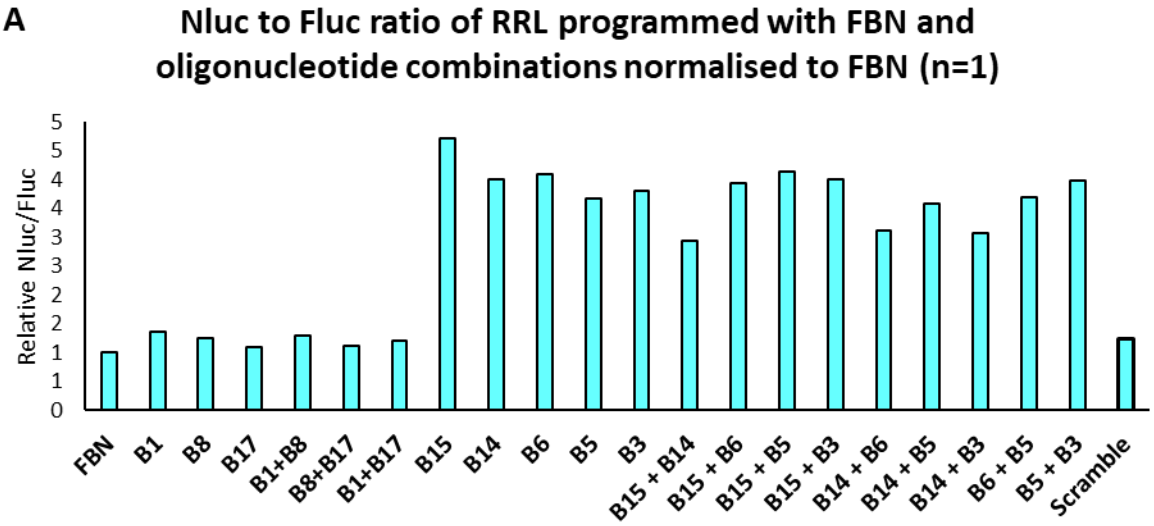

B

Oligonucleotide	avg Nluc/Fluc normalised to FBN
B15	4.71
B15 + B5	4.14
B6	4.09
B14	4.01
B15 + B3	4.01
B5 + B3	3.98
B15 + B6	3.93
B3	3.80
B6 + B5	3.69
B5	3.67
B14 + B5	3.58
B14 + B6	3.11
B14 + B3	3.08
B15 + B14	2.93
B1	1.37
B1+B8	1.30
B8	1.24
Scramble	1.23
B1+B17	1.20
B8+B17	1.12
B17	1.09
FBN	1.00

Figure 6.4 **Luciferase assay results of RRL programmed with 500 ng FBN and 1 µM final concentration of oligonucleotide combinations.** A) Nluc to Fluc ratio normalised to Nluc to Fluc ratio of RRL programmed with FBN. B) List of oligonucleotides ranked from the highest to the lowest effect they had modifying the Nluc to Fluc activity in FBN.

6.3 B14 AND B15 MODIFIED OLIGONUCLEOTIDES

At this point we decided to focus on the oligonucleotides that had shown to have the ability to increase the IRES activity the most in RRL: B14 and B15. We used mfold to study the secondary

structures that B14 and B15 could form and we slightly modified the oligonucleotides to avoid the formation of any loop structures or self-binding regions (see Figure 6.5). To B14 five nucleotides were removed from the 5' end and five more were added in the 3', creating B14 AB and to B15 five nucleotides were removed from the 5' end and two more were added in the 3', creating B15 AB (see Figure 6.6 for oligonucleotide target site). We verified that B14 AB and B15 AB did not have any self-binding sites using mfold. Both B14 AB and B15 AB showed the max score and query cover for BAG1 when run on a BLAST, however some oligonucleotides showed a smaller similarities with other genes. Due to time and resource limitations, we could not study how that affected the effectivity of the oligonucleotides.

The oligonucleotides were modified with LNA monomers (see section B.4 on page 273 for oligonucleotide sequence) to make them nuclease resistant.

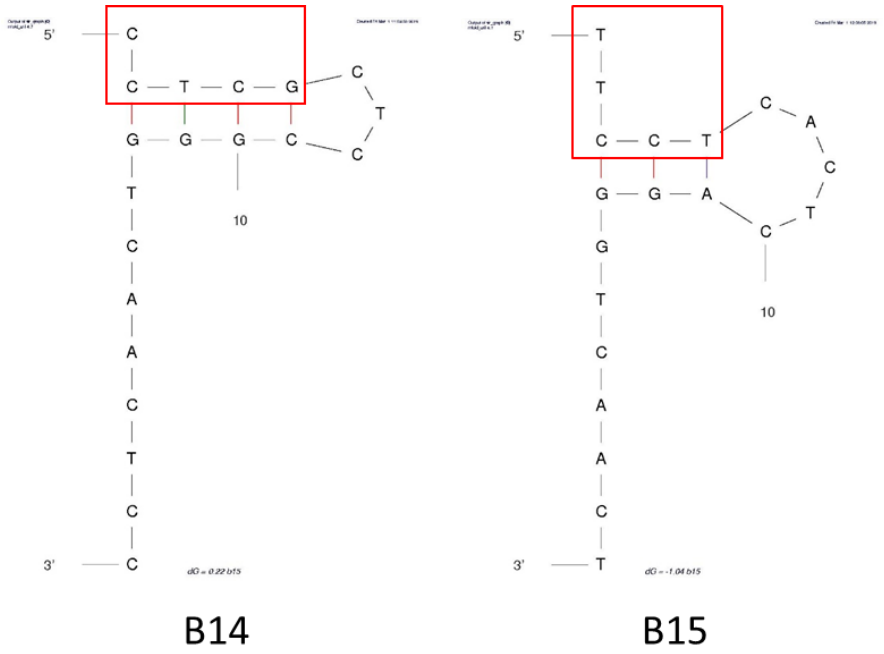

Figure 6.5 **Predicted secondary structures of B14 and B15 using mfold**. The regions selected were removed from the oligonucleotides to avoid the formation of self-binding of the oligonucleotides.

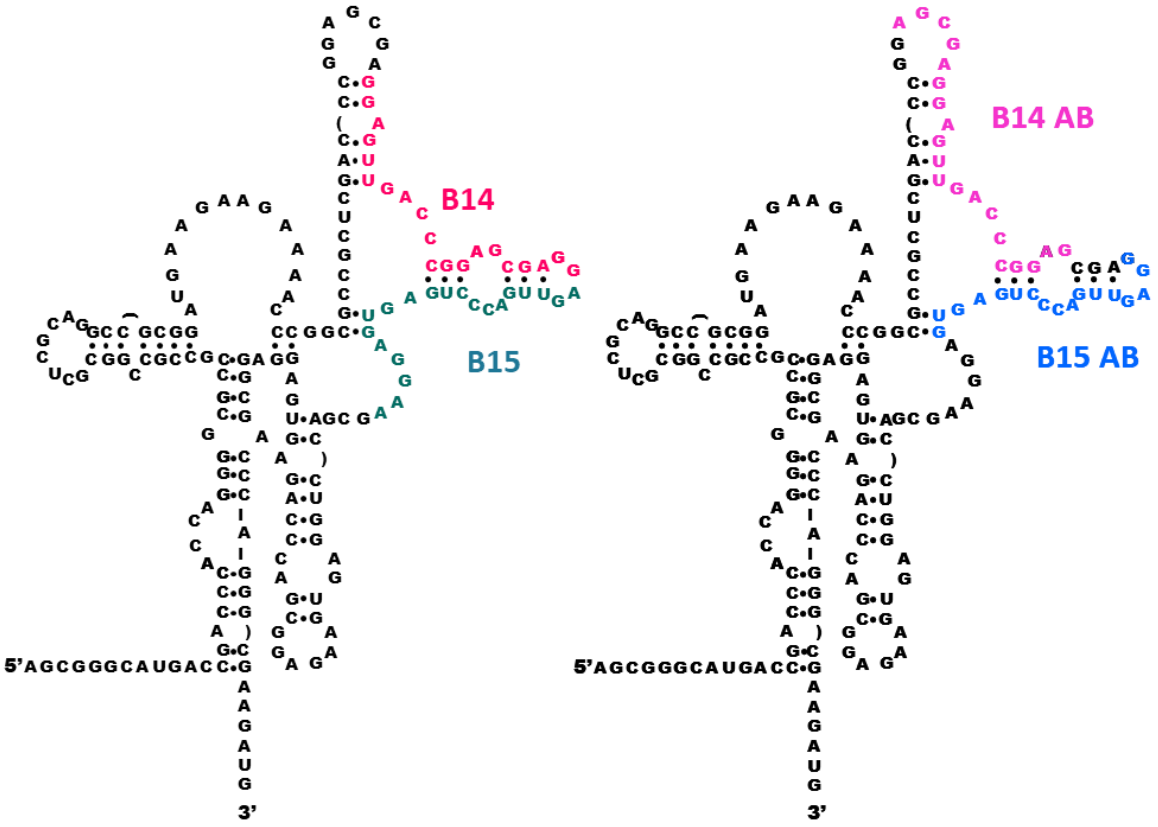

Figure 6.6 **Representation of the targeting site of B14, B15, B14 AB and B15 AB in the *BAG1* IRES.**

6.3.1 Programming RRL with the oligonucleotides

We programmed RRL as in previous experiments with FBN and unmodified B14, B14 AB, B15, B15 AB and Scramble oligonucleotides and their analogue LNA-DNA mixmers. The experiment was done twice: either heating the oligonucleotides and FBN at 65°C before starting the RRL reaction (in case the heating step was critical for the action of the modified oligonucleotides) or omitting this step. In every case RRL were programmed with a final concentration of 1 µM of oligonucleotide and 500 ng of *in vitro* synthesised FBN RNA.

In general RRL programmed with FBN and the oligonucleotides kept a constant Fluc activity when compared to RRL programmed with FBN (no oligonucleotide) (see Figure 6.7, A). In the case of the Nluc activity big differences could be observed between the modified and unmodified oligonucleotides (see Figure 6.7, B). RRL programmed with the unmodified oligonucleotides showed a very high Nluc activity compared to the Scramble and FBN (no oligonucleotide) programmed RRL, whereas RRL programmed with modified oligonucleotides and FBN showed a smaller Nluc activity than RRL programmed with Scramble and FBN (no oligonucleotide). All the RRL programmed with FBN and Scramble oligonucleotides showed a similar Nluc activity as RRL programmed with FBN (no oligonucleotide). One hypothesis that could explain these results could be a combination of the following ideas. On one hand, the 40S ribosomal subunit could consider

the LNA-DNA mixmers-RNA duplex as a double strand region (due to the strong binding of the LNAs to the RNA), not finding the single stranded region to land and start translation through the IRES. It could also happen that the ribosomal landing takes place just upstream the oligonucleotide binding site, and as the LNA-DNA mixmers bind in a very strong way to the RNA they block the ribosomal scanning. On the other hand, LNA-DNA mixmers could bind too strongly to the FBN RNA so that the ribosomes that are potentially reading through from the Fluc (if they were any) cannot continue with the reinitiation process. These would explain why an increase in the Nluc activity is not seen and why in the presence of the LNA-DNA mixmers the Nluc activity is smaller than in their absence.

The Nluc to Fluc ratio of RRL programmed with FBN and the oligonucleotides was calculated and normalised to the Nluc to Fluc ratio of RRL programmed with FBN (no oligonucleotide) (see Figure 6.7, C). RRL programmed with FBN and Scramble oligonucleotides showed an Nluc to Fluc ratio similar to the one of RRL programmed with FBN (no oligonucleotide). The RRL programmed with the unmodified oligonucleotides showed at least a tenfold increase in the Nluc to Fluc ratio when compared to the RRL programmed with Scramble. The RRL programmed with FBN and the modified oligonucleotides showed at least a 40% reduction in the Nluc to Fluc ratio when compared to the RRL programmed with Scramble. The FBN and oligonucleotide heating step at 65°C increased the Nluc to Fluc activity in most of the cases, although it was more obvious in the unmodified oligonucleotides. However, the heating step was not critical for the oligonucleotides to have an effect, as we had previously shown.

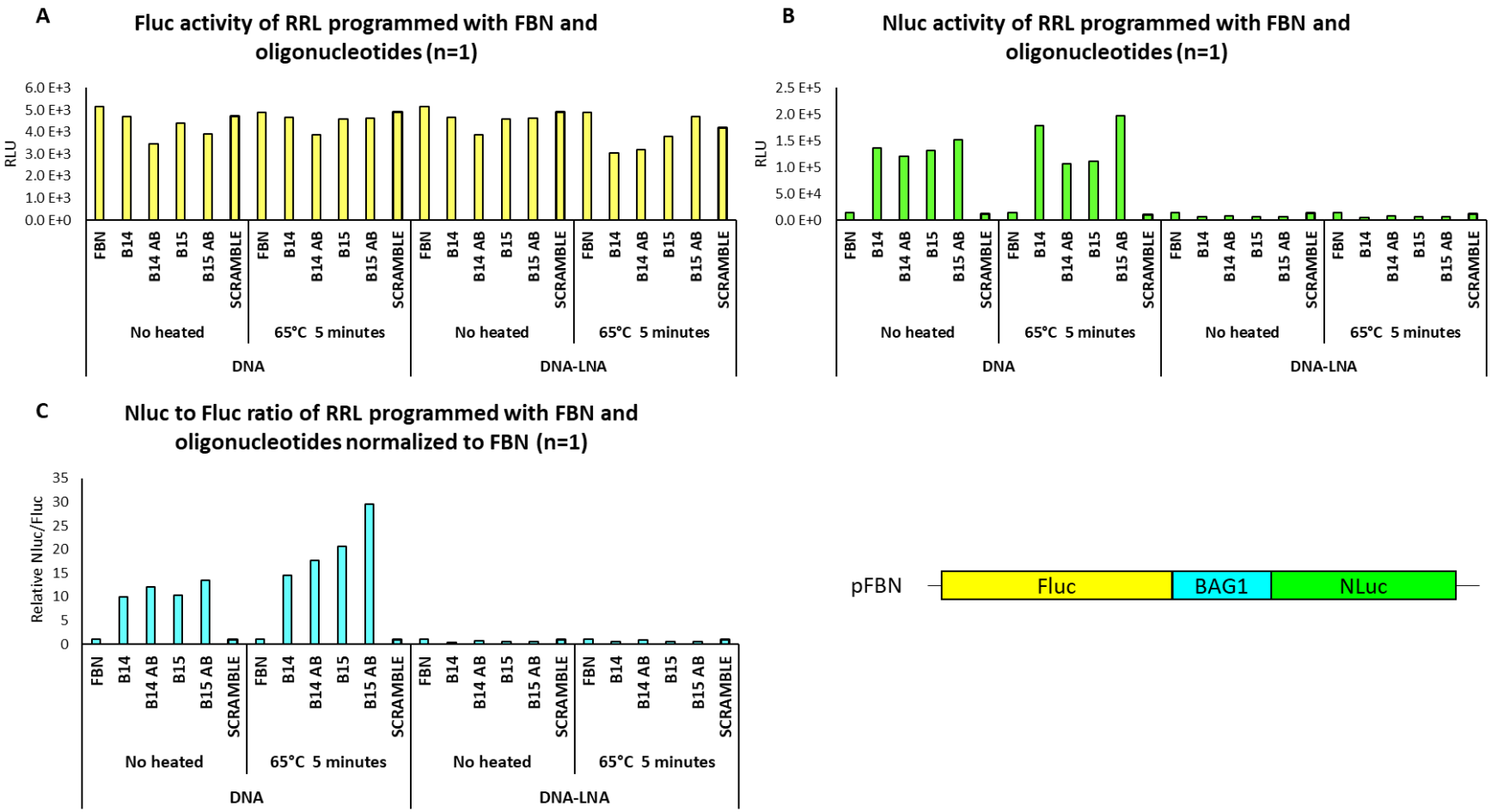

Figure 6.7 **Luciferase assay results of RRL programmed with 500 ng of FBN and 1 µM final concentration of oligonucleotides.** A) Fluc, B) Nluc activity and C) Nluc to Fluc ratio normalised to Nluc to Fluc ratio of RRL programmed with FBN.

6.3.2 HEK293 transfection with the oligonucleotides

After studying the effect of B14, B14 AB, B15 and B15 AB unmodified and LNA-DNA mixmers in cell free systems, and showing that the unmodified oligonucleotides were able to increase the *BAG1* IRES activity, the next logical step was to return to cell transfections to study if the oligonucleotides could show the same effect. To study the effect of the oligonucleotides in HEK293 cells, they were transfected alongside phpBN and pGL4.13SV40. A final concentration of 25 nM and 50 nM of oligonucleotide were transfected in each experiment (in case doubling the oligonucleotide concentration showed a higher activity), the transfection was done for two days. The results were normalised to Mock transfected cells. The experiment was done twice, each time in triplicate. A one-way ANOVA with a Dunnett's multiple comparison test was done ($P<0.05$) to compare the Nluc to Fluc ratio of oligonucleotide treated cells with the Nluc to Fluc ratio of Mock or Scramble treated cells.

The Nluc to Fluc ratio of cells transfected with the oligonucleotides was compared to the Nluc to Fluc ratio of Scramble transfected cells to study the effect of the oligonucleotides on the *BAG1* IRES activity (see Figure 6.8). None of the oligonucleotide transfected cells showed a significantly different Nluc to Fluc ratio when compared to Scramble or Mock transfected cells. We could thereby say that, with the number of replicates done, none of the oligonucleotides were able of modifying the *BAG1* IRES activity in HEK293 cells when 25 or 50 nM were transfected.

The Fluc and Nluc results of these experiments can be found in Figure D.13 on page 303.

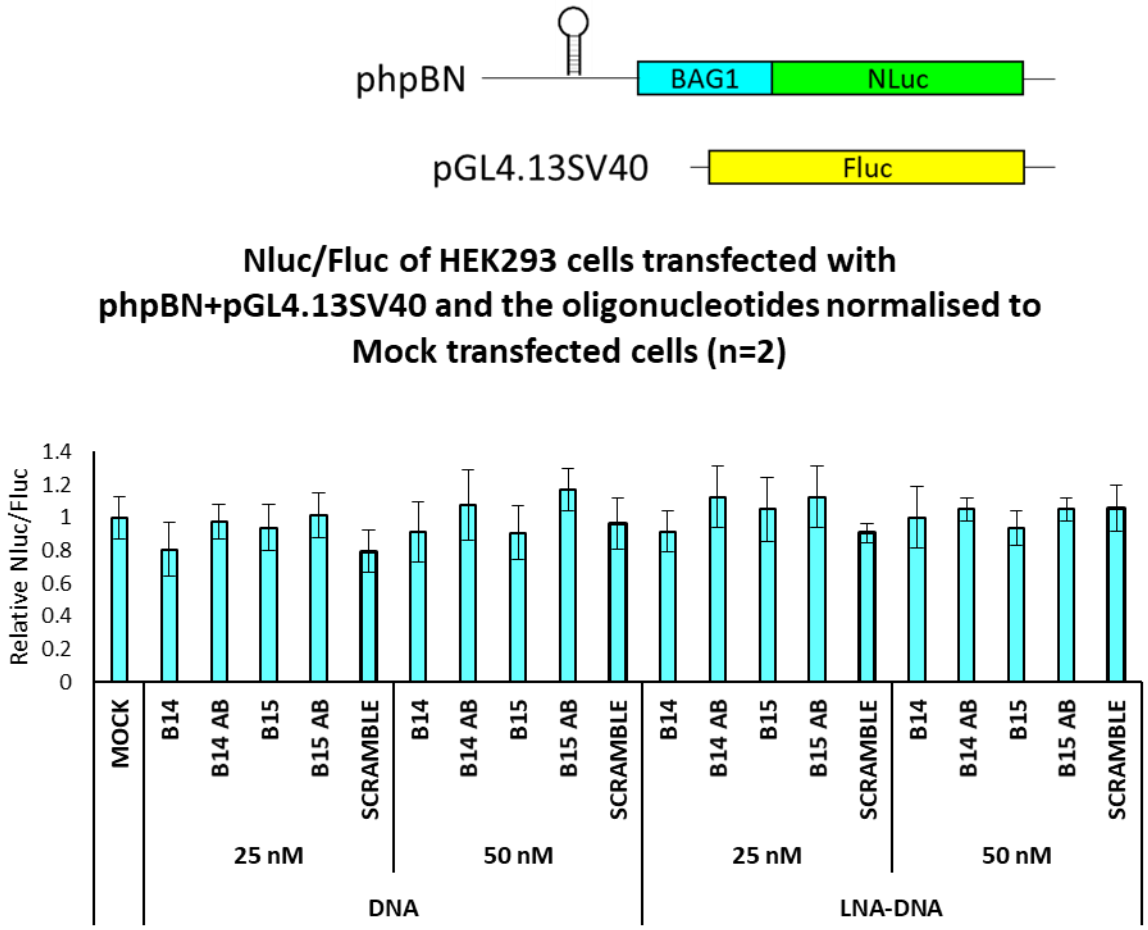

Figure 6.8 **Luciferase assay of HEK293 cells transfected with a final concentration of 25 and 50 nM of oligonucleotides for two days.** Nluc to Fluc ratio normalised to Nluc to Fluc ratio of Mock transfected cells of HEK293 cells transfected with phpBN+pGL4.13SV40 and the oligonucleotides.

6.4 NEW MODIFIED OLIGONUCLEOTIDES

Not many researchers have managed to increase protein expression using oligonucleotides targeting specific mRNAs, but Liang *et al.*[215] and Rouleau *et al.*[186] have shown some success. Roleau *et al.* managed to increase protein levels using oligonucleotides specifically designed to inhibit the folding of a G4 structure in the mRNA. For their purpose they used 2'-*O*-methyl ribonucleotides and LNA-DNA with a phosphodiester backbone. Liang *et al.* managed to increase protein expression by inhibiting upstream open reading frames (uORFs) using 2'-*O*-methyl oligonucleotides with phosphodiester linkages as well as with a phosphorothioate backbone, which they showed to enhance pharmacological properties.

Based on these two publications we decided to synthesise B14 AB and B15 AB with 2'-*O*-methyl ribonucleotides with phosphorothioate linkages. Oligonucleotides were ordered from Sigma-Aldrich.

We first tried these 2'-*O*-methyl phosphorothioate (2' OME PS) oligonucleotides in RRL. As in previous experiments, RRL were programmed with a final concentration of 1 µM of oligonucleotide and 500 ng of *in vitro* synthesised FBN RNA. Unmodified DNA oligonucleotides and modified LNA-DNA chimeras were also used to program RRL.

RRL programmed with unmodified oligonucleotides and LNA-DNA chimeras showed a similar Fluc activity, whereas RRL programmed with 2' OME PS showed a smaller Fluc activity (see Figure 6.9, A). These results made us believe that phosphorothioate oligonucleotides could degrade the RNA in RRL, somehow interact with the translation machinery or reduce the activity of the Fluc substrate in the Luciferase assay. The effect of the 2' OME PS oligonucleotides was not sequence dependent, as the Scramble oligonucleotide, which did not target any area in the whole FBN RNA showed the same results as B14 AB and B15 AB 2' OME PS.

RRL programmed with unmodified oligonucleotides showed an increase in the Nluc activity when compared to RRL programmed with FBN (no oligonucleotide), this increase was sequence dependent, as RRL programmed with Scramble DNA and FBN (no oligonucleotide) showed a similar Nluc activity (see Figure 6.9, B). RRL programmed with LNA-DNA mixmers and FBN showed a similar Nluc activity as RRL programmed with FBN (no oligonucleotide), whereas RRL programmed with 2' OME PS oligonucleotides showed a much reduced Nluc activity. RRL programmed with Scramble 2' OME PS and FBN also showed a much reduced Nluc activity, suggesting that the effect of the oligonucleotides in the Nluc activity was not sequence dependent. These results further supported our thoughts that the PS oligonucleotides could be interfering with different aspects of the assays.

Nluc to Fluc ratios of RRL programmed with the oligonucleotides were also analysed to study the effect of the oligonucleotides on the *BAG1* IRES activity (see Figure 6.9, C). RRL programmed with the unmodified oligonucleotides showed an increased Nluc to Fluc ratio, as on previous occasions. RRL programmed with LNA-DNA mixmers showed a slightly reduced Nluc to Fluc activity compared to RRL programmed with Scramble, as in previous occasions. RRL programmed with 2' OME PS showed a smaller decrease in the Nluc to Fluc ratio (weaker than the effect of the LNA-DNA mixmers), suggesting they did not have the ability to modify the *BAG1* IRES activity in RRL. However, as 2' OME PS oligonucleotides showed overall inhibition of both Fluc and Nluc activities, we did not consider them capable of specifically modifying the *BAG1* IRES activity in RRL.

To check if the oligonucleotide activity in RRL was dose dependent, and specifically if a reduction in the 2' OME PS oligonucleotide concentration could show different results in the Fluc and Nluc activities, we programmed RRL with 500 ng of FBN and a final concentration of 0.2 µM, 0.5 µM or 1 µM (as in the previous experiments) of oligonucleotides.

RRL programmed with the unmodified oligonucleotides and the LNA-DNA mixmers did not show large variabilities in the Fluc activity when different oligonucleotide concentrations were used (the increase in the Fluc activity of RRL programmed with a final concentration of 0.2 μM of B14 AB DNA could be due to human error due to the addition of a higher volume of RNA to the reaction or a higher RRL volume to the luciferase assay), however an increase in the 2' OME PS concentration decreased the Fluc activity (see Figure 6.10, A). RRL programmed with unmodified Scramble or LNA-DNA Scramble showed the same Fluc activity even if different oligonucleotide concentrations were used, as expected. However, RRL programmed with Scramble 2' OME PS decreased the Fluc activity as the oligonucleotide concentration increased. This suggested that the effect of the 2' OME PS oligonucleotides was dose dependent, but not sequence dependent.

RRL programmed with 14 AB DNA showed less Nluc activity as the oligonucleotide concentration increased, on the other hand, RRL programmed with 15 AB DNA showed an increase in the Nluc activity as the oligonucleotide concentration increased (Figure 6.10, B). RRL programmed with LNA-DNA mixmers or 2' OME PS oligonucleotides showed a decrease in the Nluc activity as the oligonucleotide concentration increased. RRL programmed with unmodified Scramble or LNA-DNA Scramble did show very similar Nluc activities, whereas RRL programmed with Scramble 2' OME PS decreased the Nluc activity as the concentration increased.

The Nluc to Fluc ratios (Figure 6.10) showed that an increase in the concentration of the unmodified oligonucleotides increased the Nluc to Fluc ratio and thereby the IRES activity. The opposite could be observed with the modified oligonucleotides: increasing the oligonucleotide concentration decreased the Nluc to Fluc ratio, and thereby the IRES activity, however the difference when the oligonucleotide concentrations were modified was not very big.

To check if the effect of 2' OME oligonucleotides was sequence dependent, we programmed RRL with 500 ng of FN and a final concentration of 1 μM of B14 AB DNA, B14 AB LNA-DNA and B14 AB 2' OME PS. RRL programmed with B14 AB DNA and B14 AB LNA-DNA and FN (no oligonucleotide) showed a very similar Fluc activity, whereas RRL programmed with B14 AB 2' OME PS showed a reduced Fluc activity (see Figure 6.11, A).

RRL programmed with B14 AB DNA showed a lower Nluc activity than RRL programmed with FN (no oligonucleotide) and RRL programmed with B14 AB LNA-DNA showed a higher Nluc activity (Figure 6.11, B). RRL programmed with B14 AB 2' OME PS showed the smallest Nluc activity, a reduction of 3.5-fold compared to FN (no oligonucleotide) programmed RRL.

These results suggest that the effect of the 2’ OME PS oligonucleotides is sequence independent. We still do not know if they degrade the RNA, if they affect the translation machinery or if they interact with the chemical reactions that take place during the luciferase assay.

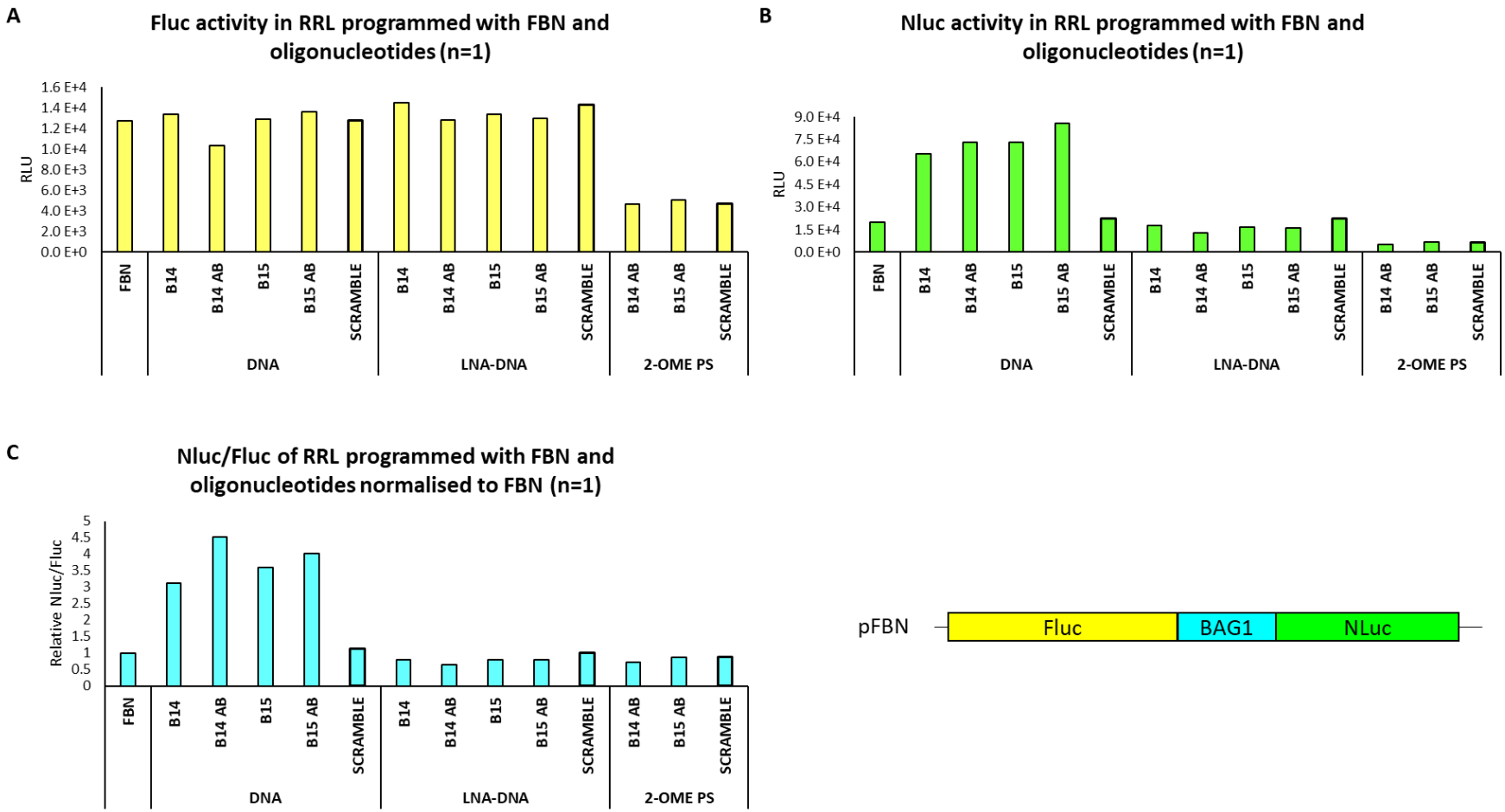

Figure 6.9 **Luciferase assay results of RRL programmed with 500 ng of FBN and a final concentration of 1 µM of DNA, LNA-DNA and 2' OME PS oligonucleotides.** A) Fluc activity, B) Nluc activity and C) Nluc to Fluc ratio normalised to Nluc to Fluc ratio of RRL programmed with FBN of RRL programmed with FBN and the oligonucleotides.

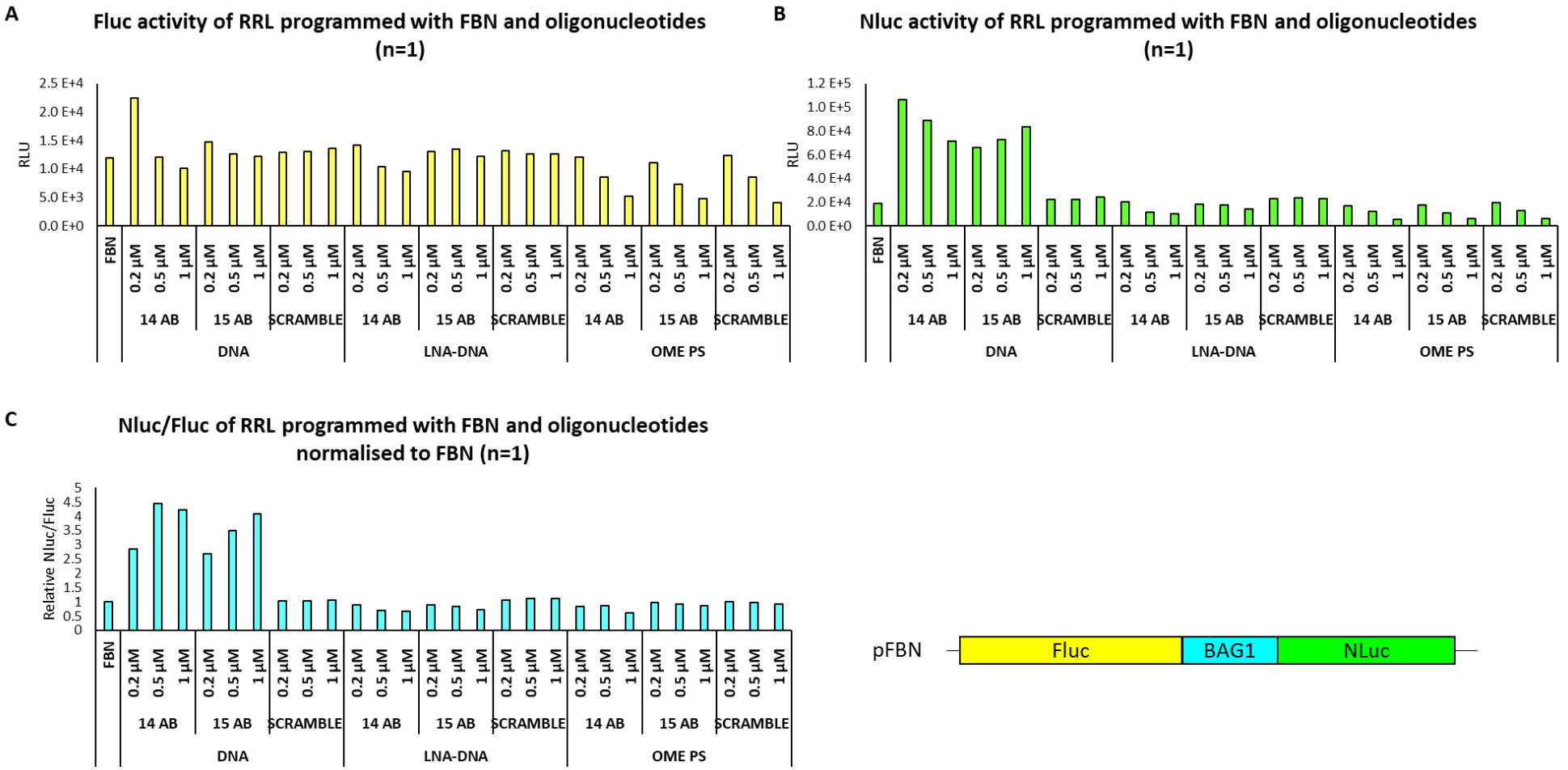

Figure 6.10 **Luciferase assay results of RRL programmed with 500 ng FBN and different final concentrations (0.2 µM, 0.5 µM and 1 µM) of DNA, LNA-DNA and 2' OME PS oligonucleotides.** A) Fluc activity, B) Nluc activity and C) Nluc to Fluc ratio of oligonucleotide programmed RRL normalised to FBN programmed RRL.

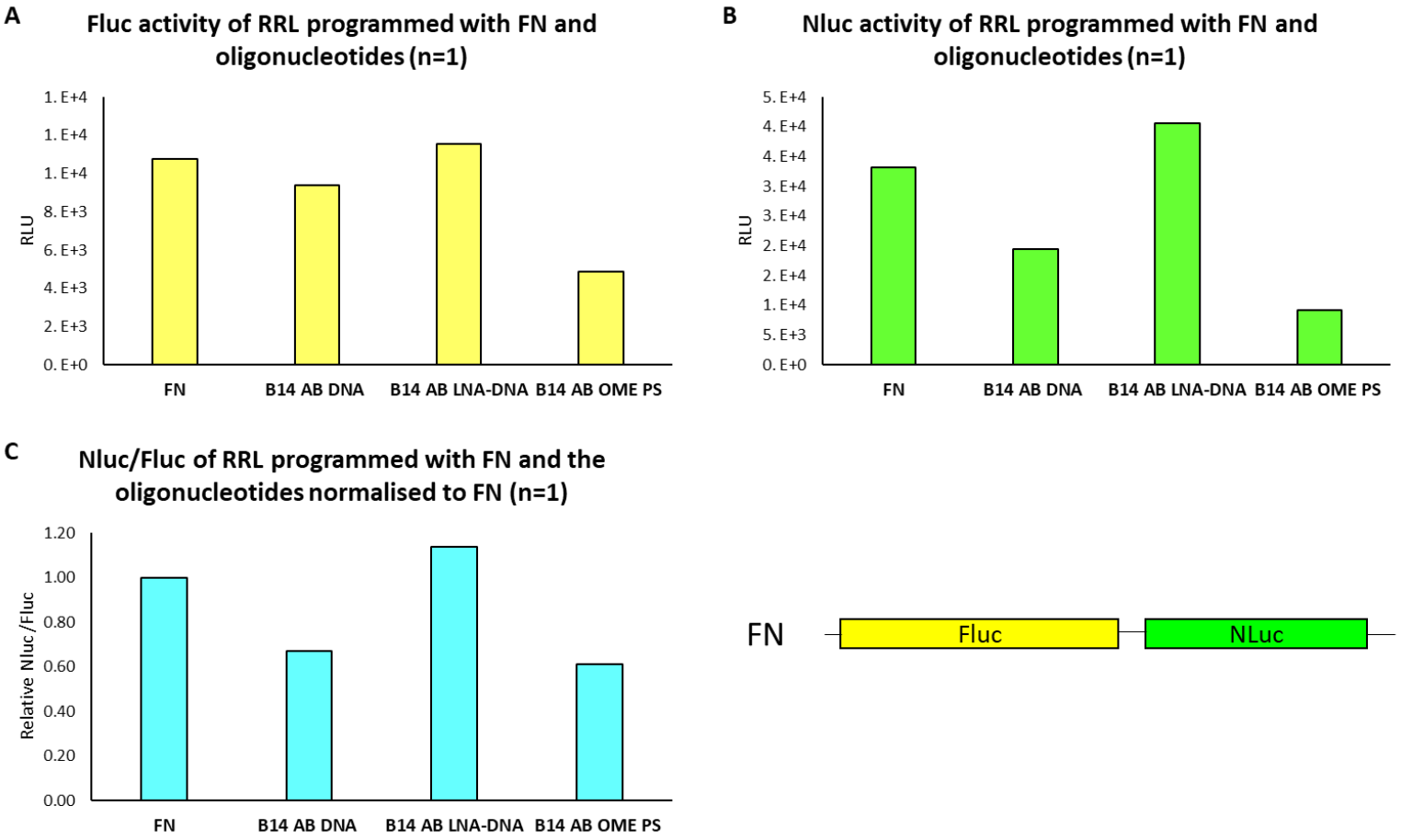

Figure 6.11 **Luciferase assay results of RRL programmed with 500 ng of FN and a final concentration of 1 µM of B14 AB DNA, LNA-DNA and 2' OME PS oligonucleotides.** A) Fluc activity and B) Nluc activity and C) Nluc to Fluc ratio of oligonucleotide programmed RRL normalised to FBN programmed RRL

6.5 DO THE OLIGONUCLEOTIDES BIND TO THE RNA?

After the confusing results obtained when programming RRL with the different oligonucleotides, it made sense to try and study if the different oligonucleotides with different chemistries were definitely binding to the RNA. The ideal experiment would show that the oligonucleotides could bind to the cellular mRNA, however, due to the limited resources, we could only show the ability of the oligonucleotides to bind to the *in vitro* synthesised RNA.

The *BAG1* 5' UTR sequence present in FBN was *in vitro* transcribed as explained in section 2.10 on page 72. That *BAG1* RNA was then reverse transcribed as explained in section 2.8.2 on page 68 using the different oligonucleotides as primers for the reverse transcription reaction. The reaction was then treated with RNase A to make sure any remaining RNA was degraded. In this way, only when the oligonucleotides had the ability to bind to the *in vitro* transcribed *BAG1* RNA the resulting cDNA would be detectable by agarose gel electrophoresis. See Figure 6.12 F for an illustration of the experiment and the different cDNA sizes expected. Note that the ladder used in the experiment showed bands in base pairs, whereas the cDNA was single stranded, hence the reason why the expected sizes do not match with what the ladder shows.

In the first experiment B14 AB DNA, LNA-DNA, 2' OME PS, Scramble DNA were used as primers. As a positive control BAG1 R primer was used, the same primer used to amplify the *BAG1* DNA before the *in vitro* transcription reaction, which should bind to the RNA. As a negative control a no oligonucleotide reaction was used, where no cDNA should be observed. The reaction where the Scramble oligonucleotide was used could also be considered as a negative control, as this oligonucleotide should not bind anywhere in the *BAG1* RNA.

As can be seen in Figure 6.12 A, only the reverse transcriptions from B14 DNA, B14 LNA-DNA and BAG1 R primers were successful as a clear cDNA band was observed on the agarose gel. Both negative controls (Scramble and no oligo) did not show any cDNA, as expected, however there were two background bands at 300-400 bp. B14 2' OME PS did not show any cDNA band either, however, in this case, no background bands could be observed.

The same experiment was repeated using B14 AB, B15 AB and Scramble 2' OME PS, and using B14 AB DNA as a positive control and a no oligonucleotide reaction as a negative control (see Figure 6.12, B). Only the reaction where B14 AB DNA was used showed a clear cDNA band. The no oligonucleotide reaction showed the same background bands as before. B14 AB 2' OME PS showed a very faint band smaller than expected, whereas B15 AB showed a very faint band of

the right size. Scramble 2' OME PS did not show any bands, as expected, not even the background bands seen in the no oligonucleotide reaction.

To check whether the 2' OME PS oligonucleotides could degrade the RNA, the *BAG1* RNA was incubated with B14 AB 2' OME PS, Scramble 2' OME PS, B14 AB DNA and Scramble DNA were incubated for 10 minutes at 37°C, followed by the reverse transcription reaction where the BAG1 R primer was added. As BAG1 R was added to the reaction, it was assured that the RNA would reverse transcribe, unless the RNA had been degraded.

In Figure 6.12 C it could be observed that the reactions where the RNA was incubated with B14 AB 2' OME PS and B14 AB DNA showed a similar pattern, however the bands from the AB DNA reactions were brighter, suggesting the reverse transcription reaction had been more successful. The reaction where the RNA was incubated with Scramble DNA showed the same band pattern as the reaction incubated only with BAG1 R, as expected. However, the reaction incubated with Scramble 2' OME PS showed a very faint band of a small size, suggesting that the RNA had not reverse transcribed. The same experiment was then repeated incubating the RNA with Scramble DNA, LNA and 2' OME PS before doing the reverse transcription reaction using BAG1 R (see Figure 6.12, D). In this case, Scramble DNA and LNA showed the same band pattern, which was similar to the band pattern of the reaction where only BAG1 R was used. Scramble 2' OME PS showed a unique faint band of a small size. This could be explained in different ways: the 2' OME PS oligonucleotides were actually degrading the RNA or, the reverse transcriptase was unable to detect or use a 2' OME PS-RNA duplex to initiate the reverse transcription reaction.

To check whether the PS oligonucleotides could somehow degrade the RNA, B14 AB, B15 AB and Scramble DNA, LNA and 2' OME PS were incubated with the *in vitro* transcribed *BAG1* RNA for 45 minutes at 37°C and then run on a 1% agarose gel (see Figure 6.12, E). All the reactions gave a unique band of the same size, suggesting that no RNA degradation had happened. The fact that Scramble 2' OME PS showed a weaker band could be due to human error, such as by pipetting a smaller amount of RNA into the reaction or when loading the gel. Most of the DNA and LNA oligonucleotides showed a very small and faint band, which could have been formed by the excess of oligonucleotides. However the 2' OME PS oligonucleotides did not show that band, although this could be because GelRed was unable to bind to the 2' OME PS oligonucleotides.

With this experiment we showed that the DNA and LNA-DNA oligonucleotides can successfully bind to the *in vitro* made RNA in a sequence specific manner. However, we could not determine their binding affinity to the mRNA in the cells.

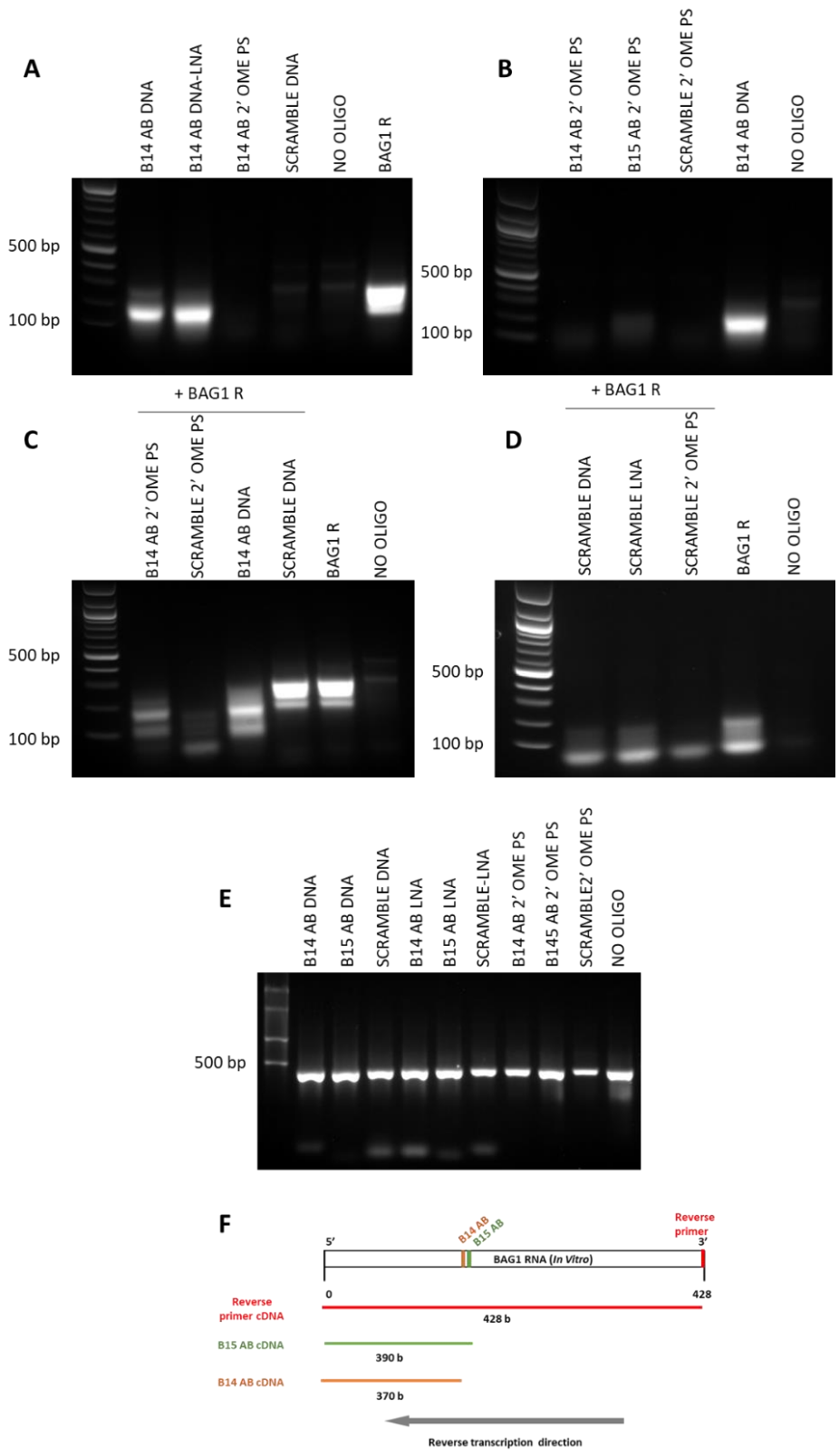

Figure 6.12 **cDNA patterns of reverse transcription reactions where the different oligonucleotides were used as primers in the reaction.** A and B) *In vitro* transcribed *BAG1* RNA was reverse-transcribed using the oligonucleotides specified. C and D) *In vitro* transcribed *BAG1* RNA was reverse-transcribed with a combination of the oligonucleotides specified. E) *In vitro* transcribed *BAG1* RNA after incubation with the oligonucleotides. F) Illustration of the reverse transcription reaction results when the different oligonucleotides are used.

6.6 2’ OME OLIGONUCLEOTIDES: RRL

To study whether the RRL results obtained with the 2’ OME PS oligonucleotides were due to the 2’ OME or due to the phosphorothioate linkages, B14 AB, B15 AB and Scramble 2’ OME oligonucleotides with phosphodiester linkages were ordered from ATD BIO. 2’ OME PS oligonucleotides were also ordered from ATD BIO to verify they showed the same results as the ones ordered from Sigma-Aldrich.

RRL were programmed as on previous occasions with 500 ng of *in vitro* made FBN RNA and a final concentration of 1 µM of B14 AB, B15 AB and Scramble oligonucleotides with the following chemistries: DNA (unmodified), LNA-DNA mixmers, 2’ OME PS and 2’ OME (phosphodiester). Fluc and Nluc activity was measured.

DNA oligonucleotides, LNA-DNA mixmers and 2’ OME oligonucleotides did not have a large effect on the Fluc activities (see Figure 6.13, A). 2’ OME PS oligonucleotides (B14 AB, B15 AB and Scramble), both the ones ordered from ATD BIO and Sigma-Aldrich showed a decrease in Fluc activity in every case. These results suggested that the effect that 2’ OME PS oligonucleotides have in RRL must be due to the presence of the phosphorothioate oligonucleotides, and that it was not sequence specific or due to the 2’ OME.

The story was a bit different in the case of Nluc activity (Figure 6.13, B). As in previous occasions, B14 AB and B15 AB DNA oligonucleotides increased the Nluc activity, whereas the Scramble DNA oligonucleotide did not have such a large effect. These results suggested that B14 AB and B15 AB DNA oligonucleotides have the ability to increase *BAG1* IRES activity. Both LNA-DNA mixmers and 2’ OME oligonucleotides showed the same results: the Scramble oligonucleotide did not have any effect in the Nluc to Fluc ratio, however both B14 AB and B15 AB decreased the Nluc to Fluc activity when compared to FBN (no oligonucleotide) programmed RRL, suggesting that these modifications could decrease the IRES activity. As explained before, this reduction in the Nluc activity could be due to the fact that 2’ OME and LNA oligonucleotides could bind to the RNA in a very strong manner, complicating the ribosomal scanning or entry and thereby inhibiting translation. All the 2’ OME PS oligonucleotides showed a very small Nluc activity, suggesting that the phosphorothioates could affect the system in a sequence independent manner.

When the Nluc to Fluc ratio was studied, and thereby the IRES activity was studied, DNA oligonucleotides showed an increase in *BAG1* IRES activity as on previous occasions, whereas both LNA-DNA mixmers and 2’ OME oligonucleotides showed decreases in the *BAG1* IRES

activity (see Figure 6.13, C). The results of the 2' OME PS oligonucleotides were not considered, as they were interfering with the system somehow.

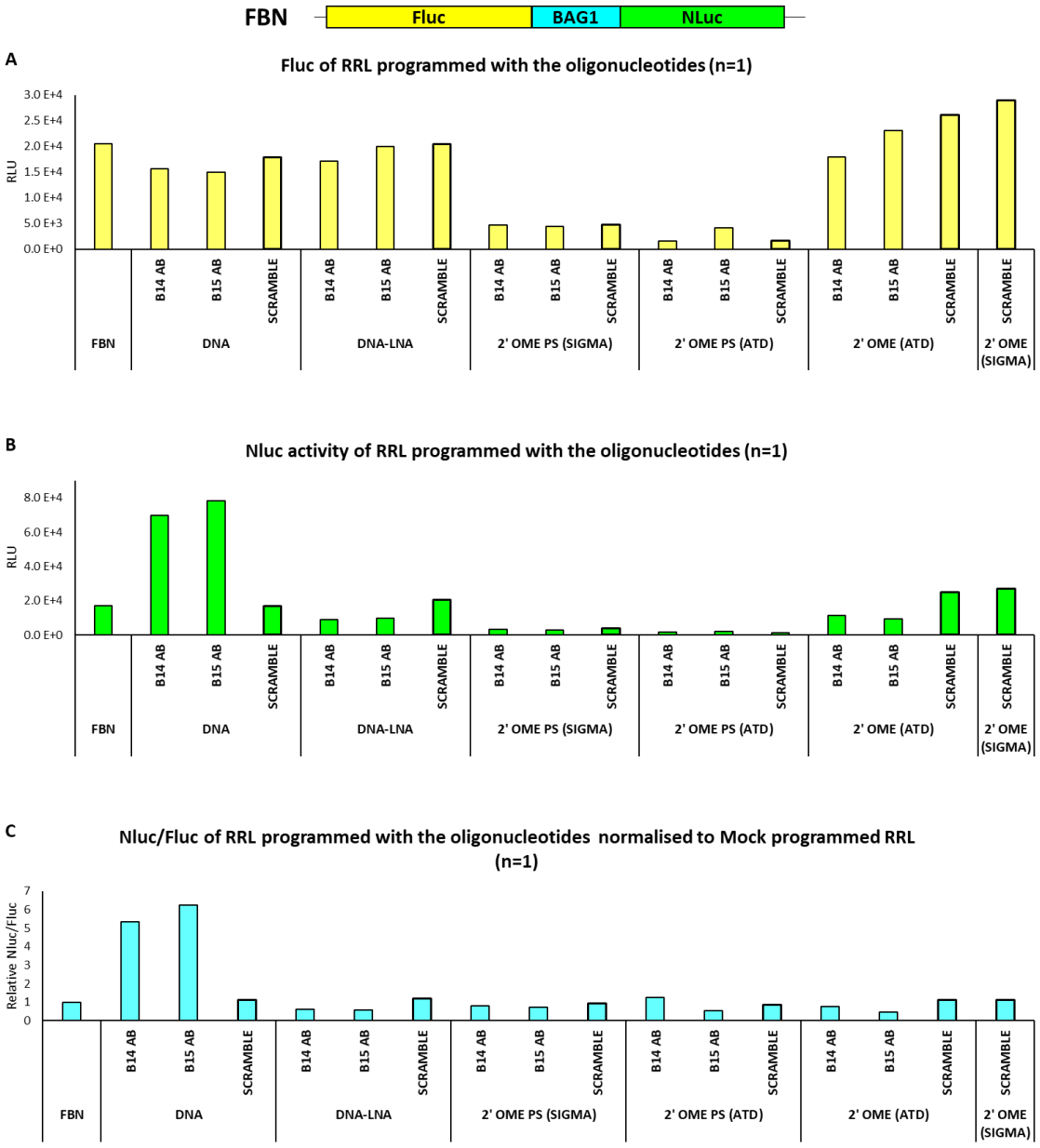

Figure 6.13 **Luciferase assay results of RRL programmed with 500 ng of FBN and a final concentration of 1 µM of oligonucleotide**. A) Fluc activity, B) Nluc activity and C) Nluc to Fluc ratio of RRL programmed with FBN and oligonucleotides normalised to the Nluc to Fluc ratio of RRL programmed with FBN.

To check whether oligonucleotides could target the *BAG1* IRES, the *BAG1* IRES was *in vitro* transcribed and all the B14 AB and Scramble oligonucleotides were used as primers for a reverse transcription reaction (as previously explained in section 6.5 on page 211), as control BAG1 R primer was used (the primer used to amplify the *BAG1* IRES by PCR prior to the *in vitro* transcription reaction). The cDNA obtained from the reverse transcription reaction was run in

an agarose gel, a band in the gel would indicate that the oligonucleotides had successfully bound to the RNA.

None of the Scramble oligonucleotides showed a band in the agarose gel (see Figure 6.14), as expected, only B14 AB DNA, B14 LNA and BAG1 R primer showed a clear band. These results suggest different possibilities: the 2' OME PS and 2' OME oligonucleotides did not bind to the *in vitro* synthesised *BAG1* RNA or that the reverse transcriptase could not detect a 2' OME PS-RNA or a 2'OME-RNA duplex and thereby could not reverse transcribe the sequence. Related to this, it needs to be said that reverse transcriptase stops transcribing when it comes across 2' OME sequences in the presence of low concentration of dNTPs, while at high dNTP concentrations it can continue with the process of transcription[297]. The fact that the 2' OME oligonucleotides behaved in RRL in a similar way as the LNA-DNA mixmers suggested that the most probable explanation was that the reverse transcriptase could not initiate reverse transcribing through a 2'OME-RNA duplex.

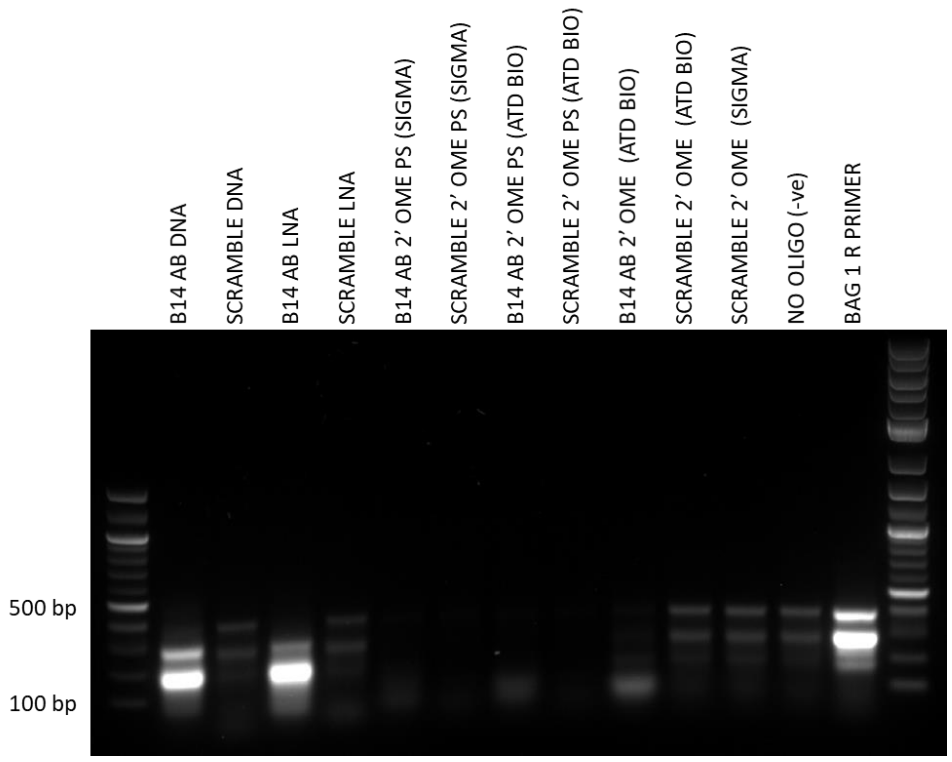

Figure 6.14 ***In vitro* transcribed *BAG1* RNA reverse transcription reaction results after using the oligonucleotides as primers for the reaction.** Only B14 AB DNA and LNA were able to successfully reverse transcribe BAG1 RNA.

6.7 DISCUSSION

EFFECT OF THE OLIGONUCLEOTIDES IN RABBIT RETICULOCYTE LYSATE

As working with HEK293 and hpBN-HEK cells did not give us the results we were hoping for, we decided to go one step backwards and study the effect of the oligonucleotides in the cell free system RRL. Having previously shown that the *BAG1* IRES was not active in RRL, this system would be particularly useful to study the ability of the oligonucleotides to increase the IRES activity.

The RRL programming protocol was optimised, and we saw that although incubating the RNA with the oligonucleotides at 65°C before the RRL reaction could increase the oligonucleotide activity, an incubation of just 37°C, mimicking what could happen in the human body, was enough to get a good oligonucleotide activity. Most of the oligonucleotides showed an increase in the Nluc to Fluc ratio, and thereby the *BAG1* IRES activity in RRL, but B5, B6, B14 and B15 were the oligonucleotides that showed the strongest activity. These four oligonucleotides targeted the same area in the *BAG1* IRES, which happened to be the ribosome landing area. When those oligonucleotides were combined in pairs we could not observe a further increase in the IRES activity.

WORKING WITH THE MOST PROMISSING OLIGONUCLEOTIDES: B14 AND B15

After all the RRL experiments done, it was concluded that B14 and B15 were the oligonucleotides with the strongest ability to modify the *BAG1* IRES activity, and we thereby decided to keep working with these two oligonucleotides. The sequence of B14 and B15 was slightly modified with the removal and addition of nucleotides in the 5' or 3' ends to avoid any secondary structure formation within the oligonucleotides and created B14 AB and B15 AB. B14, B14 AB, B15, B15 AB and Scramble oligonucleotides unmodified and LNA-DNA mixmers were synthesised and the oligonucleotides were used to program RRL alongside FBN. The unmodified oligonucleotides were more effective modifying the IRES activity in RRL than their modified LNA-DNA analogues when the FBN and the oligonucleotides were heated at 65°C (to mimic the activity of a helicase that the LNA-DNA mixmers could require) or when the heating step was skipped. None of the oligonucleotides had a major effect on the Fluc activity, however unmodified oligonucleotides showed the ability to increase the Nluc activity, whereas the LNA-DNA mixmers reduced it. Heating the RNA-oligonucleotide to 65°C did not affect the effectiveness of the LNA-DNA mixmers. In this experiment again, the unmodified B14, B14 AB, B15 and B15 AB DNA oligonucleotides drove increases in the IRES activity, whereas the LNA-DNA mixmers decreased the IRES activity in RRL. The hypothesis we have to explain this could

that LNA-DNA mixmers might bind too strongly to the RNA and block the 40S ribosomal landing and/or scanning, thereby reducing IRES-mediated translation. These results suggest that the oligonucleotide efficiency is dependent on both the sequence and the chemistry of the same.

B14, B14 AB, B15, B15 AB and Scramble oligonucleotides unmodified and LNA-DNA mixmers were also transfected in HEK293 cells at a final concentration of 25 and 50 nM for two days. In this case, none of the oligonucleotides had the ability to modify the IRES activity when compared to Scramble or Mock transfected cells. The reason behind this could be due to different reasons: an inadequate transfection timing (too long or too short) or oligonucleotide concentration used (too high or too low), the poor stability of the oligonucleotides in cells, a low oligonucleotide transfection efficiency, or the inability of the oligonucleotides to target the mRNA in the cells.

2' OME PS OLIGONUCLEOTIDES

To try to overcome some of these problems, we further consulted the existing literature on oligonucleotides and their influence on gene expression. We could only find two references where different lab groups had managed to increase protein expression using oligonucleotides. Liang *et al.*[215] managed to increase protein expression by inhibiting upstream open reading frames and Rouleau *et al.*[186] did it by inhibiting the folding of a G4 structure in the mRNA. Liang *et al.* used 2'-*O*-methyl oligonucleotides with phosphodiester linkages as well as with a phosphorothioate backbone for their purpose, whereas Rouleau *et al.* used 2'-*O*-methyl ribonucleotides and LNA-DNA with a phosphodiester backbone. We had previously shown that LNA-DNA mixmers did not work for our purpose, however we had not yet tried 2' OME oligonucleotides. We therefore decided to modify B14 AB and B15 AB with 2' OME and PS bonds.

B14 AB, B15 AB and Scramble DNA, LNA-DNA and 2' OME PS were used to program RRL alongside FBN. RRL programmed with the PS oligonucleotides showed a much reduced Fluc and Nluc activity. These results suggested that the phosphorothioates could have the ability to degrade *in vitro* synthesised RNA in RRL, or that they could somehow influence the RRL translation machinery. DNA and LNA-DNA oligonucleotides behaved in the same way as on previous occasions, DNA oligonucleotides increased the IRES activity in RRL, while LNA-DNA mixmers decreased it. LNA-DNA mixmers were designed to increase the melting temperature of the oligonucleotides and to bind to the target RNA in a stronger way, whereas DNA oligonucleotides would target the RNA in a weaker way, with more flexibility. LNA-DNA mixmers could bind so strongly to the target RNA that they could block the 40S ribosomal

landing site in the IRES or could block the scanning of any possible ribosome that had reinitiated from the Fluc.

RRL were programmed with different final concentrations of oligonucleotides (0.2 μM, 0.5 μM or 1 μM), to study if the Fluc or Nluc activity observed in RRL programmed with LNA-DNA mixmers and 2' OME PS oligonucleotides was dose dependent. An increase in the oligonucleotide concentration also increased the effects of the oligonucleotides: in the DNA oligonucleotides the increase in the IRES activity was stronger, and in the case of the LNA-DNA mixmers, the decrease was also stronger. In the case of 2' OME PS oligonucleotides we showed that the effect that the oligonucleotides had on the Fluc activity was dose dependent, as RRL programmed with 0.2 μM of oligonucleotides showed at least twice more Fluc activity than RRL programmed with 1 μM of oligonucleotide. The results were very similar for RRL programmed with B14 AB, B15 AB and Scramble 2' OME oligonucleotides, showing that even if the effects were dose dependent, they were not sequence specific.

To check whether the oligonucleotides could bind to the *in vitro* transcribed *BAG1* RNA, the RNA was reverse transcribed using the oligonucleotides and the cDNA obtained was analysed by agarose gel electrophoresis. B14 AB and B15 AB DNA and LNA-DNA showed efficient binding to the RNA, and Scramble DNA and LNA-DNA failed to do so, as expected. The 2' OME PS oligonucleotides failed to show strong cDNA bands. This could be for two reasons: the 2' OME PS oligonucleotides were unable to efficiently bind to the RNA or the reverse transcriptase was unable to detect a 2' OME PS-RNA duplex to start the reverse transcription.

2' OME oligonucleotides with phosphodiester bonds were ordered and used to program RRL alongside FBN. 2' OME oligonucleotides did not affect the Fluc activity in RRL, but reduced the Nluc activity, showing a reduced Nluc to Fluc ratio when compared to the RRL programmed with Scramble 2' OME or FBN (no oligonucleotide). The results of the 2' OME oligonucleotides was very similar to the one of the LNA-DNA mixmers, however the 2' OME oligonucleotides failed to reverse transcribe the *in vitro* synthesised *BAG1* RNA. These results suggest that the duplex 2' OME-RNA could be strong enough to block the ribosomal scanning or the 40S ribosomal subunit landing and that the reverse transcriptase might not be able to detect a 2' OME-RNA duplex. The results also showed that the results obtained in the RRL programmed with 2' OME PS was due to the phosphodiester bonds and not to the 2' OME.

Chapter 7 USING OLIGONUCLEOTIDES TO MODIFY THE *BAG1* IRES ACTIVITY IN CELLS (II)

7.1 IRES ACTIVITY IN HEK293 CELLS AND CAL51

The fact that B14 AB and B15 AB DNA could increase the activity of the *BAG1* IRES in RRL (where the *BAG1* IRES activity is non-existent), but not in HEK293 cells could be because HEK293 cells had a high IRES activity, which would make it almost impossible to increase it even more.

Pickering *et al.*[95] showed that *BAG1* IRES had different levels of activity in different cell lines. They classified HEK293 cells as cells with a medium to high *BAG1* IRES activity, whereas CAL51 cells had a smaller IRES activity. The differences in the IRES activity could be due to the difference in the ITAF concentration in different cell lines, meaning that cells with a bigger concentration of ITAFs would have a stronger IRES activity. As shown by Pickering *et al.*[95], the *BAG1* IRES requires the presence of the ITAFs PCBP1 and PTBP1 to be active. When these two proteins bind to a specific area of the *BAG1* IRES, they create a single stranded region where the 40S ribosomal subunit can land and start translation (see Figure 7.1, B).

BAG1 IRES activity was studied in HEK293 and CAL51 cells mimicking Pickering's experiment, although dosage of plasmids was hard to ascertain from the paper[95] or the related PhD thesis[298]. HEK293 and CAL51 cells were co-transfected with pFBN and pPTBP1 and/or pPCBP and the Nluc to Fluc ratio was analysed to study IRES activity. An increase in the Nluc to Fluc ratio, and thereby in the IRES activity, in the presence of pPTBP1 and pPCBP would show that the *BAG1* IRES activity in that cell line could be increased in the presence of those two proteins. As a control, the same experiment was done while transfecting cells with pFN, where no differences should be observed in the Nluc to Fluc ratio when pPTBP1 and/or pPCBP were co-transfected. One of the objectives of this project was to use oligonucleotides that could mimic the activity of PTBP1 and PCBP1 in increasing BAG1 protein expression, thereby it would be easier to obtain successful results in a cell line where we could probe that pPTBP1 and pPCBP could have an effect. pPTBP1 and pPCBP plasmids were a gift of Professor Anne Willis.

In a 96 well plate 2 000 HEK293 cells or 4 000 CAL51 cells were plated, double the amount of CAL51 were transfected as their life cycle is of 50-60 hours[299] whereas HEK293's is 24-30 hours[300] according to the DSMZ. The day after seeding the cells, they were transfected with 10 ng of pFN or pFBN and 20 ng of pPTBP1 and/or pPCBP using GeneJuice. Two days after

transfection luciferase assays were carried out. The experiment was done in triplicate three independent times. A one-way ANOVA with a Dunnett's multiple comparison test was done ($P<0.05$) to compare the Nluc to Fluc ratio of pFBN transfected cells with cells transfected with pFBN and the ITAFs.

The presence of pPTBP1 and pPCBP did not show any effect in HEK293 cells (see Figure 7.1, D). The Nluc to Fluc ratio did not change when HEK293 cells were co-transfected with pFBN and pPTBP1 and/or pPCBP. These results suggested that the concentration of PTBP1 and PCBP in HEK293 cells could be high enough to keep the IRES active, and thereby an increase in the number of these proteins would not have a significant effect in the IRES. On the other hand, in CAL51 cells, it could be observed a significant increase in the Nluc to Fluc ratio of cells in the presence of both pPTBP1 and pPCBP. These results suggested that the ITAF concentration in CAL51 cells was less, and that there may be a better cell line with even less ITAF expression in which to study an increase in the IRES activity by the oligonucleotides.

When the *BAG1* IRES expression was studied by western blot, CAL51 cells showed a smaller p36 expression than HEK293 cells (see Figure 7.1, C), which again showed that the IRES-driven translation in in these cells is likely to be less. These results suggested that increasing the *BAG1* IRES activity in HEK293 cells could be a bigger challenge than increasing it in CAL51 cells, we thereby continued working with CAL51 cells.

By normalising the Nluc to Fluc activity of FBN to the Nluc to Fluc activity of FN we could measure the IRES activity in both HEK293 and CAL51 cells. Surprisingly CAL51 cells a stronger IRES activity than HEK293 cells (see Figure 7.2). These results contradict our hypothesis that the IRES activity was smaller in CAL51 cells.

The oligonucleotide transfection efficiency of CAL51 and HEK293 cells was determined by the transfection of the fluorescent oligonucleotide B6FAM. Transfections were done in the presence of RiboJuice and in the absence of it (considered as a negative control). A final concentration of 25 nM of oligonucleotide were transfected for two days. Cell nucleus was stained with DAPI.

As it can be observed in Figure 7.3, B6FAM could not be successfully transfected in the absence of a transfection reagent as RiboJuice. However, in the presence of RiboJuice, both HEK293 and CAL51 cells showed a high transfection efficiency. These results suggest that CAL51 could be a good cell line to study the activity of the oligonucleotides in the *BAG1* IRES.

The Fluc and Nluc results of these experiments can be found in Figure D.14 and Figure D.15on pages 304 and 305.

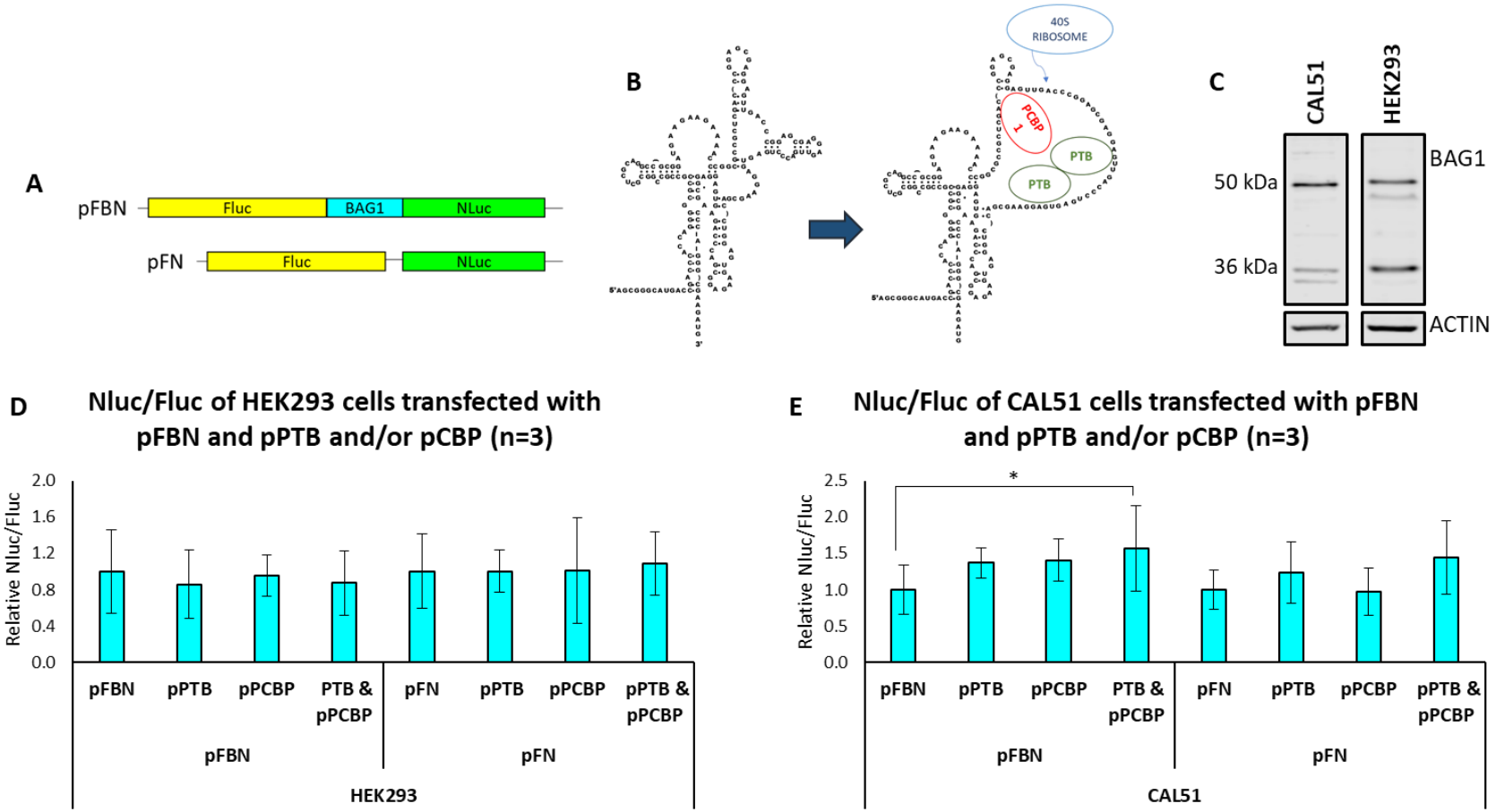

Figure 7.1 **HEK293 and CAL51 cells transfected with pPCBP and pPTBP.** A) pFBN and pFN schematic illustration. B) The binding of PTBP1 and PCBP in that specific area of the *BAG1* IRES creates a singles stranded region where the 40S ribosomal subunit can bind to and start translation. C) Western Blot showing HEK293 cells have a stronger p36 expression than CAL51 cells, and thereby a higher IRES activity. D and E) Nluc to Fluc ratio of HEK293 and CAL51 cells co-transfected with pFBN or pFN and pPTBP1 and or pPCBP.

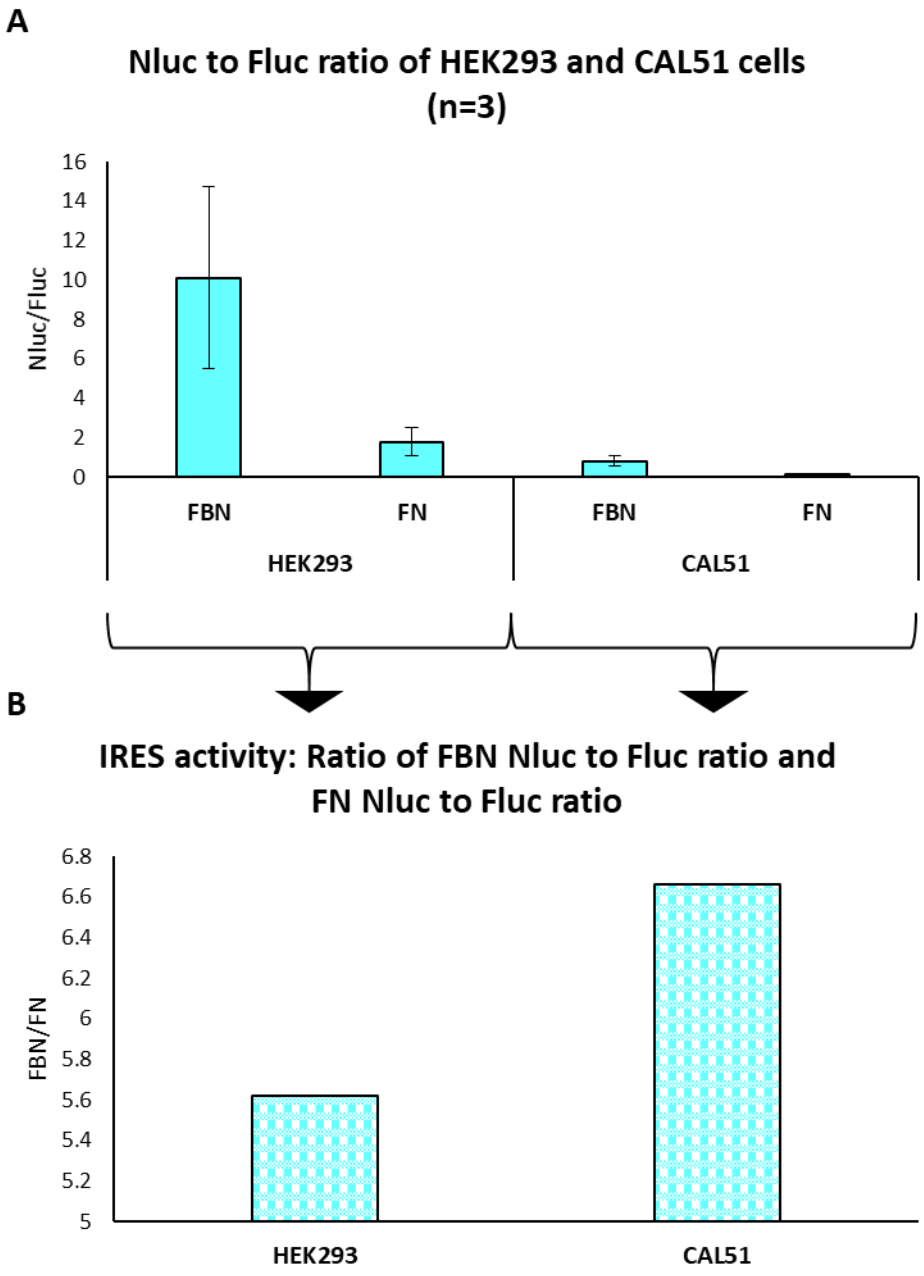

Figure 7.2 **Luciferase assay results of HEK293 and CAL51 cells transfected with FBN and FN.** A) Average of the Nluc to Fluc ratio of HEK293 and CAL51 cells transfected with FBN and FN. The experiment was done three individual times in triplicate, the error bars show the standard deviation. B) Nluc to Fluc ratio of HEK293 and CAL51 cells transfected with FBN normalised to the Nluc to Fluc ratio of cells transfected with FN to determine the IRES activity in the different cell lines.

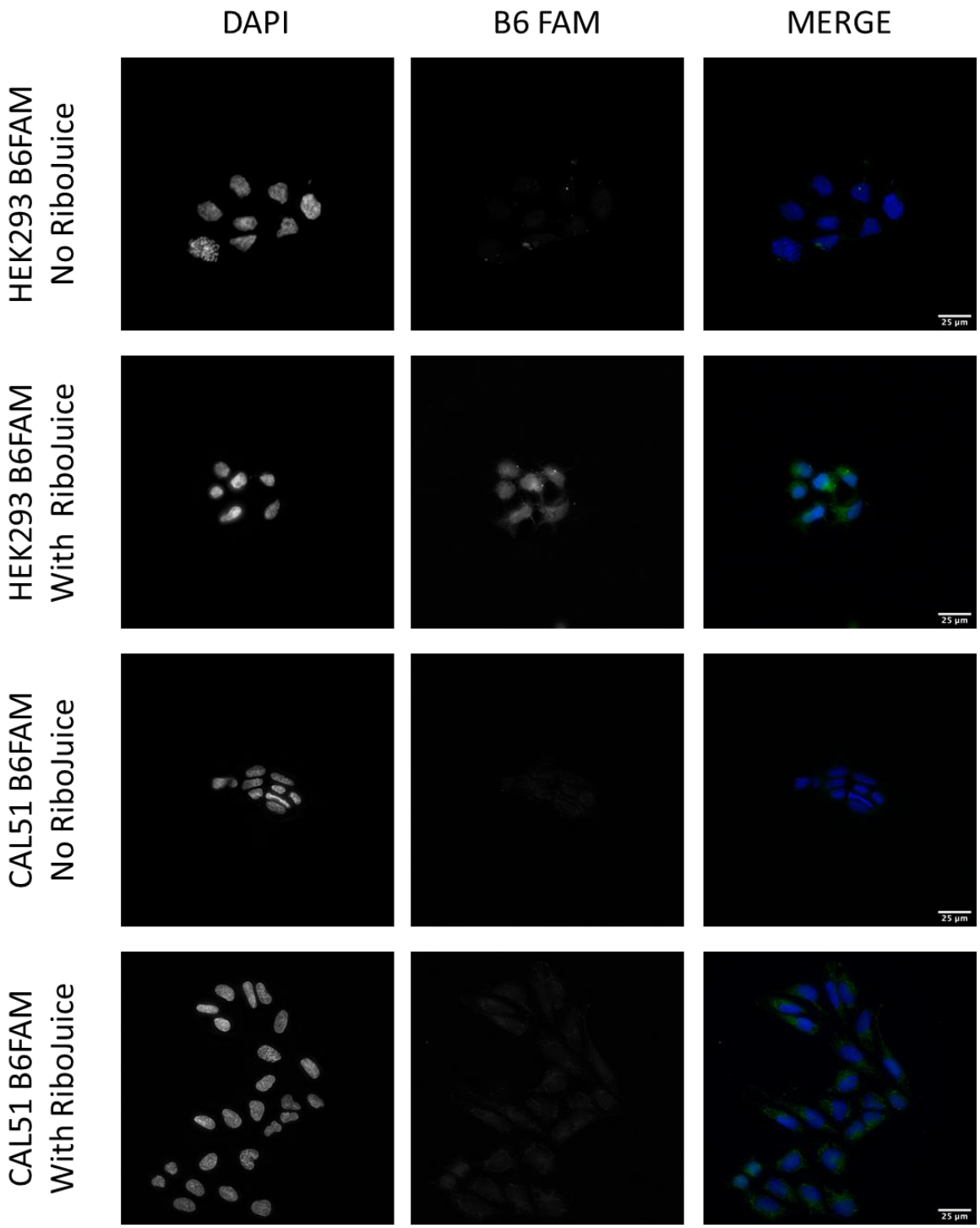

Figure 7.3 **Fluorescent microscopy images of HEK293 and CAL51 cells transfected with the fluorescent oligonucleotide B6FAM in the presence or absence of the transfection reagent RiboJuice.**

7.2 TRANSFECTING THE NEW OLIGONUCLEOTIDES IN HEK293, CAL51 AND hpBN-HEK CELLS: LUCIFERASE ASSAY

HEK293, CAL51 and hpBN-HEK cells were co-transfected with phpBN and pGL4.13SV40 and a final concentration of 25 nM of B14 AB, B15 AB and Scramble oligonucleotides with the following

chemistries: DNA, LNA-DNA mixmers, 2' OME PS and 2' OME. Transfections were done for 1 and 2 days.

On day one, 2 000 HEK293 and hpBN-HEK cells or 4 000 CAL51 cells were seeded per well in a 96 well plate. The following day transfections were carried out as explained in section 2.2.3 on page 60. A one-way ANOVA with a Dunnett's multiple comparison test was done ($P<0.05$) to check if the oligonucleotide transfected cells had a significantly different Nluc to Fluc ratio from Scramble or Mock transfected cells. However it needs to be noted that each experiment was done only once in triplicate, so the sample size was too small to undertake reliable statistical analysis.

The DNA, LNA-DNA and 2' OME PS oligonucleotides were transfected in the same experiment, 2' OME oligonucleotide transfections were carried out in a different experiment, and thereby the results will be shown in different graphs.

DNA, LNA-DNA and 2' OME PS oligonucleotides in HEK293 and CAL51 cells:

There were no large differences when the transfections were done in CAL51 and HEK293 cells for 1 or 2 days. None of the oligonucleotides had a significant effect in the Nluc to Fluc ratio when they were transfected for 1 day (Figure 7.4, A) or for 2 days (Figure 7.4, B), when compared to Scramble or Mock transfected cells.

The Fluc and Nluc results of these experiments can be found in Figure D.16 and Figure D.17 on pages 306 and 307.

DNA, LNA-DNA and 2' OME PS oligonucleotides in hpBN-HEK cells:

Until now, every experiment we had done using hpBN-HEK cells was done by co-transfecting pGL4.13SV40 and the oligonucleotides, and normalising the Nluc activity present in the cells to the activity of transfected pGL4.13SV40 (assuming the transfection efficiency of the oligonucleotides would be the same as the plasmid's). In this experiment, to reduce the variability that transfecting the pGL4.13SV40 could introduce in the system, we decided to normalise the Nluc activity to the total protein concentration in each well. To do so, the total protein concentration was measured with a Bradford assay, using 8 µl of cell lysate.

When transfections were done for one day, none of the oligonucleotides modified the Nluc expression when compared to Scramble transfected oligonucleotides (see Figure 7.5, A). However, B14 AB, B15 AB and Scramble unmodified and LNA-DNA oligonucleotides significantly increased the Nluc expression when compared to Mock transfected cells. When transfections were done for two days, none of the oligonucleotides modified in a significant way the Nluc activity when compared to Scramble or Mock transfected cells.

None of the oligonucleotides modified in a significant way the Nluc to protein ratio when compared to Scramble or Mock transfected cells for one or two days (see Figure 7.5, B).

2' OME oligonucleotides in HEK293 and CAL51 cells

Unfortunately none of the 2' OME oligonucleotides had a significant effect in the Nluc to Fluc ratio in CAL51 or HEK293 cells when compared to Scramble or Mock transfected cells when transfections were done for one or two days (Figure 7.6).

The Fluc and Nluc results of these experiments can be found in Figure D.18 and Figure D.19 on pages 308 and 309.

2' OME oligonucleotides in hpBN-HEK cells:

None of the 2' OME oligonucleotides had an effect in the Nluc activity of hpBN-HEK cells (see Figure 7.7, A) or in the Nluc to protein ratio (see Figure 7.7, B) when compared to Scramble or Mock transfected cells when transfections were done for one or two days.

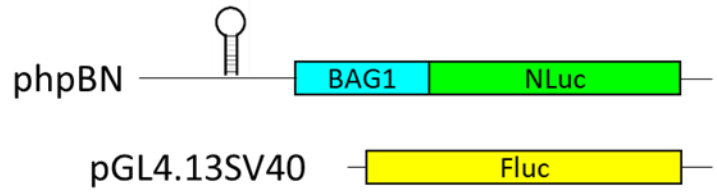

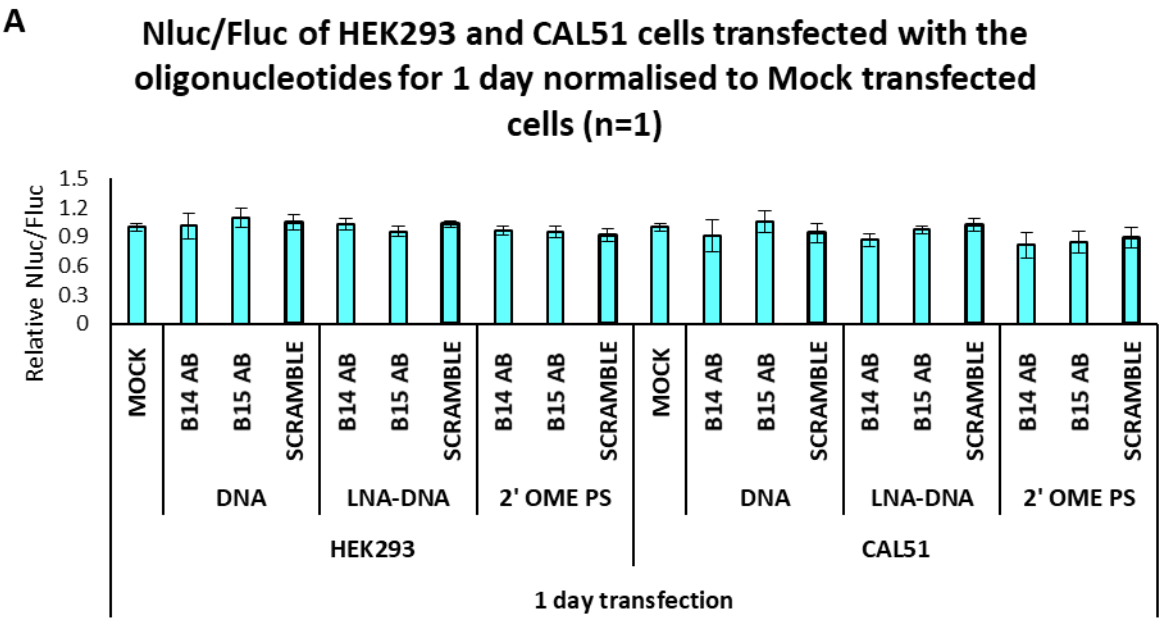

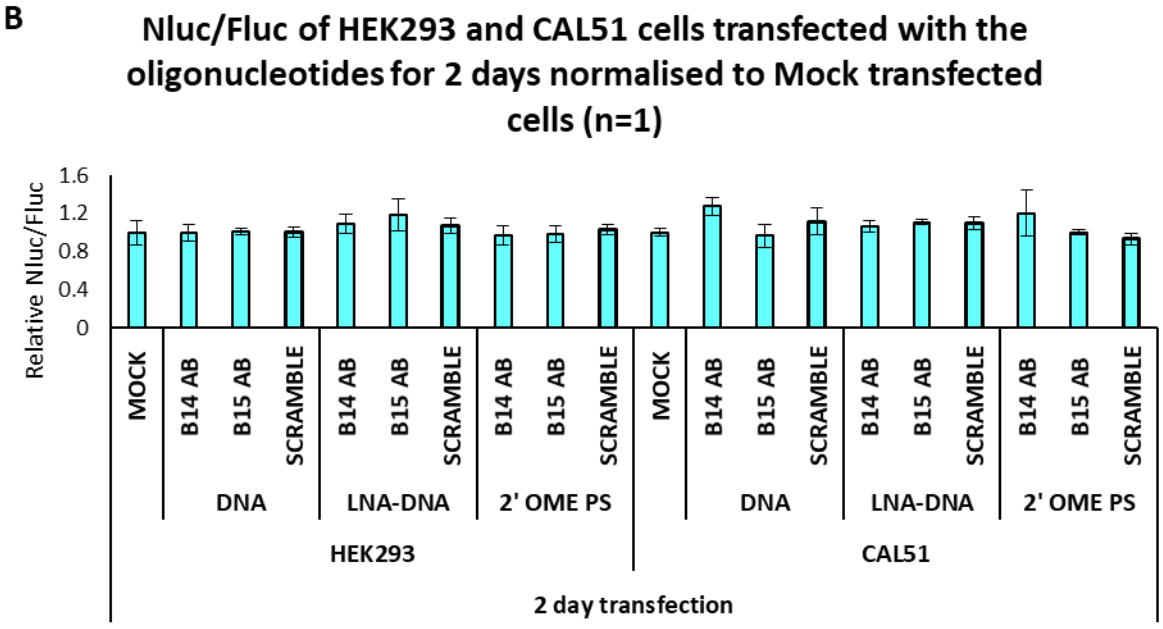

Figure 7.4 **Nluc to Fluc ratio normalised to Mock transfected cells of HEK293 and CAL51 cells transfected with a final concentration of 25 nM of oligonucleotides for one day (A) or two days (B).**

Error bars show standard deviatio values of an experiment done once in triplicate.

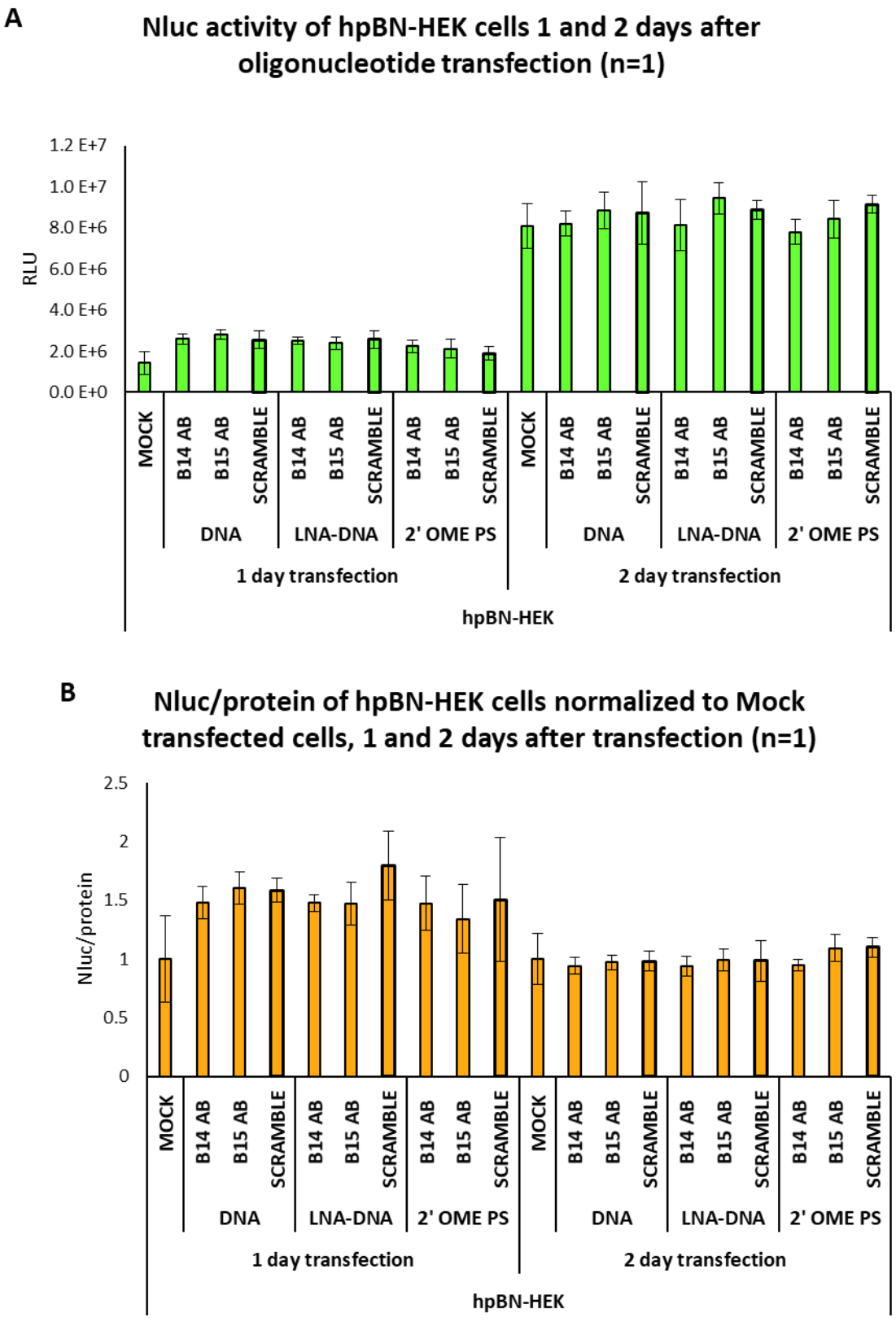

Figure 7.5 **Luciferase assay of hpBN-HEK cells transfected with the oligonucleotides.** Nluc activity (A) and Nluc activity to protein ratio normalised to Mock transfected cells (B) in hpBN-HEK cells transfected with a final concentration of 25 nM of oligonucleotides for one and two days. Error bars show ± SD of an experiment done once in triplicate.

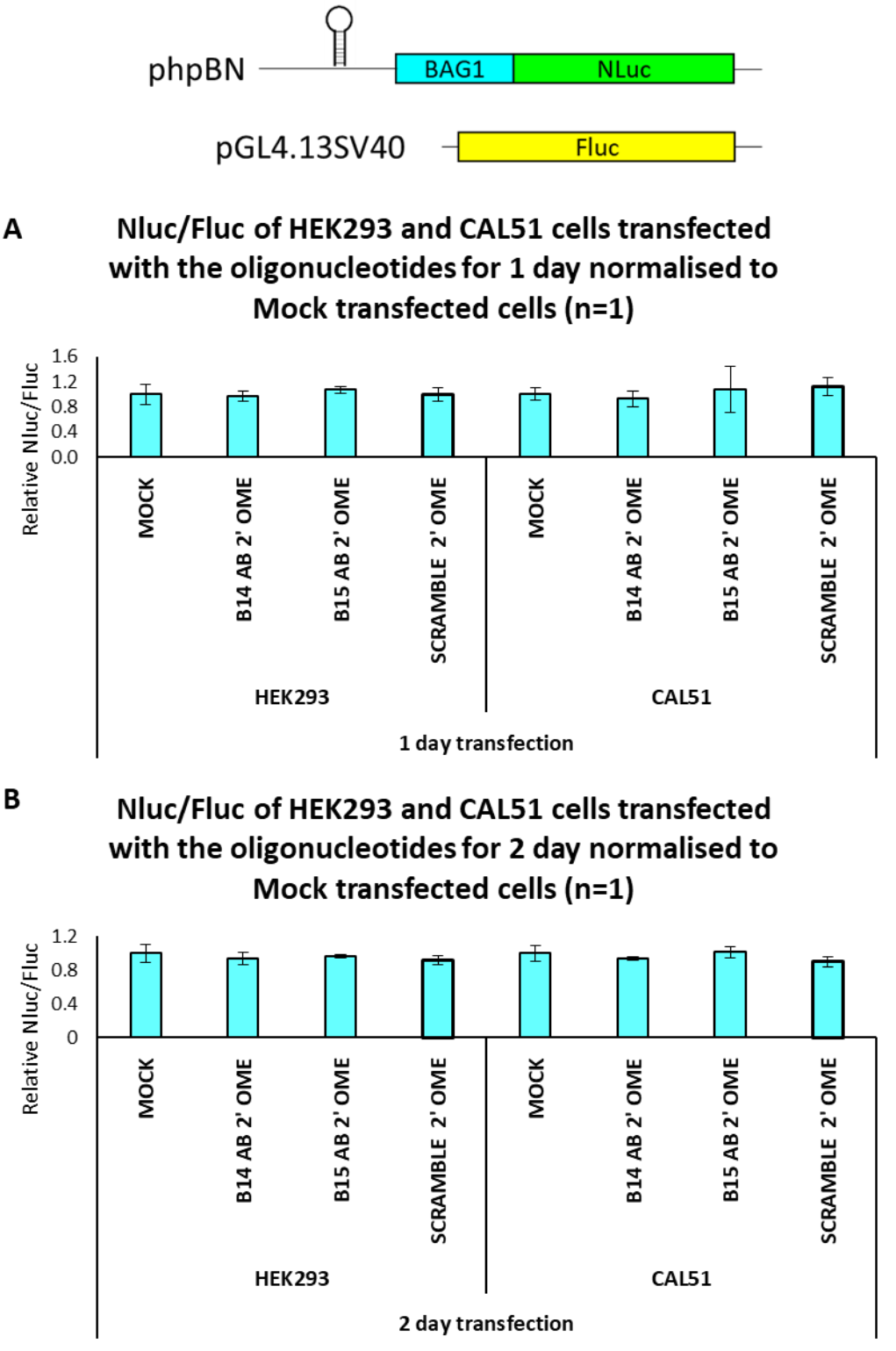

Figure 7.6 **Nluc to Fluc ratio normalised to Mock transfected cells of HEK293 and CAL51 cells transfected with a final concentration of 25 nM of 2' OME oligonucleotides for one day (A) and two days (B).** Error bars show ± SD of an experiment done once in triplicate.

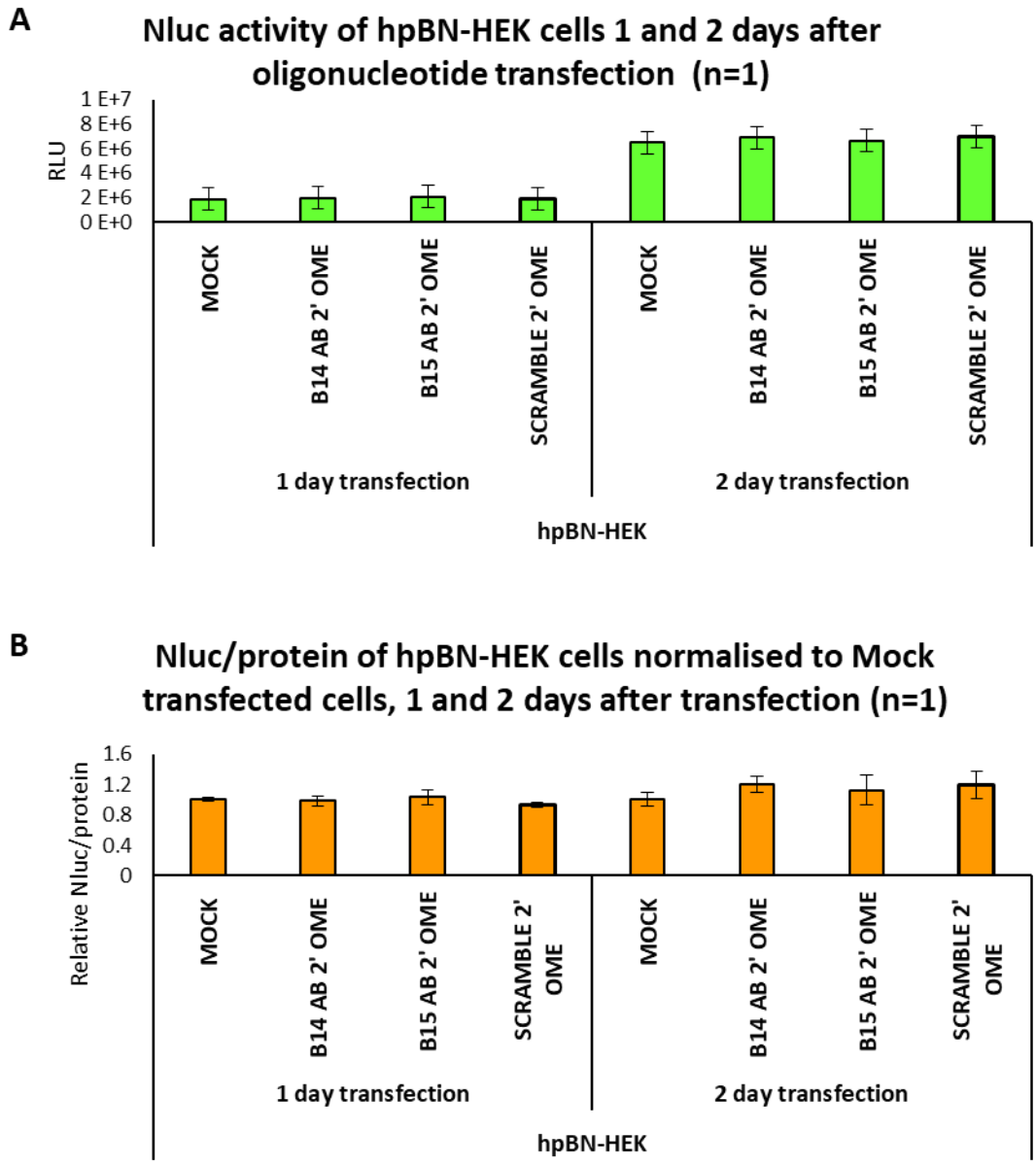

Figure 7.7 **Nluc activity (A) and Nluc activity to protein ratio normalised to Mock transfected cells (B) in hpBN-HEK cells transfected with a final concentration of 25 nM of 2' OME oligonucleotides for one and two days.** Error bars show ± SD of an experiment done once in triplicate.

7.3 STUDYING THE EFFECT OF B14 AB AND B15 AB IN CAL51 AND HEK293 CELLS BY WESTERN BLOT

The ability of the oligonucleotides to modify the endogenous *BAG1* IRES activity was also measured in CAL51 and HEK293 cells. A final concentration of 25 nM of oligonucleotide were transfected using RiboJuice (see section 2.2.3 on page 60 for a full protocol) and the BAG1 expression was studied one and two days after transfection by Western Blot (see section 2.6 on page 65 for a full protocol). To study the *BAG1* IRES activity, the expression of the p50 and p36 BAG1 isoforms was quantified and compared for each transfection, as the translation of the BAG1

p36 is partially carried out *via* the IRES, whereas the translation of the p50 isoform is cap-dependent. The total BAG1 expression (normalised to the actin expression) was also quantified. By looking at the blots we could not observe any effect produced by the oligonucleotides, we thereby will present here the quantified results. These blots and their analysis can be found on Appendix E on page 313.

When looking at the total BAG1 expression normalised to actin and to Mock transfected cells, it seems that CAL51 show a higher BAG1 expression than HEK29 cells (see Table 7.1). No conclusions could be made to decide whether increasing the transfection timing to two days helped increasing the activity of the oligonucleotides, as no consensus was found in the results, some of the oligonucleotides had a stronger effect when they were transfected for a day and others when they were transfected for two days. The oligonucleotides did not have the same effect in CAL51 or HEK293 cells either.

When the p50 and p36 expression was analysed, it was obvious that HEK293 cells showed a higher p36 expression than CAL51 cells (see Table 7.2). As the western blots were done only once no statistical analysis could be done. However, it could be observed that none of the oligonucleotides modified the p36 expression when compared to Scramble or Mock transfected cells in neither of the cell lines.

Table 7.1 Total BAG1 expression normalised to actin expression and to Mock transfected cells of CAL51 and HEK293 cells transfected with a final concentration of 25 nM of oligonucleotide for 1 or 2 days, measured by western blot.

		CAL51		HEK293	
		1 DAY TRANSFECTION	**2 DAY TRANSFECTION**	**1 DAY TRANSFECTION**	**2 DAY TRANSFECTION**
	MOCK	1.00	1.00	1.00	1.00
DNA	B14 AB	1.43	0.70	0.47	0.82
	B15 AB	1.22	1.22	0.46	0.87
	SCRAMBLE	1.64	1.15	0.34	1.06
LNA-DNA	B14 AB	0.81	0.56	0.98	1.02
	B15 AB	0.87	1.07	1.12	1.47
	SCRAMBLE	0.90	0.96	1.09	1.10
2' OME PS	B14 AB	1.40	1.41	0.66	1.21
	B15 AB	1.06	1.33	0.73	1.12
	SCRAMBLE	1.23	1.02	0.72	0.86
2' OME	B14 AB	0.86	0.68	0.95	0.84
	B15 AB	0.81	0.71	0.94	1.52
	SCRAMBLE	0.66	0.80	1.14	1.79

Table 7.2 %p50 and %p36 expression quantified from the western blots of CAL51 and HEK293 cells transfected with a final concentration of oligonucleotide of 25 nM for one or two days.

		CAL51				HEK293			
		1 DAY TRANSFECTION		2 DAY TRANSFECTION		1 DAY TRANSFECTION		2 DAY TRANSFECTION	
		%p50	%p36	%p50	%p36	%p50	%p36	%p50	%p36
DNA	B14 AB	0.54	0.46	0.64	0.36	0.63	0.37	0.55	0.45
	B15 AB	0.55	0.45	0.69	0.31	0.55	0.45	0.58	0.42
	SCRAMBLE	0.54	0.46	0.72	0.28	0.58	0.42	0.52	0.48
	MOCK	0.53	0.47	0.73	0.27	0.55	0.45	0.55	0.45
LNA-DNA	B14 AB	0.73	0.27	0.72	0.28	0.45	0.55	0.46	0.54
	B15 AB	0.69	0.31	0.71	0.29	0.41	0.59	0.43	0.57
	SCRAMBLE	0.68	0.32	0.74	0.26	0.43	0.57	0.41	0.59
	MOCK	0.61	0.39	0.73	0.27	0.41	0.59	0.44	0.56
2' OME PS	B14 AB	0.73	0.27	0.72	0.28	0.47	0.53	0.51	0.49
	B15 AB	0.66	0.34	0.76	0.24	0.49	0.51	0.48	0.52
	SCRAMBLE	0.68	0.32	0.73	0.27	0.50	0.50	0.50	0.50
	MOCK	0.61	0.39	0.73	0.27	0.48	0.52	0.51	0.49
2' OME	B14 AB	0.72	0.28	0.72	0.28	0.54	0.46	0.50	0.50
	B15 AB	0.68	0.32	0.69	0.31	0.53	0.47	0.50	0.50
	SCRAMBLE	0.70	0.30	0.71	0.29	0.49	0.51	0.48	0.52
	MOCK	0.72	0.28	0.71	0.29	0.48	0.52	0.52	0.48

7.4 CO-TRANSFECTION OF *IN VITRO* SYNTHESISED RNA WITH THE OLIGONUCLEOTIDES

At this point we could only show that the oligonucleotides could successfully modify IRES-mediated translation in RRL, unfortunately we could not show the same results in HEK293 or CAL51 cells. We decided to co-transfect *in vitro* transcribed FBN RNA and the oligonucleotides in cells and study if the oligonucleotides could modify the IRES activity as they showed in RRL. For this experiment FBN was *in vitro* synthesised with an m^7G-cap and a poly(A) tail (see section 2.10 on page 72 for a detailed protocol). The experiment was done in CAL51 cells and not in HEK293 cells, as we had previously shown that the *BAG1* IRES activity could be increased in CAL51 cells with the addition of pPTBP1 and pPCBP (see section Chapter 7 on page 221), and we wanted to show whether the oligonucleotides could have the same effect.

Oligonucleotides and FBN were transfected for 6 and 24 hours. The reason behind this was that after 24 hours both the RNA and oligonucleotides could have been degraded, however if this was not the case, the oligonucleotides would have had a longer time to have an effect. The 6 hour transfection was done in case the oligonucleotides or RNA showed degradation symptoms in the 24 hour transfection. Transfections were done as explained in section 2.14 on page 79, using Lipofectamine 2000 (Thermo Fisher Scientific). The IRES activity of oligonucleotide transfected cells was compared to Mock transfected cells (cells transfected with FBN RNA but no oligonucleotide) and Scramble transfected cells. Results were analysed by a multiple comparisons one-way ANOVA with a Dunnett's multiple comparison test ($P<0.05$) to compare the Nluc/Fluc activity of the oligonucleotide transfected cells with the Nluc/Fluc activity of Mock or Scramble transfected cells.

The Nluc to Fluc ratio was analysed to study *BAG1* IRES activity in the presence of the oligonucleotides. When transfections were done for 6 hours (see Figure 7.8, A), B14 AB DNA, B15 AB DNA, B14 AB 2' OME PS and B14 AB 2' OME transfected cells showed a significantly different Nluc to Fluc ratio than Scramble transfected cells. Cells transfected with B14 AB DNA, B14 AB LNA, B15 AB LNA and Scramble LNA showed a significantly different Nluc to Fluc ratio than Mock transfected cells. B14 AB DNA and B14 AB 2' OME PS significantly increased the Nluc to Fluc ratio and B14 AB 2' OME significantly decreased it. B14 AB DNA and B14 AB 2' OME behaved as in RRL, however they showed a smaller effect in the IRES activity in cells than in RRL.

When transfections were done for 24 hours (see Figure 7.8, B), cells transfected with B14 AB DNA, B14 AB 2' OME PS and B14 AB 2' OME showed significantly different Nluc to Fluc ratios than Scramble and Mock transfected cells. As when the oligonucleotides were transfected for 6 hours, B14 AB DNA and B14 AB 2' OME PS increased the IRES activity, but their effect was smaller when they were transfected for 24 hours, suggesting that some oligonucleotide degradation could have occurred. B14 AB 2' OME had the strongest effect decreasing the Nluc to Fluc ratio when it was transfected for 24 hours, suggesting this oligonucleotide could be more stable than the DNA and 2' OME PS oligonucleotides.

With this experiment we could show that the oligonucleotides could also have an effect in cells and that their ability to decrease or increase the IRES activity was more dependent on their chemistry rather than their sequence, as shown in RRL.

The Fluc and Nluc values of these results can be found in Figure D.20 and Figure D.21 on page 310 and 311.

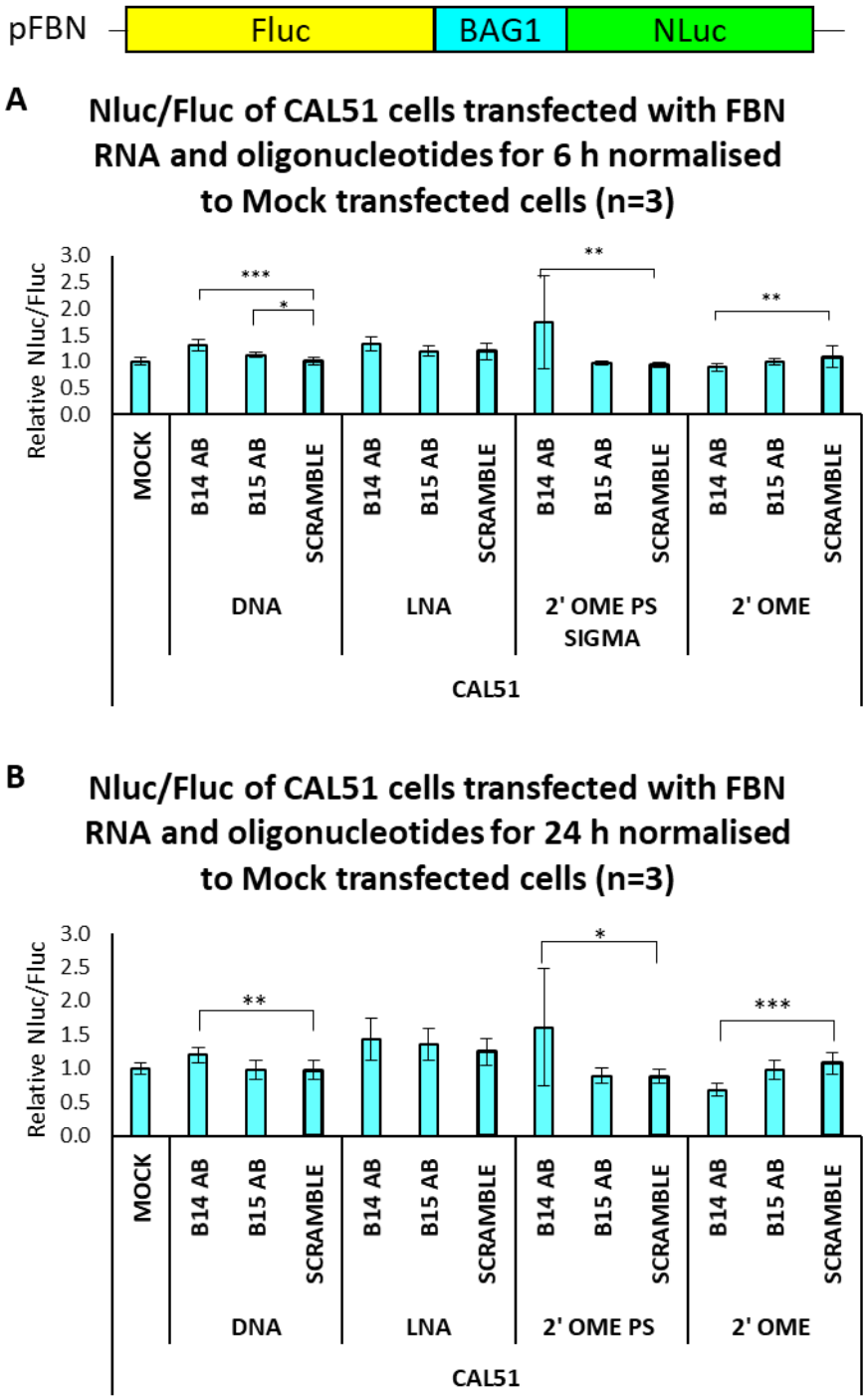

Figure 7.8 **Nluc to Fluc ratio of CAL51 cells co-transfected with 150 ng of *in vitro* transcribed m^{7}G-FBN-poly(A) RNA and a final concentration of 1 µM of oligonucleotides for 6 hours (A) and 24 hours (B).** Error bars show ±SD. Statistical analysis was done using a one-way ANOVA with Dunnett's multiple comparison test to compare the Nluc/Fluc activity of the oligonucleotide transfected cells with the Nluc/Fluc activity of Mock or Scramble transfected cells ($P<0.05$).

7.5 TRANSFECTION OF hpBN-HEK CELLS WITH LIPOFECTAMINE

On the previous experiment it was the first time that we had successfully shown that some of the oligonucleotides could significantly increase or decrease the *BAG1* IRES activity in cells. However we could only show that the oligonucleotides could modify the IRES activity of an *in vitro* synthesised RNA. We still had not succeeded in showing that the oligonucleotides could modify the IRES activity of an RNA transcribed in the cells. There were two approaches that had successfully worked in the co-transfection of RNA with the oligonucleotides that we had never tried before: doing a 6 hour transfection with the oligonucleotides and transfecting the oligonucleotides using Lipofectamine 2000.

We decided to compare the ability of the oligonucleotides to modify the *BAG1* IRES activity when transfected with Lipofectamine 2000 when transfections were done for 6 and 24 hours, oligonucleotide final concentration was 25 nM. The experiment was done in hpBN-HEK cells to avoid having to co-transfect any plasmid so that we introduced the smallest number of variables possible in the experiment. The total amount of protein was also calculated *via* a Bradford assay, and the Nluc activity was normalised to the total amount of protein in each case. B14 AB was transfected in the cells, as it had previously shown to have a stronger effect than B15 AB. Scramble oligonucleotides were also transfected as a control. The experiment was done three independent times, each of them in triplicate.

25 nM of oligonucleotide were transfected a total of three times using Lipofectamine 2000, transfections were done for 6 and 24 hours (see Figure 7.9). A one-way ANOVA with a Dunnett's multiple comparison test ($P<0.05$) was carried out to compare the Nluc activity of the oligonucleotide transfected cells with the Nluc activity of Mock transfected cells. The same test was used to compare the Nluc to protein ratio of cells transfected with oligonucleotides to the Nluc to protein ratio of Mock transfected cells. An unpaired t-test (two-tailed) ($P<0.05$) was done to check if the Nluc to protein ratio of the B14 AB transfected cells was significantly different from those of the Scramble oligonucleotide transfected cells.

When transfections were done for 6 hours, both B14 AB DNA and B14 AB LNA-DNA treatments showed a significant increase in the Nluc activity and the Nluc to protein ratio when compared to Mock transfected cells (see Figure 7.9, A and B). When transfections were done for 24 hours, all the oligonucleotides (B14 AB and Scramble) except the 2' OME modified ones significantly increased both the Nluc activity and the Nluc to protein ratio when compared to Mock transfected cells (see Figure 7.9, C and D). Unfortunately no difference was observed in any of the cases where the B14 AB transfections were compared to the Scramble transfections. However

some of the oligonucleotides, B14 AB 2' OME mostly, showed a slight increase of the Nluc to Fluc activity when compared to the Scramble transfected cells.

Even if we could show that the oligonucleotides had the ability to significantly increase the Nluc activity and thereby the IRES activity compared to Mock transfected cells, it would have been interesting to prove that B14 AB had the ability to increase the IRES activity when compared to Scramble transfected cells. Trying the same technique by modifying the oligonucleotide concentration, the transfection timing or even the cell line (repeating it in CAL51 cells) could lead to promising results.

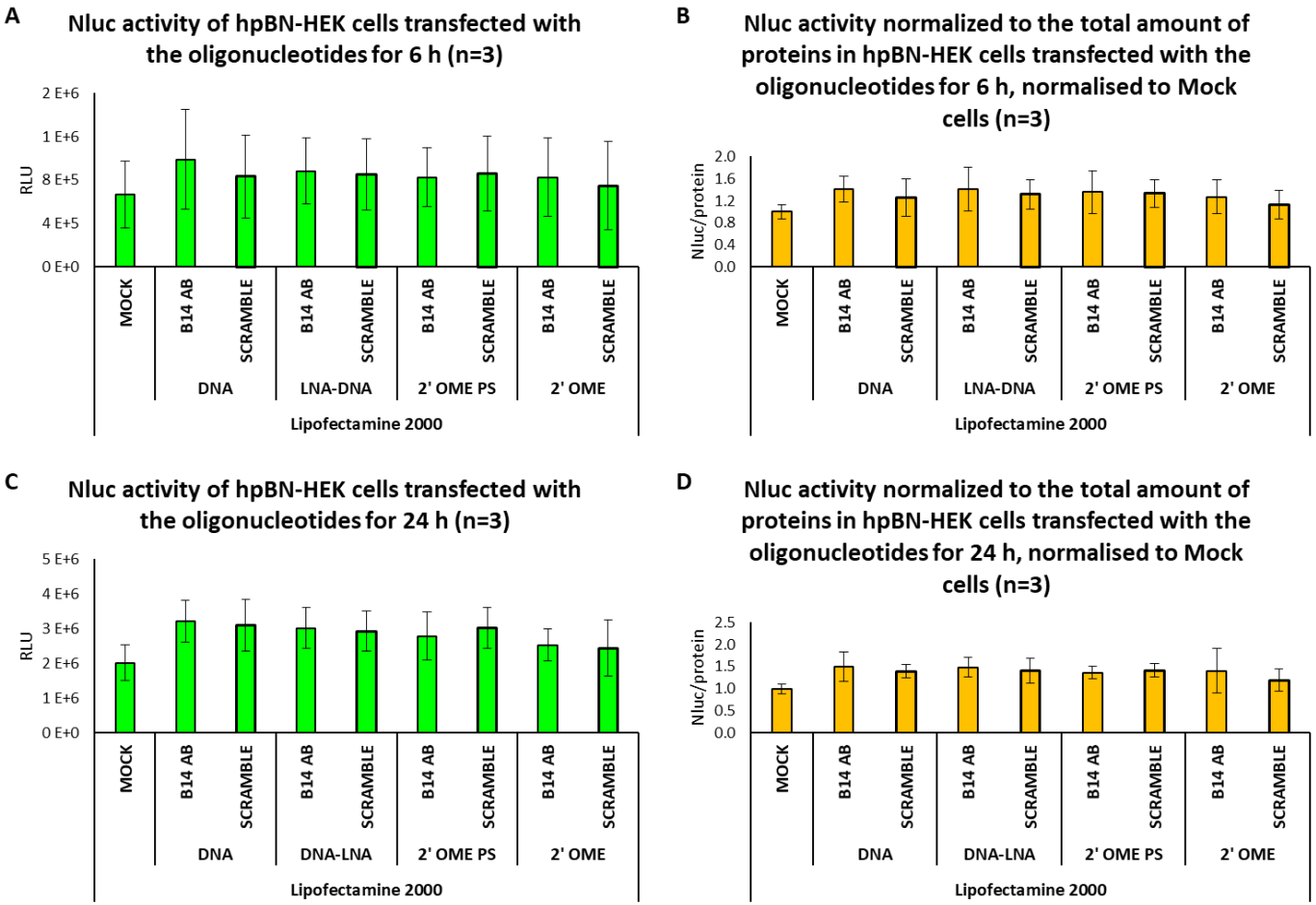

Figure 7.9 **Nluc activity (A) and Nluc activity to protein ratio (B) of hpBN-HEK cells transfected with a final concentration of 25 nM of oligonucleotide for 6 hours and 24 hours.** Error bars show ± SD of an experiment done once in triplicate.

7.6 DISCUSSION

STUDYING IRES ACTIVITY IN HEK293 AND CAL51 CELLS

Pickering *et al.*[95] studied the activity of the *BAG1* IRES in different cell lines and classified HEK293s as cells with a medium to high IRES activity. Among the cells with the lowest IRES activity they identified CAL51 cells. They also showed that by overexpressing PTBP1 and PCBP in those cells the *BAG1* IRES activity could be increased. When we overexpressed PTBP1 and PCBP in CAL51 and HEK293 cells transfected with pFBN, only CAL51 cells significantly increased the *BAG1* IRES activity. When the Nluc to Fluc ratio of pFBN transfected cells was normalised to the Nluc to Fluc ratio of pFN transfected cells to study the IRES activity in each cell line, CAL51 cells had a stronger IRES activity. Overall, CAL51 cells showed a strong *BAG1* IRES activity which could be increased if the PTBP1 and PCBP expression increased. HEK293 cells showed a smaller *BAG1* IRES activity, which did not increase its activity when PTBP1 and PCBP were overexpressed. The fact that the *BAG1* IRES could be increased in CAL51 by the overexpression of the ITAFS required for the correct *BAG1* IRES activity suggested that CAL51 cells could be a better model to study the effect of the oligonucleotides than HEK293 cells.

However, when a final concentration of 25 nM of B14 AB and B15 AB DNA, LNA-DNA, 2' OME PS and 2' OME were transfected in CAL51 cells for one and two days and the *BAG1* IRES activity was measured by luciferase assays and western blots, none of the oligonucleotides had a significant effect in the IRES activity. The same results were obtained in HEK293 cells.

CO-TRANSFECTION OF *IN VITRO* SYNTHESISED FBN AND THE OLIGONUCLEOTIDES IN CAL51 CELLS

B14 AB, B15 AB and Scramble DNA, LNA-DNA, 2' OME PS and 2' OME were incubated with *in vitro* transcribed FBN RNA and transfected in CAL51 cells for 6 and 24 hours. All the cells transfected with FBN and the oligonucleotides showed high Fluc and Nluc activities, even the cells transfected with 2' OME PS oligonucleotides. These results show that the 2' OME PS do not have the same effect in cells as in RRL, and if they have the ability to degrade RNA this is only possible in RRL. Overall, the Nluc and Fluc activities were higher when the RNA was transfected for 24 hours, suggesting that the RNA did not suffer a lot of degradation.

B14 AB had a stronger effect than B15 AB in the *BAG1* IRES activity. B14 AB DNA and 2' OME PS showed a significant increase in the Nluc to Fluc ratio when compared to Scramble or Mock transfected cells and their activity was stronger when the treatment was done for 6 hours. B14 2' OME decreased it and its activity was stronger when the transfection was done for 24 hours.

These results show that oligonucleotides with the same sequence, targeting the same RNA region could have opposite results depending on their chemical properties. The results also suggest that DNA and 2' OME PS oligonucleotides could be less stable than 2' OME oligonucleotides.

After the success of the FBN RNA and oligonucleotides co-transfection, we decided to try the two factors that had shown to work in this last experiment but never tried before: transfecting the oligonucleotides for a shorter period of time (6 hours) and using Lipofectamine 2000 as the transfection reagent instead of RiboJuice. The experiments was done in hpBN-HEK cells. If the experiment was done in HEK293 or CAL51 cells, plasmids would have to be transfected alongside the oligonucleotides. Plasmids could take over 6 hours to express, and thereby we could not study the effect of the oligonucleotides in such a short period of time. Unfortunately, none of the oligonucleotides significantly modified the *BAG1* IRES activity when compared to Scramble transfected cells.

As previously mentioned, not many people have managed to successfully increase protein expression with the use of oligonucleotides, and the ones that increased it did it by blocking inhibitory elements of the process of translation such as uORFs or G4s. Our purpose was different from this; we have tried to modify the secondary structure of an IRES using oligonucleotides to make it more active. This approach has shown to be very challenging and of a difficult approach. We have found the best area to target in the whole *BAG1* IRES and proposed an oligonucleotide (B14 AB) that has successfully shown in repeated occasions to increase *BAG1* IRES activity in RRL and when co-transfected with FBN RNA in CAL51 cells. We have also shown that the same oligonucleotide with different chemical properties could have different effects in the *BAG1* IRES activity, which could be based in the different binding properties or strengths that the oligonucleotides can bind to the RNA. Unfortunately, we have been unable to show an increase in the endogenous *BAG1* IRES activity with the use of B14 AB.

Chapter 8 FINAL DISCUSSION, CONCLUSIONS AND FUTURE WORK

TARGETING IRESs AS A THERAPEUTIC APPROACH

Since IRESs were discovered in viruses, several researchers have tried to use drugs and small molecules to inhibit the IRES activity. Researchers have taken two mayor approaches in this sense: disrupting the IRES structure itself or preventing interactions of the IRES with the ribosome or ITAFs, in most occasions by targeting the ITAFs themselves[115]. Since IRESs were discovered in cellular mRNAs and their implication in cancer development was observed[116], targeting IRESs has been considered an attractive possibility for anticancer therapy[117].

The main aim of this project was to use oligonucleotides to control gene expression of IRES elements by modifying their secondary structure. We focussed on the *BAG1* IRES as it had been previously studied by members of the supervisory group, its structure had been experimentally determined, and the ITAFs required for its proper functioning had been identified[82]. We spent some time verifying the presence of an IRES in *BAG1*, as the existence of cellular IRESs has generated controversies among some researchers[79,110,112,273] (see Chapter 3 for a full discussion on this topic). We have successfully shown modification of IRES-mediated translation in the cell free system RRL using oligonucleotides, in this case unmodified B14 AB was the most successful candidate. However, we did not manage to get the same results *in cellulo* (see Chapter 5 for more information).

FUTURE APPROACHES

We focused on the *BAG1* IRES structure proposed by Pickering *et al.*[82] in 2004 for the initial design of the oligonucleotides. It would be interesting to do some extra work on the secondary structure of the *BAG1* IRES. Doing a SHAPE analysis or using higher resolution techniques such as X-ray crystallography, Nuclear Magnetic Resonance (NMR) spectroscopy or Cryo-electron microscopy (Cryo-EM) we could further determine the structure of the *BAG1* IRES, to see if these techniques gave a structure similar to that previously proposed. It could then be further studied if there are any changes in the structure of the IRES in the presence of B14 AB or any of the other oligonucleotides. Furthermore, B14 AB with the different chemistries could be studied to find out if these have the same ability to modify the IRES structure. Some researchers have created algorithms that claim to be useful to detect IRES structures in mRNAs[301–303], unfortunately they are not straight forward to use and some training is needed to understand the different

algorithms and the number of possible variables. Nevertheless, running the *BAG1* IRES sequence on these algorithms could help us get a better idea of its structure.

We showed that we could modify the Nluc to Fluc ratio of RRL programmed with both *in vitro* synthesised FBN RNA and the oligonucleotides. To be 100% sure that by modifying the Nluc to Fluc ratio what we are modifying is the *BAG1* IRES activity, we could programme RRL with an *in vitro* synthesised RNA containing the two reporter genes Fluc and Nluc and a sequence of the same length and nucleotide composition as the *BAG1* 5' UTR in FBN, containing the targeting sequence of the oligonucleotide to test, but that does not form the predicted IRES structure (see Figure 8.1). Only when the RRL programmed with that RNA and the oligonucleotide showed the same Nluc to Fluc ratio when compared to RRL programmed just with the RNA we could confidently argument that the oligonucleotides are specifically affecting the *BAG1* IRES activity.

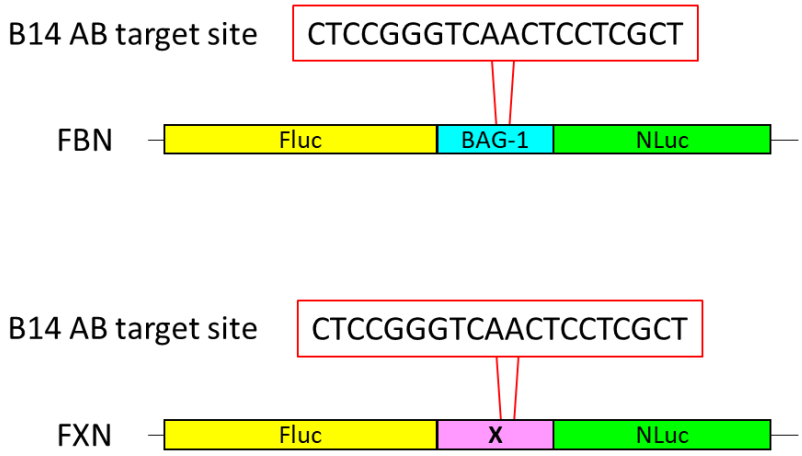

Figure 8.1 **FBN RNA showing the targeting point of B14 AB.** FXN RNA is composed by the reporter genes Fluc and Nluc, and between both of them we can find the sequence X, which has the same length as the *BAG1* 5' UTR cloned in FBN. Sequence X will not form an IRES, but it will still have the target site for B14 AB. If FXN showed a different Nluc to Fluc ratio in the presence of B14 AB, it would mean that the effect observed in the modification of the Nluc to Fluc ratio in FBN in the presence of the oligonucleotides is not due to the *BAG1* IRES activity.

Continuing with the research on the cell free systems, the oligonucleotide activity could also be tested in TnT. With RRL we could only measure the levels of translation of the *BAG1* IRES, however in TnT both the processes of transcription and translation take place, creating a more similar environment to the one in the cells. To do so, TnT could be programmed with the FBN PCR product containing the T7 promoter alongside the oligonucleotides. A modification of the Nluc to Fluc ratio of oligonucleotide programmed TnT would verify the ability of the oligonucleotides to modify the *BAG1* IRES activity. For the same purpose, experiments carried out in RRL could be done in a different cell free system such as Wheat Germ Extract.

One interesting approach would be to study whether the oligonucleotides are able to bind to the *BAG1 IRES* in cells. Due to its highly structured conformation, oligonucleotides may be unable to efficiently interact with IRESs; and in this sense, some IRESs might be harder to target than others. This is a very challenging approach and we have not been able to find any evidence in the literature where it has been determined if a certain oligonucleotide successfully binds to the mRNA other than *via* observations on effects on the levels of protein expression. Biotinylated oligonucleotides could be designed to contain biotin on their 5' or 3' extremes or in their internal sequence. The biotin could be attached during the process of synthesis, or could also be added to the 3' terminus by attaching a biotin-dUTP using *E.coli* DNA polymerase I (Klenow fragment) or using one of the available commercial kits for this purpose. The addition of biotin to oligonucleotides for research purposes has been widely done for different purposes such as to study helicase mechanisms[304] or as hybridization probes to study the presence of a specific DNA[305,306]. Hassan *et al.* used this very same approach to isolate cell-specific micro RNAs[307]. For our purpose, we could use a similar protocol to the one developed by Hassan *et al.* After transfection of the cells with biotinylated oligonucleotides, these would be lysed and the RNA bound to the biotinylated oligonucleotides isolated using streptavidin beads. Beads would be washed with proteinase and DNase to get rid of the proteins and DNA bound to the RNA and the RNA sequences could be analysed by qRT-PCR for the presence of *BAG1* mRNA. A positive amplification of *BAG1* would show the successful binding of the oligonucleotides to the *BAG1* IRES. A failure would not necessarily mean the failure of the oligonucleotides to target the *BAG1* IRES, but the fact that the system proposed is not the ideal one for our purpose. With this method, we could not only study whether the oligonucleotides bind to the IRES or not, but also the effects that modifying the oligonucleotide concentration could have: increasing the oligonucleotide concentration would increase the efficiency of the system (would we recover more *BAG1* mRNA?) or would we be just saturating the system? We could also study the effect that the oligonucleotides could have in different cell lines: are we recovering the same amount of RNA when transfecting different cell lines with the same amount of oligonucleotide? By the biotinylation of the different modified oligonucleotides we could also study which one is the most efficient at targeting the IRES.

We decided to do the experiments in HEK293 cells due to their high transfection efficiency. However Pickering *et al.* already showed that different cell lines had different *BAG1* IRES activities[95], and we have corroborated those results. In fact the research they did was not very extensive as they only studied three human breast cancer cell lines (CAL51, MCF7 and CAMA-1), a human lung cancer cell line (CALU1), HEK293 cells (human embryonic kidney cell line immortalised with adenovirus) and HeLa S3 cells (human cervical epithelioid carcinoma), although

in the original thesis work on the *BAG1* IRES, a wider panel of cell lines was used[298]. After this information was published, the implication of *BAG1* in different cancers such as Acute Myeloid Leukemia was discovered, where an increase in BAG1 expression has been observed associated with resistance to chemotherapy[308] or in colorectal tumour cells, where BAG1 has shown to supress the key regulatory cytokine transforming growth factor beta [TGF-β1], which is associated with a malignant phenotype[166]. The expression of BAG1 has also been studied in a wide variety of breast cancer cell lines others than the ones studied by Pickering *et al.*[163]. The *BAG1* IRES activity could be measured in all these cell lines by western blot, and as p36 is the isoform whose translation is driven by the IRES, it is relatively easy to measure the IRES *versus* cap-mediated translation. We should still keep in mind that p36 is translated both *via* the canonical translation and the IRES, with the latter being less effective, and that we cannot differentiate 100% how much protein is translated *via* each method. As the idea of the use of the oligonucleotides was to mimic the activity of PTBP1 and PCBP1 in aiding ribosome recruitment to the IRES, it would also make sense to study the expression of those two proteins in these cell lines to check if a direct relationship could be observed between *BAG1* IRES activity and the PCBP-1 and PTBP1 protein levels. Once the BAG1 activity in different cell lines was determined, we could choose the best cell lines to work with depending on our aim: we would use cell lines with a lower IRES activity to try and increase it using oligonucleotides and cell lines with a higher IRES activity to try and decrease it.

One of the biggest difficulties found in antisense therapy (the use of oligonucleotides to control gene expression) is the poor delivery of oligonucleotides in cells, which is increased in *in vivo* experiments. A poor delivery could explain why we could not see an effect when oligonucleotides were used in cells. We used RiboJuice for the delivery of the oligonucleotides, as it was the most effective one, with the best transfection efficiency and toxicity balance among all the transfection reagents we were able to try. However, we could consider modifying the oligonucleotides in different ways to increase their uptake by the cells. Gymnotic delivery (oligonucleotide delivery without the use of transfection reagents) of the phosphorothioate oligonucleotides could be a solution to this problem, however this technique requires a higher oligonucleotide concentration and much longer transfection timing[309]. In addition, phosphorothioate oligonucleotides were not found to be very efficient in our experiments. Different approaches could be used that have already shown to increase the cellular uptake, such as the addition of a lipid[310,311], a cholesterol group[312] or fluorocarbon chain[313] to the oligonucleotides. Oligonucleotides can also be encapsulated in nanoparticles, which are usually based on positively charged polymers and metal nanomaterials, to improve their potential. The nanoparticles need to have the ability to deliver the oligonucleotides to the targeting cells, while keeping them safe from nuclease degradation or

serum protein adsorption. Once in the cells, the nanocarriers need to ensure that the oligonucleotides can escape the nanocarriers[314].

It would also be interesting to study with higher precision the best transfection timing. To do so hpBN-HEK cells could be transfected with the oligonucleotides and directly add one of the new nanoluciferase substrates, Endurazine or Vivazine (Promega) which can be added directly to cells and monitored for extended periods[263]. A luminometer which maintains the correct temperature and CO_2 level could then be programmed to measure the Nluc activity (bioluminescence) at every set time (for example every hour for 48 hours). This could allow us to study the exact time at which the oligonucleotides have the greatest effect. Every element in the experiment, such as the cell line used, number of cells seeded, transfection reagent used and concentration of the same, could be modified to determine in a more precise way the perfect transfection protocol.

Once the best transfection protocol is determined and at least one oligonucleotide has shown to modify the IRES activity, the ultimate experiment to verify the ability of the oligonucleotides to modify levels of translation could be to use polysome profiling. This technique consists of a sucrose-gradient separation where the polysomes (mRNA with two or more ribosomes), monosomes (mRNA molecule with a unique ribosome), small and large ribosomal subunits and unbound mRNA will be separated according to their density. mRNAs that are translated at low levels will be mainly towards the monosome region of the gradient, whereas highly translated mRNAs will appear towards the "heavier" polysomal region. The levels of a specific mRNA extracted from fractions of the gradient can be analysed by qPCR. By comparing the polysomal profiles and the levels of *BAG1* mRNA in the "heavier" fractions of the polysome profile of cells treated with the Scramble oligonucleotide and the IRES targeting oligonucleotide, we could check whether there is an increase in the presence of the *BAG1* mRNA in the polysome fraction, and thereby an increase in translation, in the IRES targeting oligonucleotide treated cells.

Once the oligonucleotide transfection is optimised, cell viability studies should be done, as well as cell stress studies. *BAG1* is an anti-apoptotic gene, in this sense inhibiting the *BAG1* IRES activity should lead to an increase in apoptosis and thereby cell viability should decrease, whereas an increase in the *BAG1* IRES activity should decrease apoptosis, thereby cell viability should increase. However these effects might not be seen as *BAG1* is not the only gene implicated in apoptosis regulation. In addition, we would have to study whether the IRES activity has such a big influence in the expression of BAG1, as *BAG1*'s principal translation pathway is the canonical one[143,144,146].

It would also be beneficial to study the half-life of the oligonucleotides in serum to determine the best transfection timing and the stability of the oligonucleotides. Oligonucleotides could be

incubated in serum for different periods of time, cleaned-up and run on a polyacrylamide denaturing gel to determine their degradation levels.

It is known that IRES-mediated activity takes place when cap-mediated translation is compromised, as in hypoxia, nutrition deprivation or heat shock. In this case we know that p36 can maintain its expression thanks to the IRES during heat shock[144]. It would be interesting to study the levels of IRES-mediated translation in the situations when IRES-mediated translation is the strongest, and study if we could modify that activity during those situations with the use of oligonucleotides.

If these future approaches that we are proposing here were successful, the next logical step would be to move on to doing some *in vivo* assays. New challenges would be encountered then, such as the delivery of the oligonucleotides to the cells of interest, making sure the stability of the oligonucleotides is high once they have been delivered and reducing the possible toxic effects they could cause among others.

INSTRUCTIONS FOR SOMEONE TRYING TO TARGET IRESs WITH OLIGONUCLEOTIDES

One of the positive aspects of this project is that, if proven successful, the same approach could be used to target different IRESs implicated in different diseases. Overall, I would say that the correct way to overcome a challenge like this is the following: design an oligonucleotide pool covering the whole sequence of interest and design a dual luciferase vector where the sequence of interest (the IRES) can be cloned between two reporter genes. Start by trying the oligonucleotides in an *in vitro* system like RRL to determine the exact sequence that should be targeted, prior to this the activity of the IRES in RRL should be assessed. Subsequently, work to study the IRES activity in different cell lines would determine which is the best cell line to work with, always considering if the final goal is to increase or decrease the IRES activity, the transfection efficiency of that cell line should also be studied. Further parameters to be optimised would be to determine the best transfection protocol by using a luminometer where the temperature and CO_2 level can be controlled, and study which is the best transfection protocol in terms of the number of cells to be seeded, the transfection reagent to use and its concentration, the concentration of oligonucleotide and the length of the transfection process. Once the best protocol is determined, it should be repeated at least three times to have enough data for the statistical analysis. The modification in the IRES activity can be determined in several ways: i) by studying protein expression using western blot (if antibodies are present for the gene of interest). ii) By measuring mRNA levels by qPCR to verify that the effect seen in the protein levels is at the level of translation and not due to modifications on the mRNA levels. iii) By a polysome profiling assay in the presence and in the absence of oligonucleotides. An important aspect of these kind of

experiments is the appropriate use of controls. In this sense, a scramble oligonucleotide that does not target any sequence in the whole genome should be used, with the same properties in terms of length and chemistry that the proposed oligonucleotides, to verify that the effect seen is exclusive of the oligonucleotide of interest.

Appendix A **OLIGONUCLEOTIDES SYNTHESISED IN THE LABORATORY**

The first set of oligonucleotides used (BAG 1 DNA, BAG 2 DNA, BAG 3 DNA, BAG 4 DNA, BAG 1 LNA, BAG 2 LNA, BAG 3 LNA and BAG 4 LNA) were synthesised in the laboratory.

A.1 MATERIAL AND METHODS

A.1.1 Unmodified DNA oligonucleotide synthesis

Table A.1.1 Unmodified oligonucleotide sequences.

Name	Sequence
BAG 1 DNA	5'-GGT CGA GCG G-3'
BAG 2 DNA	5'-GGT CTG AGC GG-3'
BAG 3 DNA	5'-CTT CTT CAC TCA GGG TCA ACT-3'
BAG 4 DNA	5'-CTC GAG CGG CGC-3'
BAG 3 NEW	5'-CTT CCT CAC TCA GGG TCA ACT-3'
BAG 4 NEW	5'-GTC GAG CGG CGC-3'
SCRAMBLE	5'-ACT ACC GTT GTT ATA GGT GT-3'

The oligonucleotides were synthesised on a DNA Synthesiser (Applied Biosystems 392). DNA strands were synthesised by solid phase synthesis on a 1 µmole scale using standard protocols. The nucleotide phosphoramidites, solvents and reagents used were purchased from Link Technologies (UK) or Tides Services (GER).

Following the synthesis, DNA strands were cleaved from the column manually by washing the column with syringes containing 1ml of aqueous ammonia for at least one hour. After one hour, one last wash was done with 500 µl of aqueous ammonia. The ammonia solution containing the cleaved DNA strands (total volume of 1.5 ml of aqueous ammonia) were transferred to a screw cap tube. The strands were deprotected by heating at 40°C overnight (or at least 5 hours). Deprotected strands were then purified by Glen-Pak™ Cartridges (Glenresearch) following the recommendations of the manufacturer.

After the purification, oligonucleotides were concentrated on a speed-vac concentrator (Eppendorf) and stored at 4°C.

A.1.2 LNA-DNA mixmers synthesis

Table A.1.2 LNA-DNA mixmers sequences. LNA modifications are marked in bold and underlined.

Name	Sequence
BAG 1 LNA	5'-**G**G**T** CGA **G**C**G** G-3'
BAG 2 LNA	5'-**G**G**T** CTG A**G**C **G**G-3'
BAG 3 LNA	5'-C**T**T CT**T** CAC **T**CA G**G**G TCA AC**T** C-3'
BAG 4 LNA	5'-C**T**C **G**AG CG**G** C**G**C-3'

Nucleotides in bold letters represent the LNA modifications.

The oligonucleotides were synthesised in a DNA synthesiser (Expedite 8900 Nucleic Acid Synthesis System). DNA strands were synthesised by solid phase synthesis on a 1 µmole scale. The LNA nucleosides were purchased from Rasayan Inc (US).

- ***SYNTHESIS OF LNA PHOSPHORAMIDITES***

CEP-CI had to be added to the LNA modifications so that they could couple to the next nucleotide (Figure A.1.1).

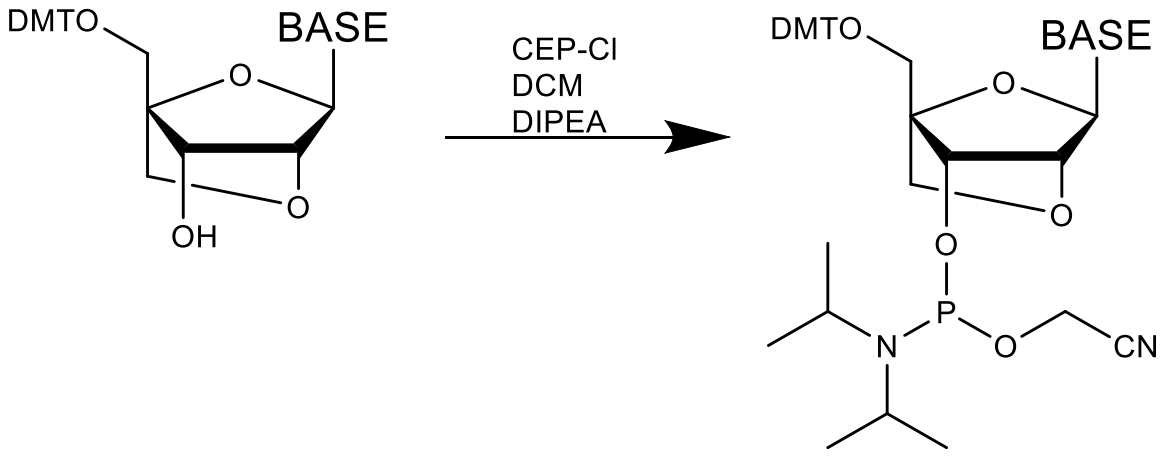

Figure A.1.1 **Reaction showing the addition of CEP-CI to the 5'-O-DMT-LNA to generate LNA phosphoramidite.**

5'-O-DMT-T-LNA (200 mg 349 µmol, 1 equivalence) was weighted into an oven dried flask and dried overnight by vacuum (25 ml in a two neck round-bottom flask (RBF) with a stirrer bar). The T-LNA was dissolved in DCM (5 ml) and molecular sieves were added to the flask. The reaction

was put under argon. DIPEA (242 µl, 1396 µmol, 4 equivalences) was added to the reaction. The reaction was purged with argon for 10 minutes. CEP-CI (234 µl, 1047 µmol, 3 equivalences) was added to the reaction. The reaction was stirred in the dark for two hours under argon. The reaction was monitored by TLC (DCM + 10% MeOH). TLC showed a small amount of starting material remained, however the reaction was taken forward.

The solution was transferred to another two neck RBF (oven dried) *via* cannula system. A small amount of 1 ml DCM was added to wash the flask. The volume was decreased to around 1 ml. In parallel, hexane was purged with argon and molecular sieves. Hexane (5ml) was added and the reaction was put on ice. A yellow oily precipitate formed. A cannula was used to remove the hexane and the flask was placed under vacuum for 10 minutes. This gave a light yellow oily solid. This was dissolved in 0.5 ml acetonitrile and transferred to an oven dried DNA synthesiser vial. The flask was washed with 1.5 ml acetonitrile and added to the vial. This was used directly on the synthesiser. Coupling time was extended to 7 minutes. After deprotection (following the LNA coupling) a bright orange colour was observed which indicated good coupling efficiency.

In tandem:

5'-O-DMT-G-LNA (250 mg, 383 µmol, 1 equivalence) was weighted into a two-neck oven dried flask and dried overnight by vacuum (25 ml in a two neck RBF with a stir bar). The G-LNA was dissolved in anhydrous DCM (5 ml) and molecular sieves were added to the flask. The reaction was placed under argon. DIPEA (267 µl, 153.2 µmol, 4 equivalences) was added to the reaction. The reaction was purged with argon for 10 minutes. CEP-CI (256 µl, 149 µmol, 3 equivalences) was added to the reaction. The reaction was stirred in the dark for two hours under argon. The reaction was monitored by TLC (DCM + 10% MeOH). TLC showed lots of starting material. More CEP-CI was added (85 µl). The other reaction was worked up while this continued to react for around one hour. TLC showed more product, but it was taken forward.

The solution was transferred to another two neck RBF (oven dried) *via* cannula system. A small amount of 1 ml of DCM was used to wash the sieves.

The volume was reduced to around 1 ml using argon and exhaust. In parallel, hexane (molecular sieves plus purged) (5 ml) was added to the flask and put on ice. An oily precipitate was formed. Hexane was removed by cannula.

The precipitate was washed with 2ml of hexane. The precipitate was put under vacuum for 10 minutes. The solid was dissolved in 0.5 ml acetonitrile and transferred to oven dried DNA synthesiser vial. Flask was washed with 1 ml acetonitrile. Acetonitrile (1.5 ml) was added to the vial (total volume 3 ml). The formed material was used directly on the synthesiser. After

deprotection (following the LNA coupling) a bright orange colour was observed which indicated good coupling efficiency.

Following the synthesis, DNA strands were cleaved from the column manually by washing the column with syringes containing 1 ml of aqueous ammonia for at least one hour. After one hour, one last wash was done with 500 µl of aqueous ammonia. The ammonia containing the cleaved DNA strands in 1.5 ml of aqueous ammonia were transferred to a screw cap tube. The strands were deprotected by heating them at 40°C overnight (or at least 5 hours). Deprotected strands were then purified by Glen-Pak™ Cartridges (Glenresearch) following the indications of the manufacturer.

After the purification, oligonucleotides were concentrated on a speed-vac and stored at 4°C.

A.1.3 UV-VIS spectroscopy

To determine yield and purity of the DNA strands, absorbance was measured at 260 nm (A260) using a UV-VIS spectrometer. A blank measurement was done with 120 µl of MilliQ water. The absorbance was measured in a total volume of 121 µl of sample diluted in water.

All the absorbance readings at 260 nm were between 0.1 and 1.

The amount of DNA in nmoles and the concentration was calculated using the absorbance values.

A.1.4 Mass Spectrometry

Mass spectrometry analysis was carried out using the School of Chemistry's mass spectrometry facilities. Sample submission was done diluting 40 µM of oligonucleotide in 20 µl of MilliQ water.

A.2 ANALYTICAL ANALYSIS: ULTRAVIOLET–VISIBLE SPECTROSCOPY

The oligonucleotide yield and rough purity was measured by UV spectroscopy. The results obtained were used to calculate the oligonucleotide concentration in the sample using the Beer Lambert law:

$$\boldsymbol{A = \varepsilon l c}$$

Where A is the absorbance, $\boldsymbol{\varepsilon}$ is the molar absorptivity, l is the length of the solution the light passes through and c is the concentration of the solution.

Absorbance readings were performed at 260 nm (A_{260}). All the absorbance readings were within the spectrometers linear range (0.1-1) to ensure they were reliable.

Table A.1.3 Calculated molar absorptivity of the synthesised oligonucleotides and the yield obtained.

	CALCULATED ε*	**CONCENTRATION µM**
BAG 1 DNA	98300	643
BAG 2 DNA	105800	392.5
BAG 3 DNA	188100	472
BAG 4 DNA	106200	238
BAG 1 LNA	98300	899
BAG 2 LNA	105800	470
BAG 3 LNA	188100	1850
BAG 4 LNA	106200	1860

*ε was calculated using the following web page: https://www.atdbio.com/tools/oligo-calculator

A.3 MASS SPECTROMETRY

Table A.1.4 Expected mass *vs* obtained mass of the oligonucleotides in the mass spectrometry analysis.

	EXPECTED MASS	**OBTAINED MASS**
BAG 1 DNA	3109.0344	3108.3
BAG 2 DNA	3413.2276	3412.3
BAG 3 DNA	6332.1045	6330.8
BAG 4 DNA	3647.3740	3646.4
BAG 1 LNA	3221	3220.3
BAG 2 LNA	3525	3525.6
BAG 3 LNA	6761	6761.2
BAG 4 LNA	3759	3758.7

All the oligonucleotides showed the expected mass. The spectrum of BAG 1 showed some impurity, including guanosine deletion. The spectrum of BAG 2 overall looked good with some excess of sodium or potassium. BAG 3 and BAG 4 both showed some cytosine deletion. BAG 1 LNA, BAG 2 LNA and BAG 4 LNA showed a pure spectrum. BAG 3 LNA showed some guanosine deletion. All the oligonucleotides showed enough purity to be used (over 85%).

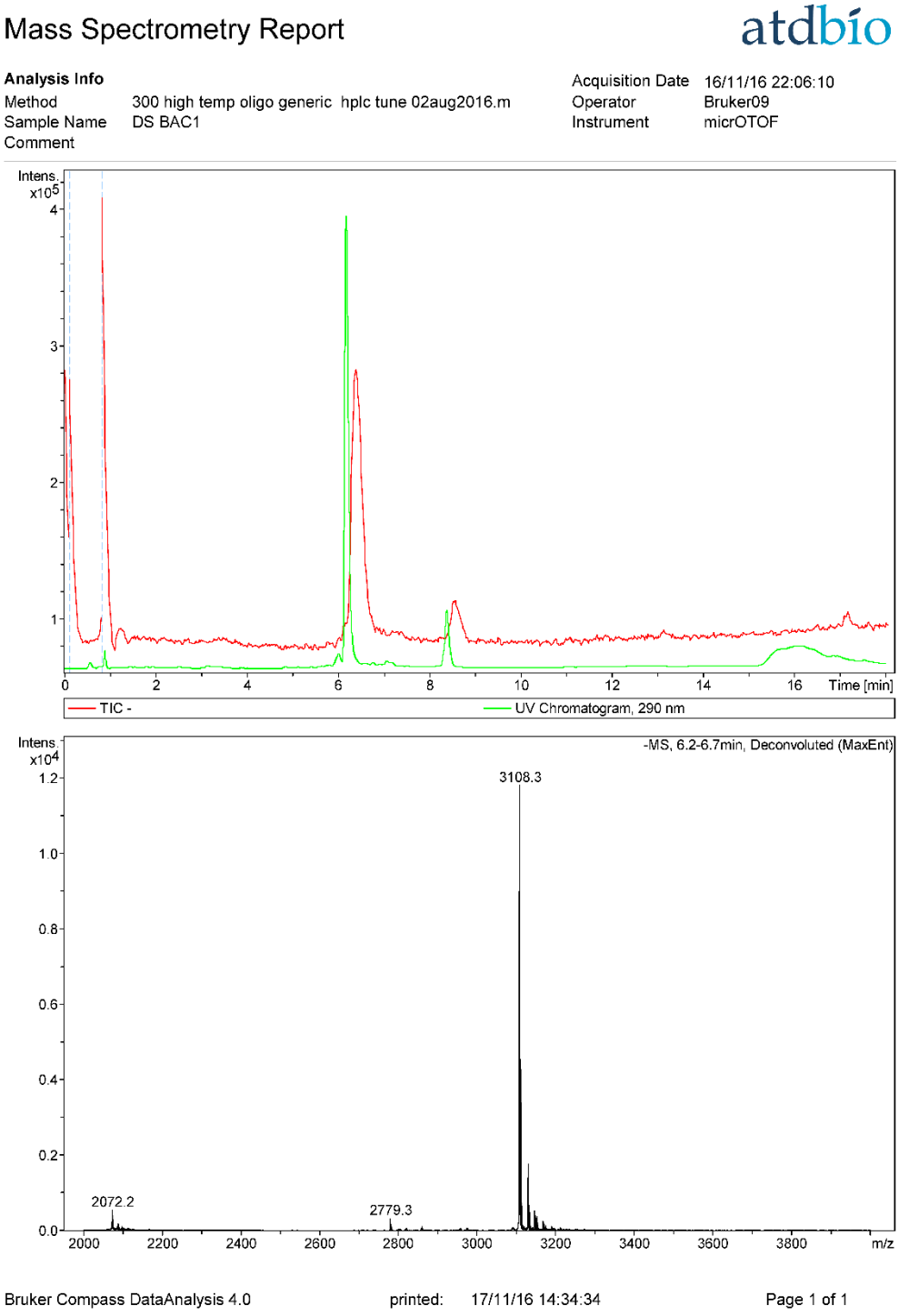

Figure A.1.2 BAG 1 DNA oligonucleotide mass spectrometry result.

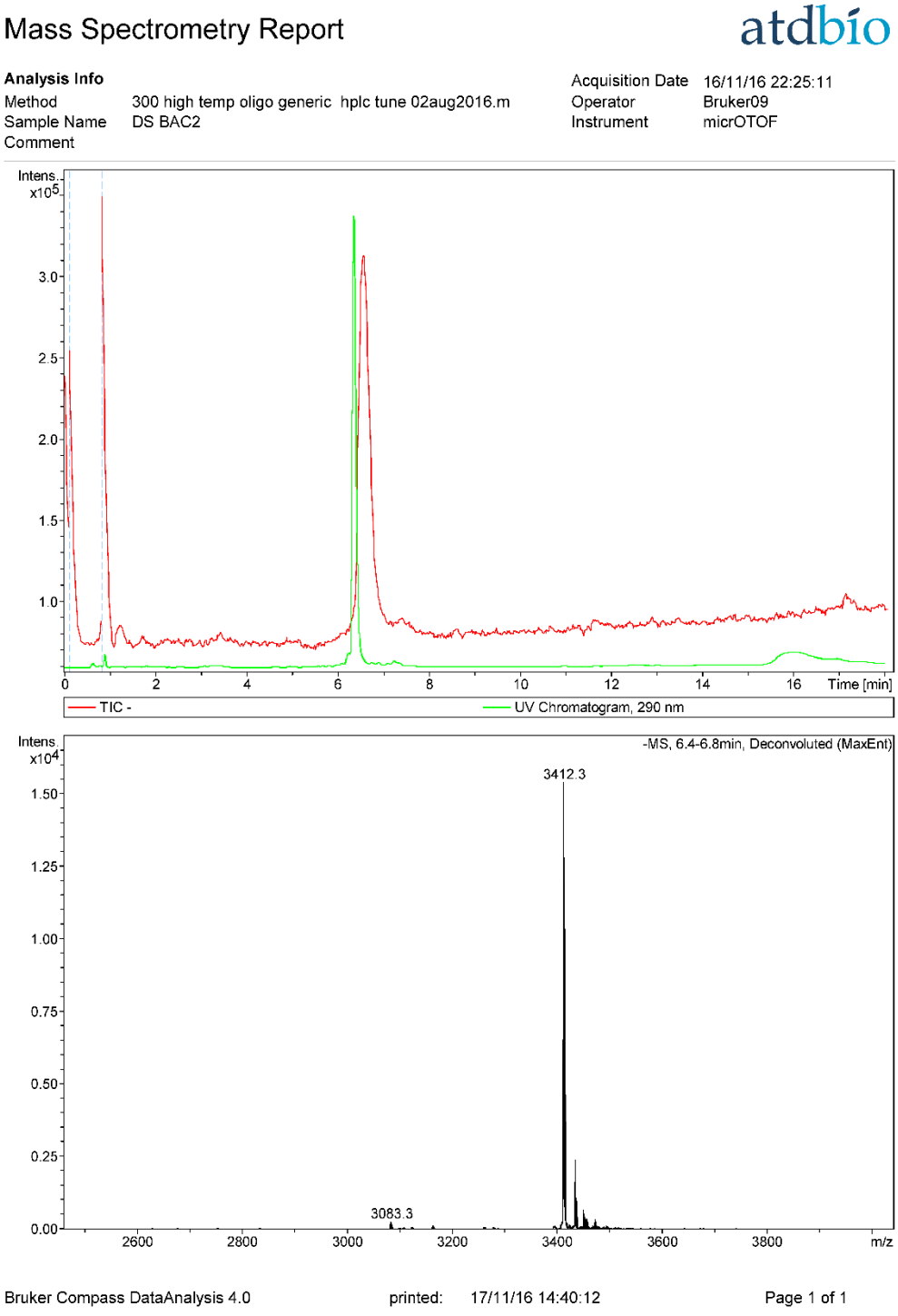

Figure A.1.3 BAG 2 DNA oligonucleotide mass spectrometry result.

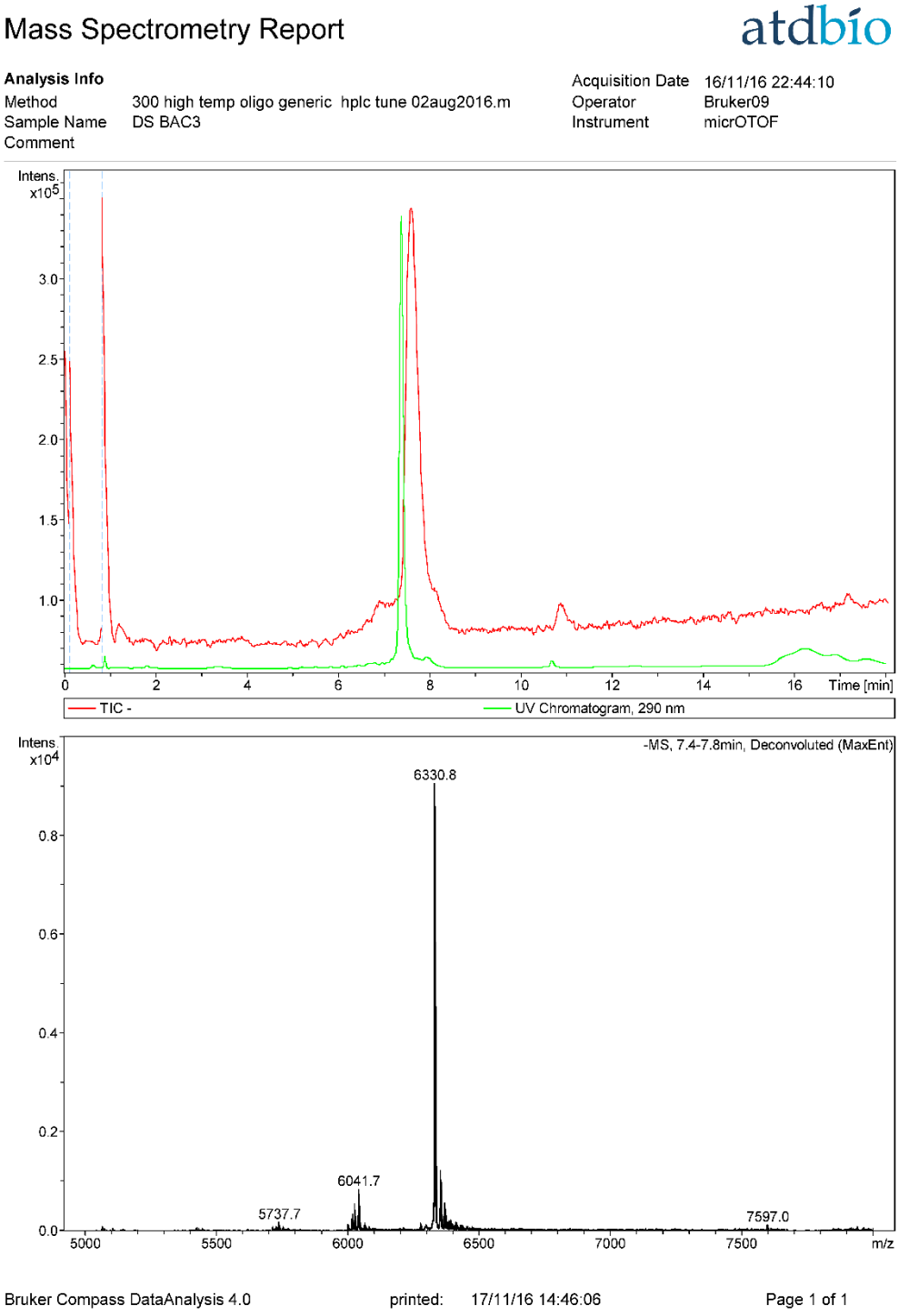

Figure A.1.4 BAG 3 DNA oligonucleotide mass spectrometry result.

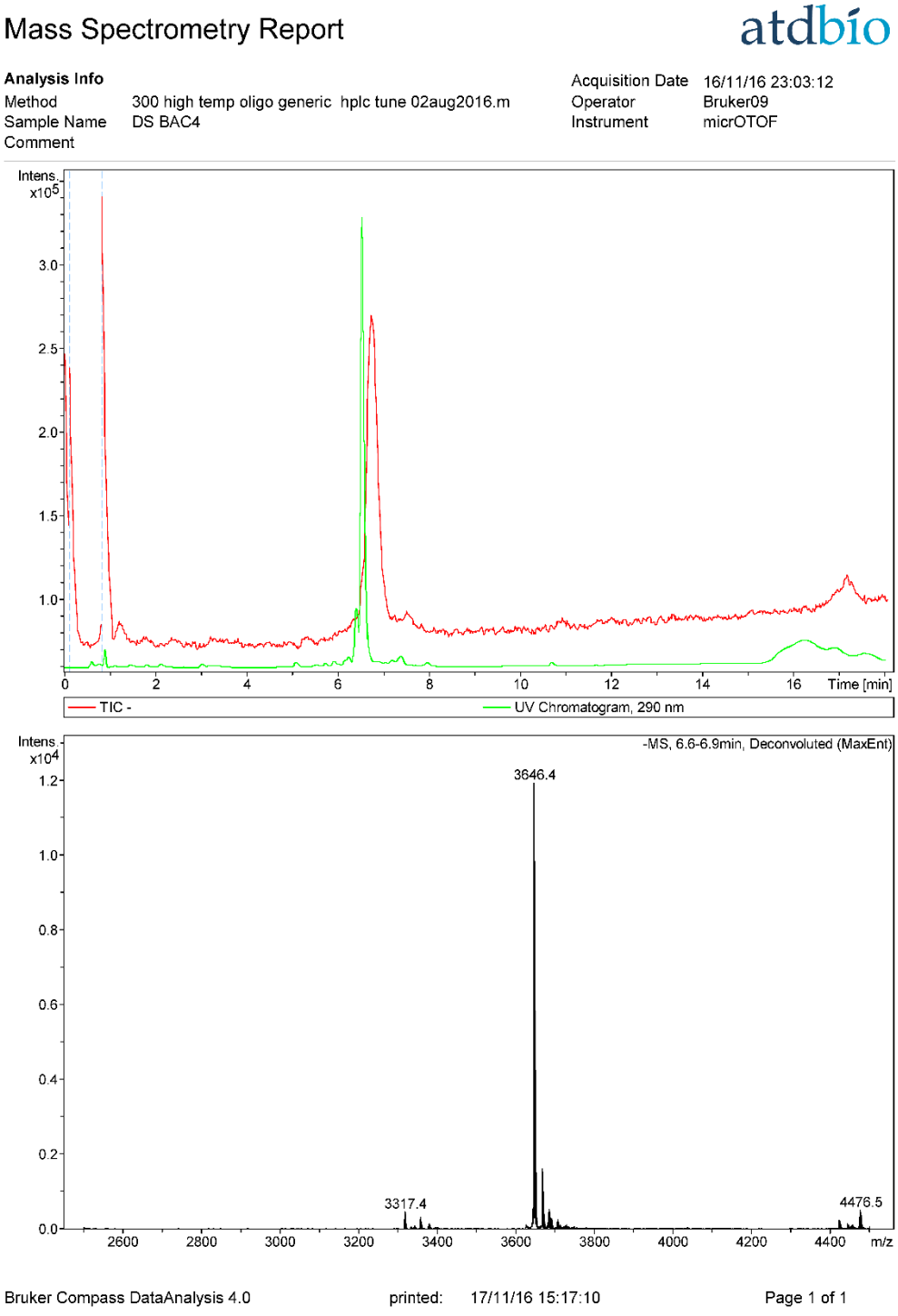

Figure A.1.5 BAG 4 DNA oligonucleotide mass spectrometry result.

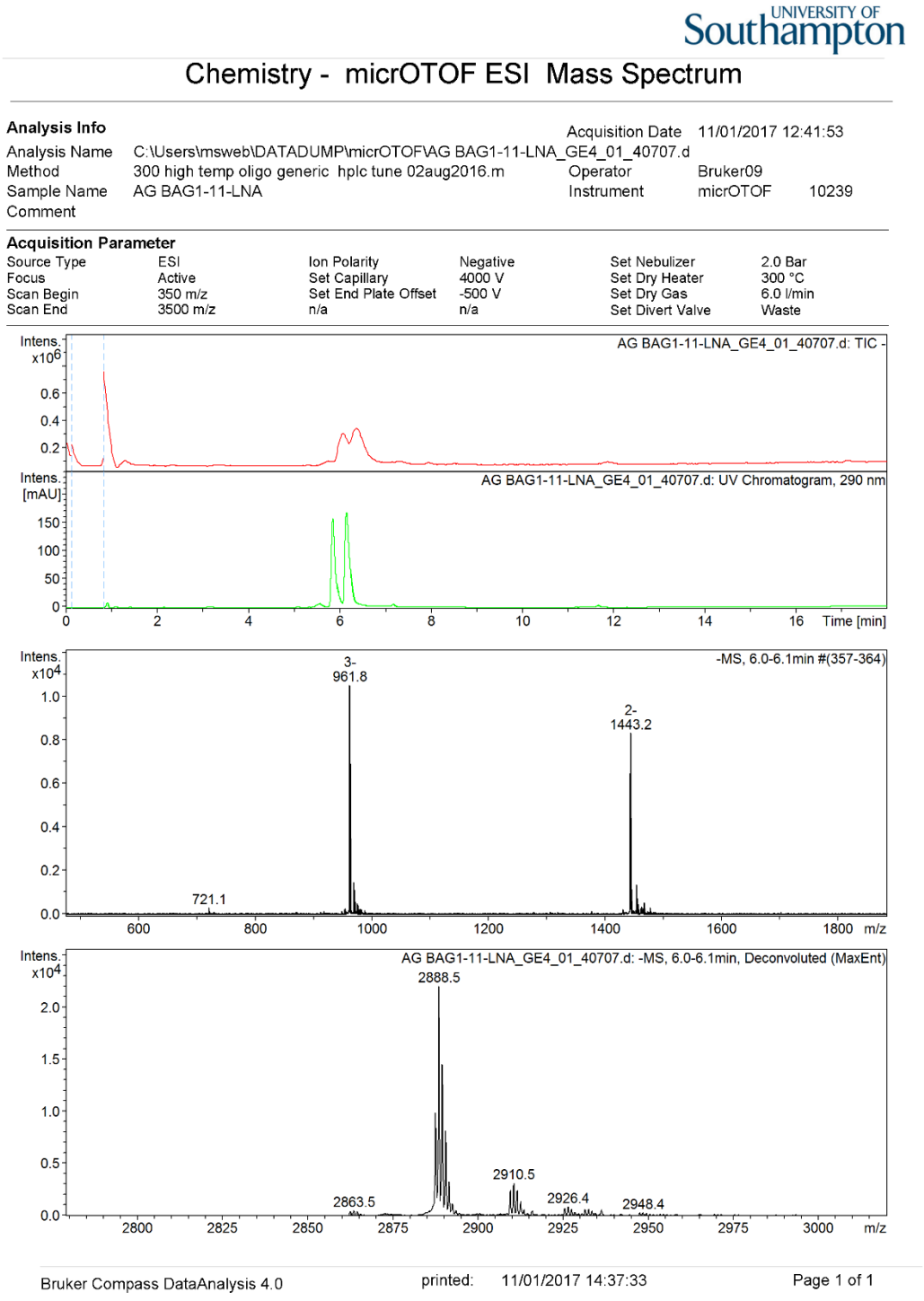

Figure A.1.6 BAG 1 LNA oligonucleotide mass spectrometry result, peak 1.

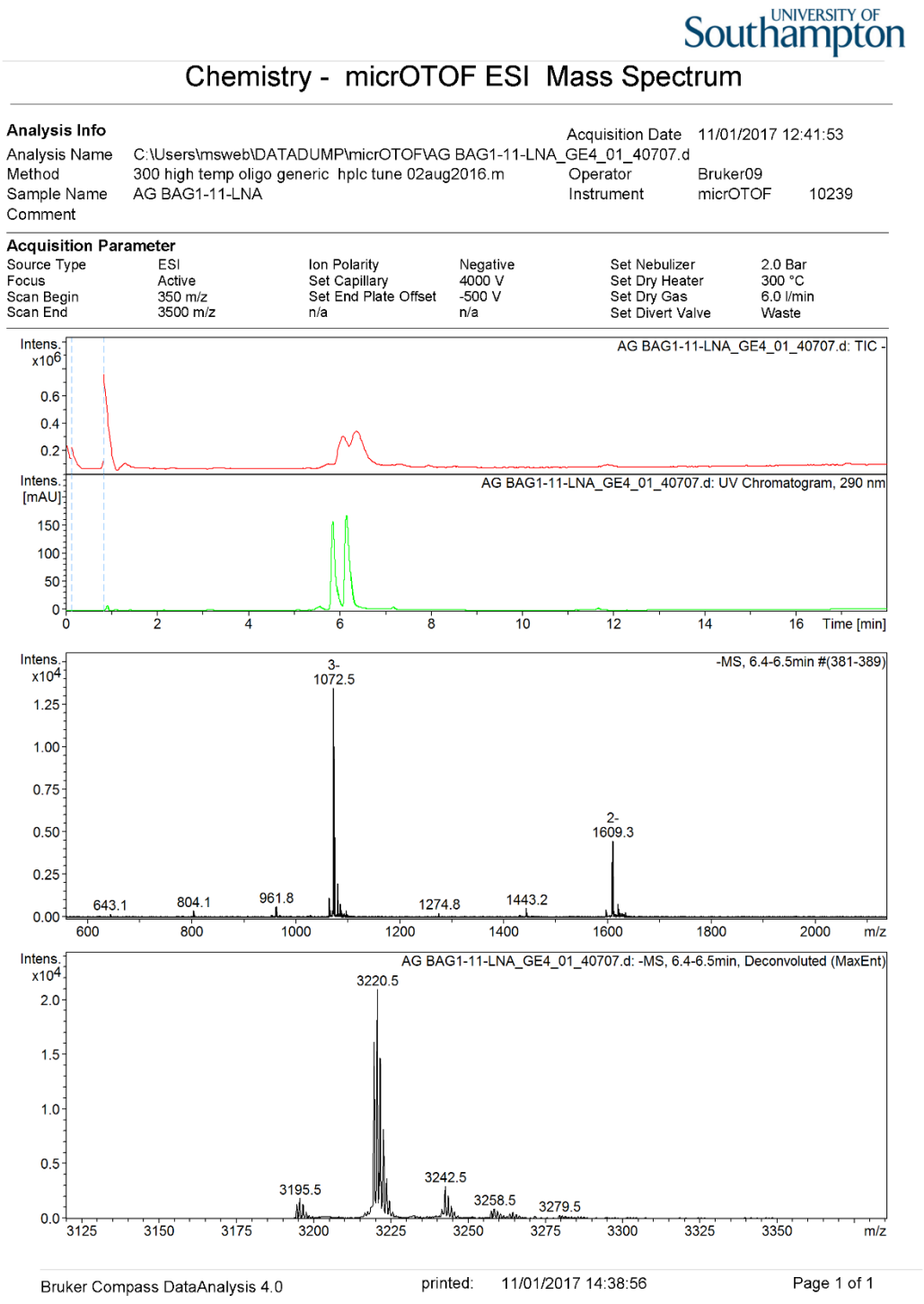

Figure A.1.7 BAG 1 LNA oligonucleotide mass spectrometry result, peak 2.

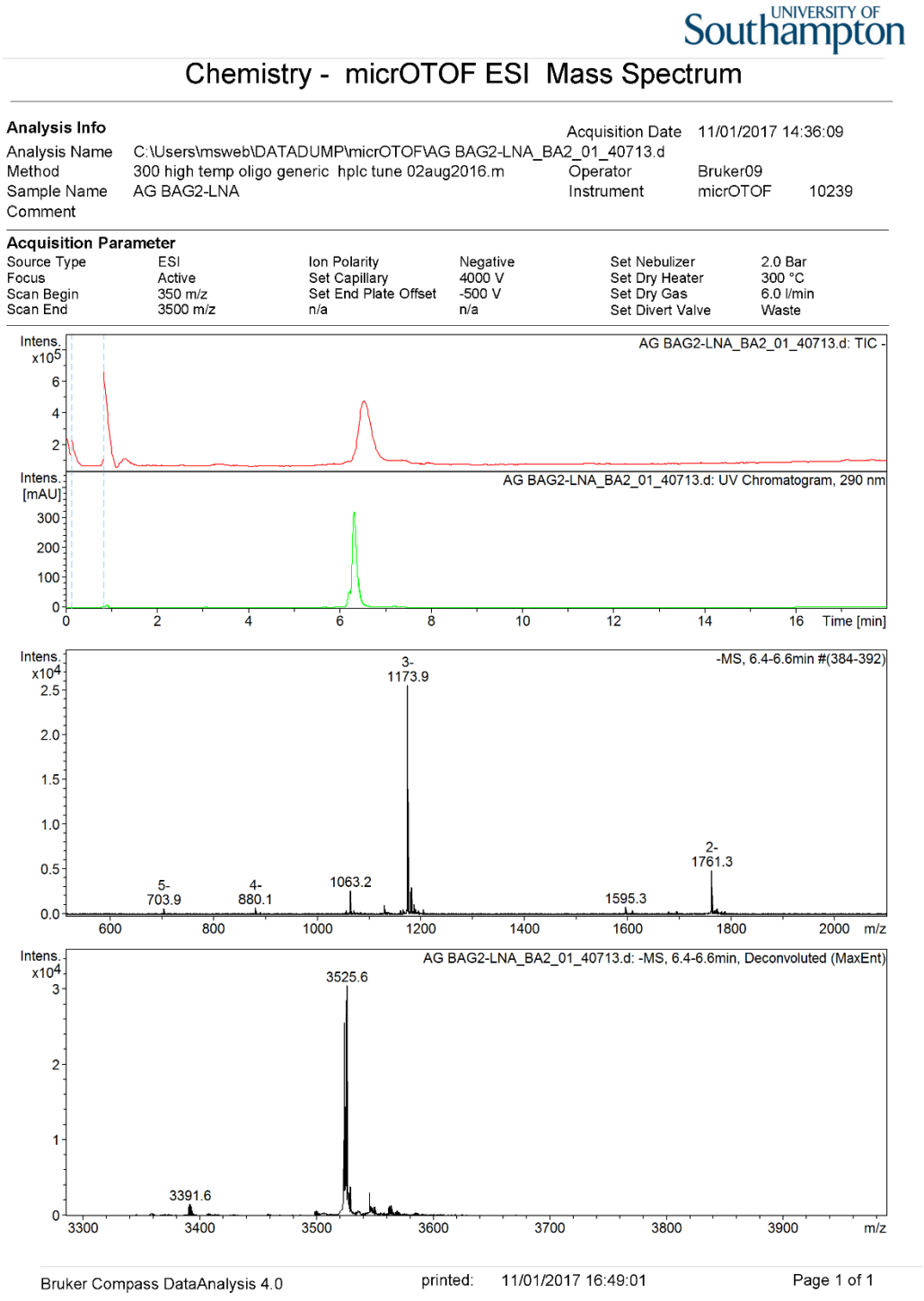

Figure A.1.8 BAG 2 LNA oligonucleotide mass spectrometry result.

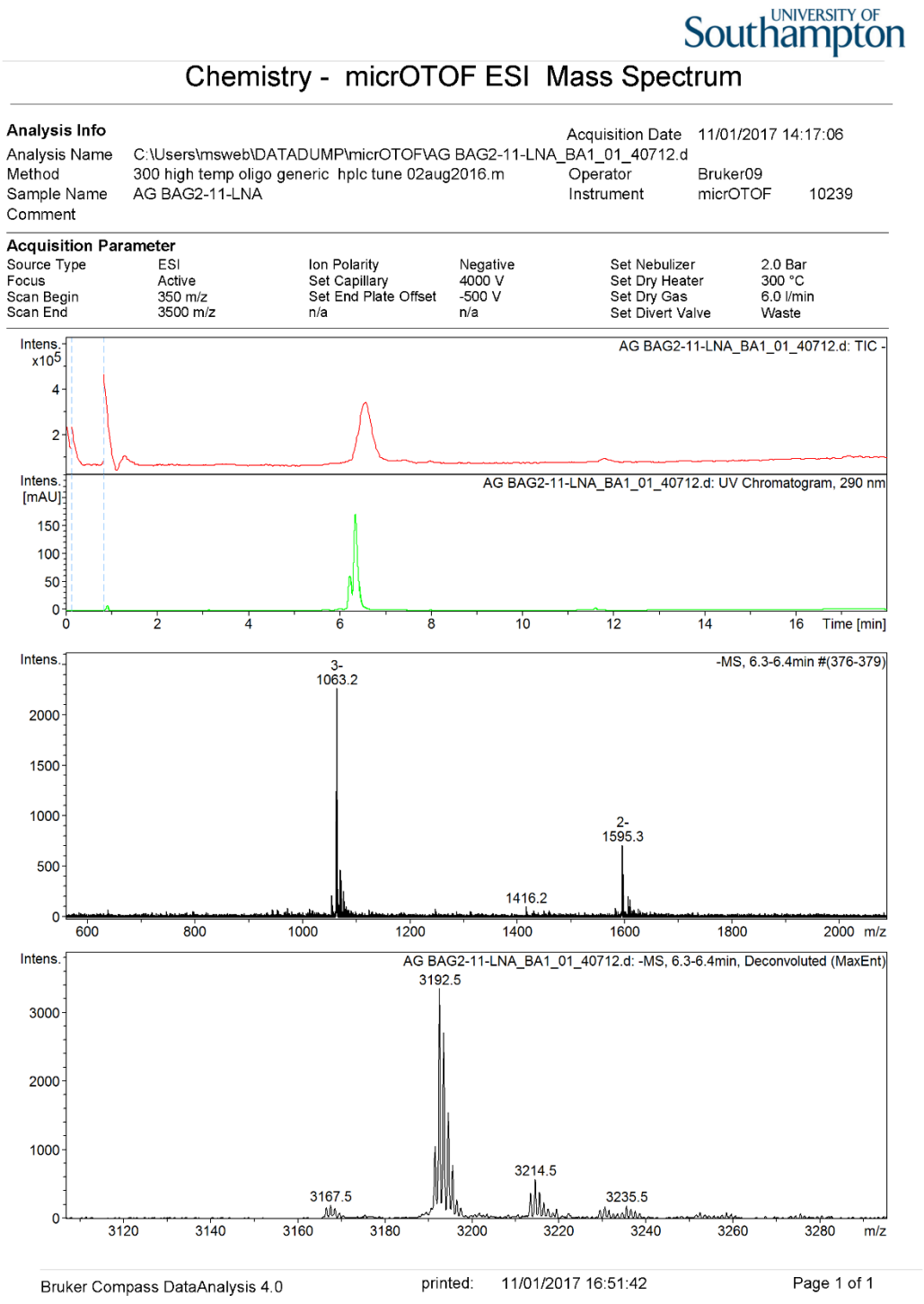

Figure A.1.9 BAG 2 LNA oligonucleotide mass spectrometry result, peak 1.

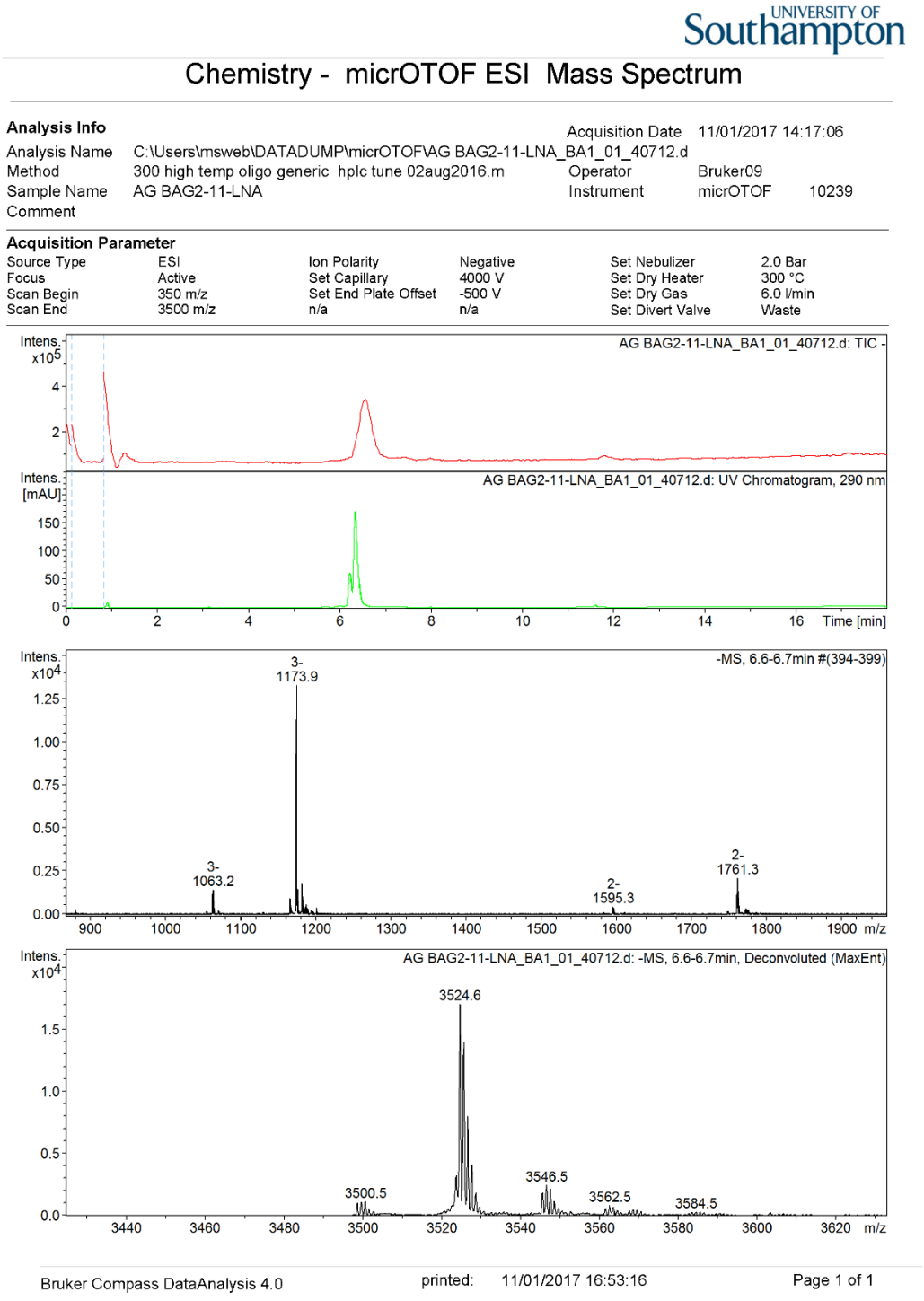

Figure A.1.10 BAG 2 LNA oligonucleotide mass spectrometry result, peak 2.

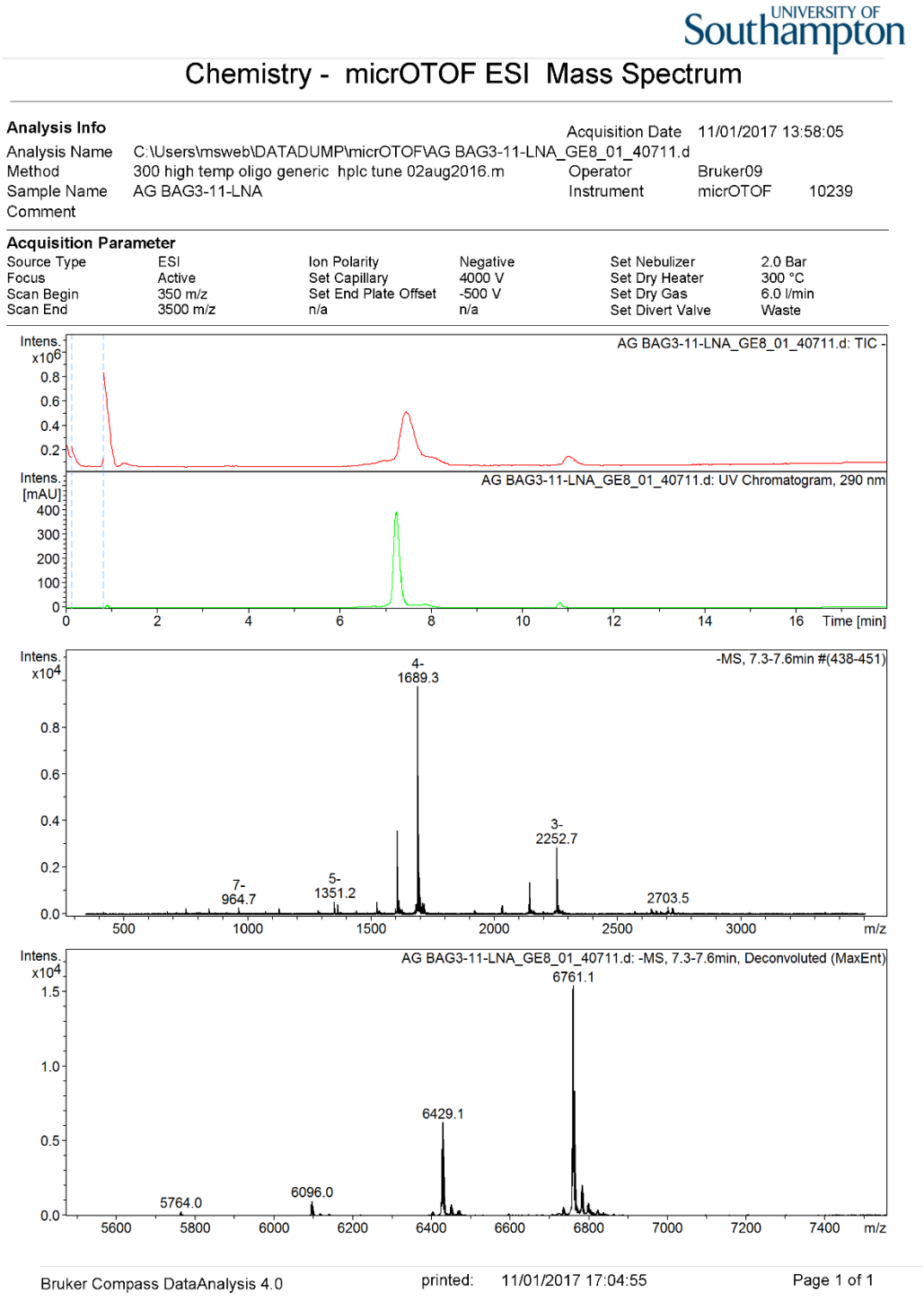

Figure A.1.11 BAG 3 LNA oligonucleotide mass spectrometry result.

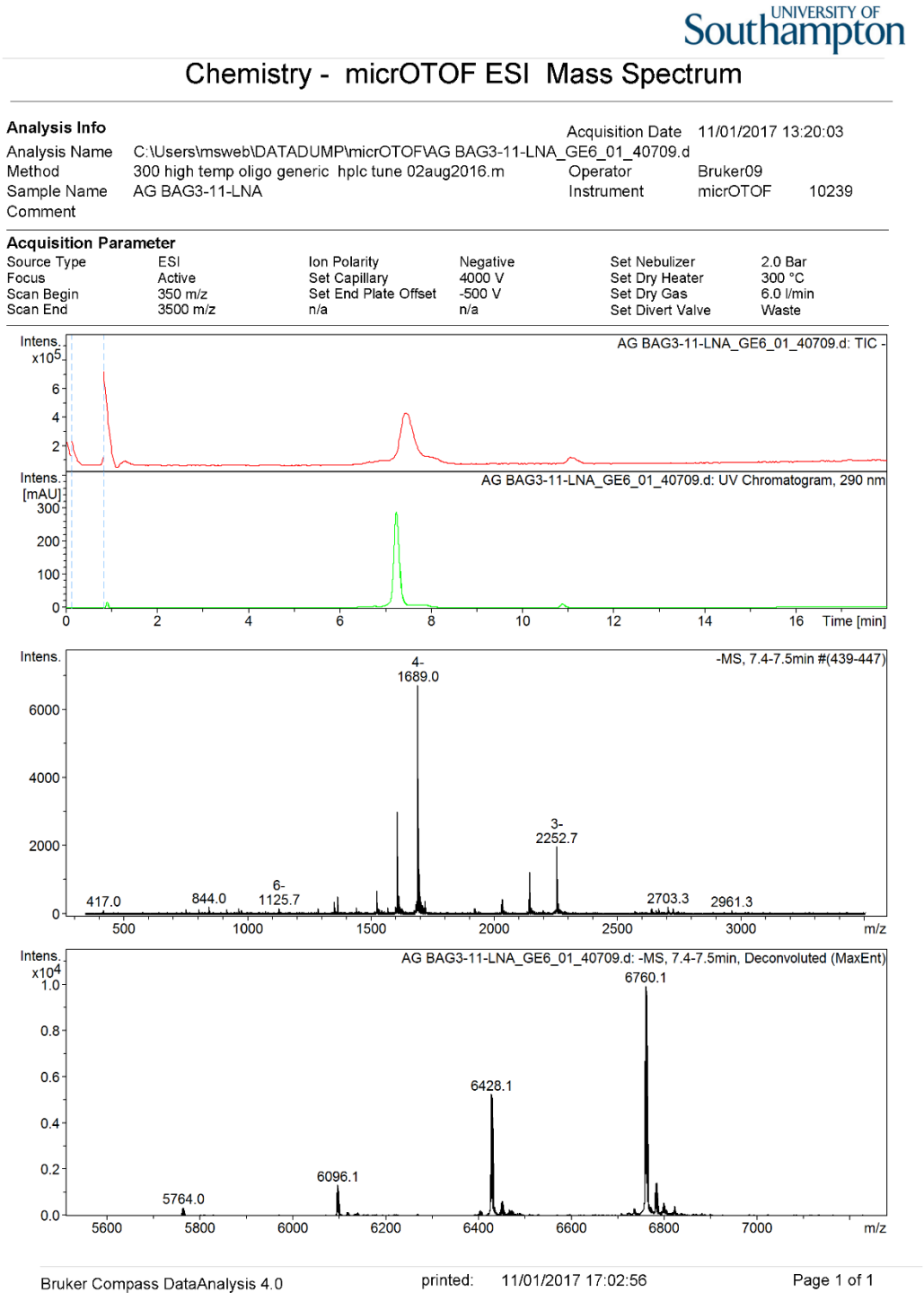

Figure A.1.12 BAG 3 LNA oligonucleotide mass spectrometry result.

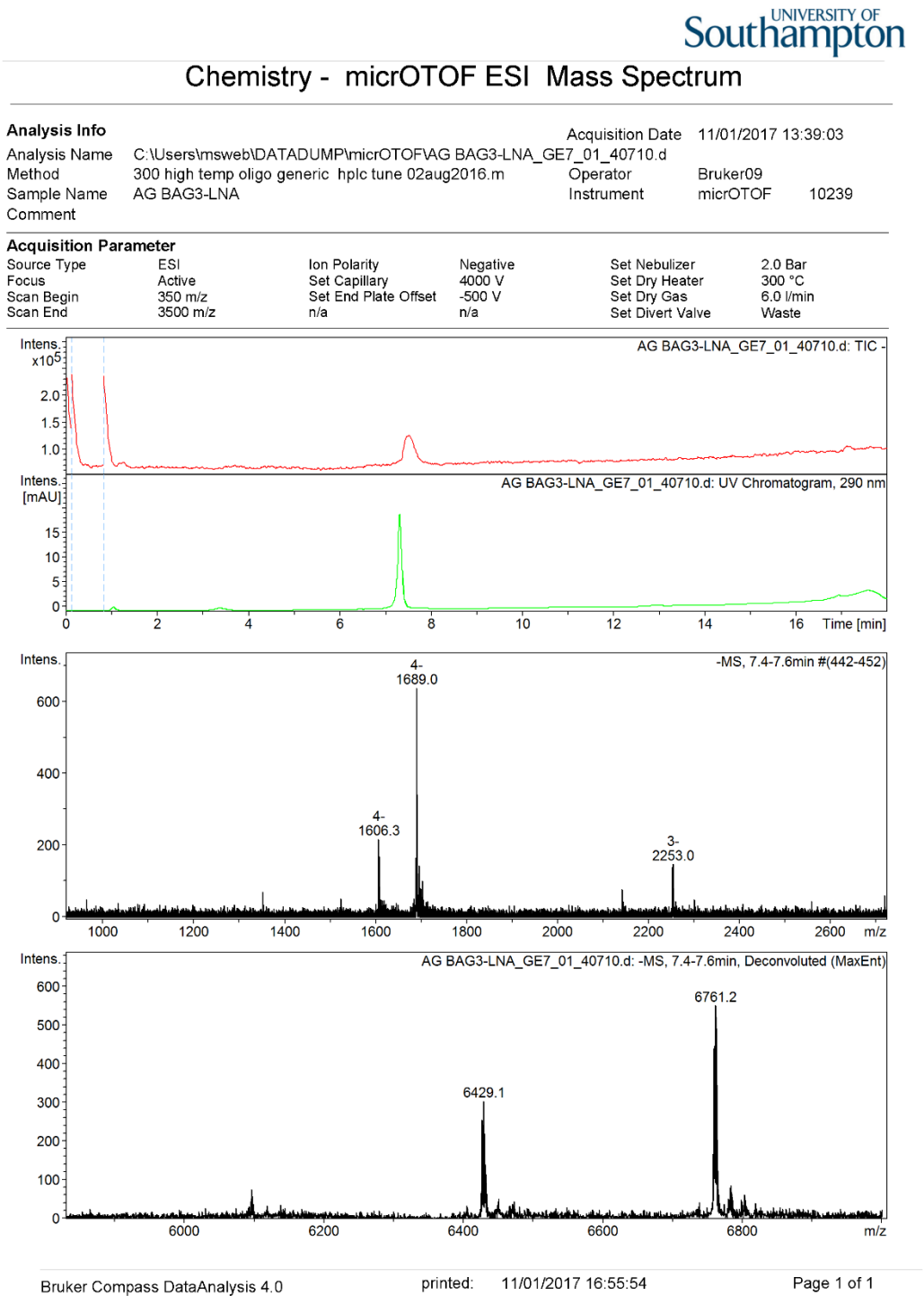

Figure A.1.13 BAG 3 LNA oligonucleotide mass spectrometry result.

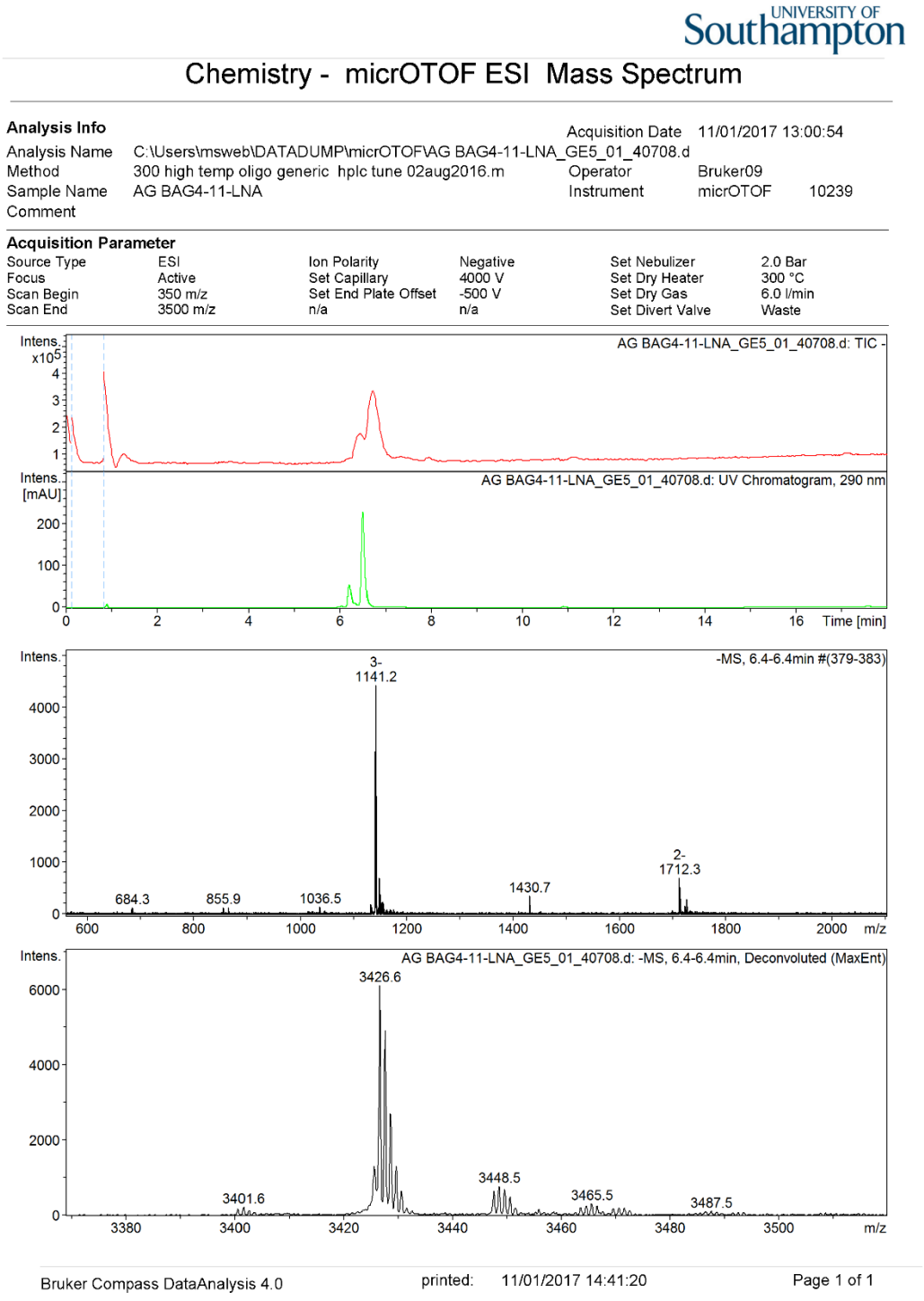

Figure A.1.14 BAG 4 LNA oligonucleotide mass spectrometry result, peak 1.

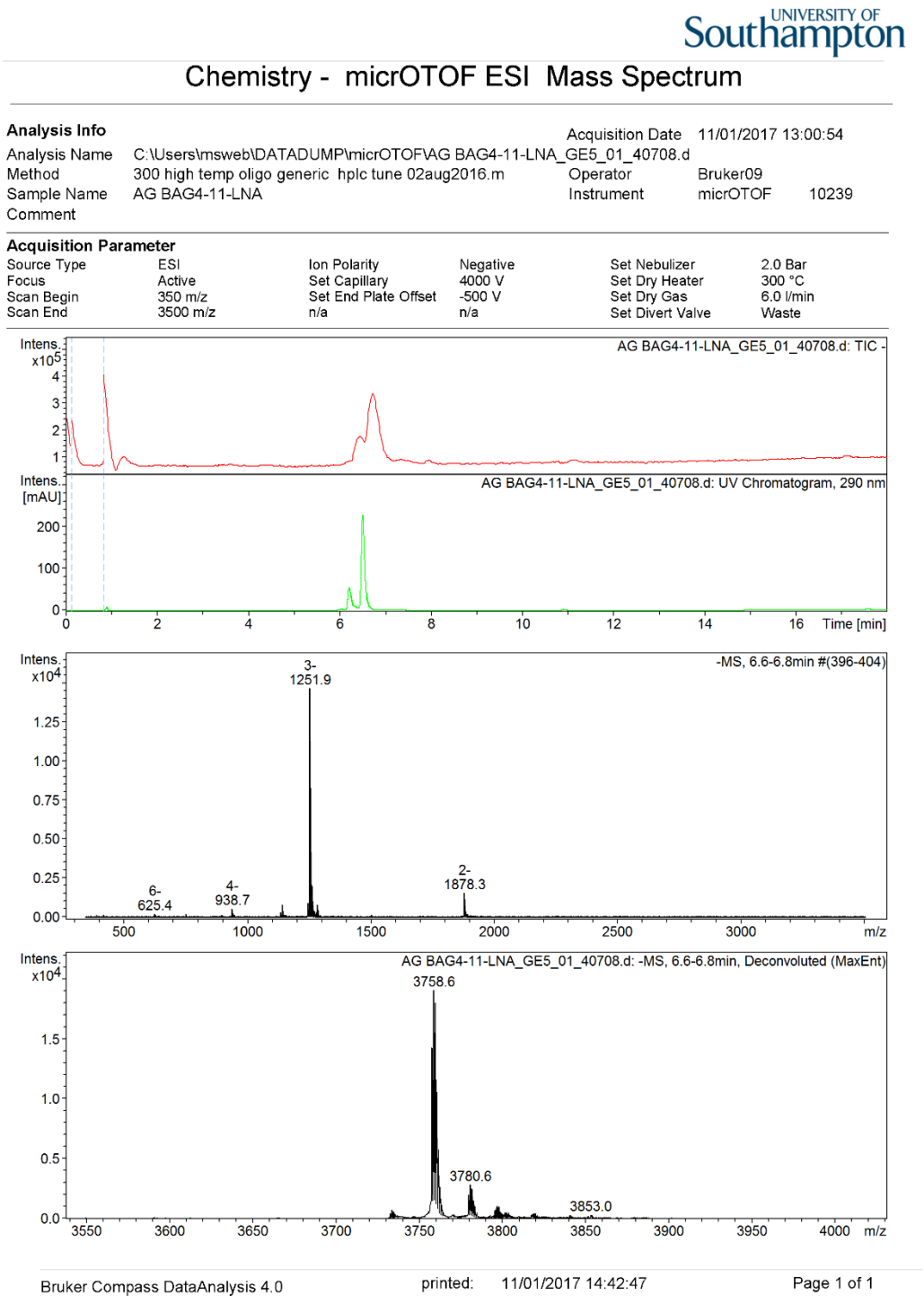

Figure A.1.15 BAG 4 LNA oligonucleotide mass spectrometry result, peak 2.

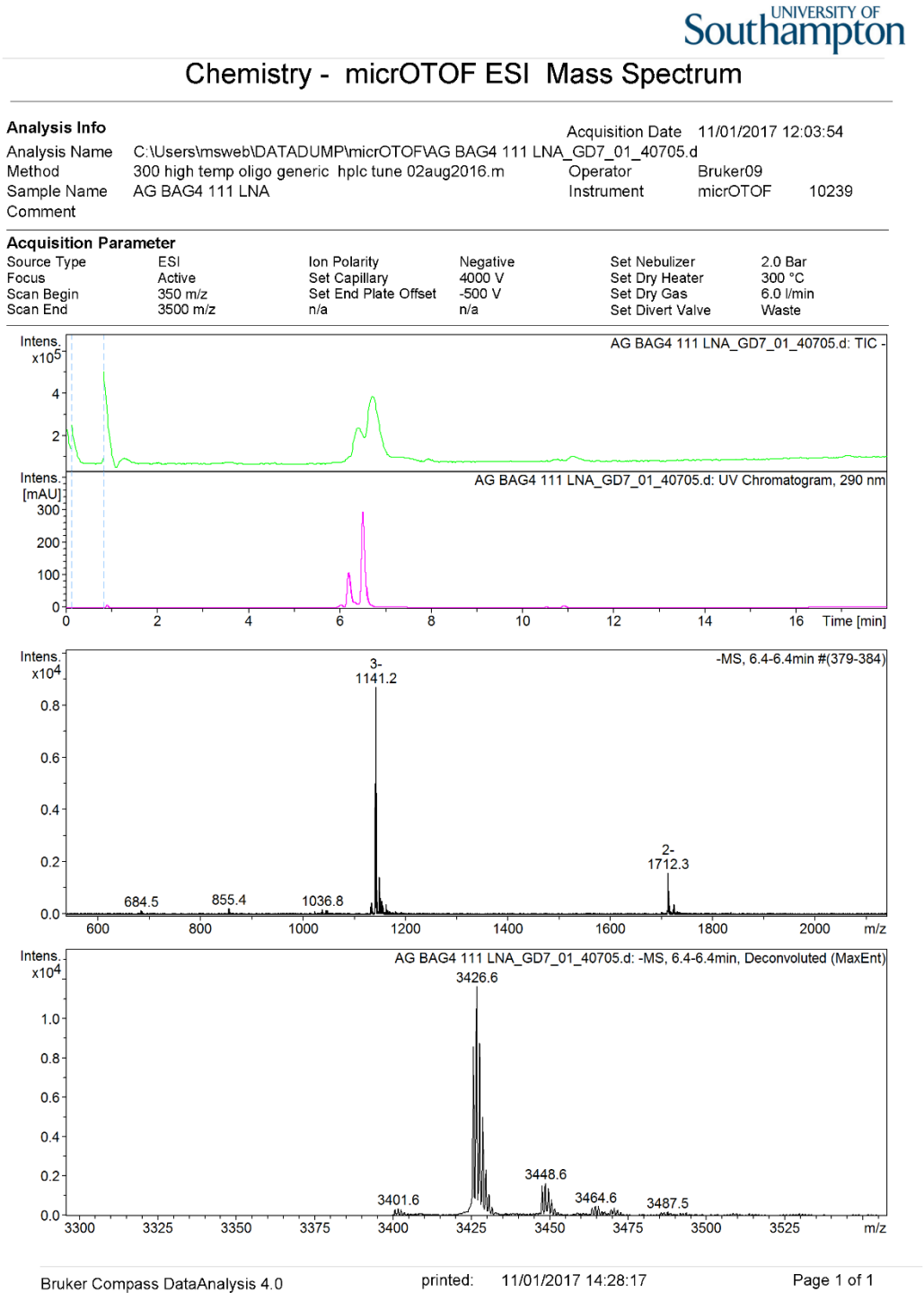

Figure A.1.16 BAG 4 LNA oligonucleotide mass spectrometry result, peak 1.

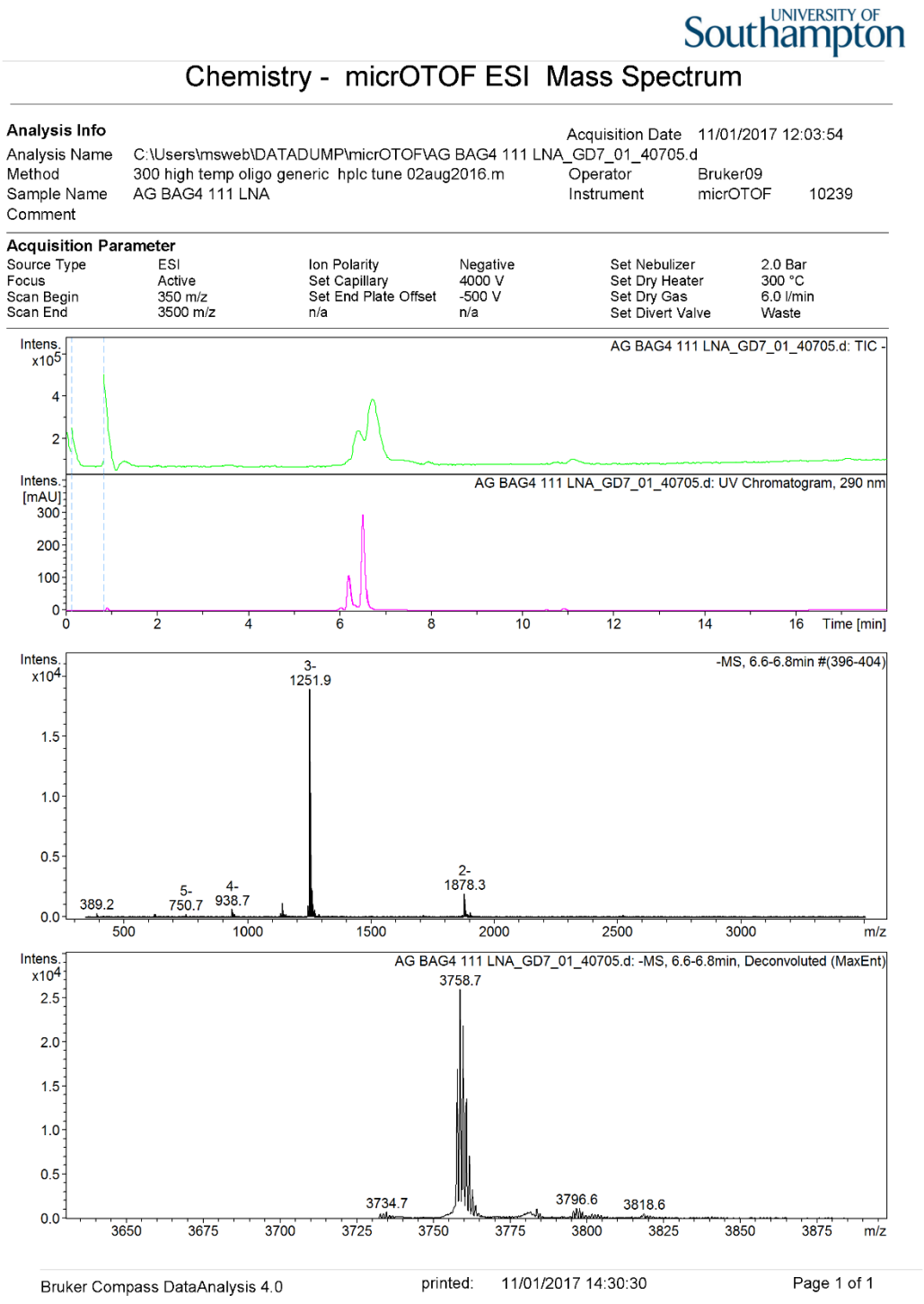

Figure A.1.17 BAG 4 LNA oligonucleotide mass spectrometry result, peak 2.

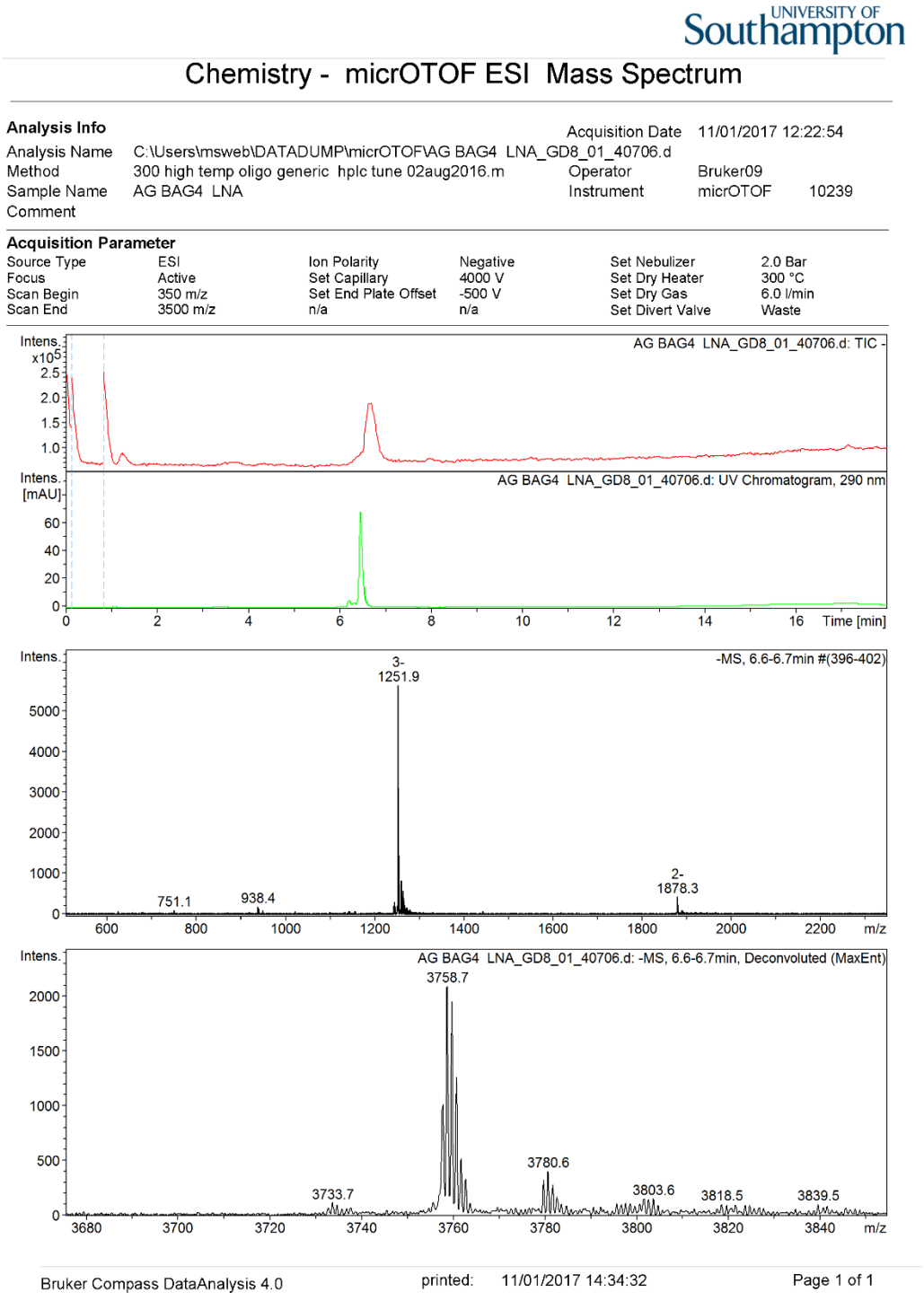

Figure A.1.18 BAG 4 LNA oligonucleotide mass spectrometry result.

Appendix B **SEQUENCE OF THE OLIGONUCLEOTIDES USED**

B.1 Oligonucleotides synthesised in the laboratory. LNA modifications are highlight in bold and underlined letters.

Name	**OLIGONUCLEOTIDE SEQUENCE 5'-3'**
BAG 1 DNA	GGTCGAGCGG
BAG 2 DNA	GGTCTGAGCGG
BAG 3 DNA	CTTCTTCACTCAGGGTCAACT
BAG 4 DNA	CTCGAGCGGCGC
BAG 3 NEW	CTTCCTCACTCAGGGTCAACT
BAG 4 NEW	GTCGAGCGGCGC
SCRAMBLE	ACTACCGTTGTTATAGGTGT
BAG 1 LNA	**G**G**T**CGA**G**C**G**G
BAG 2 LNA	**G**G**T**CTGA**G**C**G**G
BAG 3 LNA	C**T**TCT**T**CAC**T**CAG**G**GTCAAC**T**C
BAG 4 LNA	C**T**C**G**AGCG**G**C**G**C

B.2 Oligonucleotide pool targeting the reduced sequence of the *BAG1* IRES. These oligonucleotides were ordered from Sigma-Aldrich.

NAME	**OLIGONUCLEOTIDE SEQUENCE 5'-3'**
B1	TGGTGGGTCGGTCATGCCCG
B2	AGCGCCGGCGGCGGCGCCCC
B3	TTCTTCATCCGCGGCCTGCG
B4	TCGAGCGGCGCCGGGTTTTC
B5	GGTCAACTCCTCGCTCCGGG
B6	AGGGTCAACTCCTCGCTCCG
B7	TCCAGGTCGCTTCCTCACTC

B8	ACTCTGGGTCGCCTCTTCAC
B9	CTTCGCCCTGGGTCGCCTCCTC
B10	GCGGCGCCCCTGGTGGGTCG
B11	GCGGCCTGCGAGCGCCGGCG
B12	CCGGGTTTTCTTCTTCATCC
B13	TCGCTCCGGGTCGAGCGGCG
B14	CCTCGCTCCGGGTCAACTCC
B15	TTCCTCACTCAGGGTCAACT
B16	GCCTCTTCACTCCAGGTCGC
B17	TCGCCTCCTCACTCTGGGTC
B 6 FAM	FAM-AGGGTCAACTCCTCGCTCCG

B.3 B1, B9, B10, B11 and BAG 4 oligonucleotides with different modifications: PS DNA, PS LNA-DNA and LNA. LNA nucleotides are represented highlighted in bold and underlined, PS linkages are presented with an asterisk.

B1 PS DNA	T*G*G*T*G*G*G*T*C*G*G*T*C*A*T*G*C*C*C*G*A*
B9 PS DNA	C*T*T*C*G*C*C*C*T*G*G*G*T*C*G*C*C*T*C*C*T*C
B10 PS DNA	G*C*G*G*C*G*C*C*C*C*T*G*G*T*G*G*G*T*C*G
B11 PS DNA	G*C*G*G*C*C*T*G*C*G*A*G*C*G*C*C*G*G*C*G
BAG 4 PS DNA	G*T*C*G*A*G*C*G*G*C*G*C
SCRAMBLE PS DNA	A*C*T*A*C*C*G*T*T*G*T*T*A*T*A*G*G*T*G*T
B1 PS LNA	**T***G*G*T***G***G*G***T***C*G*G***T***C*A*T***G***C*C*C***G***A
B9 PS LNA	C***T***T*C***G***C*C*C***T***G*G*G***T***C*G*C*C***T***C*C***T***C
B10 PS LNA	**G***C*G*G*C***G***C*C*C*C***T***G*G***T***G*G*G***T***C*G
B11 PS LNA	**G***C*G***G***C*C***T***G*C***G***A*G*C***G***C*C*G***G***C*G
BAG 4 PS LNA	**G***T*C***G***A*G*C***G***G*C***G***C
SCRAMBLE PS LNA	A*C***T***A*C*C***G***T*T*G***T***T*A*T*A***G***G*T***G***T
B1 LNA	**T**GGT**G**GG**T**CGG**T**CAT**G**CCC**G**A

B9 LNA	C**T**TC**G**CCC**T**GGG**T**CGCC**T**CC**T**C
B10 LNA	**G**CGGC**G**CCCC**T**GG**T**GGG**T**CG
B11 LNA	**G**CG**G**CC**T**GC**G**AGC**G**CCG**G**CG
BAG 4 LNA	**G**TC**G**AGC**G**GC**G**C
SCRAMBLE LNA	AC**T**ACC**G**TTG**T**TATA**G**GT**G**T

B.4 B14, B14 AB, B15, B15 AB and Scramble sequences, unmodified and LNA-DNA mixmers. LNA nucleotides are represented highlighted in bold and underlined, 2' OME nucleotides represented in italics and phosphorothioate bonds represented with an asterisk.

Oligonucleotide name	Sequence 5'-3'
B14 DNA	CCTCGCTCCGGGTCAACTCC
B14 AB DNA	CTCCGGGTCAACTCCTCGCT
B15 DNA	TTCCTCACTCAGGGTCAACT
B15 AB DNA	CACTCAGGGTCAACTCC
SCRAMBLE DNA	ACTACCGTTGTTATAGGTGT
B14 LNA-DNA	CCTCGCTCCGGGTCAACTCC
B14 AB LNA-DNA	CTCCGGGTCAACTCCTCGCT
B15 LNA-DNA	TTCCTCACTCAGGGTCAACT
B15 AB LNA-DNA	CACTCAGGGTCAACTCC
SCRAMBLE LNA-DNA	ACTACCGTTGTTATAGGTGT
B14 AB 2' OME PS	*C*T*C*C*G*G*G*T*C*A*A*C*T*C*C*T*C*G*C*T*
B15 AB 2' OME PS	*C*A*C*T*C*A*G*G*G*T*C*A*A*C*T*C*C*
SCRAMBLE OME PS	*A*C*T*A*C*C*G*T*T*G*T*T*A*T*A*G*G*T*G*T*

Appendix B

B14 AB 2’ OME	*CTCCGGGTCAACTCCTCGCT*
B15 AB 2’ OME	*CACTCAGGGTCAACTCC*
SCRAMBLE OME	*ACTACCGTTGTTATAGGTGT*

Appendix C **SEQUENCING RESULTS**

In each of the chromatographs the start and end of the ORF of interest have been marked with a square, and the sequence has been underlined using different colours:

- Yellow: Fluc ORF
- Green: Nluc ORF
- Blue: BAG1 5’ UTR
- Red: CMV promoter
- Pink: hairpin

Appendix C

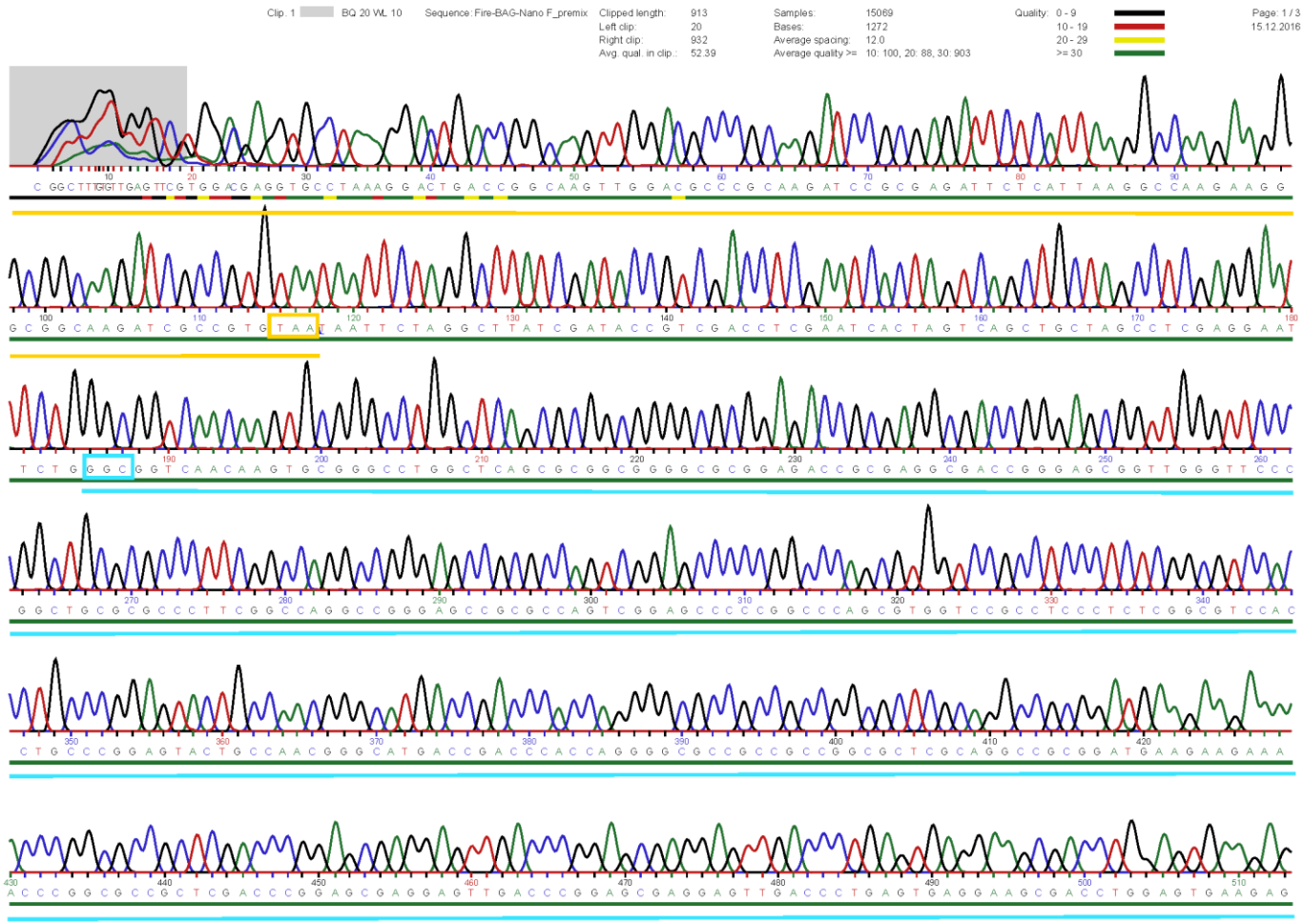

Figure C. 1 pFBN sequencing results sequenced with 3'Luc2 seq F forward primer. In the chromatograph it can be observed the end of the Fluc ORF (yellow), the whole BAG1 5' UTR (in blue) and most of the Nluc ORF (in green), however some mismatches could be observed at the end of the sequence.

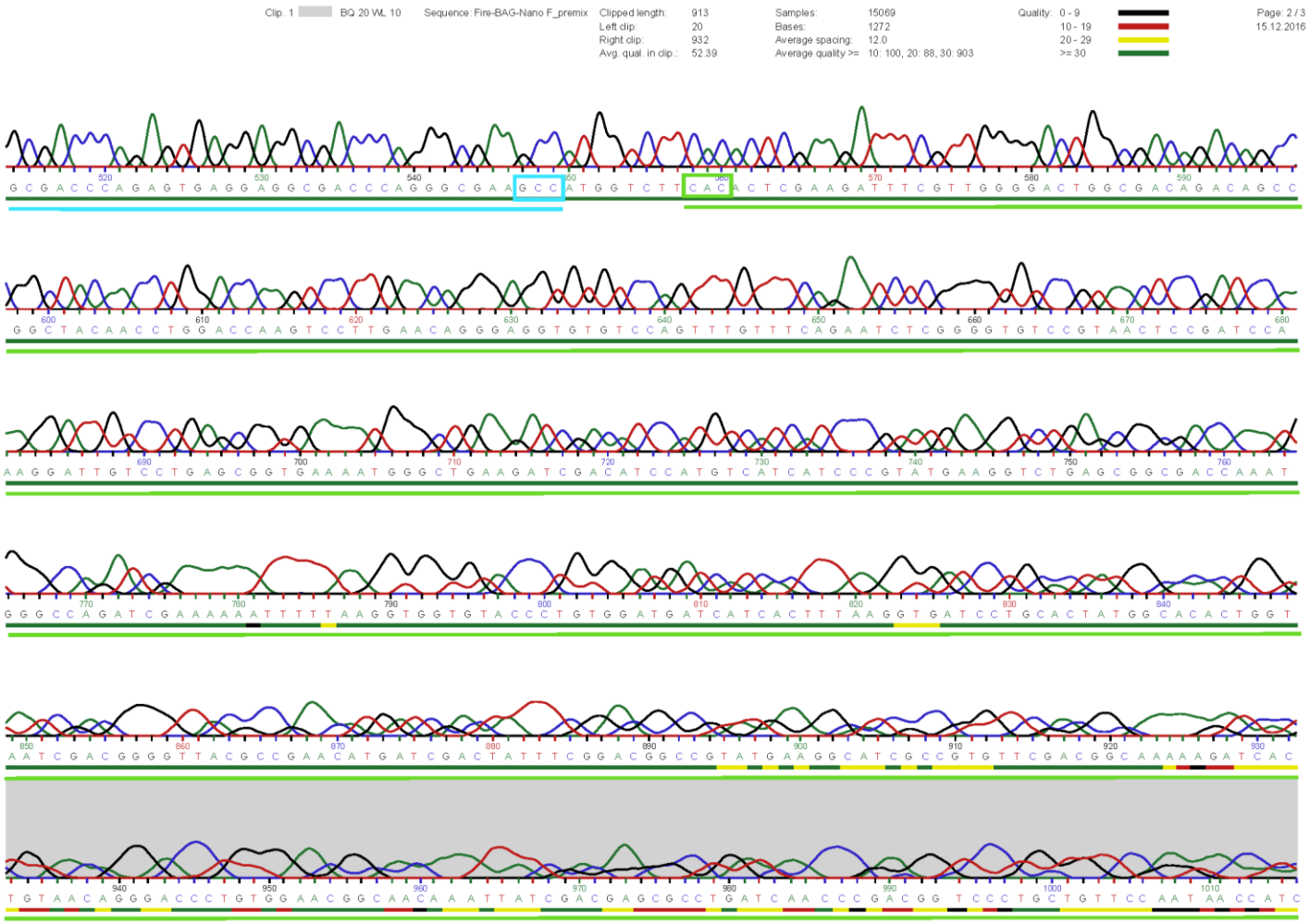

Figure C. 2 pFBN sequencing results sequenced with 3'Luc2 seq F forward primer. In the chromatograph it can be observed the end of the Fluc ORF (yellow), the whole BAG1 5' UTR (in blue) and most of the Nluc ORF (in green), however some mismatches could be observed at the end of the sequence.

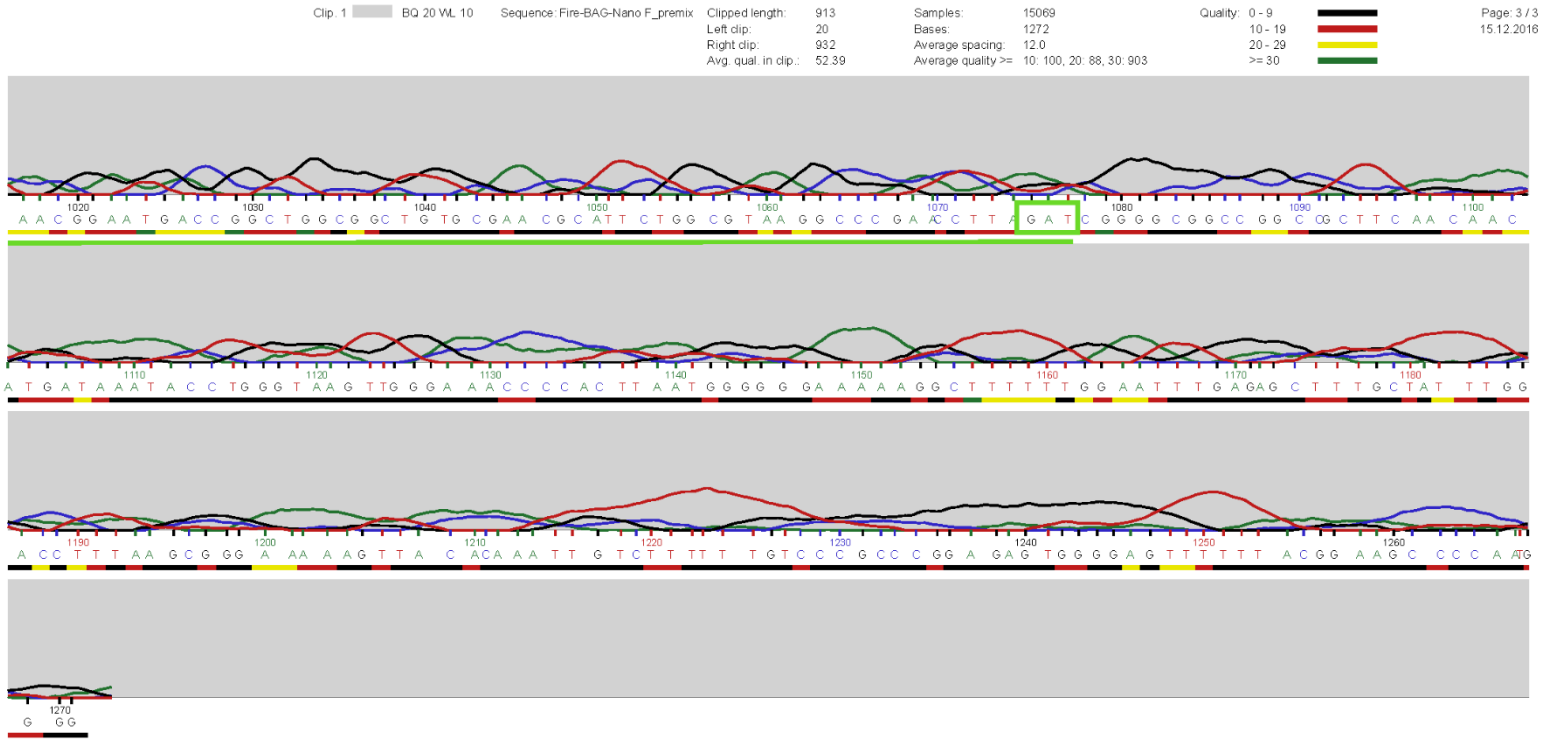

Figure C. 3 pFBN sequencing results sequenced with 3'Luc2 seq F forward primer. In the chromatograph it can be observed the end of the Fluc ORF (yellow), the whole BAG1 5' UTR (in blue) and most of the Nluc ORF (in green), however some mismatches could be observed at the end of the sequence.

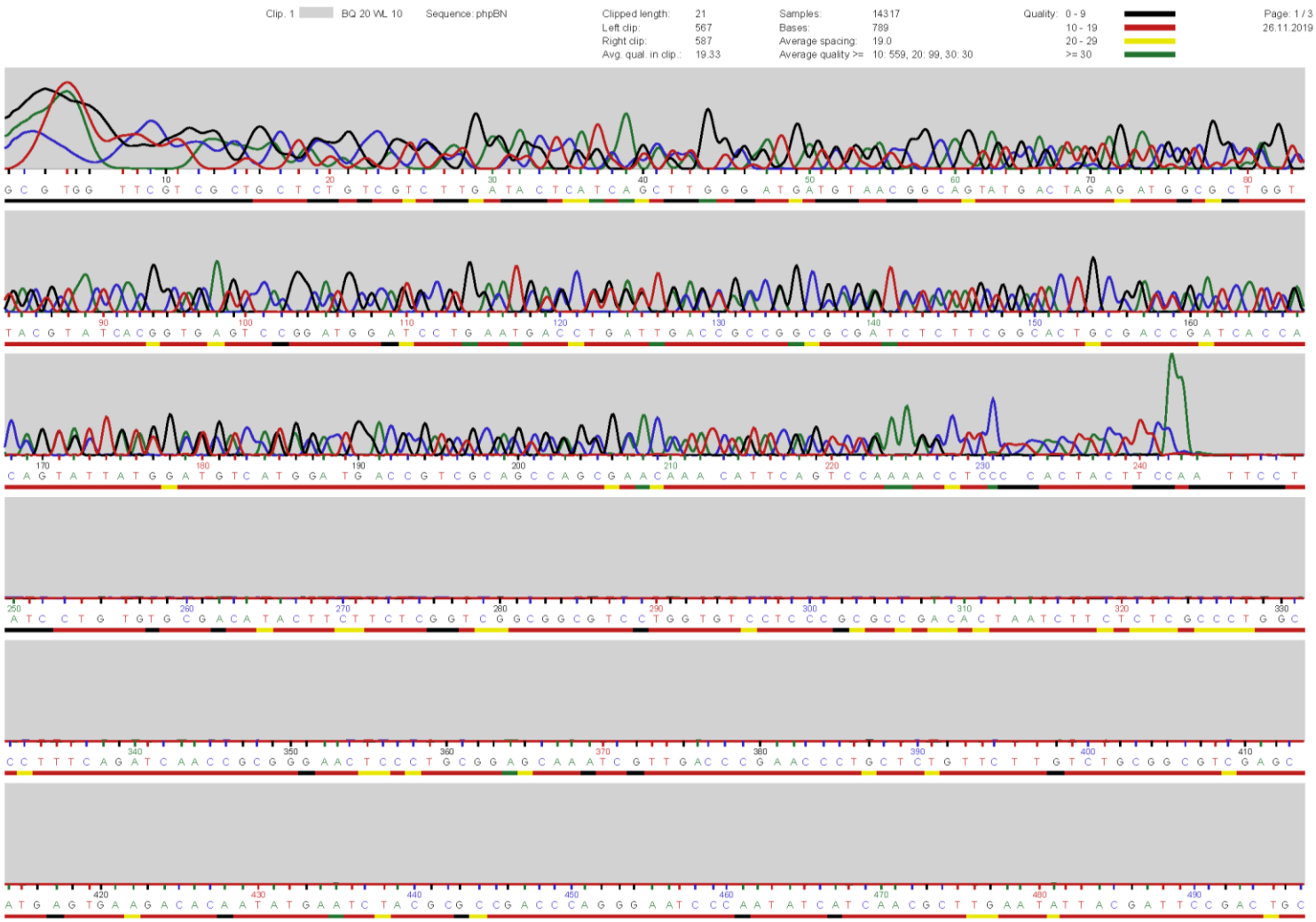

Figure C. 4 phpBN sequencing results sequenced with AfterSV40 F forward primer. Sequencing failed due to the hairpin present in phpBN.

Appendix C

Figure C. 5 phpBN sequencing results sequenced with AfterSV40 F forward primer. Sequencing failed due to the hairpin present in phpBN.

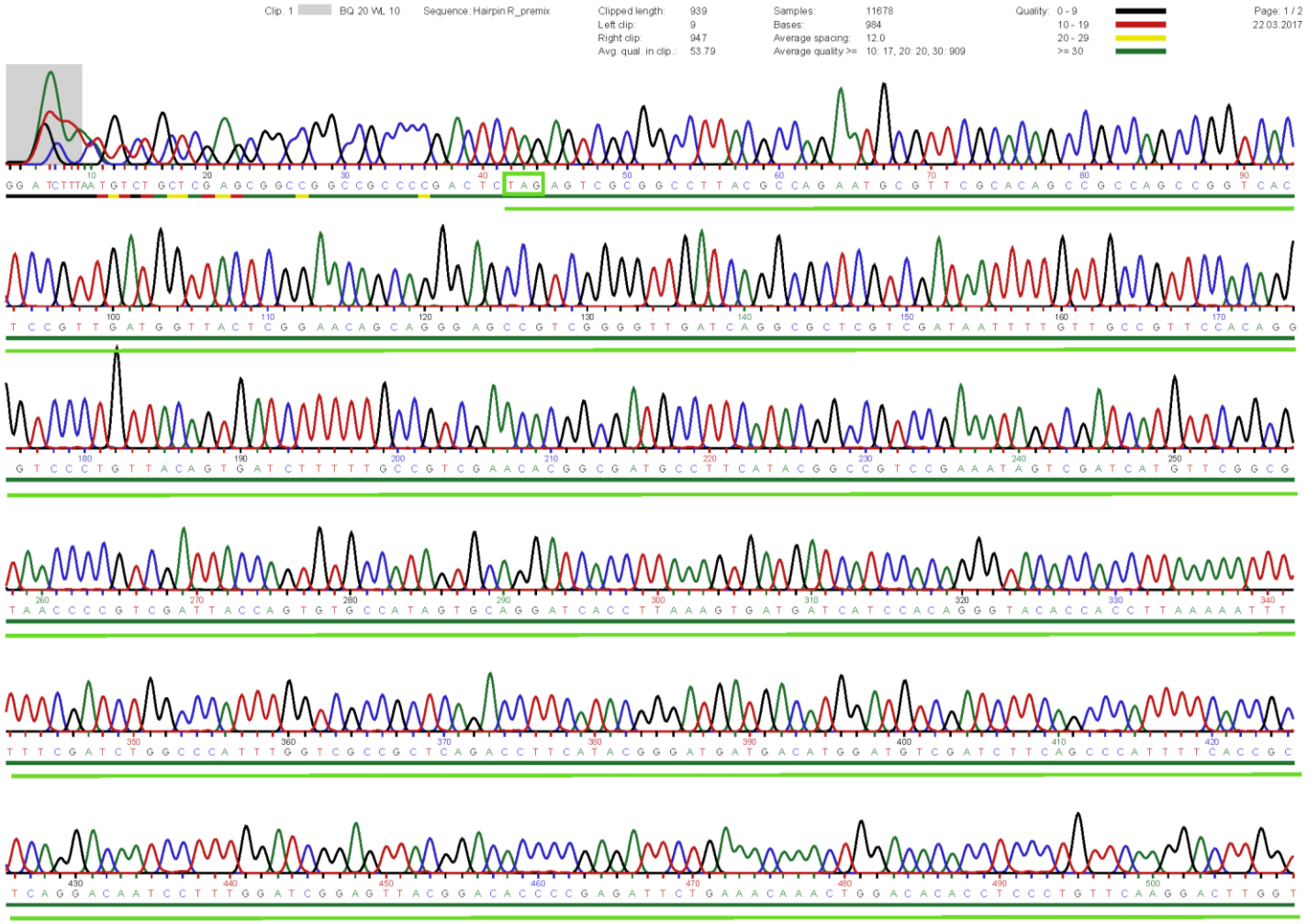

Figure C. 6 phpBN sequencing results sequenced with SV40pAseR2 reverse primer. In the chromatograph it can be observed the whole Nluc ORF (in green), the whole BAG1 5' UTR (in blue) and the start of the hairpin (in pink).

Appendix C

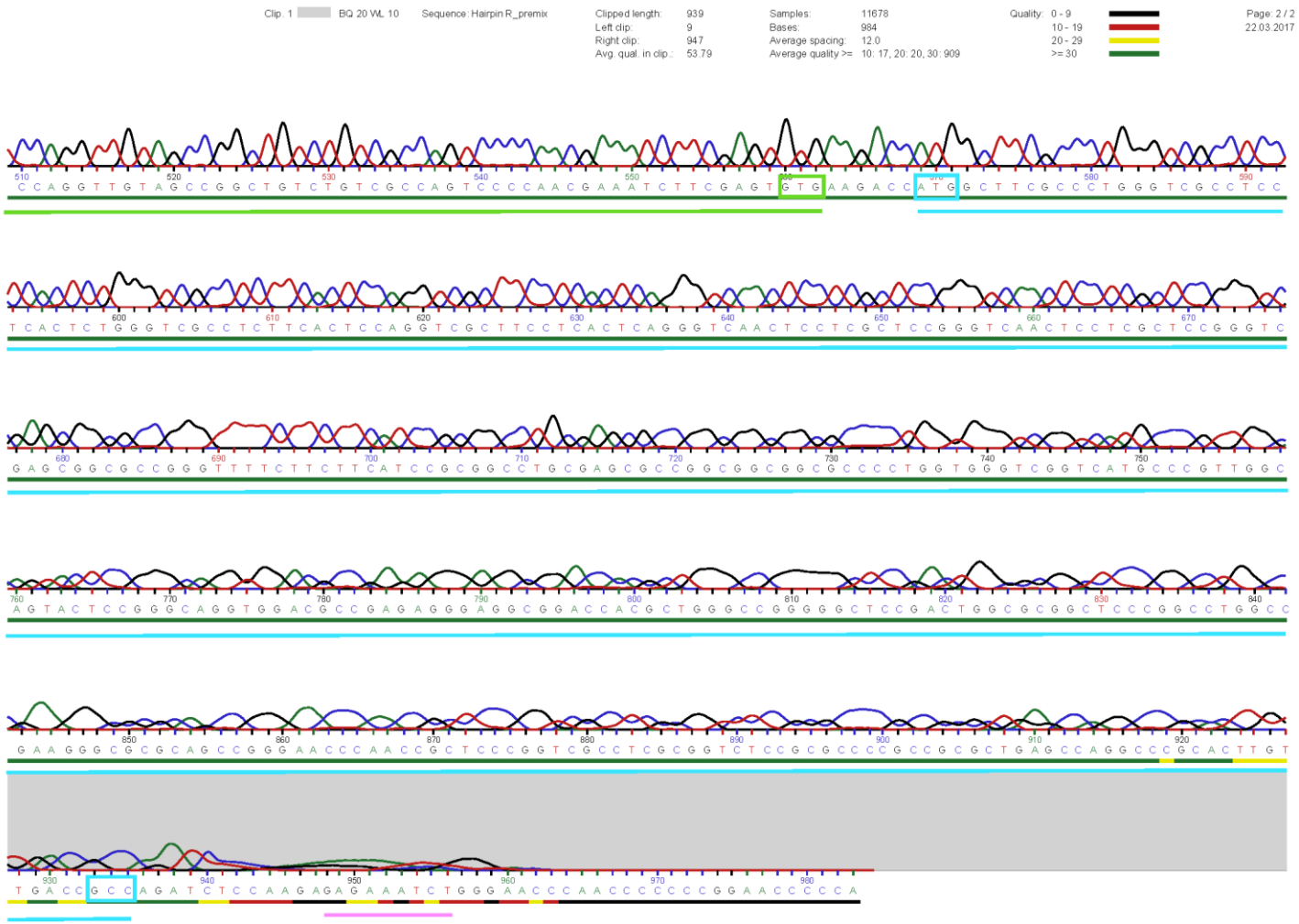

Figure C. 7 phpBN sequencing results sequenced with SV40pAseR2 reverse primer. In the chromatograph it can be observed the whole Nluc ORF (in green), the whole BAG1 5' UTR (in blue) and the start of the hairpin (in pink).

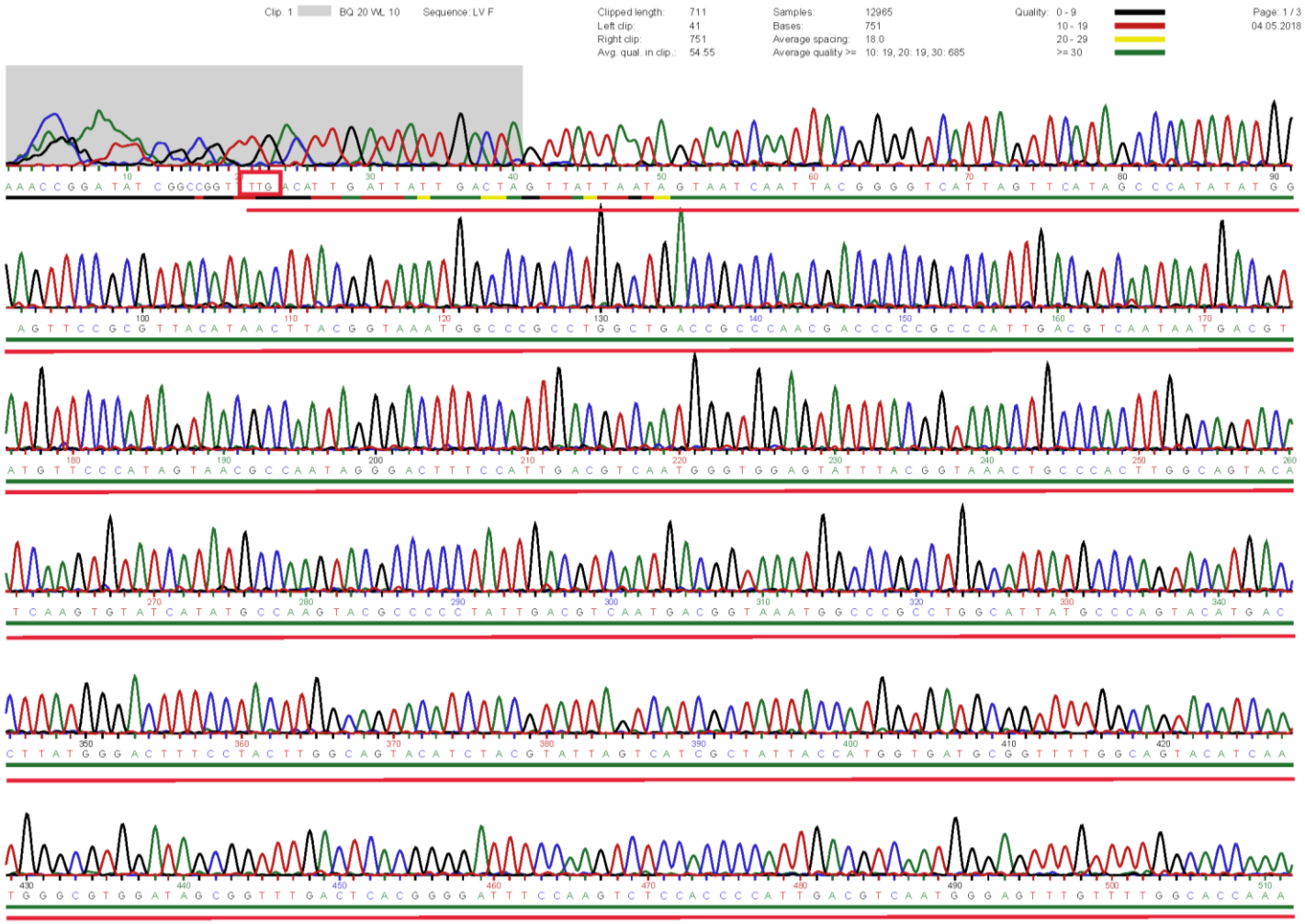

Figure C. 8 pLVTHM-phpBN sequencing results sequenced with CMV-phpBN insert F forward primer. In the chromatograph it can be observed the whole CMV promoter ORF (in red),) and the start of the hairpin (in pink).

Appendix C

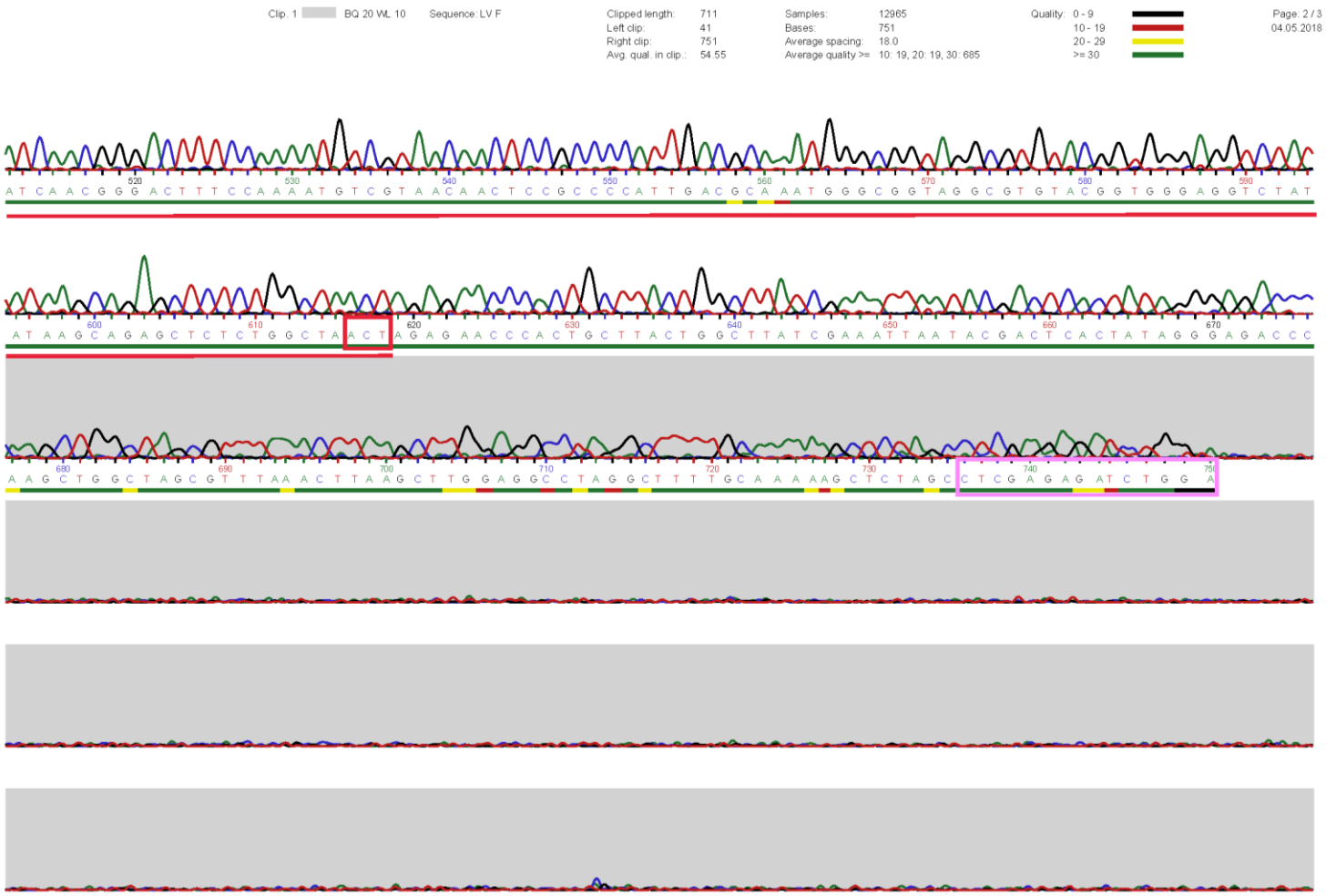

Figure C. 9 pLVTHM-phpBN sequencing results sequenced with CMV-phpBN insert F forward primer. In the chromatograph it can be observed the whole CMV promoter ORF (in red),) and the start of the hairpin (in pink).

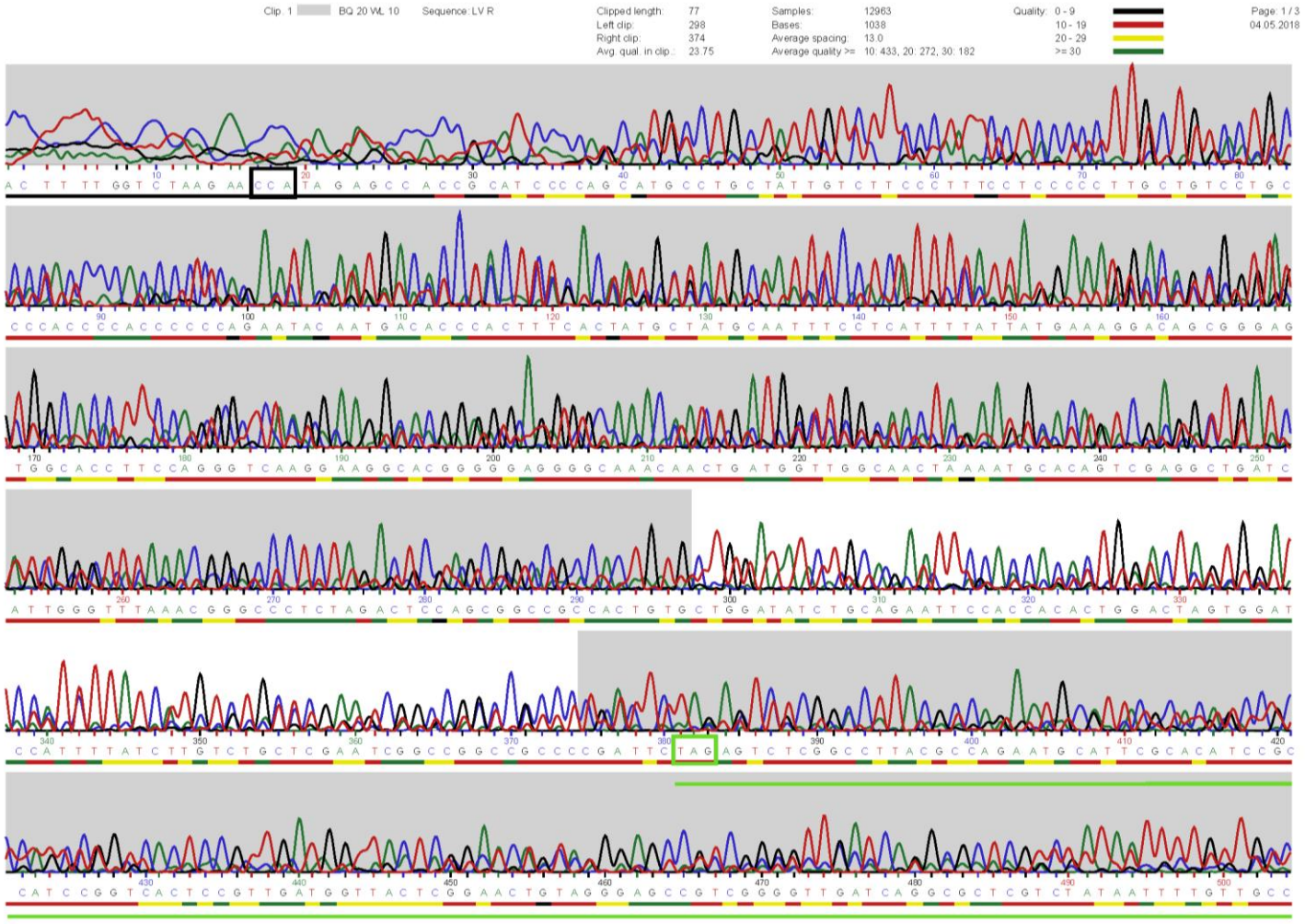

Figure C. 10 pLVTHM-phpBN sequencing results sequenced with R-CMVPA-ClaI reverse primer. In the chromatograph it can be observed the whole Nluc ORF (in green),) and the end of *BAG1* 5' UTR (in blue). In black it is marked the point where the sequence starts matching the pLVTHM lentivirus.

Appendix C

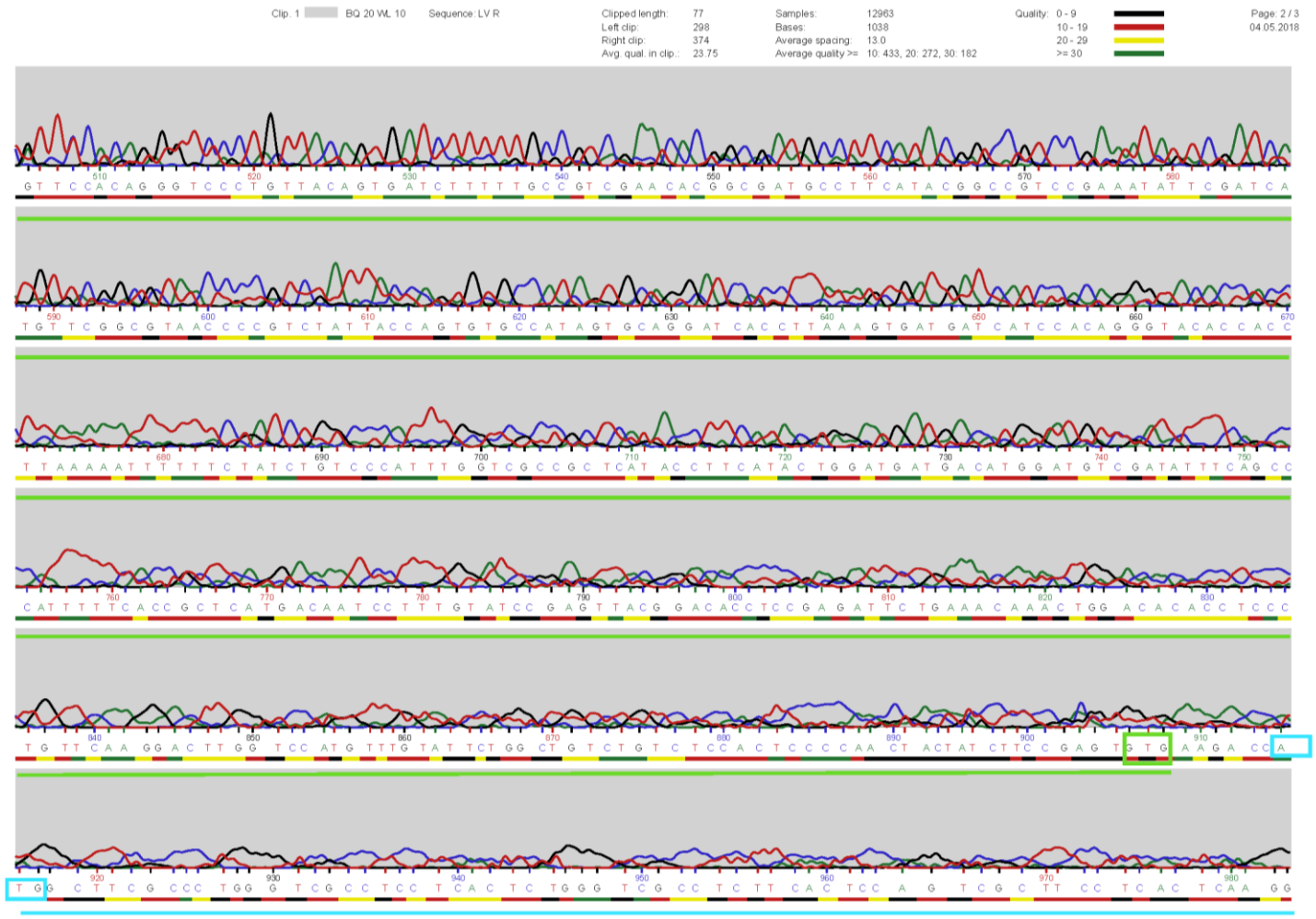

Figure C. 11 pLVTHM-phpBN sequencing results sequenced with R-CMVPA-ClaI reverse primer. In the chromatograph it can be observed the whole Nluc ORF (in green),) and the end of *BAG1* 5' UTR (in blue). In black it is marked the point where the sequence starts matching the pLVTHM lentivirus.

Appendix D **SUPPLEMENTARY Fluc AND Nluc VALUES**

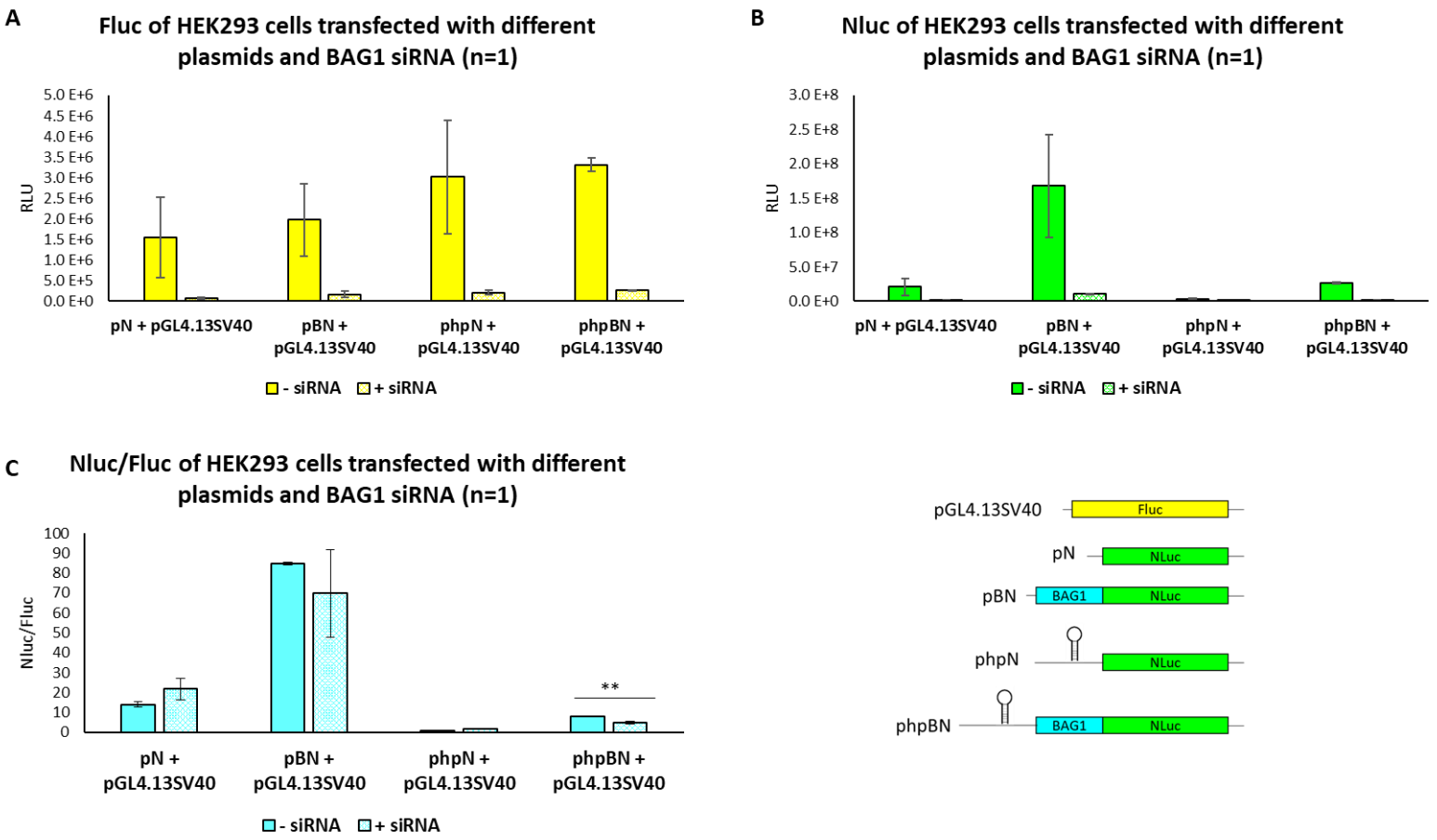

Figure D.1 **Luciferase results of HEK293 cells transfected with the different constructs previously made and the BAG1 siRNA to check efficiency of the siRNA.** A) Fluc activity, B) Nluc activity and C) Nluc to Fluc ratio of HEK293 cells. Error bars showing standard deviation values of the triplicate values. Statistical analysis was done with an unpaired T-test (two-tailed) ($p<0.05$).

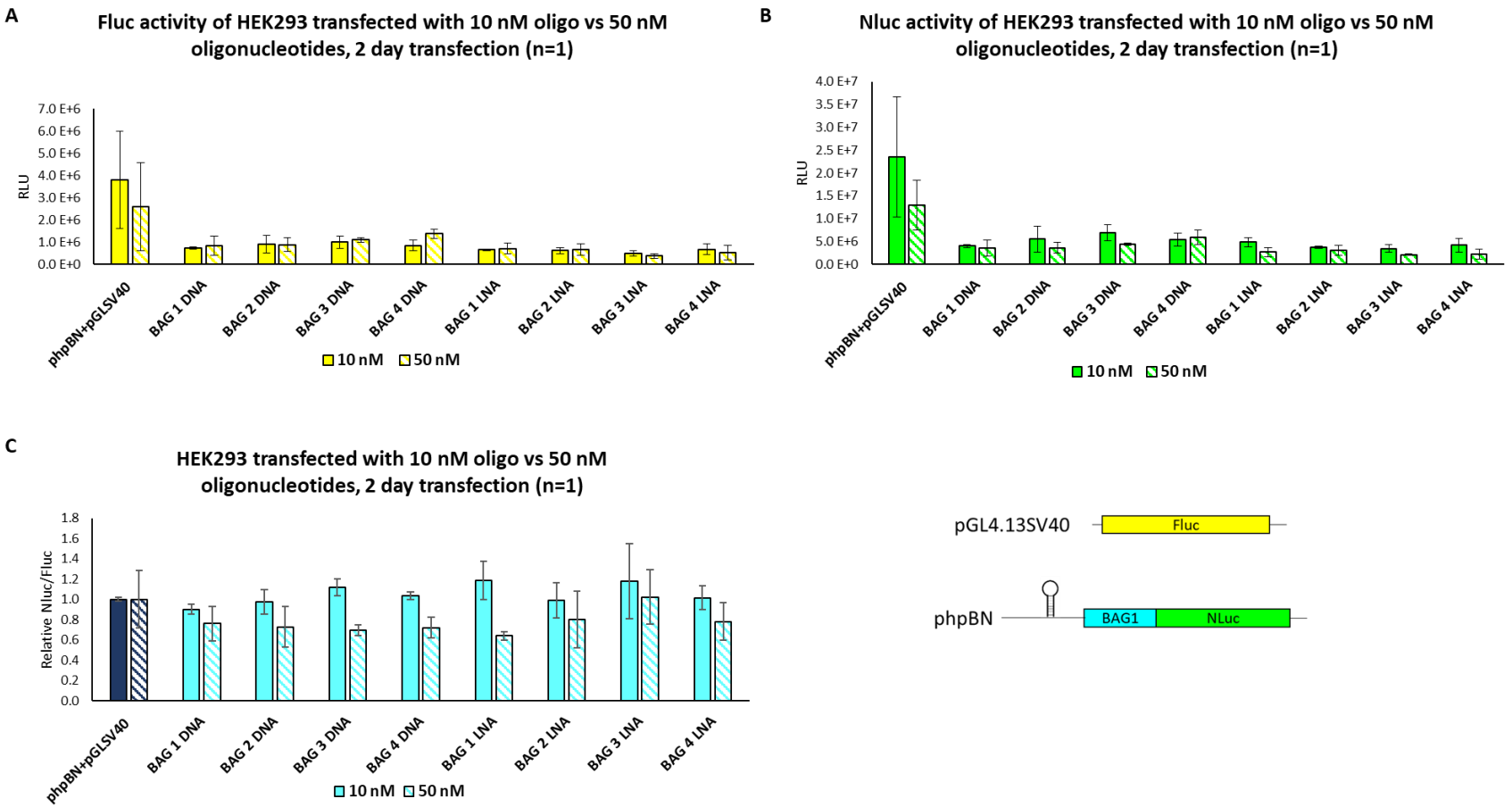

Figure D.2 **Luciferase assay result of HEK293 cells transfected with a final concentration of 10 nM and 50 nM of oligonucleotides for 2 days.** A) Fluc, B) Nluc, C) Nluc to Fluc ratio normalised to phpBN+pGL4.13SV40 transfected cells. Error bars showing standard deviation values.

Appendix D

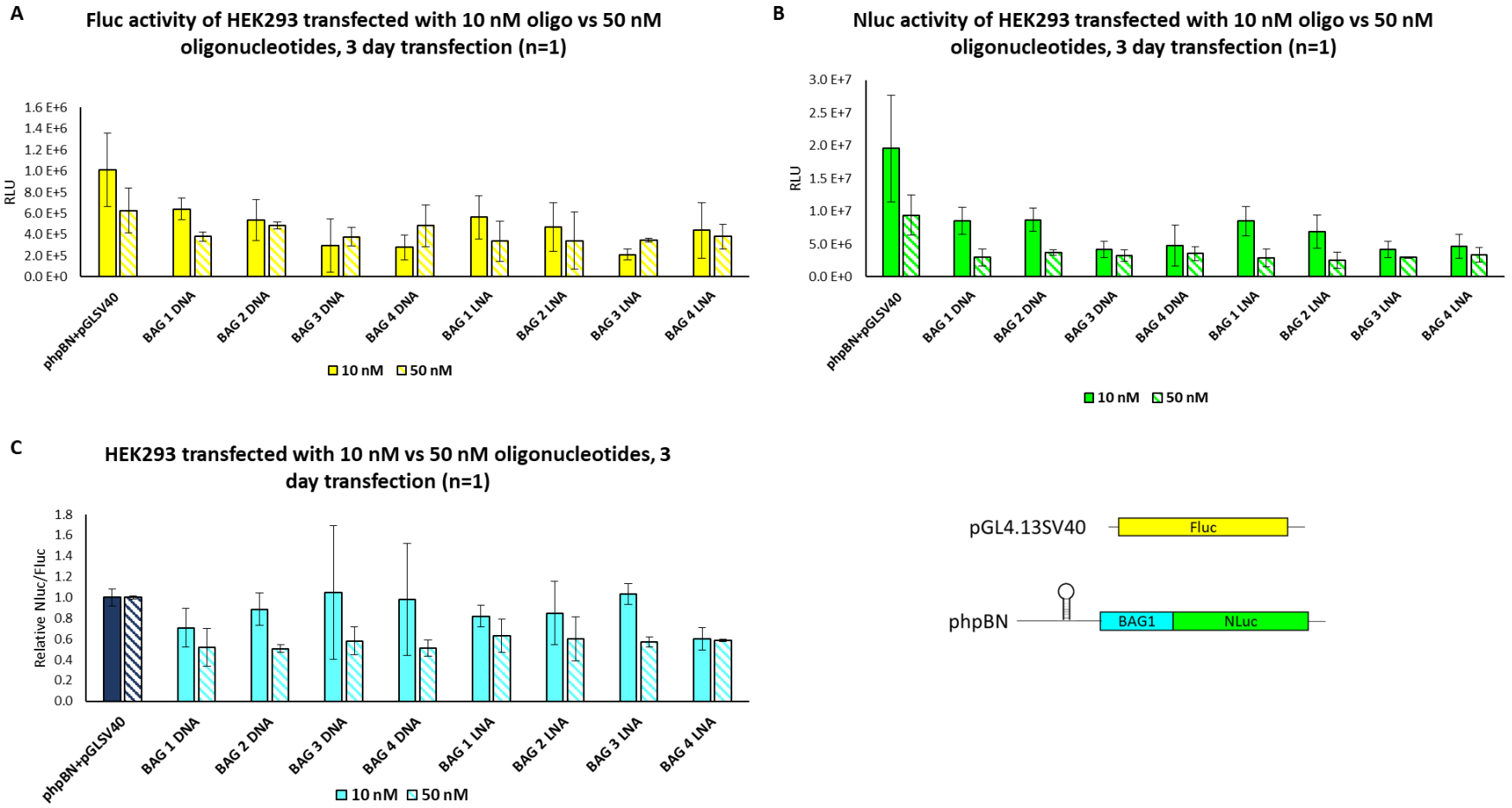

Figure D.3 **Luciferase assay result of HEK293 cells transfected with a final concentration of 10 nM and 50 nM of oligonucleotides for 3 days.** A) Fluc, B) Nluc, C) Nluc to Fluc ratio normalised to phpBN+pGL4.13SV40 transfected cells. Error bars showing standard deviation values.

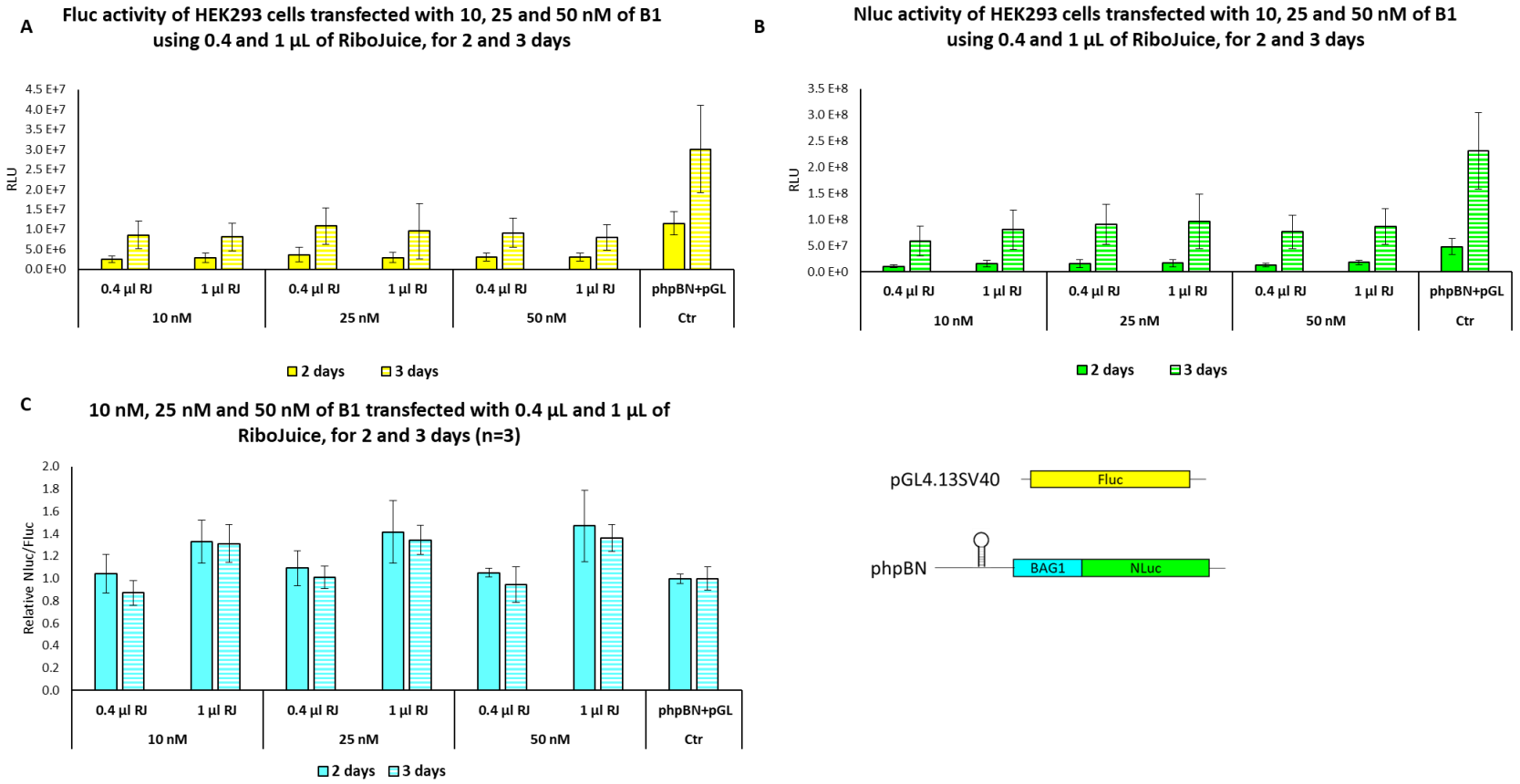

Figure D.4 **Luciferase assay results of HEK293 cells transfected with a final concentration of 10 nM, 25 nM and 50 nM of B1 using 0.4 µl, 1 µl and 2 µl of RiboJuice.** A) Fluc activity, B) Nluc activity and C) Nluc to Fluc ratio normalised to the Nluc to Fluc ratio of phpBN+pGL4.13SV40. Error bars show standard deviation values of each of the three independent replicates, each of them done in triplicate

Appendix D

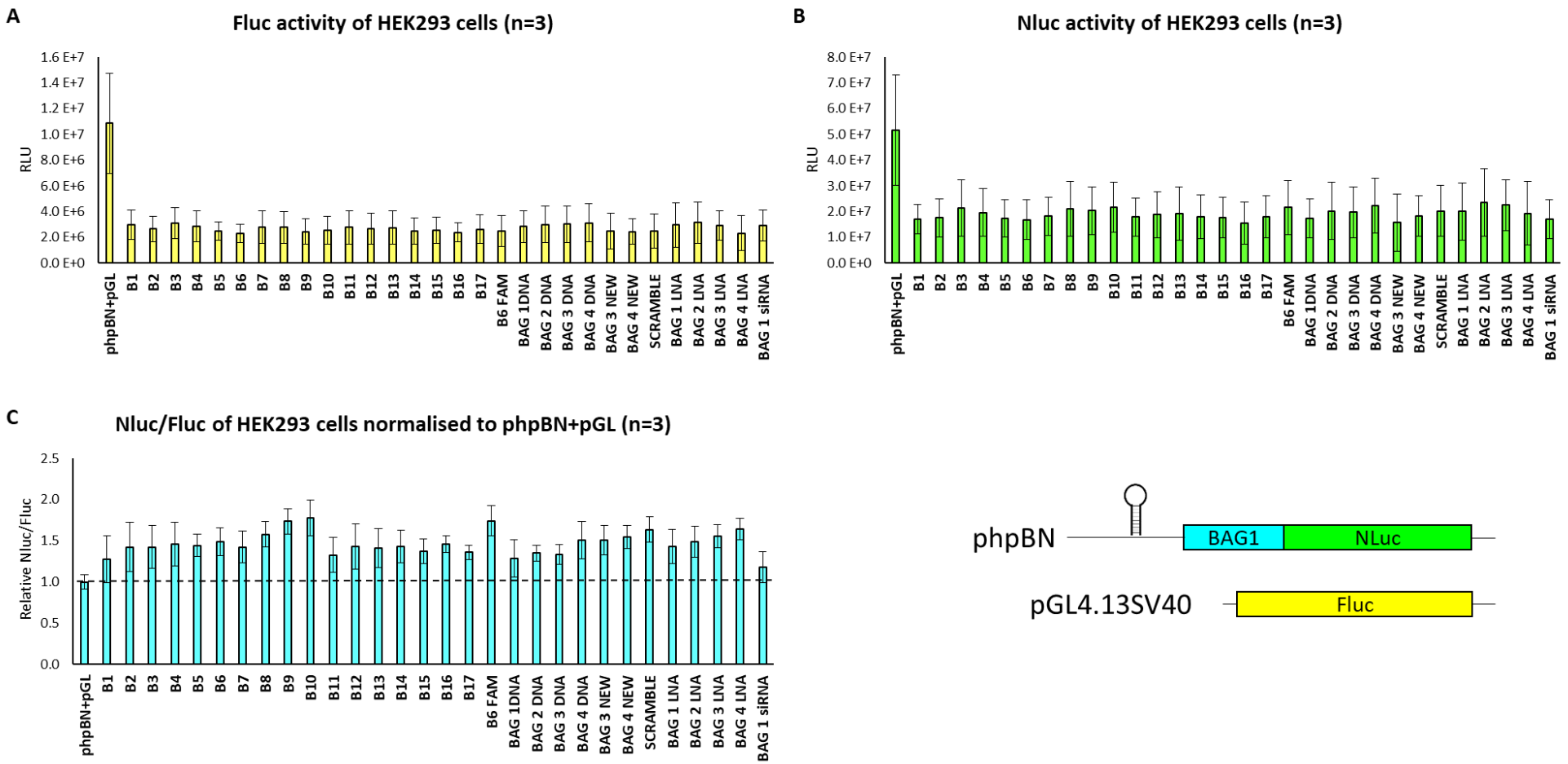

Figure D.5 **Dual luciferase reporter assay results of HEK293 cells transfected with a final concentration of 25 nM of oligonucleotides for two days.** Fluc (A) and Nluc (B) activity and Nluc/Fluc normalised to phpBN+pGL4.13SV40 transfected cells (C). Results from three independent experiments each done in triplicates. Error bars show ±SD.

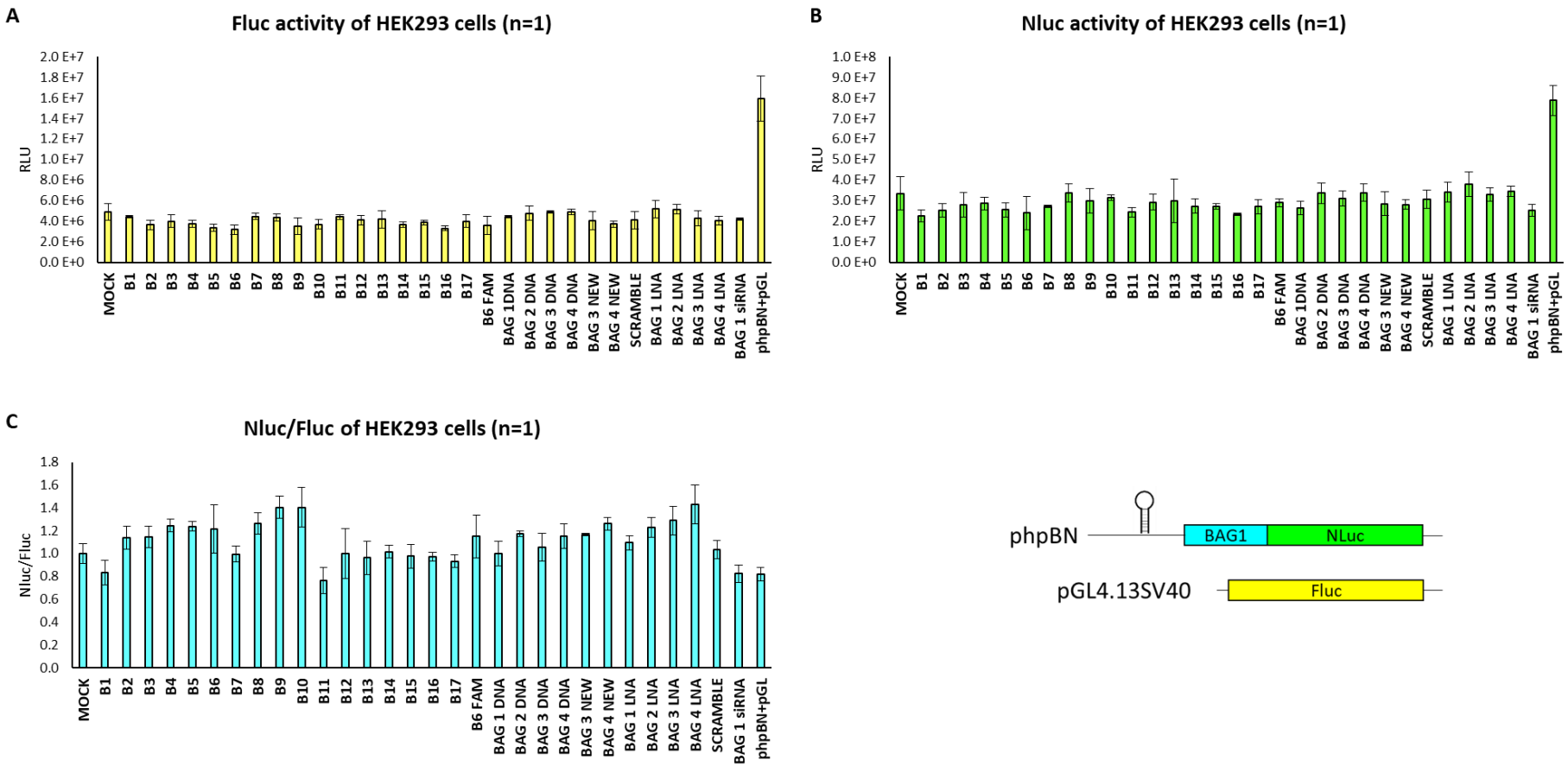

Figure D.6 **Dual luciferase reporter assay results of HEK293 cells transfected with a final concentration of 25 nM of oligonucleotides for two days.** Fluc (A) and Nluc (B) activity and Nluc/Fluc normalised to Mock transfected cells (C). Error bars show ±SD.

Appendix D

Table D 1 Statistical analysis of Nluc to Fluc ratios of HEK293 cells transfected with a final concentration of 25 nM of oligonucleotides for 2 days normalised to the Nluc to Fluc ratio of phpBN+pGL4.13SV40 (no oligonucleotide cells) analysed by a one-way ANOVA with a Tukey's multiple comparison test. P<0.05. Transfections in A showed to be significantly different from transfections in B.

Transfection A	Transfection B	Significance
phpBN + pGL4.13SV40	B2	*
	B3	*
	B4	**
	B5	**
	B6	**
	B7	*
	B8	****
	B9	****
	B10	****
	B12	*
	B13	*
	B14	*
	B16	**
	BAG 4 DNA	***
	BAG 4 NEW	****
	BAG 1 LNA	*
	BAG 2 LNA	**
	BAG 3 LNA	****
	BAG 4 LNA	****
	SCRAMBLE	****
B9	B1	*
	B11	*
	BAG 1 DNA	**
	BAG 4 DNA	*
	BAG 3 NEW	*
B10	B1	***
	B11	**
	B15	*
	B17	*
	BAG1 siRNA	****
	BAG 1 DNA	***
	BAG 2 DNA	*
	BAG 3 DNA	**
	BAG 3 NEW	**
B6 FAM	B1	**
	B11	*
	BAG1 siRNA	****
	BAG 1 DNA	**
	BAG 3 DNA	*
	BAG 3 NEW	*
BAG1 siRNA	B8	*
	B9	****
	BAG 4 LNA	**
	SCRAMBLE	**

Table D 2 Statistical analysis of Nluc to Fluc ratios of HEK293 cells transfected with a final concentration of 25 nM of oligonucleotides for 2 days normalised to the Nluc to Fluc ratio of phpBN+pGL4.13SV40 (no oligonucleotide cells) analysed by a one-way ANOVA with a Dunnett's test to compare the oligonucleotides against phpBN+ pGL4.13SV40. (P<0.05).

Transfection A	Transfection B	Significance
phpBN + pGL4.13SV40	B2	**
	B3	**
	B4	***
	B5	***
	B6	****
	B7	**
	B8	****
	B9	****
	B10	****
	B11	*
	B12	***
	B13	**
	B14	***
	B15	**
	B16	***
	BAG 2 DNA	*
	BAG 3 DNA	*
	BAG 4 DNA	****
	BAG 3 NEW	*
	BAG 4 NEW	****
	BAG 1 LNA	***
	BAG 2 LNA	****
	BAG 3 LNA	****
	BAG 4 LNA	****
	SCRAMBLE	****

Table D 3 Statistical analysis of Nluc to Fluc ratios of HEK293 cells transfected with 25 a final concentration of 25 nM of oligonucleotides for 2 days normalised to the Nluc to Fluc ratio of Mock transfected cells analysed by a one-way ANOVA with a Tukey's multiple comparison test. P<0.05. Transfections in A showed to be significantly different from transfections in B

Transfection A	Transfection B	Significance		Transfection A	Transfection B	Significance
phpBN + pGL4.13SV40	B2	**		B9	B12	**
	B3	**			B13	**
	B4	****			B14	*
	B5	****			B15	**
	B6	****			B16	*
	B8	****			B17	***
	B9	****			BAG 1 DNA	**
	B10	****			BAG 3 DNA	*
	BAG 2 DNA	***			SCRAMBLE	*

	BAG 3 NEW	***		B10	B12	**
	BAG 4 NEW	**			B13	**
	BAG 4 DNA	**			B14	*
	BAG 3 DNA	*			B15	**
	BAG 1 LNA	*			B16	*
	BAG 2 LNA	****			B17	***
	BAG 3 LNA	****			SCRAMBLE	*
	BAG 4 LNA	****			SIRNA	****
BAG1 SIRNA	B4	*			BAG 1 DNA	**
	B5	**			BAG 3 DNA	*
	B8	**		B11	B 2	*
	B9	****			B3	*
	B10	****			B4	***
	BAG 2 DNA	*			B5	***
	BAG 4 NEW	**			B6	***
	BAG 2 LNA	**			B8	****
	BAG 3 LNA	***			B9	****
	BAG 4 LNA	****			B10	****
MOCK	B9	**			BAG 2 DNA	**
	B10	**			BAG 4 DNA	*
	BAG 4 LNA	**			BAG 3 NEW	**
B1	B4	**			BAG 4 NEW	***
	B5	**			BAG 2 LNA	***
	B6	*			BAG 3 LNA	****
	B8	**			BAG 4 LNA	****
	B9	****		BAG 4 LNA	B12	**
	B10	****			B13	***
	BAG 4 NEW	**			B14	**
	BAG 2 LNA	**			B15	***
	BAG 3 LNA	***			B16	**
	BAG 4 LNA	****			B17	***
B7	B9	**			SCRAMBLE	**
	B10	**			BAG 1 DNA	**
	BAG 4 LNA	**			BAG 3 DNA	*
				B17	BAG 3 LNA	*

Table D 4 Nluc to Fluc ratios of HEK293 cells transfected with a final concentration of 25 nM of oligonucleotides for 2 days normalised to the Nluc to Fluc ratio of Mock transfected cells analysed by a one-way ANOVA with a Dunnett's test to compare the oligonucleotides against Mock transfected cells. ($P<0.05$).

Transfection A	**Transfection B**	**Significance**
MOCK	B9	***
	B10	***
	BAG 3 LNA	*
	BAG 4 LNA	***

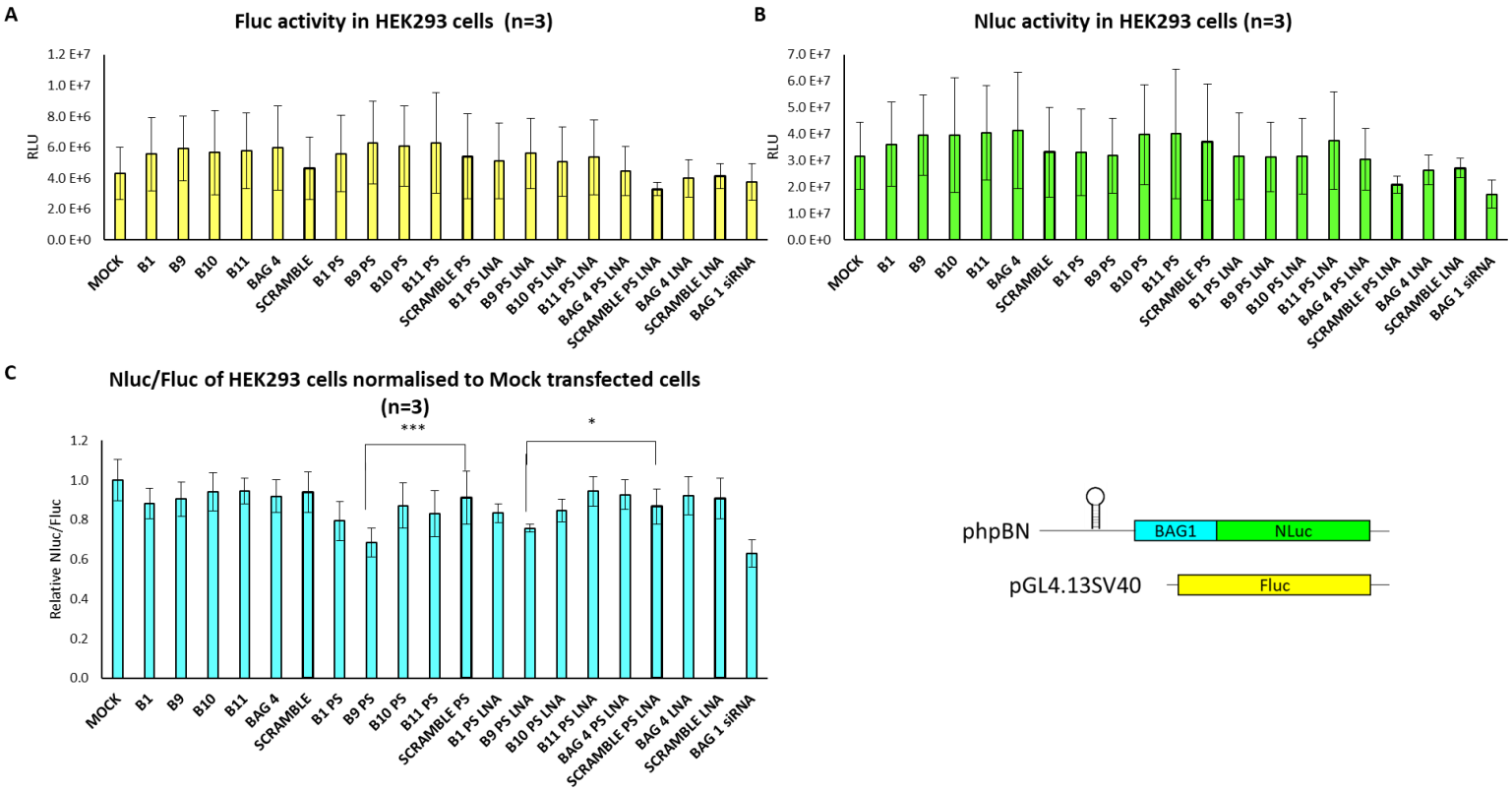

Figure D.7 **Dual luciferase assay results of HEK293 cells transfected with a final concentration of 25 nM of the selected oligonucleotides for two days.** A) Fluc and B) Nluc activities and C) Nluc to Fluc ratio normalised to Mock transfected cells. Results from three independent experiments, each done in triplicates. Error bars show ± SD. Statistical analysis was done using a one way ANOVA with a Dunnett's multiple comparison test ($P<0.05$), where the means of the Nluc to Fluc ratio of each oligonucleotide treated cells normalised to Mock transfected cells were compared against the Nluc to Fluc ratio of Scramble transfected cells.

Appendix D

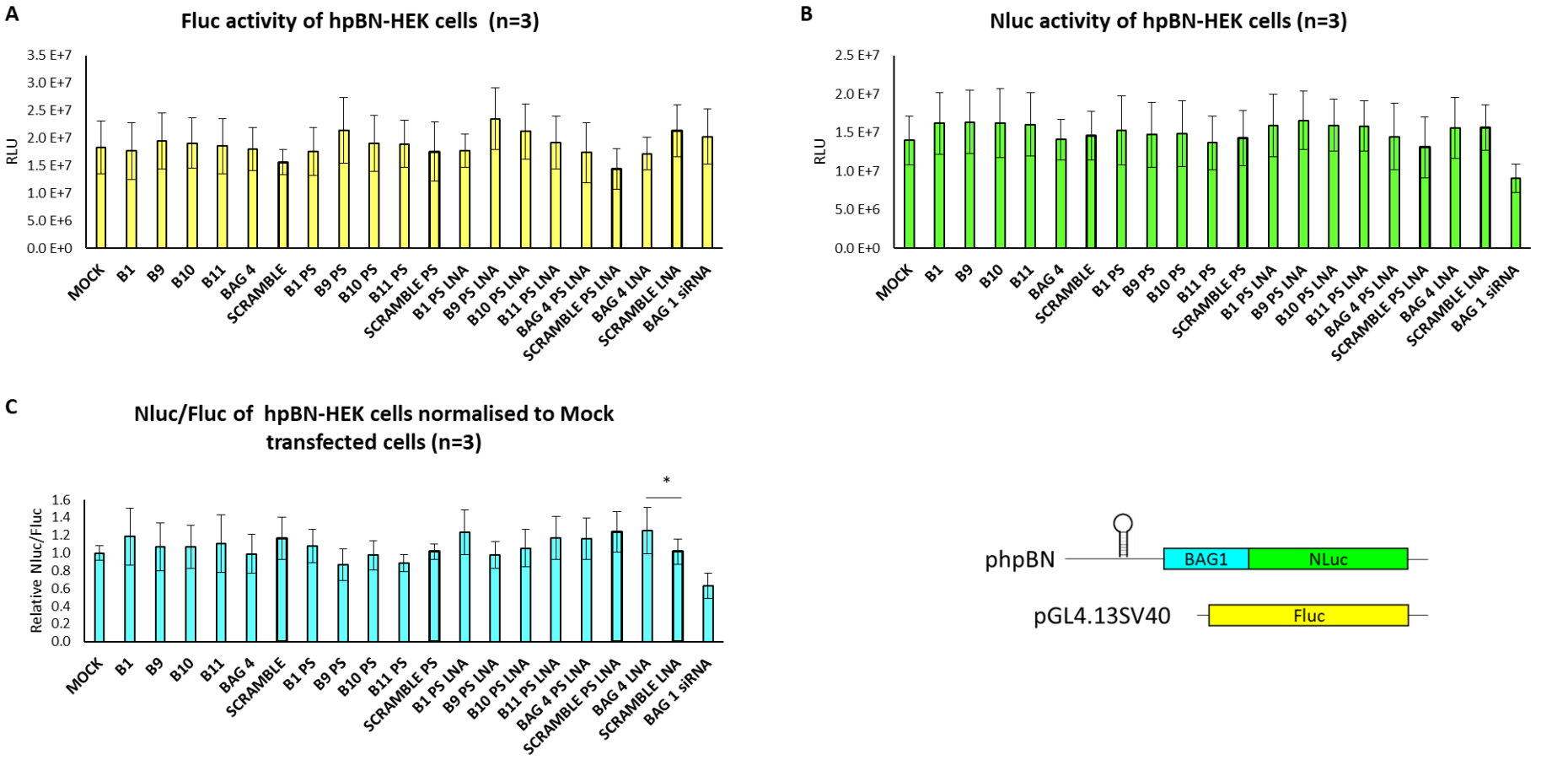

Figure D.8 **Dual luciferase assay of hpBN-HEK cells transfected with a final concentration of 25 nM of the selected oligonucleotides for two days.** A) Fluc and B) Nluc activity of hpBN-HEK cells was measured and C) Nluc to Fluc ratio was calculated and normalised to the Nluc to Fluc of Mock transfected cells. Error bars represent ± SD. Statistical analysis was done using a one-way ANOVA with a Dunnett's multiple comparison test ($P<0.05$), where the means of the Nluc to Fluc ratio of each oligonucleotide treated cells normalised to Mock transfected cells were compared against the Nluc to Fluc ratio of Scramble transfected cells.

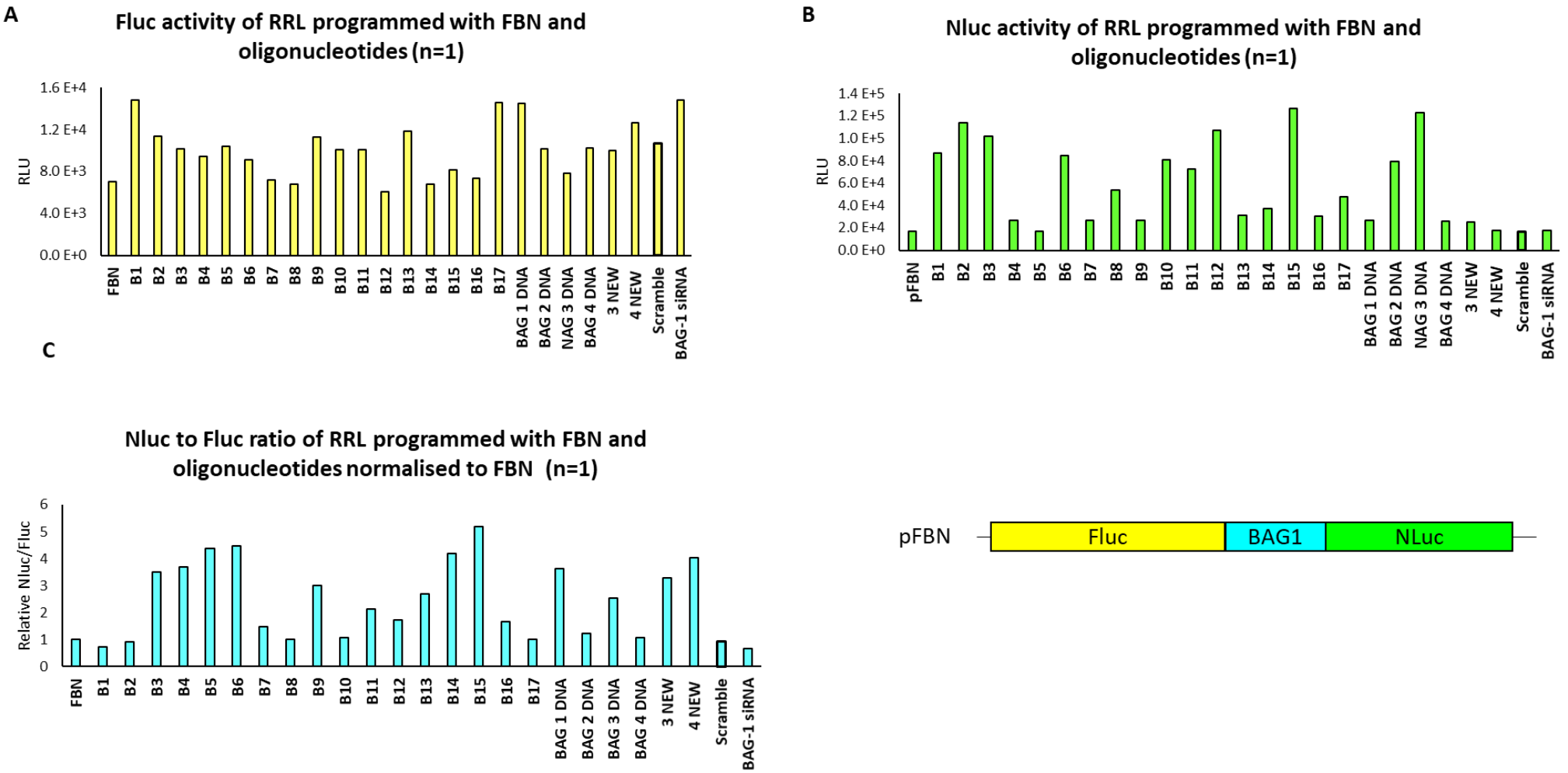

Figure D.9 **Luciferase assay results of RRL programmed with 500 ng FBN and 1 µM of final concentration unmodified oligonucleotides (heated at 65°C).** A) Fluc and B) Nluc activities and D) Nluc to Fluc ratio normalised to Nluc to Fluc ratio of RRL programmed with FBN.

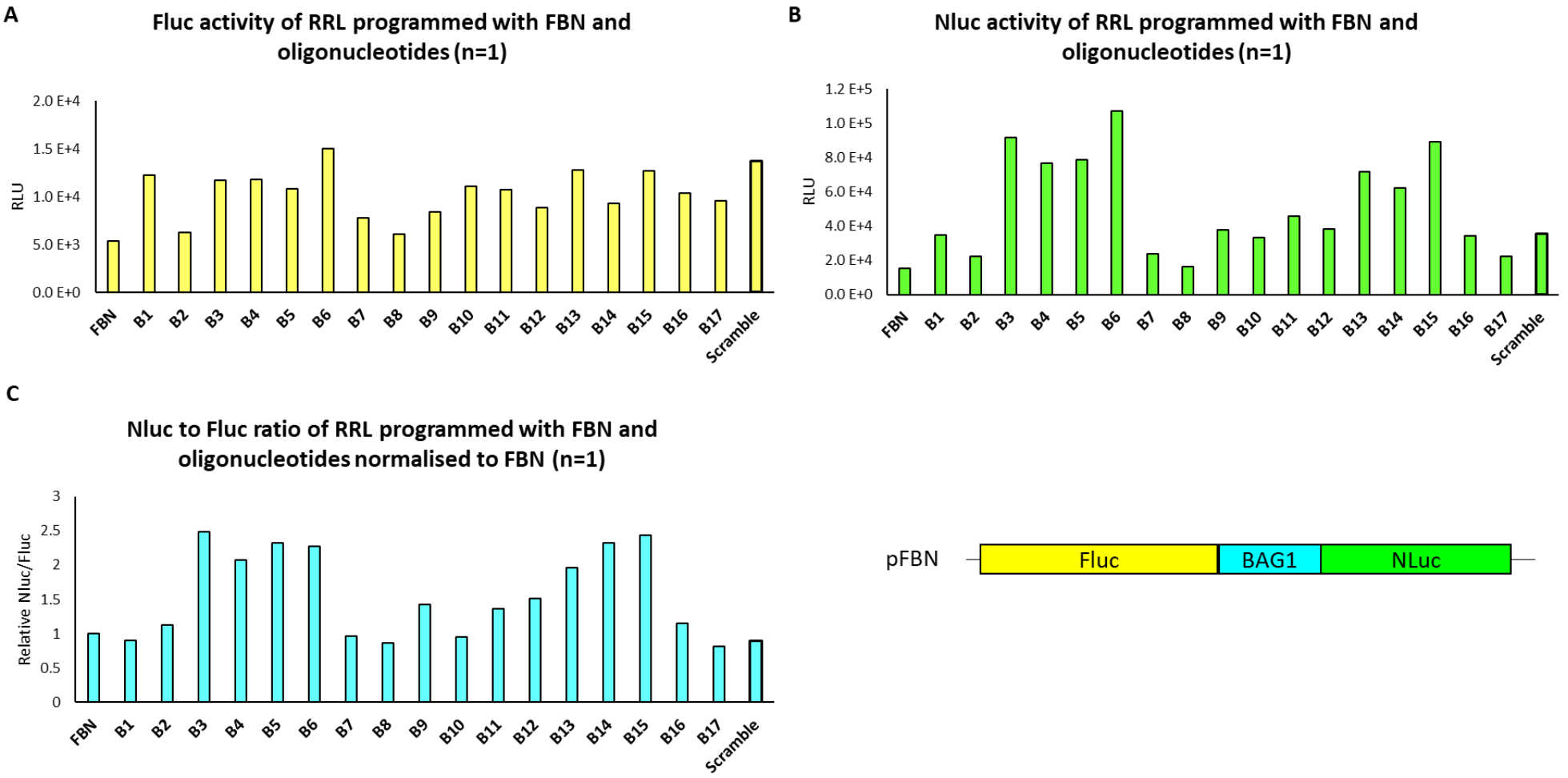

Figure D.10 **Luciferase assay results of RRL programmed with 500 ng FBN and 1 µM final concentration of oligonucleotides, not heated at 65°C.** A) Fluc and B) Nluc activities and D) Nluc to Fluc ratio normalised to Nluc to Fluc ratio of RRL programmed with FBN.

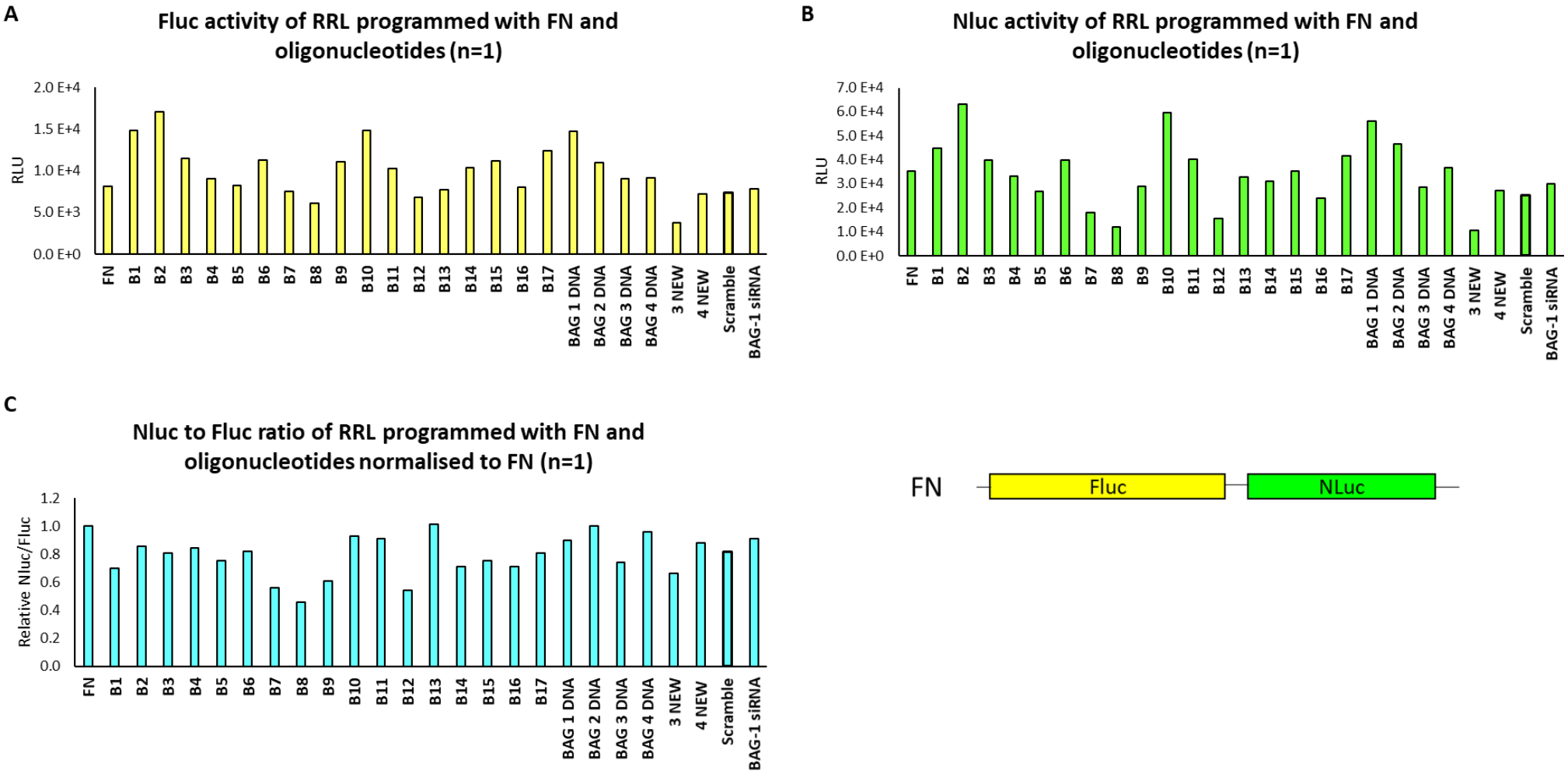

Figure D.11 **Luciferase assay results of RRL programmed with 500 ng FN and 1 µM final concentration of unmodified oligonucleotides (heated at 65°C). A**) Fluc and B) Nluc activities and D) Nluc to Fluc ratio normalised to RRL programmed with FN.

A

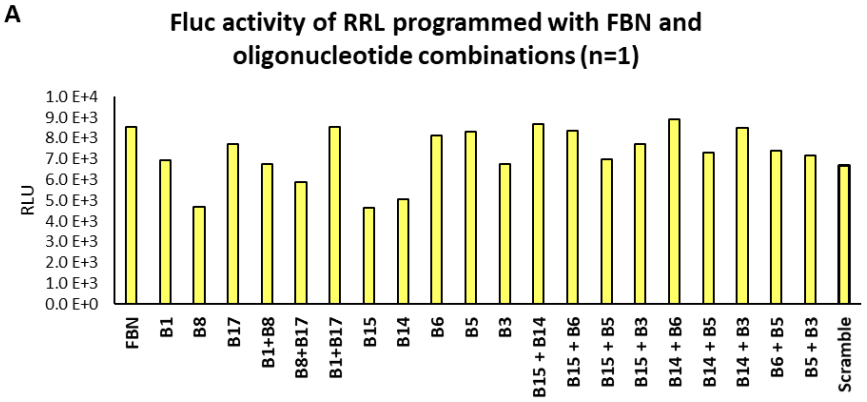

B

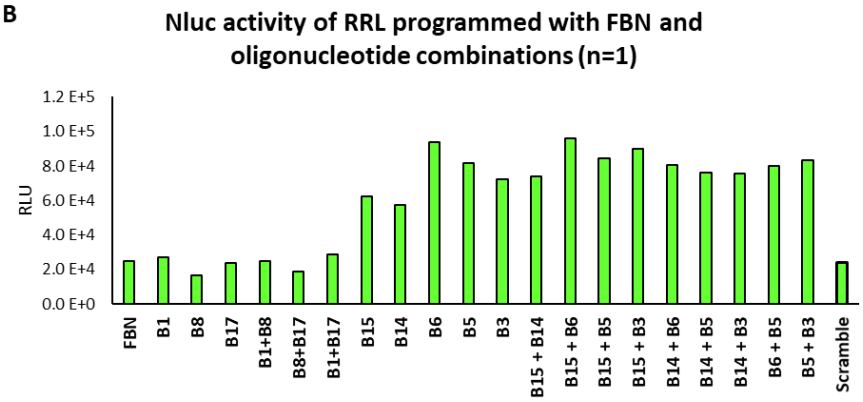

C

Oligonucleotide	avg Nluc/Fluc normalised to FBN
B15	4.71
B15 + B5	4.14
B6	4.09
B14	4.01
B15 + B3	4.01
B5 + B3	3.98
B15 + B6	3.93
B3	3.80
B6 + B5	3.69
B5	3.67
B14 + B5	3.58
B14 + B6	3.11
B14 + B3	3.08
B15 + B14	2.93
B1	1.37
B1+B8	1.30
B8	1.24
Scramble	1.23
B1+B17	1.20
B8+B17	1.12
B17	1.09
FBN	1.00

D

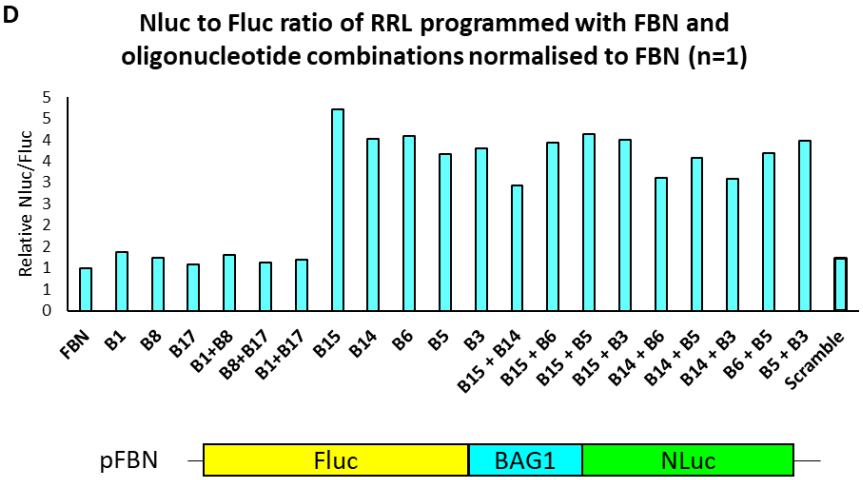

Figure D.12 **Luciferase assay results of RRL programmed with 500 ng FBN and 1 µM final concentration of oligonucleotide combinations.** A) Fluc and B) Nluc activities and D) Nluc to Fluc ratio normalised to Nluc to Fluc ratio of RRL programmed with FBN. C) List of oligonucleotides ranked from the highest to the lowest effect they had modifying the Nluc to Fluc activity in FBN.

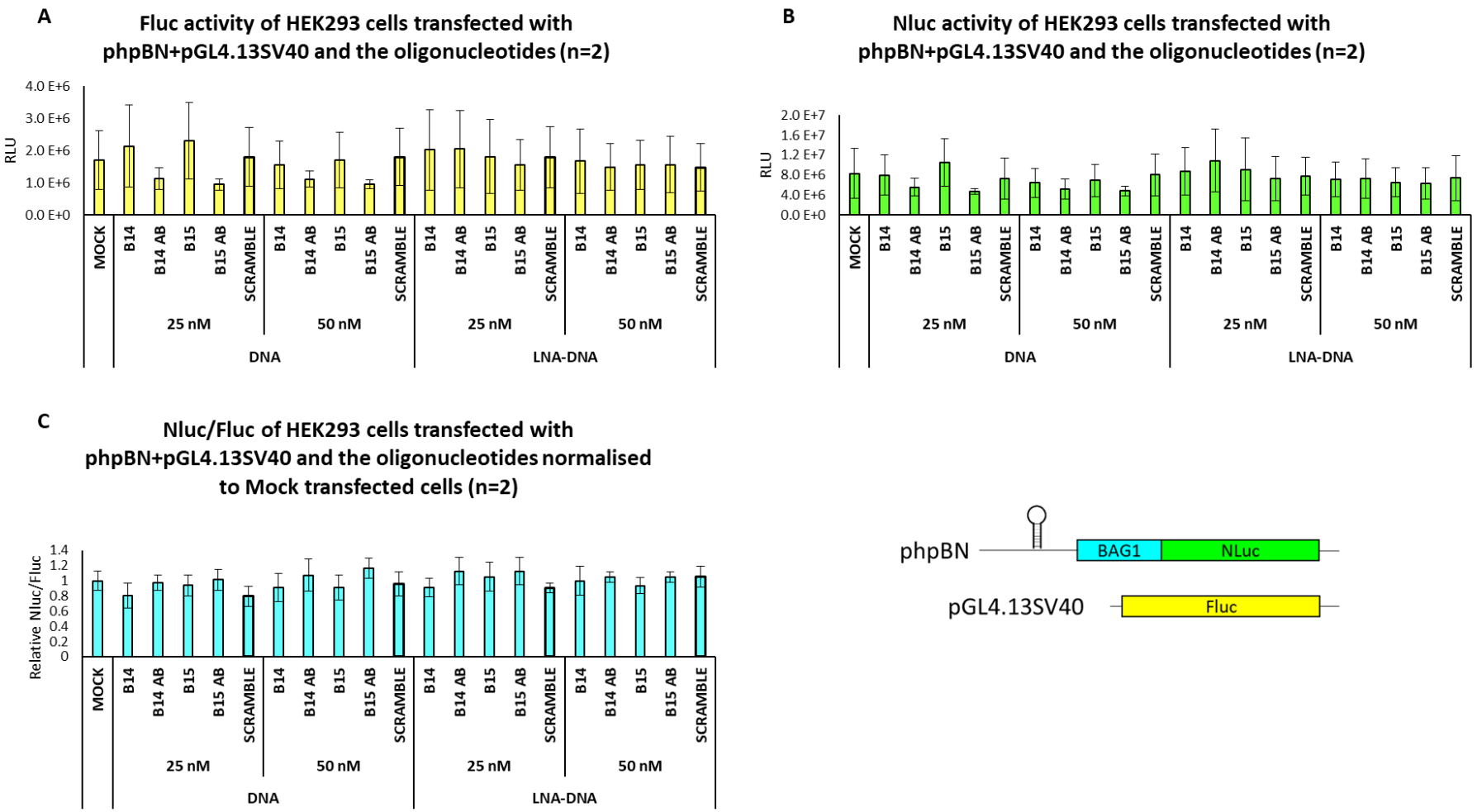

Figure D.13 **Luciferase assay of HEK293 cells transfected with a final concentration of 25 and 50 nM of oligonucleotides for two days.** A) Fluc activity, B) Nluc activity and C) Nluc to Fluc ratio normalised to Nluc to Fluc ratio of Mock transfected cells of HEK293 cells transfected with phpBN+pGL4.13SV40 and the oligonucleotides.

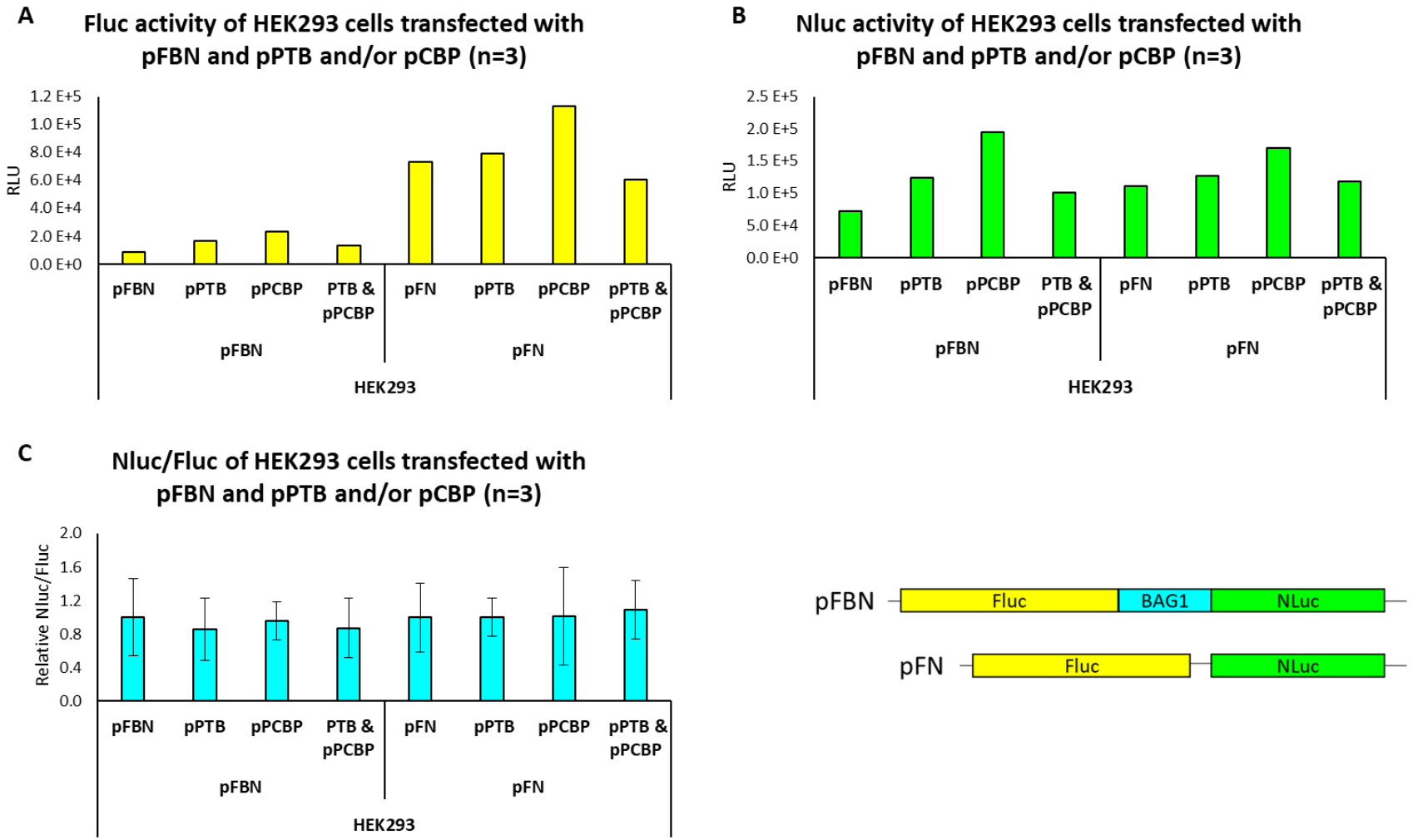

Figure D.14 **Luciferase assay results of HEK293 cells transfected with pFBN or pFN and pPCBP and/or pPTB.** A) Fluc and B) Nluc activity. C) Nluc to Fluc ratio of HEK293 cells co-transfected with pFBN or pFN and pPTBP1 and or pPCBP. Error bars show ± SD. The experiment was done in triplicate 3 individual times.

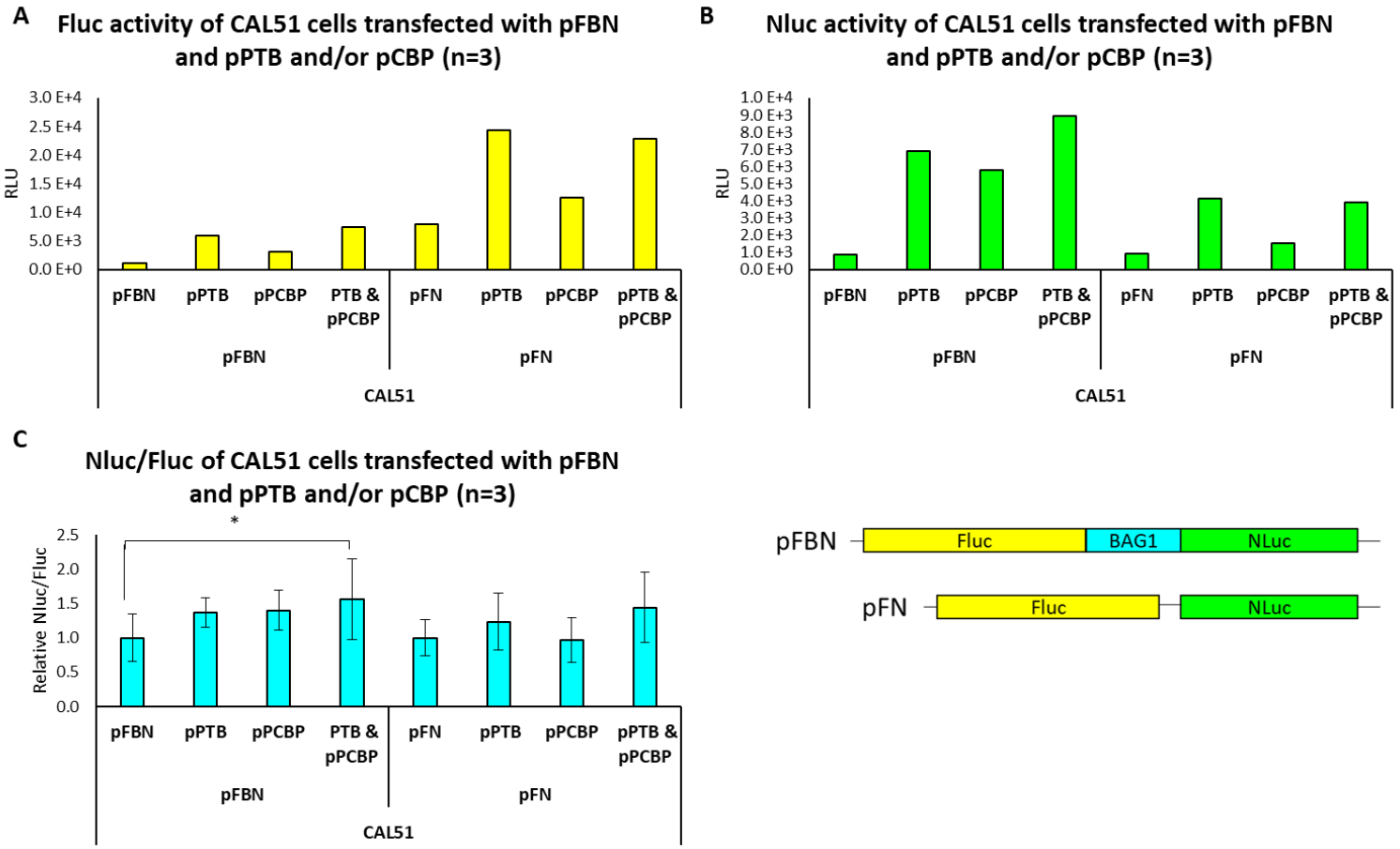

Figure D.15 **Luciferase assay results of CAL51 cells transfected with pFBN or pFN and pPCBP and/or pPTB.** A) Fluc and B) Nluc activity. C) Nluc to Fluc ratio of HEK293 cells co-transfected with pFBN or pFN and pPTBP1 and or pPCBP. Error bars show ± SD. The experiment was done in triplicate 3 individual times. Statistical analysis was done using a one-way ANOVA with a Dunnett's multiple comparison test ($P<0.05$), where the means of the Nluc to Fluc ratio of each transfection normalised to pFBN or pFN transfected cells was compared against the Nluc to Fluc ratio of pFBN or pFN transfected cells.

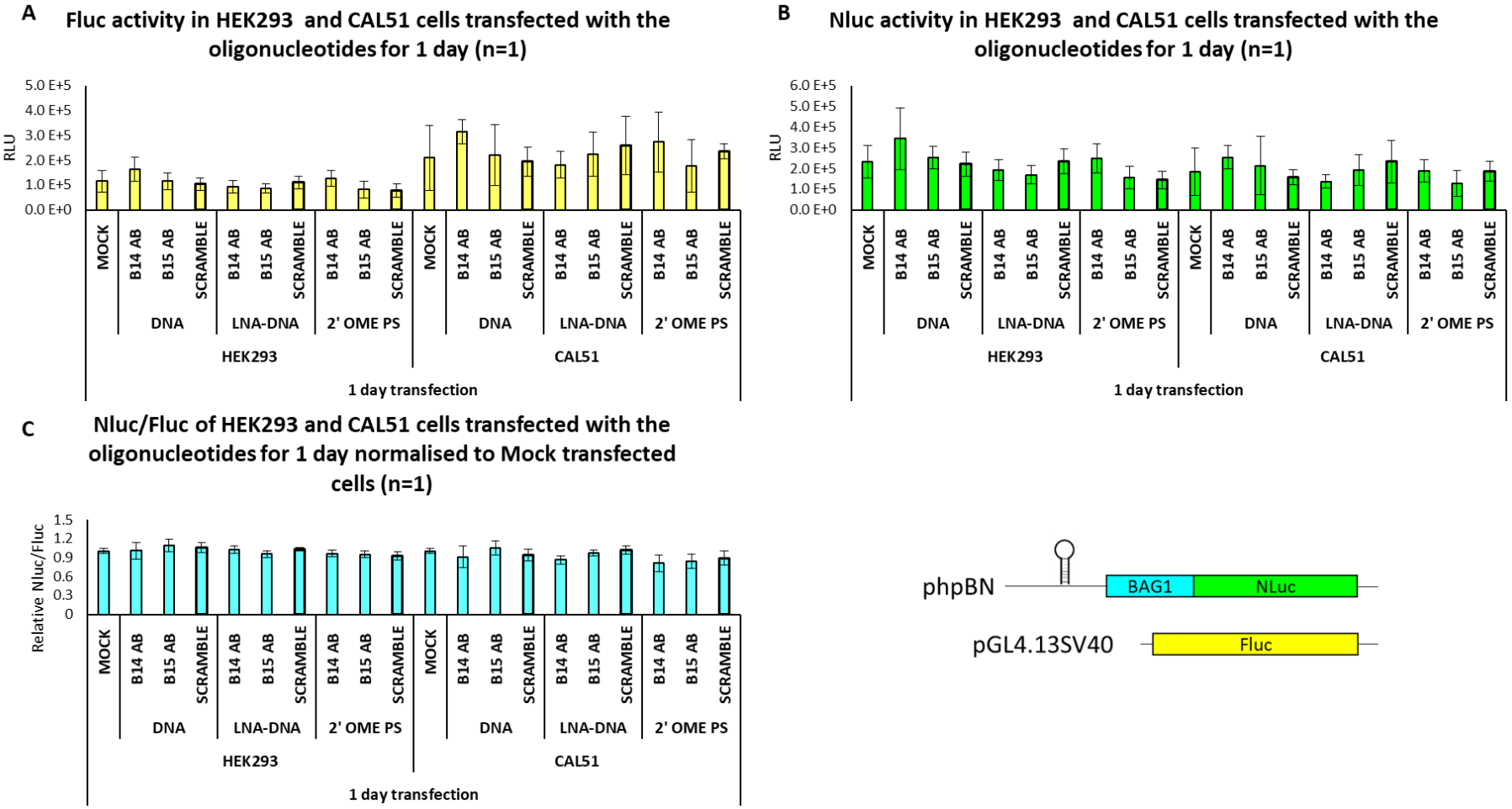

Figure D.16 **Fluc activity (A), Nluc activity (B) and Nluc to Fluc ratio normalised to Mock transfected cells (C) of HEK293 and CAL51 cells transfected with a final concentration of 25 nM of oligonucleotides for one day.** Error bars show standard deviatio values of an experiment done once in triplicate.

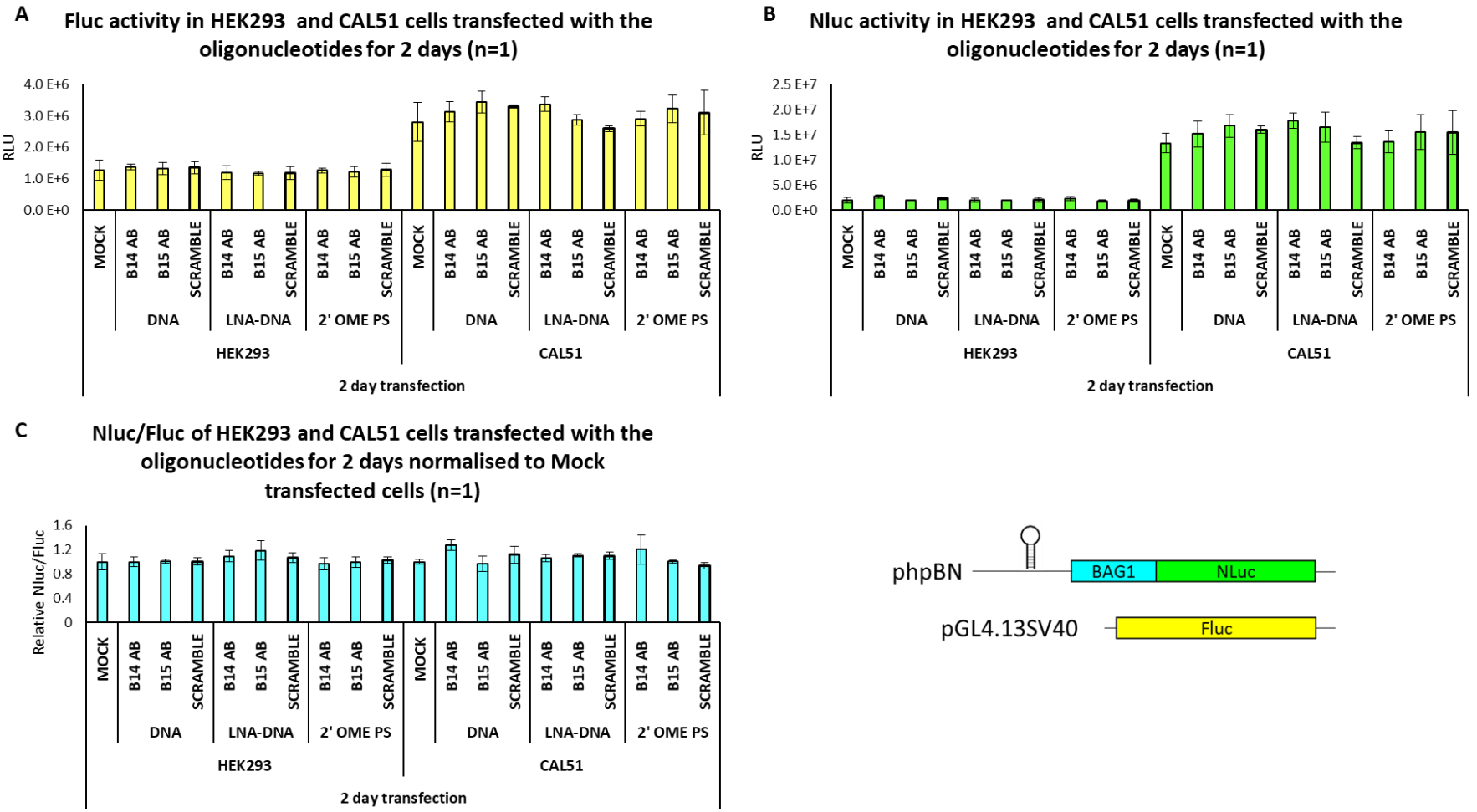

Figure D.17 **Fluc activity (A), Nluc activity (B) and Nluc to Fluc ratio normalised to Mock transfected cells (C) of HEK293 and CAL51 cells transfected with a final concentration of 25 nM of oligonucleotides for two days.** Error bars show standard deviatio values of an experiment done once in triplicate.

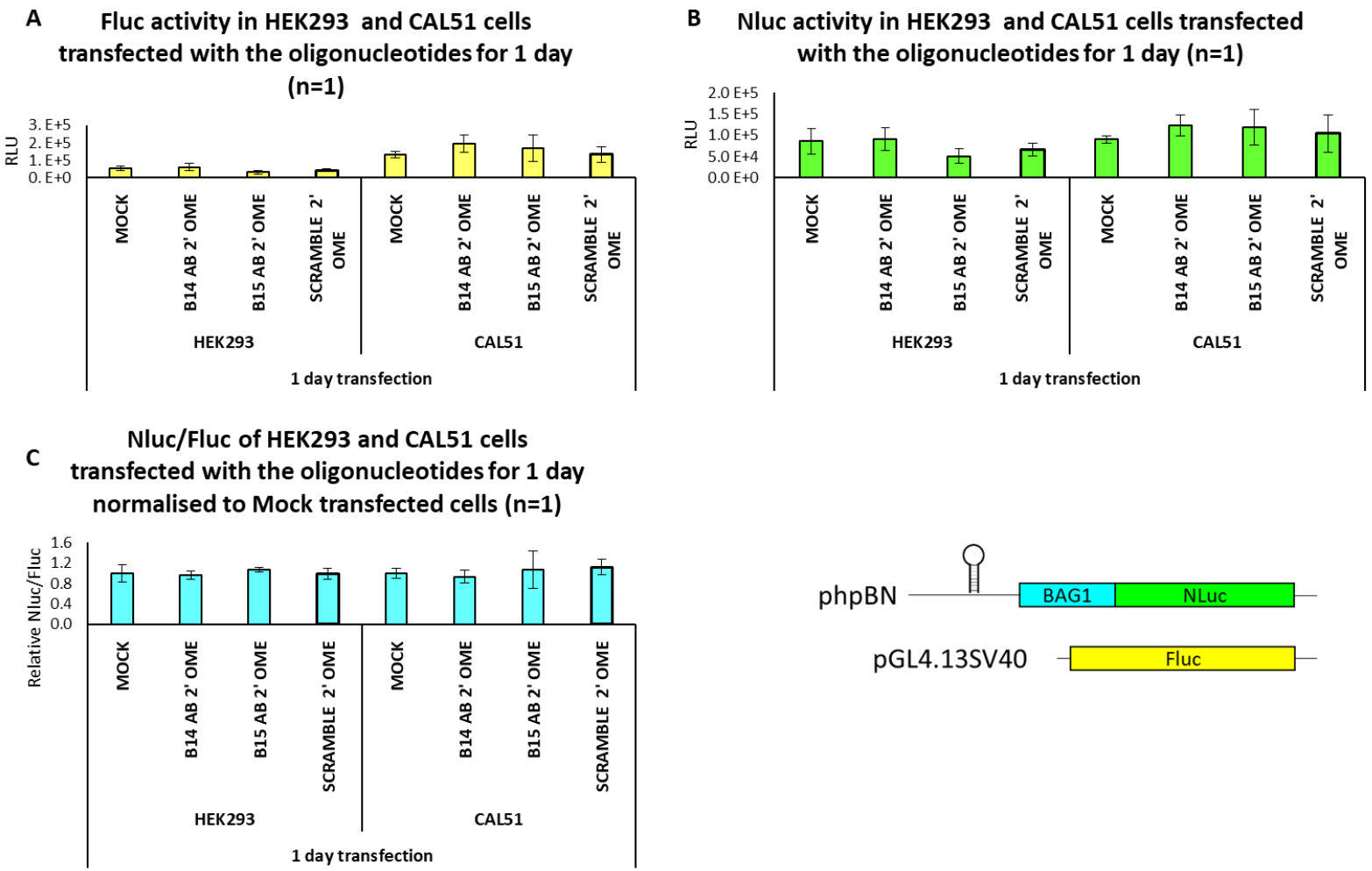

Figure D.18 **Fluc activity (A), Nluc activity (B) and Nluc to Fluc ratio normalised to Mock transfected cells (C) of HEK293 and CAL51 cells transfected with a final concentration of 25 nM of 2' OME oligonucleotides for one day.** Error bars show standard deviatio values of an experiment done once in triplicate.

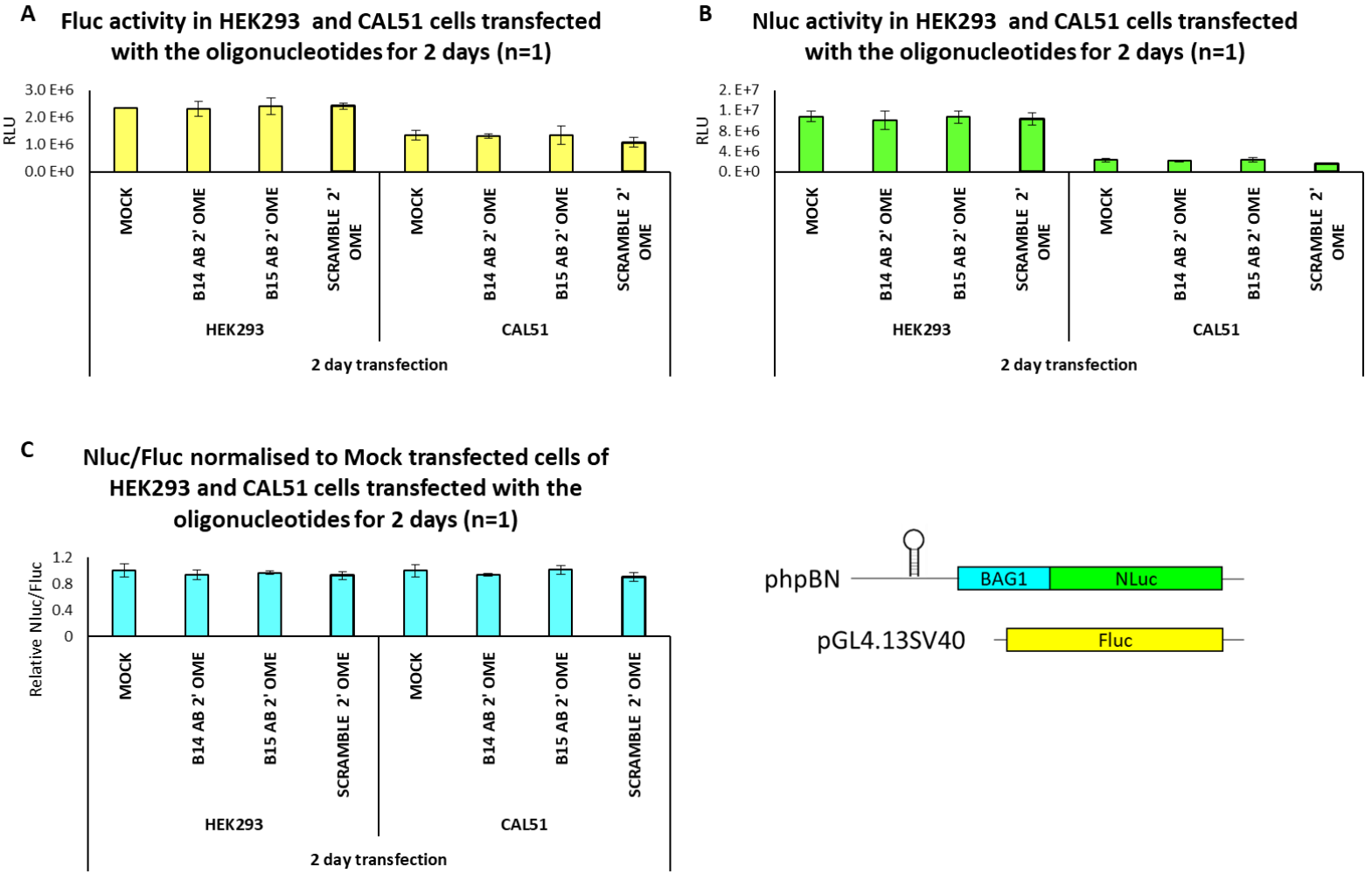

Figure D.19 **Fluc activity (A), Nluc activity (B) and Nluc to Fluc ratio normalised to Mock transfected cells (C) of HEK293 and CAL51 cells transfected with a final concentration of 25 nM of 2' OME oligonucleotides for two days.** Error bars show standard deviatio values of an experiment done once in triplicate.

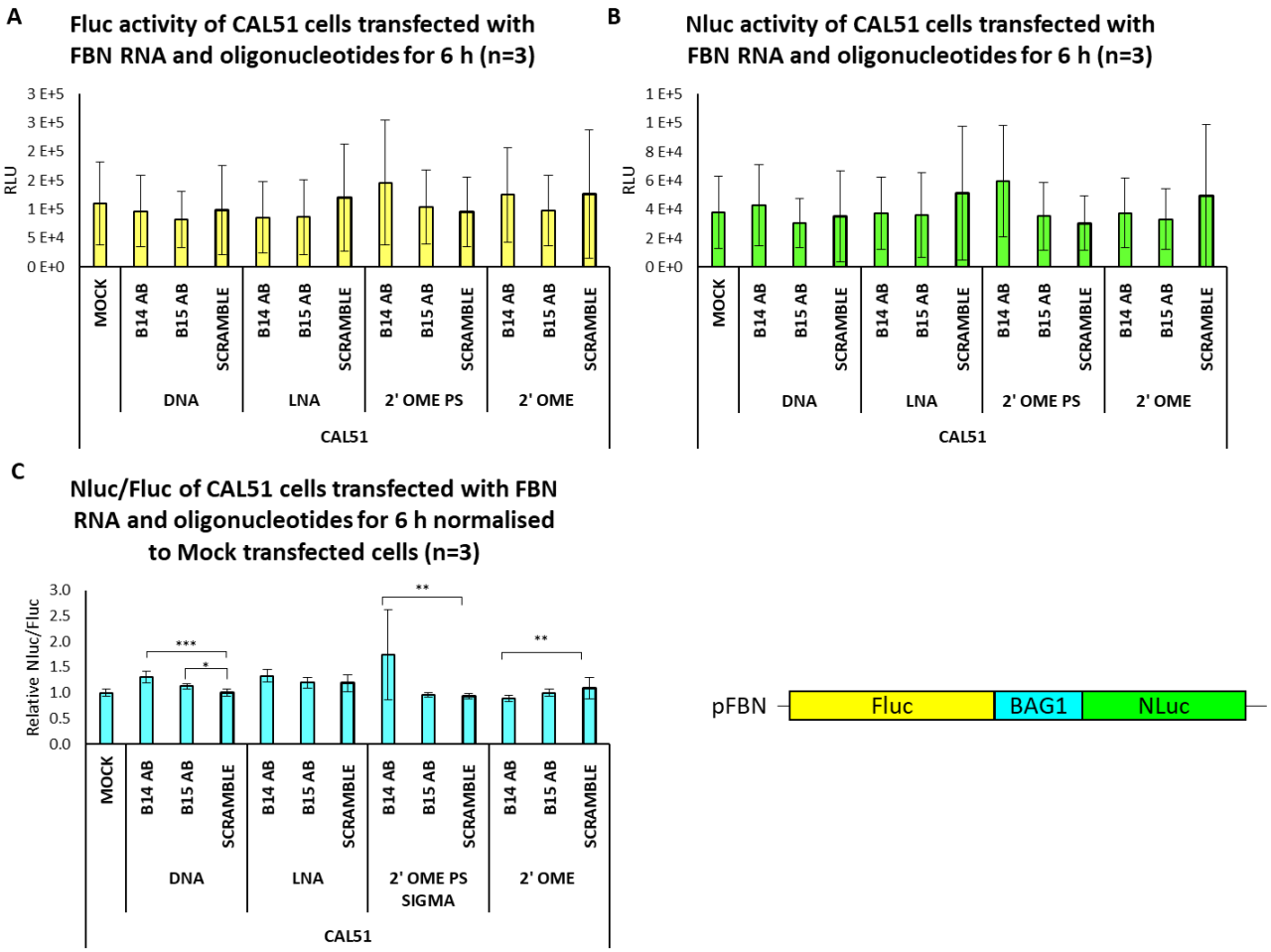

Figure D.20 **Fluc (A), Nluc (B) and Nluc to Fluc ratio (C) of CAL51 cells co-transfected with 150 ng of *in vitro* transcribed m^{7}G-FBN- poly(A) RNA and a final concentration of 1 µM of oligonucleotides for 6 hours.** Error bars show ±SD. Statistical analysis was done using a one-way ANOVA with Dunnett's multiple comparison test to compare the Nluc/Fluc activity of the oligonucleotide transfected cells with the Nluc/Fluc activity of Mock or Scramble transfected cells ($P<0.05$).

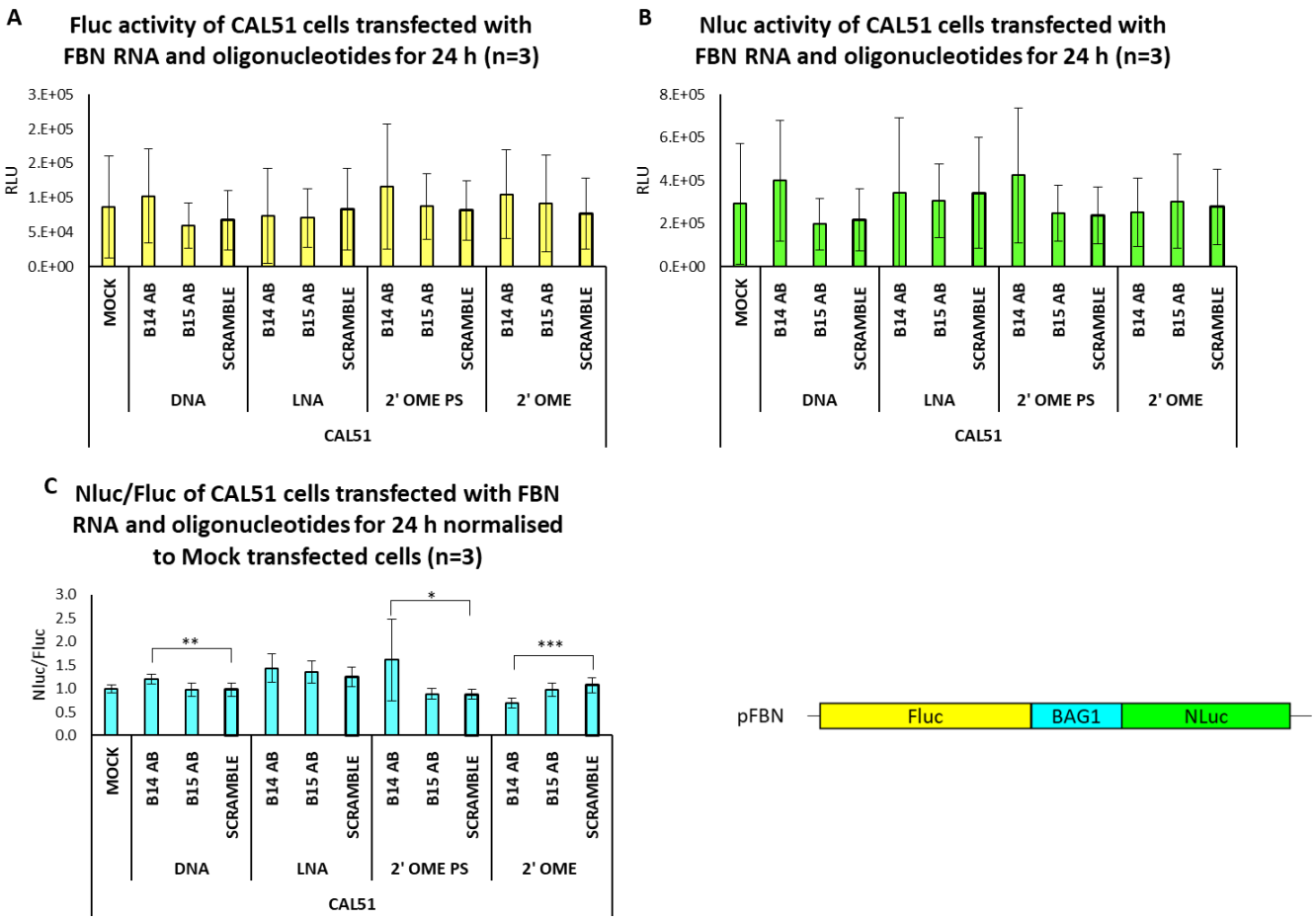

Figure D.21 **Fluc (A), Nluc (B) and Nluc to Fluc ratio (C) of CAL51 cells co-transfected with 150 ng of *in vitro* transcribed m^{7}G-FBN- poly(A) RNA and a final concentration of 1 µM of oligonucleotides for 24 hours.** Error bars show ±SD. Statistical analysis was done using a one-way ANOVA with Dunnett's multiple comparison test to compare the Nluc/Fluc activity of the oligonucleotide transfected cells with the Nluc/Fluc activity of Mock or Scramble transfected cells ($P<0.05$)

Appendix E **SUPPLEMENTARY WESTERN BLOT RESULTS**

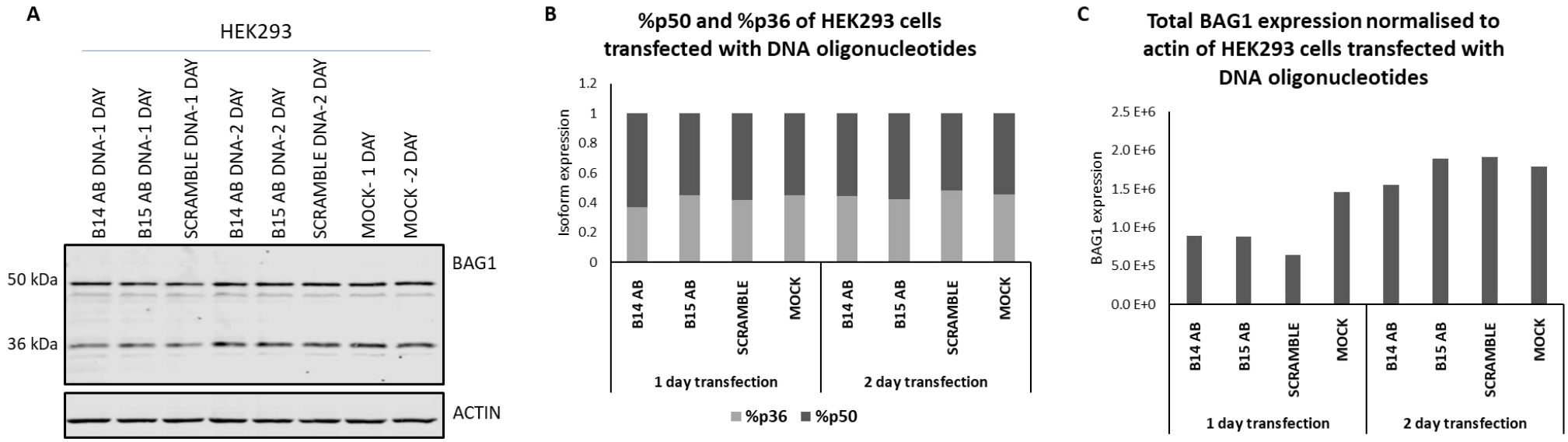

Figure E. 1 W**estern Blot of HEK293 cells transfected with a final concentration of 25 nM of unmodified oligonucleotides for one and two days** . A) Blot, B) %p50 and %p36 expression and C) total BAG1 expression normalised to actin expression.

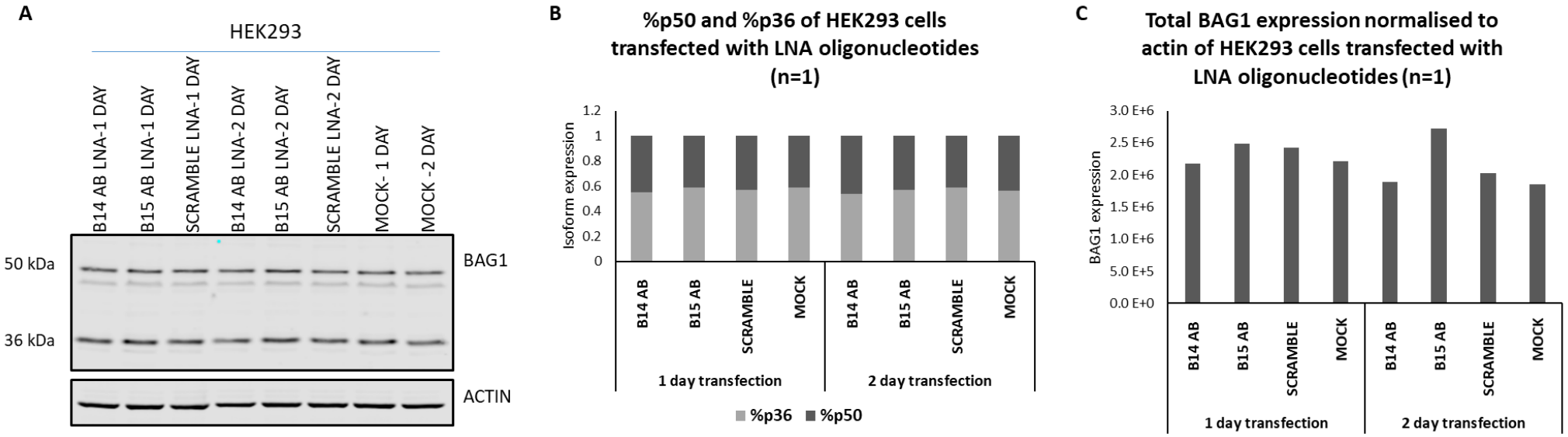

Figure E. 2 **Western Blot of HEK293 cells transfected with a final concentration of 25 nM of LNA oligonucleotides for one and two days** . A) Blot, B) %p50 and %p36 expression and C) total BAG1 expression normalised to actin expression.

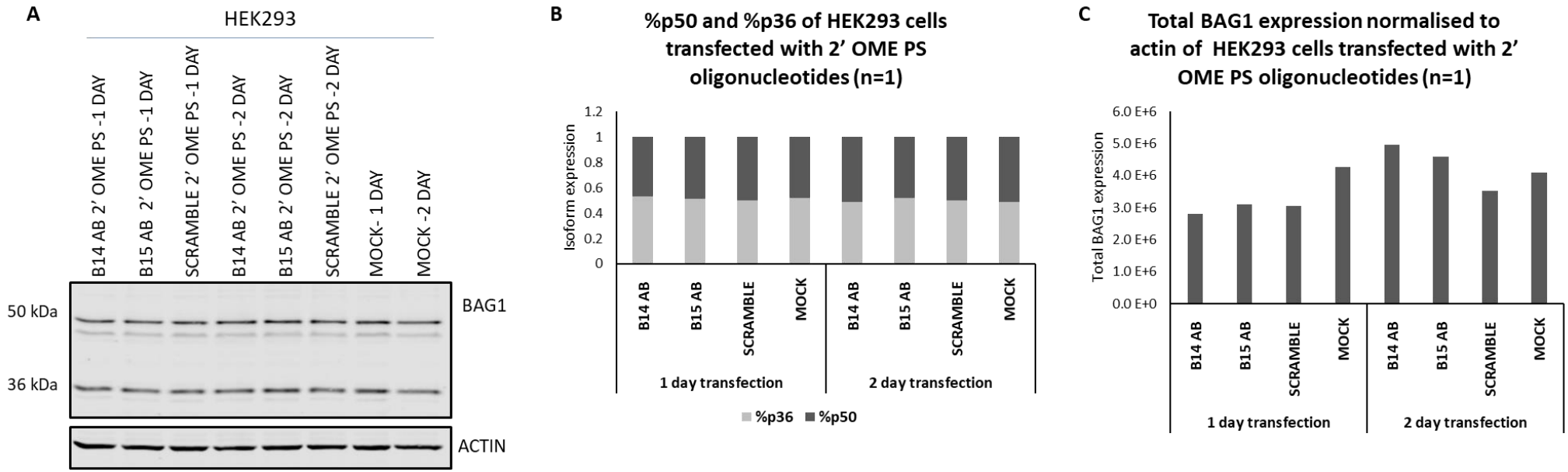

Figure E 3**. Western Blot of HEK293 cells transfected with a final concentration of 25 nM of 2' OME PS oligonucleotides for one and two days** . A) Blot, B) %p50 and %p36 expression and C) total BAG1 expression normalised to actin expression.

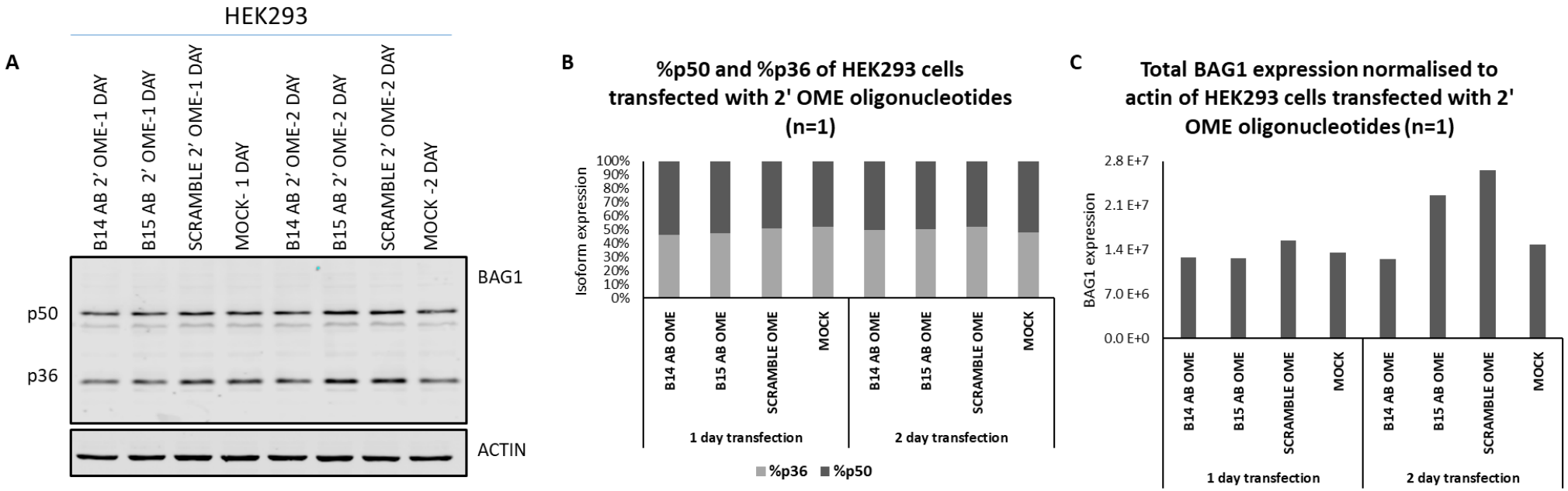

Figure E. 4 **Western Blot of HEK293 cells transfected with a final concentration of 25 nM of 2' OME oligonucleotides for one and two days** . A) Blot, B) %p50 and %p36 expression and C) total BAG1 expression normalised to actin expression.

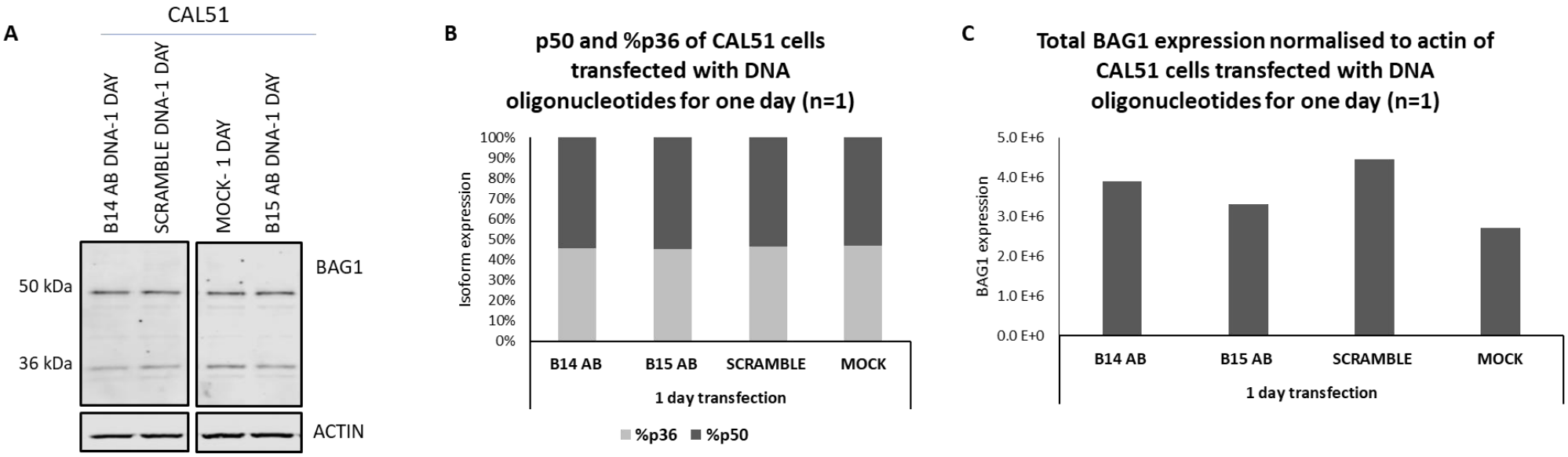

Figure E. 5 **Western Blot of CAL51 cells transfected with a final concentration of 25 nM of unmodified oligonucleotides for one day** . A) Blot, B) %p50 and %p36 expression and C) total BAG1 expression normalised to actin expression.

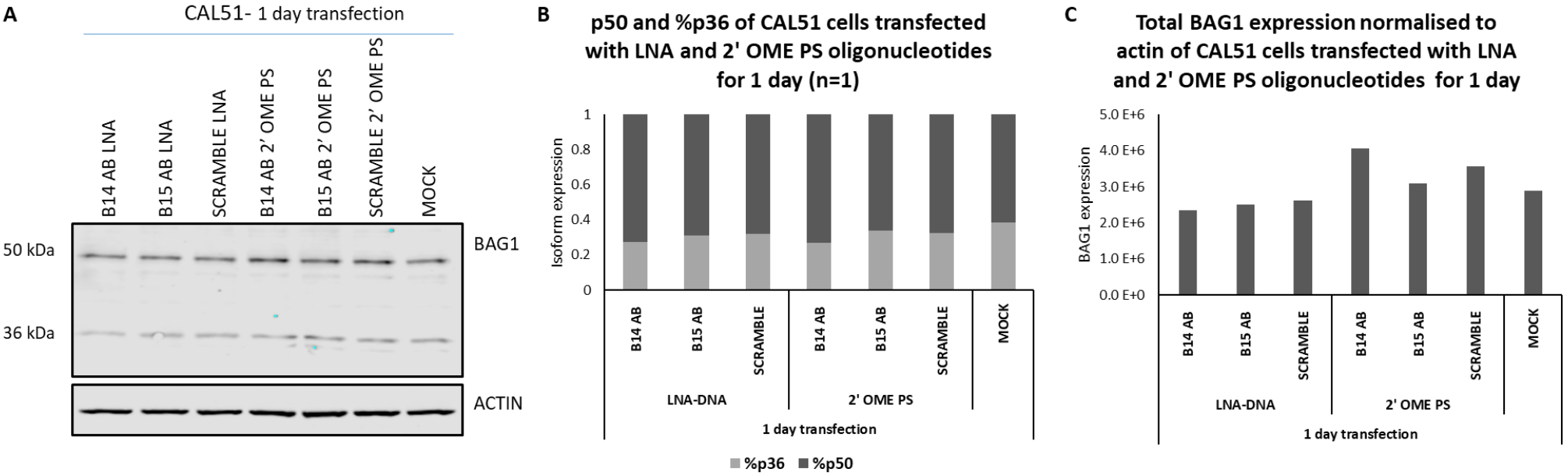

Figure E. 6 **Western Blot of CAL51 cells transfected with a final concentration of 25 nM of LNA and 2' OME PS oligonucleotides for one day** . A) Blot, B) %p50 and %p36 expression and C) total BAG1 expression normalised to actin expression.

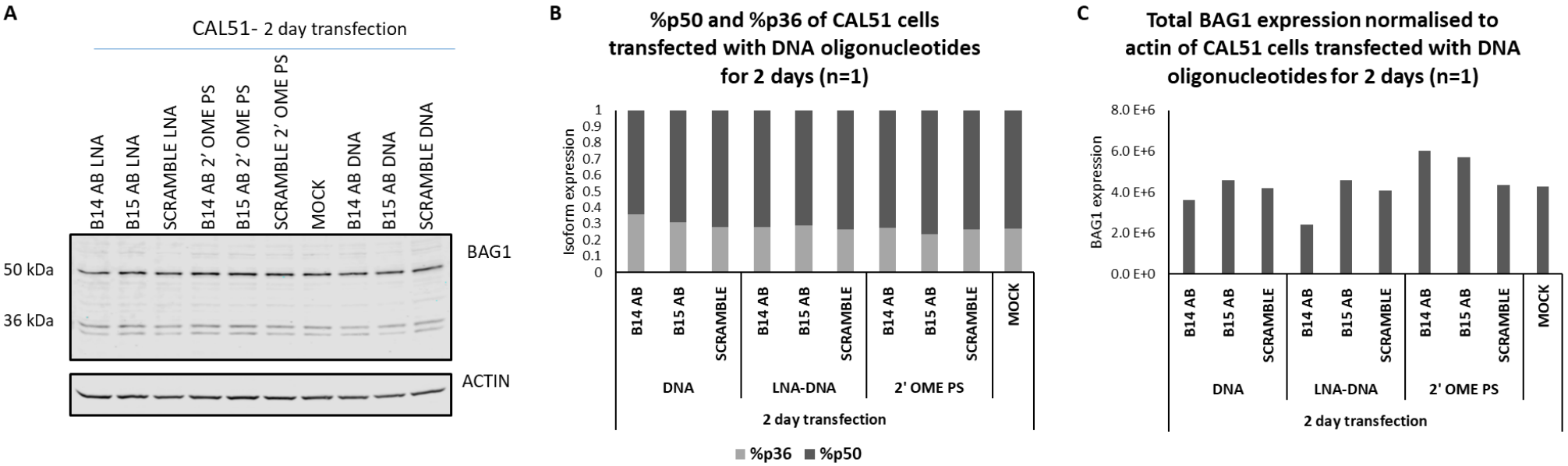

Figure E. 7 **Western Blot of CAL51 cells transfected with a final concentration of 25 nM of LNA and 2' OME PS and DNA oligonucleotides for two days** . A) Blot, B) %p50 and %p36 expression and C) total BAG1 expression normalised to actin expression.

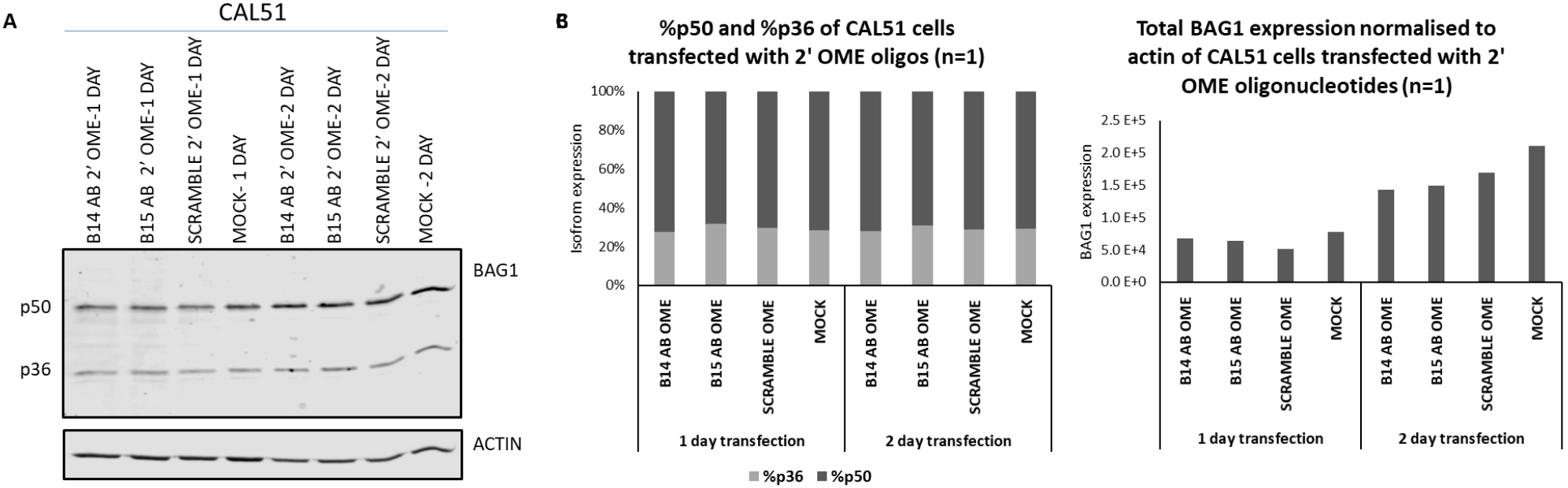

Figure E. 8 **Western Blot of CAL51 cells transfected with a final concentration of 25 nM of LNA and 2' OME oligonucleotides for one and two days** . A) Blot, B) %p50 and %p36 expression and C) total BAG1 expression normalised to actin expression.

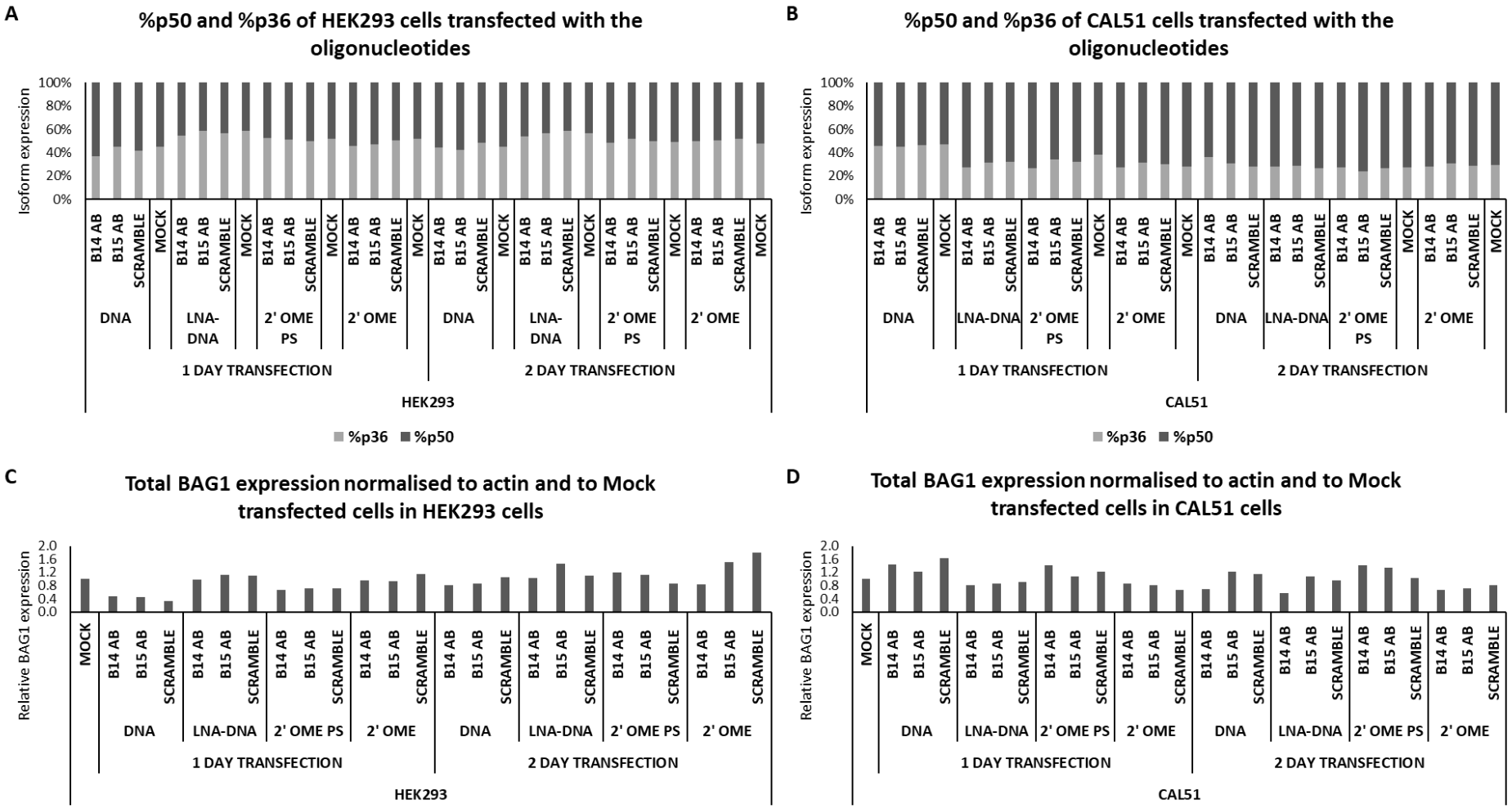

Figure E. 9 **HEK293 and CAL51 western blot quantification results, after being transfected with a final concentration of 25 nM of the oligonucleotides for one and two days.** %p36 and %p51 expression in HEK293 (A) and CAL51 (B) cells and total BAG1 expression normalised to actin, normalised to Mock transfected cells in HEK293 (C) and CAL51 (D) cells.

Bibliography

1. Crick, F. Central dogma of molecular biology. *Nature* **227,** 561–563 (1970).

2. Egli, M., Flavell, A., Pyle, A. M., Wilson, W. D., Haq, S. I., Luisi, B., Fisher, J., Laughton, C., Allen, S., Engels, J., Blackburn, G. M., Gait, M. J., Loakes, D. & Williams, D. M. *Nucleic Acids in Chemistry and Biology*. (The Royal Society of Chemistry, 2006). doi:10.1039/9781847555380

3. Shing, P. & Carter, M. DNA Structure: Alphabet Soup for the Cellular Soul. in *DNA Replication-Current Advances* (InTech, 2011). doi:10.5772/18536

4. Watson, J. D., Smith, J. D., Hamilton, L., White, J., Wyatt, G. R., F Wilkins, M. H. & Wilson, H. R. *Molecular Configuration in Sodium Thymonucleate*. *Biochim. et Bwph11s. Acta* **1,** (Cambridge Univ. Press, 1947).

5. Watson, J. D. & Crick, F. H. C. Molecular Structure of Nucleic Acids: A Structure for Deoxyribose Nucleic Acid. *Nature* **171,** 737–738 (1953).

6. Hoogsteen, K. The structure of crystals containing a hydrogen-bonded complex of 1-methylthymine and 9-methyladenine. *Acta Crystallogr.* **12,** 822–823 (1959).

7. Hoogsteen, K. The crystal and molecular structure of a hydrogen-bonded complex between 1-methylthymine and 9-methyladenine. *Acta Crystallogr.* **16,** 907–916 (1963).

8. Hodes, M. E.; Charlotte, G.; Rakoma, L.; Erwin, C. The composition of the deoxyribonucleic acid of salmon sperm. *J. Biol. Chem.* **192,** 223–230 (1951).

9. Berg, Jeremy M., John L. Tymoczko, L. S. *Biochemistry*. (2012).

10. Wang, A. H.-J., Quigley, G. J., Kolpak, F. J., Crawford, J. L., van Boom, J. H., van der Marel, G. & Rich, A. Molecular structure of a left-handed double helical DNA fragment at atomic resolution. *Nature* **282,** 680–686 (1979).

11. Berg, J. M., Tymoczko, J. L. & Stryer, L. *DNA Can Assume a Variety of Structural Forms*. (W H Freeman, 2002).

12. Nielsen, S., Yuzenkova, Y. & Zenkin, N. Mechanism of eukaryotic RNA polymerase III transcription termination. *Science (80-.).* **340,** 1577–1580 (2013).

13. Latchman, D. S. *Gene Control*. (Garland Science, 2010).

14. Mongan, N. P., Emes, R. D. & Archer, N. Detection and analysis of RNA methylation. *F1000Research* **8,** (2019).

15. Choi, J., Ieong, K. W., Demirci, H., Chen, J., Petrov, A., Prabhakar, A., O'Leary, S. E., Dominissini, D., Rechavi, G., Soltis, S. M., Ehrenberg, M. & Puglisi, J. D. N6-methyladenosine in mRNA disrupts tRNA selection and translation-elongation dynamics. *Nat. Struct. Mol. Biol.* **23,** 110–115 (2016).

16. Chen, X. Y., Zhang, J. & Zhu, J. S. The role of m6A RNA methylation in human cancer. *Molecular Cancer* **18,** (2019).

17. Lin, S., Choe, J., Du, P., Triboulet, R. & Gregory, R. I. The m6A Methyltransferase METTL3 Promotes Translation in Human Cancer Cells. *Mol. Cell* **62,** 335–345 (2016).

18. Merino, E. J., Wilkinson, K. A., Coughlan, J. L. & Weeks, K. M. RNA structure analysis at single nucleotide resolution by Selective 2'-Hydroxyl Acylation and Primer Extension (SHAPE). *J. Am. Chem. Soc.* **127,** 4223–4231 (2005).

19. Motorin, Y. & Massenet, S. RNA structure, maturation, interactions and functions. *Biochimie* **164,** 13–14 (2019).

20. Dethoff, E. A., Chugh, J., Mustoe, A. M. & Al-Hashimi, H. M. Functional complexity and regulation through RNA dynamics. *Nature* **482,** 322–330 (2012).

21. Mauger, D. M., Siegfried, N. A. & Weeks, K. M. The genetic code as expressed through relationships between mRNA structure and protein function. *FEBS Lett.* **587,** 1180–1188 (2013).

22. Lai, D., Proctor, J. R. & Meyer, I. M. On the importance of cotranscriptional RNA structure formation. *Rna* **19,** 1461–1473 (2013).

23. Woodson, S. A. Taming free energy landscapes with RNA chaperones. *RNA Biol.* **7,** 677–686 (2010).

24. Dethoff, E. A. & Weeks, K. M. Effects of Refolding on Large-Scale RNA Structure. *Biochemistry* **58,** 3069–3077 (2019).

25. Yang, X., Yang, M., Deng, H. & Ding, Y. New era of studying RNA secondary structure and its influence on gene regulation in plants. *Front. Plant Sci.* **9,** 1–7 (2018).

26. Spitale, R. C., Crisalli, P., Flynn, R. A., Torre, E. A., Kool, E. T. & Chang, H. Y. RNA SHAPE analysis in living cells. *Nat. Chem. Biol.* **9,** 18–20 (2013).

27. Van Der Velden, A. W. & Thomas, A. A. M. The role of the 5' untranslated region of an mRNA in translation regulation during development. *International Journal of Biochemistry and Cell Biology* **31,** 87–106 (1999).

28. Jansen, R. P. mRNA localization: Message on the move. *Nature Reviews Molecular Cell Biology* **2,** 247–256 (2001).

29. Bashirullah, A., Cooperstock, R. L. & Lipshitz, H. D. Spatial and temporal control of RNA stability. *Proc. Natl. Acad. Sci. U. S. A.* **98,** 7025–7028 (2001).

30. Mignone, F., Gissi, C., Liuni, S. & Pesole, G. Untranslated regions of mRNAs. *Genome Biology* **3,** (2002).

31. Kozak, M. An analysis of 5'-noncoding sequences from 699 vertebrate messenger rNAS. *Nucleic Acids Res.* **15,** 8125–8148 (1987).

32. Pesole, G., Liuni, S., Grillo, G. & Saccone, C. Structural and compositional features of untranslated regions of eukaryotic mRNAs. in *Gene* **205,** 95–102 (1997).

33. Graziano Pesolea, Flavio Mignonea, Carmela Gissia, Giorgio Grillob, Flavio Licciullib, S. L. Structural and functional features of eukaryotic mRNA untranslated regions. *Gene* **276,** 73–81 (2001).

34. Rodriguez, C. M., Chun, S. Y., Mills, R. E. & Todd, P. K. Translation of upstream open reading frames in a model of neuronal differentiation. *BMC Genomics* **20,** (2019).

35. Kozak, M. Circumstances and mechanisms of inhibition of translation by secondary structure in eucaryotic mRNAs. *Mol. Cell. Biol.* **9,** 5134–42 (1989).

36. Terenin, I. M., Smirnova, V. V., Andreev, D. E., Dmitriev, S. E. & Shatsky, I. N. A researcher's guide to the galaxy of IRESs. *Cell. Mol. Life Sci.* **74,** 1431–1455 (2017).

37. Locker, N., Chamond, N. & Sargueil, B. A conserved structure within the HIV gag open reading frame that controls translation initiation directly recruits the 40S subunit and eIF3. *Nucleic Acids Res.* **39,** 2367–2377 (2011).

38. Karginov, T. A., Pastor, D. P. H., Semler, B. L. & Gomez, C. M. Mammalian Polycistronic mRNAs and Disease. *Trends Genet.* **33,** 129–142 (2017).

39. Jodoin, R., Carrier, J. C., Rivard, N., Bisaillon, M. & Perreault, J. P. G-quadruplex located in the 5'UTR of the BAG-1 mRNA affects both its cap-dependent and cap-independent translation through global secondary structure maintenance. *Nucleic Acids Res.* **47,** 10247–

10266 (2019).

40. Millevoi, S., Moine, H. & Vagner, S. G-quadruplexes in RNA biology. *Wiley Interdisciplinary Reviews: RNA* **3,** 495–507 (2012).

41. Beaudoin, J. D. & Perreault, J. P. 5′-UTR G-quadruplex structures acting as translational repressors. *Nucleic Acids Res.* **38,** 7022–7036 (2010).

42. Bugaut, A. & Balasubramanian, S. 5′-UTR RNA G-quadruplexes: Translation regulation and targeting. *Nucleic Acids Research* **40,** 4727–4741 (2012).

43. Morris, M. J., Negishi, Y., Pazsint, C., Schonhoft, J. D. & Basu, S. An RNA G-quadruplex is essential for cap-independent translation initiation in human VEGF IRES. *J. Am. Chem. Soc.* **132,** 17831–17839 (2010).

44. Bonnal, S., Schaeffer, C., Créancier, L., Clamens, S., Moine, H., Prats, A. C. & Vagner, S. A single internal ribosome entry site containing a G quartet RNA structure drives fibroblast growth factor 2 gene expression at four alternative translation initiation codons. *J. Biol. Chem.* **278,** 39330–39336 (2003).

45. Clarke IV, T. F. & Clark, P. L. Rare codons cluster. *PLoS One* **3,** (2008).

46. Vlasova, I. A., Tahoe, N. M., Fan, D., Larsson, O., Rattenbacher, B., SternJohn, J. R., Vasdewani, J., Karypis, G., Reilly, C. S., Bitterman, P. B. & Bohjanen, P. R. Conserved GU-Rich Elements Mediate mRNA Decay by Binding to CUG-Binding Protein 1. *Mol. Cell* **29,** 263–270 (2008).

47. Holcik, M. & Sonenberg, N. Translational control in stress and apoptosis. *Nature Reviews Molecular Cell Biology* **6,** 318–327 (2005).

48. Cole, C. N. & Scarcelli, J. J. Transport of messenger RNA from the nucleus to the cytoplasm. *Curr. Opin. Cell Biol.* (2006). doi:10.1016/j.ceb.2006.04.006

49. Schmeing, T. M. & Ramakrishnan, V. What recent ribosome structures have revealed about the mechanism of translation. *Nature* **461,** 1234–1242 (2009).

50. Sonenberg, N. & Hinnebusch, A. G. Regulation of Translation Initiation in Eukaryotes: Mechanisms and Biological Targets. *Cell* **136,** 731–745 (2009).

51. Kozak, M. Regulation of translation via mRNA structure in prokaryotes and eukaryotes. *Gene* **361,** 13–37 (2005).

52. Richard J. Jackson, Christopher U.T. Hellen, and T. V. P. The mechanism of eukaryotic translation initiation and principles of its regulation. *Nat Rev Mol Cell Biol* **11(2),** 113–127 (2010).

53. Hann, S. R., King, M. W., Bentley, D. L., Anderson, C. W. & Eisenman, R. N. A non-AUG translational initiation in c-myc exon 1 generates an N-terminally distinct protein whose synthesis is disrupted in Burkitt's lymphomas. *Cell* **52,** 185–195 (1988).

54. Clements, J. M., Laz, T. M. & Sherman, F. Efficiency of translation initiation by non-AUG codons in Saccharomyces cerevisiae. *Mol. Cell. Biol.* **8,** 4533–4536 (1988).

55. Peabody, D. S. Translation initiation at non-AUG triplets in mammalian cells. *J. Biol. Chem.* **264,** 5031–5 (1989).

56. Jackson, R. J. The ATP requirement for initiation of eukaryotic translation varies according to the mRNA species. *Eur. J. Biochem.* **200,** 285–294 (1991).

57. Svitkin YV, Pause A, Haghighat A, Pyronnet S, Witherell G, Belsham GJ, S. N. The requirement for eukaryotic initiation factor 4A (eIF4A) in translation is in direct proportion to …. *RNA* 382–394 (2001).

58. Luukkonen, B. G., Tan, W. & Schwartz, S. Efficiency of reinitiation of translation on human immunodeficiency virus type 1 mRNAs is determined by the length of the upstream open reading frame and by intercistronic distance. *J. Virol.* **69,** 4086–94 (1995).

59. Kozak, M. Constraints on reinitiation of translation in mammals. *Nucleic Acids Res.* **29,** 5226–5232 (2001).

60. Rowlands, A. G., Panniers, R. & Henshaw, E. C. The catalytic mechanism of guanine nucleotide exchange factor action and competitive inhibition by phosphorylated eukaryotic initiation factor 2. *J. Biol. Chem.* **263,** 5526–33 (1988).

61. Baird, T. D., Palam, L. R., Fusakio, M. E., Willy, J. A., Davis, C. M., McClintick, J. N., Anthony, T. G. & Wek, R. C. Selective mRNA translation during eIF2 phosphorylation induces expression of IBTKα. *Mol. Biol. Cell* **25,** 1666–1675 (2014).

62. Gingras, A.-C., Raught, B. & Sonenberg, N. eIF4 Initiation Factors: Effectors of mRNA Recruitment to Ribosomes and Regulators of Translation. *Annu. Rev. Biochem.* **68,** 913–963 (1999).

63. Kozak, M. At least six nucleotides preceding the AUG initiator codon enhance translation in

mammalian cells. *J. Mol. Biol.* **196,** 947–950 (1987).

64. Kozak, M. The scanning model for translation: An update. *J. Cell Biol.* **108,** 229–241 (1989).

65. Hatzoglou, A. A. K. and M. Cellular IRES-mediated translation: the war of ITAFs in pathophysiological states. *Cell Cycle* **10:2,** 229–240 (2011).

66. Wilson, J. E., Pestova, T. V, Hellen, C. U. . & Sarnow, P. Initiation of Protein Synthesis from the A Site of the Ribosome. *Cell* **102,** 511–520 (2000).

67. Jang, S. K., Kräusslich, H. G., Nicklin, M. J., Duke, G. M., Palmenberg, A. C. & Wimmer, E. A segment of the 5' nontranslated region of encephalomyocarditis virus RNA directs internal entry of ribosomes during in vitro translation. *J. Virol.* **62,** 2636–43 (1988).

68. Pelletier, J. & Sonenberg, N. Internal initiation of translation of eukaryotic mRNA directed by a sequence derived from poliovirus RNA. *Nature* **334,** 320–325 (1988).

69. Lozano, G., Francisco-Velilla, R. & Martinez-Salas, E. Ribosome-dependent conformational flexibility changes and RNA dynamics of IRES domains revealed by differential SHAPE. *Sci. Rep.* **8,** 1–13 (2018).

70. Martinez-Salas, E., Francisco-Velilla, R., Fernandez-Chamorro, J. & Embarek, A. M. Insights into structural and mechanistic features of viral IRES elements. *Front. Microbiol.* **8,** 1–15 (2018).

71. Godet, A. C., David, F., Hantelys, F., Tatin, F., Lacazette, E., Garmy-Susini, B. & Prats, A. C. IRES Trans-Acting Factors, Key Actors of the Stress Response. *Int. J. Mol. Sci.* **20,** (2019).

72. Lu, H.-H., Wimmert, E. & Purcell, H. *Poliovirus chimeras replicating under the translational control of genetic elements of hepatitis C virus reveal unusual properties of the internal ribosomal entry site of hepatitis C virus Communicated by Robert*. **93,** (1996).

73. Wang, C., Le, S. Y., Ali, N. & Siddiqui, A. An RNA pseudoknot is an essential structural element of the internal ribosome entry site located within the hepatitis C virus 5' noncoding region. *RNA* **1,** 526–37 (1995).

74. Pestova, T. V, Shatsky, I. N., Fletcher, S. P., Jackson, R. J. & Hellen, C. U. T. *A prokaryotic-like mode of cytoplasmic eukaryotic ribosome binding to the initiation codon during internal translation initation of hepatitis C and classical swine fever virus RNAs*. (1998).

75. Costantino, D. & Kieft, J. S. A preformed compact ribosome-binding domain in the cricket paralysis-like virus IRES RNAs. *RNA* **11,** 332–343 (2005).

76. Balvay, L., Rifo, R. S., Ricci, E. P., Decimo, D. & Ohlmann, T. Structural and functional diversity of viral IRESes. *Biochim. Biophys. Acta - Gene Regul. Mech.* **1789,** 542–557 (2009).

77. Kozak, M. Leader length and secondary structure modulate mRNA function under conditions of stress. *Mol. Cell. Biol.* **8,** 2737–2744 (1988).

78. Johannes, G. & Sarnow, P. Cap-independent polysomal association of natural mRNAs encoding c-myc, BiP, and eIF4G conferred by internal ribosome entry sites. *Rna* **4,** 1500–1513 (1998).

79. Gilbert, W. V. Alternative ways to think about cellular internal ribosome entry. *J. Biol. Chem.* **285,** 29033–29038 (2010).

80. Macejak, Dennis G; Sarnow, P. *Internal initiation of translation mediated by the 5' leader of a cellular mRNA*. *12. Catterall, W. A. A. Rev. Biochem* **70,** (1984).

81. Komar, A. A. & Hatzoglou, M. Internal ribosome entry sites in cellular mRNAs: Mystery of their existence. *J. Biol. Chem.* **280,** 23425–23428 (2005).

82. Pickering, B. M., Mitchell, S. A., Spriggs, K. A., Stoneley, M. & Willis, A. E. Bag-1 internal ribosome entry segment activity is promoted by structural changes mediated by poly(rC) binding protein 1 and recruitment of polypyrimidine tract binding protein 1. *Molecular and cellular biology* **24,** 5595–605 (2004).

83. Jackson, R. J. Alternative mechanisms of initiating translation of mammalian mRNAs. *Biochem. Soc. Trans.* **33,** 1231–1241 (2005).

84. Holcik, M. & Korneluk, R. G. Functional characterization of the X-linked inhibitor of apoptosis (XIAP) internal ribosome entry site element: role of La autoantigen in XIAP translation. *Mol. Cell. Biol.* **20,** 4648–57 (2000).

85. Holcík, M., Gordon, B. W. & Korneluk, R. G. The internal ribosome entry site-mediated translation of antiapoptotic protein XIAP is modulated by the heterogeneous nuclear ribonucleoproteins C1 and C2. *Mol. Cell. Biol.* **23,** 280–8 (2003).

86. Nevins, T. A., Harder, Z. M., Korneluk, R. G. & Holčík, M. Distinct regulation of internal ribosome entry site-mediated translation following cellular stress is mediated by apoptotic fragments of eIF4G translation initiation factor family members eIF4GI and p97/DAP5/NAT1. *J. Biol. Chem.* **278,** 3572–3579 (2003).

87. Evans, J. R., Mitchell, S. a, Spriggs, K. a, Ostrowski, J., Bomsztyk, K., Ostarek, D. & Willis, A.

E. Members of the poly (rC) binding protein family stimulate the activity of the c-myc internal ribosome entry segment in vitro and in vivo. *Oncogene* **22,** 8012–8020 (2003).

88. Mitchell, S. A., Brown, E. C., Coldwell, M. J., Jackson, R. J. & Willis, A. E. Protein factor requirements of the APAF-1 internal ribosome entry segment: roles of polypyrimidine tract binding protein and upstream of N-ras. *Mol. Cell. Biol.* **21,** 3364–74 (2001).

89. Créancier, L., Morello, D., Mercier, P. & Prats, A. C. Fibroblast growth factor 2 internal ribosome entry site (IRES) activity ex vivo and in transgenic mice reveals a stringent tissue-specific regulation. *J. Cell Biol.* **150,** 275–281 (2000).

90. Prévôt, D., Darlix, J. L. & Ohlmann, T. Conducting the initiation of protein synthesis: The role of eIF4G. *Biol. Cell* **95,** 141–156 (2003).

91. Spriggs, K. A., Cobbold, L. C., Jopling, C. L., Cooper, R. E., Wilson, L. A., Stoneley, M., Coldwell, M. J., Poncet, D., Shen, Y.-C., Morley, S. J., Bushell, M. & Willis, A. E. Canonical Initiation Factor Requirements of the Myc Family of Internal Ribosome Entry Segments. *Mol. Cell. Biol.* **29,** 1565–1574 (2009).

92. Komar, A. A. & Hatzoglou, M. Cellular IRES-mediated translation: The war of ITAFs in pathophysiological states. *Cell Cycle* **10,** 229–240 (2011).

93. Pisarev, A. V, Shirokikh, N. E. & Hellen, C. U. T. Translation initiation by factor-independent binding of eukaryotic ribosomes to internal ribosomal entry sites. *C. R. Biol.* **328,** 589–605 (2005).

94. Xia, X. & Holcik, M. Strong eukaryotic IRESs have weak secondary structure. *PLoS One* **4,** 4–6 (2009).

95. Pickering, B. M., Mitchell, S. A., Evans, J. R. & Willis, A. E. Polypyrimidine tract binding protein and poly r(C) binding protein 1 interact with the BAG-1 IRES and stimulates its activity in vitro and in vivo. *Nucleic Acids Res.* **31,** 639–646 (2003).

96. Schepens, B., Tinton, S. A., Bruynooghe, Y., Parthoens, E., Haegman, M., Beyaert, R. & Cornelis, S. A role for hnRNP C1/C2 and Unr in internal initiation of translation during mitosis. *EMBO J.* **26,** 158–169 (2007).

97. Pyronnet, S., Pradayrol, L. & Sonenberg, N. A cell cycle-dependent internal ribosome entry site. *Mol. Cell* **5,** 607–616 (2000).

98. Coldwell, M. J., Cowan, J. L., Vlasak, M., Mead, A., Willett, M., Perry, L. S. & Morley, S. J.

Phosphorylation of eIF4GII and 4E-BP1 in response to nocodazole treatment: A reappraisal of translation initiation during mitosis. *Cell Cycle* **12,** 3615–3628 (2013).

99. Stoneley, M., Chappell, S. A., Jopling, C. L., Dickens, M., Farlane, M. M. A. C. & Willis, A. E. c-Myc Protein Synthesis Is Initiated from the Internal Ribosome Entry Segment during Apoptosis. *Mol. Cell. Biol.* **20,** 1162–1169 (2000).

100. Stein, I., Itin, A., Einat, P. A. Z., Skaliter, R., Grossman, Z. & Keshet, E. Translation of Vascular Endothelial Growth Factor mRNA by Internal Ribosome Entry : Implications for Translation under Hypoxia. *Mol. Cell. Biol.* **18,** 3112–3119 (1998).

101. Qin, X. & Sarnow, P. Preferential Translation of Internal Ribosome Entry Site-containing mRNAs during the Mitotic Cycle in Mammalian Cells *. *J. Biol. Chem.* **279,** 13721–13728 (2004).

102. Van Den Beucken, T., Koritzinsky, M. & Wouters, B. G. Translational control of gene expression during hypoxia. *Cancer Biology and Therapy* **5,** 749–755 (2006).

103. Hantelys, F., Godet, A.-C., David, F., Tatin, F., Renaud-Gabardos, E., Pujol, F., Diallo, L., Ader, I., Ligat, L., Henras, A. K., Sato, Y., Parini, A., Lacazette, E., Garmy-Susini, B. & Prats, A.-C. Vasohibin1, a new IRES trans-acting factor for induction of (lymph)angiogenic factors in early hypoxia. *bioRxiv* 260364 (2019). doi:10.1101/260364

104. Renaud-Gabardos, E., Tatin, F., Hantelys, F., Lebas, B., Calise, D., Kunduzova, O., Masri, B., Pujol, F., Sicard, P., Valet, P., Roncalli, J., Chaufour, X., Garmy-Susini, B., Parini, A. & Prats, A. C. Therapeutic Benefit and Gene Network Regulation by Combined Gene Transfer of Apelin, FGF2, and SERCA2a into Ischemic Heart. *Mol. Ther.* **26,** 902–916 (2018).

105. Weingarten-Gabbay, S., Elias-Kirma, S., Nir, R., Gritsenko, A. A., Stern-Ginossar, N., Yakhini, Z., Weinberger, A. & Segal, E. Systematic discovery of cap-independent translation sequences in human and viral genomes. *Science (80-.).* **351,** (2016).

106. Chappell, S. A., Lequesne, J. P. C., Paulin, F. E. M., DeSchoolmeester, M. L., Stoneley, M., Soutar, R. L., Ralston, S. H., Helfrich, M. H. & Willis, A. E. A mutation in the c-myc-IRES leads to enhanced internal ribosome entry in multiple myeloma: A novel mechanism of oncogene de-regulation. *Oncogene* **19,** 4437–4440 (2000).

107. Hudder, A. & Werner, R. Analysis of a Charcot-Marie-Tooth disease mutation reveals an essential internal ribosome entry site element in the connexin-32 gene. *J. Biol. Chem.* **275,** 34586–34591 (2000).

108. Marcel, V., Ghayad, S. E., Belin, S., Therizols, G., Morel, A. P., Solano-Gonzàlez, E., Vendrell, J. A., Hacot, S., Mertani, H. C., Albaret, M. A., Bourdon, J. C., Jordan, L., Thompson, A., Tafer, Y., Cong, R., Bouvet, P., Saurin, J. C., Catez, F., Prats, A. C., Puisieux, A. & Diaz, J. J. P53 Acts as a Safeguard of Translational Control by Regulating Fibrillarin and rRNA Methylation in Cancer. *Cancer Cell* **24,** 318–330 (2013).

109. Gehring, U. Biological activities of HAP46/BAG-1. The HAP46/BAG-1 protein: Regulator HSP70 chaperones, DNA-binding protein and stimulator of transcription. *EMBO Rep.* **5,** 148–153 (2004).

110. Kozak, M. A second look at cellular mRNA sequences said to function as internal ribosome entry sites. *Nucleic Acids Research* **33,** 6593–6602 (2005).

111. Kozak, M. Alternative ways to think about mRNA sequences and proteins that appear to promote internal initiation of translation. *Gene* **318,** 1–23 (2003).

112. Kozak, M. Lessons (not) learned from mistakes about translation. *Gene* **403,** 194–203 (2007).

113. Kozak, M. New Ways of Initiating Translation in Eukaryotes? *Mol. Cell. Biol.* **21,** 8238–8246 (2001).

114. Merrick, W. C. Cap-dependent and cap-independent translation in eukaryotic systems. *Gene* **332,** 1–11 (2004).

115. Komar, A. A. & Hatzoglou, M. Exploring internal ribosome entry sites as therapeutic targets. *Article* **5,** 1 (2015).

116. Stoneley, M. & Willis, A. E. Cellular internal ribosome entry segments: structures, trans-acting factors and regulation of gene expression. *Oncogene* **23,** 3200–3207 (2004).

117. Holcík, M. Targeting translation for treatment of cancer--a novel role for IRES? *Current cancer drug targets* **4,** 299–311 (2004).

118. Dibrov, S. M., Parsons, J., Carnevali, M., Zhou, S., Rynearson, K. D., Ding, K., Garcia Sega, E., Brunn, N. D., Boerneke, M. A., Castaldi, M. P. & Hermann, T. Hepatitis C virus translation inhibitors targeting the internal ribosomal entry site. *Journal of Medicinal Chemistry* **57,** 1694–1707 (2014).

119. Davis, D. R. & Seth, P. P. Therapeutic targeting of HCV internal ribosomal entry site RNA. *Antiviral Chemistry and Chemotherapy* **21,** 117–128 (2011).

120. Dasgupta, A., Das, S., Izumi, R., Venkatesan, A. & Barat, B. Targeting internal ribosome entry site (IRES)-mediated translation to block hepatitis C and other RNA viruses. *FEMS Microbiol. Lett.* **234,** 189–199 (2004).

121. Nulf, C. J. & Corey, D. Intracellular inhibition of hepatitis C virus (HCV) internal ribosomal entry site (IRES)-dependent translation by peptide nucleic acids (PNAs) and locked nucleic acids (LNAs). *Nucleic Acids Res.* **32,** 3792–3798 (2004).

122. Martinand-Mari, C., Lebleu, B. & Robbins, I. Oligonucleotide-based Strategies to Inhibit Human Hepatitis C Virus. *Oligonucleotides* **13,** 539–548 (2003).

123. Gallego, J. & Varani, G. The hepatitis C virus internal ribosome-entry site: a new target for antiviral research. *Biochem. Soc. Trans.* **30,** 140–5 (2002).

124. Jubin, R. Hepatitis C IRES: translating translation into a therapeutic target. *Curr. Opin. Mol. Ther.* **3,** 278–87 (2001).

125. Wakita, T. & Wands, J. R. Specific inhibition of hepatitis C virus expression by antisense oligodeoxynucleotides. In vitro model for selection of target sequence. *J. Biol. Chem.* **269,** 14205–14210 (1994).

126. Hanecak, R., Brown-Driver, V., Fox, M. C., Azad, R. F., Furusako, S., Nozaki, † Chikateru, Ford, C., Sasmor, ‡ Henri & Anderson, K. P. *Antisense Oligonucleotide Inhibition of Hepatitis C Virus Gene Expression in Transformed Hepatocytes Downloaded from*. *JOURNAL OF VIROLOGY* **70,** (1996).

127. Stone, J. K., Rijnbrand, R., Stein, D. A., Ma, Y., Yang, Y., Iversen, P. L. & Andino, R. A morpholino oligomer targeting highly conserved internal ribosome entry site sequence is able to inhibit multiple species of picornavirus. *Antimicrob. Agents Chemother.* **52,** 1970–1981 (2008).

128. Lin, M. V., King, L. Y. & Chung, R. T. Hepatitis C Virus–Associated Cancer. *Annu. Rev. Pathol. Mech. Dis.* **10,** 345–370 (2015).

129. Subramanian, N., Mani, P., Roy, S., Gnanasundram, S. V., Sarkar, D. P. & Das, S. Targeted delivery of hepatitis C virus-specific short hairpin RNA in mouse liver using Sendai virosomes. *J. Gen. Virol.* **90,** 1812–1819 (2009).

130. Kanda, T., Steele, R., Ray, R. & Ray, R. B. Small interfering RNA targeted to hepatitis C virus 5’ nontranslated region exerts potent antiviral effect. *J. Virol.* **81,** 669–76 (2007).

131. Shi, Y., Yang, Y., Hoang, B., Bardeleben, C., Holmes, B., Gera, J. & Lichtenstein, A. Therapeutic potential of targeting IRES-dependent c-myc translation in multiple myeloma cells during ER stress. *Oncogene* **35,** 1015–1024 (2016).

132. Du, X., Wang, J., Zhu, H., Rinaldo, L., Lamar, K. M., Palmenberg, A. C., Hansel, C. & Gomez, C. M. Second cistron in CACNA1A gene encodes a transcription factor mediating cerebellar development and SCA6. *Cell* **154,** 118 (2013).

133. Pastor, P. D. H., Du, X., Fazal, S., Davies, A. N. & Gomez, C. M. Targeting the CACNA1A IRES as a Treatment for Spinocerebellar Ataxia Type 6. *Cerebellum* **17,** 72–77 (2018).

134. Vaklavas, C., Meng, Z., Choi, H., Grizzle, W. E., Zinn, K. R. & Blume, S. W. Small molecule inhibitors of IRES-mediated translation. *Cancer Biol. Ther.* **16,** 1471–1485 (2015).

135. Takayama, S., Sato, T., Krajewski, S., Kochel, K., Irie, S., Millan, J. A. & Reed, J. C. Cloning and Functional Analysis of BAG-l : A Novel BCL2-Binding Protein with Anti-Cell Death Activity. *Cell* **80,** 279–284 (1995).

136. Zeiner, Matfhias & Gehring, U. A protein that interacts with members of the nuclear hormone receptor family : Identification and cDNA cloning. *pRoc. Natl. Acad. Sci. USA* **92,** 11465–11469 (1995).

137. Takayama, S., Bimston, D. N., Matsuzawa, S., Freeman, B. C., Aime-sempe, C., Xie, Z., Morimoto, R. I. & Reed, J. C. BAG-1 modulates the chaperone activity of Hsp70 / Hsc70. *EMBO J.* **16,** 4887–4896 (1997).

138. Wang, H., Rapp, U. R. & Reed, J. C. BCL2 Targets the Protein Kinase Raf-1 to Mitochondria. *Cell* **87,** 629–638 (1996).

139. Zeiner M., N. Y. & & Gehring U. The hsp70-associating protein Hap46 binds to DNA and and stimulates transcription. *Biol. Cell* **96,** 10194–10199 (1999).

140. Bardelli, A., Longati, P., Albero, D., Goruppi, S., Schneider, C., Ponzetto, C. & Comoglio, P. M. HGF receptor associates with the anti-apoptotic protein BAG-1 and prevents cell death. *EMBO J.* **15,** 6205–6212 (1996).

141. Townsend, P. A., Cutress, R. I., Sharp, A., Brimmell, M. & Packham, G. BAG-1 : a multifunctional regulator of cell growth and survival. *Biochim. Biophys. Acta* **1603,** 83–98 (2003).

142. Townsend, P. A., Stephanou, A., Packham, G. & Latchman, D. S. BAG-1: A multi-functional

pro-survival molecule. *Int. J. Biochem. Cell Biol.* **37,** 251–259 (2005).

143. Yang, X., Chernenko, G., Hao, Y., Ding, Z., Pater, M. M., Pater, A. & Tang, S. Human BAG-1 / RAP46 protein is generated as four isoforms by alternative translation initiation and overexpressed in cancer cells. *Oncogene* **17,** 981–989 (1998).

144. Coldwell, M. J., deSchoolmeester, M. L., Fraser, G. a, Pickering, B. M., Packham, G. & Willis, a E. The p36 isoform of BAG-1 is translated by internal ribosome entry following heat shock. *Oncogene* **20,** 4095–100 (2001).

145. Homo sapiens BAG cochaperone 1 (BAG1), transcript variant 1, mRNA - Nucleotide - NCBI. Available at: https://www.ncbi.nlm.nih.gov/nuccore/NM_004323.6. (Accessed: 21st March 2020)

146. Packham, G., Brimmell, M. & Cleveland, J. L. Mammalian cells express two differently localized Bag-1 isoforms generated by alternative translation initiation. *Biochem. J.* **813,** 807–813 (1997).

147. Takayama, S., Krajewski, S., Krajewska, M., Kitada, S., Zapata, J. M., Kochel, K., Knee, D., Scudiero, D., Tudor, G., Miller, G. J., Miyashita, T., Yamada, M. & Reed, J. C. Expression and Location of Hsp70 / Hsc-Binding Anti-Apoptotic Protein BAG-1 and Its Variants in Normal Tissues and Tumor Cell Lines1. *CANCER Res.* **58,** 3116–3131 (1998).

148. Schmidt, U., Wochnik, G. M., Rosenhagen, M. C., Young, J. C., Hartl, F. U., Holsboer, F. & Rein, T. Essential role of the unusual DNA-binding motif of BAG-1 for inhibition of the glucocorticoid receptor. *J. Biol. Chem.* **278,** 4926–4931 (2003).

149. Yang, X., Hao, Y. & Ding, Z. Differential Expression of Antiapoptotic Gene BAG-1 in Human Breast Normal and Cancer Cell Lines and Tissues Differential Expression of Antiapoptotic Gene BAG-1 in Human Breast Normal and Cancer Cell Lines and Tissues 1. *Clin. Cancer Res.* **5,** 1816–1822 (1999).

150. Niyaz, Y., Zeiner, M. & Gehring, U. Transcriptional activation by the human Hsp70-associating protein Hap50. *J. Cell Sci.* **114,** 1839–45 (2001).

151. Alberti, S., Esser, C. & Höhfeld, J. BAG-1—a nucleotide exchange factor of Hsc70 with multiple cellular functions. *Cell Stress Chaperones* **8,** 225 (2003).

152. Wang, H.-G., Takayama, S., Ra, U. R., Reed, J. C. & Vogt, P. K. *BCL2 interacting protein, BAG-1, binds to and activates the kinase Raf-1 Communicated by*. *Cell Biology* **93,** (1996).

153. Song, J., Takeda, M. & Morimoto, R. I. Bag1-Hsp 70 mediates a physiological stress signalling pathway that regulates Raf-1/ERK and cell growth. *Nat. Cell Biol.* **3,** 276–282 (2001).

154. Elmore, S. Apoptosis: A Review of Programmed Cell Death. *Toxicologic Pathology* **35,** 495–516 (2007).

155. Clevenger, C. V., Thickman, K., Ngo, W., Chang, W. P., Takayama, S. & Reed, J. C. Role of Bag-1 in the survival and proliferation of the cytokine- dependent lymphocyte lines, Ba/F3 and Nb2. *Mol. Endocrinol.* **11,** 608–618 (1997).

156. Oorschot, A. A. A. M. D., Hollander, A. I. Den, Danen-van Oorschot, A. A. A. M., den Hollander, A. I., Takayama, S., Reed, J. C., van der Eb, A. J. & Noteborn, M. H. M. BAG-1 inhibits p53-induced but not apoptin-induced apoptosis. *Apoptosis* **2,** 395–402 (1997).

157. Tang, B. S., Shaheta, N., Chernenko, G., Khalifa, M. & Wang, X. Expression of BAG-1 in invasive breast carcinomas. *J. Clin. Oncol.* **17,** 1710–1719 (1999).

158. Townsend, P. A., Cutress, R. I., Sharp, A., Brimmell, M. & Packham, G. BAG-1 Prevents Stress-induced Long-term Growth Inhibition in Breast Cancer Cells via a Chaperone-dependent Pathway 1. *CANCER Res.* **63,** 4150–4157 (2003).

159. Terada, S., Fukuoka, K., Fujita, T., Komatsu, T., Takayama, S., Reed, J. C. & Suzuki, E. Anti-apoptotic genes, bag-1 and BCL2, enabled hybridoma cells to survive under treatment for arresting cell cycle. *Cytotechnology* **25,** 17–23 (1997).

160. Tang, S., Beck, J., Murphy, S., Chernenko, G., Robb, D., Watson, P. & Khalifa, M. BAG-1 Expression Correlates with BCL2, p53, Differentiation, Estrogen and Progesterone Receptors in Invasive Breast Carcinoma. *Breast Cancer Res. Treat.* 203–213 (2004).

161. Kilbas, P. O., Akcay, I. M., Doganay, G. D. & Arisan, E. D. Bag-1 silencing enhanced chemotherapeutic drug-induced apoptosis in MCF-7 breast cancer cells affecting PI3K/Akt/mTOR and MAPK signaling pathways. *Mol. Biol. Rep.* **46,** 847–860 (2019).

162. Liu, H., Lu, S., Gu, L., Gao, Y., Wang, T., Zhao, J., Rao, J., Chen, J., Hao, X. & Tang, S. C. Modulation of BAG-1 expression alters the sensitivity of breast cancer cells to tamoxifen. *Cell. Physiol. Biochem.* **33,** 365–374 (2014).

163. Papadakis, E., Robson, N., Yeomans, A., Bailey, S., Laversin, S., Beers, S., Emre Sayan, A., Ashton-Key, M., Schwaiger, S., Stuppner, H., Troppmair, J., Packham, G. & Cutress, R. A combination of trastuzumab and BAG-1 inhibition synergistically targets HER2 positive

breast cancer cells. *Oncotarget* **7,** 18851–18864 (2016).

164. Clemo, N. K., Collard, T. J., Southern, S. L., Edwards, K. D., Moorghen, M., Packham, G., Hague, A., Paraskeva, C. & Williams, A. C. BAG-1 is up-regulated in colorectal tumour progression and promotes colorectal tumour cell survival through increased NF-κB activity. *Carcinogenesis* **29,** 849–857 (2008).

165. Southern, S. L., Collard, T. J., Urban, B. C., Skeen, V. R., Smartt, H. J., Hague, A., Oakley, F., Townsend, P. A., Perkins, N. D., Paraskeva, C. & Williams, A. C. BAG-1 interacts with the p50-p50 homodimeric NF-B complex: Implications for colorectal carcinogenesis. *Oncogene* **31,** 2761–2772 (2012).

166. Skeen, V. R., Collard, T. J., Southern, S. L., Greenhough, A., Hague, A., Townsend, P. A., Paraskeva, C. & Williams, A. C. BAG-1 suppresses expression of the key regulatory cytokine transforming growth factor β (TGF-β1) in colorectal tumour cells. *Oncogene* **32,** 4490–4499 (2013).

167. Barnes, J. D., Arhel, N. J., Lee, S. S., Sharp, A., Al-Okail, M., Packham, G., Hague, A., Paraskeva, C. & Williams, A. C. Nuclear BAG-1 expression inhibits apoptosis in colorectal adenoma-derived epithelial cells. *Apoptosis* **10,** 301–311 (2005).

168. Kikuchi, R., Noguchi, T., Takeno, S., Funada, Y., Moriyama, H. & Uchida, Y. Nuclear BAG-1 expression reflects malignant potential in colorectal carcinomas. *Br. J. Cancer* **87,** 1136–1139 (2002).

169. Huang, W., Liu, Z., Zhou, G., Ling, J. & Tian, A. Silencing Bag-1 gene via magnetic gold nanoparticle-delivered siRNA plasmid for colorectal cancer therapy in vivo and in vitro. *Tumor Biol.* 10365–10374 (2016). doi:10.1007/s13277-016-4926-0

170. Stewart, J. D., Cowan, J. L., Perry, L. S., Coldwell, M. J. & Proud, C. G. ABC50 mutants modify translation start codon selection. *Biochem. J.* **467,** 217–229 (2015).

171. Wegrzyn, J. L., Drudge, T. M., Valafar, F. & Hook, V. Bioinformatic analyses of mammalian 5'-UTR sequence properties of mRNAs predicts alternative translation initiation sites. *BMC Bioinformatics* **9,** 1–16 (2008).

172. Stoneley, M., Subkhankulova, T., Le Quesne, J. P., Coldwell, M. J., Jopling, C. L., Belsham, G. J. & Willis, A. E. Analysis of the c-myc IRES; a potential role for cell-type specific trans-acting factors and the nuclear compartment. *Nucleic Acids Res.* **28,** 687–94 (2000).

173. Coldwell, M. J., Mitchell, S. a, Stoneley, M., MacFarlane, M. & Willis, a E. Initiation of

APAF-1 translation by internal ribosome entry. *Oncogene* **19,** 899–905 (2000).

174. Jodoin, R., Bauer, L., Garant, J. M., Laaref, A. M., Phaneuf, F. & Perreault, J. P. The folding of 5'-UTR human G-quadruplexes possessing a long central loop. *RNA* **20,** 1129–1141 (2014).

175. MacLeod, A. R. & Crooke, S. T. RNA Therapeutics in Oncology: Advances, Challenges, and Future Directions. *J. Clin. Pharmacol.* **57,** S43–S59 (2017).

176. Paterson, B. M., Robertst, B. E. & Kuff, E. L. Structural gene identification and mapping by DNA * mRNA hybrid-arrested cell-free translation. *Proc. Natl. Acad. Sci. U. S. A.* **74,** 4370–4374 (1977).

177. Zamecnik, P. C. & Stephenson, M. L. Inhibition of Rous sarcoma virus replication and cell transformation by a specific oligodeoxynucleotide. *Proc. Natl. Acad. Sci. U. S. A.* **75,** 280–284 (1978).

178. Vickers, T. A. & Crooke, S. T. The rates of the major steps in the molecular mechanism of RNase H1-dependent antisense oligonucleotide induced degradation of RNA. *Nucleic Acids Res.* **43,** 8955–8963 (2015).

179. Baker, B. F., Lot, S. S., Condon, T. P., Cheng-Flournoy, S., Lesnik, E. A., Sasmor, H. M. & Bennett, C. F. 2'-O-(2-methoxy)ethyl-modified anti-intercellular adhesion molecule 1 (ICAM-1) oligonucleotides selectively increase the ICAM-1 mRNA level and inhibit formation of the ICAM-1 translation initiation complex in human umbilical vein endothelial cells. *J. Biol. Chem.* **272,** 11994–12000 (1997).

180. Faria, M., Spiller, D. G., Dubertret, C., Nelson, J. S., White, M. R. H., Scherman, D., Hélène, C. & Giovannangeli, C. Phosphormidate oligonucleotides as potent antisense molecules in cells and in vivo. *Nat. Biotechnol.* **19,** 40–44 (2001).

181. Vickers, Timothy A.; Wyatt, R. Jacqueine; Burckin, Todd; Bennett, C. Frank; Freier, S. M. Fully modified 2' MOE oligonucleotides redirect polyadenylation. *Nucleic Acids Res.* **29,** 1293–1299 (2001).

182. Havens, M. A. & Hastings, M. L. Splice-switching antisense oligonucleotides as therapeutic drugs. *Nucleic Acids Research* **44,** 6549–6563 (2016).

183. Singh, N. N., Luo, D. & Singh, R. N. Pre-mRNA Splicing Modulation by Antisense Oligonucleotides. in *Methods in Molecular Biology* **1828,** 415–437 (Humana Press Inc., 2018).

184. Liang, X., Shen, W., Sun, H., Migawa, M. T., Vickers, T. A. & Crooke, S. T. Translation efficiency of mRNAs is increased by antisense oligonucleotides targeting upstream open reading frames. *Nat. Biotechnol.* **34,** 875–880 (2016).

185. Master, A., Wójcicka, A., Gizewska, K., Popławski, P., Williams, G. R. & Nauman, A. A novel method for gene-specific enhancement of protein translation by targeting 5'UTRs of selected tumor suppressors. *PLoS One* **11,** 1–23 (2016).

186. Rouleau, S. G., Beaudoin, J. D., Bisaillon, M. & Perreault, J. P. Small antisense oligonucleotides against G-quadruplexes: Specific mRNA translational switches. *Nucleic Acids Res.* **43,** 595–606 (2015).

187. Gagnon, K. T. & Corey, D. R. Guidelines for Experiments Using Antisense Oligonucleotides and Double-Stranded RNAs. *Nucleic Acid Ther.* **00,** 1–7 (2019).

188. Lipinski, C. A. Drug-like properties and the causes of poor solubility and poor permeability. *J. Pharmacol. Toxicol. Methods* **44,** 235–249 (2000).

189. Greene, C. M. *MicroRNAs and other non-coding RNAs in inflammation*. *MicroRNAs and Other Non-Coding RNAs in Inflammation* (Springer International Publishing, 2015). doi:10.1007/978-3-319-13689-9

190. Koziolkiewicz, M., Gendaszewska, E., Maszewska, M., Stein, C. A. & Stec, W. J. The mononucleotide-dependent, nonantisense mechanism of action of phosphodiester and phosphorothioate oligonucleotides depends upon the activity of an ecto-5'-nucleotidase. *Blood* **98,** 995–1002 (2001).

191. Vaerman, J. L., Moureau, P., Deldime, F., Lewalle, P., Lammineur, C., Morschhauser, F. & Martiat, P. Antisense oligodeoxyribonucleotides suppress hematologic cell growth through stepwise release of deoxyribonucleotides. *Blood* **90,** 331–339 (1997).

192. Milligan, J. F., Matteucci, M. D. & Martin, J. C. Current Concepts in Antisense Drug Design. *J. Med. Chem.* **36,** 1923–1937 (1993).

193. Kára, J. & Duschinsky, R. Inhibition of thymidylate kinase and DNA synthesis in HeLa cells by 5'-deoxythymidine. *BBA Sect. Nucleic Acids Protein Synth.* **186,** 223–225 (1969).

194. Frazier, K. S. Antisense Oligonucleotide Therapies: The Promise and the Chanllenges from a Toxicologic Pathologist's Perspective. *Toxicol. Pathol.* **43,** 78–89 (2015).

195. Guvakova, M. A., Yakubov, L. A., Vlodavsky, I., Tonkinson, J. L. & Stein, C. A.

Phosphorothioate oligodeoxynucleotides bind to basic fibroblast growth factor, inhibit its binding to cell surface receptors, and remove it from low affinity binding sites on extracellular matrix. *J. Biol. Chem.* **270,** 2620–7 (1995).

196. Chan, J. H. P., Lim, S. & Wong, W. S. F. Antisense oligonucleotides: From design to therapeutic application. *Clin. Exp. Pharmacol. Physiol.* **33,** 533–540 (2006).

197. Eckstein, F. Phosphorothioates, essential components of therapeutic oligonucleotides. *Nucleic Acid Therapeutics* **24,** 374–387 (2014).

198. Stec, W. J., Zon, G., Egan, W. & Stec, B. Automated Solid-Phase Synthesis, Separation, and Stereochemistry of Phosphorothioate Analogues of Oligodeoxyribonucleotides. *J. Am. Chem. Soc.* **106,** 6077–6079 (1984).

199. Oka, N., Yamamoto, M., Sato, T. & Wada, T. Solid-phase synthesis of stereoregular oligodeoxyribonucleoside phosphorothioates using bicyclic oxazaphospholidine derivatives as monomer units. *J. Am. Chem. Soc.* **130,** 16031–16037 (2008).

200. Stec, W. J., Karwowski, B., Boczkowska, M., Guga, P., Koziołkiewicz, M., Sochacki, M., Wieczorek, M. W. & Błaszczyk, J. Deoxyribonucleoside 3'-O-(2-thio- and 2-oxo-'spiro'-4,4-pentamethylene- 1,3,2-oxathiaphospholane)s: Monomers for stereocontrolled synthesis of oligo(deoxyribonucleoside phosphorothioate)s and chimeric PS/PO oligonucleotides. *J. Am. Chem. Soc.* **120,** 7156–7167 (1998).

201. Boczkowska, M., Guga, P. & Stec, W. J. Stereodefined phosphorothioate analogues of DNA: Relative thermodynamic stability of the model PS-DNA/DNA and PS-DNA/RNA complexes. *Biochemistry* **41,** 12483–12487 (2002).

202. Koziolkiewicz, M., Krakowiak, A., Kwinkowski, M., Boczkowska, M. & Stec, W. J. Stereodifferentiation-the effect of P chirality of oligo (nucleoside phosphorothioates) on the activity of bacterial RNase H. *Nucleic Acids Res.* **23,** 5000–5005 (1995).

203. Stec, W. J., Cierniewski, C. S., Okruszek, A., Kobylańska, A., Pawłowska, Z., Koziołkiewicz, M., Pluskota, E., Maciaszek, A., Rebowska, B. & Stasiak, M. Stereodependent inhibition of plasminogen activator inhibitor type 1 by phosphorothioate oligonucleotides: proof of sequence specificity in cell culture and in vivo rat experiments. *Antisense Nucleic Acid Drug Dev.* **7,** 567–73 (1997).

204. Rockwell, P., O'Connor, W. J., King, K., Goldstein, N. I., Zhang, L. M. & Stein, C. A. Cell-surface perturbations of the epidermal growth factor and vascular endothelial growth

factor receptors by phosphorothioate oligodeoxynucleotides. *Proc. Natl. Acad. Sci. U. S. A.* **94,** 6523–6528 (1997).

205. Stein, C. A., Tonkinson, J. L., Zhang, L. M., Yakubov, L., Gervasoni, J., Taub, R. & Rotenberg, S. A. Dynamics of the internalization of phosphodiester oligodeoxynucleotides in HL60 cells. *Biochemistry* **32,** 4855–61 (1993).

206. Stein, C. A. The experimental use of antisense oligonucleotides : a guide for the perplexed. **108,** 641–644 (2001).

207. Stein, C. A., Hansen, J. B., Lai, J., Wu, S. J., Voskresenskiy, A., Høg, A., Worm, J., Hedtjärn, M., Souleimanian, N., Miller, P., Soifer, H. S., Castanotto, D., Benimetskaya, L., ørum, H. & Koch, T. Efficient gene silencing by delivery of locked nucleic acid antisense oligonucleotides, unassisted by transfection reagents. *Nucleic Acids Res.* **38,** (2009).

208. de Smet, M. D., Meenken, C. J. & van den Horn, G. J. Fomivirsen - a phosphorothioate oligonucleotide for the treatment of CMV retinitis. *Ocul. Immunol. Inflamm.* **7,** 189–198 (1999).

209. Venkateswarlu, D., Lind, K. E., Mohan, V., Manoharan, M. & Ferguson, D. M. *Structural properties of DNA:RNA duplexes containing 2′-O-methyl and 2′-S-methyl substitutions: a molecular dynamics investigation*. *Nucleic Acids Research* **27,** (1999).

210. Agrawal, S. & Goodchild, J. Oligodeoxynucleoside methylphosphonates: synthesis and enzymic degradation. *Tetrahedron Lett.* **28,** 3539–3542 (1987).

211. Giles, R. V & Tidd, D. M. *Increased specificity for antisense oligodeoxynucleotide targeting of RNA cleavage by RNase H using chimeric methylphosphonodiester/phosphodiester structures*. *Nucleic Acids Research* **20,** (1992).

212. Dias, N. & Stein, C. a. Antisense Oligonucleotides : Basic Concepts and Mechanisms. *Mol. Cancer Ther.* **1,** 347–355 (2002).

213. Shen, X. & Corey, D. R. Chemistry , mechanism and clinical status of antisense oligonucleotides and duplex RNAs. **46,** 1584–1600 (2019).

214. An ASO modification that enhances nuclease resistance, lowers toxicity, and increases binding affinity. Available at: https://www.idtdna.com/pages/education/decoded/article/an-aso-modification-that-enhances-nuclease-resistance-lowers-toxicity-and-increases-binding-affinity. (Accessed: 4th October 2019)

215. Liang, X. H., Sun, H., Shen, W., Wang, S., Yao, J., Migawa, M. T., Bui, H. H., Damle, S. S., Riney, S., Graham, M. J., Crooke, R. M. & Crooke, S. T. Antisense oligonucleotides targeting translation inhibitory elements in 5' UTRs can selectively increase protein levels. *Nucleic acids research* **45,** 9528–9546 (2017).

216. Bronson, J., Black, A., Dhar, M., Ellsworth, B. & Robert Merritt, J. To Market, To Market—2013. *Annu. Rep. Med. Chem.* **49,** 437–508 (2014).

217. Nielsen, P., Egholm, M., Berg, R. & Buchardt, O. Sequence-selective recognition of DNA by strand displacement with a thymine-substituted polyamide. *Science (80-.).* **254,** 1497–1500 (1991).

218. Mologni, L., Nielsen, P. E. & Gambacorti-Passerini, C. In vitro transcriptional and translational block of the BCL2 gene operated by peptide nucleic acid. *Biochem. Biophys. Res. Commun.* **264,** 537–543 (1999).

219. Summerton, J. E. Morpholinos and PNAs Compared. in *Peptide Nucleic Acids, Morpholinos and Related Antisense Biomolecules* 89–113 (Springer US). doi:10.1007/0-387-32956-0_6

220. Gryaznov, S. & Chen, J. K. Oligodeoxyribonucleotide N3'→P5' Phosphoramidates: Synthesis and Hybridization Properties. *J. Am. Chem. Soc.* **116,** 3143–3144 (1994).

221. Gryaznov, S. M. Oligonucleotide N3'→P5' phosphoramidates as potential therapeutic agents. *Biochimica et Biophysica Acta - Gene Structure and Expression* **1489,** 131–140 (1999).

222. Gryaznov, S., Skorski, T., Cucco, C., Nieborowska-Skorska, M., Ying Chiu, C., Lloyd, D., Chen, J.-K., Koziolkiewicz, M. & Calabretta, B. *Oligonucleotide N3'!P5' phosphoramidates as antisense agents*. *Nucleic Acids Research* **24,** (Oxford University Press, 1996).

223. Braasch, D. a & Corey, D. R. Locked nucleic acid (LNA): fine-tuning the recognition of DNA and RNA. *Chem. Biol.* **8,** 1–7 (2001).

224. Petersen, M., Nielsen, C. B., Nielsen, K. E., Jensen, G. A., Bondensgaard, K., Singh, S. K., Rajwanshi, V. K., Koshkin, A. A., Dahl, B. M., Wengel, J. & Jacobsen, J. P. The conformations of locked nucleic acids (LNA). *J. Mol. Recognit.* **13,** 44–53

225. Kurreck, J., Wyszko, E., Gillen, C. & Erdmann, V. a. Design of antisense oligonucleotides stabilized by locked nucleic acids. *Nucleic Acids Res.* **30,** 1911–1918 (2002).

226. Petersen, M. & Wengel, J. LNA: A versatile tool for therapeutics and genomics. *Trends*

Biotechnol. **21,** 74–81 (2003).

227. Darfeuille, F., Hansen, J. B., Orum, H., Di Primo, C. & Toulmé, J. J. LNA/DNA chimeric oligomers mimic RNA aptamers targeted to the TAR RNA element of HIV-1. *Nucleic Acids Res.* **32,** 3101–3107 (2004).

228. Grünweller, A., Grünweller, G. & Hartmann, R. K. Locked Nucleic Acid Oligonucleotides: The Next Generation of... : BioDrugs. *Biodrugs* **21,** 235–243 (2007).

229. Wahlestedt, C., Salmi, P., Good, L., Kela, J., Johnsson, T., Hökfelt, T., Broberger, C., Porreca, F., Lai, J., Ren, K., Ossipov, M., Koshkin, A., Jakobsen, N., Skouv, J., Oerum, H., Jacobsen, M. H. & Wengel, J. Potent and nontoxic antisense oligonucleotides containing locked nucleic acids. *Proc. Natl. Acad. Sci. U. S. A.* **97,** 5633–5638 (2000).

230. Grünweller, A., Wyszko, E., Bieber, B., Jahnel, R., Erdmann, V. A. & Kurreck, J. Comparison of different antisense strategies in mammalian cells using locked nucleic acids, 2'-O-methyl RNA, phosphorothioates and small interfering RNA. *Nucleic Acids Res.* **31,** 3185–3193 (2003).

231. Swayze, E. E., Siwkowski, A. M., Wancewicz, E. V, Migawa, M. T., Wyrzykiewicz, T. K., Hung, G., Monia, B. P. & Bennett, C. F. Antisense oligonucleotides containing locked nucleic acid improve potency but cause significant hepatotoxicity in animals. doi:10.1093/nar/gkl1071

232. Tabernero, J., Shapiro, G. I., LoRusso, P. M., Cervantes, A., Schwartz, G. K., Weiss, G. J., Paz-Ares, L., Cho, D. C., Infante, J. R., Alsina, M., Gounder, M. M., Falzone, R., Harrop, J., White, A. C. S., Toudjarska, I., Bumcrot, D., Meyers, R. E., Hinkle, G., Svrzikapa, N., Hutabarat, R. M., Clausen, V. A., Cehelsky, J., Nochur, S. V., Gamba-Vitalo, C., Vaishnaw, A. K., Sah, D. W. Y., Gollob, J. A. & Burris, H. A. First-in-humans trial of an RNA interference therapeutic targeting VEGF and KSP in cancer patients with liver involvement. *Cancer Discov.* **3,** 406–417 (2013).

233. Bader, A. G., Brown, D., Stoudemire, J. & Lammers, P. Developing therapeutic microRNAs for cancer. *Gene Ther.* **18,** 1121–1126 (2011).

234. Lam, J. K. W., Chow, M. Y. T., Zhang, Y. & Leung, S. W. S. siRNA Versus miRNA as Therapeutics for Gene Silencing. *Mol. Ther. - Nucleic Acids* **4,** e252 (2015).

235. Bernstein, E., Caudy, A. A., Hammond, S. M. & Hannon, G. J. Role for a bidentate ribonuclease in the initiation step of RNA interference. *Nature* **409,** 363–366 (2001).

236. Hammond, S. M., Bernstein, E., Beach, D. & Hannon, G. J. An RNA-directed nuclease

mediates post-transcriptional gene silencing in Drosophila cells. *Nature* **404,** 293–296 (2000).

237. Song, J. J., Smith, S. K., Hannon, G. J. & Joshua-Tor, L. Crystal structure of argonaute and its implications for RISC slicer activity. *Science (80-.).* **305,** 1434–1437 (2004).

238. Zamore, P. D., Tuschl, T., Sharp, P. A. & Bartel, D. P. RNAi: Double-Stranded RNA Directs the ATP-Dependent Cleavage of mRNA at 21 to 23 Nucleotide Intervals. **101,** 25–33 (2000).

239. Meister, G., Landthaler, M., Patkaniowska, A., Dorsett, Y., Teng, G. & Tuschl, T. Human Argonaute2 mediates RNA cleavage targeted by miRNAs and siRNAs. *Mol. Cell* **15,** 185–197 (2004).

240. Ahmadzada, T., Reid, G. & Mckenzie, D. R. Fundamentals of siRNA and miRNA therapeutics and a review of targeted nanoparticle delivery systems in breast cancer. doi:10.1007/s12551-017-0392-1

241. Rothschild, S. I. microRNA therapies in cancer. *Mol. Cell. Ther.* **2,** 7 (2014).

242. Juliano, R. L. The delivery of therapeutic oligonucleotides. *Nucleic Acids Research* **44,** 6518–6548 (2016).

243. Moreno, P. M. D. & PÃªgo, A. P. Therapeutic antisense oligonucleotides against cancer: hurdling to the clinic. *Front. Chem.* **2,** 1–7 (2014).

244. Stein, C. A. Keeping the biotechnology of antisense in context. **17,** 1999 (1999).

245. Vollmer, J., Jepsen, J. S., Uhlmann, E., Schetter, C., Jurk, M., Wader, T., Wüllner, M. & Krieg, A. M. Modulation of CpG Oligodeoxynucleotide-Mediated Immune Stimulation by Locked Nucleic Acid (LNA). *Oligonucleotides* **14,** 23–31 (2004).

246. Uhlmann, Eugen; Vollmer, J. *Recent advances in the development of immunostimulatory oligonucleotides*.

247. Marquis, J. K. & Grindel, J. M. Toxicological evaluation of oligonucleotide therapeutics. *Curr. Opin. Mol. Ther.* **2,** 258–63 (2000).

248. Stein, C. A. & Castanotto, D. FDA-Approved Oligonucleotide Therapies in 2017. *Mol. Ther.* **25,** 1069–1075 (2017).

249. Kim, R., Emi, M., Tanabe, K. & Toge, T. Therapeutic potential of antisense BCL2 as a chemosensitizer for cancer therapy. *Cancer* **101,** 2491–502 (2004).

250. Matsui, M. & Corey, D. R. Non-coding RNAs as drug targets. *Nature Reviews Drug Discovery* **16,** 167–179 (2017).

251. Corey, D. R. Telomeres and Telomerase: From Discovery to Clinical Trials. *Chemistry and Biology* **16,** 1219–1223 (2009).

252. Ouellette, M. M., Wright, W. E. & Shay, J. W. Targeting telomerase-expressing cancer cells. *Journal of Cellular and Molecular Medicine* **15,** 1433–1442 (2011).

253. Promega. *GloMax®-Multi Detection System INSTRUCTIONS*. **15,** (2004).

254. Jacobs, J. L. Systematic analysis of bicistronic reporter assay data. *Nucleic Acids Res.* **32,** e160–e160 (2004).

255. Radonić, A., Thulke, S., Mackay, I. M., Landt, O., Siegert, W. & Nitsche, A. Guideline to reference gene selection for quantitative real-time PCR. *Biochem. Biophys. Res. Commun.* **313,** 856–862 (2004).

256. Livak, K. J. & Schmittgen, T. D. Analysis of relative gene expression data using real-time quantitative PCR and the 2-ΔΔCT method. *Methods* **25,** 402–408 (2001).

257. Wang, Z., Weaver, M. & Magnuson, N. S. Cryptic promoter activity in the DNA sequence corresponding to the pim-1 5???-UTR. *Nucleic Acids Res.* **33,** 2248–2258 (2005).

258. Hall, M. P., Unch, J., Binkowski, B. F., Valley, M. P., Butler, B. L., Wood, M. G., Otto, P., Zimmerman, K., Vidugiris, G., MacHleidt, T., Robers, M. B., Benink, H. A., Eggers, C. T., Slater, M. R., Meisenheimer, P. L., Klaubert, D. H., Fan, F., Encell, L. P. & Wood, K. V. Engineered luciferase reporter from a deep sea shrimp utilizing a novel imidazopyrazinone substrate. *ACS Chem. Biol.* **7,** 1848–1857 (2012).

259. Swanson, B., Fan, F. & Wood, K. Enhanced response dynamics for transription analysis using new pGL4 reporter vectors. *Cell Notes* **17,** 3–5 (2007).

260. Stansfield, I., Jones, K. M. & Tuite, M. F. The end in sight: terminating translation in eukaryotes. *Trends Biochem. Sci.* **20,** 489–491 (1995).

261. Li, C. & Zhang, J. Stop-codon read-through arises largely from molecular errors and is generally nonadaptive. *PLoS Genet.* **15,** (2019).

262. Corporation, P. *Technical Manual pGL4 Luciferase Reporter Vectors*.

263. *Nano-Glo ® Endurazine™ and Vivazine™ Live Cell Substrates Instructions for Use of*.

264. Pickering, B. M. & Willis, A. E. The implications of structured 5' untranslated regions on translation and disease. *Seminars in Cell and Developmental Biology* **16,** 39–47 (2005).

265. Stoneley, M., Paulin, F. E., Le Quesne, J. P., Chappell, S. a & Willis, a E. C-Myc 5' untranslated region contains an internal ribosome entry segment. *Oncogene* **16,** 423–428 (1998).

266. Brown, B. A. Translation of Poliovirus RNA in Vitro : Changes in Cleavage Pattern and Initiation Sites by Ribosomal Salt Wash. **405,** 396–405 (1979).

267. Dorner, A. J., Semler, B. L., Jackson, R. J. & Hanecak, R. In Vitro Translation of Poliovirus RNA : Utilization of Internal Initiation Sites in Reticulocyte Lysate. **50,** 507–514 (1984).

268. Clark, A. T., Robertson, M. E. M., Conn, G. L. & Belsham, G. J. Conserved Nucleotides within the J Domain of the Encephalomyocarditis Virus Internal Ribosome Entry Site Are Required for Activity and for Interaction with eIF4G. **77,** 12441–12449 (2003).

269. Kang, S. T., Leu, J. H., Wang, H. C., Chen, L. L., Kou, G. H. & Lo, C. F. Polycistronic mRNAs and internal ribosome entry site elements (IRES) are widely used by white spot syndrome virus (WSSV) structural protein genes. *Virology* **387,** 353–363 (2009).

270. Thakor, N. & Holcik, M. IRES-mediated translation of cellular messenger RNA operates in eIF2α- independent manner during stress.pdf. (2011). doi:10.1093/nar/gkr701

271. Hooper, K. *Applications of a smaller, brighter, more versatile luciferase: NanoLuc ™ Luciferase Technology*. (2012).

272. Thompson, S. R. So you want to know if your message has an IRES? *Wiley Interdisciplinary Reviews: RNA* **3,** 697–705 (2012).

273. Jackson, R. J. The current status of vertebrate cellular mRNA IRESs. *Cold Spring Harb. Perspect. Biol.* **5,** 1–20 (2013).

274. Han, B. & Zhang, J. Regulation of Gene Expression by Internal Ribosome Entry Sites or Cryptic Promoters : the eIF4G Story Regulation of Gene Expression by Internal Ribosome Entry Sites or Cryptic Promoters : the eIF4G Story. *Mol. Cell. Biol.* **22,** 7372–7384 (2002).

275. Vopálenský, V., Mašek, T., Horváth, O., Vicenová, B., Mokrejš, M. & Pospíšek, M. Firefly luciferase gene contains a cryptic promoter. *RNA* **14,** 1720–1729 (2008).

276. Johnson, L. F., Levis, R., Abelson, H. T., Green, H. & Penman, S. Changes in rna in relation to growth of the fibroblast: IV. Alterations in the production and processing of mRNA and

rRNA in resting and growing cells. *J. Cell Biol.* **71,** 933–938 (1976).

277. Elbashir, S. M., Martinez, J., Patkaniowska, A., Lendeckel, W. & Tuschl, T. Functional anatomy of siRNAs for mediating efficient RNAi in Drosophila melanogaster embryo lysate. *EMBO J.* **20,** 6877–6888 (2001).

278. Wiznerowicz, M. & Trono, D. Conditional suppression of cellular genes: lentivirus vector-mediated drug-inducible RNA interference. *J. Virol.* **77,** 8957–61 (2003).

279. Gao, Z., Herrera-Carrillo, E. & Berkhout, B. Delineation of the Exact Transcription Termination Signal for Type 3 Polymerase III. *Mol. Ther. - Nucleic Acids* **10,** 36–44 (2018).

280. Belitsky, J. M., Leslie, S. J., Arora, P. S., Beerman, T. A. & Dervan, P. B. Cellular uptake of N-methylpyrrole/N-methylimidazole polyamide-dye conjugates. *Bioorganic Med. Chem.* **10,** 3313–3318 (2002).

281. Elbashir, S. M., Harborth, J., Weber, K. & Tuschl, T. Analysis of gene function in somatic mammalian cells using small interfering RNAs. *Methods* **26,** 199–213 (2002).

282. Touznik, A., Maruyama, R., Hosoki, K., Echigoya, Y. & Yokota, T. LNA/DNA mixmer-based antisense oligonucleotides correct alternative splicing of the SMN2 gene and restore SMN protein expression in type 1 SMA fibroblasts. *Sci. Rep.* **7,** 1–9 (2017).

283. Braasch, D. A., Liu, Y. & Corey, D. R. Antisense inhibition of gene expression in cells by oligonucleotides incorporating locked nucleic acids: Effect of mRNA target sequence and chimera design. *Nucleic Acids Res.* **30,** 5160–5167 (2002).

284. Torres, A., Kozak, J., Korolczuk, A., Wdowiak, P., Domańska-Glonek, E., Maciejewski, R. & Torres, K. In vitro and in vivo activity of miR-92a–Locked Nucleic Acid (LNA)–Inhibitor against endometrial cancer. *BMC Cancer* **16,** 822 (2016).

285. Gupta, N., Fisker, N., Asselin, M. C., Lindholm, M., Rosenbohm, C., Ørum, H., Elmén, J., Seidah, N. G. & Straarup, E. M. A locked nucleic acid antisense oligonucleotide (LNA) silences PCSK9 and enhances LDLR expression In Vitro and In Vivo. *PLoS One* **5,** 1–9 (2010).

286. Nulf, C. J. & Corey, D. Intracellular inhibition of hepatitis C virus (HCV) internal ribosomal entry site (IRES)-dependent translation by peptide nucleic acids (PNAs) and locked nucleic acids (LNAs). *Nucleic Acids Res.* **32,** 3792–3798 (2004).

287. Varshavsky, A. The N-end rule pathway of protein degradation. *Genes to Cells* **2,** 13–28 (1997).

288. Rahman, M. & Sadygov, R. G. Predicting the protein half-life in tissue from its cellular properties. *PLoS One* **12,** (2017).

289. ExPASy - ProtParam documentation. Available at: https://web.expasy.org/protparam/protparam-doc.html. (Accessed: 6th November 2019)

290. Zhou, P. Determining protein half-lives. *Methods Mol. Biol.* **284,** 67–77 (2004).

291. Kao, S.-H., Wang, W.-L., Chen, C.-Y., Chang, Y.-L., Wu, Y.-Y., Wang, Y.-T., Wang, S.-P., Nesvizhskii, A., Chen, Y.-J., Hong, T.-M. & Yang, P.-C. Analysis of Protein Stability by the Cycloheximide Chase Assay. *BIO-PROTOCOL* **5,** (2015).

292. Hägerlöf, M., Papsai, P., Hedman, H. K., Jungwirth, U., Jenei, V. & Elmroth, S. K. C. Cisplatin and siRNA interference with structure and function of Wnt-5a mRNA: Design and in vitro evaluation of targeting AU-rich elements in the 3′ UTR. *Journal of Biological Inorganic Chemistry* **13,** 385–399 (2008).

293. Taylor, M. F., Paulauskis, J. D., Weller, D. D. & Kobzik, L. In vitro efficacy of morpholino-modified antisense oligomers directed against tumor necrosis factor-α mRNA. *Journal of Biological Chemistry* **271,** 17445–17452 (1996).

294. Gorska, A., Swiatkowska, A., Dutkiewicz, M. & Ciesiolka, J. Modulation of p53 expression using antisense oligonucleotides complementary to the 5′-terminal region of p53 mRNA in vitro and in the living cells. *PLoS ONE* **8,** (2013).

295. Tallet-Lopez, B., Aldaz-Carroll, L., Chabas, S., Dausse, E., Staedel, C. & Toulme, J. J. Antisense oligonucleotides targeted to the domain IIId of the hepatitis C virus IRES compete with 40S ribosomal subunit binding and prevent in vitro translation. *Nucleic Acids Res.* **31,** 734–742 (2003).

296. Yu, C. H., Noteborn, M. H. M. & Olsthoorn, R. C. L. Stimulation of ribosomal frameshifting by antisense LNA. *Nucleic Acids Res.* **38,** 8277–8283 (2010).

297. Maden, B. E. H., Corbett, M. E., Heeney, P. A., Pugh, K. & Ajuh, P. M. Classical and novel approaches to the detection and localization of the numerous modified nucleotides in eukaryotic ribosomal RNA. *Biochimie* **77,** 22–29 (1995).

298. Coldwell, M. J. *Identification and functional analysis of internal ribosome entry segments in APAF-1 and BAG-1 mRNAs by*. (2000).

299. German Collection of Microorganisms and Cell Cultures GmbH: Details. Available at:

https://www.dsmz.de/collection/catalogue/details/culture/ACC-302. (Accessed: 28th October 2019)

300. German Collection of Microorganisms and Cell Cultures GmbH: Details. Available at: https://www.dsmz.de/collection/catalogue/details/culture/ACC-305. (Accessed: 28th October 2019)

301. Weingarten-Gabbay, S., Elias-Kirma, S., Nir, R., Gritsenko, A. A., Stern-Ginossar, N., Yakhini, Z., Weinberger, A. & Segal, E. Comparative genetics: Systematic discovery of cap-independent translation sequences in human and viral genomes. *Science (80-.).* **351,** (2016).

302. Gritsenko, A. A., Weingarten-Gabbay, S., Elias-Kirma, S., Nir, R., de Ridder, D. & Segal, E. Sequence features of viral and human Internal Ribosome Entry Sites predictive of their activity. *PLoS Comput. Biol.* **13,** (2017).

303. Wang, J. & Gribskov, M. IRESpy: an XGBoost model for prediction of internal ribosome entry sites. *BMC Bioinformatics* **20,** 409 (2019).

304. Morris, P. D., Tackett, A. J. & Raney, K. D. Biotin-streptavidin-labeled oligonucleotides as probes of helicase mechanisms. *Methods* **23,** 149–159 (2001).

305. Murasugi, A. & Wallace, R. B. Biotin-labeled oligonucleotides: enzymatic synthesis and use as hybridization probes. *DNA* **3,** 269–77 (1984).

306. Cook, A. F., Vuocolo, E. & Brakel, C. L. Synthesis and hybridization of a series of biotinylated oligonucleotides. *Nucleic Acids Res.* **16,** 4077–4095 (1988).

307. Hassan, T., Smith, S. G. J., Gaughan, K., Oglesby, I. K., O'Neill, S., McElvaney, N. G. & Greene, C. M. Isolation and identification of cell-specific microRNAs targeting a messenger RNA using a biotinylated anti-sense oligonucleotide capture affinity technique. *Nucleic Acids Res.* **41,** (2013).

308. Aveic, S., Pigazzi, M. & Basso, G. BAG1: The guardian of anti-apoptotic proteins in acute myeloid leukemia. *PLoS One* **6,** (2011).

309. Soifer, H. S., Koch, T., Lai, J., Hansen, B., Hoeg, A., Oerum, H. & Stein, C. A. Silencing of gene expression by gymnotic delivery of antisense oligonucleotides. *Methods Mol. Biol.* **815,** 333–346 (2012).

310. Karaki, S., Benizri, S., Mejías, R., Baylot, V., Branger, N., Nguyen, T., Vialet, B., Oumzil, K.,

Barthélémy, P. & Rocchi, P. Lipid-oligonucleotide conjugates improve cellular uptake and efficiency of TCTP-antisense in castration-resistant prostate cancer. *J. Control. Release* **258,** 1–9 (2017).

311. Godeau, G., Staedel, C. & Barthélémy, P. Lipid-conjugated oligonucleotides via 'click chemistry' efficiently inhibit hepatitis C virus translation. *J. Med. Chem.* **51,** 4374–6 (2008).

312. Epa, W. R., Rong, P., Bartlett, P. F., Coulson, E. J. & Barrett, G. L. Enhanced downregulation of the p75 nerve growth factor receptor by cholesteryl and bis-cholesteryl antisense oligonucleotides. *Antisense Nucleic Acid Drug Dev.* **8,** 489–498 (1998).

313. Godeau, G., Arnion, H., Brun, C., Staedel, C. & Barthélémy, P. Fluorocarbon oligonucleotide conjugates for nucleic acids delivery. *Medchemcomm* **1,** 76–78 (2010).

314. Sun, Y., Zhao, Y., Zhao, X., Lee, R. J., Teng, L. & Zhou, C. Enhancing the Therapeutic Delivery of Oligonucleotides by Chemical Modification and Nanoparticle Encapsulation. *Molecules* (2017). doi:10.3390/molecules22101724